



10th IAG INTERNATIONAL CONFERENCE ON GEOMORPHOLOGY

Photo by Sérgio Brito

COIMBRA - PORTUGAL
« GEOMORPHOLOGY AND GLOBAL CHANGE »

FIELDTRIP GUIDEBOOK

Arouca Geopark

14 September 2022

Artur A. Sá
António Vieira
Daniela Rocha



Artur A. Sá
António Vieira
Daniela Rocha

10th International Conference on Geomorphology Fieldtrip Guidebook – Arouca Geopark

14 September 2022



Coimbra, 2022

Edition notice:

Title: *10th International Conference on Geomorphology. Fieldtrip Guidebook – Arouca Geopark*

Authors: *Artur A. Sá (UTAD), António Vieira (UMinho) and Daniela Rocha (Arouca Geopark)*

Fieldtrip guided by: *Artur A. Sá (UTAD), António Vieira (UMinho) and Daniela Rocha (Arouca Geopark)*

Edition: *Universidade de Coimbra, Faculdade de Letras*

Fieldtrip and Guidebook Coordination: *António Vieira (University of Minho)*

Cover: *Perspective from the Detrelo da Malhada viewpoint (photograph by António Vieira)*

ISBN: 978-989-8511-02-7

Introductory Note

The 10th International Conference on Geomorphology will take place in Coimbra (Portugal) from 12th to 16th September 2022, under the theme "Geomorphology and Global Change" and it is organized by the International Association of Geomorphologists (IAG) and the Portuguese Association of Geomorphologists (APGeom).

As in previous international conferences on Geomorphology, and as is the tradition in many geomorphological events organized around the world, the organizing committee of the 10th International Conference on Geomorphology proposed several fieldtrips to the participants, occurring before, during and after the main event.

These fieldtrips intend, above all, to show to geomorphologists from all over the world the diversity and richness of the geomorphological elements of the Portuguese territory (and also from Cape Verde) and to allow an exchange of experiences between the specialists that investigate these territories and the visitors, contributing for mutual scientific enrichment and for the valorization of this international conference.

The pre-conference fieldtrip is dedicated to the islands of Santiago and Fogo, in the Archipelago of Cape Verde. It will take place from 6th to 9th September and will be led by colleagues from the University of Cape Verde (Vera Alfama, Sónia Victória, Sílvia Monteiro, José Maria Semedo and Romualdo Correia). The volcanic geomorphology will dominate the visit (including well conserved structural volcanic forms such as cones, domes, craters and calderas), especially in the island of Fogo where recent volcanic activity has been registered.

The one-day mid-conference fieldtrips will take the visitors around the Portuguese mainland territory, the 14th September, allowing the visit of four different geomorphological realities.

In the Arouca UNESCO Global Geopark, internationally recognized territory since 2009, participants will be able to visit unique geological and geomorphological features (such as planation surfaces, bowl-shaped valleys and narrow river valleys) and witness the remarkable effort of protection and promotion of natural (abiotic and biotic) and cultural (tangible and intangible) heritage. The visit to the "516 Arouca" suspension bridge will be an excellent opportunity to observe the magnificent landscapes of this mountainous territory. This fieldtrip will be led by Artur A. Sá, António Vieira and Daniela Rocha.

The field trip to coastal areas of central Portugal will be led by Pedro Dinis and António Campar Almeida. Their proposal is to observe the different morphotectonic units of central west Portugal, namely the Coastal Mountain of Serra da Boa Viagem (revealing karstification features), the littoral plain (with aeolian dunes associated with some

reliefs with higher elevation), the Cértima subsiding area (structurally-controlled morphology), and the Buçaco region (with the Syncline of Buçaco).

The visit to the Schist Mountains of Central Portugal will be centered in the mountains of Lousã and Açor, and will be conducted by Luciano Lourenço and Bruno Martins. It is proposed the observation of the main contrasts of the landscape, especially in terms of its physical geography, translated into geological, hypsometric, geomorphological, and hydrographic differentiation, or the land use and occupation and evolution of vegetation cover, namely following the recurrent large forest fires and the subsequent erosive processes they caused.

The fourth one-day fieldtrip will be oriented to the Estrela UNESCO Global Geopark, and led by Gonçalo Vieira, Emanuel Castro and Fábio Loureiro. The main geoheritage significance of the Estrela UGGp is the extent and richness of the Late Pleistocene glaciation(s) landforms and deposits (with spectacular morphological features such as the Zêzere glacial valley or the glacial cirques, moraine boulders, erratics or *roches moutounnées*) as well as the peculiar long-term geological evolution (revealing a significant diversity of granite types and landforms).

The three post-conference fieldtrips include a visit to the Lisbon Region, Serra da Estrela and, finally, Minho and Galicia (Spain), and will take place from 17th to 19th September.

The fieldtrip to the Lisbon Region will be guided by José Luís Zêzere, César Andrade, Sérgio Oliveira, Jorge Trindade and Ricardo Garcia, and will cover topics related with slope instability and landslides that affect the region of Lisbon, the floods occurring in the area north of Lisbon, and the coastal dynamics, morphology, cliff instability and beach erosion at north and south of Lisbon.

The three days field trip to the Serra da Estrela is led by Gonçalo Vieira, Emanuel Castro and Fábio Loureiro. Participants will be taken to visit some of the Geopark's most inaccessible geosites and observe breathtaking landscapes during two hikes: one in the Zêzere valley and the other between Penhas Douradas and Lagoa Comprida. The different geosites to visit include features of glacial, periglacial, granite weathering, fluvial, hydrogeological, petrological and tectonic themes, and aspects related with the management of a UNESCO Global Geopark will be discussed.

The third three-days fieldtrip is destined to the northwestern part of Portugal and the Spanish region of Galicia. Guided by Alberto Gomes and Antonio Perez Alberti, will be mainly devoted to the coastal area and to the observation and discussion of issues related to coastal dynamics, marine terrace staircases, differential uplift of coastal blocks, coastal geoheritage, coastal geoarchaeology, coastal erosion and coastal land planning.

It is our expectation that these visits will please all participants and promote the scientific enrichment of all involved, allowing a better understanding of the topics covered in each one.

We also hope that this set of fieldtrip guidebooks can help in the understanding of the themes discussed and that they can be a testimony of the commitment and dedication shown by all the scientific responsible for the several visits, to whom the organizing committee of the International Conference on Geomorphology expresses its greatest recognition and gratitude.

have a good fieldtrip!

Lúcio José Sobral da Cunha
António Vieira

on behalf of the ICG2022 Organizing Committee

ITINERARY AND SCHEDULE

Itinerary (Fig. 1 and 2)

07h00 – Departure from Coimbra

09h00 – 09h15 – Montemuro Doors (Castro Daire)

10h00 – 10h30 – S. Pedro do Campo viewpoint and Pedra Posta geosite

11h00 – 12h30 – “516 Arouca” suspension bridge and Paiva Walkways

13h00 – Senhora da Mó viewpoint – lunch pick-nick

14h30-15h00 – Detrelo da Malhada viewpoint (Freita Mountain)

15h30-16h00 - São Pedro Velho bornhardt

16h30-17h00 – Frecha da Mizarela waterfall

19h00 – Arrival to Coimbra

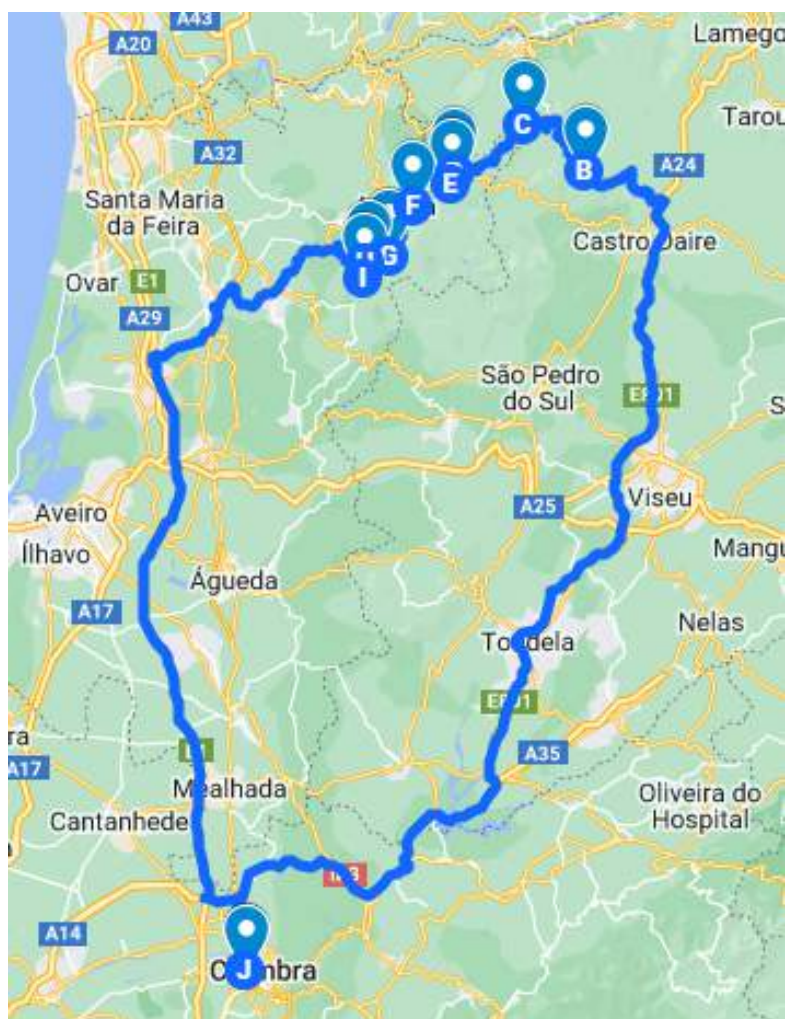


Figure 1. General itinerary

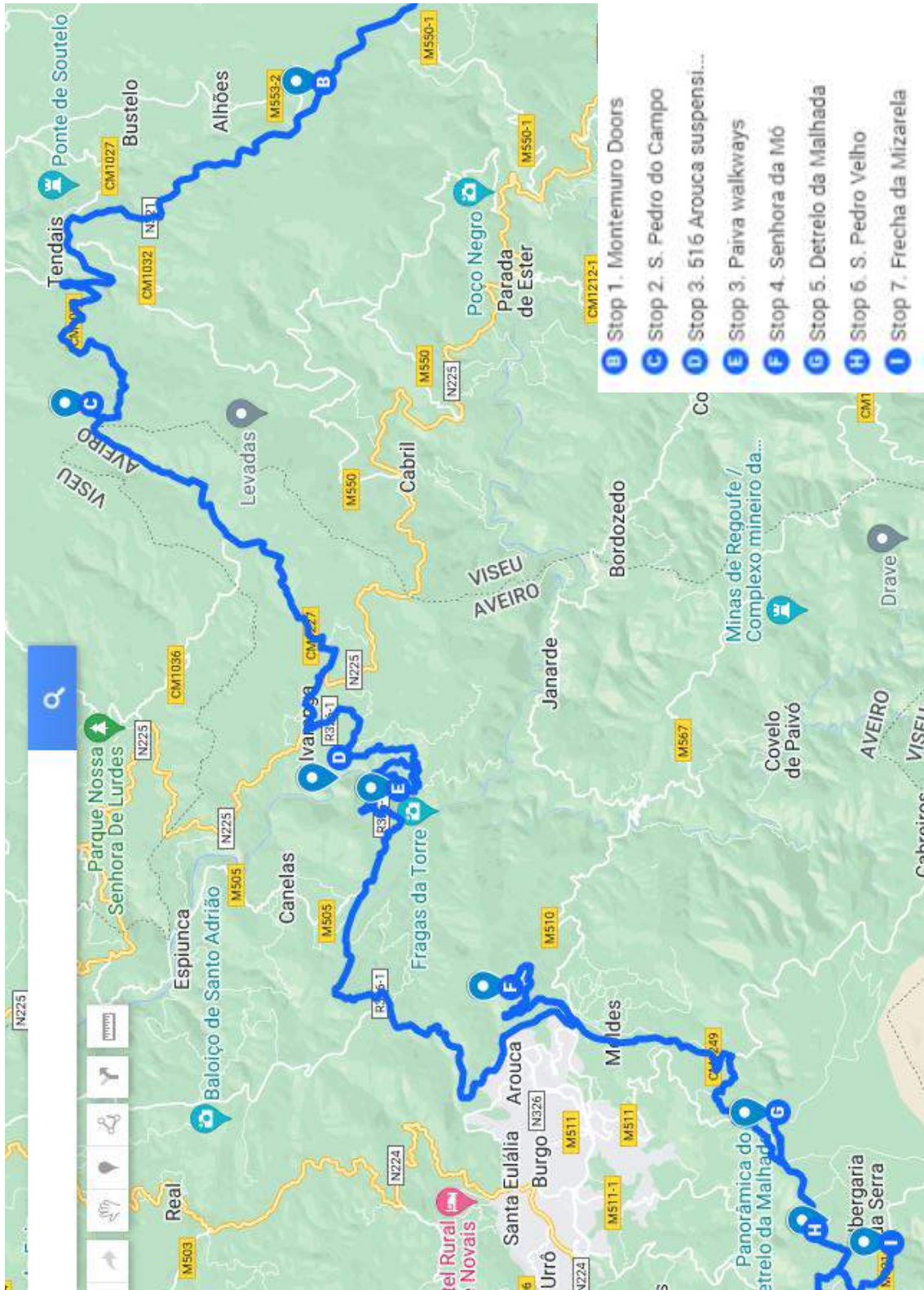


Figure 2. Partial itinerary with stops.

Introduction

The Arouca UNESCO Global Geopark (Arouca UGGp) is an internationally recognized territory since 2009, comprising a total of 328 km² and 21.154 inhabitants (INE, 2021). This recognition is due to its unique geological heritage promoted through a strategy for territorial development. This involves the protection and promotion of natural (abiotic and biotic) and cultural (tangible and intangible) heritage. The sustainable regional development strategy entails a holistic approach based on the development and implementation of educational, scientific, cultural and/or geotouristic activities. Local communities are involved in these activities and in working together in order to contribute for the achievement of a territorial sustainable economic development. To date were identified, characterized and evaluated 41 geosites in the Arouca UGGp. Among them, 24 are of geomorphological interest. Mostly they correspond to major landforms including planation surfaces, bowl-shaped valleys and narrow river valleys (Sá & Rocha, 2020).

The landforms of the Arouca UGGp have been valued in recent years as fundamental elements of the regional landscape, having assumed educational and geotourism importance. In this sense, its advertising and dissemination promoted by the Arouca Geopark Association (AGA) have allowed visitors to know and understand the processes that gave rise to the geomorphology and landscapes of this territory. Visits to geosites during educational programs, guided tours or tourist events provided visitors with close contact with the region and its people, stimulating the revitalization of communities, the knowledge and promotion of locally based products and the development of a sense of place. This reality has significantly contributed to the economic development of the Arouca UGGp.

Currently and taking into account a set of economic macro-indicators, the dynamics associated with promotion and visitation activities, directly and indirectly involving the reality of Arouca UGGp, represent an estimated annual financial return of at least 15 million euros (Rebelo *et al.*, 2014).

The visit to Arouca UGGp as part of the 10th International Conference on Geomorphology will allow participants to get in touch with this mountainous territory, carved by deep and narrow valleys. The geology of this territory (Fig. 3), almost exclusively constituted by metasedimentary rocks from the Neoproterozoic-Carboniferous periods and by Variscan granites, shaped the landscapes, conditioned the population settlements and even moulded the people, influencing their constructions and their habits of use of land. In this sense, we hope that despite the brevity of the visit, the participants will be able to enjoy it and feel the desire to return, perhaps to develop research in this territory of Education, Science and Culture.

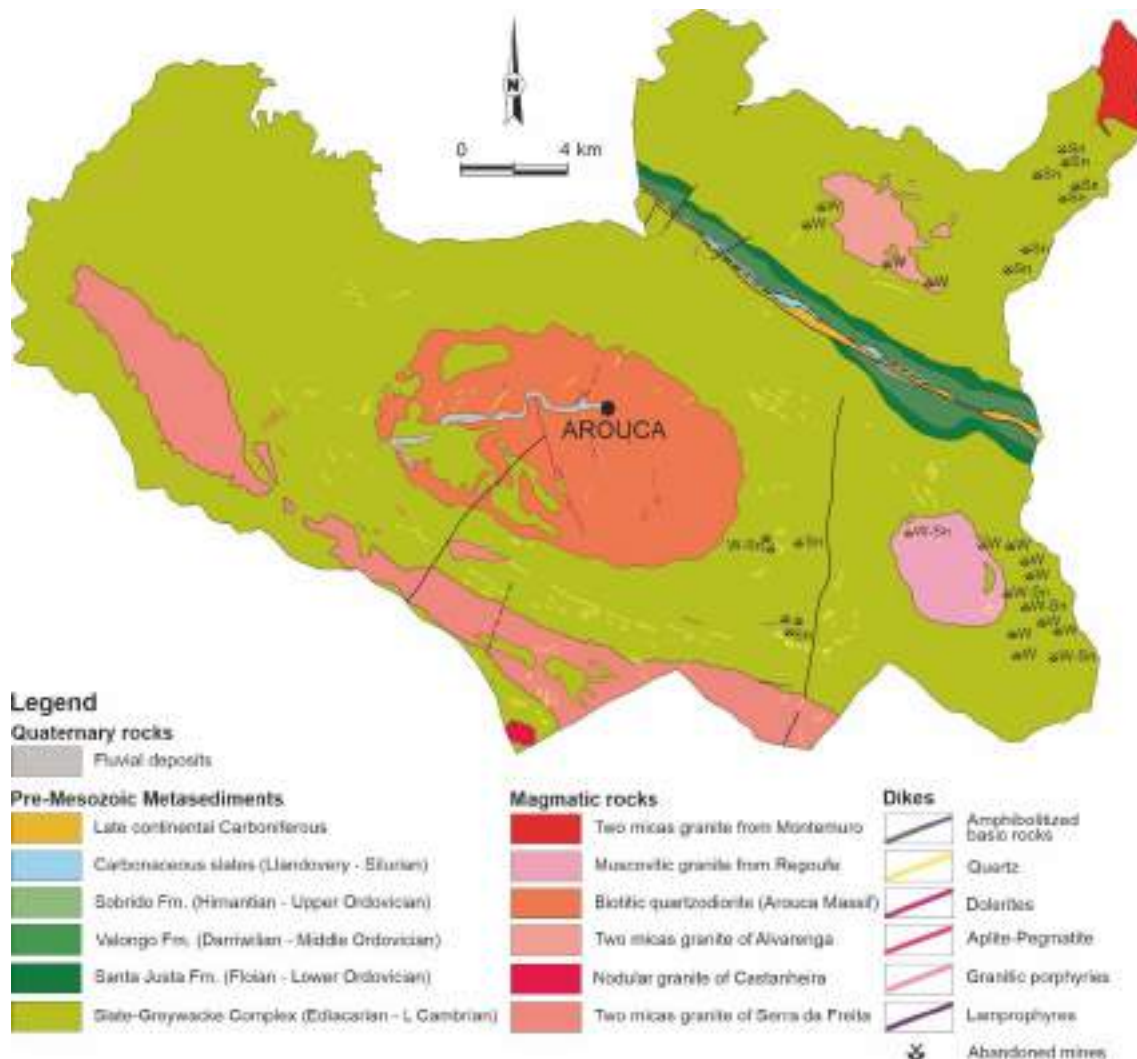


Figure 3. Simplified Geological map from Arouca Geopark and schematic geological profile. Adapted from the pages 13-B (Castelo de Paiva), 13-D (Oliveira de Azeméis), 14-A (Lamego) e 14-C (Castro Daire) of the Geological Map of Portugal, 1:50 000 scale.

According to the large morphostructural units of the Iberian Peninsula, the Arouca UGGp is geologically framed in the so-called Hesperian or Iberian Massif. This is characterized, in general terms, for being composed of metamorphic and magmatic rocks, which extend in age from the Neoproterozoic to the late Palaeozoic.

The Hesperic Massif is divided into several zones, according to its tectonic characteristics, with the Arouca UGGp being inserted in the Central Iberian Zone (Fig. 4).

Of all the differentiated structural and palaeogeographic zones within the Hesperian Massif, the most extensive portion corresponds to the so-called Central-Iberian Zone, whose central-southern sectors are characterized by extensive outcrops of ancient materials (Neoproterozoic to middle Cambrian?), which separate quartzite mountains, aligned according to the previously mentioned orientations. These mountain ranges, remarkably elongated and narrow, are the ones that preserve the rest of the Palaeozoic succession, formed by marine sediments of the Ordovician-lower Carboniferous age,

which are associated with continental deposits rich in terminal Carboniferous charcoal, formed synchronously with the folding and fracturing and associated with mountain lifting.

At Arouca UGGp, metamorphic and magmatic rocks outcrop with ages between approximately 600 Ma and 300 Ma. In this territory, the geological diversity is expressed in a unique way in its landscapes, punctuated by mountains sculpted by rivers that open their way through embedded valleys.

It is the above mentioned reality that, in a general way, we intend to make known during this brief visit to Arouca UGGp.

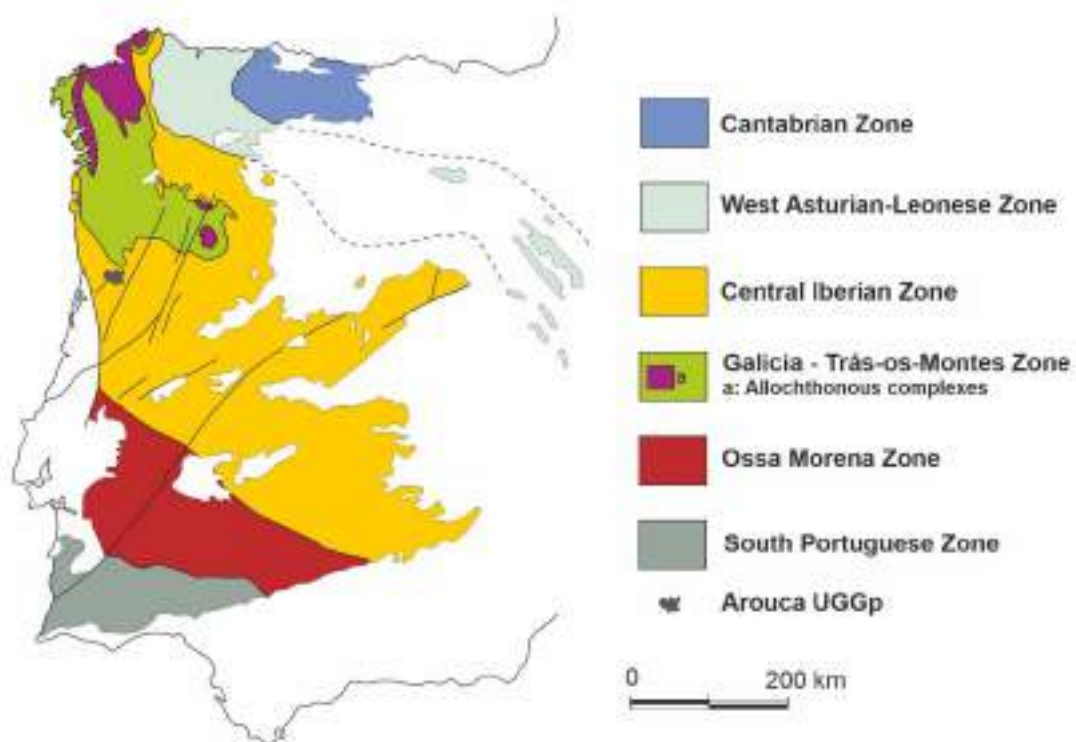


Figure 4. Division of the Hesperic Massif according to its tectono-stratigraphic characteristics, with reference to the location of the Arouca UGGp.

Stop 1. “Montemuro Doors” viewpoint

The designation of this viewpoint derives, according to Girão (1940), from the existence of a “work to defend an important population centre contemporary perhaps with the Roman conquest” (p. 10). Indeed, the ruins of the “Wall of the Montemuro Doors” are classified as an archaeological site and have been classified as a Property of Public Interest since 1974. In the 13th century, it was already mentioned in the Inquiries of 1258. According to several authors, the site has scant traces of a village fortified from the Iron Age, and can be considered as part of the Castro culture. “Doors” refers to a crossing point and “Wall” to the village wall. It was also called by shepherds and hunters as “Wall of Doors” or just “Wall” (C.M. Castro Daire, s.d.) (Fig. 5).



Figure 5. Wall of the Montemuro Doors. ©CM Cinfães

From “Montemuro Doors”, we have an impressive perspective of the morpho-structural units that characterize the north and littoral-center of Portugal: to the north, the Douro valley and the Marão mountain range; the highest sector of the Montemuro Mountain and the Central Plateaus to the east; the Gralheira Massif and Serra do Caramulo to the south; and to the west, the gradual descent towards the coast.

The “Montemuro Doors” viewpoint coincides with the passage between the south and southwest slopes of the Montemuro Mountain, well marked by the Paiva River valley, and the north slope, facing the Douro River. It also corresponds to the transition between the western sector, from S. Pedro do Campo – Perneval, and the culminating sector of the Montemuro Mountain and the Eastern Plateaus, which here give continuity to the Central Plateaus. (Vieira & Sá, 2019).

Among the geomorphological elements present in the Montemuro Mountain observable from this point, the Bestança River fracture valley and the immense diversity of granitic geofoms that outcrop here are worth mentioning. The Bestança River fracture valley (Fig. 6). It extends in a straight line, with a NW-SE direction and for more than 20 km, from the highest sectors of the Montemuro Mountain, next to the “Montemuro Doors”, to the Douro River.

The spectacularity of this valley is accentuated by the granite foothills of the Serra de Montemuro, more imposing on the left bank of the Bestança River, which contrast with the lower altitudes and less steep slopes to the East, associated with the movement of the fault.

The fracture valleys in the granitic regions are directly related to the exploitation, by the watercourses, of the structural weaknesses due to the fracturing of these rocks.

From the point of view of its valorization, we emphasize its scientific, aesthetic and ecological value. From these geomorphological elements we can observe the influence of the structure on the morphological evolution, allowing us to clearly identify the areas

of fragility of the granite massifs and the preferential action of the erosion processes. In addition to these aspects, they are excellent places for the observation of well-preserved riparian galleries, characterized by important ecosystem values. In addition to all this, it has an aesthetic value, provided by the high beauty of the landscape (Vieira, 2008; Vieira & Sá, 2019).



Figure 6. Fracture valley of the Bestança River. © António Vieira

Regarding the examples of granitic morphology observable in the area surrounding the “Montemuro Doors”, the rocky domes of Perneval (Fig. 7) and Montemuro stand out, the latter corresponding to the highest point of the Montemuro Mountain (1382 m).



Figure 7. Rocky dome of Perneval. © António Vieira

These two forms correspond to larger granitic residual forms that reach kilometric dimensions. In the granitic literature they are often called bornhardt, constituting the most common and widespread type of inselberg. The bornhardt form is delineated by predominantly vertical or subvertical fractures, which are part of the orthogonal system (Twidale, 1982; Vidal Romaní & Twidale, 1998). The domic shape is defined, however, by the scaling, arched and convex structures, which give rise to essentially convex slopes.

Stop 2. S. Pedro do Campo viewpoint and Pedra Posta geosite

The viewpoint of S. Pedro do Campo is located in the western sector of the Serra de Montemuro, at about 1130 meters of altitude. It is close to the chapel of S. Pedro, in the middle of the summit of the Montemuro mountain range, where the Pedra Posta geosite is identified. This corresponds to a tor in the Montemuro granite, characterized by being a biotite-muscovitic granite, porphyroid with medium to medium-fine grains, sometimes becoming coarse. The SW of the chapel of S. Pedro do Campo develops a set of detailed granite forms that constitute a geomorphological nucleus of high interest. Located at an altitude of about 1150 meters, it incorporates forms of the tafoni type (Moor's House), "swinging stones", slabs, gnammas, pseudo-stratifications, cannelures and polygonal cracks ("Corn bread" rock of Montemuro) (Fig. 8).



Figure 8. 'Swinging stones' located SW of the chapel of S. Pedro do Campo. © Tiago Martins / visitarouca.pt

The varied granitic morphology that can be observed here is a relevant aspect for the scientific valorization of this site. However, it is the aesthetic and landscape value that are assumed to be most important in this place (Fig. 9). The granitic landscapes of Montemuro Mountain, the Douro River valley and the Marão Mountain, to the north or the Gralheira massif to the SW, are elements of high scenic beauty that can be enjoyed from this location. Here, you can also appreciate the contrasting landscapes of the various landscape units of the Montemuro Mountain. Here, cultural aspects are also associated with natural ones, with this place of religious worship being associated with the geomorphological elements that stand out in this typically granitic landscape. (Vieira, 2008; Rocha, 2016, Vieira & Sá, 2019).



Figure 9. Landscape and granitic forms in the Pedra Posta geosite. © Tiago Martins / visitarouca.pt

Stop 3. “516 Arouca” suspension bridge and Paiva Walkway

This stop will require a walk of about 2,5 km, mostly downhill. Departing from Alvarenga, we will walk on a medium-grain, two-mica granite known as Alvarenga Granite. In contact with the formations of the Dúrico-Beirão Schist-Greywacke Supergroup, an aureole of metamorphism originated essentially formed by pelitic hornfels. This granitic intrusion, intensely eroded and giving rise to a bowl-shaped valley where the village of Alvarenga is located, is associated with a left shear zone and important tungsten mineralization, which were intensively exploited in placer deposits, essentially during the Second World War. (Medeiros *et al.*, 1964)

The path takes us to the “516 Arouca” suspension bridge, which is currently the third longest infrastructure of this type in the world. It is an iconic work in the Arouca UGGp, consisting of 127 trays of metallic railings and steel cables, with a span of 516 meters, 1.20 meters wide and 175 meters high above the Paiva River. Each of the decks that make up the bridge works as a kind of independent capsule. In this way, the feeling of security and comfort becomes greater (Fig. 10).



Figure 10. “516 Arouca” suspension bridge, with view for the Aguieiras waterfall. Alvarenga village in the background. © Publituris.pt

As this area is also classified as part of the Natura 2000 protected areas network, visitors can immediately observe a rich and diversified fauna and flora, where there are several endemic species and even endangered species.

When crossing the bridge it is possible to observe the Aguieiras waterfall, one of the geosites of the Arouca UGGp. It is formed by the Aguieiras stream, the result of the confluence of several water lines that drain the bowl-shaped valley of Alvarenga, which falls precipitously by the granite cliffs that flank the right bank of the Paiva River, through a set of gaps totalling about of 160 m. The origin of this waterfall is entirely conditioned by the orthogonal fracturing network of this granitic massif (Rocha, 2008; 2016; Sá *et al.*, 2008).

This waterfall is properly equipped for canyoning, an adventure sport, which is characterized by a controlled progression in the bed of a river/stream, through the transposition of vertical obstacles using different techniques. When going through this canyoning, it is need to overcome nine gaps in rappel, the largest of which has a gap of 65 m, for a period of time that can extend between 2 to 3 hours. It is classified as a slightly difficult canyon (Class 3, for a maximum of 7) (Paz *et al.*, 2014).

In the middle of the bridge, it is still possible to observe, upstream of the bridge, the valley excavated in a canyon, with vertical walls, locally known as “Paiva Gorge” and which is a geosite, of linear typology, of the Arouca UGGp. Downstream of the bridge, it can be seen that the Paiva River valley opens in a wide V. This marked geomorphological variation is entirely associated with the bedrock that the river intersects, in the first case the granites and in the second the schists and greywackes, with the latter being more deformed and fractured and less resistant to erosion. Various differences in levels between tight gorges and rocks make the Paiva River one of the best rivers for practicing white water activities in the winter months, such as rafting, kayaking, hydrospeeding and canoeing. It is considered by experts as one of the best whitewater tracks nationally and a reference at an international level.

During and after crossing the bridge, it is possible to observe on the left bank of the Paiva River a wooden infrastructure that corresponds to the famous “*Passadiços do Paiva*” (= Paiva walkways). This infrastructure are currently the most popular tourist infrastructure in Arouca UGGp. Designed to allow visitors to access and enjoy the beauty of the pristine nature existing in the canyon section of the Paiva River, mainly in its section excavated in the Alvarenga Granite, this walkway quickly took on a media coverage that, since its opening in June 2015, more than 2.000.000 visitors have requested this infrastructure. The mission of this walkway is to preserve, enhance and publicize the Paiva River and its surroundings (landscape, geosites, ecosystems and biodiversity), making the territory more sustainable and resilient. As a corollary of this impact on local tourism, the Paiva Walkways have been awarded since 2016 with eleven World Travel Awards, considered the “tourism Oscars”, in categories such as “Best European Tourism Development Project”, “Best European Tourist Attraction of Adventure” or “Best Adventure Tourism Attraction in the World”. Currently, daily access to the infrastructure is limited to 2.000 visitors, who must previously register and purchase the necessary access ticket via the internet (<https://reservas.passadicosdopaiva.pt/en/bilhetes>).

Travel along the approximately 8.6 km of this infrastructure built in wood along the left bank River Paiva (Fig. 11) allows visitors not only to enjoy a healthy walk in contact with nature, but also to learn about the geological (visit to five geosites of Arouca UGGp) and biological heritage (biodiversity station) of the territory (Vieira & Sá, 2019).

We will walk upstream along the left bank, going down the walkways to the Alvarenga bridge, a masonry road structure that is right at the entrance to the Paiva Gorge. From this is possible to observe the open V-shaped valley upstream, the hornfels marking the geological contact, and the giant potholes at different levels on the banks and riverbed (Rocha, 2008; 2016; Sá *et al.*, 2008; Sá & Rocha, 2020).



Figure 11. Paiva walkways, in the left bank of the Paiva River. © AGA

The bridge, dating from the 18th century, was ordered to be built by the Bishop of Lamego (D. João) and completed in 1791, by charter of D. Maria I (Oliveira *et al.*, 1999). It is made up of three arches with its main arch spanning seven meters (Fig. 12).



Figure 12. Alvarenga bridge, seen from the Paiva walkways, marking the entrance to the Paiva Gorge geosite. © AGA

Stop 4. Senhora da Mó viewpoint

Senhora da Mó is the best-known viewpoint of the Geopark, located in a position overlooking Arouca; it provides an excellent site to view the general geomorphological pattern of the region within a 360° panorama. The landscape is characterized by the occurrence of igneous, metamorphic and sedimentary rocks with differential resistance to weathering and erosion.

The Arda Valley, excavated in the Arouca bowl-shaped valley with its fertile soil, is a symbol of the main economic activity developed in the region for centuries (Sá & Rocha, 2020).

In this place, there is a small chapel with Arab features (Fig. 13), built in honor of *Senhora da Mó* (= Our Lady of the Millstone) who, according to legend, saved a Christian from slavery by the Moors. Trapped inside a wooden box, with a millstone on top, he took advantage of the knots in the rope to pray fervently, achieving the miracle of deliverance. Therefore, on the night of the 7th to the 8th of September, the men of Arouca bring to life the *Casa da Ceia* (= supper house), located next to the chapel, preparing codfish and all the delicacies of the feast in honour of the patroness. In Arouca, Our Lady of the Millstone is considered a lawyer for the fields, crops and animals and a protector against droughts and thunderstorms. It is also said that the Lady «has six more sisters», as the hermitages of Marian invocation can be seen from her chapel, located in the surrounding hills: Our Lady of the Hill; Our Lady of the Slab; Our Lady of the Blackberries; Our Lady of the Castle; Our Lady of the Guidance and Sainte Marie of the Hill (Costa, 2003).



Figure 13. Our Lady of the Millstone chapel. © European Atlantic Geotourism Route.

Lunch will be a pick-nick with products bearing the seal “GEOFood®”. The initiative and registered trademark “GEOfood®” appeared in 2015, coordinated by Magma UGGp in

Norway, Odsherred UGGp in Denmark, Rokua UGGp in Finland and Rejkyanes UGGp in Iceland. Today it constitutes an International Network, which brings together several UGGps and which aims to promote and enhance the relationship between its unique geological heritage and local food traditions. The AGA has been stimulating and promoting the agricultural sector and its food chain through the municipal project “Arouca Agrícola” (= Agricultural Arouca), articulating it with the principles of the GEOfood® network. The main goal is to link food and territory, tourism and health, sustainability and flavour and, in this way, bring the consumer closer to nature, local products and their origin and culture.

Currently GEOfood® International Network is an international movement that promotes the connections between local food and geological heritage, so that these can be used to enhance sustainable development in UNESCO Global Geoparks. GEOfood aims to increase the awareness of geological heritage and its connection to peoples’ livelihoods. GEOfood products are branded to make consumers aware of the strong connection between food production and geodiversity. The “IGCP 726 GEOfood for sustainable development in UNESCO Global Geoparks Project” (Fig. 14), supported by UNESCO, proposes a scientific approach to GEOfood, starting from the connection between geoheritage, geodiversity, ecosystem services, food production and sustainable development (UNESCO, 2022).



Figure 14. Official logo of the “IGCP 726 GEOfood for sustainable development in UNESCO Global Geoparks” Project.

Arouca UGGp is part of the GEOfood® International Network, offering locally a network of participating restaurants, which include a greater variety of local products in their menus; tourist visits to producers - «Arouca Agrícola Itineraries», awareness actions, with the school community, through the pedagogical restaurant and canteens or through dedicated educational programs and projects.

Stop 5. Detrelo da Malhada viewpoint

Accessing the existing visitor platform at the Detrelo da Malhada viewpoint (Fig. 15), it is possible to see a significant part of the territory designated as Arouca UGGp and many

of the main features of its geomorphology. In this context, the geological contact between the Ante-Ordovician metasediments (schists and greywackes) and the Arouca quartz-diorite can be observed in a very distinct way. The northern slope of this mountain preserves a set of different levels of erosion, which prove the movement of displacement of the blocks, which raised this mountain. The Arouca valley, geomorphologically known as the complex alveolus of Arouca, is a bowl-shaped valley carved into quartzodioritic rock, very prone to chemical weathering, and its bottom has accumulated sediments resulting from erosion of the surrounding area, which were retained here due to the hardness and resistance to erosion of the «*Pedra Má*» (= bad rock), a hornfels outcrop located on the limits of the villages of Rossas and Várzea (Brum Ferreira, 1978; Rochette Cordeiro, 2004) (Fig. 15).



Figure 15. Bowl-shaped valley of Arouca from Detrelo da Malhada viewpoint. © AGA

On clear days, a close look at this landscape allows us to identify the geological contact between the mica schists and the quartz-diorite from Arouca. To the North, it is possible to easily observe the elevations of Gamarão, the Paiva River valley, the Montemuro Mountain, the Douro valley socket, the mountain ranges of the Valongo region, and the Marão, Larouco and Gerês mountains. To the west, the coastal region between Espinho and Porto, and, to the east, the Côtó do Boi and the Serra da Arada, where the São Macário hill stands out (Rocha, 2008; 2016; Sá *et al.*, 2008).

The structuring of this territory occurred mostly during the upper Miocene, due to movements of large lithospheric blocks, which defined plateaus and diverse erosion levels identified in the landscape and exhumed the Andalusite-rich schists (Acciaioli Mendes, 1997; Acciaioli Mendes & Munhá, 1998) here observed and that mark some hardness reliefs in the surroundings of Detrelo da Malhada and Côtó do Boi.

The occurrence of periglacialism in this region, during the last glacial cycle, left its mark both on the flattened and eroded surface of the Serra da Freita, as well as on the alteration of rocks and soil formation, essentially in the alveoli of Arouca and Moldes (Rochette Cordeiro, 2004; Rocha, 2016). The incision of the Arda River that took place at the end of the Cenozoic, as well as the formation of the fertile soils we know today, was decisive for the implantation of the Monastery of Arouca, in the 10th century, as well as for the development of this region.

Stop 6. S. Pedro Velho bornhardt

This site is a bornhardt landform, a type of inselberg developed on the Freita Mountain granite together with diverse granitic boulders with weathering pits (Fig. 16).

At its top there is a 1st order geodesic landmark whose base is located at an altitude of 1077 m a.s.l.



Figure 16. Geodesic landmark of S. Pedro Velho, on top of a bornhardt in the Freita Mountain.

© AGA

Having undergone a geoconservation intervention, this geosite is equipped with a 360° observation deck and four interpretive panels directed to the four main cardinal points (Sá & Rocha, 2020). Allowing its visitation in safe conditions, while providing basic information to visitors, this Arouca UGGp geosite is assumed as one of the unique viewpoints in this territory. In fact, the landscape that can be seen from here on clear days is impressive, and its all-around panoramic view allows observing from the mountains of Gerês to Estrela, or from the coastline to the distant Peña de Francia, near

Salamanca, already in Spain, in an imaginary line that crosses the entire width of the Portuguese mainland.

However, a closer look at the landscape, with the help of the information contained in the railing of the balcony protecting the visitation platform, makes possible to observe the coastline from the vicinity of Póvoa de Varzim (NW) until the vicinity of Cape Mondego (SW), easily distinguishing from the W the different arms of the Estuary of Aveiro. Towards the N-NE it is still possible to distinguish the mountains of Larouco, Montesinho, Padrela, Cabreira, Alvão, Marão and Montemuro. To the E-SE it is still possible to see the Marofa and Estrela mountains and, to the S, the Caramulo and Buçaco mountains. A true compendium of the mountains of northern and central Portugal (Fig. 17).



Figure 17. Panoramic view over the degraded plateau of Freita Mountain and the distant mountains located to the E and SE, from the observation platform of S. Pedro Velho. © AGA.

In addition, a closer and detailed observation will also allow us to point out the typical villages of the mountains, especially Albergaria da Serra, with its pasture and rye fields and small subsistence vegetable gardens. From here leave every day to graze, independently, the 'Arouquesa' cows, where they also return of their own accord at the end of the afternoon.

Stop 7. Frecha da Mizarela viewpoint

The Frecha da Mizarela waterfall (Fig. 18), considered the highest in mainland Portugal, occurs in the upper section of the Caima River and is projected in a gap of about 70

meters in height, defined in the geological contact between the Granite da Serra da Freita and the Ante-Ordovician metasediments that outcrop downstream. The occurrence of this waterfall is closely linked to the Serra da Freita fault system and the movements associated with the Alpine Orogeny. However, the geological contact by fault where the waterfall is observed will correspond to a very old fault associated with the Freita Mountain shear zone, having already been identified the occurrence of movement during the Caledonian and Variscan orogenies.

From this location it is possible to see the mountain geomorphology, associated with different lithologies, with emphasis on the granitic landscape marked by chaos of blocks and bornhardts. To the West, it is possible to observe the Meso-Cenozoic border, where the Estuary of Aveiro is clearly identified in the section between Aveiro and Ílhavo (Vieira & Sá, 2019; Sá & Rocha, 2020).



Figure 18. Aspect of the Frecha da Mizarela waterfall at the end of the day. © Tiago Martins / visitarouca.pt

References

- Acciaioli Mendes, H. (1997). Processos metamórficos variscos na Serra da Freita (Zona Centro Ibérica – Portugal). Unpubl. PhD Thesis. Universidade de Aveiro. 288 pp.
- Acciaioli Mendes, H. & Munhá, J.M. (1998). O regime metamórfico da Serra da Freita. Com. Inst. Geol. Min. Actas do V Congresso Nacional de Geologia, B161 - B163.
- Brum Ferreira, A. (1978). Planaltos e Montanhas do Norte da Beira – Estudo de Geomorfologia. Memórias do Centro de Estudos Geográficos, 4, 1-374.

- CM Castro Daire (s.d.) Património. Disponível em agosto, 1, 2022 em <https://www.cm-castrodaire.pt/index.php> .
- Costa, S.M. (2003). Festas e Tradições Portuguesas. Círculo de Leitores, 7º vol., 255 pp.
- INE (2021). Censos 2021. Lisboa, Portugal: INE, Instituto Nacional de Estatística. Disponível em agosto, 1, 2022 em <https://censos2021.ine.pt/> .
- Medeiros, A.C., Pilar, L. & Fernandes, A.P. (1964). Carta e notícia explicativa da folha 13 – B (Castelo de Paiva) da Carta Geológica de Portugal à escala 1:50.000. D.G.G.M. Serviços Geológicos de Portugal, 58 pp.
- Oliveira, A., Gomes, C. A., Silva, F., Paiva, J. & Silveira, P. (1999). Rio Paiva. Águas do Douro e Paiva, S.A., Associação de Defesa do Património Arouquense & Campo de Letras – Editores, S.A, 250 pp.
- Paz, A., Brandão, A., Duarte, A., Varela, A., Sá, A., Rocha, D. & Quaresma, L. (2014). Guia de Canyoning – Arouca Geopark. Associação Geoparque Arouca (Ed.), 57 p. ISBN: 978-989-96055-9-6.
- Rebello, J., Lourenço-Gomes, L. & Ribeiro, C. (2014). Estudo sobre o valor económico da ligação às redes da UNESCO em Portugal. Sítios do Património Mundial, Reservas da Biosfera, Geoparques e Cátedras UNESCO. Comissão Nacional da UNESCO/ Ministério dos Negócios Estrangeiros, Lisboa, 84 pp.
- Rocha, D. (2016). Rota dos geossítios do Arouca Geopark. AGA - Associação Geoparque Arouca (Ed.), 159 pp., ISBN: 978-989-99633-1-3.
- Rocha, D.M.T. (2008). Inventariação, Caracterização e Avaliação do Património Geológico do concelho de Arouca. Unpubl. Master Dissertation, Departamento de Ciências da Terra, Universidade do Minho, Braga, Portugal, 159 pp. + CD-ROM.
- Rochette Cordeiro, A.M. (2004). Dinâmica de Vertentes em Montanhas Ocidentais do Portugal Central. Unpubl. PhD Thesis in Geography. Faculdade de Letras. Universidade de Coimbra, 566 pp.
- Sá, A.A. & Rocha, D. (2020). Arouca UNESCO Global Geopark: Geomorphological Diversity Fosters Local Development. In: G. Vieira, J.L. Zêzere & C. Mora (Eds.). Landscapes and Landforms of Portugal. Springer Nature, Switzerland, 329-340.
- Sá, A.A., Brilha, J., Rocha, D., Couto, H., Rábano, I., Medina, J., Gutiérrez-Marco, J.C., Cachão, M. & Valério, M. (2008). Geoparque Arouca: Geologia e Património Geológico. Câmara Municipal de Arouca (Ed.), Arouca, Portugal, 127 pp. (ISBN 978-972-8978-03-7).
- Twidale, C.R. (1982). Granite Landforms. Elsevier, Amsterdam, 372 pp.
- UNESCO (2022). International Geoscience Programme. Disponível em agosto, 2, 2022 em <https://en.unesco.org/international-geoscience-programme/projects/726> .
- Vidal Romani, J.R. & Twidale, C.R. (1989). Formas y paisajes graníticos. Universidad da Coruña. Monografías nº 55, 416 pp.
- Vieira, A. (2008). Serra de Montemuro. Dinâmicas geomorfológicas, evolução da paisagem e património natural. Unpubl. PhD Thesis in Geography. Universidade de Coimbra, Coimbra, 689 pp.

Vieira, A. & Sá, A.A. (2019). O geopatrimónio de montanhas ocidentais do Norte-Centro de Portugal e da falha Verín-Penacova. Livro-guia da visita do III Encontro Luso-Brasileiro de Património Geomorfológico e Geoconservação. CEGOT-UMinho, Centro de Estudos de Geografia e Ordenamento do Território da Universidade do Minho, Guimarães, 41 pp. (ISBN 978-989-54317-4-8)

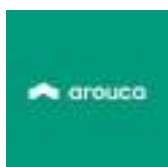
Index

Itinerary and schedule	7
Introduction	9
Stop 1. “Montemuro Doors” viewpoint	11
Stop 2. S. Pedro do Campo viewpoint and Pedra Posta geosite	14
Stop 3. “516 Arouca” suspension bridge and Paiva Walkway	15
Stop 4. Senhora da Mó viewpoint	19
Stop 5. Detrelo da Malhada viewpoint	20
Stop 6. S. Pedro Velho bornhardt	22
Stop 7. Frecha da Mizarela viewpoint	23
References	24



Photo by Sérgio Brito

ORGANIZATION AND SUPPORTERS:





10th IAG INTERNATIONAL CONFERENCE ON GEOMORPHOLOGY

Photo by Sérgio Brito

COIMBRA - PORTUGAL
« GEOMORPHOLOGY AND GLOBAL CHANGE »

FIELDTRIP GUIDEBOOK **Cape Verde (Santiago and Fogo Islands)** 06–09 September 2022

Vera Alfama
Sónia Silva Victória
Sílvia Monteiro
José Maria Semedo
Romualdo Correia



Vera Alfama
Sónia Silva Victória
Sílvia Monteiro
José Maria Semedo
Romualdo Correia

10th International Conference on Geomorphology
Fieldtrip Guidebook – Cape Verde (Santiago and
Fogo Islands)

06-09 September 2022



Coimbra, 2022

Edition notice:

Title: *10th International Conference on Geomorphology. Fieldtrip Guidebook – Cape Verde (Santiago and Fogo Islands)*

Authors: *Vera Alfama, Sónia Silva Victória, Sílvia Monteiro, José Maria Semedo and Romualdo Correia (University of Cape Verde)*

Fieldtrip guided by: *Romualdo Correia, Sílvia Monteiro and Adélio Moreno (University of Cape Verde)*

Edition: *Universidade de Coimbra, Faculdade de Letras*

Fieldtrip and Guidebook Coordination: *António Vieira (University of Minho)*

Cover: *Perspective of Santiago Island (photograph by Vera Alfama)*

ISBN: 978-972-95222-8-4

Introductory Note

The 10th International Conference on Geomorphology will take place in Coimbra (Portugal) from 12th to 16th September 2022, under the theme "Geomorphology and Global Change" and it is organized by the International Association of Geomorphologists (IAG) and the Portuguese Association of Geomorphologists (APGeom).

As in previous international conferences on Geomorphology, and as is the tradition in many geomorphological events organized around the world, the organizing committee of the 10th International Conference on Geomorphology proposed several fieldtrips to the participants, occurring before, during and after the main event.

These fieldtrips intend, above all, to show to geomorphologists from all over the world the diversity and richness of the geomorphological elements of the Portuguese territory (and also from Cape Verde) and to allow an exchange of experiences between the specialists that investigate these territories and the visitors, contributing for mutual scientific enrichment and for the valorization of this international conference.

The pre-conference fieldtrip is dedicated to the islands of Santiago and Fogo, in the Archipelago of Cape Verde. It will take place from 6th to 9th September and will be led by colleagues from the University of Cape Verde (Vera Alfama, Sónia Victória, Sílvia Monteiro, José Maria Semedo and Romualdo Correia). The volcanic geomorphology will dominate the visit (including well conserved structural volcanic forms such as cones, domes, craters and calderas), especially in the island of Fogo where recent volcanic activity has been registered.

The one-day mid-conference fieldtrips will take the visitors around the Portuguese mainland territory, the 14th September, allowing the visit of four different geomorphological realities.

In the Arouca UNESCO Global Geopark, internationally recognized territory since 2009, participants will be able to visit unique geological and geomorphological features (such as planation surfaces, bowl-shaped valleys and narrow river valleys) and witness the remarkable effort of protection and promotion of natural (abiotic and biotic) and cultural (tangible and intangible) heritage. The visit to the "516 Arouca" suspension bridge will be an excellent opportunity to observe the magnificent landscapes of this mountainous territory. This fieldtrip will be led by Artur A. Sá, António Vieira and Daniela Rocha.

The field trip to coastal areas of central Portugal will be led by Pedro Dinis and António Campar Almeida. Their proposal is to observe the different morphotectonic units of central west Portugal, namely the Coastal Mountain of Serra da Boa Viagem (revealing karstification features), the littoral plain (with aeolian dunes associated with some

reliefs with higher elevation), the Cértima subsiding area (structurally-controlled morphology), and the Buçaco region (with the Syncline of Buçaco).

The visit to the Schist Mountains of Central Portugal will be centered in the mountains of Lousã and Açor, and will be conducted by Luciano Lourenço and Bruno Martins. It is proposed the observation of the main contrasts of the landscape, especially in terms of its physical geography, translated into geological, hypsometric, geomorphological, and hydrographic differentiation, or the land use and occupation and evolution of vegetation cover, namely following the recurrent large forest fires and the subsequent erosive processes they caused.

The fourth one-day fieldtrip will be oriented to the Estrela UNESCO Global Geopark, and led by Gonçalo Vieira, Emanuel Castro and Fábio Loureiro. The main geoheritage significance of the Estrela UGGp is the extent and richness of the Late Pleistocene glaciation(s) landforms and deposits (with spectacular morphological features such as the Zêzere glacial valley or the glacial cirques, moraine boulders, erratics or *roches moutounnées*) as well as the peculiar long-term geological evolution (revealing a significant diversity of granite types and landforms).

The three post-conference fieldtrips include a visit to the Lisbon Region, Serra da Estrela and, finally, Minho and Galicia (Spain), and will take place from 17th to 19th September.

The fieldtrip to the Lisbon Region will be guided by José Luís Zêzere, César Andrade, Sérgio Oliveira, Jorge Trindade and Ricardo Garcia, and will cover topics related with slope instability and landslides that affect the region of Lisbon, the floods occurring in the area north of Lisbon, and the coastal dynamics, morphology, cliff instability and beach erosion at north and south of Lisbon.

The three days field trip to the Serra da Estrela is led by Gonçalo Vieira, Emanuel Castro and Fábio Loureiro. Participants will be taken to visit some of the Geopark's most inaccessible geosites and observe breathtaking landscapes during two hikes: one in the Zêzere valley and the other between Penhas Douradas and Lagoa Comprida. The different geosites to visit include features of glacial, periglacial, granite weathering, fluvial, hydrogeological, petrological and tectonic themes, and aspects related with the management of a UNESCO Global Geopark will be discussed.

The third three-days fieldtrip is destined to the northwestern part of Portugal and the Spanish region of Galicia. Guided by Alberto Gomes and Antonio Perez Alberti, will be mainly devoted to the coastal area and to the observation and discussion of issues related to coastal dynamics, marine terrace staircases, differential uplift of coastal blocks, coastal geoheritage, coastal geoarchaeology, coastal erosion and coastal land planning.

It is our expectation that these visits will please all participants and promote the scientific enrichment of all involved, allowing a better understanding of the topics covered in each one.

We also hope that this set of fieldtrip guidebooks can help in the understanding of the themes discussed and that they can be a testimony of the commitment and dedication shown by all the scientific responsible for the several visits, to whom the organizing committee of the International Conference on Geomorphology expresses its greatest recognition and gratitude.

have a good fieldtrip!

Lúcio José Sobral da Cunha
António Vieira

on behalf of the ICG2022 Organizing Committee

ITINERARY AND SCHEDULE

Itinerary

Day 1: Santiago Island

Plateau of Praia; Monte das Vacas; Ribeira de São Domingos; Ribeira Seca (Poilão Dam) - Orgãos; Mountainous massif of Pico de Antonia; Santa Catarina Plateau; Mountainous massif of Serra Malagueta; Tarrafal - Baía Verde (Lunch break); Tarrafal- Monte Graciosa; Biscainhos (S. Miguel).

Day 2: Departure for the island of Fogo (Fig. 1)

Praia de S. Filipe; Ponta de Salina; Monte Sambango (Mosteiros); Corvo's lava; Valley of Ribeira de Caiada; Alto Espigão viewpoint; entrance to Fogo's Natural Park.

Day 3: Fogo Island

Trail in the area of Chã das Caldeiras (within the boundaries of the Natural Park)

Option 1: Visit at Chã das Caldeiras

1. Entrance to the Natural Park of Fogo (PNF)
2. Crater of explosion, Curral de Asno
3. Lava flows from the 2014 eruption, Lantisco
4. Slag cone from the 2014 eruption
5. Bordeira
6. Lava field
7. Main façade of the old winery, Boca Fonte
8. Contact between the lava flows of 1995 and those of 2014, Cabo Nhô Ernesto
9. Villages of Chã das Caldeiras
10. Monte Preto volcanic cave
11. Hornitos, north of the volcano, Monte Preto
12. Monte Velha Forest Perimeter

Option 2: Climb to Pico do Fogo (those who want to go will have to get up at 4am to make the climb and can be back before 12am) – need to contract a local guide Pico do Fogo Volcano: For those more inclined to physical activity, you can make a climb to the volcano, duly accompanied by one of the local guides, from where you can observe a unique and unforgettable landscape.

Option 3: Climb to the Peak of the 2014 eruption (those who want to go will have to get up at 7am to make the climb and can be back before 11am) need to contract a local guide Slag cone from the 2014 eruption.

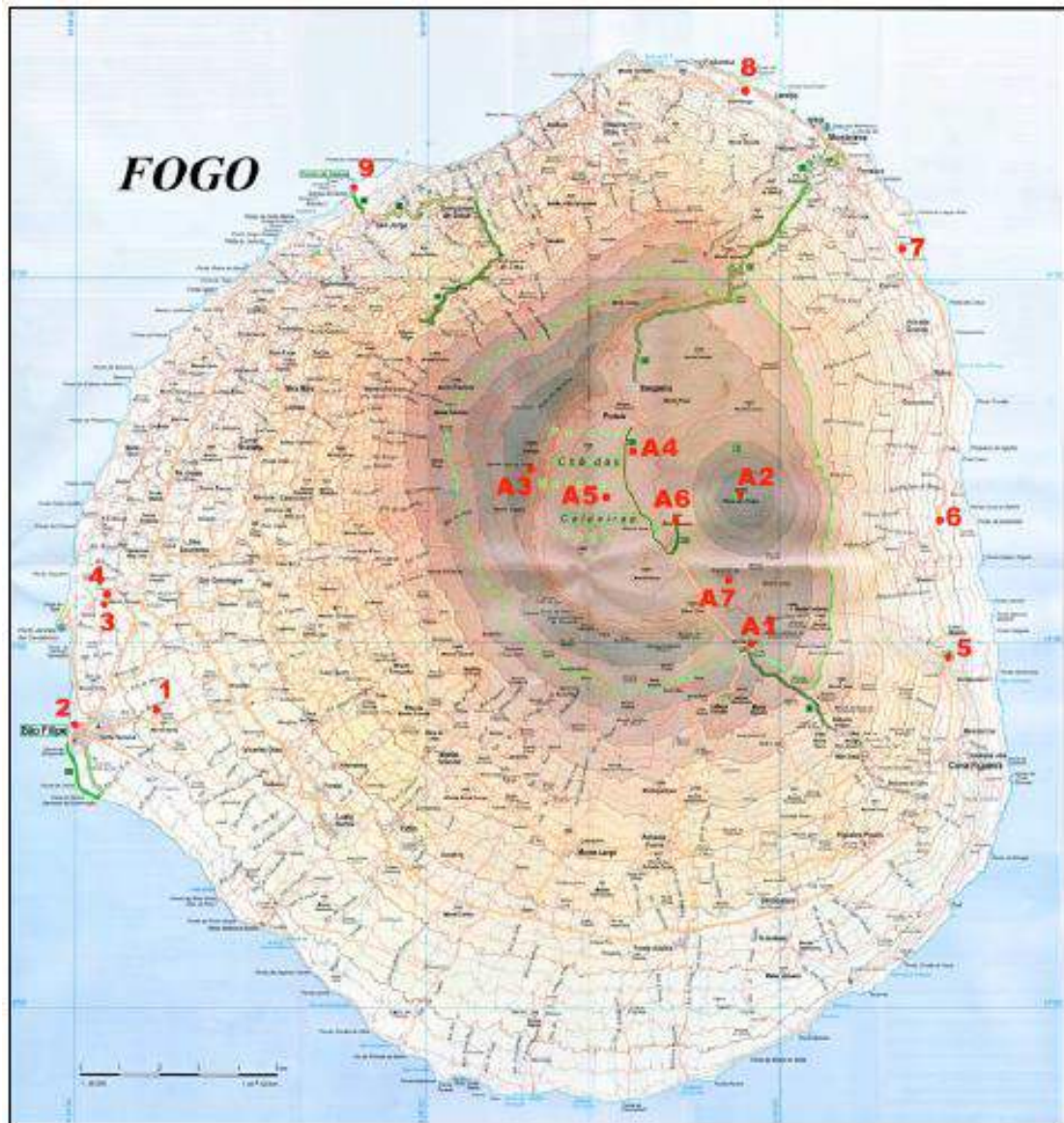


Figure 1. Itinerary of the field trip in Fogo island (Source: Alfama, 2007).

Introduction

The archipelago of Cape Verde is part of the group of islands called Macaronesia (Chevalier, 1935), which also includes the archipelagos of Madeira, the Canary Islands and the Azores and is in the Atlantic Ocean, about 500 km W of the coast of Senegal, between 14°N and 18°N latitude and 22°W and 26°W longitude. The archipelago is made up of 10 main islands and some islets (Fig. 2) that emerge from a topographic elevation with approximately 3 km of vertical extension and about 1,000 km in diameter known as Cape Verde Rise (McNUTT, 1988) and covers a total area of 4,033 km².

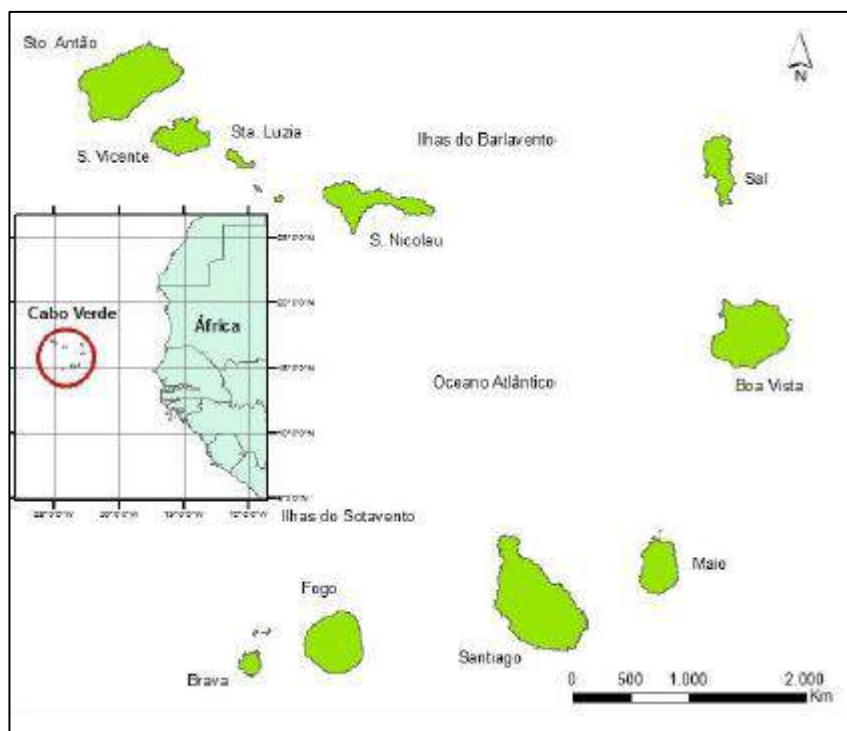


Figure 2. Localização geográfica do arquipélago de Cabo Verde (Alfama, 2016).

The group of islands forms an open arch facing west and is divided into two main groups: north and south, depending on the prevailing winds coming from the NE quadrant: Windward and Leeward. The first group is made up of the islands of Santo Antão, São Vicente, Santa Luzia, São Nicolau, Sal and Boa Vista and the leeward group is made up of the islands of Maio, Santiago, Fogo and Brava. The islands of Cape Verde are of volcanic origin, although there are also important sedimentary deposits on the islands of Sal, Boavista and Maio. They also exhibit distinct geological and geomorphological characteristics. The largest island, Santiago, is 991 km² and the smallest, Santa Luzia, is only 35 km².

The origin of the Cape Verde islands is associated with intraplate volcanism (Ernst & Buchan, 2003). According to some authors who defend its origin from mantle plumes

(hotspot), as is the case of Holm et al. (2008), they consider the existence of a cretal connection of the socle between the archipelagos of Cape Verde and Canary Islands, as well as an enormous similarity in the volcanic episodes as to its nature and composition. The hotspot type activity would have started about 19 to 22 Ma, which resulted in a large crustal uplift zone (Cape Verde Swell) in which the Cape Verde islands are embedded (Plesner et al., 2002), with volcanic activity remaining until the present day.

As for their morphological characteristics, the islands have very diversified relief forms, with each island having its own specificity. As they are volcanic islands, the relief is generally very rugged. However, in the oriental islands, also called shallow islands (Sal, Boavista and Maio), flattened forms and small elevations are predominant. There are numerous geofoms of volcanic, erosive and sedimentary origin whose study and characterisation are essential to help understand the geological history of the archipelago.

The original volcanic forms have been altered by erosive action, giving rise to a landscape dominated by deep and narrow valleys, peaks, narrow and elongated summits (locally called "*cutelos*") and wide plateau surfaces formed by basaltic flows: the "*achadas*" (tablelands). These often form true structural platforms and are found practically on all the islands well conserved structural volcanic forms such as cones, domes, craters and calderas. It is on Fogo Island that the most recent and best-preserved volcanic forms are found due to active volcanism.

The island of Santiago, much like the entire archipelago, is made up almost exclusively of morphologies, structures and rocks of volcanic origin, basaltic in nature, which were spilled by a main crater that occupies the site of the Pico de Antónia massif. The main structure of the island was formed in several phases, alternating with periods of greater quietness in the volcanic activity.

The island of Fogo displays important morphological aspects, the Chã das Caldeiras depression with 9 km of diameter, located at 1760 m of altitude, and whose base is surrounded by an escarpment (Bordeira) a 1000 m high. The highest point, the stratovolcano called Pico do Fogo, with 2829 m of altitude, reaches 1100 m of height. The current name of the island comes from the historical record of about 30 eruptions since its discovery in the 15th century.

1. Brief characterization of the area

a. Santiago Island

Santiago Island is the largest of the 10 islands of the Archipelago of Cape Verde with 991 Km² and the most densely populated with 273,988 inhabitants (INE, 2021). Its geological record is made up of volcanic materials, predominantly basalts and pyroclastic materials (breccias, lapilli, tuffs), which cover an area of 909 Km² and other basic lavas, such as limburgite, which cover 57 Km². With a long history of uplift (Ramalho, 2009), which led to the exposure of extensive sequences of volcanic seamounts and marine sediments, the presence of intrusive and extrusive carbonatites, a geomorphological evolution characterised by successive cycles of torrential flooding and valley filling by sequences of igneous rocks.

The island of Santiago displays a very fragmented morphology of volcanic origin evident from the coastal areas to the mountainous inland; it features diversified relief forms and large slopes of land, sometimes from large ravines and canyons to extensive tablelands (Ferreira, 1987). According to Assunção (1968) the intense erosion has affected the original forms resulting from the volcanic activity, so that many times it is not possible to identify in the island the old volcanic centres. The erosion acts with greater expression on the east-facing slope, the one that is more widely exposed to the action of the north-easterly trade winds; the water erosion is the process which affects more extensive areas. The average altitude of the island of Santiago is 278.5 m, with a maximum altitude of 1,392 m (Pico da Antonia Massif), to the South, and 1,063 m (Serra da Malagueta), to the North, separated by a plateau at an average altitude of 550 m, with cones and other reliefs in various states of evolution, known as the Assomada Plateau (Amaral, 1964).

To the South, there is a series of small tablelands spread out between sea level and 300-500m altitude. To the West, the coast is normally rugged, and, to the East, it is flattened and made up of tablelands. In the North of the island, Tarrafal stands out. It is an extensive region of tablelands with altitudes varying between 20 and 300 m, which develops from the northern foot of the Serra da Malagueta. This diversified relief includes a relatively dense temporary hydrographic network, which in most cases runs in embedded valleys with torrential longitudinal profiles (Marques, 1990, Gomes & Pina, 2003).

b. Fogo Island

Fogo Island belongs to the Leeward group of islands, located in the southwest of the archipelago, it has a circular shape, an area of 470 Km², and it is the fourth largest island of the Archipelago of Cape Verde. It has a population of 33,754 inhabitants (INE, 2021).

Chã das Caldeiras, where the Fogo Natural Park (PNF) can be found, the largest protected area in the country, is in the central area of the island of Fogo, Cape Verde, encompassing the Volcano, the Crater, Bordeira and the Monte Velha Forest Perimeter. It covers approximately 85 km² (Fig. 3) (Alfama, 2007).



Figure 3. Location of the Chã das Caldeiras area.

The Fogo Island (476 km²), located NW of Santiago Island, is one of the 10 islands that make up the Archipelago of Cape Verde. It has an eccentric trunco-conical shape, whose centre is displaced to the Northeast. Its flanks, particularly steep on the east side, are less steep on the west and south sides (Ribeiro, 1960), formed by recent lava flows interspersed with pyroclastics. An important morphological aspect is the Chã das Caldeiras depression (9 km in diameter) whose base is at about 1700 m of altitude, and which is bordered by a vertical wall (Bordeira) that reaches 1000 m. It is believed that the depression results from the collapse of the north-eastern flank of the island, which may have occurred in two stages. In the eastern side of Chã das Caldeiras there is a stratovolcano with 1100 metres of altitude and that reaches the maximum altitude of 2829 m, the highest point of the archipelago. The island owes its current name to the fact that 30 volcanic eruptions have occurred on it since its discovery in the 15th century, with recurrence periods varying between 1 and 98 years. The volcanic materials, alkaline mafic in nature and reflecting both explosive and effusive activity, represent most of the outcropping rocks. Also worth mentioning is the existence of carbonatite rocks integrated in the basal complex of the island, which have been dated at ages greater than 3.5 Ma. Among the rocks that outcrop on the island, the volcanic ones are worth highlighting. These are present in the form of flows, lodes and pipes, which correspond to the effusive phase, while the volcanic cones of pyroclastic material, also basaltic, correspond to the explosive phase of eruptions. One can also find sedimentary rocks such as beach sand and gravel, alluvium, slope deposits and torrential deposits.

In the archipelago of Cape Verde, the island of Fogo is the only one with historical eruptions, that is, with eruptions witnessed by the inhabitants. Since the discovery of Cape Verde (1460) about 30 eruptions have been recorded (Table 1) (Ribeiro, 1960;

Silveira et al., 1997; Silva et al., 2015). The first recorded eruption was in the year 1500, and the last was in 2014/15.

Regarding topography, it is the island with the most rugged relief, with a maximum altitude of 2829 m for a maximum diameter of only 25 Km. The basic shape of the island is an asymmetrical cone whose centre is displaced to the Northeast. The top of the conical edifice was shortened and in its place we can find a hemisphere-shaped caldera, locally referred to as the "Chã das Caldeiras", with a diameter of about 9 km and opening facing east. The escarpment that goes around the base of the caldera has a slope close to vertical, reaching about 1000 m at its highest point. In the inner side of the "Bordeira", as the escarpment is locally known, one can observe countless lodes that in some cases can be correlated with parasitic cones in its outer side (Ribeiro, 1960).

Table I. Record of eruptions that occurred in Fogo Island since its settlement.

Year			
1500	1683	1721 to 1725	1852
1564	1689	1761	1857
1569	1693	1769 and/or 1774	1858
1604	1695	1785	1909 (?)
1606 (?)	1697	1799	1951
1664	1699	1815/1816 (?)	1995
1675	1712	1817 (?)	2014/15
1680	1713	1847	

A remarkable geomorphologic feature is the absence of the eastern part of the Bordeira, as well as the presence of escarpments arranged in échelon and NW-SE direction (in the region of Cova Matinho) and a morphological step near the village of Corvo (Silveira et al., 1997). On the east flank of the island, in an area delimited by two scarps that appear in the continuation of the North and South "Bordeira" sections, no parasitic cones can be found, and both scarps coincide with the terminations of the two platform/cliff sets of the east zone (Ribeiro, 1960).

This zone is composed solely of materials emitted by the volcanic system that formed inside Chã das Caldeiras. From the interior of Chã das Caldeiras, with a flat bottom, only roughened by several scoria cones and lava flows, rises the main eruptive cone that, with about 1100 m of height, reaches the maximum altitude of 2829 m (corresponding to the highest point of the island and of the archipelago). The "Pico do Fogo" occupies, relatively to the surface of the island, an even more eccentric position than the caldera, and its eastern flank falls directly to the sea in an approximate slope of 32° (Ribeiro, 1960).

2. The geological constitution of Santiago Island

The geology of Santiago Island is essentially composed of volcanic materials, dominantly outcropping basalts, basanites, tephrites and limburgites, pyroclastic materials and lodes, basaltic dykes and limburgites. Phonolites, trachytes, gabbro, syenites, pyroxenites and sedimentary rocks can also be found in smaller extensions. The growth of the island is thought to have occurred first through a main emitting centre, later turning to fissures. The main volcanic activity must have occurred from the main crater of a volcano which would occupy the Pico de Antónia. Throughout the island there are recent and well-preserved craters. The oldest formations are observed in heavily exposed areas, usually in the bed of the most deeply excavated streams.

Tour around the Santiago Island

Stop 1. Praia Plateaus

The plateaus of Cidade da Praia lying between the altitudes of 0-200 meters, are made up of the Eruptive Complex of Pico de Antónia (PA), in which its rocks are responsible for the largest elevations and structural platforms on the island of Santiago. One can also find pyroclastic materials of explosive and effusive activities, subaerial (predominant) and submarine basaltic flows.



Stop 2. Monte das Vacas

Monte das Vacas is located near Ribeirão Chiqueiro (S. Domingos) and consists of a pyroclastic cone (tuffs, lapilli, scoria, bombs and blocks) intercalated with lava flows. It is part of the volcanic unit - Monte das Vacas Formation. The top of the volcanic cone is at about 437 m of altitude and its inclination ranges from 25°-35°. It is often easier to observe the materials that constitute the cone, due to the collapse of the flanks, resulting from the erosive action of the water lines, or from the subsidence of the cornice on which they stand.



Stop 3. Ribeira de São Domingos

The São Domingos valley is very open and eroded, with vast cultivated fields, presenting quite weathered materials of the basaltic (base) series. One can also find in this valley quite fractured and weathered lodes from the Old Eruptive Complex (CA). Usually, we may find at the top of the sequence the basaltic series of the Pico de Antónia (PA), of subaerial facies. Monte Chaminé stands out in the landscape.



Stop 4. Ribeira Seca (Poilão Dam) – Órgãos

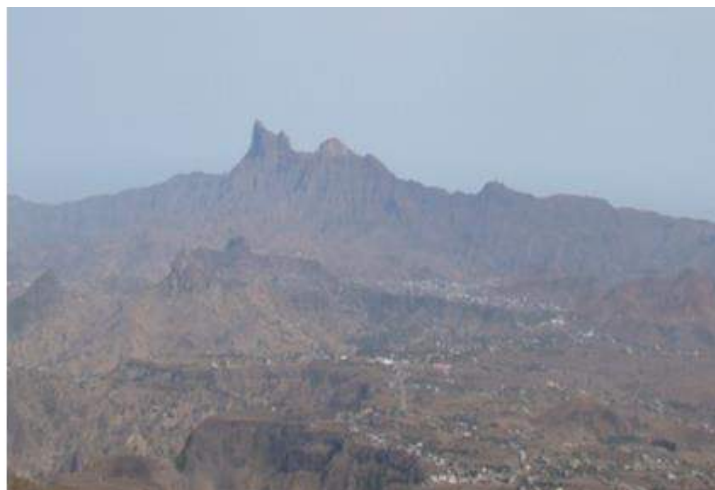
Embedded in the valley formed by the pillow lavas of the PA and the Órgãos Formation (CB) at the base of the sequence, basaltic in nature with flows, pyroclasts and hyaloclasts, this geological unit represents an important period of erosion. The Poilão Dam is a gravity dam, made of masonry, with reinforced concrete in the central core; it is intended for water storage for irrigation. With the construction of the dam, the area currently irrigated downstream of the dam is about 100 hectares.



Stop 5. Pico de Antónia Massif

Where the highest altitude of the island is reached, (1392 m), it extends in a SE-NW direction and is located facing south and west. It extends northeastwards, through the João Teves spur and southwards through the Boca Larga spur.

With altitudes above 700 m, it is overlaid by imposing peaks, besides Pico de Antónia (1392 m), Gambôa (1099 m), Tagarrinho (1035 m) and Grande (878 m). It is made up of subaerial mantles of the Pico de Antónia Formation. The massif features a dissymmetrical shape, strongly eroded, with jagged and pointed summits, to the east with the vigorous escarpment of the Pico de Antónia over the valleys of Orgãos and Picos.



Stop 6. Santa Catarina Plateau

Broad plain located at about 500 m of altitude, between the Pico da Antónia and Malagueta massifs, to the south and north, respectively; it features some volcanic cones (Monte das Vacas Formation), somewhat flattened by erosion. It leans slightly westwards, towards the coast, where it is limited by cliffs. To the West, the reliefs of Palha Carga, Monte Brianda and Pedroso are also prominent. The plateau is cut by some canyon valleys - the hydrographic basins of Águas Belas and Sansão, at the bottom of which there are irrigated areas.



Stop 7. Serra da Malagueta Massif

The Pico de Antónia and Serra da Malagueta massifs may represent the flanks of volcanic devices that had greater development in this complex, which must have covered the whole island. This massif is formed by layers of thick basalts, interspersed with pyroclasts, filled by a dense network of lodes. It displays a vigorous escarpment on the Santa Catarina plateau, broadly E-W oriented from Ponta Talho in São Miguel to the western coast of the island at Pontas Ruim and Água Doce, ending in cliffs.



Stop 8. Tarrafal - Baía Verde

Baía Verde consists of light-coloured beach sands of calcarenite and/or phonolitic nature. There occur deposits of phonolitic flows and pyroclasts from the Pico de Antónia (PA) Principal Eruptive Complex, which can be observed on the platform that forms the City of Tarrafal. The limestones, calcarenites and conglomerates of Pliocene age, constitute beach deposits, fossilised by the outflows of phonolitic flows from the PA overlying the calcarenites and conglomerates. In a section of Baía Verde, on the Presidente beach, one can observe from the bottom to the top, a sequence of conglomerates with rounded to subrounded basaltic pebbles, dispersed in a light-coloured cement of calcareous sandstone.



Stop 9. Tarrafal - Monte Graciosa

The northern side of the Serra da Malagueta massif slopes gently down towards Tarrafal, and is carved by deep ravines that enclose rows of hills in elongated ridges. The highest point of the Mountain (Serra) reaches 1064 m, and the central alignment has altitudes between 700 and 1000 m. Monte Graciosa (643 m) features a dome of phonoliths and trachytes formed by effusive and explosive volcanic phases, surrounded by basaltic mantles.



Stop 10. Biscainhos (S. Miguel)

A dense network of valleys that descend from the high areas of the Serra da Malagueta and Pico de Antónia massifs to the east of the island, ending in relatively lowlands that form flat-bottomed floodplains. Black sand or gravel beaches and relatively low cliffs. There is a predominance of high tablelands that descend gently to the sea, limited by vigorous cliffs. The valleys with subvertical slopes are numerous and deep. The coastline is quite indented with recesses and small coves.

A stop at Biscainhos allows one to observe pillow lavas outcrops from the Pico de Antónia Principal Eruptive Complex (PA) in an angular discrepancy of about 45° with subaerial flows from the PA.



3. The geological constitution of Fogo Island

On Fogo Island, specifically in the region of Chã das Caldeiras there is an active volcano that annually attracts many tourists, especially after the occurrence of the last two eruptions in 1995 and 2014. The island encompasses a complete series of geological and landscape phenomena that illustrate the formation of a landslide caldera and a pre-caldera explosive volcanic edifice, as well as a complete magmatic series with well-preserved volcanic materials, forms and structures such as lava flows of various types, varied pyroclastic materials, pyroclastic volcanic cones, etc. Visitors are attracted by the peculiarity of the landscapes, by the interest in observing an active volcano and by the magnificence and beauty of the site.

Tour around the Fogo Island

Stop 1. S. Filipe Beach

The black sands of S. Filipe beach easily giveaway the presence of basalts and other dark-coloured volcanic materials in the vicinity. In fact, on the cliffs surrounding the beach, one can observe a mixture of basalts and pyroclasts. Basaltic rocks, due to their particular nature of lava cooling, often show a columnar structure (prismatic disjunction). Sometimes basalts also display a structure resulting from their alteration (spheroidal disjunction), which causes scaling of the rock with an onion-shell appearance. This interlayering of basalts with pyroclasts represents changes in the type of volcanic activity (basalts: effusive activity; pyroclasts: explosive activity).



Stop 2. Ponta da Salina

Heading north, one arrives at Ponta da Salina, a place where the sea crashes vigorously against the cliffs formed by very old lava flows and with the typical columnar disjunction. The small beach has, however, one particularity that should be carefully observed.

The sand, although mostly black, has a "strange" greenish colour. A careful examination reveals the presence of small greenish grains of olivine, one of the minerals that form basalt and that are found in large quantities in the rocks on this part of the island. It is also possible to observe lava tunnels through which fluids flowed in the past.



Stop 3. Monte Sumbango (Mosteiros)

On the east side towards the town of Igreja, in Mosteiros, you reach the northern top of the island of Fogo, more precisely the village of Fajãzinha, built on a platform of coastal erosion (where the old Mosteiros aerodrome is located) and where there are also traces of pyroclastic deposits, as is the case of Monte Sumbango.



Mount Sumbango is a volcanic cone that is partially dismantled allowing to see the set of pyroclastic materials that form it and its internal structure. One of the main geological fault lines that cross Fogo Island from north to south runs along this point, which may possibly explain the dismantling of the volcanic cone. Coastal erosion may have contributed to the destruction of this edifice.

Stop 4. Corvo's Pahoehoe Lava Flows

Near the village of Corvo, along the road, we cross some lavas dating back to historic times, which can easily be identified by the few signs of alteration and the incipient vegetation. This stop, over one of these lava flows, allows us to contemplate magnificent examples of ropy structures. These structures develop during the cooling phase of quite fluid lavas (pahoehoe lavas), which are still moving as they slowly cool down.

The exceptional properties of these pahoehoe lava flows give them great scientific and didactic relevance, as their study allows us to understand how this phenomenon occurs. Occasionally, in this same place, some flows occur that, on account of having had a greater viscosity, gave rise to distinct structures, with a more fragmented appearance (aa type lavas). The presence of some small lava tunnels is noteworthy. In some of these tunnels the roofs have already collapsed.



Stop 5. Vale da Ribeira de Caiada

As the tour continues southeast, we cross several river valleys deeply carved by floodwater. The Ribeira de Caiada is an example of such streams, which occasionally carry water and sediment from the higher parts of the island (in the west) to the sea (in the east).

Although the climate on Fogo Island is predominantly dry for most of the year, occasional rains cause a remarkable water seepage at the surface, giving rise to violent

torrents with destructive effects that can lead, on occasion, to the cutting of roads and bridges. These relatively sinuous valleys are typical of this type of violent but short-lived phenomenon.



Stop 6. Alto Espigão Viewpoint

At an altitude of about 450m, this viewpoint is located a little south of the village of Cova Matinho, at a place on the road where a panoramic viewpoint has been built. From this spot, majestic black lava flows can be observed to the North, flowing down the slope of the volcano to the coast to the East. This lava flow dated 1951, having travelled along the eastern slope of the volcano, buried the village of Bombardeiro (built on a platform of coastal erosion known locally as "fajã") and reached the sea.

From here, one can easily distinguish, due to the difference in colour, the lava flows of the 20th century (black) and the preceding ones, already altered and, consequently, with brownish tones. From this viewpoint one can also observe slope deposits, quite thick, on the eastern flank of the volcano which overlies the entire island.



Stop 7. Entrance to the Fogo Natural Park

We continue west to the village of Achada Furna, where we head north, gradually overcoming the steep slope that leads us to the entrance of the Fogo Natural Park (PNF). Next to the wooden sign that announces the entrance to the Park, allow yourself to be fascinated by the landscape that surrounds you. From here we have a magnificent overview of the huge volcanic caldera with an area of about 60 km² as well as of the various lava flows that completely fill the bottom of the caldera. These lava flows formed during volcanic eruptions that occurred over time, after the formation of the caldera, originate a flattened bottom from where the Pico volcano and two parasitic cones (Monte Rendall and Monte Orlando, both formed during the 1951 eruption) stand out. The caldera, locally known as "Chã das Caldeiras", was formed by the circular collapse of an old volcanic edifice, seemingly in two successive episodes of collapse. This collapse gave origin to a wall, almost vertical, that surrounds almost all the caldera. Locally, this wall is known as Bordeira and, in it, it is possible to observe the internal structure of the old volcanic edifice, which has since collapsed, namely sequences of lava flows and pyroclastic deposits, as well as lodes that intersect these materials.

Option 1 - Tour inside Chã das Caldeiras - Fogo Natural Park

Stop 1a. Entrance to the Fogo Natural Park

This point coincides with the last stop on the circular tour around the island. At this point, next to the entrance to the Fogo National Park, the visitor can enjoy a first glimpse of the magnificent landscape and geodiversity of Chã das Caldeiras.



Stop 2a. Explosion crater, Curral de Asno

On the west side of Chã das Caldeiras, a shallow and rounded scoria cone explosion crater may be observed in Curral de Asno. The crater may have been altered by erosion. On the way up the cone one may observe pyroclastics of different sizes (ash, lapilli and bombs) and black colour that were deposited during the 2014 eruption. From this point there is a panoramic view of the southern side of the Fogo Island, where one may observe numerous pyroclastic cones, lava flows from historical eruptions (e.g., the 1951 eruption).



Stop 3a. Lava flows from the 2014 eruption, Lantisco

This point is where one of the first lava flows of the 2014 eruption can be found. It was over 4 meters thick and cut the access road to the communities of Chã das Caldeiras. The lava flows started at 10 am and took two directions: one towards the southwest (Monte Beco) and the other towards the southeast (Cova Tina) having destroyed the road 3 hours after the eruption started. The lava flow observed at this site is dark in colour and stony in appearance. Blocks of variable shapes and dimensions can be found.

Stop 4a. Scoria cone from the 2014 eruption

This scoria cone is the most recent volcanic structure on the island and the country and was formed during the last eruption in 2014. Its shape was moulded in accordance with the direction in which the materials were expelled.

The cone lies to the west of the volcano and features an elongated crater 245 metres long and 109 metres wide. A distinctive feature of this cone is the fact that it is located next to (east) the scoria cone formed in the 1995 eruption. It is formed by dark-coloured pyroclasts that display light shades in the crater area.



Stop 5a. Bordeira

Once you enter the Fogo National Park, the sight of the Bordeira is constant throughout the entire tour of Chã das Caldeiras. Indeed, the caldera is surrounded by an extensive wall that can reach altitudes of around 1000m, which forms a semicircle since it is open on the eastern side. The missing of the eastern part of the Bordeira is thought to have been caused by a large landslide that, due to gravity, moved the volcanic materials towards the sea and caused a tsunami that hit the island of Santiago.



Stop 6a. Lava field

Throughout the tour one may observe several lava flows originated by eruptions of different ages, the most recent being in 2014. In this field of lavas several types of lavas can be observed, with different colours ranging from black to brown. As for the types of lavas, the aa lavas are predominant, and pahoehoe and ropy lavas can also be found.

Stop 7a. Main façade of the old wine cellar, Boca Fonte

In Boca Fonte next to the road that leads to Cabo de Nhô Ernesto, one can see the façade of an old wine cellar that was affected by the lava flows of the 1995 eruption. With the waning of the eruption the flow ceased and only the front part of the wine cellar remained. The wine cellar, which had been built and equipped by German cooperatives, was swallowed by aa type lava. Interestingly, the last two eruptions partially destroyed the existing wine cellars. The 2014 eruption partially destroyed the Portela wine cellar, leaving it unfit for wine production.



Stop 8a. Contact between the lava flows of 1995 and those of 2014, Cabo Nhô Ernesto

At this point, one may observe the contact between the lava flows of 1995 and those of 2014. Both have a dark colour, but you may notice that the ones from 1995 show a more eroded aspect (). This point is of didactic interest since it displays aa type lavas of the 1995 eruption (in the form of loose blocks) and pahoehoe type lavas of the 2014 flows (with a smoother surface).



Stop 9a. Villages of Chã das Caldeiras

Chã das Caldeiras is divided into 5 locations (Cova Tina, Ilhéu de Losna, Boca Fonte, Portela and Bangaeira). Although the communities of Ilhéu de Losna, Portela and Bangaeira were left completely destroyed by the 2014 eruption, since 2016 the local population, which was evacuated at the time of the eruption, is slowly returning to Chã das Caldeiras to develop their activities. This return reflects the resilience of these people in the face of adversity. The population is engaged in agriculture, livestock, tourism and handicrafts (using lava material).

Stop 10a. Monte Preto Volcanic Cave

Volcanic caves, while not common geological phenomena, are present in the territory of the Fogo National Park. This volcanic cave is found under the scoria cone of Monte Preto, formed in the volcanic eruption of 1951.

To access this cave, it is necessary to walk on top of the lava expelled during the eruption of 1951. The cave is about 50 metres long, 18 metres wide and 10 to 15 metres deep. Volcanic stalactites can be found inside. One may enter the cave by descending with the help of a steel cable ladder and walking in humid conditions for about 50 metres.



Stop 11a. Hornitos, north of the Volcano, Monte Preto

To the north of the volcano one can find 3 lined hornitos that are still well preserved, with a height of more than 4 metres (from the surface around them). These are cone-shaped with a small opening at the top. Hornitos are geological structures that result

from lava spills and are formed on the surface of a basaltic lava flow. "Hornitos" in Spanish means small horns.



Stop 12a. Monte Velha Forest Perimeter

The route to the Northeast, from the village of Bangaeira to the area of Monte Velha, allows the visitor to carry on enjoying the magnificent landscapes of Chã das Caldeiras, as well as enabling a more detailed observation of the materials that make up Bordeira and its volcanic structures. The Monte Velha area represents the only forest perimeter on the island, developed from forestry campaigns carried out in the 1950's that introduced, on a large scale, exotic trees to all the islands, to the detriment of the endemic highland flora. The 800-hectare Monte Velha Forest boasts an exuberant vegetation of trees and shrubs. Due to its altitude, humidity and fertile soil, it has the ideal conditions for the multiplication of several endemic species in the highest levels of the whole island. Of the 87 endemic species of higher plants existing in the archipelago, Fogo Island preserves 37 species, 5 of which are exclusive to the island.

Option 2 - Climb to Pico do Fogo (between 5am and 12pm)

Stop 1b. Pico do Fogo Volcano

The Pico or Fogo Volcano, as it is locally known, is the crowning jewel of both the archipelago and the island's geodiversity. It is the main cone of an active volcano that constitutes the highest point of the country (2829 m). This volcano represents a gigantic cone of volcanic ash and scoria interspersed with lava material. On its slopes there are some parasitic cones, smaller in size, resulting from various eruptions (including the last one in 2014), formed by accumulations of pyroclasts. For those more inclined to physical activity, it is possible to climb the volcano, duly accompanied by one of the local guides. From there, one can enjoy a unique and unforgettable landscape.

Option 3 - Climb to the Peak of the 2014/15 eruption (between 7am and 11am)

Stop 1c. Scoria cone from the 2014/15 eruption

This scoria cone is the most recent volcanic structure on the island and the country and was formed during the last eruption in 2014. Its shape was moulded in accordance with the direction in which the materials were expelled. The cone lies to the west of the volcano and features an elongated crater 245 metres long and 109 metres wide. A distinctive feature of this cone is the fact that it is located next to (east) the scoria cone formed in the 1995 eruption. It is formed by dark-coloured pyroclasts that display light shades in the crater area. During the eruption that gave rise to this cone there were as many as 4 vents through which the materials were expelled. Later these vents coalesced and formed the current crater of the scoria cone.

Final notes

This Guidebook allows to make geological tours to Santiago and Fogo islands located in the archipelago of Cape Verde, where the geology is made up of rocks of basic nature and composition (e.g., basalts and similar rocks) and evolved rocks (e.g., phonoliths and nepheline syenites) resulting from magmatic evolution and differentiation processes. The landforms in Cape Verde are quite diverse, with each island presenting a specific geodiversity. Santiago Island features 10 stops where it is possible to observe recent and well-preserved volcanic structures (mainly scoria cones and craters); original volcanic forms have been altered by erosive action, giving rise to a landscape dominated by deep and narrow valleys, or open and flat valleys, and wide plateau surfaces formed by basaltic flows (folds or plateau). In Fogo Island there are about 13 stops available to observe important morphological aspects of the geology and geomorphology. From the Chã das Caldeiras depression with 9 km of diameter, located at 1760 m of altitude and whose base is surrounded by an escarpment (Bordeira) with 1000 m of height and intersected by lodes, to the highest point, the stratovolcano, called Pico do Fogo, which reaches 2829 m of altitude. The record of 30 historic eruptions since its discovery in the 15th century is evidenced by the extensive aa and pahoehoe lava fields, in addition to numerous scoria and ash cones, and well-preserved craters.

References

- Alfama, V. (2007). Património Geológico da ilha do Fogo (Cabo Verde): Inventariação, Caracterização e Propostas de valorização, Tese de Mestrado em Património Geológico e Geoconservação, Departamento Ciências da Terra, Escola de Ciências da Universidade do Minho: 114pp.
- Amaral, I. (1964). Santiago de Cabo Verde: A Terra e os Homens. Memórias da Junta de Investigação do Ultramar, nº 48: 444 p. Lisboa.
- Assunção, C. T. de (1968) – Geologia da Província de Cabo Verde: Curso de Geologia do Ultramar, Junta de Investigação do Ultramar, Lisboa, 3 - 52.
- Chevalier, A. (1935). Les îles du Cap-Vert. Flore de l'archipel. Rev. Bot. Appl., 15:733-1090.
- Ernst, R. & Bucha, K. (2003). Recognizing Mantle Plumes in the Geological Record. Annual Review of Earth Planet Sciences (31), pp. 469-523.
- Ferreira, D. (1987). La crise climatique actuelle dans L'Archipel du Cap Vert. Quelques aspects du problème dans l'île de Santiago. Finisterra, XXII(43):113-152.
- Gomes, A. & Pina, A. (2003). Problemas de recursos hídricos em ilhas. Exemplo da ilha de Santiago. Caso da bacia hidrográfica da ribeira grande da Cidade velha. Caso da bacia hidrográfica da ribeira seca. 6º Simpósio de Hidráulica e Recursos Hídricos dos PALOP, Praia.
- Holm, P. M., Grandvuinet, T., Friis, J., Wilson, J. R., Barker, A. K. & Plesner, S. (2008). An $^{40}\text{Ar}/^{39}\text{Ar}$ study of the Cape Verde hot spot: Temporal evolution in a semistationary plate environment. Journal of Geophysical Research: Solid Earth (1978 – 2012) 113:(B8).
- Marques, M. (1990). Caracterização das grandes unidades geomorfológicas da ilha de Santiago (República de Cabo Verde). Contribuição para o estudo da compartimentação da paisagem. Gracia da Orta, Centro de Estudos de Pedologia (IICT), Lisboa.
- McNutt, M. (1988). Thermal and Mechanical Properties of the Cape Verde Rise. Journal of Geophysical Research 93: 2784-2794.
- Plesner, S., Holm, P. M., & Wilson, J. R. (2002). ^{40}Ar - ^{39}Ar geochronology of Santo Antão, Cape Verde Islands, Journal of Volcanology and Geothermal Research 120(1-2): 103-121.
- Ramalho, R. (2009). Building the Cape Verde Islands. Dissertation of doctor in Philosophy. Department of Earth Sciences. University of Bristol, 251 p.
- Ribeiro, O. (1960). Ilha do Fogo e as Suas Erupções. JIU, Mem. Ser. Geográfica nº 1, 2ª edição. Lisboa.
- Silva, S. M., Cardoso, N. Alfama, V., Cabral, J., Semedo, H., Pérez, N., Dionis, S., Hernández, P., Barrancos, J., Melián, G., Pereira, J. & Rodríguez, F. (2015).

Chronology of the 2014 volcanic eruption on the island of Fogo, Cape Verde. Geophysical Research Abstracts Vol. 17, 2015 EGU General Assembly 2015.

Silveira, A. B., Serralheiro, A., Martins, I., Cruz, J., Madeira, J., Munhá, J., Pena, J., Matias, L. & Senos, M. L. (1995). A erupção da Chã das Caldeiras (Ilha do Fogo) de 2 de Abril de 1995. Lisboa, Protecção Civil, Orgão do Serviço Nacional de Protecção Civil, II Série, 7, pp. 3-14.B..

Torres, P. C., Silva, L. C., Brum da Silveira, A., Serralheiro, A. & Mota Gomes, A. (1997). Carta Geológica das Erupções Históricas da ilha do Fogo: Revisão e actualização. In "A erupção vulcânica de 1995 na ilha do Fogo, Cabo Verde", Lisboa, 119 - 132.

Index

Itinerary and schedule	7
Introduction	9
1. Brief characterization of the area	11
a. Santiago Island	11
b. Fogo Island	11
2. The geological constitution of Santiago Island	14
Tour around the Santiago Island	14
Stop 1. Praia Plateaus	14
Stop 2. Monte das Vacas	15
Stop 3. Ribeira de São Domingos	15
Stop 4. Ribeira Seca (Poilão Dam) – Órgãos	16
Stop 5. Pico de Antónia Massif	16
Stop 6. Santa Catarina Plateau	17
Stop 7. Serra da Malagueta Massif	17
Stop 8. Tarrafal - Baía Verde	18
Stop 9. Tarrafal - Monte Graciosa	18
Stop 10. Biscainhos (S. Miguel)	19
3. The geological constitution of Fogo Island	20
Tour around the Fogo Island	20
Stop 1. S. Filipe Beach	20
Stop 2. Ponta da Salina	21

Stop 3. Monte Sumbango (Mosteiros)	21
Stop 4. Corvo's Pahoehoe Lava Flows	22
Stop 5. Vale da Ribeira de Caiada	22
Stop 6. Alto Espigão Viewpoint	23
Stop 7. Entrance to the Fogo Natural Park	24
Option 1 - Tour inside Chã das Caldeiras - Fogo Natural Park	24
Stop 1a. Entrance to the Fogo Natural Park	24
Stop 2a. Explosion crater, Curral de Asno	25
Stop 3a. Lava flows from the 2014 eruption, Lantisco	25
Stop 4a. Scoria cone from the 2014 eruption	25
Stop 5a. Bordeira	26
Stop 6a. Lava field	26
Stop 7a. Main façade of the old wine cellar, Boca Fonte	27
Stop 8a. Contact between the lava flows of 1995 and those of 2014...	27
Stop 9a. Villages of Chã das Caldeiras	28
Stop 10a. Monte Preto Volcanic Cave	28
Stop 11a. Hornitos, north of the Volcano, Monte Preto	28
Stop 12a. Monte Velha Forest Perimeter	29
Option 2 - Climb to Pico do Fogo (between 5am and 12pm)	29
Stop 1b. Pico do Fogo Volcano	29
Option 3 - Climb to the Peak of the 2014/15 eruption...	30
Stop 1c. Scoria cone from the 2014/15 eruption	30
Final notes	30
References	31



Photo by Sérgio Brito

ORGANIZATION AND SUPPORTERS:





10th IAG INTERNATIONAL CONFERENCE ON GEOMORPHOLOGY

Photo by Sérgio Brito

COIMBRA - PORTUGAL
« GEOMORPHOLOGY AND GLOBAL CHANGE »

FIELDTRIP GUIDEBOOK **The Estrela UNESCO Global Geopark: from planation surfaces to glaciations** 17-19 September 2022

Gonçalo Vieira
Emanuel de Castro
Fábio Loureiro



Gonçalo Vieira
Emanuel de Castro
Fábio Loureiro

10th International Conference on Geomorphology
Fieldtrip Guidebook – The Estrela UNESCO Global
Geopark: from planation surfaces to glaciations

17-19 September 2022



Coimbra, 2022

Edition notice:

Title: *10th International Conference on Geomorphology. Fieldtrip Guidebook – The Estrela UNESCO Global Geopark: from planation surfaces to glaciations*

Authors: *Gonçalo Vieira (University of Lisbon), Emanuel de Castro (Estrela Geopark) and Fábio Loureiro (Estrela Geopark)*

Fieldtrip guided by: *Gonçalo Vieira (University of Lisbon), Emanuel de Castro (Estrela Geopark) and Fábio Loureiro (Estrela Geopark)*

Edition: *Universidade de Coimbra, Faculdade de Letras*

Fieldtrip and Guidebook Coordination: *António Vieira (University of Minho)*

Cover: *Zêzere glacial valley (photograph by António Vieira)*

ISBN: *978-972-95222-9-1*

Introductory Note

The 10th International Conference on Geomorphology will take place in Coimbra (Portugal) from 12th to 16th September 2022, under the theme "Geomorphology and Global Change" and it is organized by the International Association of Geomorphologists (IAG) and the Portuguese Association of Geomorphologists (APGeom).

As in previous international conferences on Geomorphology, and as is the tradition in many geomorphological events organized around the world, the organizing committee of the 10th International Conference on Geomorphology proposed several fieldtrips to the participants, occurring before, during and after the main event.

These fieldtrips intend, above all, to show to geomorphologists from all over the world the diversity and richness of the geomorphological elements of the Portuguese territory (and also from Cape Verde) and to allow an exchange of experiences between the specialists that investigate these territories and the visitors, contributing for mutual scientific enrichment and for the valorization of this international conference.

The pre-conference fieldtrip is dedicated to the islands of Santiago and Fogo, in the Archipelago of Cape Verde. It will take place from 6th to 9th September and will be led by colleagues from the University of Cape Verde (Vera Alfama, Sónia Victória, Sílvia Monteiro, José Maria Semedo and Romualdo Correia). The volcanic geomorphology will dominate the visit (including well conserved structural volcanic forms such as cones, domes, craters and calderas), especially in the island of Fogo where recent volcanic activity has been registered.

The one-day mid-conference fieldtrips will take the visitors around the Portuguese mainland territory, the 14th September, allowing the visit of four different geomorphological realities.

In the Arouca UNESCO Global Geopark, internationally recognized territory since 2009, participants will be able to visit unique geological and geomorphological features (such as planation surfaces, bowl-shaped valleys and narrow river valleys) and witness the remarkable effort of protection and promotion of natural (abiotic and biotic) and cultural (tangible and intangible) heritage. The visit to the "516 Arouca" suspension bridge will be an excellent opportunity to observe the magnificent landscapes of this mountainous territory. This fieldtrip will be led by Artur A. Sá, António Vieira and Daniela Rocha.

The field trip to coastal areas of central Portugal will be led by Pedro Dinis and António Campar Almeida. Their proposal is to observe the different morphotectonic units of central west Portugal, namely the Coastal Mountain of Serra da Boa Viagem (revealing karstification features), the littoral plain (with aeolian dunes associated with some

reliefs with higher elevation), the Cértima subsiding area (structurally-controlled morphology), and the Buçaco region (with the Syncline of Buçaco).

The visit to the Schist Mountains of Central Portugal will be centered in the mountains of Lousã and Açor, and will be conducted by Luciano Lourenço and Bruno Martins. It is proposed the observation of the main contrasts of the landscape, especially in terms of its physical geography, translated into geological, hypsometric, geomorphological, and hydrographic differentiation, or the land use and occupation and evolution of vegetation cover, namely following the recurrent large forest fires and the subsequent erosive processes they caused.

The fourth one-day fieldtrip will be oriented to the Estrela UNESCO Global Geopark, and led by Gonçalo Vieira, Emanuel Castro and Fábio Loureiro. The main geoheritage significance of the Estrela UGGp is the extent and richness of the Late Pleistocene glaciation(s) landforms and deposits (with spectacular morphological features such as the Zêzere glacial valley or the glacial cirques, moraine boulders, erratics or *roches moutounnées*) as well as the peculiar long-term geological evolution (revealing a significant diversity of granite types and landforms).

The three post-conference fieldtrips include a visit to the Lisbon Region, Serra da Estrela and, finally, Minho and Galicia (Spain), and will take place from 17th to 19th September.

The fieldtrip to the Lisbon Region will be guided by José Luís Zêzere, César Andrade, Sérgio Oliveira, Jorge Trindade and Ricardo Garcia, and will cover topics related with slope instability and landslides that affect the region of Lisbon, the floods occurring in the area north of Lisbon, and the coastal dynamics, morphology, cliff instability and beach erosion at north and south of Lisbon.

The three days field trip to the Serra da Estrela is led by Gonçalo Vieira, Emanuel Castro and Fábio Loureiro. Participants will be taken to visit some of the Geopark's most inaccessible geosites and observe breathtaking landscapes during two hikes: one in the Zêzere valley and the other between Penhas Douradas and Lagoa Comprida. The different geosites to visit include features of glacial, periglacial, granite weathering, fluvial, hydrogeological, petrological and tectonic themes, and aspects related with the management of a UNESCO Global Geopark will be discussed.

The third three-days fieldtrip is destined to the northwestern part of Portugal and the Spanish region of Galicia. Guided by Alberto Gomes and Antonio Perez Alberti, will be mainly devoted to the coastal area and to the observation and discussion of issues related to coastal dynamics, marine terrace staircases, differential uplift of coastal blocks, coastal geoheritage, coastal geoarchaeology, coastal erosion and coastal land planning.

It is our expectation that these visits will please all participants and promote the scientific enrichment of all involved, allowing a better understanding of the topics covered in each one.

We also hope that this set of fieldtrip guidebooks can help in the understanding of the themes discussed and that they can be a testimony of the commitment and dedication shown by all the scientific responsible for the several visits, to whom the organizing committee of the International Conference on Geomorphology expresses its greatest recognition and gratitude.

have a good fieldtrip!

Lúcio José Sobral da Cunha
António Vieira

on behalf of the ICG2022 Organizing Committee

ITINERARY AND SCHEDULE

Itinerary

Day 1

08:00 Departure from Coimbra (Largo D. Dinis) (Fig.1)

Stop 1 – Folgoso

Stop 2 – Linhares da Beira

Stop 3 – Videmonte

Stop 4 – Quinta da Taberna

Overnight in Manteigas

Day 2

Stop 1 – Hike from Penhas Douradas to Lagoa Comprida (all day)

Stop 2 – Sabugueiro

Overnight in Manteigas

Day 3

Stop 1 – Barroca d'Água – Zêzere valley (easy hike - 2h30)

Stop 2 – Covão da Ametade

Stop 3 – Piornos

Stop 4 – Covão do Boi

Stop 5 – Alto da Torre

Stop 6 – Salgadeiras

18:00 - Return to Coimbra

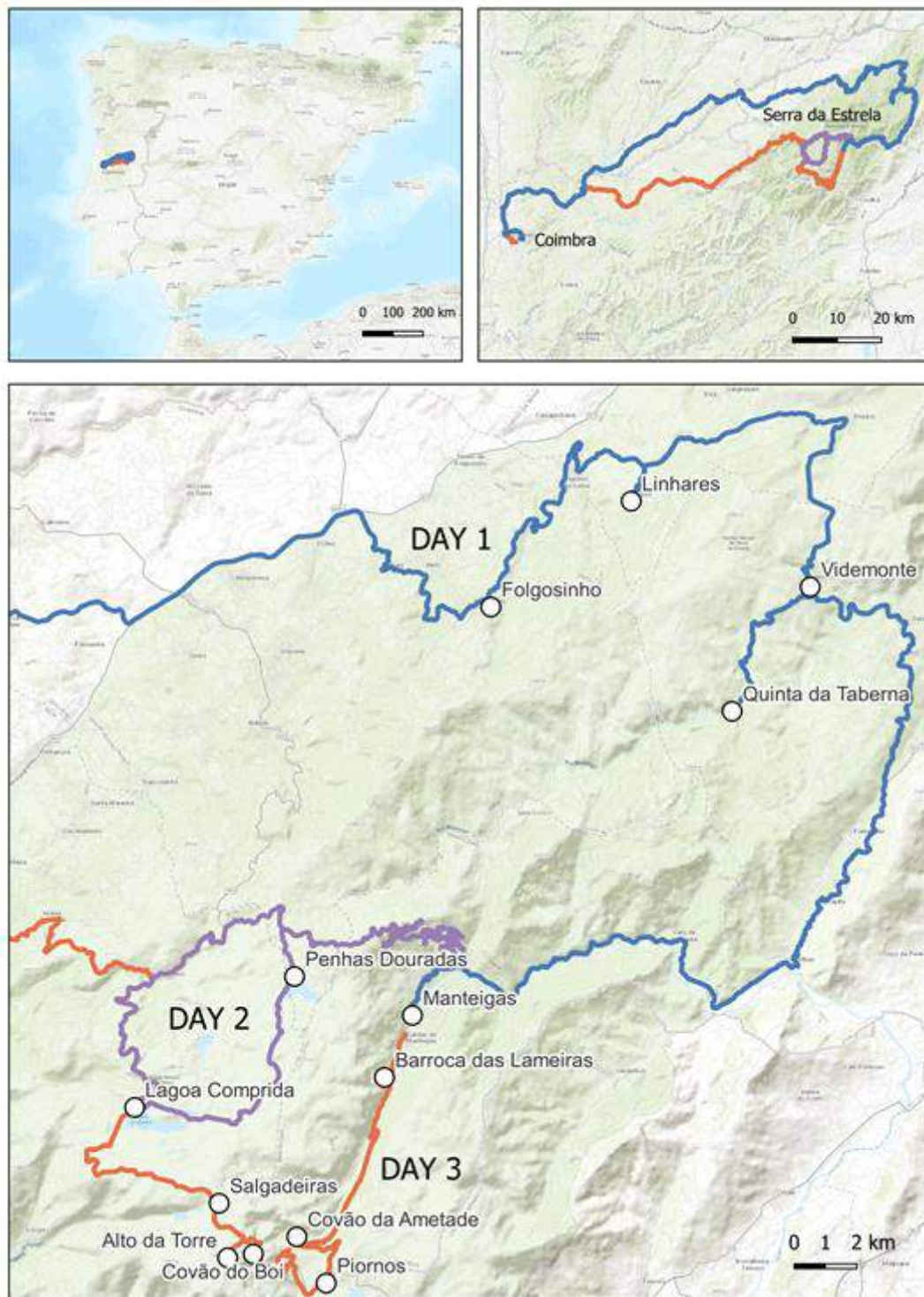


Figure 1. Itinerary of the field trip to the Serra da Estrela.

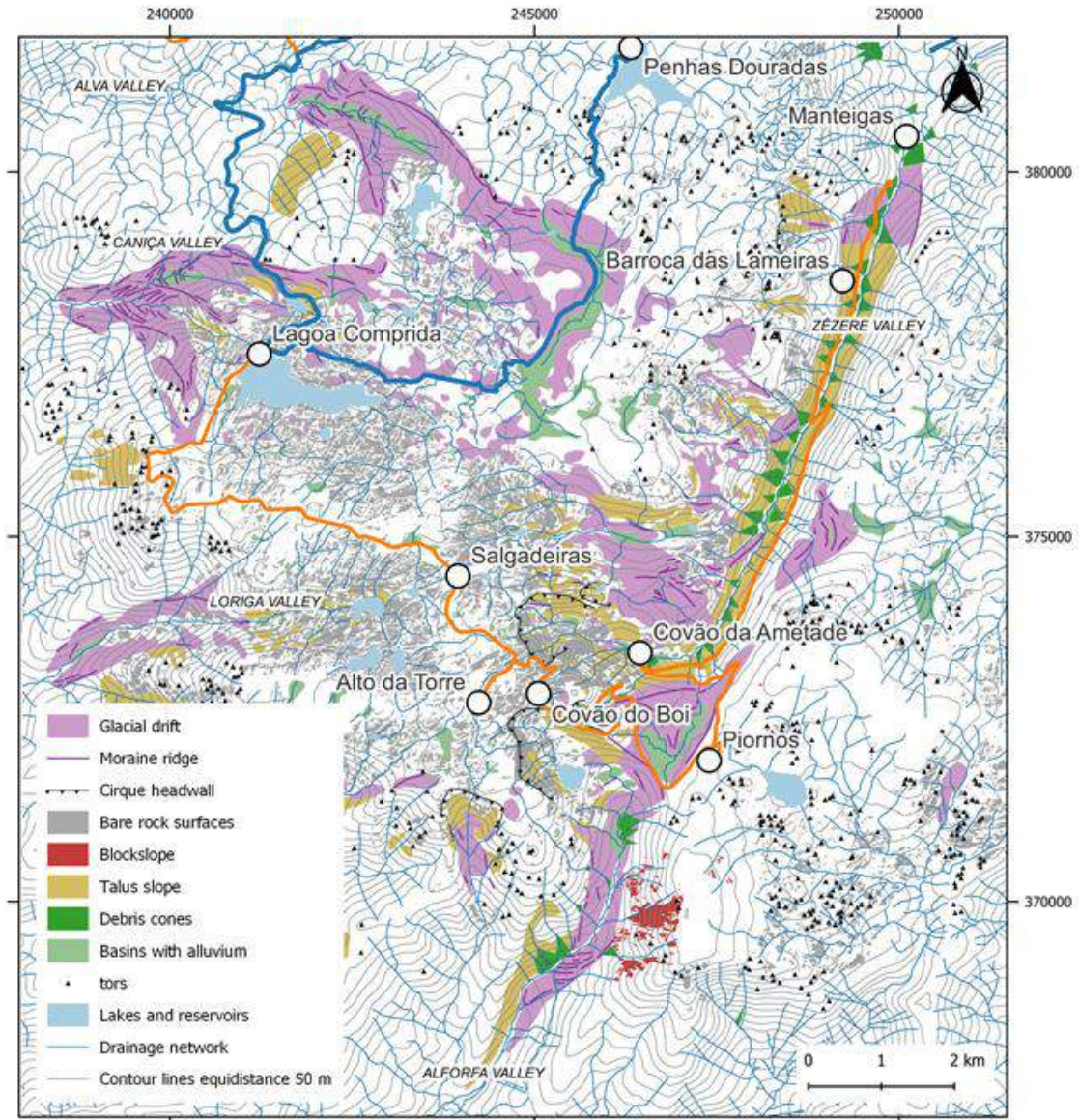


Figure 2. Glacial geomorphology of the Central area of the Serra da Estrela and itineraries in days 2 and 3.

1. The geology and geomorphology of the Serra da Estrela

1.1. Introduction

The Estrela UNESCO Global Geopark (Estrela UGGp) is located in Central Portugal and is part of the Iberian Central System, a mountain range that extends from Guadarrama, north of Madrid, to Montejunto, northeast of Lisbon. The Serra da Estrela is the highest mountain in mainland Portugal, rising to 1993 m a.s.l. at Alto da Torre, but the Estrela UGGp is a larger and encompassing area. Its boundaries include the major elements of the geology that contributed to the present-day landforms, but also to reflect how geology shaped the human nature of the Estrela inhabitants and the regional socio-economy (Fig. 3). The Estrela UGGp integrates the Estrela mountain range from its SW limits at the border with the Açor mountain, to the NE contact with the Meseta surface, as well as the piedmont regions that bound the Estrela to the NW and SE and where, for millennia humans lived in an intimate relationship with the mountain and with what it had to offer (Fig. 4).

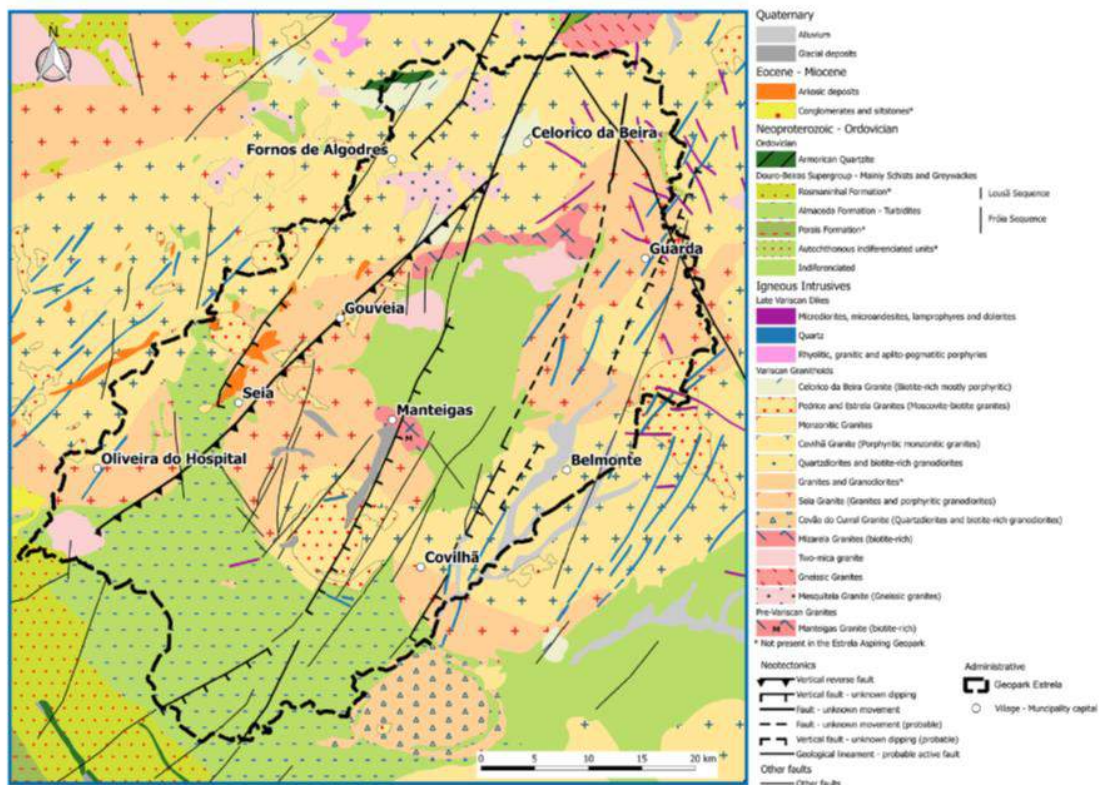


Figure 3. Geology of the Estrela UNESCO Global Geopark (based on Geological Map of Portugal 1:500.000).

The main geological originality of the Estrela UGGp is the breadth and richness of the Late Pleistocene glaciation(s) landforms and deposits, of high pedagogical and scenic values and with a remarkable scientific value, when considering the geographical

position at the SW limit of Europe. However, the glaciation and geodiversity of the Estrela UGGp would not have been possible without the peculiar long-term geological evolution from the distant past to the recent landscape evolution (Table I).

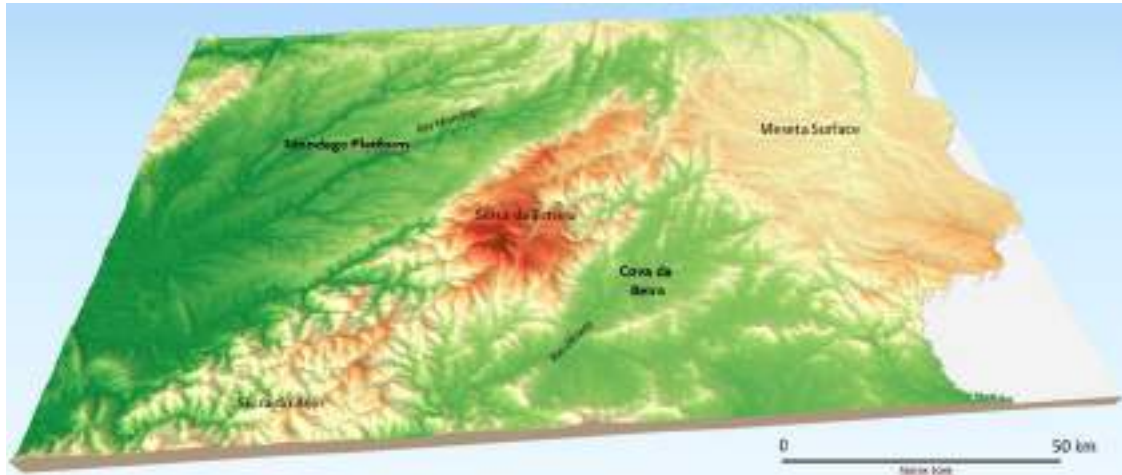


Figure 4. Overview of the Serra da Estrela topography from south to north. The Estrela rises to almost 2000 m asl and the Mondego platform averages 400-500 m asl.

1.2. The Variscan orogen heritage: a precursor of the present-day dynamics

After over 270 million years, the Variscan orogeny still shows a significant imprint in the geology of Western Iberia and jointly with the effects of Paleogene planation and Alpine tectonics, is responsible for the major features of the large-scale morphostructures and hence, for the major patterns of ecosystems, history and cultural heritage in Central Portugal.

The Estrela UGGp is located in the Central Iberian Zone (CIZ), which represents in the tectonic and paleogeographic zoning of the Iberian Peninsula, the axial zone of the Variscan orogen. This large scale orogen resulted from continental collision after the opening and subsequent closing of the Rheic and Paleothethys oceans (Ribeiro, 2013), within the context of a passage from an active continental margin (Late Precambrian) to a continental collision (Martínez-Catalán *et al.*, 2009). The resulting amalgamation of the continental masses of Laurentia, Baltica and Gondwana gave origin to the Pangea supercontinent.

In Iberia, the Variscan basement is named Iberian or Hesperian Massif and due to its paleogeographic setting is a key sector in the definition of the Palaeozoic peri-Atlantic orogens (Ribeiro, 2013). At the end of the Palaeozoic, Iberia occupied a position at the junction of the Appalachians (to the SW), the Caledonides (to the NW) and the Variscan (to the NE) (Martínez-Catalán *et al.*, 2009). Today, the Iberian Massif is present in most of the Western part of the Iberian Peninsula, with the tectono-stratigraphic model of Jullivert *et al.* (1974)(Fig. 5) dividing it into five broadly parallel zones following the Variscan structures:

- The Cantabrian and the South Portuguese zones are the external zones of the Iberian Variscan belt, with well-developed upper Palaeozoic sedimentary sequences, low-grade metamorphic and scarce sin-orogenic granite intrusions. The former is a Gondwanan overthrust foreland belt, while the later initially developed as a foredeep basin and later as an accretionary complex (Martínez-Catalán *et al.*, 2009).

Table I. Synthesis of the geological history of the Estrela UNESCO Global Geopark (EAG in the table) (AGE, 2017).

eon	era	Period	Epech	Age (Ma)	Wilson cycles	Paleogeography	Geoheritage phenomena in the EAG	
Phanerozoic	Cenozoic	Quaternary	Holocene	0.01 - today	Alpine Cycle	Fluvial erosion and slope processes (alluvial, colluvial, and debris cones), human action in the landscape, soil erosion.	Climate stability and recent human-induced climate change.	Alluvial and slope deposits.
			Pleistocene	2.6 - 0.01		Quaternary glaciations, uplift, sea-level change, fluvial erosion and stream piracy.	General cooling trend.	Glacial, fluvioglacial and periglacial deposits and landforms, active fault systems.
		Neogene	Pliocene	5.3 - 2.6		Beginning of incision of the present-day river system.	Hot climate with marked seasonality.	Formation of the main valley systems, piedmont deposition.
			Miocene	23 - 5.3		Reactivation of Variscan fault systems with main uplift of Estrela.		
		Paleogene		66 - 23		Beginning of the Alpine compression - reverse faulting. Erosion of the deep weathering mantles and retouching of the glanation surfaces.	Tropical climate with dry season.	Deposition of Arkosic clays. Planation surfaces and inselbergs.
	Mesozoic	Cretaceous		145 - 66		Opening of the Gulf of Gascony. Formation of the Iberian microplate.	No evidence in the EAG.	
		Jurassic		201 - 145		Opening of the Atlantic (Upper Jurassic). Fragmentation of the Pangeo and basic volcanism with dolerites and lamprophyres.	Pre-Cretaceous glanation surface. Wet and warm climate with deep weathering and regolith formation.	Intrusion of aplitic pegmatite and siliceous (quartz) veins.
		Triassic		252 - 201		Brittle deformation of the Variscan basement (faults NNE-SSW to ENE-WSW and NNW-SSC to NW-SE) formation of the basement.	Bragança - Vilaça - Mantegás fault and other lineaments.	
	Palaeozoic	Permian		299 - 252		Variscan Cycle	Erosion and full planation of the Variscan Belt with sedimentation in the Dúrcio-Beirão Carboniferous zone (Late Permian). D3 compressive phase (315-305 Ma) with Granite intrusions (310-290 Ma).	No evidence in the EAG. Contact metamorphic: hornfels and schists. Faults and folds in metasedimentary rocks. Most granite types of Serra da Estrela.
		Carboniferous		359 - 299			D2 extensional phase (335-315 Ma) with crustal thinning and exhumation with regional metamorphism. D1 compressive phase (360-350 Ma) with Barrovian.	Gneissic-migmatitic complex and Dúrcio Beirão metamorphic Supergroup.
		Devonian		419 - 359			Formation of the Parípea.	No evidence in the EAG.
		Silurian		443 - 419			Deposition of quartz sands in coastal environments. Granite intrusions.	Quartzites with Skolithos. Mantegás Granite.
		Ordoevician		485 - 443			Sediment deposition in the Rheic and Paleotethys oceans.	Douro-Beiras Supergroup (SGC).
		Cambrian		541 - 485				
Proterozoic	Neoproterozoic			1000 - 541	Sediment deposition in marine environment, that will become the metasedimentary rocks.	Undifferentiated Neoproterozoic units of schists, greywackes, conglomerates and quartzite rocks.		
				2500 - 1000				
Archaean			4000 - 2500		First life forms on Earth.			
	Hadaic		4550 - 4000		Earth planet formation.			

- The West Asturian-Leonese, the Central Iberian and the Ossa-Morena zones, are the internal zones, with prevailing terrains of Pre-Cambrian and Lower Palaeozoic ages. In these zones, the Variscan deformation was stronger, while high-grade metamorphism is present and sin-orogenic granite plutons are frequent.

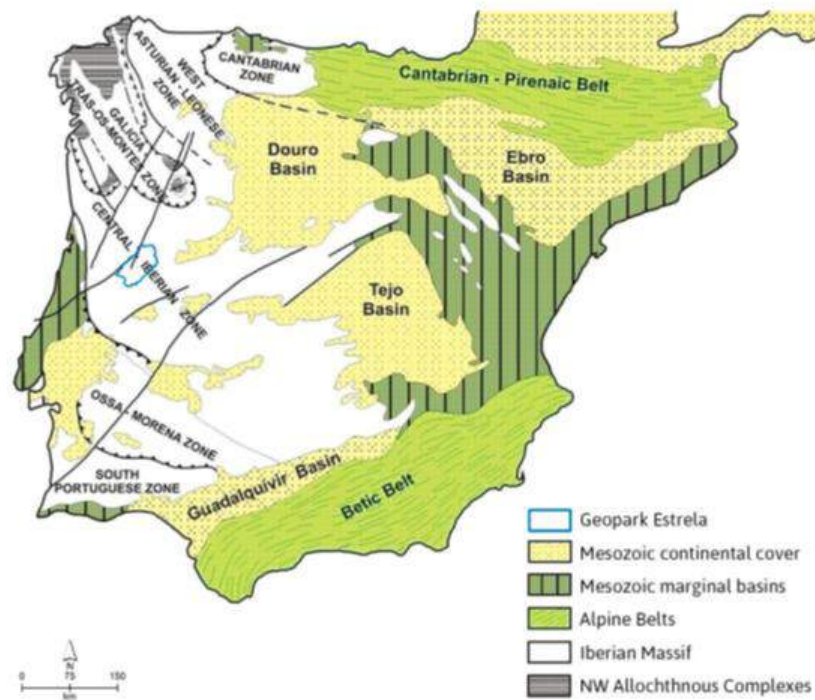


Figure 5. Tectonic and stratigraphic zoning of the Iberian Peninsula according to Julivert *et al.* 1974 (adapted from Santos and Tassinari, 2012).

1.3. The Pre-Ordovician autochthonous

The Central Iberian Zone, of special significance to the Estrela UGGp, extends from northwest to central Spain, covering most of the centre and north of Portugal and is ca. 400 km wide in the centre of the massif. Based in stratigraphic criteria and on the lithology of the autochthonous sequences underlying the Lower Ordovician quartzites, the CIZ is divided into (Martínez-Catalán *et al.*, 2009):

- The Schist-Greywacke Complex Domain (Complexo Xisto-Grauváquico, Carrington da Costa, 1950; Teixeira, 1955), a thick terrigenous sequence, currently named in Portugal the Douro-Beiras Supergroup, Sousa e Sequeira, 1987; Oliveira *et al.*, 1992). This sedimentary sequence from the Upper Precambrian to the Lower Cambrian is divided into the Douro (to the N) and the Beiras Groups (to the S), characterized as turbiditic lithofacies accumulated in two basins (Neiva *et al.*, 2013). The former shows calciturbitic occurrences and is probably upper Neoproterozoic to lower (middle?) Cambrian, while the latter is traditionally considered as monotonous non-carbonated deeper facies sequence dating from

the Neoproterozoic. Recent studies reported the existence of two distinct stratigraphic sequences bounded by a first rank unconformity (Meireles *et al.*, 2014), which is confirmed in the current 1:200.000 geological map of Portugal.

- The Ollo de Sapo Domain, a volcano-sedimentary complex, located to the N and NE of the CIZ.
- The Meridional allochthonous unit, composed by Upper Neoproterozoic to Lower Cambrian rocks with close relation to the Ossa-Morena Zone.

1.4. A wealth of granite intrusions at the late stages of the orogeny

The Variscan orogen was active in Iberia from the lower Devonian to the end of the Carboniferous and showed three major phases of deformation (D1, D2 and D3). The crustal thickening generated metamorphism and synorogenic magmatism, resulting in extensive formation of granitic rocks. Late and post-tectonic magmatism was widespread from 310 to 290 Ma, with the CIZ being the section of the European Variscan chain where granitic rocks show a wider diversity and outcrop in larger areas (Azevedo and Aguado, 2006).

The classical petrographical and geochemical classification for the granitoids of northwest Iberia groups the Variscan granites in two large categories (Capdevila and Floor, 1970; Capdevila *et al.*, 1973):

- Two mica granitoids related with migmatites and high-grade metamorphic terrains.
- Granodiorites and biotitic calc-alkaline granites (sin- and late-post-kinematic), frequently associated to mafic and intermediate igneous rocks.

Recent studies showed that the Variscan plutonism is associated with the last ductile deformation stage (D3). Hence, the Variscan granites can be divided into four groups [32]: pre-D3, sin-D3, late-D3 and post-D3. As for the scarce intrusions dating from the upper Proterozoic to the lower Palaeozoic, they are broadly classified as pre-Variscan [29] (Table II). Pre-D3 granites show similar characteristics to sin-D3 but are almost lacking in Portugal. Most of the large batholiths of peraluminous two-mica granites and leucogranites, as well as some granodiorite and biotitic granite masses are sin-D3 (320-310 Ma). The late-post-D3 granites (310-290 Ma) frequently form composite zoned massifs with contact metamorphism zones and are mainly non-deformed granodiorites and biotitic granites. They are low to moderate peraluminous, showing frequent association with basic and intermediate composition rocks. Intrusions of biotite-muscovite granites and two-mica granites, which are late- to post-D3 are also included in this group (Azevedo and Aguado, 2006).

Table II. Granites of the Estrela UNESCO Global Geopark following (Oliveira *et al.*, 1992) (* Not mapped at 1:500000 Geological map of Portugal).

Main granite types	Regional classification	Orogenic phase	
Porphyritic biotite granites	Celorico da Beira granite	late- to post-D3	Fragile fractures
Muscovite-biotite granites	Pedrice and Estrela granites	late to post-D3	Ductile shears
Monzonitic granites with megacrysts	-		
Porphyritic monzonitic granite	Covilhã granite		
Quartzdiorites and biotite granodiorites	-		
Granites and granodiorites	-		
Porphyritic granites and granodiorites	Seia granite	sin-D3 (intermediate series)	Two-mica granitoids with xenoliths
Quartzdiorites and biotite granodiorites	Covão do Curral granite		
Biotite granodiorites	Mizarela granite	sin-D3 (early series)	
Two-mica granites	-	sin-D3	
Granites and Migmatites*	-		
Gneissic granites	-	sin-D2	
Gneissic granites	Mesquitela granite	pre- to sin-D1	
Ortogneisses and granites	Manteigas granite	pre-Variscan	-

A large area of the Estrela UGGp is in the granitic batholith of the Beiras that intrudes metasediments from the Upper Proterozoic/Lower Cambrian to the Upper Carboniferous, which were variously affected by the polyphasic Variscan deformation (D1, D2 and D3). The tectono-magmatic evolution of the Beiras Batholith during the Variscan Orogeny showed the following phases (Azevedo and Aguado, 2006):

- Deformation phase D1 (~360-335 Ma), with a compressive regime inducing crustal thickening and Barrovian type metamorphism of the pre-Carboniferous metasediments, with partial crustal melting.
- Extensional phase D2 (~335-315 Ma) marked by a large-scale gravitational collapse, generating crustal thinning, exhumation of the orogen, which was the climax of the regional metamorphism with intense migmatization.
- Compressive phase D3 (~315-305 Ma), marked by significant crustal melting, which allowed for separation from the solid residuum. At this stage, peraluminous granite magmas (type-S) rose, suffered differentiation and consolidated, forming large two-mica leucogranite batholiths. Simultaneously, the lithospheric mantle,

separated from the crust inducing the ascension of basaltic magmas that intruded the interface crust-mantle in a process of underplating. This heat source induced the melting of the lower crust rocks and mixing and mingling of mantle and crustal magmas, generating I-S type magmas, forming calc-alkaline granodiorites and biotitic monzogranites (sin-D3). This pulse is present at the Estrela UGGp at the Maceira massif installed sin-cinematically at the Juzbado-Penalva do Castelo shear zone and is interpreted as evidence of the continuation of the tectonic exhumation. At the late D3 with the continuation of isostatic rebound and exhumation, the decompression of the asthenosphere generated basic magmas that hybridized with the molten felsic crust, forming calc-alkaline metaluminous to slightly peraluminous magmas. Their ascension occurred post-D3 generating the late-post-kinematic composite hybrid biotitic granite massifs of the Beiras batholith at 306 Ma. A period of ca. 20 Ma dominated by hydrothermal activity followed the deformation acting mainly along the major Variscan fault zones (Sant'Ovaia *et al.*, 2013).

Despite the Variscan age of most granitic rocks in the CIZ, the Manteigas granite, a medium to coarse-grained slightly porphyritic biotite granodiorite, outcropping in a small mass at the Estrela UGGp, is Ordovician (481.1 ± 5.9 Ma), hence completely unrelated with the Variscan Orogeny (Neiva *et al.*, 2009). This granite and the Mizarela granite are considered the same unit in the geological map of Portugal (Oliveira *et al.*, 1992), which was the base map for the Estrela UGGp. The current 1:200.000 map in the works, with the support of LNEG, will allow the differentiation of several of these lithologies.

1.5. The planation at the end of the Variscan cycle

The full cycle of the Variscan orogeny ended in the Late Permian with the planation of the mountain belt. This erosional phase is marked in continental sedimentation in intramontane basins such as the Dúrico-Beirão Carboniferous zone (Ferreira, 2005). This pre-Triassic planation surface is currently very deformed in Portugal, where it only occurs fossilized by Triassic sedimentation, while in Spain is still visible at the surface.

At the end of the orogenesis the Iberian Massif was affected by brittle tectonic deformation, giving origin to two main fault systems: an older set of NNE-SSW to ENE-WSW sinistral lateral strike-slip faults, and a younger set of NNW-SSE to NW-SE dextral lateral strike-slip faults. The former was much more significant for the subsequent geomorphological evolution in the Estrela UGGp (Ferreira, 2005), which reflects the changing tectonic and paleogeographical conditions following faulting at the end of the Variscan cycle.

In the Mesozoic, a new Wilson cycle started with rifting south and west of the present boundaries of the Iberian Massif initiating the breakup of Pangea. The stage lasted from

the Triassic to the Middle Jurassic, while a second stage associated with the opening of the Atlantic, started at the Upper Jurassic. The continuous formation of oceanic lithosphere west of Iberia and the opening of the Gulf of Gascony induced the anticlockwise rotation of Iberia, forming the Iberian microplate in the Lower Cretaceous (Ribeiro, 2013).

The current relief of the Estrela UGGp is mainly a result of the evolution since the Paleogene and particularly of the interplay between climate and tectonics, controlled by the Variscan structures. During large part of the Jurassic, the western part of the Iberian Massif was subject to intense chemical and biochemical weathering in a warm and wet climate, generating thick regoliths and the deposition of carbonates in the continental margin (Ferreira, 2005). These conditions lasted until the end of the Mesozoic (Martin-Serrano, 1988), with the deep weathering probably being the cause for the pre-Cretaceous planation surface, as an etch surface. Following tectonic activity and lasting until the Middle Tortonian (Pais *et al.*, 2012), climate changed to a tropical climate with dry season, and an erosional regime installed, removing the weathering mantles (Ferreira, 2005).

The pre-Cretaceous surface was retouched during the Paleogene and gave origin to subsequent planation surfaces that are key geomorphological features of the Iberian Massif today, with the oldest correlative deposits being the Coja arkoses (Upper Eocene). These deposits cover patches of the Paleogene planation surface, which is present from northern to southern Portugal and from which the main present-day mountains in the Iberian Massif developed. In the Estrela UGGp, these Paleogene deposits occur in the NW piedmont, mainly in the Seia-Pinhanços graben where they were protected from erosion.

Planation surfaces are divided in two major types (Ferreira, 1978, 2005): i. polygenic surfaces formed in tectonically stable areas, where deformation was consistently planated by prevailing erosional processes, and ii. stepped surfaces, where deformation was stronger and the various planation phases did not fully erode the newly formed relief, resulting in several planation surfaces forming at lower positions.

Polygenic surfaces are well represented in the Iberian Massif, with good examples being the Meseta Surface and the Mondego Platform, while stepped surfaces are also frequent, for example in the Central Portuguese Plateaux in the northern edge of the Estrela UGGp (Ferreira, 1978, 1991). Stepped surfaces prevail to the north of the Estrela UGGp, where uplift has been stronger, while polygenic surfaces prevail to the south, such as is the case of the Castelo Branco Surface (Ribeiro, 1949) in the Naturtejo Geopark or the Baixo Alentejo Penplain (Feio, 1952). The planation surfaces, especially to the south of the Serra da Estrela, show some good examples of residual reliefs (inselbergs) such as the Belmonte inselberg at the Estrela UGGp.

1.6. Collision with Africa and the rise of a new mountain

Regional compression in the Oligocene caused by the collision with the African plate initiated crustal shortening and rejuvenation of the Variscan tectonic structures (De Vicente and Vegas, 2009). One of the main features uplifting from the Central Iberian Zone Paleogene planation surface was the Iberian Central System (Cordilheira Central in Portugal), taking place possibly from the Middle to Upper Miocene (Martin-Gonzalez, 2009). Some authors, consider that the westernmost part of the Iberian Massif maintained continuous uplift during the whole Cainozoic (De Vicente *et al.*, 2007), while others place the peak of the Alpine compression in the Portuguese mainland in the Tortonian (Pais *et al.*, 2012, Cunha *et al.*, 2000). These changes were drastic for the continental topography of Iberia, which had an elevation close to the sea-level until the end of the Cretaceous [Cunha and Pena dos Reis, 1995; Dinis *et al.*, 2008) and suffered a general uplift of the planation surface between 100 and 600 m (De Vicente *et al.*, 2011).

During the so-called Alpine compression, several fault directions were reactivated: i. NE-SW to ENE-WSW oriented, as thrusts, ii. NNE-SSW, as sinistral strike-slip faults, and iii. NW-SE, as dextral strike-slip faults (Pais *et al.*, 2012). Thrusts controlled the uplift of the Central System, since they were reactivated as reverse faults. South of the Central System, the SE-verging and NW-dipping Ponsul fault flattens at depth while converging with the Seia-Lousã fault that is NW-verging and SE-dipping and located in the north (Fig. 6). The result was the formation of a large horst uplifting as a pop-up structure along a system of parallel faults (Ribeiro *et al.*, 1990). A whole section of the planation surface was displaced and is still visible in the summits of the Estrela forming a plateau, which dips slightly to the northeast, but which is well-preserved in granites. This plateau is quintessential for the Pleistocene evolution of the Estrela, due to its controls on climate and snow regime, influencing the glaciation style, dynamics and geomorphological features, key elements of the Estrela UGGp.

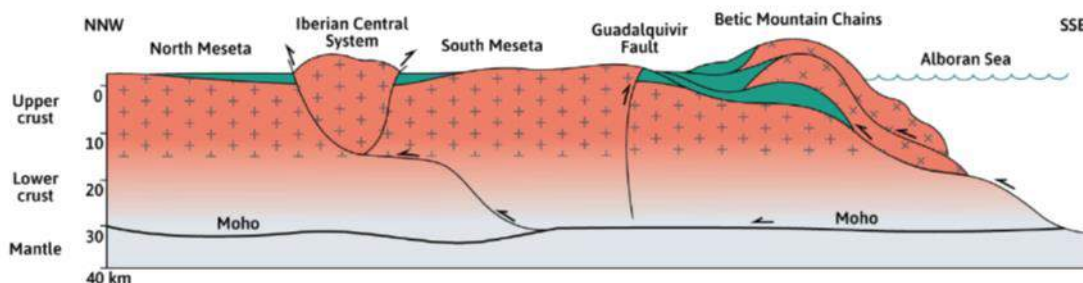


Figure 6. Schematic cross-section showing the pop-up structure of the Iberian Central System following the reactivation of Variscan faults (adapted from Ribeiro 1988).

The strike-slip fault systems show predominantly horizontal displacements that weakened the basement rocks, enabling differential erosion to carve long, deep and

linear valleys, especially where the faults affect granites. One of such examples is the 250 km long Bragança-Vilariça-Manteigas fault (BVMF) that cross-cuts the Estrela along a NNE-SSW direction giving origin to the valleys of the Zêzere and Alforfa (Daveau, 1969, Migon and Vieira, 2014) (Fig. 7). The BVMF also suffered a vertical component in the deformation that displaced the upper Estrela plateaus by about 150-200 m (Ribeiro *et al.*, 1990).

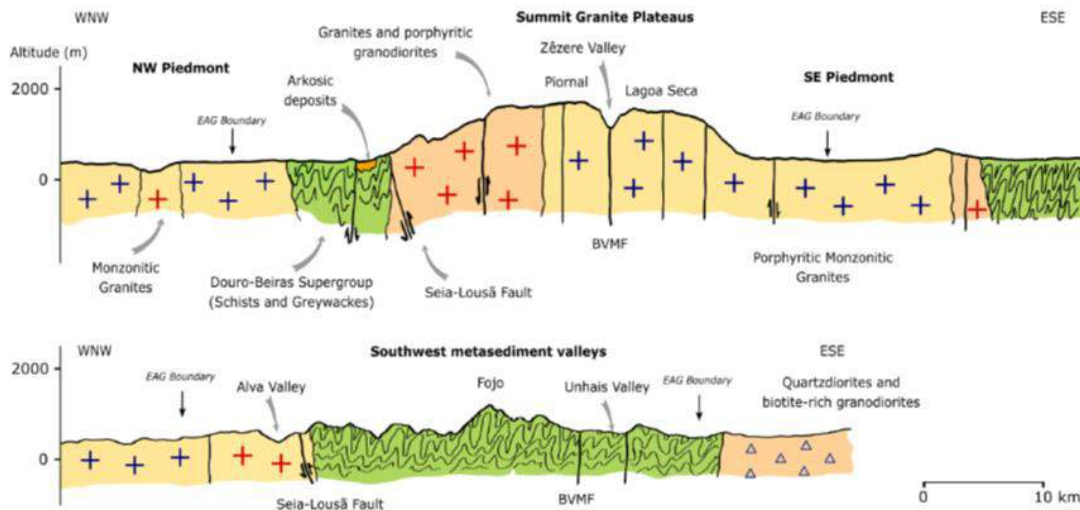


Figure 7. Simplified geological cross-sections of the Estrela UNESCO Global Geopark showing the controls of tectonics and rock type on morphology (base data from the Geological map of Portugal 1:500.000).

1.7. Towards the present-day relief organization

The Late Miocene and the Zanclean were characterized by a hot climate with marked seasonality, resulting in sedimentation occurring mainly at the foot of the fault scarps (Pais *et al.*, 2012). At the time, the main fluvial systems were endorheic draining into the interior of Iberia. In the Piacenzian the climate became hot and very wet and an exorheic fluvial network developed, with broad valleys developing in the mountains and numerous catchments forming in endorheic inland basins. In the Upper Pleistocene, the climate became colder and the continuing uplift and sea-level changes promoted a strong fluvial incision, regressive erosion and stream piracy (Pais *et al.*, 2012), defining the landform organization in Central Portugal and in the Estrela UGGp.

The tectonic deformation continued during the Quaternary with vertical movements resulting both from large scale folding and isostatic adjustments, and from active faulting. Inferred uplift rates for the last 3 Ma are of 0.1-0.2 mm/yr, with the largest deformation occurring in the centre and north of Portugal, with the Estrela UGGp territory showing values of up to 600 m, especially in the higher parts of the Estrela (Cabral, 2012; Rockwell *et al.*, 2009). Active faulting shows a predominance of ~E-W to NE-SW faults with reverse component and left-lateral strike-slip faults ~N-S to NNE-SSW.

The Seia-Lousã fault that bounds the Serra da Estrela in the north is an example of the former, while the BVMF fault is an example of the later.

The long-term geological evolution explains the general organization of the landforms in the Estrela UGGp, with the important control exerted by Alpine tectonics over reactivated Variscan faults, which generated the segmentation of the Paleogene planation indifferent steps up to the summit of the mountain (Fig. 8). One of the main geomorphological differences within the Estrela UGGp is the contrast between granites and the shales, schists and greywackes (Ribeiro, 1954; Daveau, 1969). Granite terrains show typically well-preserved remnants of the planation surfaces, both in the summit areas and in steps and erosional terraces. The valleys are rectilinear, with sharp bends, reflecting the tectonic control. On the other hand, metasedimentary terrains show sharp ridges and a dense drainage network, with scarce remnants of planation surfaces and deeply incised meandering valleys.

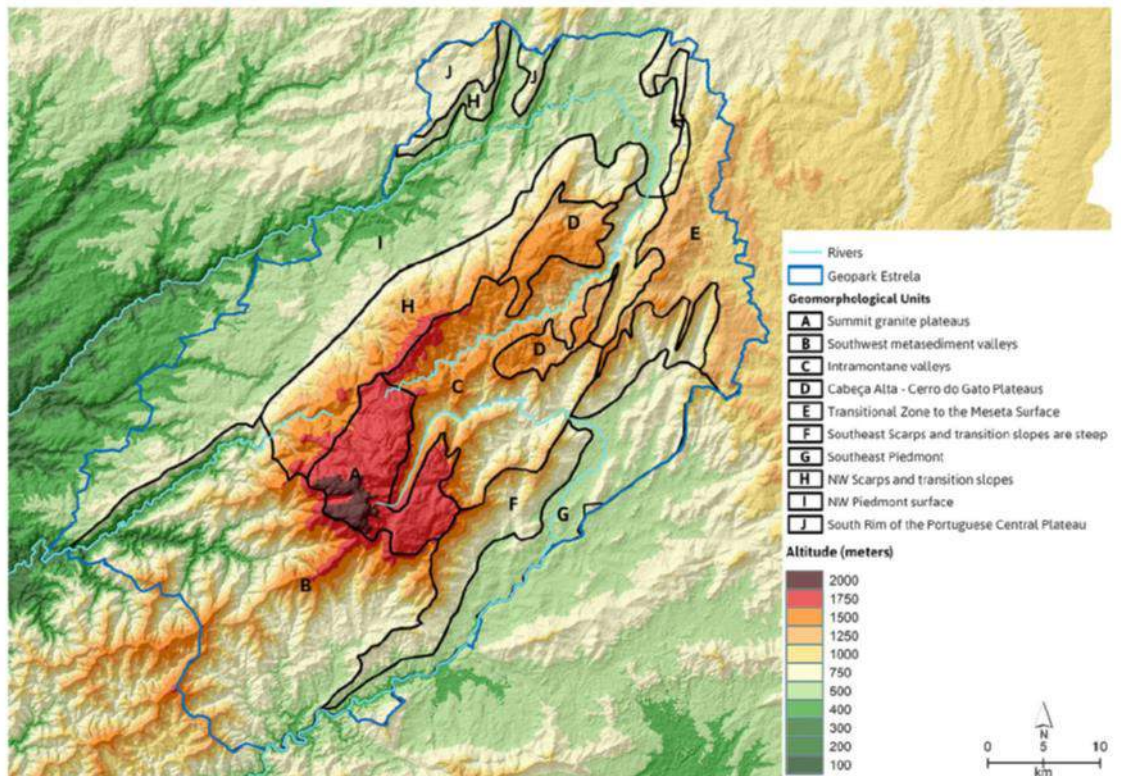


Figure 8. Geomorphological units of the Estrela UNESCO Global Geopark.

1.8. The richness of granite types and the diversity of landforms

The richness of the Estrela UGGp in granite types (Table II) with different geochemistry, age and tectonic history has allowed researchers to dig deeper into rock control on the granite geomorphology across different spatial scales. Such a granite diversity within a small area facing similar climate conditions makes the Estrela unique for assessing the effects of rock control on landforms (Migon and Vieira, 2014). Differences in granite

texture were shown to exert a major control on the occurrence of relict periglacial phenomena (Vieira, 2004), an observation with important impacts for paleoenvironmental reconstruction in granite terrains. At similar topographical settings, fine-grained granite variants show the development of blockfield and blockslopes, while coarse-grained granites show evidence of granular weathering, generating stratified slope deposits instead. Granite types also result in different tor morphologies (Migon and Vieira, 2014) (Fig. 9).



Figure 9. Examples of granite landforms in the Estrela Geopark: A. Fraga das Penhas tor and castle-koppie, B. Penedo do Sino pedestal rock, C. Terroeiro.

Although tors are not unique to the Estrela UGGp they provide, together with other granite landforms, an excellent setting for research. In the Estrela plateaus, the interplay between long-term weathering in different granite variants and the Late Pleistocene glaciation, generated important landscape differences, as well as a good dating framework. Lautensach (1929) noted that tor distribution in the Estrela showed clearly the controls of glacial erosion, with tors almost completely absent within the Pleistocene glacier boundaries. Vieira (2004) mapped over 600 tors in the plateaus confirming Lautensach's observations. However, tors were also found within the glacial limits, such as is the case of the Covão do Boi columns or the tors at the upper Candieira catchment. These formed by post-glacial erosion of the granite weathering mantle which survived under the Pleistocene glaciers (Ferreira and Vieira, 1999; Vieira, 2004). In fact, the singularity of the geomorphological setting and evolution of the Covão do Boi area, makes it one of the key geosites of international significance at the Estrela UGGp.

1.9. The originality of the last glaciation in the Serra da Estrela

a) History of research

Evidence of a glaciation at the Estrela UGGp was mentioned for the first time in 1884 by Cabral in a study about glaciations in Portugal. According to Lautensach (1929), Penck, also in 1884, had pointed evidence of glaciations in the Central System, both in Estrela and Guadarrama. In 1916, Fleury worked on Cabral's observations and described the general features of the Estrela glaciation. However, the first systematic scientific analysis of the Estrela glaciation was only made in 1929 by Hermann Lautensach, a German

geographer that spent three months in area in 1927 and 1928. He identified several features of the glaciation and mapped glacier extent and thickness. Following this work and for almost four decades, the Estrela glaciation did not attract new research, until the important paper by Suzanne Daveau in 1971 – “La glaciation de la Serra da Estrela”. Daveau added up to previous works based on better topographic maps, on field work and on systematic aerial photo interpretation. Most of the results of Daveau’s mapping are still valid today, especially in what concerns to the glacial extent outside the Zêzere valley. In the mid-1990’s, Gonçalo Vieira continued Daveau’s research and in the framework of a doctoral dissertation, using GIS, aerial photography, digital high resolution orthophotos and sedimentological analysis, supported by field work, presented the current view of the Estrela glaciation (Fig. 10). After the works of Vieira [2004, 2008), research on the glaciation has been more sporadic and deeply affected by research funding shortage. The implementation of the Estrela UGGp has resulted in increased research in the Estrela, with several recent publications and projects (Nieuwendam *et al.*, 2020; Santos *et al.*, 2020; Vieira *et al.*, 2020, 2021; Vieira and Woronko, 2021; Raab *et al.*, 2022).

b) Characteristics of the glaciation

Contrary to other mountains in Portugal, such as the Gerês and Peneda, where the glaciation generated controversies that lasted for decades (Ferreira, 1993), the glaciation of the Serra da Estrela shows widespread clear glacial geoheritage, of high scenic, pedagogical and scientific significance. For example, the remarkable U-shaped Zêzere valley has been frequently used in national and international scientific publications and is a text book example of a glacial trough.

The glaciation style of the Estrela is a result of both: i. its geographical setting in the western margin of Iberia, being the first mountain to affect the inland movement of the moist Atlantic air masses, but also, ii. of the altitude of the plateau between 1400 and ~2000 m. This altitudinal range, just above the paleo-equilibrium line altitude (ELA) of ~1650 m for the last maximum glacial extent, was perfect for the development of the Late Pleistocene glaciers (Vieira, 2008). The western plateau was especially significant for the glaciation and very sensitive to snow accumulation (as it is today) and hence to glacial inception. This is because once the ELA descends below the plateau surface, a very large accumulation area develops, providing enough ice mass for an ice-field to form. Since several valleys radiate from the plateau, conditions existed for ice streams to channel into valley glaciers (e.g. Zêzere, Alforfa, Alvoco, Loriga, Caniça and Covão do Urso).

However, the plateau also induces a large sensitivity for glacial retreat. A decrease in winter precipitation or an increase in summer ablation, with a resulting increase in the ELA, show rapid impacts in glacier mass balance, inducing the fast starvation of the valley glaciers and of the plateau ice-field. Hence, the Estrela has functioned in the

Pleistocene cold phases has a perfect « barometer » for climate variability in Western Iberia. On the contrary, if it would be a ridge style mountain (as most Alpine and Iberian mountains), it wouldn't show this behaviour that makes it unique.

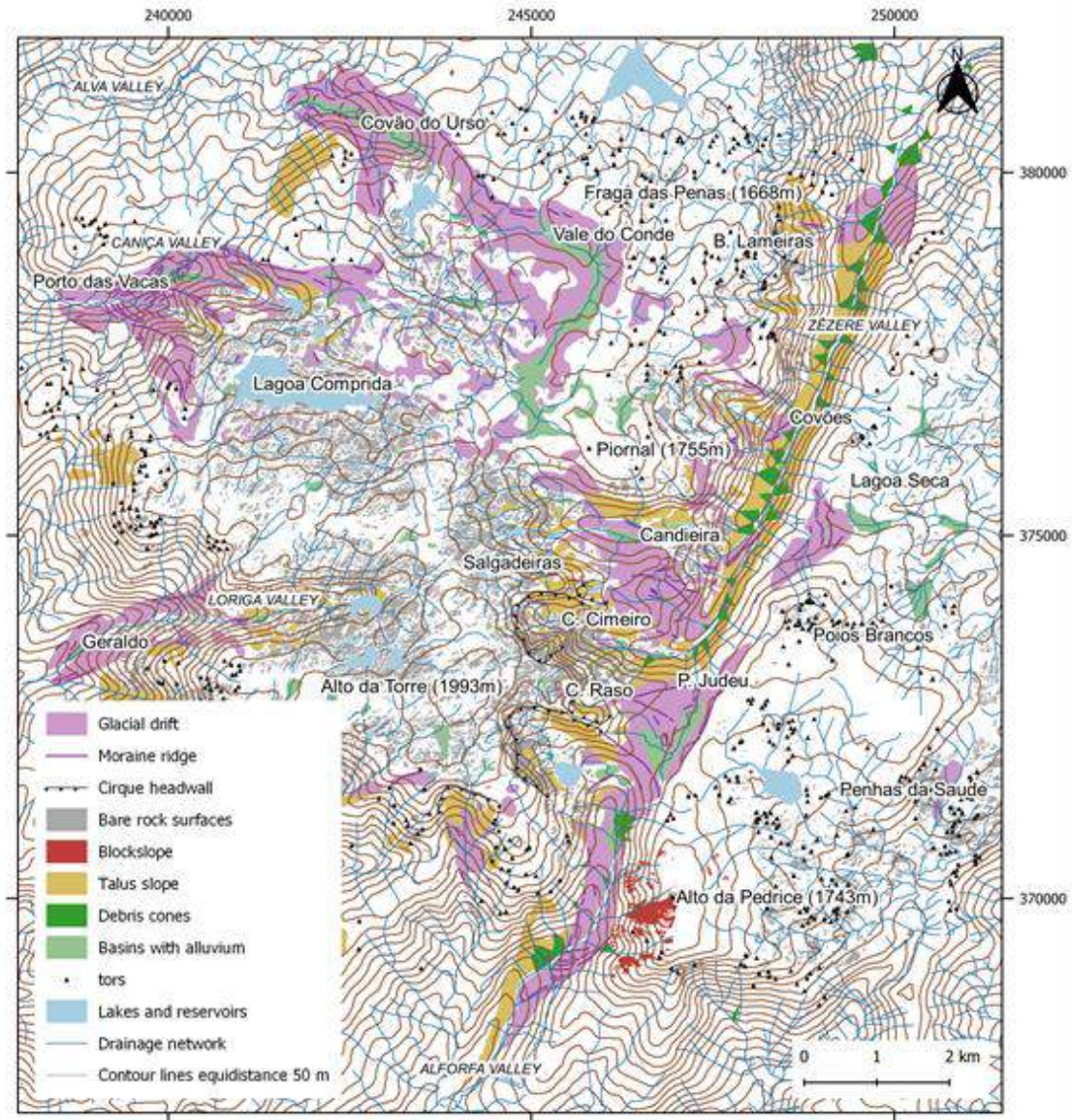


Figure 10. Main features of the glacial and periglacial geomorphology of the Serra da Estrela (after Vieira, 2004).

The Last Maximum of the Glaciation of the Serra da Estrela (LMGSE) was initially dated using thermoluminescence of fluvio-glacial sediments from the Lagoa Seca at ~30 ka BP (Fig. 11, Vieira, 2004). More recent cosmogenic isotope exposure dating from moraine boulders at the same site, support a similar age (Vieira *et al.*, 2021). This shows that the LMGSE pre-dates the LGM, a fact also supported by glacial evidence from southwest Europe and Iberia, showing that the LGM was probably cold and dry in Iberia, thus generating glacier recession.



Figure 11. The Lagoa Seca intermoraine basin and moraine ridges.

At the LMGSE, the western plateau of the Estrela had a plateau ice-field with several valley glaciers, from which the Zêzere glacier, ending close to the village of Manteigas, was the longest, with 11.3 km. The ice-field and glaciers were 66 km², with about 90 m ice thickness at the Alto da Torre and with ice thickness reaching 340 m at the Zêzere glacier (Vieira, 2008).

Glaciers left clear erosional marks in the extensive bare granite outcrops of the western plateau and valley heads, originating diverse glacial landforms, such as roches moutonnées, polished surfaces, grooves and striations (e.g. Salgadeiras and Lagoa Comprida). The contact zones between the western plateau and the main glacial valleys are marked by steep and deep cirques, especially in the eastern side, where snow accumulation was favoured by the prevailing west-winds. The best examples, are the Covão do Ferro and Covão Cimeiro, which are over 1 km wide, 240 to 290 m deep.

The glacial valleys of the Estrela show steep slopes and frequently U-shape cross-section, with the most typical being the Zêzere valley. Overdeepenings occur especially above the paleo-ELA and are infilled by post-glacial deposits that are a mixture of moraine boulders, rockfalls and sandy-gravels washed from the slope taluses. Organic sediments from overdeepenings in the plateau and at Charco da Candieira enabled the paleoenvironmental reconstruction since 14.8 ka BP. Peaks rising above the glacier surface where the ice-field drained into the Zêzere and Alforfa valleys, with nunataks at the Cântaros (pots) Gordo (fat), Raso (flat) and Magro (thin) and Piornal.

Moraines are widespread in the Estrela UGGp, occurring both along the glacial valleys and in several sectors of the western plateau (Lagoa Comprida and Vale do Conde), away from the dispersion centres of the ice-field. Most moraines are composed of large boulders (1 to over 5 m), lying on a coarse sandy-gravelly-bouldery deformation till. Most moraines show the effects of post-glacial runoff that eroded fines, sands and gravels.

Four types of moraines occur in the Estrela UGGp: i. lateral moraines, present along the larger valleys, with the best examples at Covão do Urso (4 km long), Covão Grande and Nave de Santo António, ii. Latero-frontal moraines, close to the terminus of the main valley glaciers (e.g. Manteigas and Alforfa), iii. Recessional moraine groups, present in most valleys as a series of frontal moraines, forming sets of up to 12 ridges (Caniça, Nave Travessa, Alforfa, Loriga and Lagoa Seca), iv. Marginal moraine complexes (Vale do Conde and Teleférico moraine at Nave de Santo António), and v. Sparse moraine covers, normally below 1650 m and without ridges (e.g. Lagoa Comprida, Azimbres, Vale do Conde).

Till exposures occur at the Estrela UGGp, but due to the mountain setting, limited number of outcrops and fast shrub growth, most are not easily to observe. Key outcrops such as the Cerro Rebolado flow till at the northern margin of the plateau ice-field, the Alforfa lodgement and flow tills, and the Lagoa Seca lodgement and flow tills, are excellent examples of mountain tills and of the wet-based dynamics of the glacial environment. The analysis of quartz grains from the later provided evidence that subglacial transport and erosion mobilised grains that had previously evolved in the regolith, controlled by chemical weathering (Vieira, 2004). This supports Daveau's interpretation for the saprolitic origin of the very large rounded boulders, so typical of the Estrela moraines. Such saprolites are still visible at some sites outside the glaciated area, even in the highest parts of the mountain.

Kame terraces that allow to infer the paleo valley glacier position are present in many valleys and their relation to human occupation is noteworthy, being typically used for agriculture, due to their gentle sloping surfaces, soil development and water availability.

Fluvioglacial terraces occur in Manteigas, Unhais da Serra, Alvoco and in the Alva valleys, being formed by decametric sub-rounded boulders, gravels and coarse sands, poorly stratified and forming terraces (used for agriculture and more recently to urban settlements) a few meters above the current valley floor. Three terrace generations occur in Manteigas, with a post-glacial fluvial incision of about 6 to 8 m. Fluvioglacial deposits in filling the intermorainic depression of Lagoa Seca allowed to identify the age of the last maximum glacial extent in the Estrela (Vieira, 2004).

But the glacial geoheritage of the Estrela UGGp is not limited to the LMGSE, as evidence shows ages from an earlier glacial (Vieira, 2004, 2021). At Penhas da Saúde the micromorphological analysis of a diamicton showed the presence of probably subglacial deformation microstructures. The lack of clear landforms associated to glacial erosion in the area, suggest a pre-LMGSE age for the deposit. At the Cântaro Raso and Barroca das Lameiras, linear accumulations of boulders without matrix have been interpreted as possible earlier moraines. At the Lagoa Seca, the most external of five moraine ridges, showing deeper weathering pits than the three internal ridges, was recently dated using ^{36}Cl , providing minimum ages of 138.9 ± 14.1 to 146.7 ± 17.8 ka, supporting a pre-Weichselian age (Vieira *et al.*, 2021).

c) Chronology

The following main stages in the Estrela glaciation may be (Vieira, 2004; Vieira *et al.*, 2021):

- The **external stage**, oldest and pre-Weichselian (c. 140 ka), without clear glacial landforms, but identified based on the presence of sectors of large boulders interpreted as moraines, on the till of Penhas da Saúde and with absolute age datings.
- The **Last Maximum of the Serra da Estrela Glaciation (LMGSE)**, corresponding to the maximum extent of the glaciers, as seen in well-preserved moraine features and kame terraces (c. 30 ka BP).
- The **Internal stage 1**, marked by numerous moraine ridge complexes in the valleys in positions inside the LMGSE maximum.
- The **Internal stage 2**, identifiable at some latero-frontal moraines in the Zêzere and Alforfa valleys.
- The **deglaciation of the plateau** at the Bølling-Allerød Interstadial (14.6–12.9 ka).

Contrary to other mountains in Iberia, at the Estrela UGGp moraines close to or inside the glacial cirques are very scarce. This fact should be related to the style of deglaciation associated to the plateau ice-field, which given a rise in the ELA would have quickly been affected by an ablation regime in a large area, inducing ice-stagnation in the valleys and areolar melting resulting in abandoned bodies of dead-ice. These condition would have seen limited erosion in the cirques and consequently, no significant moraine deposits.

d) The Periglaciation

The significance of relict periglacial phenomena in the Estrela UGGp area was reported for the first time by Daveau (1973, 1978) that described the Pedrice blockslope, stratified slope deposits and screes in the Zêzere Valley and showed that frost action played a role in Late Pleistocene morphogenesis. Since most phenomena occurred outside the glaciated area and very few inside it, they should be, at least, synchronous to the LMGSE or older. More recently, Vieira (2004) presented a systematic survey and analysis of the periglacial deposits and landforms and identified a wider relict periglacial activity in Estrela, with block fields, stone-banked solifluction lobes, head-type, stratified slope deposits and debris-flow deposits. Traces of permafrost action, possibly of Late Pleistocene age are present in lamellar structures in slope deposits above 1200 m (Vieira, 2004; Nieuwendam *et al.*, 2019; Vieira and Nieuwendam, 2020), together with other features, such as a bouldery accumulation interpreted as a paleorockglacier at Alforfa.

1.10. Postglacial evolution

The Charco da Candieira deposits from the Candieira valley at 1409 m offer a good insight into the paleoenvironmental evolution of the Estrela UGGp since about 14.8 ka BP (Van den Brink and Janssen, 1985; Vand der Knaap and Van Leeuwen, 1997):

- At 14.8 ka BP glaciers were still present at the upper areas of the catchment.
- Until the Younger Dryas, climate conditions varied, with altitudinal shifting of the periglacial zone, which was more active in the Bølling and in the Younger Dryas, with open grassland formations. Between both these stadials, in warmer and wetter conditions, open woodlands occupied the valleys.
- At the onset of the Holocene, open woodlands expanded in the mountain and Quercus forests colonized the lower valleys.
- Around 7.6 ka BP Cerealia pollen increased and the forest became less dense. At 5.6 ka BP humans became the main driving force on forest dynamics.
- At 3.3 ka BP large-scale deforestation took place, first at 1400 m, climbing to 1750 m at 2.8 ka BP.
- Subsequent phases reflected successive waves of deforestation, especially at 0.8 and 0.6 ka BP, culminating at 0.34 BP with increased soil erosion.

2. Introduction to the itinerary and description of the stops

The three-day field trip will allow for a very good overview of the main highlights of the ~2,200 km² of the Estrela Geopark. It will include visits to the main geosites, spreading over glacial, periglacial, granite weathering, fluvial, hydrogeological, petrological and tectonic themes, as well as a discussion of several issues related to the objectives and management of a UNESCO Global Geopark. We will highlight on the scientific value of the geosites, but will promote the links with cultural aspects of many of them. We will emphasize on how a rich geological heritage can be the basis for promoting sustainable development in a territory of a low-density and ageing population, suffering from complex socio-economic and environmental issues. The field trip will include 2 days based on bus travelling around the Geopark with short walks and 1 full-day of hiking in the plateau (easy but long). For those not willing to do the hike, an alternate program may be prepared.

In Day 1 we will surround the Serra da Estrela from the west and will enter it from the northwest, crossing the intramontane valleys carved in metasediments. The day will be dedicated to an introduction to the geological and geomorphological setting of the range, and to the links between the local communities and the geological heritage. We will discuss the implementation of the Estrela UNESCO Global Geopark and practical issues and challenges associated to its management.

Days 2 and 3 will be dedicated to the core of the Serra da Estrela and will focus on exploring the glacial heritage of the mountain, while also discussing the relict periglacial geomorphology and contemporary landscape dynamics. For this, in day 2, we will make a hike crossing the western plateau, between Penhas Douradas and Lagoa Comprida. In day 3, we will do a short hike in the Zêzere valley and will visit by bus several geosites of high scientific relevance, which contributed to the implementation of the geopark.

Day 1

Stop 1. Folgoso

Regional geomorphological framework, quartz dike.

Folgoso is a mountain village from the municipality of Gouveia. The stop allows for a first insight into the contact between the Mondego Platform and the western fault scarp of the Serra da Estrela. A massive quartz dike with a thickness of about 10 m was the chosen location for the construction of the Folgoso castle (Fig. 12). Rising from the surrounding landscape, the dike is heavily mineralized in tin and wolfram, which were the cause of its mining in the 1940s and 1950s, with about 25 tons of wolframite and 8

of cassiterite extracted. Besides these, the dyke shows mineralizations of phosphates and sulphides, still evident in the greenish colour of the heaps.



Figure 12. Folgosinho castle atop the quartz dike.

Stop 2. Linhares da Beira

An introduction to the Estrela UNESCO Global Geopark

Built on a residual relief, the Historical Village of Linhares da Beira shows a unique architectural heritage, fruit of the legacy left by the civilizations that settled throughout the history (Fig. 13). Founded in medieval times, with foral granted in 1169 by D. Afonso Henriques, it lost this status with the liberal administrative reform, in 1855. Although the site has seen the settlement of pre-Roman peoples and there is written record of the passage of Romans, Visigoths and Muslims, the story of Linhares has its origin in the context of the Christian Reconquest. The buildings are a testimony to the use of geology by its inhabitants, with its granite constructions and medieval Castle implanted in the highest point of the residual relief. From the castle, the panorama offers views over the Mondego platform and the southern slope of the central Portuguese plateau.



Figure 13. Linhares da Beira castle.

Stop 3. Videmonte

Geological controls on landforms

Videmonte shows a clear connection between geology and the rural life of the people who live there, as testified by the houses, built in schist and granite, due to the proximity of the contact between these two rock types (Fig. 14). In the village, several traditional activities are still maintained, such as the use of the community oven to bake the tasty rye bread, with rye produced on the Videmonte plateau, with the help of the old irrigation system that was once used to distribute water through the village. Privileged by water and wind resources, the picturesque village of Videmonte also has a relevant historical and architectural heritage, such as the main church (São João Baptista Church) that was built in baroque style in the 17th century and the fountains dating from the 18th and 19th century.



Figure 14. The village of Videmonte.

Stop 4. Quinta da Taberna

Fluvial geomorphology, metasediments

The geology of Quinta da Taberna and its surroundings is characterized by the presence of metasedimentary rocks, with outcrops showing intercalations of schists and metagreywackes and microfold structures (Fig. 15). The landscape shows the typical traits of an intramontane fluvial valley, cut in metasedimentary rocks, with the linear interfluvial ridges and the meandering Mondego river. The small village provides for a glimpse into the traditional life in the mountain's interior, which prevailed until the 1970's and to the close linkage between human occupation of the mountain and geology. The future use of the Quinta da Taberna geosite as an interpretation centre and educational resource will be discussed.



Figure 15. Quinta da Taberna metasedimentary outcrops.

Day 2

Hike from Penhas Douradas to Lagoa Comprida (all day)

Granite landforms, moraines, glacial erosion, plateau ice-field

The hike will cross the western plateau of the Serra da Estrela from the non-glaciated area, in the Penhas Douradas/Vale de Rossim to the core of the glacial erosion area in the Lagoa Comprida (Fig. 16).

At Penhas Douradas (c. 1,500 m) the landforms are marked by the presence of the Seia granite, a coarse-grained porphyritic variant, which due to the stripping of the weathering mantle, generated a large number of granite landforms, such as boulders, tors and castle-koppjes. The Fragões das Penhas are an excellent example of the latter (Fig. 17).

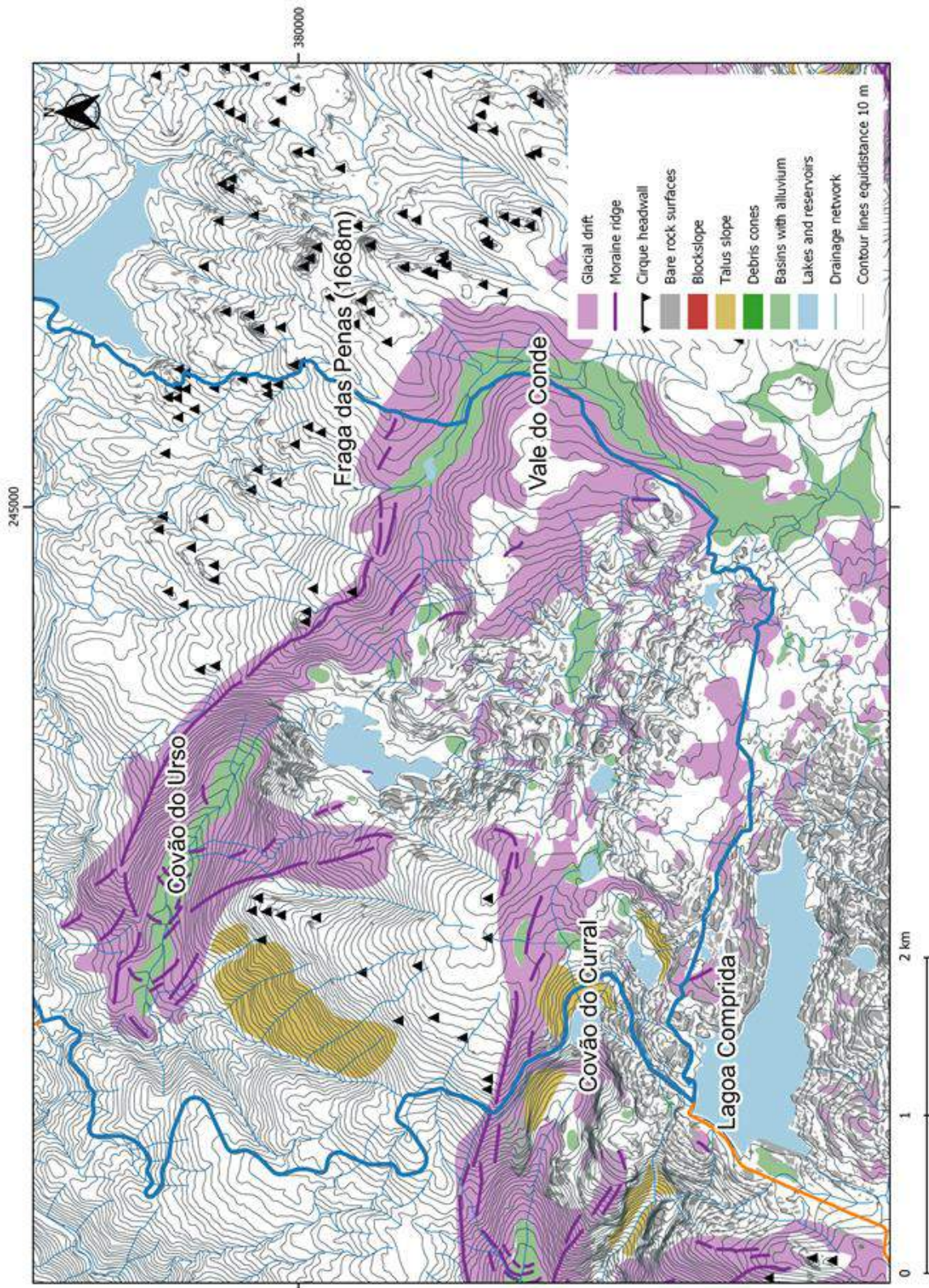


Figure 16. Main features of the geomorphology of the western plateau of the Serra da Estrela with the hike of Day 2 from P. Douradas to Lagoa Comprida (after by bus).



Figure 17. Moraine at Vale do Conde.

Stop 2. Sabugueiro/Covão do Urso Panorama

Glaciated vs non-glaciated landscape. Introduction to the Estrela glaciation. Lateral moraine of Covão do Urso and northwest limit of the plateau ice-field.

The viewpoint allows to analyse northwest sector of the plateau ice-field and the contrast between the Late Pleistocene glaciated and non-glaciated landscape. The stop is located in the non-glaciated area, where a typical granite weathering morphology prevails, with the widespread presence of boulders and tors in convex locations. Towards the southeast, the Covão do Urso valley drained the plateau ice-field, with a glacier flowing to close to the village of Sabugueiro. A 4 km long lateral moraine is visible in the north interfluvium of the valley, continuing up to the Vale do Conde in the plateau. Several lateral and frontal moraine ridges occur along the valley floor. This area is currently being mapped using drones and sampled for cosmogenic isotope exposure dating in a collaboration between the universities of Lisbon (G. Vieira) and Zurich (M. Egli).

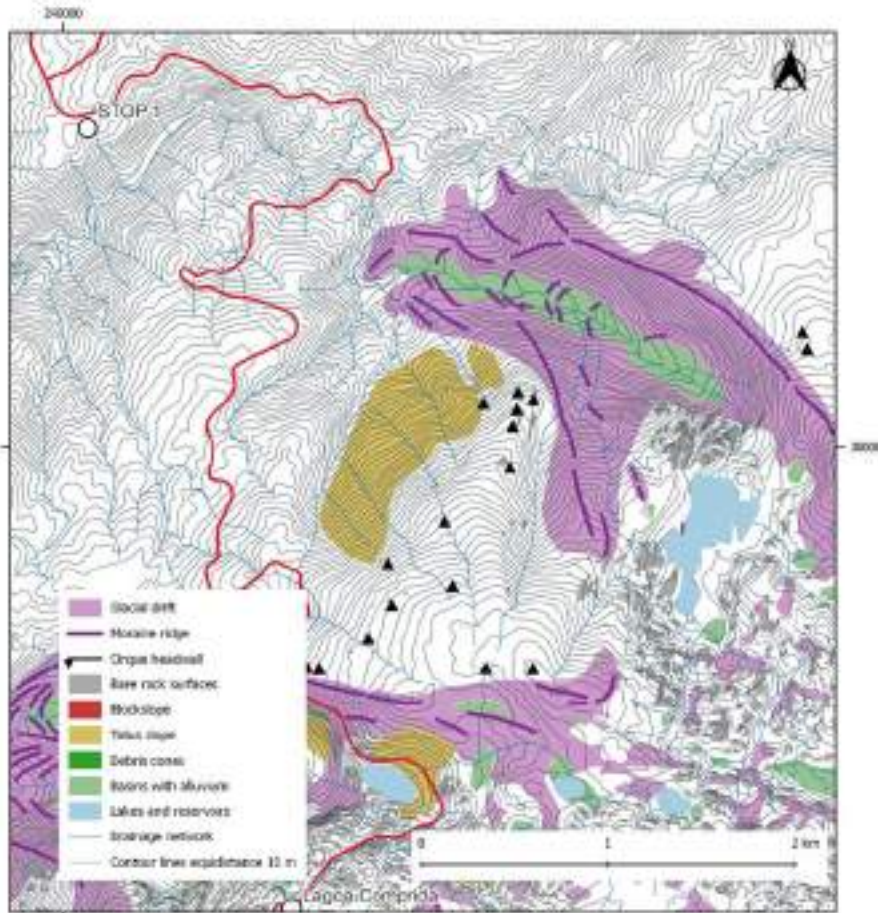


Figure 18. Main features of the glacial geomorphology of the Covão do Urso (adapted from Vieira 2004).

Day 3

Stop 1. Barroca d'Água – Zêzere valley (easy hike - 2h30)

The Barroca de Água stratified gravelly deposit shows a trough cross-bedding, revealing the evidence of debris flows (Fig. 19). The coarsest beds are open-work and constituted by polycrystalline centimetric very angular clasts of porphyritic granite of local origin. Thick massive beds of fine and coarse granite sands, with gravels prevail. Silty-sandy greyish lenses occur in some sectors and have been interpreted as reworked glacial silt. The deposit shows a convex surface morphology and develops linearly in the lower part of the slope, towards the valley floor and perpendicular to it. Smaller deposits of similar characteristics occur downstream and on the opposite site of the valley. Nieuwendam *et al.* (2020) studied the deposit's micromorphology and confirm the deposition by debris flow activity. Given it's linear morphology, debris flow genesis involving significant volumes of water and lack of any source gully upslope, the deposit was possibly formed in an ice-marginal position or in a subglacial setting under a dead-ice valley glacier (Bezembinder and Niessen, 1989; Vieira, 2004; Vieira and Nieuwendam, 2020).



Figure 19. The Barroca de Água cross-bedded gravelly deposit.

The Zêzere glacial valley is a perfect example of glacial erosion (Fig. 20). With a U-shaped cross-section profile for c. 9 km, between Covão da Ametade and the town of Manteigas, the valley presents in its upstream sector a succession of overdeepenings, riegels and hanging valleys, as well as several types of glacial, fluvioglacial and slope deposits. At the maximum of the last glaciation, the ice thickness reached 340 meters close to Covão da Albergaria, fed by the ice-field of the Torre Plateau. A little further downstream, the Zêzere valley was also fed by glaciers from the hanging valleys of Candieira and Covões. The shape of the present valley and its rectilinear character are a result of erosion processes favoured by the Bragança-Vilariça-Manteigas-Unhais da Serra tectonic lineament.



Figure 20. Zêzere glacial valley.

Stop 2. Covão da Ametade

U-shaped glacial valleys, glacial overdeepening, riegels.

Generally, in the Estrela, the so-called “covões” correspond to glacial overdeepenings, which are normally infilled by post-glacial deposition. The Covão da Ametade provides a good view towards the Cântaro Magro and marks the contrast between the zones of glacial erosion and deposition in the upper catchment of the Zêzere valley (Fig. 21).

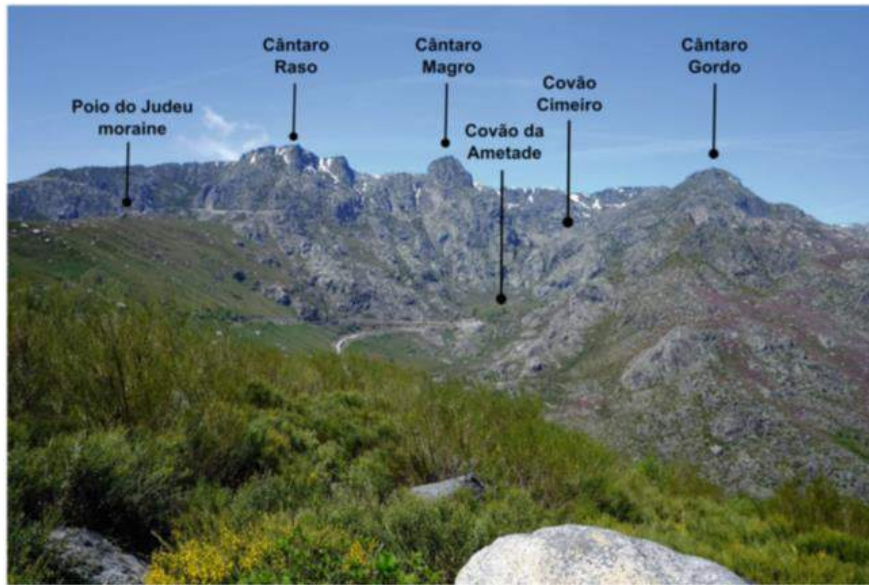


Figure 21. Zêzere glacial valley.

Stop 3. Piornos

Panorama to Nave de Santo António. Glacial cirques. Moraines. Problems of pre-Weichselian glaciations.

Piornos offers a good panorama towards the eastern margin of the Torre plateau, allowing for the observation of the Covão do Ferro glacial cirque, the three paleonunataks formed by Cântaro Raso, Cântaro Magro and Cântaro Gordo (Figs. 21 and 22), and to the complex moraine infill of the Nave de Santo António. It also allows for analyzing the contrasts of the landforms between the western (Torre) and eastern (Penhas da Saúde) plateaus, as well as an understanding of the tectonic significance of the Alforfa and Zêzere valleys.

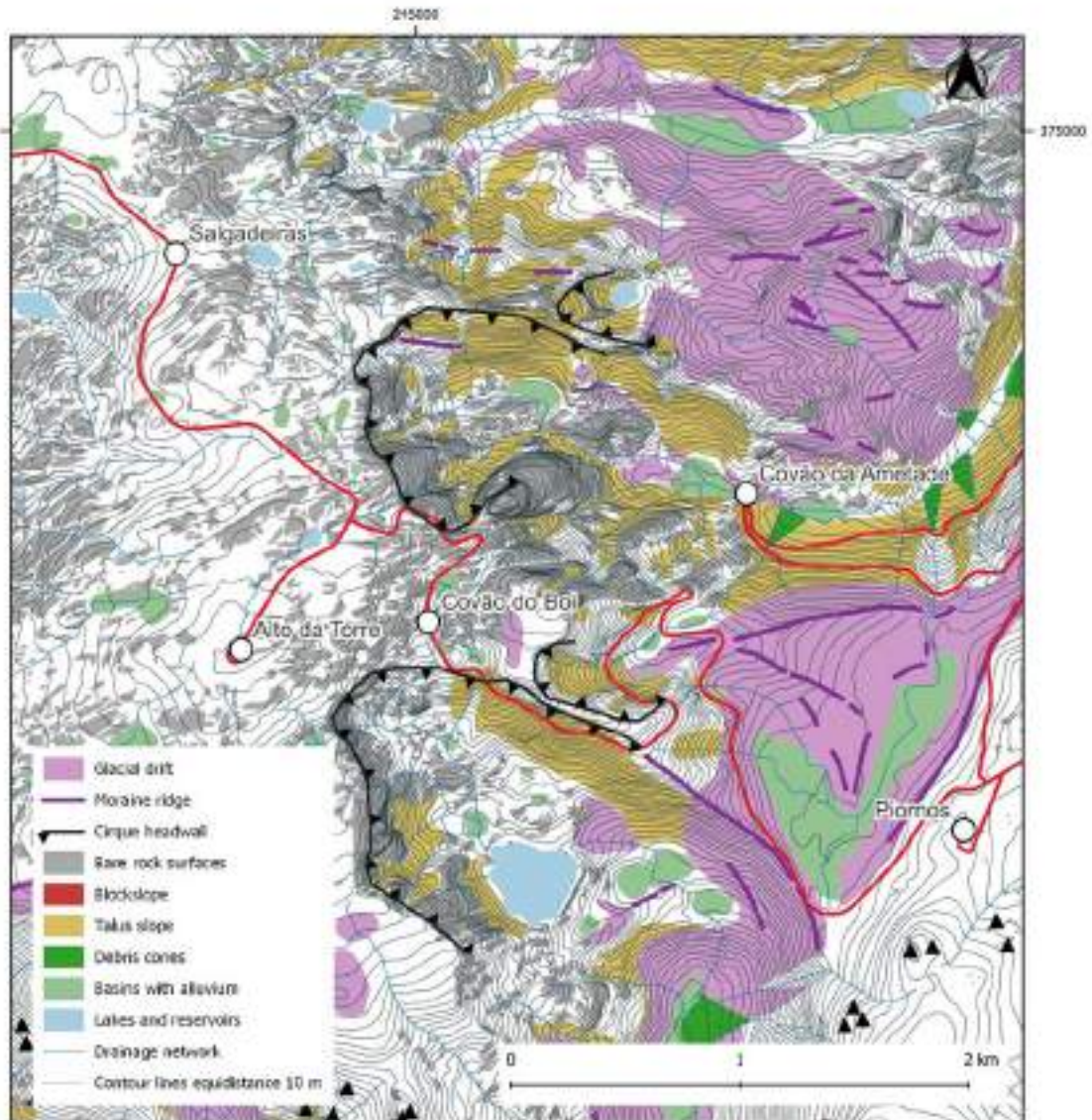


Figure 22. Main features of the glacial geomorphology of the Alto da Torre and its surroundings (adapted from Vieira 2004).

Stop 4. Covão do Boi

Granite columns, glacial and post-glacial erosion, glacial evolution of the Zêzere valley, the Lagoa Seca col, Pre-Weichselian glacial evidence.

At 1,840 m a.s.l., between the Alto da Torre, the glacial cirque of Covão do Ferro, the Zêzere glacial valley and the Cântaro Raso, a small, but very relevant col shows up - the Covão do Boi (Fig. 23). In this remarkable geosite, we find a set of granite columns, with diameters of 2 to 5 m and between 4 and 8 m in height, constituting a rare set of landforms. Before they surfaced, the granite columns were shaped under the surface due to the deep weathering of the granite, along a dense orthogonal joint network, that formed a thick weathering mantle. During the last glaciation the col was razed by glacial erosion that removed part of the weathering mantle and cut the top of fresh granite

corestones. Following glacial retreat, water erosion continued the removal of the weathering mantle and the granite columns started to form at the surface. These granite columns are locally called cheese-piles, because they resemble, in a nutshell, the form of a stack of typical Serra da Estrela cheeses. The granite columns have been sampled for cosmogenic isotope exposure dating in 2020, confirming the postglacial age of the columns, and a manuscript is currently in preparation by Raab and colleagues.



Figure 23. Granite columns of Covão do Boi.

Stop 5. Alto da Torre

Elevated planation surfaces. Panorama to the Central Iberian Cordillera.

The Western Plateau with an elevation rising from about 1,500 m in the north, at Penhas Douradas, to 1993 m at Alto da Torre, is the highest summit in mainland Portugal (Fig. 24). The area is the highest remnant of the uplifted Paleogene planation surface, which has been stripped by erosion and still preserves wide flat areas, interrupted by several steps. These are controlled by tectonics, as well as lithology. Overall in the Estrela, the differences between the metasedimentary (schists, greywackes, shales) and the granites, prevail. Wide plateaus and rectilinear valleys have developed in the latter, while the former have generated narrow linear interfluves, deeply dissected by v-shaped and irregular valley, with a dense river network and meanders. In the plateaus, the different granite-types, together with tectonics, gave origin to the different in the landscape (Migon and Vieira, 2014).



Figure 24. The Alto da Torre plateau viewed towards the north.

Stop 6. Salgadeiras – Lagoas do Covão da Clareza

Plateau ice-field, glacial erosion, hanging valleys, overdeepenings, deglaciation, Holocene evolution of the Serra da Estrela.

The Salgadeiras - Lagoas do Covão da Clareza area at c. 1800 m a.s.l. shows a typical landscape of glacial erosion in the plateau, resembling a Scandinavian fjell. The area shows extensively glacially scoured granite outcrops, marked by overdeepenings with numerous small ponds and lakes, which provide valuable sedimentary archives of the postglacial evolution of the Estrela. The area is also part of the biogenetic reserve and part of the Natura 2000 network and protected as a RAMSAR site.

The deglaciation of the Salgadeiras has occurred after 14.2 ka (Vieira *et al.* 2021), with glacierets possibly surviving in niches for longer. New rock samples from polished rock outcrops and a small moraine in the Salgadeiras are currently under investigation for cosmogenic isotope exposure dating (Vieira and Egli).

The Holocene evolution of the Serra da Estrela has been studied from a 14 m core from the Charco da Candieira at 1,410 m a.s.l. with the reconstruction of the paleoenvironmental conditions after c. 14.8 ka (Van der Knaap and Van Leeuwen, 1997). More recently, within the project HOLMODRIVE, an international team lead by the University of Lisbon, has been analyzing new sediment cores from Lagoa do Peixão between the Charco da Candieira and Salgadeiras, at c. 1,660 m a.s.l.

References

- AGE (2017). Aspiring Geopark Estrela Application Dossier for UNESCO Global Geopark. Associação Geopark Estrela, Portugal.
- Azevedo, M.R; Valle Aguado, B. (2006). Origem e Instalação de Granitóides Variscos na Zona Centro-Ibérica. In: Dias R, Araújo A, Terrinha P, Kullberg J.C, (Coord.), Geologia de Portugal no Contexto da Ibéria. 107-122p.
- Bezembinder L, Niessen A (1989) Palynologisch en geomorfologisch onderzoek langs de bovenloop van de Rio Zêzere, Serra da Estrela. Unpublished report. Laboratory of Palaeobotany and Palynology, Utrecht, The Netherlands.
- Cabral, F.A.V.P. (1884). Vestígios glaciários na Serra da Estrela. Revista de Obras Públicas e Minas, Lisboa. 435-459p.
- Cabral, J. (2012). Neotectonics of mainland Portugal: state of the art and future perspectives. Neotectónica de Portugal peninsular: estado de la cuestión y perspectivas de futuro. Journal of Iberian Geology 38 (1). 71-84p.
- Capdevila, R.; Corretge, G.; Floor, P. (1973). Les granitoides varisques de la Meseta Iberique. Bull. Soc. Geol. France. 209-228p.
- Capdevila, R.; Floor, P. (1970). Les differents types de granites hercyniens et leur distribution dans le nord-ouest de l'Espagne. Bol. Geol. Miner. Espana 81. 215-225p.
- Carrington da Costa, M. (1950). Notícia sobre uma carta geológica do Buçaco de Nery Delgado. Comunicações dos Serviços Geológicos de Portugal. 1-28p.
- Cunha P.P.; Pena dos Reis, R. (1995). Cretaceous sedimentary and tectonic evolution of the northern sector of the Lusitanian Basin (Portugal). Cretaceous Research 16. 155-170p.
- Cunha, P.P.; Pimentel, N.; Pereira, D.I. (2000). Sedimentary and tectonic signature of the betie compresión clímax in Portugal: the late Vallesian-Turolian sedimentary discontinuity. Ciências da Terra 14. Univ. Nova Lisboa. 61-72p.
- Daveau, S. (1969). Structure et relief de la Serra da Estrela. Finisterra 4(7). 33-197p.
- Daveau, S. (1971). La glaciation de la Serra da Estrela. Finisterra. Revista Portuguesa de Geografia 6 (11). 5-40p.
- Daveau, S. (1973). Quelques exemples d'évolution quaternaire des versants au Portugal. Finisterra, Lisboa. 5-45p.
- Daveau, S. (1978). Le périglaciaire d'altitude au Portugal. Colloque sur le périglaciaire d'altitude du domaine méditerranéen et abords, Strasbourg.
- De Vicente, G.; Cloetingh, S.; Van Wees, J.D.; Cunha, P.P. (2011). Tectonic classification of Cenozoic Iberian foreland basins. Tectonophysics 502(1-2). 38-61p.
- De Vicente, G.; Vegas, R.; Muñoz-Martín, A.; Silva, P.G.; Andriessen, P.; Cloetingh, S.; González-Casado, J.M.; Van Wees, J.D.; Álvarez, J.; Carbó, A.; Olaiz, A. (2007).

- Cenozoic thick-skinned and topography evolution of the Spanish Central System. *Glob. Planet. Change* 58. 335-381p.
- De Vicente, G.; Vegas, R. (2009). Large-scale distributed deformation controlled topography along the western Africa–Eurasia limit: tectonic constraints. *Tectonophysics* 474. 124-143p.
- Dias, R.; Ribeiro A. (2013). O Varisco do sector norte de Portugal. In: Dias R, Araújo A, Terrinha P, Kullberg J.C, (Eds). *Geologia de Portugal*, vol1, Escolar Edit. 59-71p.
- Dinis, J.; Rey, J.; Cunha, P.P.; Callapez, P.; Pena dos Reis, R. (2008). Stratigraphy and allogenic controls of the western Portugal Cretaceous: an updated synthesis. *Cretaceous Research* 29. 772-780p.
- Feio, M. (1952). A evolução do relevo do baixo Alentejo e algarve. *Com. ser. geológicos Portugal* 32, Lisboa.
- Ferreira A.B. (1991). Neotectonics in northern Portugal. A geomorphological approach. *Geomorph. N.F, Berlim, Estugarda, Suppl. BD.82.* 73-85p.
- Ferreira A.B. (1993). Manifestações geomorfológicas glaciárias e periglaciárias em Portugal. In: Carvalho G.S, Ferreira A.B, Senna-Martínez J.C, (eds.). *O Quaternário em Portugal: Balanço e perspectivas.* A.P.E.Q., Ed. Colibri. 75-84p.
- Ferreira A.B. (2005). *O Ambiente Físico. Vol1. Geografia de Portugal*, (coord.) Medeiros C.A, Lisboa, Círculo de Leitores. 495p.
- Ferreira, A.B. (1978). Planaltos e Montanhas da Beira, estudo de Geomorfologia. *Mem. Centro Estudos Geográficos* 4. 374p.
- Ferreira, N.; Iglésias, M.; Noronha, F.; Pereira, E.; Ribeiro, A.; Ribeiro, M.L. (1987). Granitóides da Zona Centro Ibérica e seu enquadramento geodinâmico. In: Bea F, Carnicero A, Gonzalo J, Lopez Plaza M, Rodriguez Alonso M, (Eds.) *Geologia de los Granitóides y Rocas asociadas del Macizo Hespérico*, Rueda, Madrid. 37-51p.
- Ferreira, N.; Vieira, G. (1999). Guia geológico e geomorfológico do Parque Natural da Serra da Estrela. PNSE-ICN, Ministério da Economia, Inst. Geológico e Mineiro. 111p.
- Fleury, E. (1916). Sur les anciennes glaciations de la Serra d'Estrela. *Paris*, 162. 599-601p.
- Julivert, M., Fontbote J., Ribeiro, A., Conde, L. (1974). Memória explicativa del Mapa Tectónico de la Peninsula Iberica y Baleares, Escala 1:1000000. Instituto Geológico y Minero de España, Madrid.
- Lautensach, H. (1929). Eiszeitstudien in der Serra da Estrela (Portugal). *Zeitschrift für Gletcherkunde* 17. 324-369p.
- Martínez-Catalán J.R, Aller J, Alonso J.L, Bastida F. (2009). The Iberian Variscan orogen. In: García-Cortés A, (Ed.) *Spanish Geological Frameworks and Geosites - An Approach to Spanish Geological Heritage of International Relevance.* IGME.
- Martín-González, F. (2009). Cenozoic tectonic activity in a Variscan basement: evidence from geomorphological markers and structural mapping (NW Iberian Massif). *Geomorphology* 107. 210-225p.

- Martin-Serrano, A. (1988). El relieve de la region occidental zamorana. La evolucion morfológica de um borde del macizo hespérico. Inst. Estudios Zamoranos Florien de Ocampo, Zamora. 311p.
- Meireles, C.; Castro, P.; Ferreira, N. (2014). On the presence of cadomian angular unconformity in Beiras Group (Central Portugal): cartographic, lithostratigraphic and structural evidences. *Comunicações Geológicas* 101, Esp. I. 495-498p.
- Migoñ, P.; Vieira, G. (2014). Granite geomorphology and its geological controls, Serra da Estrela, Portugal. *Geomorphology* 226. 1–14p.
- Neiva A.M.R, Teixeira R.J.S, Lima S.M, Silva P.B. (2013). Idade, Origem e Protólitos de granitos variscos de três áreas portuguesas, Academia das Ciências de Lisboa. 13p.
- Neiva, A.M.R.; Williams, I.S.; Ramos, J.M.F.; Gomes, M.E.P.; Silva, M.M.V.G.; Antunes, I.M.H.R. (2009). Geochemical and isotopic constraints on the petrogenesis of Early Ordovician granodiorite and Variscan two-mica granites from the Gouveia area, central Portugal. *Lithos* 11. 186-202p.
- Nieuwendam, A., Vieira, G.; Woronko, B., Schaefer, C., & Johansson, M. (2020). Reconstructing cold climate paleoenvironments from micromorphological analysis of relict slope deposits (Serra da Estrela, Central Portugal). *Permafrost and Periglacial Processes*.
- Oliveira J.T, Pereira E, Ramalho M, Antunes M.T, Monteiro J.H. (1992). Noticia Explicativa da Carta Geológica de Portugal, escala 1/500000, Serviços Geológicos de Portugal.
- Pais, J.; Cunha, P.P.; Pereira, D.; Legoinha, P.; Dias, R.; Moura, D., Silveira A.B, Kullberg J.C, González-Delgado J.A. (2012). The Paleogene and Neogene of Western Iberia (Portugal). A Cenozoic record in the European Atlantic domain. Springer, Heidelberg. 156p.
- Raab G., Dollenmeier W., Tikhomirov D., Vieira G., Migoñ P., Ketterer M.E., Christl M., Stutz J., Egli M. (2022). Contrasting soil dynamics in a formerly glaciated and non-glaciated Mediterranean mountain plateau (Serra da Estrela, Portugal). *Catena*. <https://doi.org/10.1016/j.catena.2022.106314>
- Ribeiro, A. (2013). A Evolução Geodinâmica de Portugal; os ciclos ante-mesozóicos. In: Dias R, Araújo A, Terrinha P, Kullberg J.C, (Eds.). *Geologia de Portugal no contexto da Ibéria*. Univ. Évora. 15-57p.
- Ribeiro, A.; Kullberg, M.C.; Kullberg, J.C.; Manuppella, G.; Phipps, S. (1990). A review of Alpine tectonics in Portugal: Foreland detachment in basement and cover rocks. *Tectonophysics* 184. 357-366p.
- Ribeiro, O. (1949). Le Portugal Central (livret-guide de l'excursion C). XVI Cong. Inter. Géogr. Lisboa.
- Ribeiro, O. (1954). Estrutura e Relevo da Serra da Estrela. *Bol. Real Soc. Esp. Hist. Nat.* (homenaje Hernández-Pacheco), Madrid. 549-566p.
- Rockwell, T.; Fonseca, J.; Madden, C.; Dawson, T.; Owen, L.A.; Vilanova, S.; Figueiredo P. (2009). Palaeoseismology of the Vilarica segment of the Manteigas-Bragança Fault in northeastern Portugal. In: Reicherter K, Michetti A.M, Silva P.G, (eds.) *Palaeoseismology: Historical and Prehistorical Records of Earthquake Ground*

- Effects for Seismic Hazard Assessment. The Geological Society London, Special Publications 316. 237-258p.
- Sant’Ovaia, H.; Martins, H.C.B.; Noronha, F. (2013). Oxidized and reduced Portuguese Hercynian granites associated with W and Sn hydrothermal mineralizations. *Comunicações Geológicas*, 100(1). 33-39p.
- Santos, J.B.; Vieira, G.; Santos-González, J.; Woronko, B.; Redondo-Vega, J.M. (2020). Macrofabric and grain size analysis of moraines and other till deposits in the Serra da Estrela Mountains, central Portugal, *Physical Geography*, <https://doi.org/10.1080/02723646.2020.1838136>
- Santos, R.M.P.; Tassinari, C.C.G. (2012). Different lead sources in an abandoned uranium mine (Urgeiriça, Central Portugal) and its environment impact, isotopic evidence. *Geochemistry: Exploration, Environment Analysis* 12. 241-252p.
- Sousa M.B, Sequeira A.J.D. (1987). Carta Geológica de Portugal à escala 1/50000, Folha 10D – Alijó. Serv. Geol. Portugal, Lisboa.
- Teixeira, C. (1955). Notas sobre a Geologia de Portugal: O Complexo Xisto-Grauváquico ante-Ordovícico. Porto (Eds.) Lisboa. 50p.
- Van Den Brink, L.M.; Janssen, C.R. (1985). The effect of human activities during cultural phases on the development of montane vegetation in the Serra da Estrela, Portugal. *Review of Palaeobotany and Palinology* 44. 193-205p.
- Van der Knaap, W.O.; Van Leeuwen, J.F.N. (1997). Holocene vegetation successions, altitudinal vegetation zonation, and climatic change in the Serra da Estrela. *Review of Palaeobotany and Palinology*, 97. 239-285p.
- Vieira, G. (2004). Geomorfologia dos planaltos e altos vales da Serra da Estrela. Ambientes frios do Plistocénico Superior e dinâmica actual. PhD in Geography. University of Lisbon, 724p.
- Vieira, G. (2008). Combined numerical and geomorphological reconstruction of the Serra da Estrela plateau ice-field, Portugal. *Geomorphology* 97. 190-207p.
- Vieira, G.; de Castro, E.; Gomes, H.; Loureiro, F.; Fernandes, M.; Patrocínio, F.; Firmino, G.; Forte, J.P. (2020). The Estrela Geopark—From planation surfaces to glacial erosion. in Vieira G., Zêzere, J.L. & Mora, C. (Eds.), *Landforms and Landscapes of Portugal*, Springer: 341-357.
- Vieira, G.; Nieuwendam, A. (2020). Glacial and Periglacial landscapes of the Serra da Estrela. in Vieira G., Zêzere, J.L. & Mora, C. (Eds.), *Landforms and Landscapes of Portugal*, Springer: 185-198.
- Vieira, G.; Palacios, D.; Andrés, N.; Mora, C.; Vázquez Selem, L.; Woronko, B.; Soncco, C.; Úbeda, J.; Go-yanes, G. (2021). Penultimate Glacial Cycle glacier extent in the Iberian Peninsula: new evidence from the Serra da Estrela (Central System, Portugal), *Geomorphology*, 388, <https://doi.org/10.1016/j.geomorph.2021.107781>.
- Vieira, G.; Woronko, B. (2021). The glaciers of Serra da Estrela, in Oliva, M., Palacios, D. & Fernández-Fernández, J.M. (Eds.), *Iberia, Land of Glaciers*, Elsevier, <https://doi.org/10.1016/B978-0-12-821941-6.00020-7>

Index

Itinerary and schedule	7
1. The geology and geomorphology of the Serra da Estrela	10
1.1. Introduction	10
1.2. The Variscan orogen heritage: a precursor of the present-day dynamics	11
1.3. The Pre-Ordovician autochthonous	13
1.4. A wealth of granite intrusions at the late stages of the orogeny	14
1.5. The planation at the end of the Variscan cycle	16
1.6. Collision with Africa and the rise of a new mountain	18
1.7. Towards the present-day relief organization	19
1.8. The richness of granite types and the diversity of landforms	20
1.9. The originality of the last glaciation in the Serra da Estrela	21
a) History of research	21
b) Characteristics of the glaciation	22
c) Chronology	26
d) The Periglaciation	26
1.10. Postglacial evolution	27
2. Introduction to the itinerary and description of the stops	28
<u>Day 1</u>	28
Stop 1. Folgoso	28
Stop 2. Linhares da Beira	29
Stop 3. Videmonte	30

Stop 4. Quinta da Taberna	31
<u>Day 2</u>	31
Hike from Penhas Douradas to Lagoa Comprida (all day)	31
Stop 2. Sabugueiro/Covão do Urso Panorama	33
<u>Day 3</u>	34
Stop 1. Barroca d'Água – Zêzere valley (easy hike - 2h30)	34
Stop 2. Covão da Ametade	36
Stop 3. Piornos	36
Stop 4. Covão do Boi	37
Stop 5. Alto da Torre	38
Stop 6. Salgadeiras – Lagoas do Covão da Clareza	39
References	40



Photo by Sérgio Brito

ORGANIZATION AND SUPPORTERS:





**10th IAG INTERNATIONAL
CONFERENCE ON GEOMORPHOLOGY** *Photo by Sérgio Brito*

COIMBRA - PORTUGAL
« GEOMORPHOLOGY AND GLOBAL CHANGE »

FIELDTRIP GUIDEBOOK

Lisbon Region

17–19 September 2022

José Luís Zêzere
César Andrade
Sérgio Oliveira
Jorge Trindade
Ricardo Garcia



José Luís Zêzere
César Andrade
Sérgio Oliveira
Jorge Trindade
Ricardo Garcia

10th International Conference on Geomorphology Fieldtrip Guidebook – Lisbon Region

17-19 September 2022



Coimbra, 2022

Edition notice:

Title: *10th International Conference on Geomorphology. Fieldtrip Guidebook – Lisbon Region*

Authors: *José Luís Zêzere (University of Lisbon), César Andrade (University of Lisbon), Sérgio Oliveira (University of Lisbon), Jorge Trindade (University of Lisbon), Ricardo Garcia (University of Lisbon)*

Fieldtrip guided by: *José Luís Zêzere (University of Lisbon), César Andrade (University of Lisbon), Sérgio Oliveira (University of Lisbon), Jorge Trindade (University of Lisbon), Ricardo Garcia (University of Lisbon)*

Edition: *Universidade de Coimbra, Faculdade de Letras*

Fieldtrip and Guidebook Coordination: *António Vieira (University of Minho)*

Cover: *Rotational slides affecting the motorway A9 (CREL) (photograph by José Luis Zêzere)*

Introductory Note

The 10th International Conference on Geomorphology will take place in Coimbra (Portugal) from 12th to 16th September 2022, under the theme "Geomorphology and Global Change" and it is organized by the International Association of Geomorphologists (IAG) and the Portuguese Association of Geomorphologists (APGeom).

As in previous international conferences on Geomorphology, and as is the tradition in many geomorphological events organized around the world, the organizing committee of the 10th International Conference on Geomorphology proposed several fieldtrips to the participants, occurring before, during and after the main event.

These fieldtrips intend, above all, to show to geomorphologists from all over the world the diversity and richness of the geomorphological elements of the Portuguese territory (and also from Cape Verde) and to allow an exchange of experiences between the specialists that investigate these territories and the visitors, contributing for mutual scientific enrichment and for the valorization of this international conference.

The pre-conference fieldtrip is dedicated to the islands of Santiago and Fogo, in the Archipelago of Cape Verde. It will take place from 6th to 9th September and will be led by colleagues from the University of Cape Verde (Vera Alfama, Sónia Victória, Sílvia Monteiro, José Maria Semedo and Romualdo Correia). The volcanic geomorphology will dominate the visit (including well conserved structural volcanic forms such as cones, domes, craters and calderas), especially in the island of Fogo where recent volcanic activity has been registered.

The one-day mid-conference fieldtrips will take the visitors around the Portuguese mainland territory, the 14th September, allowing the visit of four different geomorphological realities.

In the Arouca UNESCO Global Geopark, internationally recognized territory since 2009, participants will be able to visit unique geological and geomorphological features (such as planation surfaces, bowl-shaped valleys and narrow river valleys) and witness the remarkable effort of protection and promotion of natural (abiotic and biotic) and cultural (tangible and intangible) heritage. The visit to the "516 Arouca" suspension bridge will be an excellent opportunity to observe the magnificent landscapes of this mountainous territory. This fieldtrip will be led by Artur A. Sá, António Vieira and Daniela Rocha.

The field trip to coastal areas of central Portugal will be led by Pedro Dinis and António Campar Almeida. Their proposal is to observe the different morphotectonic units of central west Portugal, namely the Coastal Mountain of Serra da Boa Viagem (revealing karstification features), the littoral plain (with aeolian dunes associated with some

reliefs with higher elevation), the Cértima subsiding area (structurally-controlled morphology), and the Buçaco region (with the Syncline of Buçaco).

The visit to the Schist Mountains of Central Portugal will be centered in the mountains of Lousã and Açor, and will be conducted by Luciano Lourenço and Bruno Martins. It is proposed the observation of the main contrasts of the landscape, especially in terms of its physical geography, translated into geological, hypsometric, geomorphological, and hydrographic differentiation, or the land use and occupation and evolution of vegetation cover, namely following the recurrent large forest fires and the subsequent erosive processes they caused.

The fourth one-day fieldtrip will be oriented to the Estrela UNESCO Global Geopark, and led by Gonçalo Vieira, Emanuel Castro and Fábio Loureiro. The main geoheritage significance of the Estrela UGGp is the extent and richness of the Late Pleistocene glaciation(s) landforms and deposits (with spectacular morphological features such as the Zêzere glacial valley or the glacial cirques, moraine boulders, erratics or *roches moutounnées*) as well as the peculiar long-term geological evolution (revealing a significant diversity of granite types and landforms).

The three post-conference fieldtrips include a visit to the Lisbon Region, Serra da Estrela and, finally, Minho and Galicia (Spain), and will take place from 17th to 19th September.

The fieldtrip to the Lisbon Region will be guided by José Luís Zêzere, César Andrade, Sérgio Oliveira, Jorge Trindade and Ricardo Garcia, and will cover topics related with slope instability and landslides that affect the region of Lisbon, the floods occurring in the area north of Lisbon, and the coastal dynamics, morphology, cliff instability and beach erosion at north and south of Lisbon.

The three days field trip to the Serra da Estrela is led by Gonçalo Vieira, Emanuel Castro and Fábio Loureiro. Participants will be taken to visit some of the Geopark's most inaccessible geosites and observe breathtaking landscapes during two hikes: one in the Zêzere valley and the other between Penhas Douradas and Lagoa Comprida. The different geosites to visit include features of glacial, periglacial, granite weathering, fluvial, hydrogeological, petrological and tectonic themes, and aspects related with the management of a UNESCO Global Geopark will be discussed.

The third three-days fieldtrip is destined to the northwestern part of Portugal and the Spanish region of Galicia. Guided by Alberto Gomes and Antonio Perez Alberti, will be mainly devoted to the coastal area and to the observation and discussion of issues related to coastal dynamics, marine terrace staircases, differential uplift of coastal blocks, coastal geoheritage, coastal geoarchaeology, coastal erosion and coastal land planning.

It is our expectation that these visits will please all participants and promote the scientific enrichment of all involved, allowing a better understanding of the topics covered in each one.

We also hope that this set of fieldtrip guidebooks can help in the understanding of the themes discussed and that they can be a testimony of the commitment and dedication shown by all the scientific responsible for the several visits, to whom the organizing committee of the International Conference on Geomorphology expresses its greatest recognition and gratitude.

have a good fieldtrip!

Lúcio José Sobral da Cunha
António Vieira

on behalf of the ICG2022 Organizing Committee

ITINERARY AND SCHEDULE

Itinerary

Day 1 (17 September)

07:00 - Departure from Coimbra (Largo D. Dinis) (Fig. 1)

10:00 – 11:00 - Stop 1. Loures

11:30 – 12:30 - Stop 2. Trancão Valley

12:45 – 14:00 - Bucelas (Packed Lunch)

14:30 – 15:30 - Stop 3. Calhandriz

16:00 – 17:00 - Stop 4. Arruda dos Vinhos

17:30 - 18:00 - Stop 5. Quintas

19:00 - Arrival in Lisbon

20:00 - Dinner

Day 2 (18 September)

08:00 - Departure from Lisbon

09:00 – 09:45 - Stop 1. Maceira

10:00 – 11:00 - Stop 2. Santa Rita beach

11:30 – 12:40 - Stop 3. Coxos beach

12:45 – 13:30 - Lunch

13:45 – 14:00 - Ribeira de Ilhas viewpoint

14:45 – 15:15 - Stop 4. Azenhas do Mar

15:45 – 16:30 - Stop 5. Cape Roca

17:00 – 17:30 - Stop 6. Cresmina dune field

17:45 – 18:15 - Stop 7. Cape Raso

19:15 - Arrival in Lisbon

Day 3 (19 September)

08:00 - Departure from Lisbon

08:45 - 10:00 - Stop 1. Capuchos

10:15 - 11:45 - Stop 2. S. João da Caparica

12:30 - 13:45 - Setúbal

14:00 - 14:30 - Stop 3. Outão

14:45 - 15:15 - Stop 4. Arrábida mountain

16:15 - 17:00 - Stop 5. Cape Espichel

18:00 - 18:30 - Stop 6. Cristo Rei

19:00 - Arrival in Lisbon

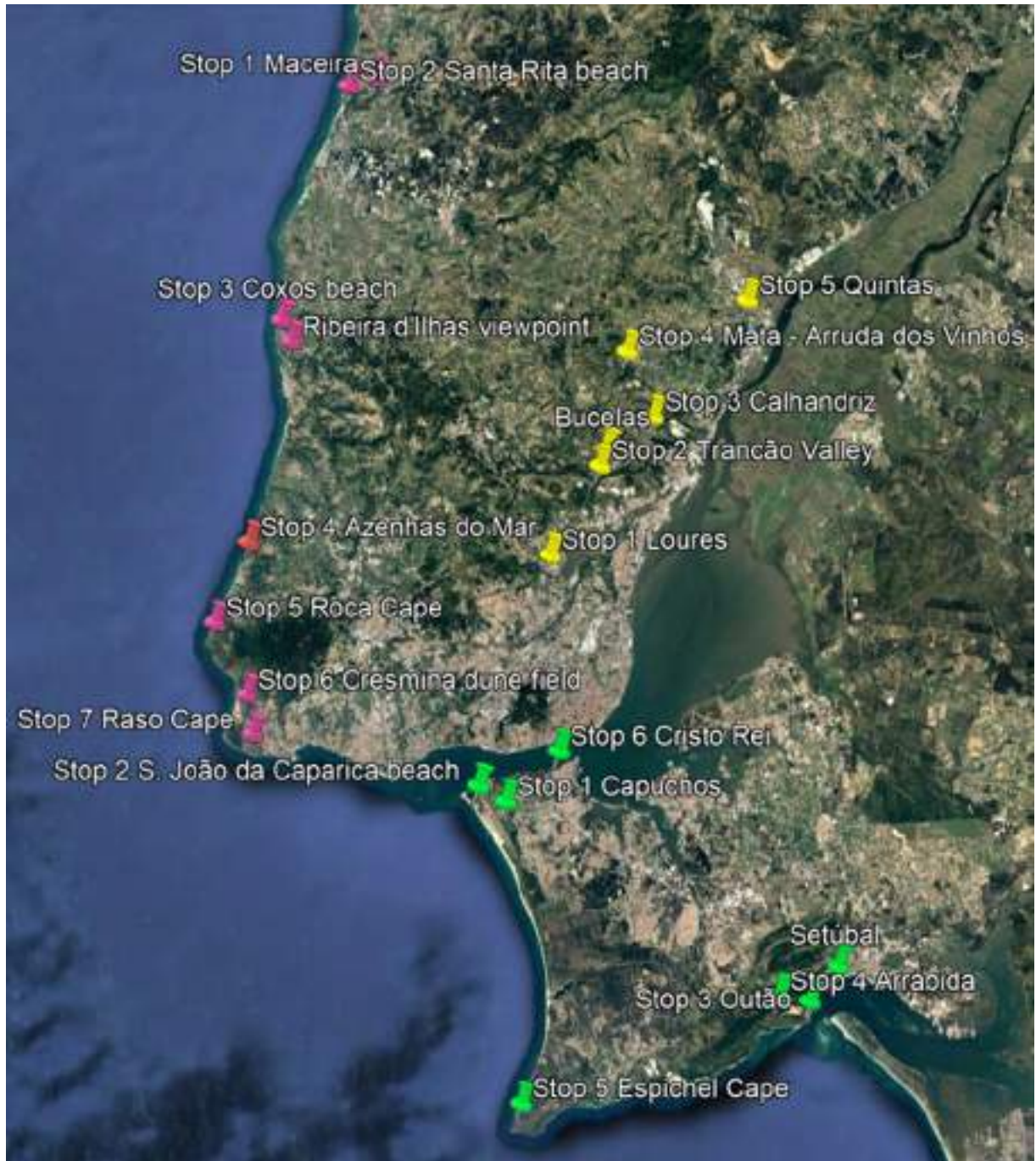


Figure 1. Itinerary of the field trip – Day 1 (yellow), Day 2 (red), Day 3 (green) (Source: Google Earth).

Introduction

Geological Setting

The Lisbon region is part of a geomorphological unit that was named “Low Mountains, Hills and Inland Plateaux of the Lusitanian Basin” by Ramos & Pereira (2020).

The Lusitanian Basin formed during the Mesozoic in relation to the open of the Atlantic Ocean (Ribeiro *et al.* 1979). It corresponds to a continental margin distensive basin extending over 200 km, following roughly NNW–SSE direction, and reaches 100 km in width, 2/3 of which are emerged (Fig. 2). The basin was infilled by sediments of Mesozoic and Cenozoic ages with a maximum thickness of about 5000 m (Kullberg *et al.* 2013; Ramos & Pereira, 2020).

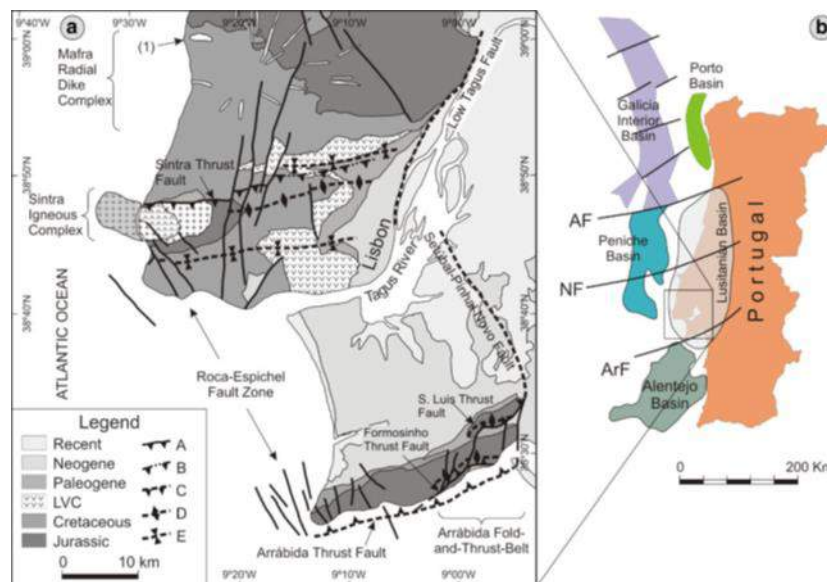


Figure 2. Geological setting and structural map of the southern part of the Lusitanian Basin: a Simplified geological framework of the region of Sintra–Lisboa–Arrábida (mod. from Ribeiro *et al.* 1990). Abbreviations for the legend: A. thrust fault, B. blind thrust fault, C. inferred thrust fault; D. anticline; E. syncline. b Location and geological context of the region represented in (a) (extracted from Kulberg & Kulberg, 2020)

In late Cretaceous, the tectonic regime changed from predominantly extensional into compressional. The Iberia went through a remarkable anti-clockwise rotation ($\sim 35^\circ$) during which seafloor spreading occurred in the Bay of Biscay, whereas Eurasia-Iberia collision started, and Africa started drifting northwards including an anti-clockwise rotation that is still occurring nowadays (Dewey *et al.* 1989; Terrinha *et al.* 2013; Righetti, 2022).

The compression started in the late Cretaceous reactivated a deep fault extending from the submarine Tore Seamount (300 km west of Peniche) to the Gulf of Cadiz (Ribeiro

2013). Magma ascended in zones of decompression along this NNW-SSE lineament in the onshore of the West Iberian Margin (Rock 1982; Kullberg and Kullberg 2000; Miranda *et al.* 2009), leading to the intrusion of the magmatic massifs of Monchique, Sines and Sintra by 94–72 Ma ago (Ramos & Pereira, 2020). Besides these three large magmatic bodies, there are other smaller contemporary magmatic occurrences located in the onshore of the Lisbon peninsula (Kulberg & Kulberg, 2020): the intrusive Ribamar diorite (88 Ma), the Mafra Radial Dyke Complex (75–72 Ma) and the extrusive Lisbon Volcanic Complex, by the same age, made by basalts and pyroclasts and reaching a maximum thickness of 400 m.

The tectonic inversion of the Lusitanian Basin was accentuated during the Miocene. Miocene compression was responsible for the creation of large ENE-WSW synclines and anticlines in the area north of Lisbon and generated the Arrábida Chain in the southern limit of the Lusitanian Basin, through the reactivation of ENE–WSW to NE–SW trending faults (Fonseca *et al.* 2020). The Arrábida Chain is a small Alpine orogenic belt, formed by south-verging ENE–WSW folds and thrust planes, connected to left-lateral NNE–SSW and N–S strike-slip faults (Kullberg *et al.* 2000).

Geomorphological Setting

Three small mountains dominate the geomorphology of the Lisbon Region (Fig. 3): The Montejunto mountain (666 m) located to the north, the Arrábida mountain (501 m) located to the south, and the Sintra mountain (529 m) located to the west.

The Montejunto mountain extends from the NE to the SW over 18 km and corresponds to a faulted anticline affecting limestones and marls of Upper Jurassic age.

The structural control on the morphology of the Arrábida Chain is strongly evidenced in the Formosinho (501 m) and São Luís (293 m) anticlines.

The Sintra mountain (528 m) is located the Atlantic Ocean just north of Cascais (Fig. 3), extending over 10 km in the W-E direction. The Sintra Mountain is formed mostly by granite, syenite and gabbro, corresponding to the intrusion of an igneous diapyr that occurred during the Late Cretaceous (Kulberg and Kulberg, 2000).

In the east zone of the area between the Montejunto mountain and Lisbon, the differential erosion was prevalent during the Quaternary allowing the formation of a hilly landscape that does not exceed 450 m asl (Fig. 3). Such landscape includes structural landforms (e.g. *cuestas*) and large depressions generated by differential erosion (e.g. Loures and Arruda dos Vinhos). In the western zone of this area, a polygenic coastal plateau was formed during the Late Pliocene and the Early Quaternary (Ferreira, 1981). This geomorphologic unit does not exceed 200 m asl (Fig. 3), and it has a gentle dip (<2°) toward the west. Fluvial erosion verified during the Quaternary promoted the degradation of the plateau.

In the Setúbal peninsula, the coastal plateau is also present extending from the base of the São Luís Mount to Cape Espichel at c. 190 – 220 m asl., where it receives the name of “Cape Platform”.

Climate setting

The climate of the Lisbon region is Mediterranean but with a significant influence of low-pressure systems originated in the Atlantic. The mean annual precipitation (MAP) ranges from less than 500 mm in Cascais zone southward the Sintra mountain up to 1350 mm in the top of Montejusto mountain (Fig. 3). At the reference rain gauge of Lisboa-Geofísico, the MAP is 726 mm, and the rainfall occurs mostly from October to March (75% of the total amount; 67% of the total rainy days). The precipitation regime is very irregular at the interannual and inter-seasonal scales, and encompasses large periods of drought, long lasting rainy periods, and very intense short rainfall episodes (Trigo *et al.*, 2004, 2005; Zêzere *et al.*, 2005; Paredes *et al.*, 2006).

Pleisto-Holocene vertical land movement and Holocene sea level changes

Net sea level variations along the central western Portuguese coast since the late Pliocene have been driven by absolute sea level (eustatic), isostatic and tectonic changes.

Evidences for regional uplift of Portuguese mainland are abundant along the coast, in the form of high marine cliffs, deeply incised fluvial channels and raised marine terraces and wave-cut platforms (cf. Cabral, 2012 and references therein). Those studies indicate rates in the range of 0.1 to 0.2 mm/year as representative of mean uplift intensity from ca. 3 million years onwards. Investigation of coastal and fluvial landforms (e.g. fluvial and marine terraces, raised marine abrasion platforms) and of geomorphic indexes in hydrographic basins confirm the small magnitude and spatial heterogeneity of uplift intensity over the Portuguese coastal fringe: Ramos-Pereira (2005) interpreted previous work by Ferreira (1984), which further investigated field evidences reported in Madeira and Dias (1982) to infer 0.125 mm/year for the Pleisto-Holocene vertical uplift rate of the Sintra igneous range, whereas Ressurreição *et al.* (2012) proposed an absolute uplift rate of ca. 0.04 mm/year for the coastal region encompassing the Sado estuary, in close agreement with the 0.05 mm/year estimate of Dias *et al.* (2016) for the whole Sado basin. More recently, Figueiredo *et al.* (2019) inferred long-term regional tilting toward the W to NW of the Sado basin since the early Pleistocene, with small or no long-term uplift of the coastal rim. Evidence of negative vertical movements also exist, although less abundant, highlighting differences in neotectonic readjustments of distinct crustal blocks. One example of this is the deformation of the Tagus fluvial basin during the last 1.7-1.5 million years. This basin experienced subsidence and tilting opposite to the inherited regional flow direction. This originated a large-scale reorganization of the drainage network, improving its hierarchic organization and promoting the capture and

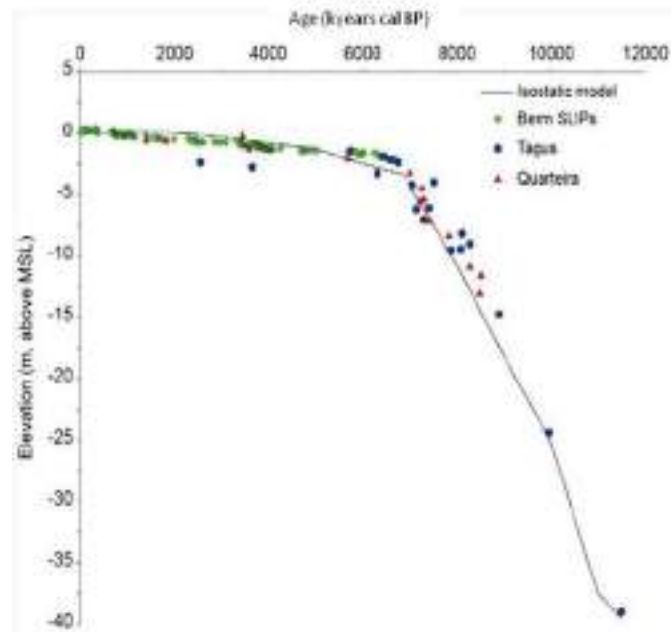


Figure 4. Plot of sea level index points (SLIPs) and isostatic sea level curve of Leorri et al. (2012) along the Atlantic Iberian margin. Berm –related SLIPs: Sado estuary, Costas et al. (2016); Tagus estuary, Vis et al. (2008); Quarteira estuaries and shelf, Teixeira et al. (2005). Adapted from Costas et al. (2016).

Despite minor differences in sea-level oscillations of shorter duration and time location of the mid-Holocene break in slope in different sea level curves, the data contain no evidence of higher-than-present sea level over the Holocene.

Contrasts between the magnitudes of vertical land motion (in the order of 10-1 mm/year) and changes in relative sea level over the Holocene (in the order of 100 mm/year) indicate that the latter have been largely dominated by eustatic components. Future rate of sea level rise (that may increase to 101 mm/year by the end of the 21st century) will enhance this contrast.

Oceanographic forcing (tides, waves and storm surge)

The west coast of mainland Portugal is fully exposed to North Atlantic waves and is a mixed-energy, high-energy and swell-dominated coast.

Tides are semidiurnal, with mean spring tidal range of 2.8 m (Andrade *et al.*, 2002). Maximum water level related to astronomical tides reaches about 1.9 m above mean sea level (msl). Deep water wave climate is characterized by mean yearly significant wave height (H_s0) of ca. 2.0 m, mean peak period (T_p) in the range of 10–12 s, and mean direction practically exclusively from the northwest quadrant (Costa & Esteves, 2009; Dodet *et al.*, 2010; Silveira, 2017; Oliveira *et al.*, 2020) (Fig. 5). Wave parameters display a seasonal pattern, shifting between higher, longer and more westerly incoming waves during winter, and lower, shorter and more northerly during summer.

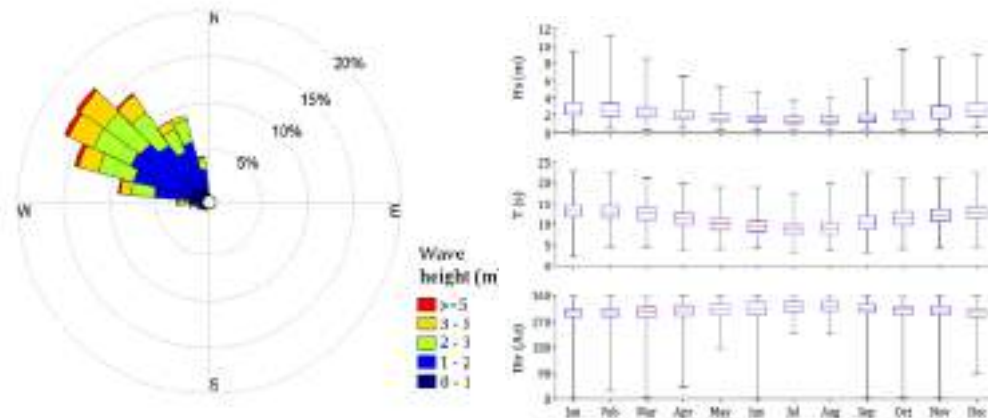


Figure 5. Left - Deepwater (>1000 m) wave record (1979 – 2014) at the latitude of Figueira da Foz showing frequency of Hs0 according to wave directions. Right – Box-plots of monthly distributions of Hs0, Tp and direction (Dir). After Silveira (2017).

Portuguese west coast is impacted annually by 9 to 12 marine storms (Ferreira *et al.*, 2009), mostly during winter and propagating from WNW. Storms last on average for 26 h and may increase maximum Hs and Tp to about 14 m and above 20s, respectively. The events of 15 February 1941, 28 February 1978 (with partial destruction of the west jetty of Sines) and, more recently, Christina (3 – 7 January 2014, with damages estimated in 6 M Euros) are examples of high-intensity storms that significantly impacted the central-western Portuguese coast throughout the 20th century (cf. Daveau *et al.*, 1978; Freitas and Dias, 2013; Pinto, 2014; Diogo *et al.*, 2014 for further details).

Storm surge-related increase in sea-level is less than 0.5 m along the open central western coast (Taborda and Dias, 1992; Gama *et al.*, 1997; Vieira *et al.*, 2012), making it a secondary driver of coastal processes, although local amplification in estuaries have been recorded (e.g. ca. 1.0 m at Viana do Castelo harbor - NW coast, Taborda and Dias, 1992, and 0.90 m in the Tagus estuary -Antunes *et al.*, 2013). Most of the coastal response to oceanographic forcing is therefore related with breaking or broken waves, rather than inundation caused by intense storm-related surges.

Nearshore wave regime, coastal sediment transport and sediment budget

Despite sharing similar deep water wave climate, the coastal sections visited in this field trip exhibit varying nearshore wave conditions. Wave propagation towards the coast over shallower water is accompanied by changes in height and direction determined by bottom morphology and coastline configuration (Fig. 6). These changes are particularly relevant when coastal segments trending N-S and W-E are compared (Fig. 7).

The coast to the north of cape Raso and extending until cape Carvoeiro forms a coastal sediment cell (Santos *et al.*, 2014), both headlands inhibiting wave-driven sediment bypassing (Fig. 7).

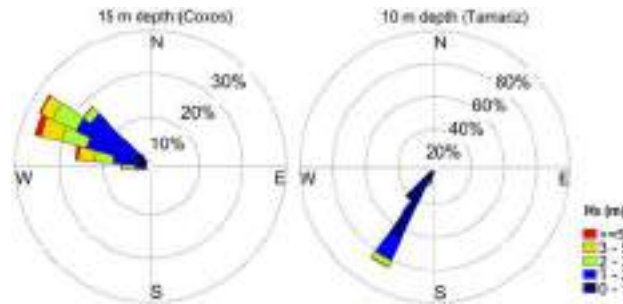


Figure 6. Nearshore wave regime (2011-2015) at Coxos (left) and Tamariz (right)(after Bastos *et al.*, 2022).

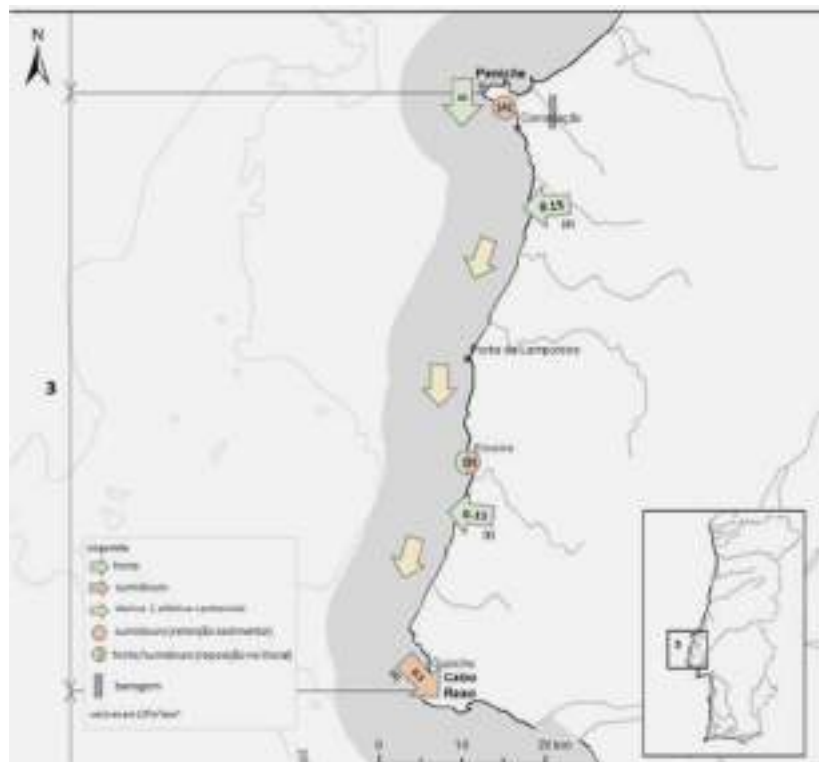


Figure 7. Sediment cell #3. Green arrows: sediment sources (streams); orange arrows: sinks (aeolian); yellow arrows: potential net > effective drift; grey rectangle: dam; circles: red (dredging) and green (beach nourishment). After Santos *et al.* (2014).

North of cape Raso the coastline is straight and bordered by submarine bottom displaying regular and broadly parallel contours (Fig. 7). Shoaling effects dominate over refraction, given the small angular offset between mean annual wave power direction (NW) and general coastline development (Fig. 6). Net potential net longshore drift is directed southward and of high magnitude (106 m³/year, cf. Ribeiro, 2017) exceeding by two orders of magnitude the effective drift (104 m³/year). This contrast is explained by the low intensity of external sediment sources, essentially consisting in solid load delivered by streams. Relevance of cliff retreat as a sediment source is very small given the prevailing carbonate nature of rocks affected by erosion. The only relevant sediment sink corresponds to the Guincho-Crismina dune complex. Guincho beach, at the downdrift end of the cell, makes the source of aeolian sand that feeds the Guincho-

Crismina dune complex and bypasses Raso headland, heading towards the updrift region of the Raso – Lisbon coast. Estimates of wind-driven sand transport potential are of ca. 104 m³/year (Rebêlo, 2004; Santos, 2006; Silva, 2015; Ferreira, 2019), matching effective littoral drift at the downdrift segment of this sediment cell.

The coast extending from cape Raso to cape Espichel (this headland also inhibiting sand bypass) consists of two distinct sectors, separated by the Tagus inlet (Fig. 8) and developing with different orientations. In addition, there is a pronounced offset in longitude of the coast developing northward of cape Raso and south of the Tagus inlet. As detailed below, this sediment cell displays an overall pattern of sand dispersion characterized by convergence towards the Tagus outer estuary.

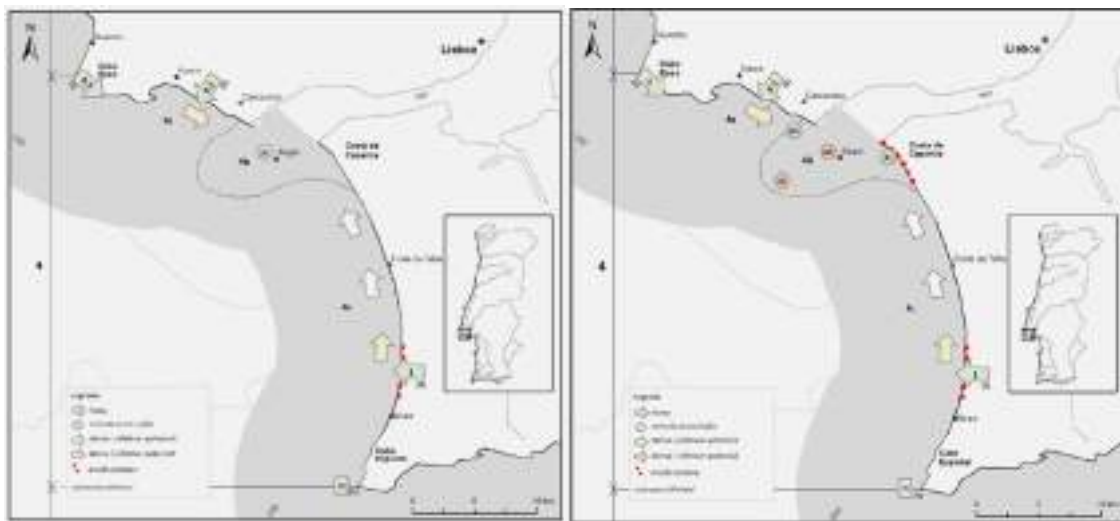


Figure 8. Sediment cell #4. Green arrows: sediment sources (aeolian +streams+cliff erosion – red squares); green circles: retention over sand shoals; yellow arrows: potential net > effective drift; white arrows: potential net \approx effective drift. Left: “natural” conditions; right: “present-day” conditions, including significant anthropic influence, e.g. sand extraction from shoals of the outer estuary and blockage of aeolian bypassing of Raso headland. After Santos et al. (2014).

The marked directional change in coastline orientation eastwards of cape Raso provides effective shelter regarding prevailing NW waves, the intensity of sheltering increasing eastwards (Fig. 9)(cf. also Silva *et al.*, 2020). Cliff retreat and small streams feed some sand to this coast but the rate of sediment supply from these external sources is insufficient to saturate the potential longshore transport rate, defining a sediment starved coastal context.

The Tagus estuary is not a relevant sand source for the coast extending northward and southward of the inlet channel, including the Cascais – Guincho reach.

In contrast, the coast southward of the Tagus estuary is oriented north-south and adopts an arcuate shape, similar to that of equilibrium bays. This coast is sandy and bordered by a sandy strandplain from Caparica to Fonte da Telha; the central region up to praia

das Bicas is dominated by sand beaches leaning against active cliffs cut in sand and soft sandstone, and further south it is sand-starved with active cliffs and developed in carbonate rocks. No permanent rivers outlet on this coastal segment.

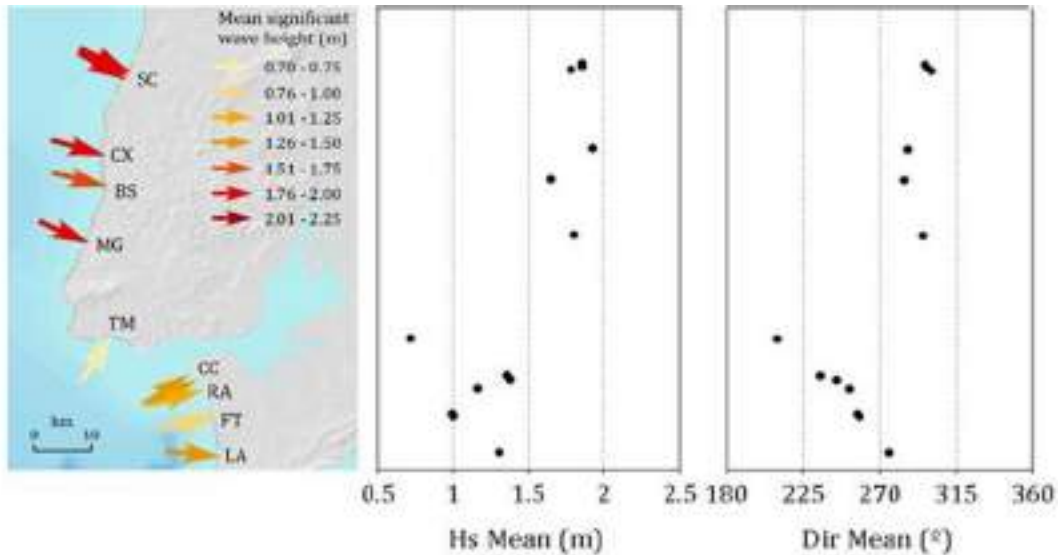


Figure 9. Nearshore mean Hs and direction in locations with contrasting exposure, related with sheltering offered by Raso headland and offset in longitude of the coast north and south of the Tagus estuary. Left –color and orientation of arrows indicate mean Hs and mean wave direction, respectively; right - mean Hs and direction at locations indicated by arrows (adapted from Silveira, 2017).

Taborda *et al.* (2014) discussed previous models of sediment dispersion along this coastal stretch, which relied to a large extent on the concept of static equilibrium bays (e.g. Abecassis 1987). Taborda *et al.* (2014) showed that potential and effective net littoral drift along the Caparica –Espichel coast are directed northwards when addressed at decadal to century time scales, thus opposite to the general trend of the western Portuguese coast. From its updrift end (close to cape Espichel) until Albufeira lagoon the magnitude of net drift increases northwards from nil to about 105 m³/year (Fig. 10) and retreat of cliffs developed in sandstone, together with active gullies, supply the amount of sand required for saturation of the longshore transport potential. Further north until Caparica no significant gradients in longshore wave power and transport were found.

Until the mid-20th century the Guincho aeolian corridor remained active and formed the main external source of sand input into the Cape Raso – Tagus estuary coastal ribbon, maintaining small pocket beaches and feeding the outer shoals of the Tagus estuary. On the other hand, cliff retreat and gullies supplied the sand required to feed and saturate littoral currents and drift between cape Espichel and Fonte da Telha, this sand heading further north and maintaining the active beach-dune system of Caparica strandplain as well as the Tagus outer shoals. Sediment convergence towards the outer estuary favored their progressive increase in volume.



Figure 10. Location of beaches referred in text and schematic of longshore drift magnitude. Adapted from Taborda et al. (2014).

This pattern changed markedly from the mid 20th century onwards, when external sediment sources were significantly reduced due to human interference. Aeolian input at the northern boundary was shut down due to urban expansion and re-vegetation of the Guincho aeolian corridor. Intensive (several million cubic meters) sand dredging of the Bugio sand shoal and Tagus inlet channel generated a huge sediment deficit that affected the sediment budget of the outer estuary and proximal beaches. Littoral drift was not able to compensate this deficit until present. Sediment scarcity led to extensive reworking and lowering of the marginal linear bars of the Tagus main channel (Cachopo do Norte and Bugio) and erosion of Caparica beaches, together with increased storm flooding of the developed areas of Costa da Caparica.

Sediment cell extending between capes Espichel and Sines shows similarities with the previous one in what relates general morphology, an estuary at a northern location, sheltering effects, patterns of coastal sediment dispersion, and organization in two contrasting sectors (Fig. 11). The sector developing to the east of cape Espichel trends W-E and extends until the inlet of the Sado estuary. It is essentially rocky, related with the Arrábida range, and low-energy given the pronounced sheltering regarding the prevailing wave regime.

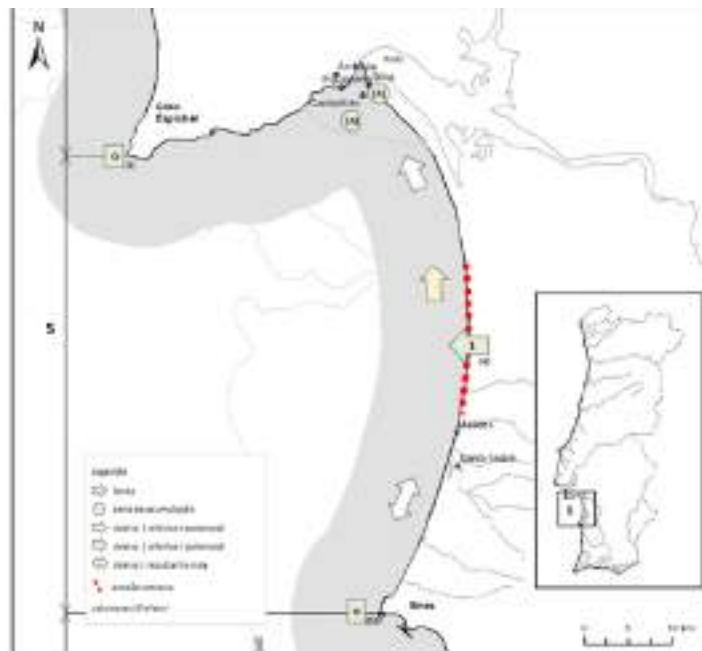


Figure 11. Sediment cell #5. Green arrows: sediment sources (streams+cliff erosion – red squares); green circles: retention over sand shoals, spit and dunes; yellow arrows: potential net > effective drift; white arrows: potential net < effective drift. After Santos et al. (2014).

Between Sado estuary and cape Sines, which is defined by a resistant sub-volcanic intrusive mass, the coast displays an arcuate planshape and consists of a sandy beach, only interrupted by inlets of small lagoons and streams featuring attached barriers. The beach is limited by fordune ridges over most of the northern extension of this coastal section and by active cliffs (developed in soft sandstones) alternating with dunes over its central and southern extension. The northern end of the sector corresponds to the Tróia sand spit, a barrier that restricts water and sediment exchanges between the estuary and the open ocean to a narrow inlet. The spit is quite protected from modal waves but more exposed to westerly and southwesterlies and net potential longshore drift magnitude was estimated to ca. 105 m³/year (Gama *et al.*, 2006), and directed from the spit root (at the latitude of Carvalhal) to its free tip. Thus, coastal sediment dispersion converges and feeds the Sado ebb delta complex, an accretionary morphological feature that contributes to reduce wave energy over the northernmost section of the spit.

Slope Instability

Due to its geological and geomorphological characteristics, the Lisbon Region, namely the zone northwards the Tagus valley, is one of the most landslide-prone areas in Portugal (Zêzere, 2001, 2020). In particular, the Upper Jurassic marls, clays and limestones, the Albian–Middle Cenomanian marls and clays and the Volcanic Complex of Lisbon have been recurrently affected by landslides in recent years. Landslides have been inventoried and mapped for over 30 years, and the landslide density is 5.8

landslides/km² along the cuesta landforms (Zêzere, 2001) and increases to 13 landslides/km² in the Grande da Pipa River basin, which develops over the Upper Jurassic rocks (Oliveira, 2012; Oliveira *et al.* 2015, Garcia and Oliveira, 2020).

The most frequent landslide types in the region are rockfalls, shallow translational slides, deep-seated translational slides, deep-seated rotational slides and composite and complex slope movements, which were summarized by Zêzere *et al.* (2005) (Fig. 12).

Most rockfalls in the region are ancient events that affected compact Cretaceous and Jurassic limestone on slopes over 30° (Zêzere, 2001). The density of rockfalls is highest along the Trancão River gorge where 192 fallen blocks were inventoried (Vaz and Zêzere, 2016). These are limestone blocks and range from 1 to 125 m³. The major rockfalls along the valley are described in historical documents as being triggered by the 1755 Lisbon earthquake (Vaz and Zêzere, 2016).

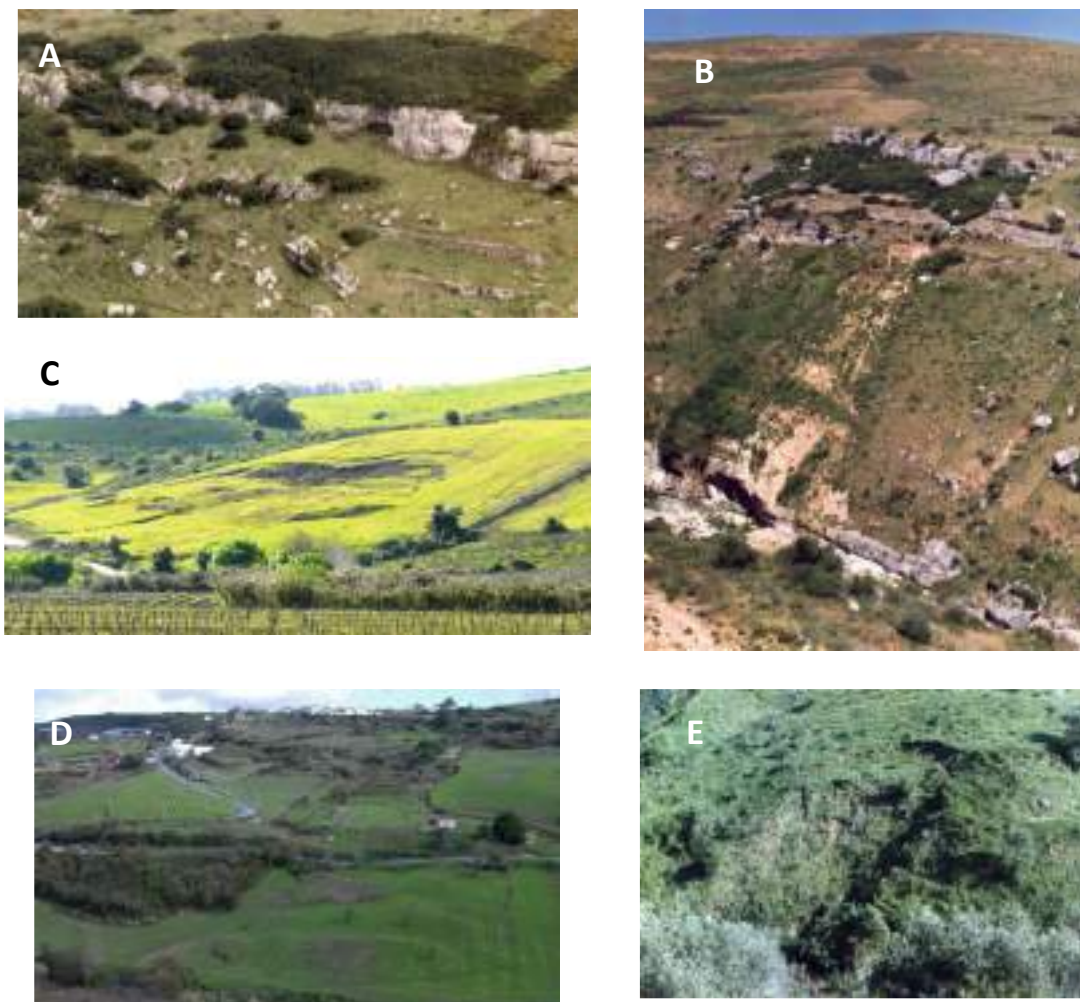


Figure 12. Examples of landslide types in the Lisbon Region. (A) Earthquake-triggered rockfalls along the Trancão valley; (B) Complex roto-translational slide in the Grande da Pipa River basin; (C) Shallow translational slide in the Trancão valley; (D) Rotational slide in Alrota (Trancão basin); (E) Translational slide in Pinheiro de Loures (Trancão basin).

Shallow translational slides are the most frequent landslides in the region. These are slope movements with planar slip surfaces with a typical depth of up to 1.5 m, and a small dimension (mean area, 550 m²; mean volume, 290 m³). In most cases, shallow landslides occur on steep valley slopes (mean slope angle = 23°) and affect colluvium covering impermeable rocks, such as volcanic tuffs, marls and clays.

Deep-seated translational slides are at least one order of magnitude larger than shallow movements (mean area, 4059 m²; mean volume, 5232 m³). These landslides are more frequent on marls and marly limestones of Jurassic and Cretaceous age. They occur on structural slopes following stratification, along shear surfaces coincident with impermeable bedding planes. As a rule, the gradient of slopes affected by deep-seated translational slides (17° in average) exceeds the dip of strata.

Deep-seated rotational slides show the highest average depth (5 m) and are larger than translational slides (mean area, 9407 m²; mean volume, 34843 m³). These landslides are more common in areas where Upper Jurassic formations crop out, like the Calhandriz area and the Grande da Pipa River basin. The Jurassic clays and marls are very prone to rotational sliding, which includes single, confined and multiple retrogressive sub-types.

Composite and complex slope movements present at least two types of mechanism, simultaneously (composite slope movement) or in sequence (complex slope movement). In many cases, particularly for old landslides, it is impossible to distinguish between composite and complex slope movements. In the Lisbon Region, most composite/ complex slope movements combine rotational slides with translational slides and rotational slides with flows, and affect mostly marls, clays and marly limestones dated from Jurassic and Cretaceous. Landslides in this group show the largest average area (27011 m²) and volume (42998 m³).

Rainfall Thresholds for Landslide Occurrence

Landslide events that occurred in the Lisbon Region in the last decades were triggered by rainfall, as extensively addressed in the literature (Ferreira *et al.*, 1987; Zêzere, 1988, 2001a; Zêzere and Trigo, 2011; Zêzere *et al.*, 2015).

In a recent work, Vaz *et al.* (2018) computed the rainfall thresholds for the Lisbon region, using the centenary rain gauge of Lisboa-Geofísico and the DISASTER database (Zêzere *et al.*, 2014), which include landslides that caused fatalities, injuries, missing people, evacuated and homeless people that were collected exploring several daily and weekly newspapers, published in Portugal between 1865 and 2010. In addition, Vaz *et al.* (2018) also collected landslides that did not cause any human damage during the same period, using the same newspaper sources.

96 landslide-triggered events were identified in the 10km-buffer around the reference Lisboa-Geofísico rain gauge (Fig. 13). The rainfall-triggered landslide events occurred mainly in wet years: 89% of landslide events were registered in years with rainfall above the Mean Annual Rainfall (MAR) (Fig. 14).

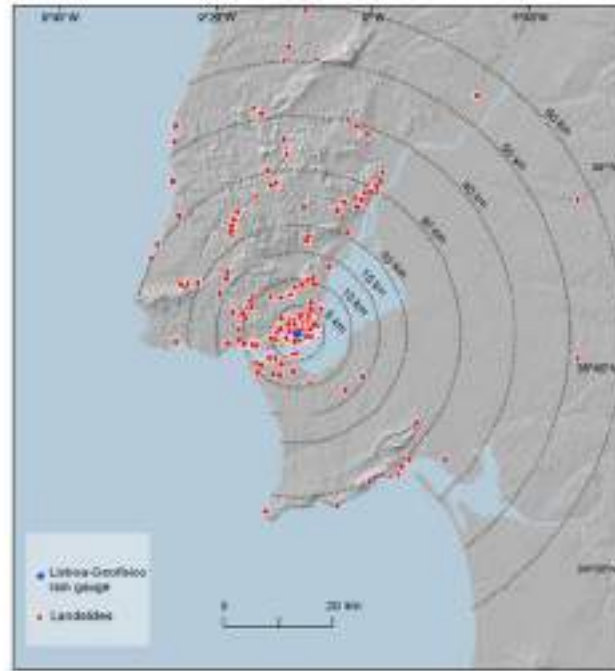


Figure 13. Distribution of landslides in the Lisbon region (1865-2010) and buffer distances from the reference rain gauge (Vaz *et al.*, 2018).

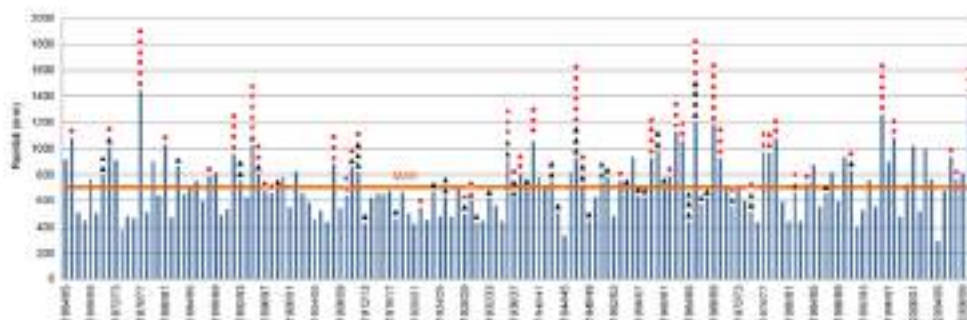


Figure 14. Annual rainfall at Lisboa-Geofísico rain gauge for the period 1864/65 – 2009/10. Red dots and black triangles symbolize rainfall-triggered events and non-rainfall-triggered landslide events, respectively, at a distance up to 10 km from the reference rain gauge (Vaz *et al.*, 2018).

The monthly distribution of landslide events follows the rainfall distribution over the year in a Mediterranean climate, with dry summers and wet winters. 92% of landslide events occurred from November to March. Within this period, January and February stand out with the highest concentration of landslide events (24 and 22.9 %, respectively). The obtained critical durations associated with landslide events range from 1 to 90 consecutive days. The monthly distribution of critical durations is shown in figure 15 for the rainfall-triggered landslide events. The shorter rainfall events (less than 20 consecutive days) occurred mainly from September to December (56 %) at the beginning of the rainy period. On the contrary, when associated with longer rainfall periods (more than 20 consecutive days) the landslide events were more frequent from January to May (86 %).

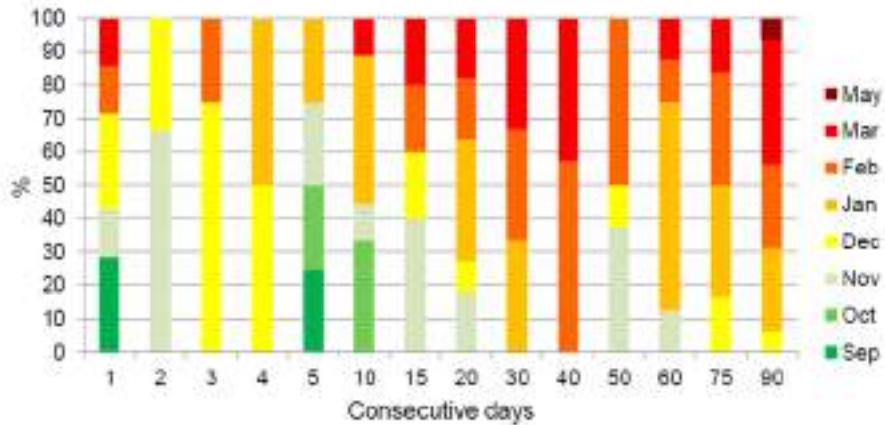


Figure 15. Monthly frequency of the rainfall-triggered landslide events against the duration of the rainfall period (Vaz *et al.*, 2018).

The rainfall thresholds for landslide initiation in the Lisbon Region are shown in figure 16. Data gathered from detailed landslide inventories in the area north of Lisbon has shown that events generating shallow translational slides have been associated to short periods (1–15 days) of intense rainfall, while deep-seated rotational and translational slides as well as composite/complex slope movements relate to longer periods (4–12 weeks) of less intense rain.

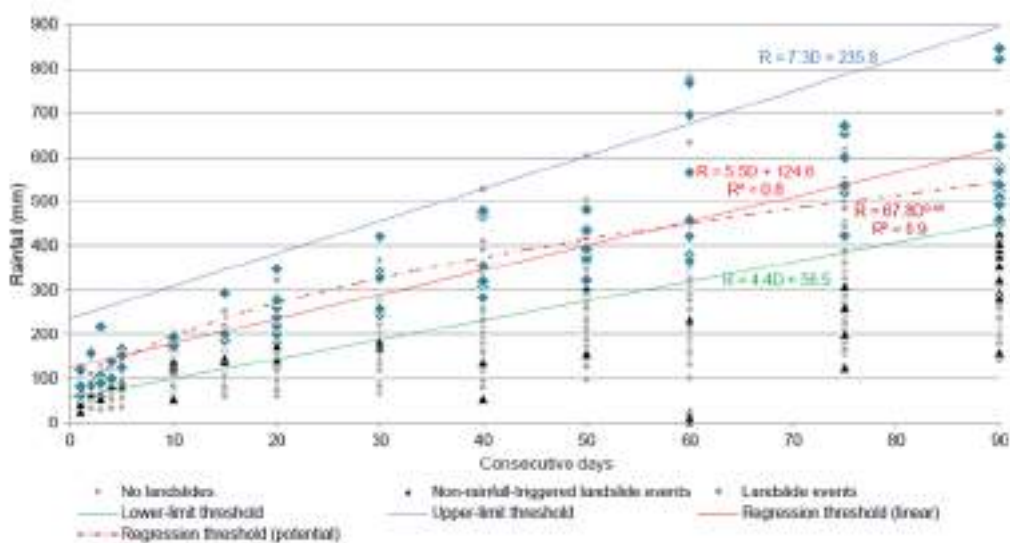


Figure 16. Cumulated rainfall duration thresholds for landslide events in the Lisbon region (1865 to 2010). Distance up to 10 km from the reference rain gauge (Vaz *et al.*, 2018).

The rainfall conditions associated with shallow and deep-seated landslides are in accordance with the hydrological processes acting on the affected slopes (Zêzere and Trigo, 2011). The shallow translational slides occur at the contact of the shallow soil with the underlying more impermeable bedrock, or within the soil material in response to the prompt growth of pore water pressure and the decrease of soil’s apparent cohesion, following intense rainfall events. In contrast, deep-seated landslides occur due to the

reduction of shear strength of soils and soft rocks, resulting from the steady rise of the groundwater table and the development of positive pore water pressures in the affected material, as a consequence of long-lasting rainfall episodes.

DAY 1. LANDSLIDES AND FLOODS IN THE NORTH OF LISBON

Stop 1. Loures - Cuestas landscape and the Loures basin

The North of Lisbon Region is part of the Lusitanian Basin of Meso-Cenozoic age and is located close to the contact between this old basin and the much younger Tagus Cenozoic Basin. The geological setting is a monocline with layers dipping from 5° to 25° towards south and south-east. These layers form the southern flank of a large anticline centred northwards in the Arruda dos Vinhos Basin. Rocks are of sedimentary and volcanic origin, dating from the Upper Jurassic to the Quaternary (Fig. 17).

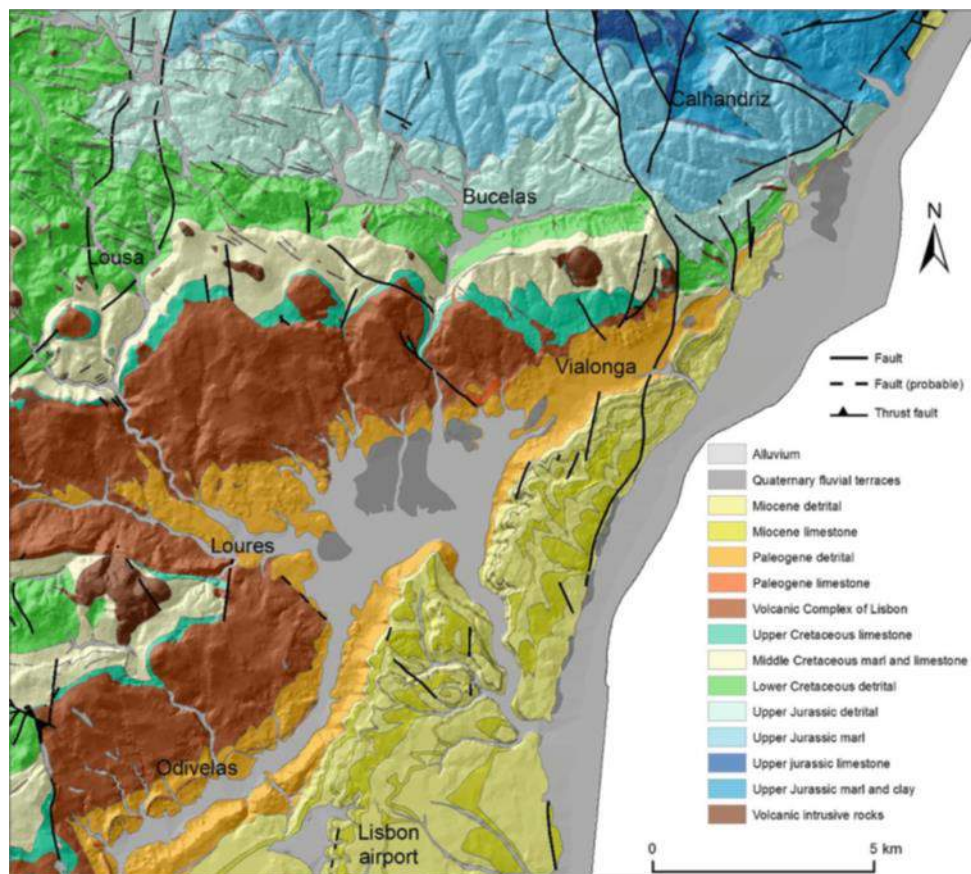


Figure 17. Geological setting of the North of Lisbon Region.

The alternating lithology, together with the low-to-moderate monocline dipping, promoted the development of cuesta landforms that were shaped by differential erosion associated to the fluvial system during the Quaternary. From north to south,

two cuestas are prominent landforms in the regional geomorphology (Fig. 18): the Lousa–Bucelas Cuesta, which shows a W-E direction and has developed along 12 km over Cretaceous formations; the Odivelas–Vialonga Cuesta, which shows a SW-NE direction and has developed along 18 km over Paleogene and Miocene formations.

Northwards, the steep slope of the Odivelas–Vialonga Cuesta is overlooking the Loures Basin, whose floor is a flat area with elevation ranging typically from 1 to 20 m asl. This basin was shaped in poorly consolidated geological formations of Paleogene age—the Benfica Complex.

The uplift of the North of Lisbon Region relative to the Tagus Basin is proven by the non-existence of any significant sedimentation in the region since the Late Miocene up to the recent times (Ferreira *et al.*, 1987; Zêzere, 1991, 2001). Moreover, the tectonic uplift explains the development of stepwise pattern of several erosional levels, in relation to the general lowering of the base level, as well as the strong fluvial erosion that generated very steep valley slopes, despite the typically low elevation of the region.

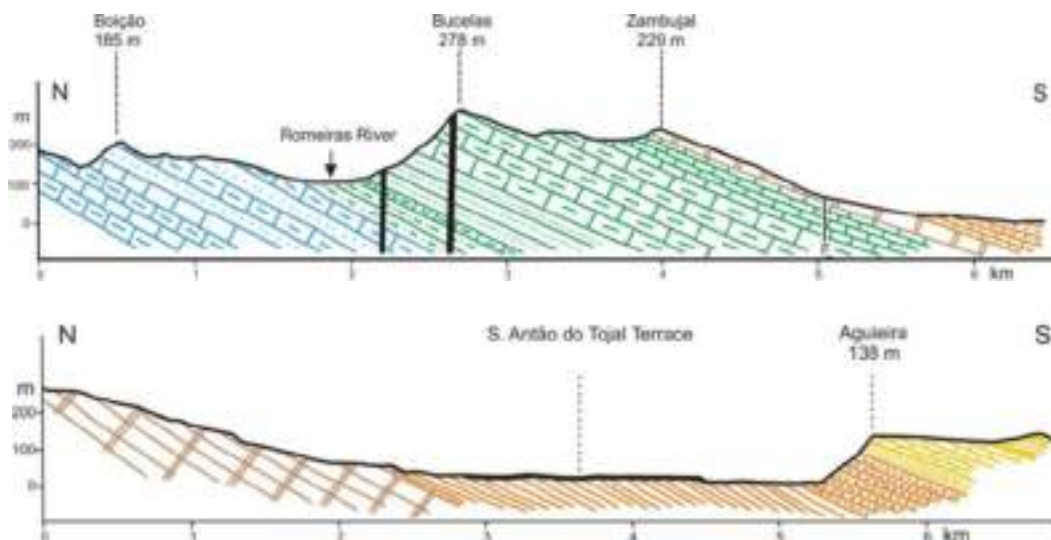


Figure 18. Geological profiles of the Lousa-Bucelas cuesta (A) and the Odivelas-Vialonga cuesta (B). Blue – Jurassic formations; Green – Cretaceous formations; Brown – Volcanic Complex of Lisbon; Orange – Paleogene; Yellow – Miocene; Grey – Quaternary.

The Loures Basin extends along 7 km in the SW-NE direction, whereas its width in NW-SE direction is less, 3 km. The basin is partially covered by alluvium that is named locally as ‘Várzea’, which formed during the higher sea level stands recorded in the Holocene (Zbyszewski, 1964). In addition, the Loures Basin includes the most important Quaternary terrace levels of the region (Fig. 17, Fig. 19): Quinta do Infantado (QI), Santo Antão do Tojal (SAT), São Julião do Tojal (SJT) and Quintanilho (Q). These terraces have been assigned to a transgression prior to the last cold period of the Quaternary (Breuil and Zbyszewski, 1943).

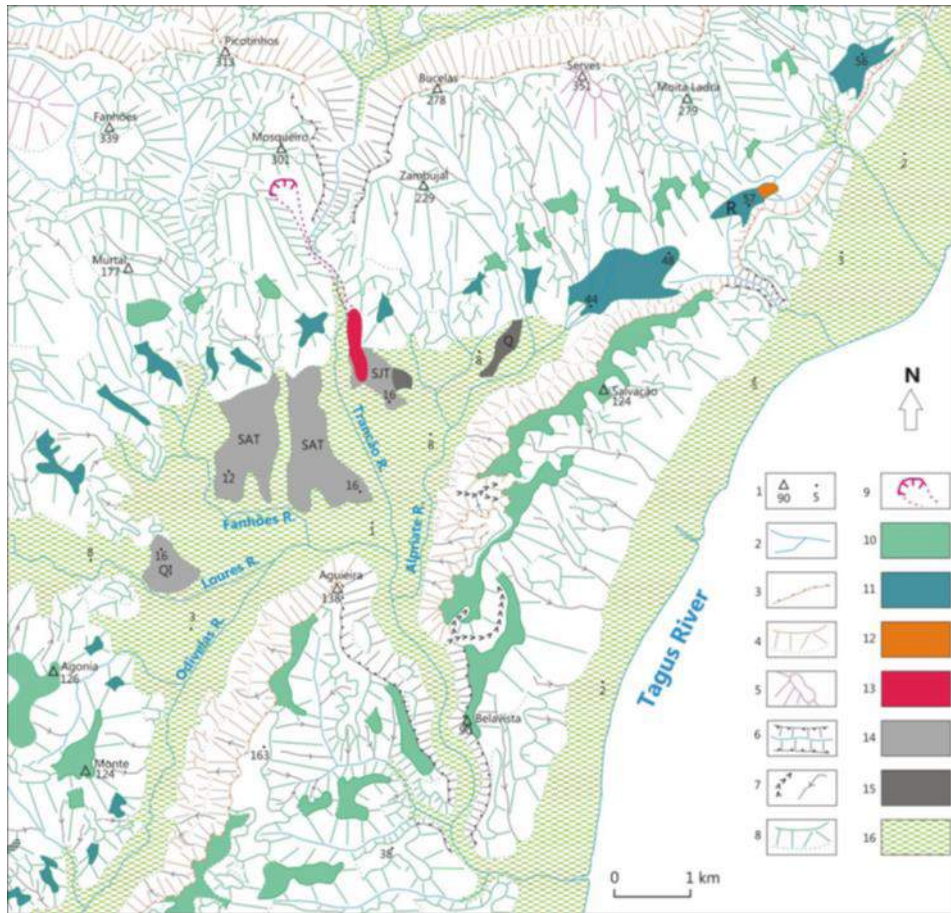


Figure 19. Geomorphological map of the Loures Basin and surrounding area.

Legend: 1 elevation (m asl), 2 river, 3 face slope of cuesta, 4 structural slope (rectilinear, concave), 5 volcanic intrusion, 6 fluvial gorge, 7 V-shaped valley and gully, 8 slope (rectilinear, concave), 9 scarp and path of old debris flow, 10 erosional level (100–130 m), 11 erosional level (40–50 m), 12 old terrace, 13 old debris flow deposit, 14 sandy terrace, 15 coarse terrace, 16 alluvial plain. Fluvial terraces: QI Quinta do Infantado, SAT Santo Antão do Tojal, SJT São Julião do Tojal, Q Quintanilho and R Reentrante.

Terraces of QI, SAT and SJT have similar sedimentological characteristics and stratigraphic position and should be contemporaneous. They are made by fine texture deposits constituted by clay, silt, sand and fine gravel that suffered short fluvial transport, starting mostly on the Paleogene formation that surrounds the basin. The terrace of SAT provided remains of *Elephas antiquus* and *Equus caballus* together with several Mousterian (Middle Palaeolithic) artefacts, which support the last interglacial age proposed by Breuil and Zbyszewski (1943).

The Quintanilho terrace (Q) is in the NE border of the Loures Basin and is composed of cobbles of limestone, basalt and quartz, within fine- and medium-carbonated sandy matrix. A deposit with similar characteristics was found in the eastern sector of the SJT terrace, embedded in the fine-textured terrace deposit. The coarser character of the Quintanilho terrace testifies to a more energetic fluvial system in comparison with the one that generated the fine-textured terrace deposits. It indicates reactivation of fluvial

erosion in the NE margin of the Loures Basin, starting mostly on the surrounding outcrops of the Upper Cenomanian limestone and the Volcanic Complex of Lisbon.

In the SJT terrace, in addition to the fine-textured deposits and deposits with characteristics similar to the Quintanilho terrace, an older thick debris flow deposit was found beneath the fine-textured deposits. It is poorly sorted and massive, containing basalt pebbles and boulders, enveloped in an abundant clay matrix and is probably associated with the large landslide rupture zone identified by Ferreira (1984) on the Volcanic Complex of Lisbon, 1.5 km upstream (Fig. 19).

The oldest Quaternary sediment found in the North of Lisbon Region is a terrace deposit located at Reentrante in an ancient fluvial valley floor at 40–50 m asl (Fig. 19). It shows a well-defined structure, with alternating fine (sand and clay) and coarse (limestone and basalt cobble) beds, that cannot be associated to the small tributary of the Tagus River that currently flows near Reentrante. In addition, the Reentrante zone is located within an erosional level located at 40–50 m asl that extends the Loures Basin towards NE without any geomorphological constraint. Therefore, when the erosional level at 40–50 m asl was shaped, the Loures Basin should have been open towards the NE direction, and the Reentrante terrace is a remnant of a former fluvial system flowing north-eastwards to the Tagus River.

Assuming the old drainage towards NE, Zêzere (1988) concluded that the breach in the Odivelas–Vialonga Cuesta, where the Trancão valley is found nowadays, occurred after the formation of the erosional level located at 40–50 m asl, probably due to the headward erosion of a former river flowing southwards to the Tagus, which modified the former fluvial system of the Loures Basin through stream piracy.

Stop 2. Trancão Valley - Landslides and landslide susceptibility assessment in the Fanhões-Trancão area

Geomorphological setting

The Fanhões–Trancão area (20 km²) is a part of the Lousa-Bucelas cuesta, being located in the dip slope of the cuesta, where there is a general coincidence between the topographical surface and the dip of the geological layers (12° towards SE). The Trancão river cuts the cuesta in two parts along a cataclinal valley where the river flows roughly in the in the same direction of the dip of strata.

From the lithological point of view, five units are distinguished (Fig. 20), apart from Quaternary terraces on the north section of the Loures basin, and alluvial deposits which partly fill the main valleys. The sandstones of upper Barremian-Aptian only appear in the north sector of the Trancão river valley. This geological formation is covered by a heterogeneous formation mainly formed by marls, with marly limestone and limestone intercalations of Albian-middle Cenomanian age. In the Trancão valley, this lithological

unit is usually covered by slope deposits with a thickness generally higher than 0.5 m. The compact limestones of upper Cenomanian age, although limited in area, are clearly perceptible in the landscape, appearing as prominent rock walls on the middle part of the Trancão valley. The Volcanic Complex of Lisbon (Upper Cretaceous age) lies above the Cenomanian limestones in more than half of the Fanhões-Trancão area. This volcanic formation is very heterogeneous including compact and weathered basalts, and volcanic tuffs. The Paleogene formations outcrop to the south of the eruptive rocks and are formed by lacustrine limestones, conglomerates, and sandstones.

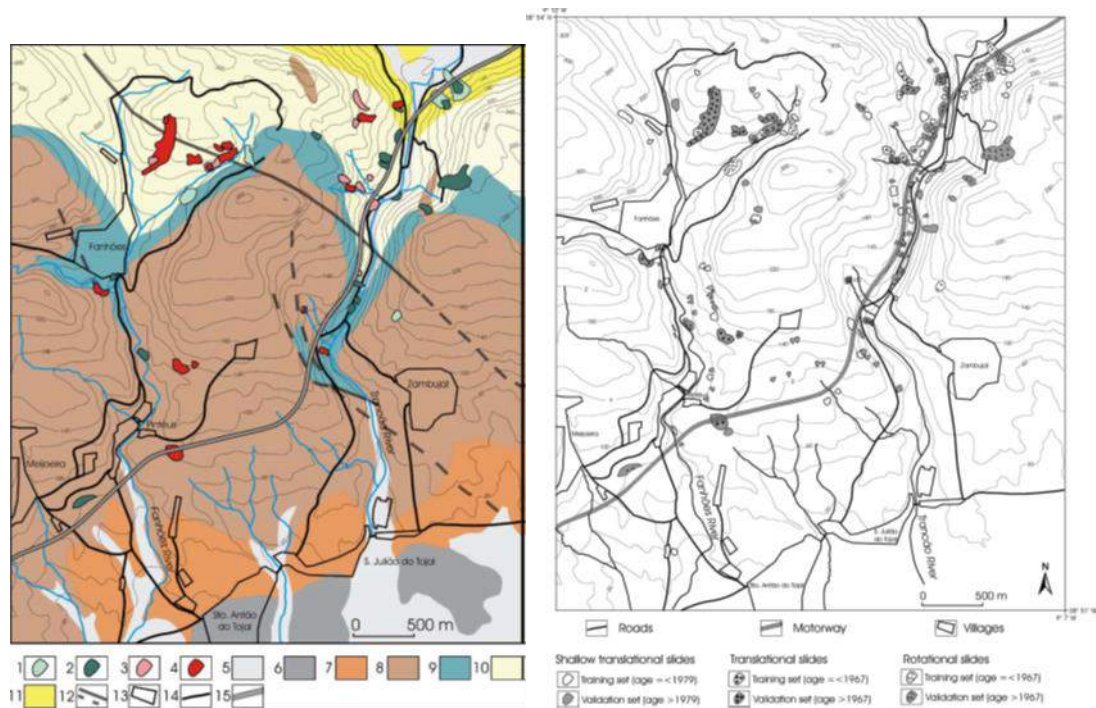


Figure 20. Geology, topography and landslide type, age and distribution in the Fanhões–Trancão area (adapted from Zêzere *et al.*, 2007, 2008).

Legend: 1 Rotational slides (age<1979), 2 rotational slides (age≥1979); 3 translational slides (age<1979); 4 translational slides (age≥1979); 5 alluvium; 6 terrace deposits; 7 Palaeogene conglomerates, sandstones and limestones; 8 Upper Cretaceous Volcanic Complex of Lisbon (basalts and volcanic tuffs); 9 Upper Cenomanian limestones; 10 Albian– Middle Cenomanian marls and marly limestones; 11 Upper Barremian–Aptian sandstones; 12 fault, uncertain (dashed); 13 villages; 14 roads; 15 motorway A9 (CREL).

Landslide incidence

The Fanhões-Trancão area is characterized by active landsliding, mainly on valley slopes (Fig. 20). Landslides were recognized and mapped at the 1:2000 scale applying standard field techniques. A field form was completed for each landslide including landslide typology, absolute age, state of activity, morphometric parameters and slope properties. Landslides were classified according to the type of mechanism and the geometry of the slip surfaces.

The complete landslide inventory of the Fanhões-Trancão area includes 147 slope movements and a total unstable area of 450,000 m². The landslide density is 7.4 per km² and the unstable area corresponds to 2% of the total surface. Inventoried landslides are shallow translational (100 cases), translational slides (26 cases), and rotational slides (21 cases). Although the small number of translational and rotational slides, differences among landslide types are statistically significant at the 1% level for landslide depth, landslide area, landslide volume, and gradient of unstable slopes.

Shallow translational slides have small dimensions in the test site (mean area, 1422 m²) and involve minor volume of materials (mean volume, 357 m³). Planar slip surfaces of these slope movements are located below the topographical surface typically from 0.5 m to 1.5 m. Failure develops mostly along contact between the permeable colluvium and the underlying impermeable bedrock composed of claystone, marl or volcanic tuff. Landslide velocity typically ranges from rapid (1.8 m/h to 3 m/min) to very rapid (3 m/min to 3 m/s). Therefore, the affected material frequently moves outside the rupture limit, but the downslope flowing of such material is limited in extent, due to the low relief energy of the area.

Translational slides are deeper seated and larger than shallow movements (mean depth 3.4 m; mean area 6429 m²; mean volume 6699 m³). These landslides involve the bedrock (namely marls and clays with limestone and marly limestone intercalations), and typically occur along shear surfaces controlled by impermeable bedding planes, on slopes that follow the dip of the strata. Slopes affected by translational slides present the lowest average gradient (16°) when compared with the other types of landslides. The moderate slope gradient does not favour the rapid overland and sub-surface drainage, thus contributing to landslide occurrence.

Rotational slides have the highest average depth, area and volume (5 m, 6544 m², and 14,650 m³, respectively) within the landslide inventory. Rotational movements were identified dominantly in the north part of the test site both in the Trancão valley and in the Fanhões valley, on slopes with gradient moderate to high (slope average=21°). Most of these landslides affect lithologic units composed by sandstones, marls and marly limestones.

Landslides in the study area are an important source of risk as a set of villages, scattered houses and infrastructure (e.g. motorways and national roads) are present in hazardous zones. There is no information about people directly injured by landslides in the area. This fact is related, on the one hand, with the low velocity of the larger and deeper slope movements (rotational and translational slides) allowing people to escape, and on the other hand, with the small size of shallow translational slides, despite their usually high velocity. Nevertheless, during the last four decades landslides have produced damages to property as well as the widespread disruption of roads, which were responsible for significant direct and indirect economic losses.

Landslide disruption of Motorway A9 (CREL) in the Trancão Valley

Landslide susceptibility was first assessed for the Trancão Valley in 1988 using a qualitative geomorphological approach (Fig. 21). This approach allows the construction of a susceptibility map directly derived from landslide distribution (Fig. 20), which clearly shows the landslide-prone character of large areas within the valley. Today, the Trancão River valley is crossed by the metropolitan motorway A9 (CREL), which is the most important strategic infrastructure existing within the study area. This motorway has a total length of 34.4 km and has a path circular in relation to the city of Lisbon, crossing the northern part of the metropolitan zone of the city.

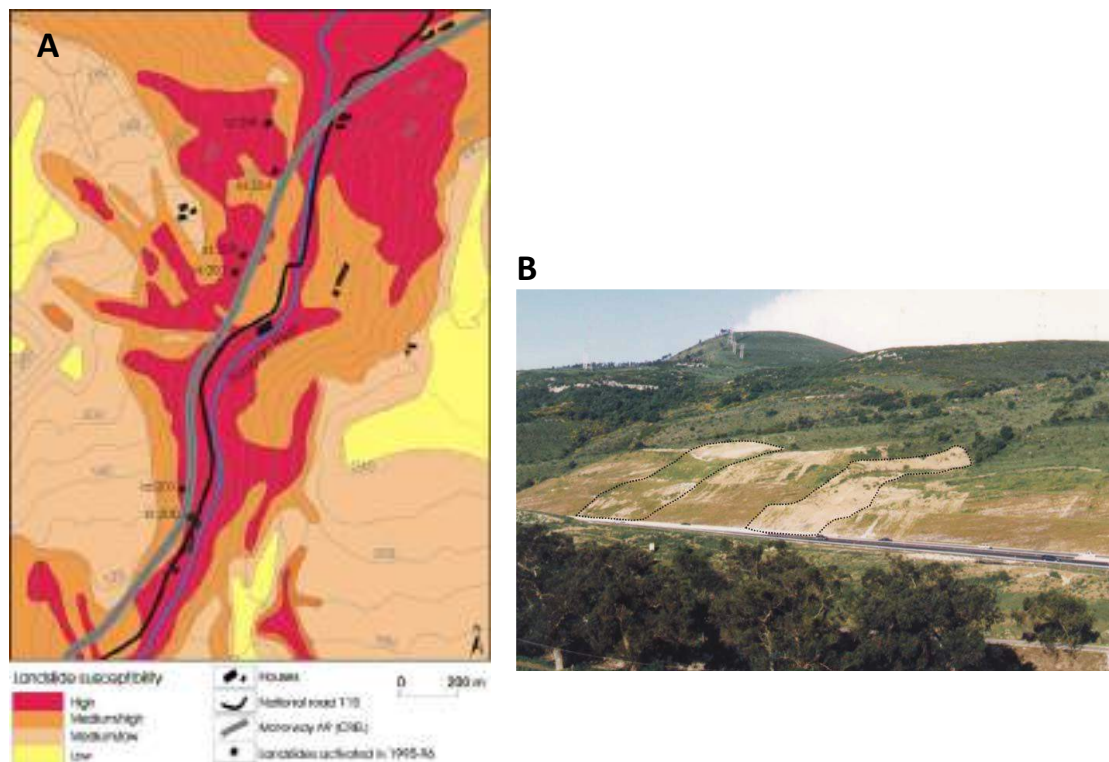


Figure 21. (A) Qualitative geomorphological landslide susceptibility assessed before the construction of motorway A9 (adapted from Zêzere, 1988); (B) Rotational slides (Id: 202 and 203) activated during the winter 1995–1996 and affecting the motorway A9 (CREL) (Zêzere et al., 2007).

The motorway A9 was constructed from 1993 to 1995 with a total investment of 240 million euros (7 million euros per km). Such amount was a national record at that time and was justified by the amount of geotechnical and engineering works. In the particular case of the Trancão River valley, a huge artificial cut was opened on the west side of the valley, in an upslope position compared to the National road 115. Within the valley, the path of the motorway crosses slopes that were previously classified as very susceptible to landslides (Fig. 21).

The motorway A9 was opened to traffic in September 1995, but experienced strong landslide-induced disruption in December 1995 and January 1996 after a heavy rainfall period. On the west slope of the Trancão Valley, six landslides occurred, five of them directly affecting the motorway A9. It is worth noticing that all these landslides occurred in areas previously classified as very susceptible to slope instability, according to geomorphological criteria. The most problematic case corresponds to a rotational slide–earthflow (landslide Id: 200) which completely destroyed three lanes of the motorway. Three other rotational slides (landslide Id: 202, 203 and 204) also affected the motorway, but were less extensive. The depletion zone of these landslides is located upslope from the position of the motorway (Fig. 21), and the road was partially buried by debris forming the landslide foot. The recovery of the motorway was very expensive and lasted for 6 months in the case of stabilization of landslide Id: 200.

Landslide susceptibility assessment and mapping

The evaluation and mapping of the landslide susceptibility was made independently for each type of landslide using the Joint Conditional Probability Function (Chung and Fabbri, 1993; Fabbri *et al.*, 2002; Zêzere *et al.*, 2004). Seven thematic layers were used as landslide predisposing factors: slope angle, slope aspect, slope curvature, lithology, superficial deposits, geomorphology, and land use. The prediction method was firstly applied independently to the total sets of shallow translational slides (100 cases), translational slides (26 cases) and rotational slides (21 cases) allowing to compute success rate curves for susceptibility models. In addition, the three original landslide data sets were partitioned into two groups using a temporal criterion. In order to obtain comparable samples, the temporal cut was made in 1979 for shallow translational slides, and in 1967 for translational and rotational slides. The first sub-set (landslide training set) was used to generate a new prediction map, and the second sub-set (landslide validation set) was compared with the prediction results for validation. The obtained temporal-based prediction rates for the three landslide types are shown in figure 22. Charts on figure 22 also includes for comparison the success-rates computed using the total set of each landslide type both for training and validation, as well as the prediction rates based on the random partition of the landslide data sets.

The computed prediction rate curves based on the landslide temporal partition were used to interpret and classify the three susceptibility maps obtained using the complete landslide data sets. Additionally, as the predictive power of the susceptibility models is shown by the slope in the prediction rate curve, variations on that slope were used to define five landslide susceptibility classes, with boundaries corresponding to the main breaks of slope on the prediction rate curve (Fig. 22). Lastly, percentage of predicted validation landslides corresponding to previous referred boundaries was used to assign empirical probabilities to each landslide susceptibility class (Fig. 22), assuming that the behaviour of future slope instability will be similar to that measured in the past.

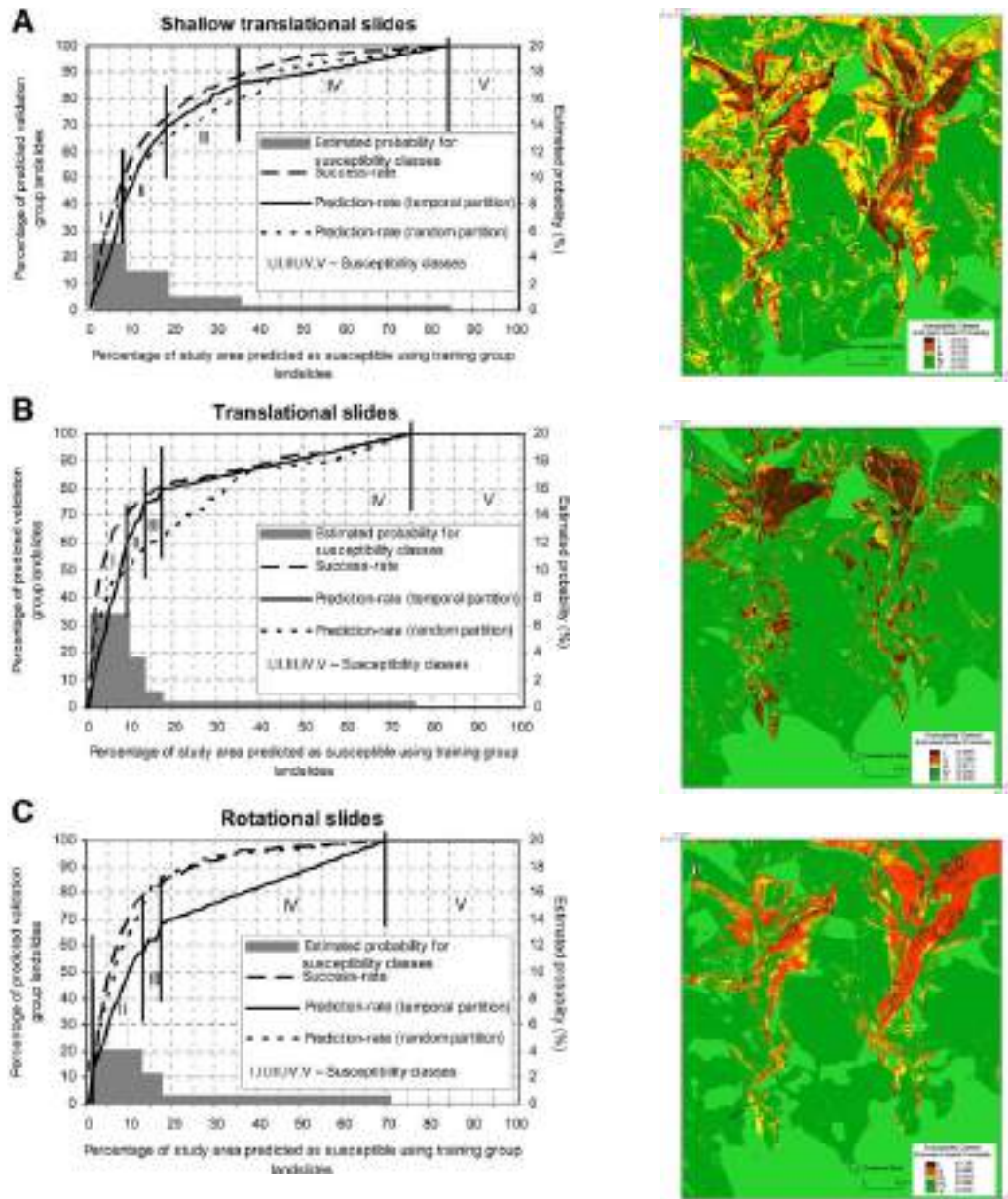


Figure 22. Landslide susceptibility maps of the Fanhões-Trancão area, validation curves (success and prediction rates); I, II, III, IV, and V, landslide susceptibility classes defined according to breaks of slope of prediction rate curves obtained by the temporal partition of landslide data sets. A – Shallow translational slides; B – Translational slides; C – Rotational slides (adapted from Zêzere *et al.*, 2008).

Stop 3. Roucas - Calhandriz – The Calhandriz Landslide

The Calhandriz landslide (Fig. 23) occurred on the 9-10th February 1979 and moved during about 36 hours. Among the landslides recently occurred in the region North of Lisbon this one mobilised the greatest volume of materials and caused the most extensive damage (Coelho, 1979; Ferreira, 1984).



Figure 23. Location of the Calhandriz landslide (Source of image: World imagery, ESRI) (Garcia & Oliveira, 2020).

Geologic and climatic conditions

In the Calhandriz area the rocks are of upper Jurassic age, and are organized as follows, from bottom to top: a complex of clays and marls with detrital intercalation (Abadia layers), reaching a thickness of 800 m; narrow benches (10-20 m) of coralline limestone (Amaral beds); complex of marls, marly limestones and limestones, with sandstone intercalations, of reaching a thickness of 350 m. The local geological structure is monocline with layers dipping SSE from 8° to 12°.

The Calhandriz landslide occurred after a very rainy late Autumn and Winter. Taking the rainfall registered at the Lisbon airport as a reference, on the date of the Calhandriz landslide the rainfall accumulated from the beginning of September 1978 had reached 700 mm a score that was never before recorded at that site (in 30 years of records) and which was above the 90th percentile at the Lisbon Geophysical station (150 years of records). The critical rainfall triggering conditions estimated for the S. Julião do Tojal rain gauge (located 8.5 km Southwest) were 694 mm in 75 consecutive days, for which a return period of 22 years was computed (Zêzere *et al.*, 2015).

It should be highlighted that when the landslide occurred the soil was saturated due to the rise of the water table level up to the topographic surface, as proved by the presence of several pools coincident with the depressed zones within the landslide mass, the days after the landslide.

Description of the landslide

The Calhandriz landslide (Fig. 24, Table I), with an area in excess of 180,000 m², affected about 1,300,000 m³ of materials, taking into account a maximum depth of 12 m to the slip surface. The possible reconstruction of the landslide morphology renders it possible

to individualize two major sections in the landslide, whose boundary is a break of slope located close to the road running from the village of Calhandriz to Mato da Cruz.

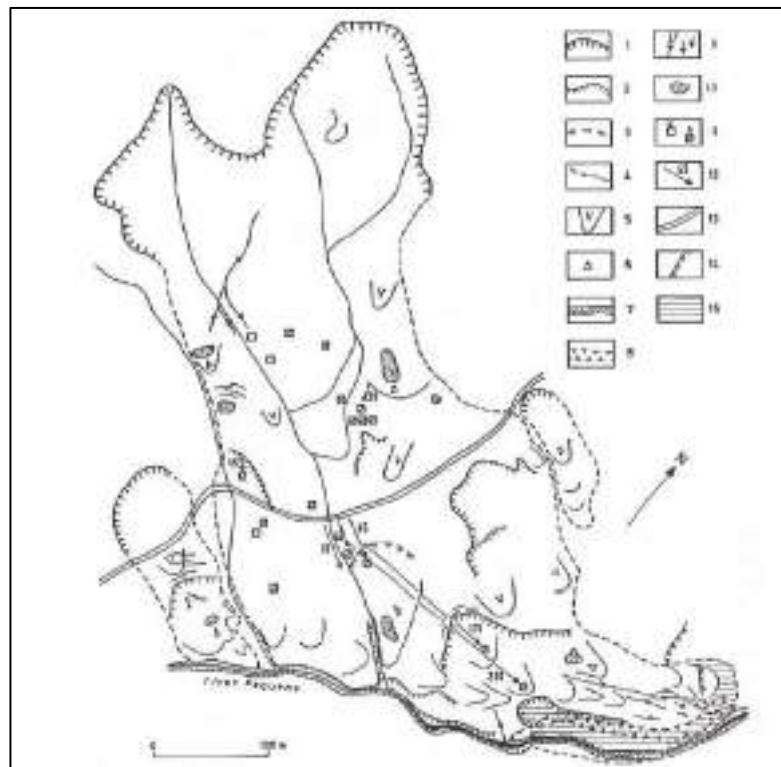


Figure 24. Simplified geomorphological map of the Calhandriz landslide (Ferreira *et al.*, 1996).
 Legend: 1 – main scarp; 2 – secondary scarp; 3 – probable secondary scarp; 4 – landslide boundary; 5 – accumulation lobe; 6 – reverse slope angle; 7 – present fluvial channel; 8 – former fluvial channel; 9 – gully and rill; 10 – pool; 11 – affected houses, a) repaired; b) destroyed; 12 – horizontal displacements (in meters); 13 – road; 14 – wall; 15 – flow.

The sector upslope from the road presented a less active landslide dynamics and comprised two subareas. The subarea to the North displayed a more pronounced main scarp with a height of 1 to 3 m. The horizontal displacement in this sector reached 30 m and several houses were destroyed. The subarea to the South is bounded by a smaller scarp up to 1 m height. The horizontal displacement reached here 15 m and 4 houses were affected, two of them later repaired.

The section downslope from the road was the most dynamic and complex. Here two major depletion zones were formed, reaching up to -8.5 m in relation to the original topography (Fig. 25). The major accumulation sector is located at the downslope part of the landslide reaching a maximum value of 12 m above the original topographic surface. The horizontal displacements were the highest in this section. The houses standing by the road and the road itself suffered displacement ranging from 45 to 50 m, and two further houses located few meters downslope were displaced 170m and 230m. At total, 7 houses were destroyed in this section of the landslide.

The Pequeno river was blocked and suffered a horizontal displacement southward reaching 28 to 30m. The river is now entrenched in the affected material.

Table I. Morphometric parameters of Calhandriz landslide

Slope Characteristics	Dipping of layers	12°N176°
	Slope aspect	136°
	Slope height	210 m
	Slope length	1036 m
	Slope angle	9°
Landslide morphometry	Max. length	1010 m
	Max. width	316 m
	Estimated depth	12 m
	Total area	181,360 m ²
	Estimated volume	1297,850 m ³

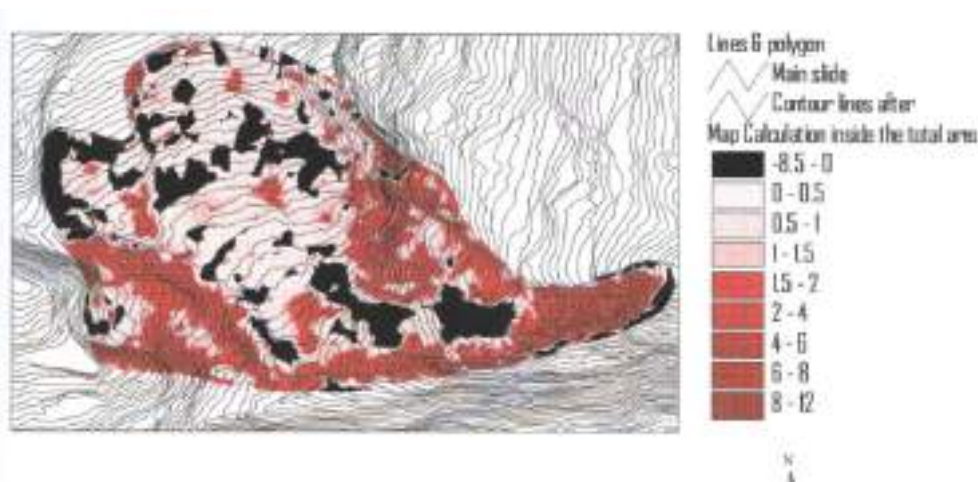


Figure 25. Topographic changes produced by the Calhandriz landslide (van Drunen, 2000).

Landslide typology and dynamics

The Calhandriz landslide is a complex slope movement, with a main slide (translational) component forwarded by the presence of relatively permeable rocks and soils (marly limestones and slope deposits) overlying a clay bench that will act as slip surface. The near concordance between the value and direction of the dipping of the layers and the slope angle and aspect is impressive (Fig. 26).

Within the displaced material there occurred localised rotational slide movements, as confirmed by the backward tilting of some houses and by the numerous reverse slope angles that were preserved few days after the landslide occurrence.

In the downslope part of the landslide, where the original fluvial channel was blocked by the displaced material, an earthflow occurred.

In the 9th February 1979, the landslide is likely to have been initiated in its downslope section, probably in relation with higher pore-water pressures next to the Pequeno river. The failure will then have progressed in retrogression. The retrogressive failure was accompanied by successive reactivations in the downslope section, with new scarps

opening within the displaced material, which explains for the greater amplitude of the horizontal displacements that occurred there.

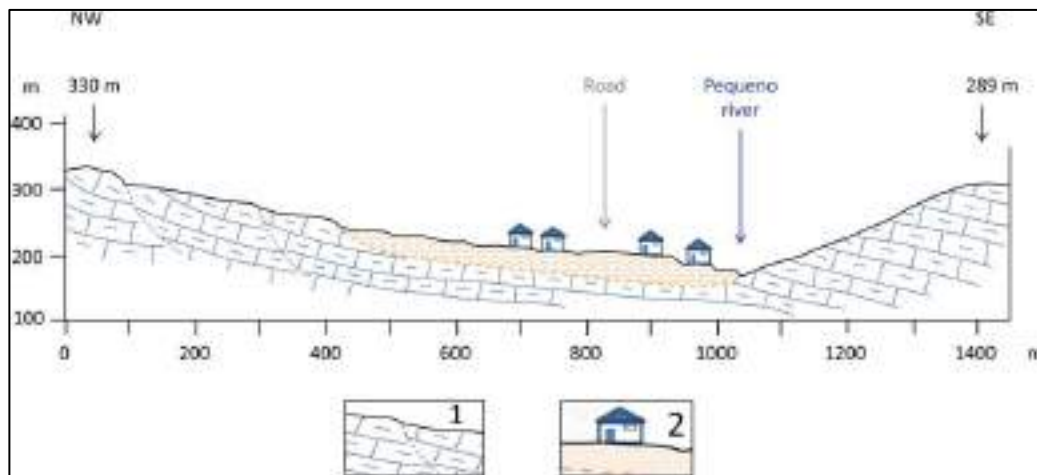


Figure 26. Schematic profile of the Calhandriz landslide. 1. Old landslide scars in marls and marly limestones; 2. Calhandriz landslide mass and affected houses (adapted from Ferreira 1984; Garcia & Oliveira, 2020).

Stop 4. Mata - Landslides and landslide susceptibility assessment in the Grande da Pipa River (GPR) basin, Arruda dos Vinhos

Geological and Geomorphological setting

The Grande da Pipa River basin (Arruda dos Vinhos) has 110.6 km² and is elongated 15 km in the west-east direction (Fig. 27). The elevation ranges from 440 m asl at the west to 5 m asl at the east, near the confluence of the GPR mouth with the Tagus River alluvial plain (Oliveira *et al.*, 2015). The regional geology is dominated by sedimentary materials of Upper Jurassic age (Fig. 27), which are deformed by a wide curvature angle tectonic rebound centred in the Arruda dos Vinhos region (Zbyszewski and Assunção, 1965). In detail, eleven lithological units (LU) were identified in the GPR basin, dated from the Oxfordian (?)–Lower Kimmeridgian to the Holocene. From these, the alternation of limestone, marl, clay, and sandstone dated from the Kimmeridgian to the Lower Thitonian is prevalent in 95.7 % of the study area and represent four major lithological units (Zbyszewski and Assunção 1965): (i) LU 5 (5.8 %) - limestones and marls (150 to 250 m thickness, lower Thitonian; Kullberg *et al.*, 2006); (ii) LU 6 (16.1 %) - mudstones, sandstones, marls, and limestones dated from the upper Kimmeridgian (65 to 130 m thick; Kullberg *et al.*, 2006); (iii) LU 7 (16 %) - coralline limestones (30 to 80 m thick, strongly variable vertically and laterally, upper Kimmeridgian, Kullberg *et al.*, 2006); and (iv) LU 8 (57.8 %) - marl, clay, and sandstone complex (800 m thick, Kimmeridgian); the marls are frequently sandy and micaceous, with calcareous or limonitic nodules and sandstone intercalations (Zbyszewski and Assunção, 1965).

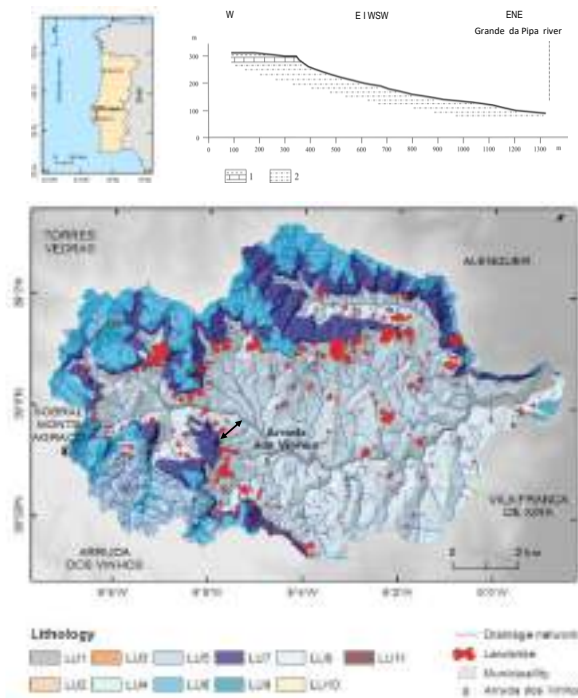


Figure 27. Map showing geology and landslide distribution in the Grande da Pipa River (GPR) basin. Lithological units are classified according to age criteria: LU1—Alluvium; LU2—Limestone intercalations; LU3—Conglomerates, sandstones and mudstones; LU4—Sandstones, marls and limestones; LU5—Limestones and marls; LU6—Mudstones, sandstones, marls and limestones; LU7—Coralic limestones; LU8—Limestones; LU9—Marls, mudstones and sandstones; LU10—Conglomerates; and LU11—Dykes and magmatic intrusions (adapted from Garcia & Oliveira 2020; Oliveira, 2012, Oliveira *et al.*, 2015).

The alternation of rocks, with different permeability and resistance to mechanical and chemical erosion, defines nowadays the presence of an important erosive basin with a significant fraction of the older and softer rocks (LU 8) lying in the central part of the basin (differential erosion promotes a structural relief inversion), where gentle slopes are dominant (slope angle lower than 15° occurs in 87.5 % of the study area). Above this unit, the coralline limestones (LU 7) originate the steepest slopes within the basin (limestone walls - 10–20 m high rock faces). Because of this geomorphological control, slopes within the GPR basin are essentially of the anacinal type, as the layers dip gently to the exterior of the basin in relation with the timeless erosion of the tectonic rebound structure.

Landslide incidence

The Grande da Pipa River basin (GPR) is recognized as a major landslide prone area within the north of Lisbon region (Oliveira, 2012). The landslide inventorying of the study area was mainly based on the systematic geomorphological field survey at the 1:2000 scale (2006-2010) and on the interpretation of aerial photographs and ortophotomaps obtained in different time periods (e.g., 1983, 1989, 2007, 2012). The analysis was complemented with the field interpretation of landslide morphometric features, and with a shadow relief model from a 1:10 000 digital elevation model (DEM). Landslide

morphologic evidence tend to disappear in 10 to 20 years, and even early if the unstable terrain is subject to agricultural activity (e.g., vineyards or cereals) or to development activities (e.g., urbanization). Therefore, landslide typology and landslide limits were defined sometimes through the identification of geomorphological features that were frequently degraded or even completely obliterated by human action (modification of surface runoff and subsurface drainage and changes in topography in the unstable areas as well in the surrounding areas are common practices in the region). Field survey allows to build a list of landslide fracture types and deformation patterns, essentially in the built elements (houses, roads) helping to map the different landslide types that occur in the GPR basin (Fig. 28).



Figure 28. (A) Damage and deformation patterns associated to landslide activity in the GPR basin. (A) Oblique fractures in building, (B) translational/vertical displacement fractures in building, (C) Building back tilting; (D) Vertical fractures in building, (E) Lateral displacement of wall, (F) Vertical fractures in wall; (G) Translational displacement on wall vertical fracture; (H) Hummocky deformation on wall and road, (I) Leaning trees; (J) Fractures and deformation of wells; (K) parabolic fractures on road, (L) lateral displacement on road fractures (M) Fractures perpendicular to the road track, (N) fractures parallel to the road track; and (O) Cross fractures on road (adapted form Oliveira *et al.*, 2015).

The historical landslide inventory for the Grande da Pipa River basin includes 1434 landslides (Fig. 27), mainly of the slide type (96% of the total landslide inventory), affecting 5.9% (6,484,402 m²) of the basin (Oliveira, 2012; Oliveira *et al.*, 2015). The landslide density is of 13 landslides/km², one of the highest in the north of Lisbon region. Landslides are typically small (from 7 to 262,000 m²) with a mean area of approximately 4500 m². The largest and most destructive landslides are deep-seated rotational slides

with a slip surface depth >1.5 m. 570 landslides of this type were inventoried, representing 93% of the total unstable area in the GPR basin. The shallow slides (slip surface depth ≤ 1.5 m) are dominant in number (799 shallow rotational and translational slides, both in natural and artificial slopes—cuts and fills) but represent only 6% of the total unstable area in the basin.

The causes of the landslides affecting the clays and marls of the Abadia complex (LU9) were summarized by Alonso *et al.* (2010) and are mainly related to changes in water content (effective stresses) and changes in soil suction, after heavy rain periods, which degrade the clays and marls in terms of their mechanical properties (strength, cohesion, loss of cementation, bonding and stiffness). This physical disaggregation, together with the succession of wetting and drying cycles that induce plastic deformation, promotes the water entering the rock, thus reducing shear strength. In addition, modifications of surface run-off, subsurface drainage (e.g. use of drains) and topography (e.g. terrain landfills and excavations) in the unstable surrounding areas are common practices in the region and contribute to the occurrence of new landslides or reactivation of the old ones. Most of the landslides inventoried in the GPR basin were triggered by rainfall. However, the landslides are not more frequent in the lower part of the slopes, where the ground water table is typically higher. The largest landslides show their main landslide scarp near the contact between the clays and marls (LU9) and the limestones (LU7) that outcrops in the upper part of the slopes. The intense fracturing that exists in the ductile limestone formation allows for their high permeability, whereas slow percolation of water along the clays and marls underneath it allows for deep soil saturation in the upper part of the slope after long-lasting rainfall events.

Landslide susceptibility assessment and mapping

Landslide susceptibility maps were produced for the main landslide types that occur in the GPR study area: deep-seated rotational slides; shallow rotational slides and shallow translational slides. A similar susceptibility modelling approach to the one applied to susceptibility maps of STOP 2 – Trancão Valley was used in the GPR study area. Seven thematic layers were used as landslide predisposing factors: slope, aspect, slope plan curvature, lithology, soil thickness, Slope Over Area Ratio (SOAR), and Topographic Position Index (TPI). The Information Value bivariate statistical method was selected to weight variable classes. For training and validation purposes each landslide type inventory was divided in a training and a validation subset, based on a random partition 70/30 % of the landslides number, respectively.

Classified and non-classified susceptibility maps are shown in figure 29**Figure**. Five landslide susceptibility classes were defined based on the prediction rate curves (Fig. 30). These five classes should include the area necessary to cumulatively validate 50%, 70%, 85%, 95% and 100% of the slide area of the validation group and were designated as “Very High Susceptibility”, “High Susceptibility”, “Moderate Susceptibility”, “Low Susceptibility” and “Very Low Susceptibility”.

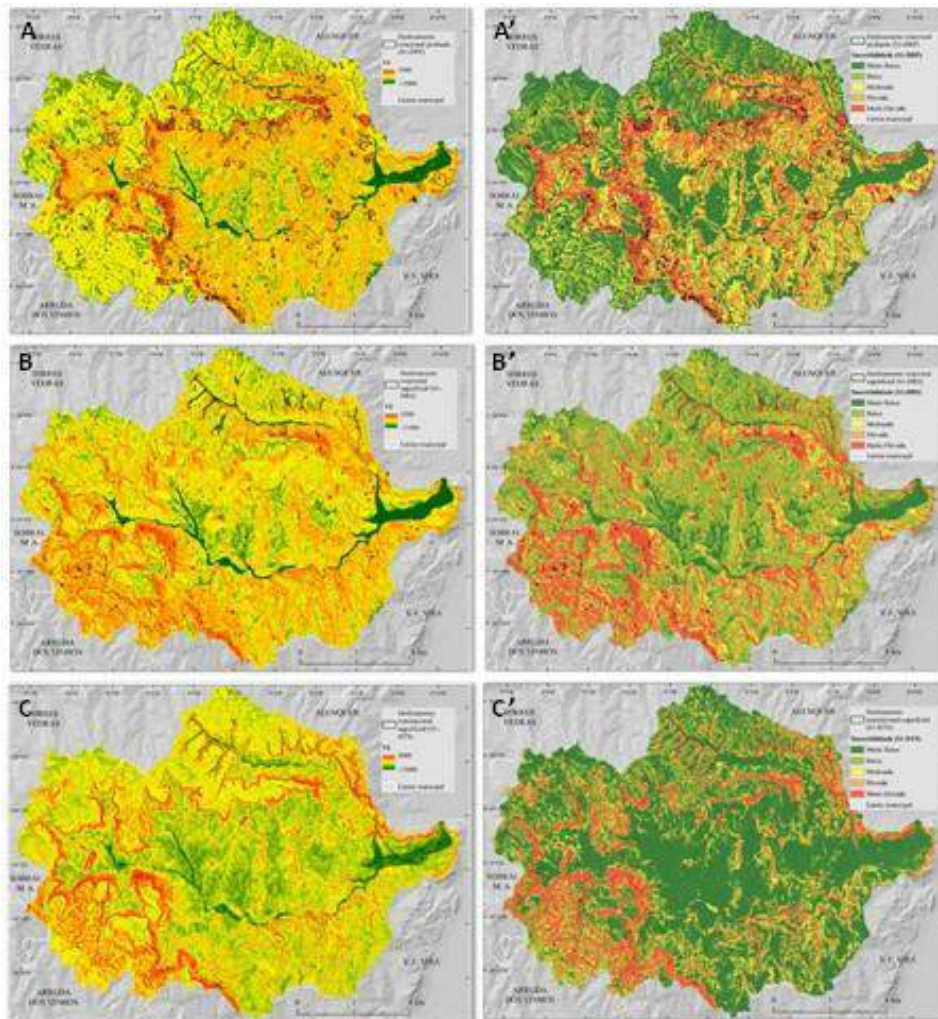


Figure 29. Landslide susceptibility maps of the GPR study area – A / A') Susceptibility maps to deep-seated rotational slides (classified/not classified map); B / B') Susceptibility maps to shallow rotational slides (classified/not classified map); C / C') Susceptibility maps to shallow translational slides (classified/not classified map).

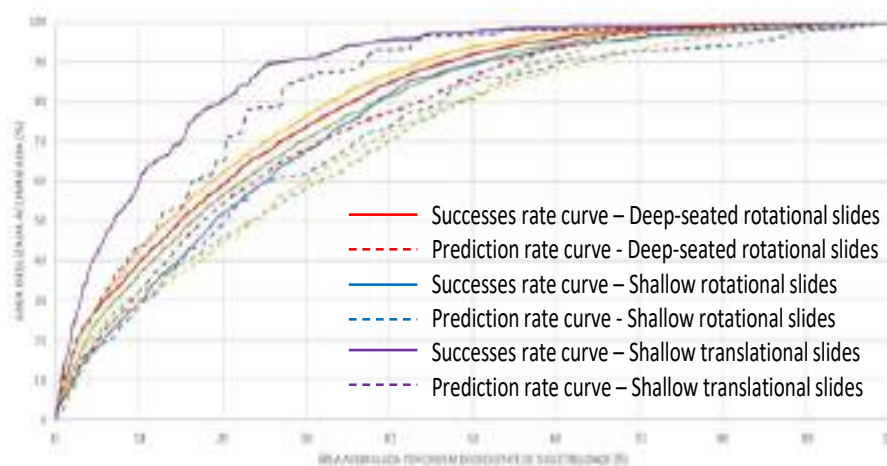


Figure 30. Successes and prediction rate curves of the different landslide susceptibility maps of the GPR study area – A / A') Susceptibility maps to deep-seated rotational slides (classified/not classified map); B / B') Susceptibility maps to shallow rotational slides (classified/not classified map); C / C') Susceptibility maps to shallow translational slides (classified/not classified map).

Different spatial susceptibility patterns are recognized for the different slide types, reflecting the different the spatial distribution of shallow and deep slides within the GPR study area and the different predisposing conditions that promote these types of slope instability phenomena.

As in STOP 2 – Trancão Valley, landslides in the GPR basin are also an important source of risk. A significant number/part of villages, scattered houses, and infrastructure (road network) are present in hazardous zones. Also, during the last decades, landslides have produced significant damages to property as well as the widespread disruption of roads (Fig. 31), which were responsible for significant direct and indirect economic losses. Even so, some increase in exposure is possible to depict for recent years, with the widespread construction (scattered houses or recent urbanizations) over high and very high deep-seated rotational slides susceptible areas (Fig. 32).

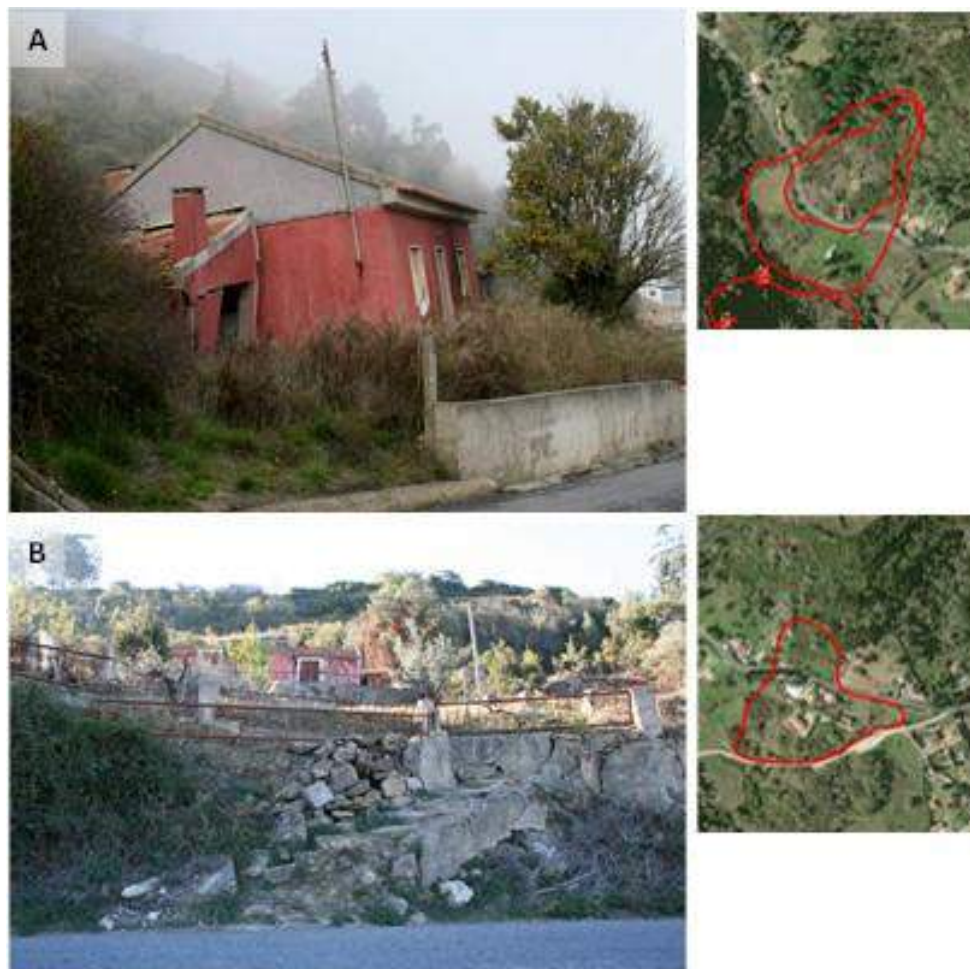


Figure 31. Buildings affected by deep-seated rotational slides in the GPR basin. A) House back tilting; B) House affected by the slide right flank (2015).



Figure 32. Exposure to Deep-Seated rotational slides for 2004 (upper figure) and 2021 (bottom figure). Red polygons indicate high to very high susceptibility to deep-seated rotational slides. Yellow line polygons represent the landslide limits (adapted from Oliveira *et al.*, 2015).

PSInSAR spatial distribution and deformation velocities (LOS) of landslides in the GPR basin

The potential contribution of PS deformation maps to landslide hazard in the Grande da Pipa River basin was evaluated by exploring a TerraSAR-X SAR data set of PSs. The terrain deformation was measured between April 2010 and March 2011 for the small test site of Laje-Salema, which is in the south-central part of the study area. The resulting data set (Fig. 33) have 1,468,999 PSs, from which 10,749 PSs are in the GPR basin. The ground deformation is given by the PS velocity, measured in mm/year and the estimated PS velocities are the mean velocity for the period covered by the interferograms. PS terrain deformation data allows to identify 13 new potential landslides and to redraw new landslide limits for 13 previously mapped landslides using also aerial photo and topographic interpretation helping to identify potential landslide features. The landslide state of activity was updated for 39 landslides (11 % of the 344 inventoried landslides).

The number of PSs per landslide ranges from 1 PS (17 cases) to 69 PSs (1 case). This result indicates that the number of PSs is more dependent on the presence of human

elements (non-natural terrain reflectors) than on the landslide area, even considering the detailed ground range resolution of TerraSAR-X (1.7–3.5 m).

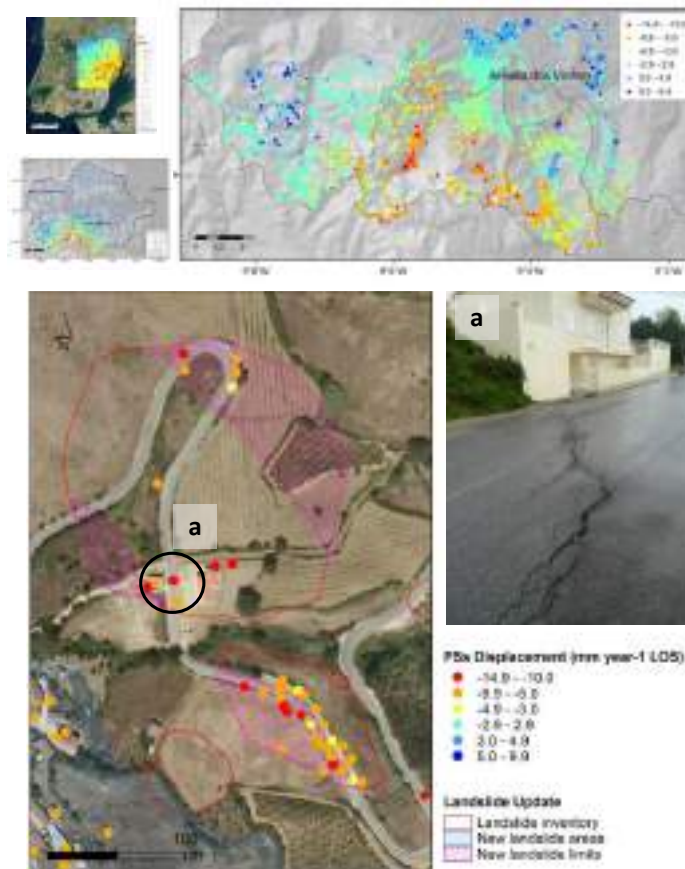


Figure 33. PSInSAR spatial distribution and deformation velocities (LOS) in the GPR basin (upper maps) and landslide field deformation in hotspot landslide areas identified by PSInSAR monitoring (bottom) (Oliveira *et al.*, 2015).

In fact, a substantial fraction of the large landslides in the test site occurs on cultivated or abandoned agricultural terrains, which explains the relatively low number of PSs. Furthermore, the reduced number of PSs may also be related with the deformation velocity inside the landslide mass. Landslide activity in the Lisbon region is strongly dependent on the rainfall (irregular) regime. Consequently, the deformation of landslide mass in any moment in time can be larger than limits of deformation imposed by the PSInSAR technique, in this case 3.1 cm of deformation at each 11 days. During the PSInSAR monitoring period, the large majority of the 39 landslides, which are extremely slow-moving landslides with mean deformation velocities (LOS) between 2 and 10 mm/year⁻¹, typically occurred over 20/ 30 years ago, have registered some deformation in a certain point or in a particular landslide section, compatible with the dynamic behaviour of slow-moving landslides. The post-rupture creep deformation is not enough to generate superficial evidence of landslide displacement, such as tension cracks or secondary landslide scarps on natural terrains, but is sufficient to produce rupture signs in rigid structures and infrastructures like buildings and roads (Fig. 33).

Vegetation evolution by ecological succession as a potential bioindicator of landslides relative age in Southwestern Mediterranean region

Landslides have a direct impact in the ecosystem's dynamics being considered one of the main vegetation perturbation processes. The relation between vegetation cover evolution and time period after landslide disturbance was assessed, as well as the potential use of vegetation evolution within landslide areas as temporal bioindicators of landslide activity, in order to determine landslide relative age. Four rotational slides of known relative age, located in the Grande da Pipa River basin (Arruda dos Vinhos) were selected. The methodology includes four main steps: (1) to identify the flora and vegetation differences between the main landslide sectors (scarp, body, foot); (2) to find out if the differences in floristic composition and vegetation structure are reflected in the succession process; (3) to find out if the succession process has produced different seral stages along the longitudinal gradients; (4) to compare the succession process in landslide affected areas with the undisturbed adjacent areas. The data points towards a slow evolution of the vegetation in the period following the disturbance, being necessary long periods for the perturbed area reach vegetation characteristics similar to the ones of the unperturbed areas (Fig. 34). The progressive succession is rapid in the foot, slow in the body and extremely slow in the scarp. The presence of orchids in the body may be considered as an age bioindicator of more than 15 years since landslide disturbance. These landslides could be understood as unique habitats that function as biodiversity hotspots for rare and/or protected species. In the case of the older landslide (> 50 years), it corresponds to the evolved stage close to the potential natural vegetation (Lopes *et al.*, 2020)

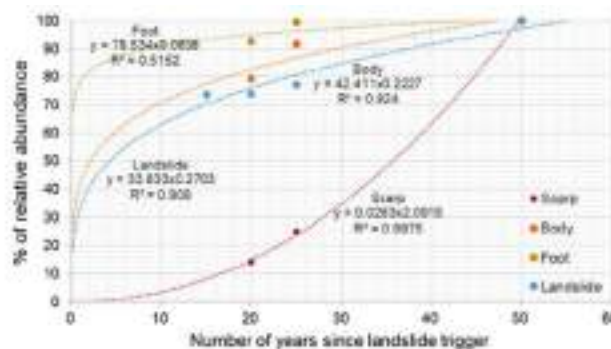


Figure 34. Trends of relationship between time from disturbance by landslide occurrence and vegetation relative abundance for the studied landslides and landslide sectors (Lopes *et al.*, 2020).

Stop 5. Quintas - Disastrous flash flood occurred in November 1967

The flash flood disaster

On the night of 25 November 1967 and early morning hours of the following day, the Lisbon area suffered the deadliest natural hazard since the ill-famed 1755 earthquake.

The occurred flash floods took everybody by surprise as most of the victims were at home sleeping and did not notice the rapid accumulation of water in small streams.

According to the DISASTER database (Zêzere *et al.*, 2014), 2045 people were directly affected by the November 1967 flash floods. The number of confirmed fatalities is 522, but this is certainly underestimated, because of censorship on newspapers imposed at that time by the Portuguese dictatorial political regime. In addition, 330 injured, 885 homeless, 307 evacuated and one missing people were reported.

Rainfall event and hydrologic context of the flash flood

The main cause for the disastrous floods is related to the large amount of precipitation concentrated during a few hours on the night of 25–26 November. According to the IB02 database the pattern of intense precipitation (above 75 mm) is oriented with a SW–NE axis and crosses roughly the central region of Portugal (Fig. 35A). Moreover, it is possible to observe an area where the daily precipitation surpassed the 120 mm threshold located over the metropolitan region of Lisbon. In addition, this extreme value corresponds to an anomaly above 8 standard deviation from the long term climatology (1950–2008).

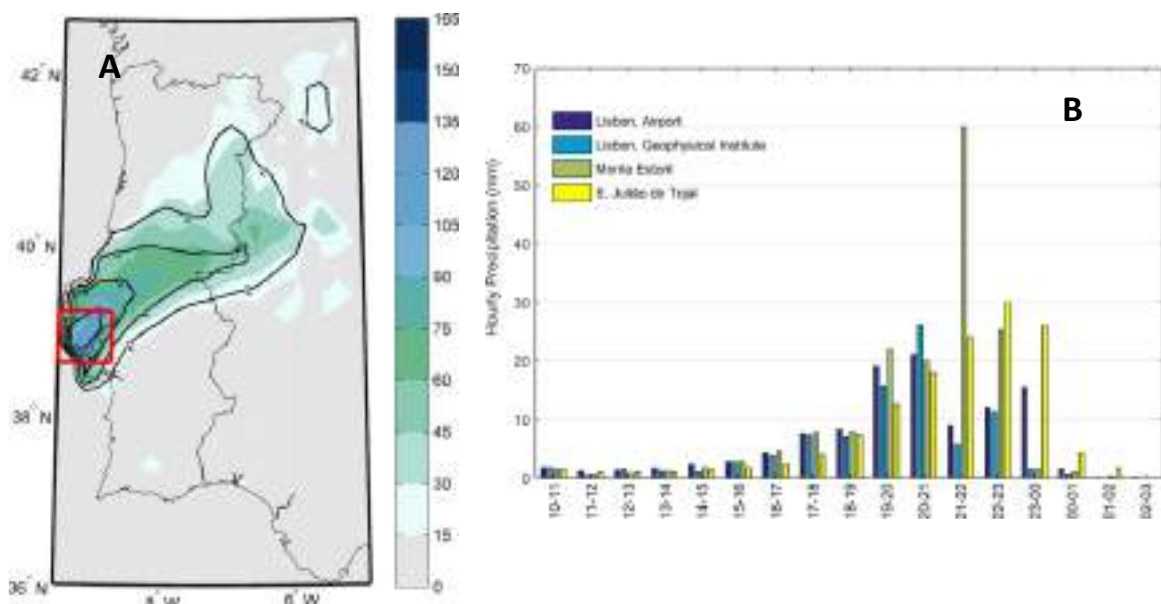


Figure 35. (A) Daily accumulated precipitation (mm, shaded) and corresponding standard deviation anomalies (black contour) for the 25 November 1967; (B) Hourly precipitation registered at four rain gauges located over the Lisbon region (see Fig. 35 for location) starting at 1000UTC of 25 November and ending at 0300UTC of 26 November 1967. Source: Portuguese National Weather Service (Instituto Português do Mar e da Atmosfera) (Adapted from Trigo *et al.*, 2016).

The 25–26 November 1967 flash flood event was triggered by an extreme rainfall event that reached 137 mm in 24 h, almost 1/5 of the mean annual rainfall at S. Julião do Tojal. Figure 35B shows the hourly rainfall registered at four rain gauges in the Lisbon region, starting at 1000UTC on the 25 November and finishing at 0300UTC on the 26 November.

The hourly data shows that most of the rainfall was concentrated in just five hours (between 1900UTC and midnight).

Twenty small and medium size hydrographic basins were affected, covering 14 municipalities (Fig. 36). The maximum elevation within the hydrographic basins is 360 m asl. The main rivers have a slope comprised in the range 10–60 m/km and most of them (80%) are contained in the range 10–30 m/km. The prevalent low to very low permeable geological formations hinders the infiltration of water and increases the stormflow. As a consequence, the hydrographic network is well developed and the average drainage density is 3 km/km². The response times for the terminal section of the hydrographic basins range between 4 h and 5 h 40 m.

Another factor that increased the magnitude of the November 1967 flash flood was the tide that influenced the terminal sections of the hydrographic basins. According to the Portuguese Hydrographic Institute, the high tide was registered at 2150UTC on the 25 November and the highest levels of the tide occurred between 1835UTC and 0046UTC, thus matching the occurrence time of the flash flood.

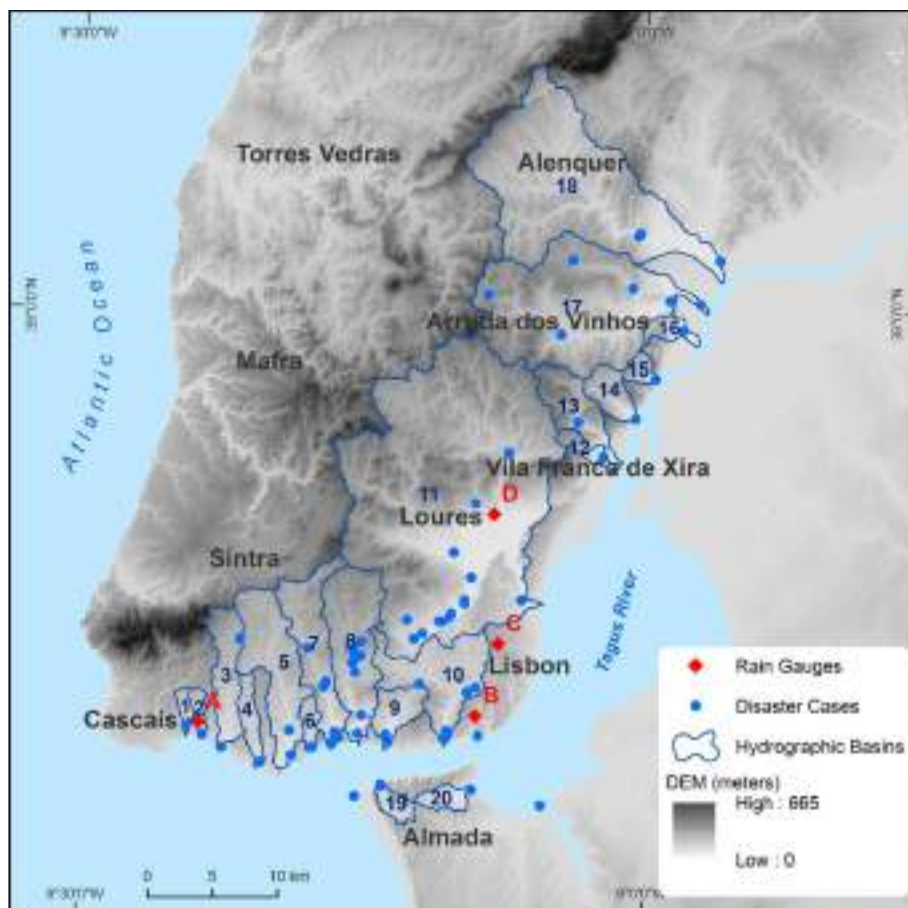


Figure 36. Location of the drainage basins affected by the November 1967 flash flood (blue numbers), the DISASTER cases (blue dots) and the rain gauges (red). 17 – Grande da Pipa. Rain gauges (red): A – Monte Estoril; B – Lisbon, Geophysical Institute; C – Lisbon, Airport; D – São Julião do Tojal (Trigo *et al.*, 2016).

The Quintas village case

The deadliest place of the 1967 flash flood occurred on a rural area, in the small village of Quintas (Fig. 37) where local conditions constituted a “trap” for the population. Quintas village is located in the terminal sector of the Grande da Pipa river basin, on the right bank of the river, between the floodplain and the slope bottom (Fig. 37). The hydrographic basin upstream Quintas village has an area of 108.7 km² (93% of the total basin), the river has a stream order 5 according to Strahler classification and 403 tributaries. The most important tributary is the Carnota stream that converges only 2240 m upstream of Quintas village.

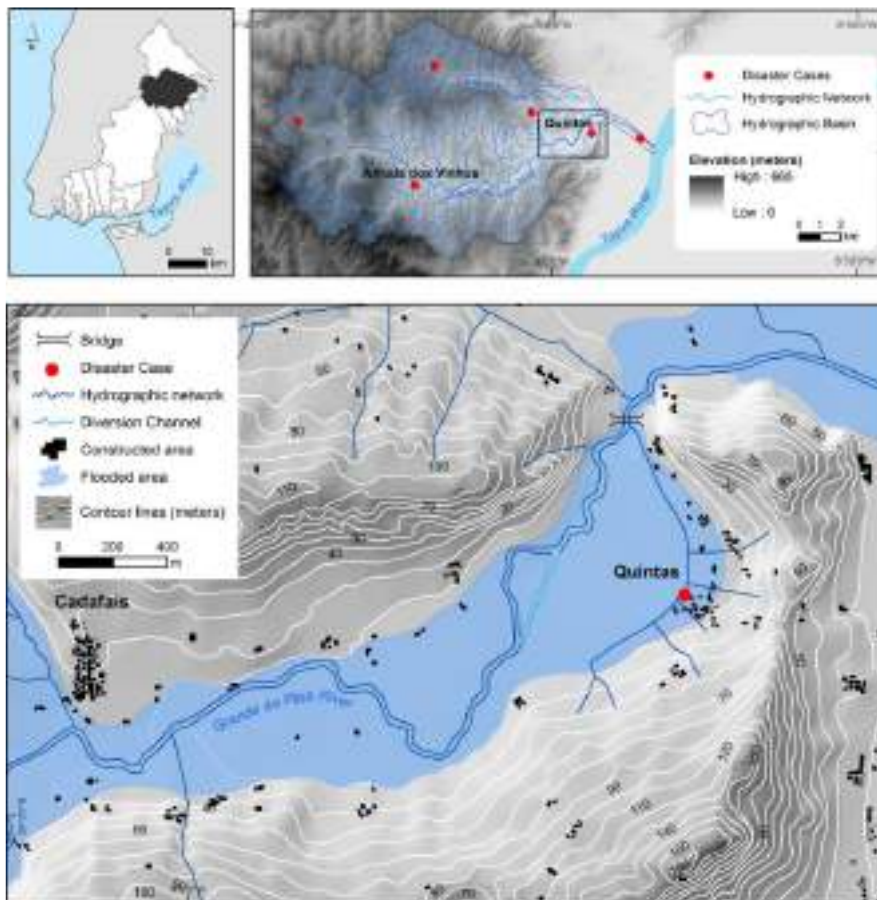


Figure 37. Details of Grande da Pipa basin (upper right panel) and Quintas village morphologic context and flooded area (lower panel) during the November 1967 flash flood along with the location of the human damages highlighted with a blue dot. Source: DISASTER database (Zêzere *et al.*, 2014; Trigo *et al.*, 2016).

The estimated peak discharge reached 441.5 m³/s, corresponding to 100-year return period. However, the disaster of Quintas is mostly explained by adverse local geomorphologic and hydrographic conditions, which have raised the height of water column at the bottom of the valley. In this sector, the floodplain is approximately 580 m width, with a slight slope towards the southeast. The most depressed area of the floodplain had a small yazoo stream, very close to the village, located near the concave

sector of the meander (Fig. 37). During the flood, this was a preferred corridor for the floodwaters circulation that swept through the central part of the village. Nevertheless, what exacerbated the flood height and affected area was the narrowing of the valley, 720 m downstream of the village (Fig. 37). This bottleneck is caused by interbedded limestone layers within the sandy clay complexes that make up the geological substratum of the region. In the narrow place the bottom of the valley is only 130 m wide and had a small bridge over the river, which was a barrier to the flood water circulation, loaded with debris and mud. The elevation of the water column was inevitable, and the flood covered the ground floors of the houses, many of which had only one floor.

According to the DISASTER database, in this village about 103 people died (70% of the total inhabitants). The resultant trauma led to the non-construction of houses where whole families died, extending the village, today, along the slope overhanging the valley. After the 1967 flash flood, a diversion channel was built to protect the village.

DAY 2 – THE COAST NORTH OF LISBON

Stop 1. Maceira – Structural and erosional landforms

Introduction

Portuguese Extremadura is rich in "subjects" for geomorphological research not only regarding the dynamics of current coastal systems, but also of inherited environmental systems. This is directly related its geographic coastal position. This situation gives it sedimentary characteristics related to the limits of the Portuguese Western Mesocenoic Rim (cf Introduction Chapter).

The coastal Quaternary of the Portuguese Western Mesocenoic Rim, and particularly the rocky coast between Cabo Carvoeiro and Cabo da Roca, stands out with geomorphological evidence resulting from the action of that mixed dynamics. Some of these evidences are not exclusive of the Quaternary. The littoral platform, which develops north from Serra de Sintra to Lagoa de Óbidos, has deposits of complex origin and is generally designated as polygenic (Cabral, 1993; Daveau *et al*, 1985; Vanney and Mougnot, 1981), and whose age will not go beyond the Palaeogene (Cabral, 1993).

Other evidence exists whose genesis is not associated with the concept of platform polygyny, but with the notching of the hydrographic network. Such geomorphological evidence corresponds to terraces and terrace deposits associated with the watercourses that cut through this sector of the coastal platform. Preliminary works carried out by Daveau (1973), in the terminal sector of the Sisandro River basin, show a succession of phases of stability and carving with very clear geomorphological testimonies such as

abandoned meanders at 70 - 60 meters (msl) or valley bottoms suspended over the present floodplain.

Representative sequences of raised beaches are also a geomorphological evidence of changes in the formation of these deposits in relation to the present day (Breuil and Zbyszewski, 1942 - 45). Rau and Zbyszewski (1949) refer to a sedimentary sequence which they call the "Grimaldienne beach" at an altitude of 16 metres, whose sedimentary testimonies they associate with ante-Würmian glaciations.

In this stretch of Extremadura coastline there is also clear and well sectorized geomorphological evidence of Quaternary chronology. The inherited dune fields and, mainly, the consolidated dunes of Magoito and S. Julião are attributed to the last maximum glacial and post glacial periods (Daveau, 1973; Daveau *et al*, 1983; Pereira, 1983; Pereira and Borges Correia, 1985).

The post-glacial period deposits is particularly disturbed in the terminal sectors of the hydrographic basins, as the sea level oscillations, in general, are known, either by direct observations or by spatial generalizations concerning nearby areas (Daveau, 1980; Dias, 1985; Dias, 1990; Dias and Taborda, 1988). The valley bottoms and the sedimentation contained therein are also important geomorphological evidences, however, these are still little studied, with few geosedimentological, palynological or geophysical studies. Much of this evidence is present in the terminal sector of the Alcabrichel River basin and associated with the Maceira diapiric depression (Fig. 38, Fig. 39).

The Alcabrichel River has a hydrographic basin at around 180km², starting in the in the western slope of the Montejunto mountain range. Carved in Mesozoic soils, with some lithological monotony (sandstones, clays and limestones), it has about 30km in length and a permanent hydrological regime, but regularly with little flow. However, the alluvial plain is more than 1 km wide in some sectors and indicates a great transport capacity during flood episodes.

The Alcabrichel River cuts the coastal platform that culminates in this sector at 160 meters of altitude, leaving its testimony in a series of other levels whose lowest is at about 20 m altitude.

From a lithostratigraphic point of view, sedimentary materials from the beginning of the Jurassic (Hetangian) to the present day can be found here, with the substratum consisting essentially of sandstones which are clayey, gravelly, but with the presence of compact limestones, a fact which naturally confers a differential and selective action to the erosive agents which shape the landscape.

The terminal sector of the Alcabrichel River basin is characterized by a particularly local and complex tectonic setting, associated with the presence of a diapiric structure at 500 meters from the river mouth, combining global (Cenozoic compression) and regional tectonic regimes. The Maceira diapir appears, thus, in the alignment of the Lourinhã fault and the Caldas da Rainha diapir, conferring a complex structural arrangement to

the materials, mainly in what concerns to the very competent rocks such as the compact limestones that border the diapiric depression.

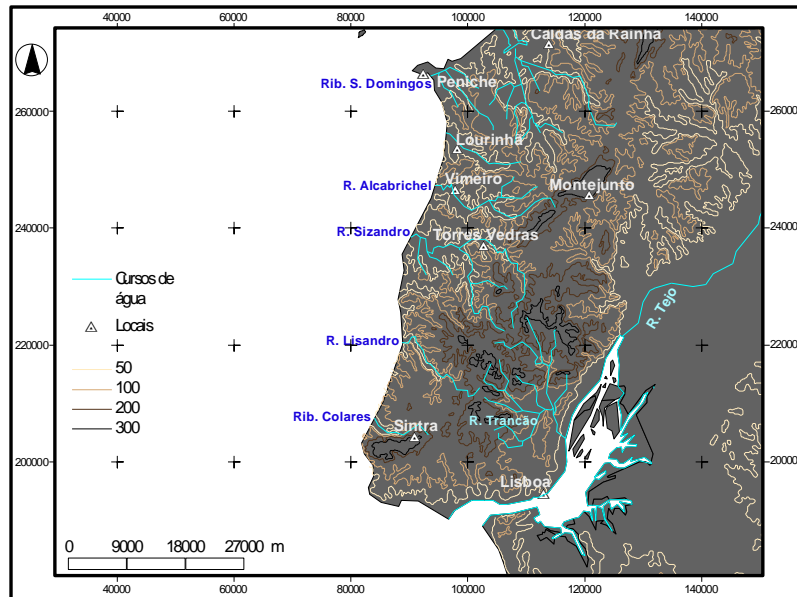


Figure 38. Location of the Alcabrichel River in Estremadura.

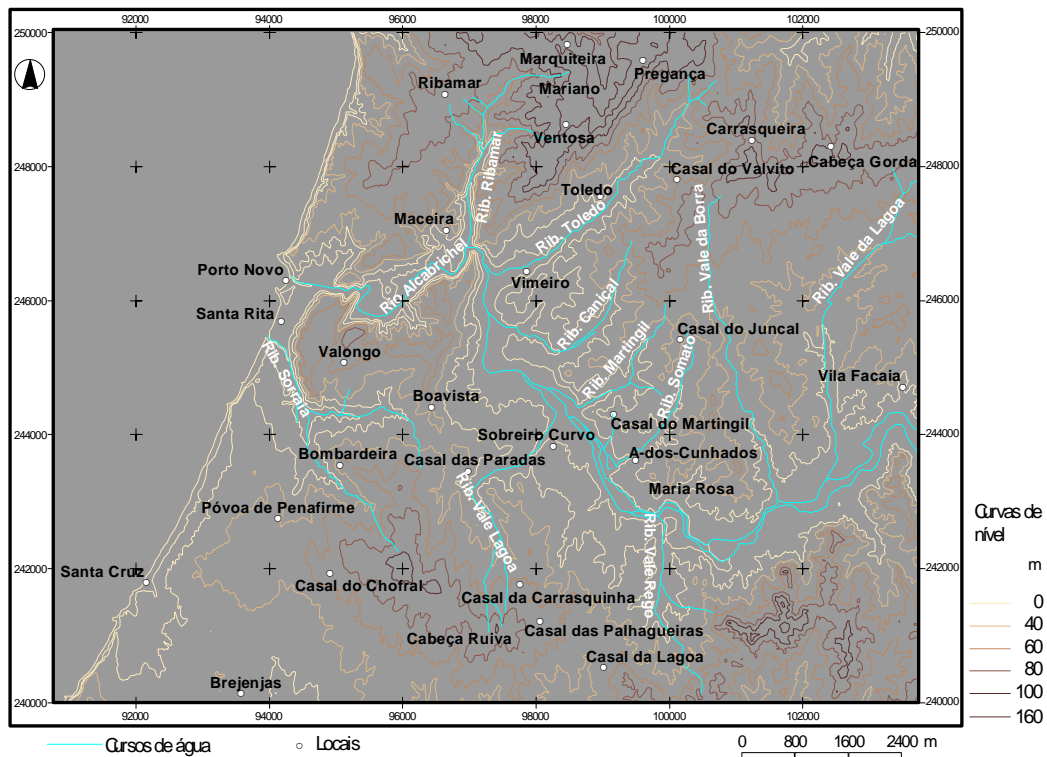


Figure 39. Terminal sector of the Alcabrichel River basin, the most important sites and watercourses.

In stratigraphic terms, we can find in this area the Mesozoic (Jurassic and Cretaceous) and Cenozoic layers, with the Jurassic formations dominating in outcrop area

(approximately 70% of the area). The Mesozoic-Cretaceous and Cenozoic formations have approximately the same area (Fig. 40).

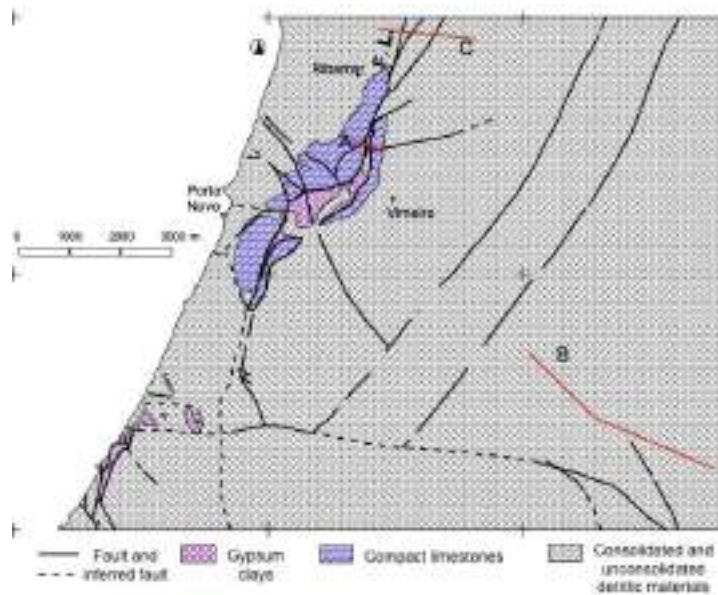


Figure 40. Lithological diversity and organization of the geological faults.
F.L. - Lourinhã fault. A – Location of the figure 39.

Jurassic lithostratigraphy

According to Manuppella, G. *et al* (1999), the oldest formation is the Hetangian that is mainly constituted by a pelitic-carbonate-evaporite complex composed essentially of gypsiferous and saliferous, deeply brecciated clays (Table II, Fig. 41). This lithological unit represents great importance from the point of view of the direct structural conditioning exerted on other units and, logically, on the morphology related to them. This conditioning is mainly due to the argillokinetic movements to which the marls are subjected (Ribeiro, 1984, p. 176). The "Dagorda clays", whose lower limit is not known, are at the origin of the diapiric alignment present between Maceira and Sta. Cruz (Fig. 39, Fig. 40), which extends northwards into the great diapiric depression of Caldas da Rainha. This alignment is installed along the great tectonic structure of approximate direction NNE - SSW, the Lourinhã fault (Fig. 3), and it is representative of the first rifting phase, preceding the opening of the Atlantic (Wilson, 1987 in Manuppella *et al*, 1999) and the first tectonic rifts.

The Lourinhã fault is, according to Manuppella (1999) "rooted in the basement" and, naturally, is conditioned by late-Variscan structures associated with it. The accidents whose direction is approximately transversal to the previous one is attributed to the activity of the diapir. One of the characteristics of the Dagorda unit is the absence of stratification and the sequences being highly tectonised.

Chronologically contemporary with the Dagorda clays, the dolomites are confined to the interior of the Maceira diapiric depression. This lithological unit is arranged in small

discontinuous nuclei underneath the Dagorda unit and, due to its superior resistance to erosion. Essentially, differential erosion processes originate a hard relief in the center of the depression. Both lithological units correspond to a marine environment where dolomite is generated by biological action or evaporation.

Table II. Simplified stratigraphy of the terminal sector of the Alcabrichel River basin.

Chrono-stratigraphic reference		Units and lithologies	
Ceno- zoic	Holocene	Alluviums, beach and dune sands (a, A, ad, d)	
	Pleistocene and Plio- pleistocene	Coastal and river terrace deposits (Q, P _s)	
Mesozoic	Cretaceous	Cenomanian	Clayey limestone with silt intercalations
		Aptian – Upper Barremian	Silts, mudstones, and sandstones
		Lower Barremian – Hauterivian	Clayey sandstones-
		Lower Hauterivian – Upper Valangian	Clayey silts
		Valangian – Upper Berriasian	Fine clayey sandstone
		Berriasian	Sandy silts, clays and coarse sandstones
	Jurassic	Titonian	Sandstones (fine and coarse), mudstones, and limestones (J ³ Bo; J ³ So)
		Kimeridgian	Compact limestones (J ³ Ap; J ³ V)
		Hetangian	Evaporitic layers of clays, dolomitic limestones (J ¹ Pl; J ¹ Da)

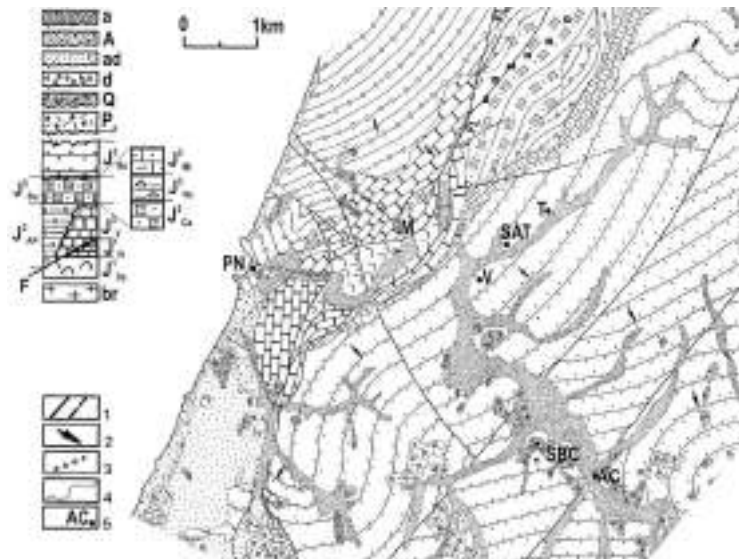


Figure 41. Lithostratigraphy of the lower Alcabrichel River. 1 – Fault and inferred fault; 2 – Layers inclination direction; Anticlinal axis; 4 – Layer limit; 5 – Site location.

The stratigraphic sequence present in the terminal sector of the Alcabrichel River basin is interrupted in the Hetangian, and there are no sedimentary traces relative to the

middle and upper Liasic and the entire Middle Jurassic. In fact, on the pelitic-carbonate-evaporite complex of the Dagorda clays settle the "Vimeiro Limestones", so called because they outcrop near that locality, with a Kimeridgian (Malm) age. The Vimeiro unit is related to the second rifting phase, where the Lourinhã fault would delimit to the W the tectonic rift created by the North Atlantic expansion process. With markedly marine lithofacies of low depth, this unit is particularly important in the definition of the Maceira diapiric depression, corresponding to quite resistant materials that form an abrupt along the depression due to differential erosion. This abrupt corresponds to a tectonic contact by reverse faulting between lower and upper Jurassic materials, whose morphological evidence reveals a fault line scarp. The fault mirror will have already been eroded on the top by the transgressive episodes which are at the origin of the coastal platform carved in the compact Vimeiro limestones and by the slope processes (essentially erosion by run-off) which nowadays affect the marls of the Hetangian unit (Fig. 41). The direct contact with the "Dagorda clays" gives to this unit a high degree of tectonic deformation that sometimes reaches values of layer tilt superior to 70°. The anticlinal alignment is established along the Lourinhã fault, having there, roughly, its axis (Fig. 42).

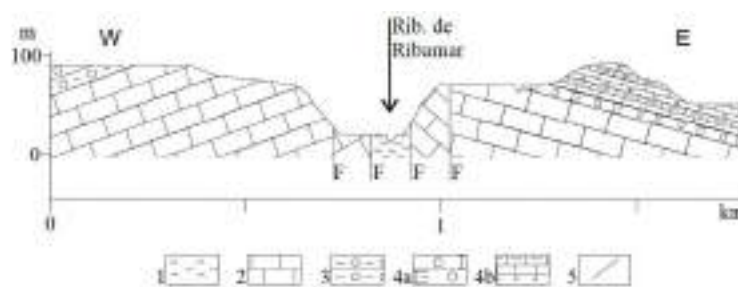


Figure 42. Anticline fold to the N of Maceira. 1 – Gypsum clays "Margas de Dagorda"; 2 - Vimeiro limestones; 3 - Praia de Amoreira and Porto Novo unit; 4 - Sobral unit: a - Clays and Sandstones of Castelhanos; b - Limestone, clayey sandstone and Miragaia marls; 5 – Fault.

Contemporary with the previous formation, the "Sandstone, marl and sand of Praia da Amoreira and Porto Novo" is a lithological unit of coastal (or transitional) and continental facies which, according to Hill (1989 in Manuppella *et al*, 1999), is attributed to the existence of a system of alluvial cones directly related to the tilting of the Lusitanian Basin margin. This unit is also important because it contains a deposit of dinosaur remains.

Cretaceous lithostratigraphy

In the terminal sector of the Alcabrichel River basin, the Cretaceous sedimentation is only represented until the beginning of the Middle Cretaceous, appearing in discordance with the Jurassic and after the second rifting episode. The definition of the transition between the Kimeridgian and the Berriasian is not consensual, as the materials present in Santa Cruz, attributed to the Upper Jurassic are the object of doubts by Wilson (1979),

who refers to a cretaceous age for them according to palynological and micropalaeontological analyses.

Based on the Bombarral unit, the Berrasian is characterized in the study area by the Serreira unit, which is essentially sandy, continental and has a fluvial facies, demonstrated by the presence of interbedded structures. The dimension diversity of the materials is high, from conglomeratic, coarse and fine sandy elements to kaolinitic clays.

Similarly, the Vale de Lobos unit also presents intercrossed structures, but the dimensional spectrum of the grains of which it is composed is restricted to sandstones, silts and clays. This unit, without facies variation, is attributed to the Upper Berriasian - Valanginian.

The sedimentation in the transition between the Valanginian and the Hauterivian is characterized by two formations whose thicknesses have little expressivity in the area. The Sta. Susana / S. Lourenço unit is composed of clays, silts of fine to coarse grains and, although assumed in the same chronostratigraphic spectrum, the S. Lourenço formation is older, being attributed by Manuppella (1999) to the Valanginian. The limits are established by the presence of deposits with ferruginous crusts between this unit, the older Vale de Lobos unit, and the more recent Lugar de Além unit.

The Lugar de Além unit also fits into the transition referred to above and is essentially made up of clayey or sandy silts. This unit encloses a sequence that can be considered globally positive, in the Lower Cretaceous, composed of the formations mentioned above.

The transition between the Hauterivian and the Barremian is represented by an increase in the energy of the deposition medium, however the sequence of the Fonte Grada unit, referred to this geological spectrum, is composed by dimensions of the materials in a positive sequence, showing towards the top the reduction of the transport energy.

The transition from the Barremian to the Aptian and the entire Aptian is characterized by the two component terms of the Almargem unit. This unit corresponds to the end of the Lower Cretaceous, in the terminal sector of the Alcabrichel River basin, and its two terms are separated by a ferruginous crust, with an increase in the caliber of the materials, essentially gresosaceous and conglomeratic, towards the top.

From the middle Cretaceous there is only the Casal do Marco unit (Cenomanian), whose expressivity in the study area is small. However, it is constituted by marly limestones, marls and sandstones, probably already framed in the transgressive environment that characterizes the early part of the Middle Cretaceous.

Although affected by some faults, the evidence of tectonic movements in the Cretaceous represented in the area seems to be small, giving rise to a structure, although undulating, almost tabular, whose layer inclination values are about 4° (Fig. 43).

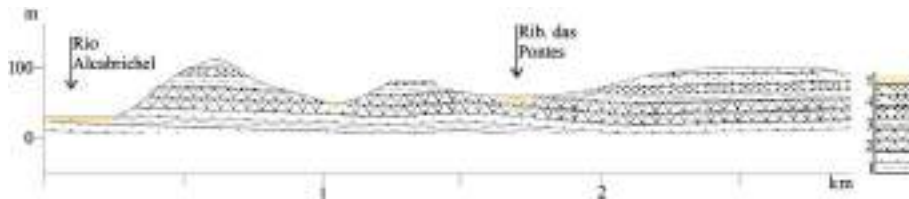


Figure 43. Cretaceous lithostructure. 1 – Serreira unit; 2 – Vale de Lobos unit; 3 – Sta. Susana e S. Lourenço units; 4 – Lugar de Além unit; 5 – unconsolidated deposits. (B in figure 40)

Cenozoic lithostratigraphy

After Mesozoic sedimentation, there is a large sedimentation hiatus that covers the entire Tertiary. In fact, from the Paleogene and Neogene eras only the discordant deposits of the late Pleistocene are represented. This hiatus of more than 60 million years poses some difficulties in the interpretation of the materials present in this area and relating to the Cenozoic era, since the intense erosion or alteration of the ante-Turonian materials leaves open not only the genesis of the discordant materials but also their chronological referencing.

Thus, the Cenozoic only provides lithological information concerning the Plio-Pleistocene transition and the Quaternary (Pleistocene and Holocene) (Mannuppella *et al*, 1999), corresponding to the oldest materials presented in the study area within this chronostratigraphic spectrum. These materials, corresponding to the Silveira Unit, outcrop in the SW sector of the area and are essentially characterized by fluvial facies, where it is sometimes possible to distinguish more clayey levels. These sands are generally very poor in macrofauna or even azoic, however, in a survey made 1 km NNE of the locality of Silveira there are two exceptions in the whole profile captured there. At about 20m from the surface it was possible to distinguish a sandier level with the presence of mollusks and at 56m depth another one with shells and scattered pebbles.

Given the lithological and faunal similarities with other deposits further north in the Caldas da Rainha region, Manuppella *et al* (1999) refer them to the transition between Pliocene and Pleistocene. The authors admit that a large part of the sequence is still in the Pliocene, but there is no reference to the dynamics that might have been responsible for the disappearance or impossibility of formation of the Paleogene and Neogene materials.

This gap raises some doubts already partially exposed above and which have to do with the fact that the origin of these materials is effectively linked to the first Fini or post-Pliocene drainage systems, resulting from a climatic cooling and a lowering of the base level, or if they result only from erosion or alteration of Mesozoic materials, enhanced during the whole Cenozoic and that with the successive lowering of the sea level during the Quaternary have degraded, suffering partial or total resettlement.

Already related to the Quaternary, pleistocene gravel deposits can be found along the Alcabrichel River and its tributaries and along the whole coastline, although with less expressiveness.

These materials have very different facies, since they are positioned in distinct sites and because they are found in discordance over distinct lithological units, which naturally affects their fundamental composition (gravelly, sandy, and clayey fractions) and mineralogical composition. Along the tributary creeks and the Alcabrichel River, the terrace unconsolidated materials, show a direct influence of previous incision phases of these rivers and the respective hydrological dynamics. However, it is possible to distinguish colluvial materials resulting from the dynamics of slopes associated to climatic frameworks different from the present day. Along the coast some raised beaches, whose facies will necessarily be different from the previous ones, reveal sand deposits with a pebble component. Both beaches have also characteristic elements of prehistoric occupation from the Palaeolithic to the Bronze Age, Manuppella *et al* (1999).

The materials present in the beach and beach-dune systems are referred by Manuppella *et al* (1999) to the Holocene.

Structural landforms

The forms linked to folded structures are, in the study area, expressed in the anticlinal Pia do Mestre (near Pregança) - Maceira - Valongo. As already mentioned, this anticlinal fold is roughly centred on the Lourinhã fault. However, to the NE of the diapiric depression, the axis shifts slightly to the east, with the fault becoming an integral part not of the axis, but of the western flank of the anticlinal in question (Trindade, 2001).

Resulting from the injection of gypsiferous and saliferous marly material along the fault (Dagorda clays), the overlying material is blistered, and some sectors can be distinguished in the same folded structure. In the first one, located to NNE of Maceira, the anticlinal is faulted in the West flank, and its axis is disposed at half slope only culminating with the summit in Pia do Mestre, North of the geodesic vertex of Mariano, being the anticlinal fold perpendicularly incised by small water courses affluent of the Ribeira de Ribamar.

The Lourinhã fault is associated with parallel faults, giving rise to tectonic compartments that helps to explain the asymmetries in the inclination values of the flanks of the anticlinal through their differential response to the kinetic energy associated to the Dagorda unit. As mentioned above, the inclination of the flanks tends to decrease towards NNE, revealing an increasingly deeper and less significant influence of the argillokinetic movements that affect the structure of the substratum. The existence of this area of fragility, derived from tectonics and structure, is related to the Ribeira de Ribamar valley.

In the SSW sector of the anticlinal, the fold is eroded, outcropping the Dagorda Margas in the center of the depression. The shape of the diapiric depression is not symmetrical,

i.e., it narrows towards NNE. Conjugating this fact with the decrease in the inclination of the anticlinal flanks in the same direction it becomes clear that the diapiric activity decreases as the thickness of the overlying materials increases and the rigidity in relation to tectonic stresses decreases.

The morphotectonic elements present in the interior of the diapir give the relief a very particular vigour in this area, expressing the consequences of its activity. In this sense, the Vimeiro unit, totally composed by compact limestones, is arranged in a hog-back or bar, reaching values of 90° inclination (Fig. 44).



Figure 44. Vimeiro limestone bars.

The difference in rock resistance to erosion has its maximum expressiveness in this sector, translated in the fault line scarps that can reach altitudes higher than 90m. As is the case of the Porto Novo gorge.

Corresponding to very resistant materials, the Vimeiro limestones, although extremely tectonised, are responsible for the confinement of the diapiric depression and for the conservation of its shape. It is a fact that the watercourses are, in these sectors, installed in areas of high tectonic fragility, but this valley is necessarily posterior to the "pliocene" levels related to the littoral platform expressed in the higher slope tops that "close" the depression. In this sense, the vigour of the gorges cannot only be explained based on the areas of tectonic fragility but, with a parallel action between this factor and a continuous uplift, the result of compressive efforts which intensify during the Pliocene. The dominance of compressive tectonics is attributed to the reapproximation of the African plate and continues through the Quaternary.

This interpretation agrees with the literature on diapiric areas in Portugal. Canérot *et al.* (1995) interpret the dynamics of the Caldas da Rainha diapir through the movement of the marls (argillokinesis) and with the consequent wrinkling of the overlying materials by base detachment, originating anticlinal structures. Another important fact is its relationship with the already mentioned Cenozoic compressive tectonics (inducing argillokinesis), which places its activity period closer to the present time in relation to what was assumed by Ribeiro *et al.* (1979), who considered, at the time of publication, its activity until the Miocene.

The polygenic coastal platform

The rates of relative rise or fall in sea level naturally cause changes in the configuration of landscapes. These effects are felt not only at the level of the marine hydrological systems and its action on the coast, but also in the whole continental hydrological system. Thus, the repercussions of the relative modification of the sea level are not limited to the range of oscillation of the coastline over thousands or millions of years but produce geomorphological evidence that often allows the assessment of significant environmental changes. This can be done by combining evidence in a particular area or by studying one piece of evidence in detail (e.g. a correlative deposit).

The study of landforms and their associated deposits, as testimonies of this oscillation, is only one of the tools frequently used to understand the impacts caused by the dynamics of the coastline on a longer time scale.

The first major evidence of this dynamic is present in the distinction of the genesis of the interfluves present in this area. These can be understood as a coastal platform geomorphologic unit. Although polygenetic, this coastal platform has its genesis in the coastal environment (interface) and in the several Quaternary levels related to the incision of the hydrographic network.

As mentioned above, the lack of information validating a clear distinction between the levels of the coastal platform and the cut of the drainage network prevents a complete approach to this problematic. However, criteria can be adopted that allow a relative approximation to this notion of transition between coastal and continental processes. In this sense, the spatial arrangement and the discontinuities in the representation of the morphological evidence (Fig. 45) of periods of base level stability, can correspond to a valid source of information concerning the transition between the littoral platform and the watercourses embedding. Following these criteria, the shelf levels were broken down into 3 morphological groups which is why they are represented as P1, P2 and P3 from the highest to the lowest in altitude respectively (Fig. 45, Fig.46).



Figure 45. Geomorphological map. 1 – Altitude; 2 - Slope top and base; 3 and 4 – Slope; 5 to 7 – “v”, “u” and planar shaped valley; 19 – town. P – Polygenic coastal platform; TI, II, III, IV, V – Fluvial terrace.

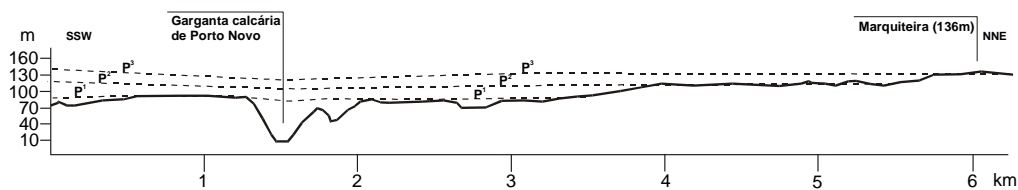


Figure 46. Topographic profile along the polygenic coastal platform levels near the Maceira depression.

Thus, the highest level of the coastal platform (P1) is found at altitudes varying between 130 and 160 metres in the NW sector of the area, corresponding to the interfluvium where the settlement of Ventosa and Pregança is located. With no traces of discordant sedimentary material correlative to this stabilisation episode of the base level, the interfluvium develops essentially on three types of Jurassic substrate: Miragaia, Nadrupe and Castelhanos units, already described above in the lithostructural framework.

Embedded in the previous, the intermediate level (Fig. 8) develops between 100 and 130 m altitude. This one, contrary to the previous one, has greater spatial expressivity, not being limited to appear associated or in the sequence of P1, as for example the interfluvium in which the locality of Ribamar is found. In fact, P2 is spatially represented by elongated patches in the NE sector of the area (Cabeça Gorda interfluvium), which constitute the headwaters of the Ribeira de Toledo. In the South sector (Fig. 8) it is also represented the level P2 but much less conserved. The materials of the substratum in which they are cut contribute to this fact, i.e., while P2 in Cabeça Gorda is cut in Jurassic-Turonian substratum (Bombarral unit), the P2 interfluviums of the SE sector

directly cut Cretaceous materials, alternating more detrital or more marly layers. The lithological change corresponds, therefore, to an essential factor in explaining the state of conservation of these levels.

The lower level of the Coastal Platform (P3) develops mainly on two quite distinct substrate types, the limestones of the Vimeiro unit and the sandstones of the Bombarral unit, being regularly found at elevations between 80 and 100 metres (Fig. 45).

On the right bank of the Alcabrichel river and at its mouth, P3 conservation is evident and two fundamental characteristics may be distinguished:

1. its spatial distribution following the highest tops (Cabeça Gorda level) from E to W, its spatial discontinuity being attributed to the progressive embedding of the drainage network. The fact that there is no evident correspondence in the left margin in relation to this level is related to a modification in the lithological nature of the materials and their different resistance to erosion, since in this margin outcrops of cretaceous materials also essentially cohesive, as is the case of the sandstones of the Bombarral titonian unit, but coarser and less cohesive;
2. the way it is disposed near the mouth of the Alcabrichel River, distributing itself perpendicularly to the river, with no traces of the progressive notching of the drainage network (Fig. 45, Fig. 47). The constitution of the materials in which the platform is carved in this sector corresponds essentially to compact and resistant Kimeridgian limestones. The power of the erosive agent necessary to create this level (P3) will have been such that lithological differences and areas of tectonic fragility would have been a minor factor in its formation (Fig. 47).

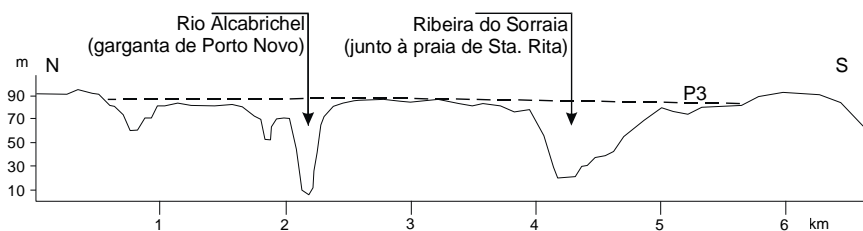


Figure 47. Topographic profile along the P3 level of the coastal platform near the Maceira depression.

Stop 2. Santa Rita beach -recent and present-day coastal dynamics

Evolution of the Sta. Rita coastal system during the last centuries

The coastal stretch between Peniche and Cascais is a wave dominated rocky coast highly conditioned by the Atlantic atmospheric circulation. This results in a clear seasonal differentiation of wave patterns.

The Peniche – Cascais coastal sector (Fig. 48) is lacking in sediment supply from longshore drift and local sources because: a – of the dominantly limestone nature of the

cliffs; b – the presence of two natural obstacles to sediment transport by longshore drift, that are the Nazaré Canyon and the Peniche headland; c – of the small sized river basins that are unable to effectively contribute to regional sediment budget.

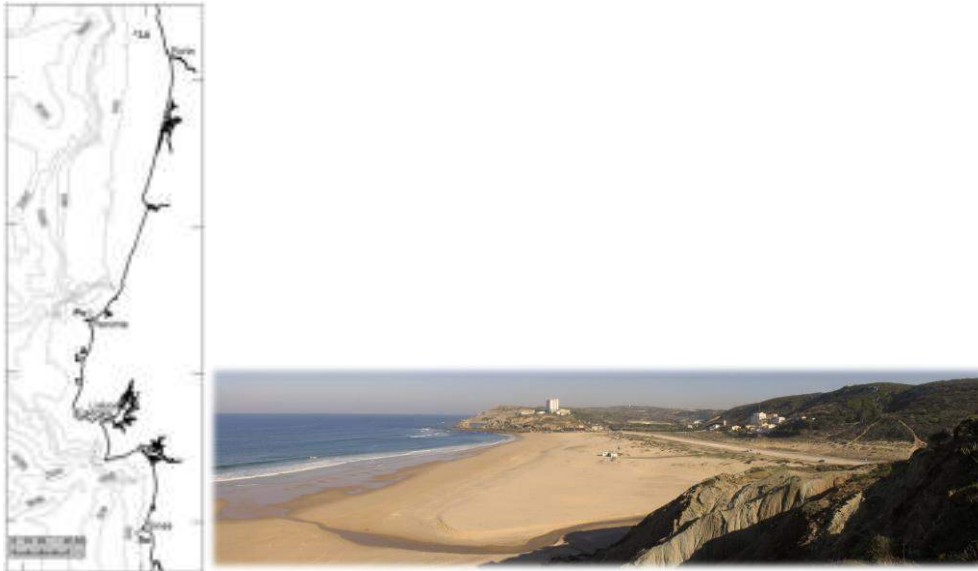


Figure 48. Portuguese coastal area. Sta. Rita beach.

In this coastal stretch beach systems are narrow, embayed and/or part of small estuaries. Sta. Rita beach is a composite beach system with two components of beach-dune in the northernmost part of the beach and a beach-cliff system in the south end. The dune field sub-component shows signs of heavy anthropogenic degradation with a dense trampling network and abundant deflation surfaces. Cliff sub-component dynamics is mainly dependent on continental erosion processes (Trindade, 2010; Trindade e Pereira, 2013).

The first documentary reference existing in relation to settlement attempts in the study area dates back to the 9th century. Around 850 a German hermit, named Ancirado, erected the first foundation of the Monastery of N. Sra. da Graça de Penafirme (later repositioned and rebuilt, it is currently in ruins and partially covered by inherited dune fields, in the Ribeira do Sorraia valley) in partnership with Benedictine monks, both fleeing from Muslim attacks in Torres Vedras and the fertile banks of the Sizandro River to the South. Here they found, besides a "deserted" and uninhabited place suitable for their retreat, the fertile lands of the Alcabrichel River valley and bases for a fishing activity based on the lacustrine fauna of the coastal lagoon in the mouth of the Alcabrichel river. This fact is evident in the chronicles of Frei António da Purificação (in Silva, 1999, p.83), when he, citing sources, described the triangle Maceira - Porto Novo - Penafirme as having large and fertile alluvial plains and the lagoon that was abundant in every kind of fish, and seafood.

Amorim Girão (1949-51), quoting the allegations of the General Attorney, Mr. Augusto Paes de Almeida e Silva, made in 1939 in the Court of Torres Vedras, and published in

Defesa do Património Nacional, by the Cultural Department of the Torres Vedras City Council, refers to the existence of a deep lagoon with outlet to the sea, which, still in the 9th century, existed sheltered on the Praia de Sta. Rita. In this sense, this stretch of coast would be characterized, around the ninth century, by a barrier lagoon system, whose depositional dynamics would still allow for the existence of a faunal diversity incompatible with advanced states of sedimentation known in the present day coastal lagoons (Fig. 49).



Figure 49. Recent secular evolution of the Sta. Rita coastal system.

After a scarcity of references between the 10th and 12th centuries, more data on the rebuilding of the monastery appears in the 13th century. The rebuilding is attributed to

the constant burial of the monastery by dunes and by reducing the amount of fish in the lagoon.

Besides direct evidence of a very recent and quite active geomorphologic dynamics, there are others that confirm it. The Monastery of Penafirme had a third rebuilding, pointed out by Júlio Vieira for the year 1597, which the ruins are still visible in the valley of the Ribeira do Sorraia. The reconstruction and repositioning of the Penafirme Monastery denounces a clear inadaptation to the geomorphologic dynamics of the place, dynamics that would have its origin not only in the strong winter winds, as stated in the descriptions, but also in the increase of the sedimentary availability to be mobilized through aeolian processes.

This whole succession of events may be seen in the context of a regional tendency towards the estuarine silting up attributed to the majority of Portuguese rivers, a fact that results from the direct action of man on the upstream slopes, deforesting them, intensified since the time of the discoveries. The main function of the port of S. Denis, today Porto Novo, denounces precisely a forestry supply activity so important that it would justify the construction of a cargo port.

The low volumetric capacity to accommodate sedimentation, derived from structural and morphological constrains, in relation to other lagoons today still in a phase of infilling (ex. S Martinho do Porto or Óbidos), mark the time lag in relation to the substitution of systems.

The whole system would have initially functioned with an erosive predominance, enhanced by the hetangian marly substrate (Margas da Dagorda) and by the morphology existing there, providing shelter from the dominant swell, but exposing a more depressed area more susceptible to mechanical erosion to southwest storms. The shelter conditions and sediment availability, associated to a dominant northwest swell, would have contributed to the development of a sandbank. This sandbank was fixed to the north and conditioned by the marine sediment transport dynamics and fluvial sediments provided the intensification of the deforestation of the surrounding areas. The abundant availability of sediment ended up being responsible, along with the exposure and morphology of the coastline and the dominant swell, for the total filling of the coastal lagoon and the replacement of this system by another with a distinct geomorphologic dynamics, the beach-dune system of Sta. Rita beach (Trindade, 2001; Trindade, 2010).

Concluding, i) the sedimentary dynamics of the coastline reported by the historical sources points to a rapid process of settlement, following the known trend in nearby systems; ii) the system dimension influenced the fast rhythm of substitution of coastal system types in Sta. Rita; iii) the sequence of coastal environments identified through the historical sources points to a deep reduction in the sediment transport energy, being

possible to anticipate the presence of: (i) an open estuary; (ii) a tombolo; (iii) a barrier lagoon system; (iv) a beach-dune/beach system.

Present day morphodynamics of the Sta. Rita beach system

Sta. Rita beach corresponds to a composite coastal system, with a dune beach component to the north and a cliff beach component to the south. A large part of this composite system lies on a small diapiric depression (Trindade, 2001), where a pelitic-carbonate-evaporite complex of Hetangian age outcrops, composed of gypsiferous and saline clays of extrusive character and named by Choffat de Margas de Dagorda (Manuppella *et al.*, 1999). The structural arrangement that this formation confers to the materials of the Vimeiro (compact bioclastic limestones) and Praia da Amoreira and Porto Novo (sandstones, marls and sandstones) units conditions the morphology and, consequently, the trapezoidal planimetric shape of the northern sector of the system (Fig. 50).

The cliff line, carved in the Unit of Praia da Amoreira and Porto Novo, is interrupted in this sector due to the presence of the mentioned diapiric depression, making possible the accumulation of sediments. These sediments and the shelter of the site from the dominant NW swell allowed the development of a sandbank and the constitution of a barrier lagoon system, which would still exist in the 9th century. The continued intervention on the slopes, through deforestation, led to an increase in sediment transport along the Alcabrichel River basin, the silting up of the Sta. Rita lagoon system, about 4 centuries ago, and its replacement by the present dune beach system (Trindade, 2001).

Beach planimetric dynamics

The planimetric shape of a beach depends primarily on the wave regime reaching the shoreline. The predominance of head and heights determines the way wave crests are refracted and diffracted and, consequently, influences the energy distribution along the coastline (Komar, 1998). This differentiation in wave energy distribution is often promoted by the presence of promontories that focus the convergence of wave crests, influencing the transport capacity along the coastline between the promontory, with higher energy dissipation, and the associated beach systems.

The frequency and magnitude of successive forwards and retreats of the shoreline and the constant modifications in the morphometric parameters of the beach plane are also influenced by the characteristics of the sediment sources that contribute to its nourishment, the rhythms of erosion/accretion and of sediment transport to and from the system.

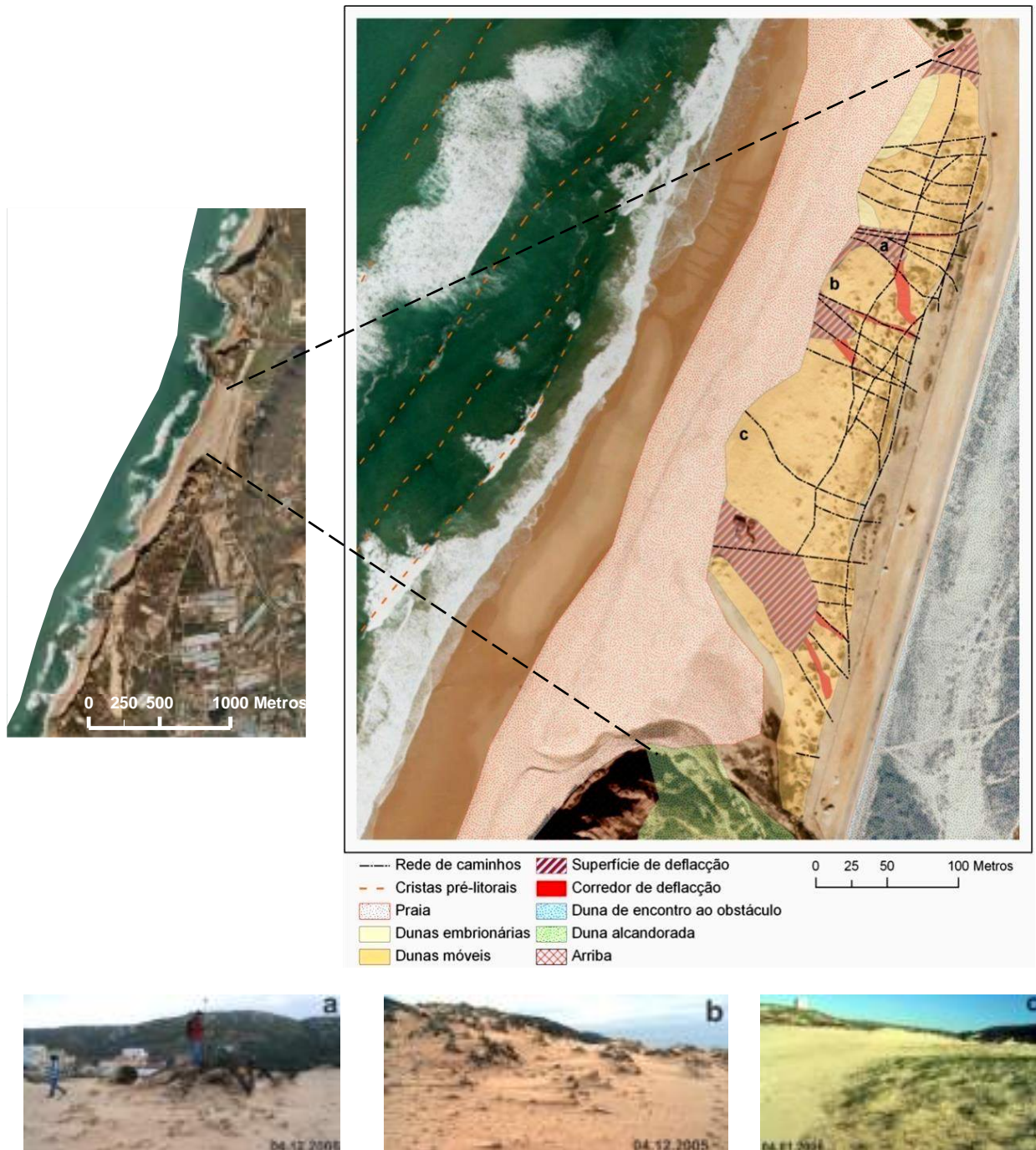


Figure 50. System components and degradation elements of the dune field at Sta. Rita beach. a - dune degraded by trampling; b - embryonic dunes; c - recent colonisation by *Elymus farctus* at the inner limit of the upper beach (2004 orthophoto map).

The average horizontal positioning of the mean sea level (nmm) observed in relation to the relative point of no mobility (pnmr – Fig. 51) is 88m at Sta. Rita beach.

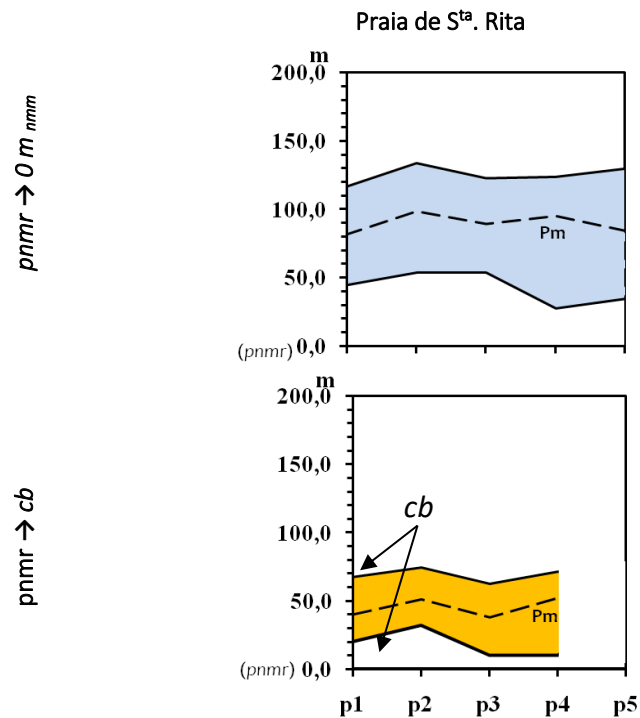


Figure 51. Planimetric dynamics of the Sta. Rita beach. pnmr - point of relative non mobility; cb - crest of the berm; nm - mean sea level; Pm - mean position.

Beach profile dynamics

The highest values of maximum altimetric differences were registered in the Sta. Rita system, reaching 6.4m (P2) and 5.5m (P1) (Fig. 52). Sand bars are almost absent from the beach profile measurements. This fact does not mean their inexistence, but rather the impossibility of their monitoring due to the measuring conditions below the predicted tide height.

The extreme vertical variation recorded on the beaches studied is essentially the result of sediment exchange between the berm and the bar.

The extreme vertical variation recorded on the Sta. Rita beach results from the exchange of sediments between the berm and the bar(s). It also can be related to the transition between a near-reflective profile with berm and a ridge and runnel system to the north (P1 and P2), which becomes a more dissipative profile towards higher exposure in the south (P4 and P5).

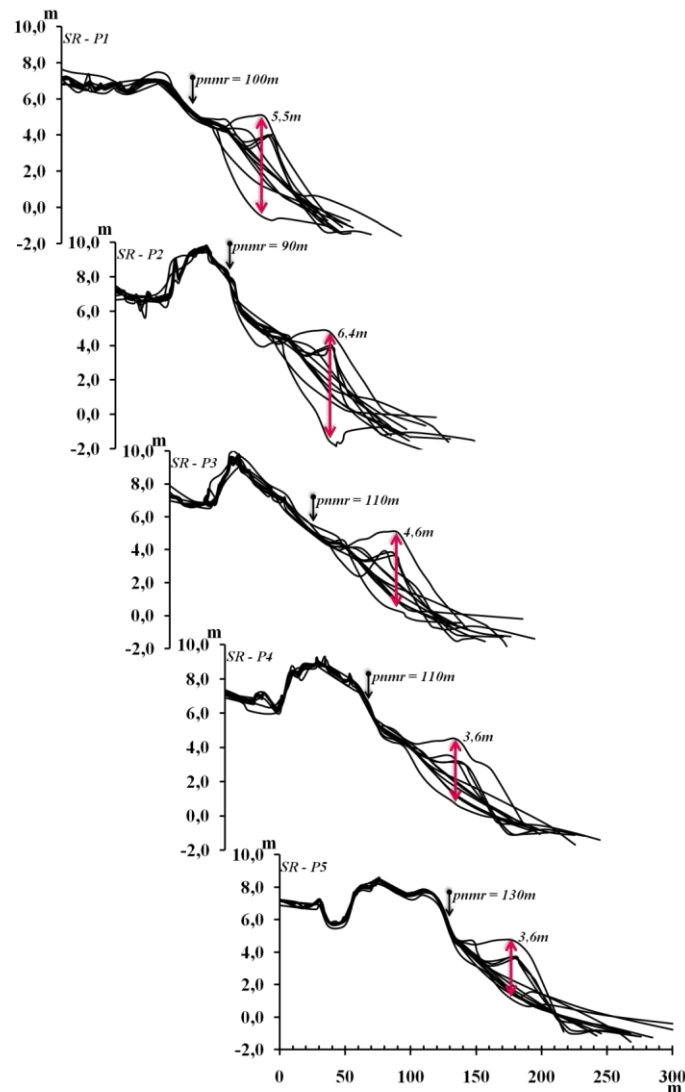


Figure 52. Maximum vertical variation per profile at Sta Rita beach, between 21.03.2004 and 28.11.2006. P1 located north of the monitored area.

Stop 3. Coxos – Sand and boulder dynamics on a rocky shore

Coxos area is a sediment-starved rocky coast, with an irregular coastline and N-S general trend, where 20-50 m-high cliffs alternate with sandy pocket beaches and structurally controlled rocky platforms. Both cliffs and platforms are cut in lower Cretaceous clays, resistant sandstone, marls and limestones (Fig. 53). These layers are gently tilted toward SSW and intercepted by faults and open joints with metric spacing.

The lateral continuity of cliffs is interrupted in this location by Coxos sandy pocket beach (Fig. 54). The beach is encased in a U-shaped fault-controlled embayment. The southern steep-sloping wall limiting the beach corresponds with a vertical, NW-SE trending fault that rose the southern Cretaceous block in relation to the northern block (vertical offset of about 20 m), and this generated repetition of the stratigraphic sequence north and south of the beach.

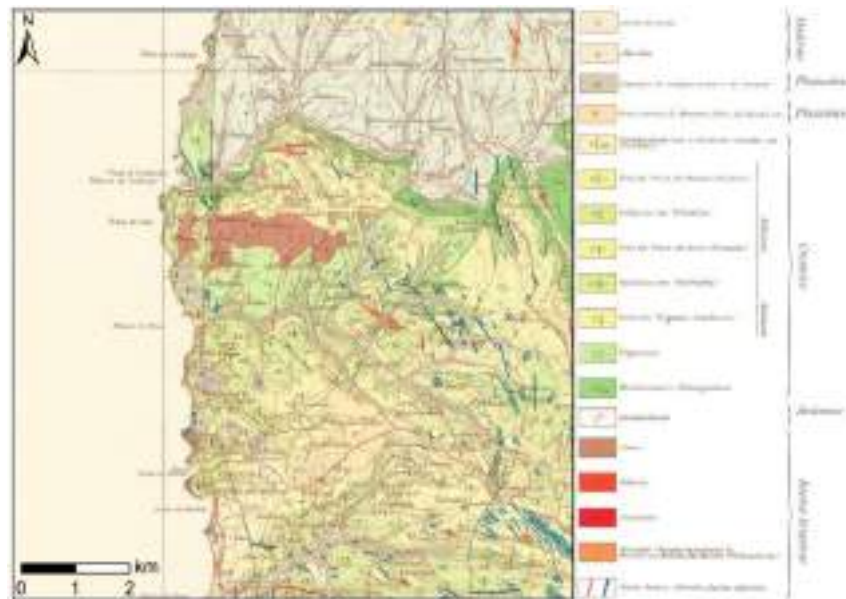


Figure 53. Geologic map of Ericeira-Coxos region (fragment of the 1:50000 30-C Torres Vedras geological map, Zbyszewski *et al.*, 1955. Image not to scale).

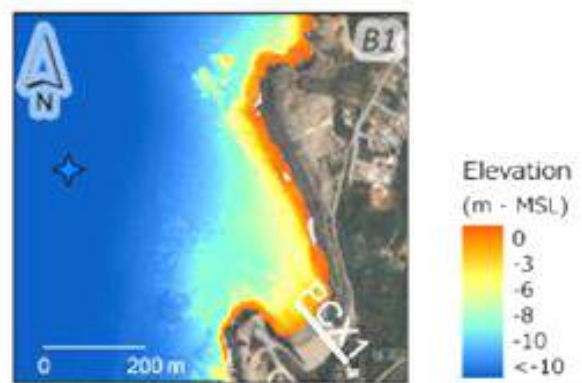


Figure 54. Digital elevation model of Coxos beach area (after Bastos *et al.*, 2022). PCX1 – beach profile in figure 55.

This stop addresses the morphodynamics of the Coxos sand beach and the boulder deposit at the southern rocky ribbon. Material on this stop summarized herein was mostly condensed from the studies of Bastos *et al.* (2022), Oliveira (2017), Oliveira and Andrade (2017) and Oliveira *et al.* (2020); the interested reader is referred to these studies and references therein.

Coxos: morphodynamics of a rock-bounded sand beach

Most sand beaches adjust their morphology in a proportional way to varying oceanographic conditions. This is especially true in bar-beach systems, where sand is abundant at the landward and seaward ends of the profile and allowed to circulate freely between the subaerial and submarine domains of the active beach profile, in tune with changes in morphology and wave energy. In contrast, rock-bounded beaches behave differently, because they exist in sand-starved coasts, they are deeply encased

between protruding headlands, they are confined landward by a hard boundary and rest on a rocky platform that extends seaward of the sand accumulation. In these cases, geomorphology plays a relevant role in determining morphodynamic patterns that depart from the more conventional continuum between of “summer” and “storm” profiles.

Coxos makes an excellent example of a rock bounded beach (Fig. 54). It faces NW and is fully exposed to the dominant offshore wave regime. The sand crescent extends seaward to about 1 m below mean sea level and is deeply encased between two rocky headlands. Its landward limit abuts a cliff about 30 m high, which cuts near horizontal limestone and resistant well-cemented sandstone layers. The beach corresponds to a small volume of sand resting on a rocky platform defined in resistant bedrock that becomes exposed in spring low tide and extends seaward to the closure depth and beyond.

Like many other rock-bounded beaches, Coxos is known to be remarkably stable at a multi-annual scale, regardless of changes in oceanographic forcing (including modal storms) (Fig. 55, Fig. 56) and only occasionally responds to storm extreme wave forcing with abrupt morphological changes. This is illustrated by profiles in figure 55. One set corresponds to pre-*Christina* surveys, showing lack of significant response to variations in incident wave conditions including winter modal storms. Seasonal response is restricted to small berm variations in height and width. *Christina*, an exceptionally high-magnitude storm induced significant lowering of beach area and volume, from 130 - 180 m³/m (pre-storm) to 30 - 80 m³/m (post-storm) (Fig. 56). *Christina* made landfall in 3 January 2014 and produced disruptive changes in the subaerial beach profile, and this behavior is markedly different from that of open beaches margined by dunes or featuring robust and wide berms on the same coast, although they all share similar deep-water wave climate and limited sediment supply (cf. Diogo *et al.*, 2014). Sediment recovery of the subaerial beach has been progressing at very low rate and the beach did not recover until present its pre-storm morphology.

The following model explains the causes and patterns of abrupt beach erosion and recovery observed in rock-bounded beaches (cf. Bastos *et al.*, 2022 for further details). To a large extent, the model was developed based on the CISML monitoring program of morphodynamics of beaches along the Western Portuguese coast (promoted by the Portuguese regional environmental authority, cf. Silveira *et al.*, 2013)) and investigation of storm morphological thresholds affecting beach stability (cf. Diogo *et al.*, 2014, Silveira, 2017).

Stability in volume, slope, shape and sediment observed over multiannual scales in Portuguese rock bounded beaches is only occasionally disrupted by abrupt and short-lived episodes of significant volume loss over their sub-aerial domain. This suggests the existence of a stability threshold modulated by both oceanographic and geological/geomorphological factors. Once this threshold is exceeded, the natural self-

reorganizing ability (resilience) of the beach is not sufficient to absorb the wave energy input without significant morphological change.

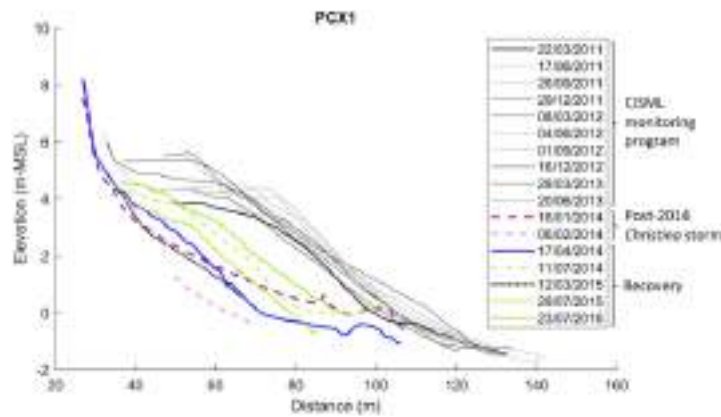


Figure 55. Beach profile PCX1 (Coxos beach) between March 2011 and July 2016. Gray lines correspond to monitoring surveys, dark gray refers to winter profiles and light gray to summer profiles (after Bastos *et al.*, 2022).

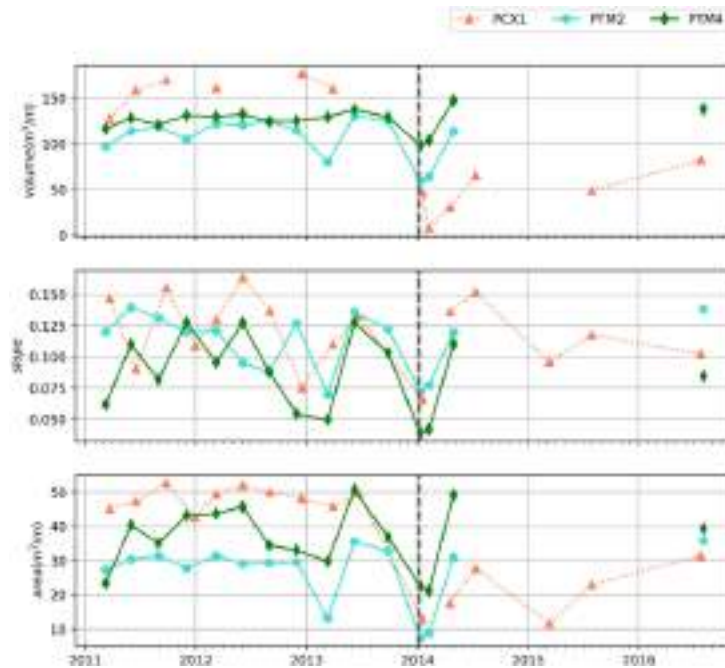


Figure 56. Morphological indicators extracted from subaerial beach profiles PCX1 (Coxos), PTM2 and PTM4 (Tamariz). Dashed gray-line indicates post-Christina survey. Data gaps correspond to profiles failing to allow computation of indicators (e.g., profiles too short) (after Bastos *et al.*, 2022).

The rocky basement outcropping at the shoreface acts as a wave energy dissipator that controls the width of the surf zone, modulates the height of incoming wave bores and limits the vertical reach of swash. In this context most sedimentary processes regulating beach morphodynamics under modal oceanographic forcing, including modal storms under threshold conditions, occur over the beach face in association to swash, with surf-related processes being less important and restricted to the sediment-barren rocky platform (Fig. 57, upper panel).

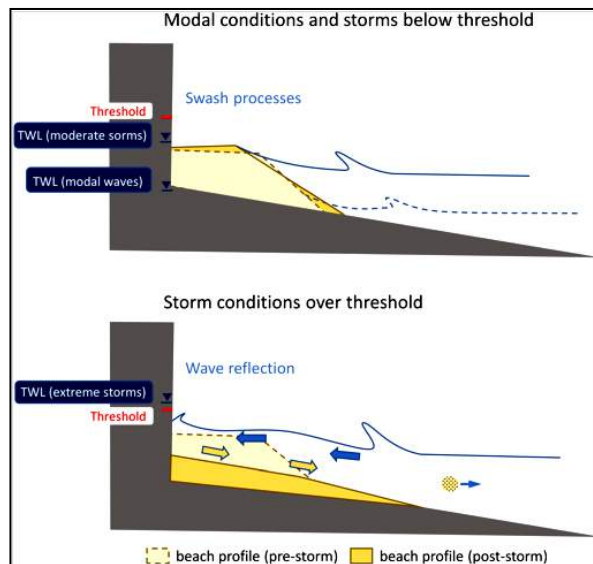


Figure 57. Conceptual model of morphological changes in geologically controlled beaches: processes driving beach responses to TWL below and above threshold. Upper panel – equilibrium stage related with modal waves and storm waves raising TWL below threshold; Lower panel – perturbation stage related with storm waves raising TWL above threshold (after Bastos *et al.*, 2022).

Minor morphological changes may also occur related to modal storms that promote limited sand transfer to the proximal nearshore and occasional overwash of the berm. Sand transferred to the submarine platform will rapidly return to the foreshore once the higher-energy conditions wane out. Overwash may cut back the berm but also build it to higher elevations, provided that sand-loaded swash overtops the berm surface while losing energy (Fig. 57, top panel). Accretion of the berm reduces the chance of overwash and further reworking of the beach, thus contributing to diminish the magnitude of beach response. Altogether, this explains why, during most of the time, variations in wave energy (including moderate storms), are not accompanied by significant morphological changes. Thus, the geomorphological setting effectively damps modal external forcing, and minor changes in subaerial beach morphology act to oppose further disturbances of the beach system, resulting in a negative feedback of geomorphology upon forcing.

Notwithstanding the above, every now and again natural resilience of the beach may be superseded during extreme (but infrequent) storms and trigger catastrophic beach response in a short time (Fig. 57, bottom panel, Fig. 58), following which a new condition takes over.

Catastrophic responses happen when combination of high tide level, storm surge, wave setup and runup (including both gravity and infragravity components) promote exceptionally high total water level within the embayment hosting the beach, raising it above a critical threshold (Fig. 57, bottom panel). Given the small magnitude of storm surge along this coast, critical water level is essentially determined by favorable combinations of tide, infragravity waves and exceptionally long-period waves.

Whenever total water level peaks over a critical threshold, broken waves overtop the entire beach and reach its landward boundary with sufficient energy to sustain reflection of incoming wave bores. The scarp at the beach landward boundary cannot supply sand, and thus the berm becomes the only source for sediment moved seaward by cross-shore currents. Reflection strengthens the undertow and rip currents over the submarine profile (Martins *et al.*, 2017) enhancing the offshore-directed sediment transport. Under this set of exceptional conditions, the beach system abruptly changes by rapid emptying of the subaerial beach.

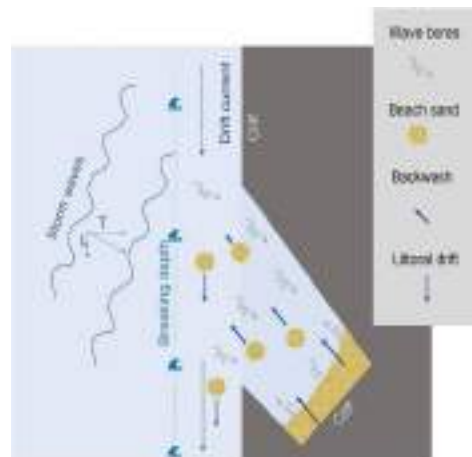


Figure 58. Coxos - Scheme showing the emptying process of the subaerial beach during extreme storms that raise TWL above critical threshold. Full inundation of the beach; wave-bores reaching the rigid inland boundary are reflected and promote backwash erosive capacity; sediment transported until the breaking depth, outside of the embayment, is captured by the drift current and transported downdrift. L (longitudinal) and T (transversal) wave power components (after Bastos *et al.*, 2022).

Geomorphology is also a relevant player in determining the timescales of post-storm beach recovery, because it contributes to determine the fate of sediment discharged over the nearshore by storm wave action. Nearshore sediments may remain within the active beach profile or be captured by longshore currents and exit the sediment cell. Geomorphological constrains play a crucial role in determining which condition will prevail (for example, protruding headlands or submarine ridges may form barriers to longshore drift, and wave direction may change over a rigid submarine platform modulating wave angle at breaking). Thus, although indirectly, geomorphology modulates the recovery time of the subaerial beach, once post-storm forcing conditions resume.

The depth of closure of Coxos profile for Christina storm waves was estimated in ca. 10 m below mean sea level. This depth is located outside the rocky embayment framing the sand beach. In addition, wave angles at breaking were persistently close to 35°, indicating that longshore drift currents were able to readily transfer nearshore sediment to nearby coastal cells located further downdrift. Coxos high indentation does not favor sediment bypassing from updrift during modal wave conditions, because of smaller

wave angles and seaward extension of active profile shorter than the reach of geomorphological barriers. In addition, the larger coastal ribbon hosting Coxos is sand starved, with no relevant external sediment sources. Poor sediment supply from updrift areas and geomorphological barriers to longshore drift combined to defer the rate of new sediment input in the embayment. Therefore, ten years after *Christina*, Coxos was still unable to fully recover the pre-storm volume.

Initial conditions surveyed under CISML program over Coxos beach (just as it may happen in many similar rock-bounded beaches worldwide) must have been achieved after many decades, and a pattern of stability of rock bounded beaches resulting from short-term monitoring programs should be taken with caution when used to inform beach management instruments.

Coxos: origin, chronology and processes of a coastal boulder accumulation

Extreme marine flooding of coasts by storms and tsunamis may result in the deposition of sediment onshore and the signature of such events along sand-starved rocky and cliffed coasts usually consists of coarse particles, ranging from a few centimeters up to several meters in length. The literature reports observations of entrainment, transport and re-deposition of large boulders landward of the shoreline during both contemporaneous tsunamis and storms, but it has proved difficult to distinguish boulders deposited by storms from those produced by tsunami when addressing pre-historical events. This stop provides an opportunity to discuss a peculiar boulder accumulation resting on a structural platform south of Coxos beach.

The Cretaceous sequence outcropping in this location is described in Zbyszewski *et al.* (1955), Rey (2007) and Rey *et al.* (2003, 2009). In broad terms, the sequence represents sedimentation during a marine transgressive + regressive cycle dated from the Upper Valanginian to the Upper Hauterivian. This cycle comprises a number of third-order complete depositional sequences, separated by evidences of exposure, erosion or interruption of sedimentation, evidenced by hardground surfaces. The cliff profile is influenced by lithology, fracture spacing and orientation, and bed thickness and attitude. Thick sets of hard limestone and sandstone layers develop subtidal to supratidal platforms limited by vertical scarps that evolve by rock fall, and they occur in the lower section of the cliff. In places where more resistant layers are inter-bedded with softer sandstones, marls or mudstones, the cliff face undergoes differential erosion and develops an irregular profile with overhangs, benches, pseudo-notches and stepped structurally-controlled surfaces (Fig. 59). The tread of stepped surfaces slopes westward and southward (seaward) in agreement with the dip of the strata. The rise of the steps is inherited from the thickness (0.5–1 m) of the harder layers and corresponds to WNW-ESE to N-S near-vertical fractures with metric spacing. Seaward of the shoreline, the cliff face plunges into the sea, allowing for modal waves to retain direction and energy just before impacting the cliff face. In contrast, a low-sloping cliff section (<40°) develops in softer sediments on the upper section of the cliff. These terms essentially evolve by

sheet erosion, gulying and mass wasting in relation with subarial processes, rather than marine-related processes.



Figure 59. (a) Northward views of Coxos area showing irregular and stepped profiles with overhangs, vertical scarps and structural notches and (b) stepped supratidal structural platforms. Scale is 3 m long. Modified after Oliveira (2017).

Five main lithostratigraphic units (Units A to E) were defined by Oliveira (2017) based on geomorphological aspects and the stratigraphical framework described by Rey (2007) (Fig. 60). Upper and lower boundaries of each unit correspond to structural surfaces (herein named surfaces S I to S IV) and benches developed by differential erosion. The visit will concentrate on Unit D, which is separated from the underlying Unit C by SIV, a hardground surface hosting most of the event-boulders and corresponding to a structural platform.

Differential erosion of lower units A to C generated an extremely irregular coastline in plan shape, with narrow and elongated headlands alternating with deeply encased and funneled embayments (referred to as indentations in Fig. 63a below), limited by steep walls and developed in relation with NW-SE vertical joints. The small embayments concentrate wave bores and increase landward flow of incoming waves.

Unit D is composed of crystalline limestone layers interbedded with soft and thin marls and siltstones, the mechanical resistance increasing towards the top. The topmost limestone layer controls the development of surface S IV and the whole set forms a pronounced step along the southern sector. Enhanced downwearing and erosion immediately below the bottom surface of the topmost layer allowed for the development of horizontal, wedge-shaped hollows, which are exploited by storm waves impacting the cliff face. At the southern end of the visited reach, transition from Unit D to Unit E is made by a lenticular body of silty, very fine micaceous sand exhibiting fluvial

facies, indicating a brief regressive episode that allowed for the development of a fingered detrital fan than invaded the otherwise shallow carbonate marine platform.

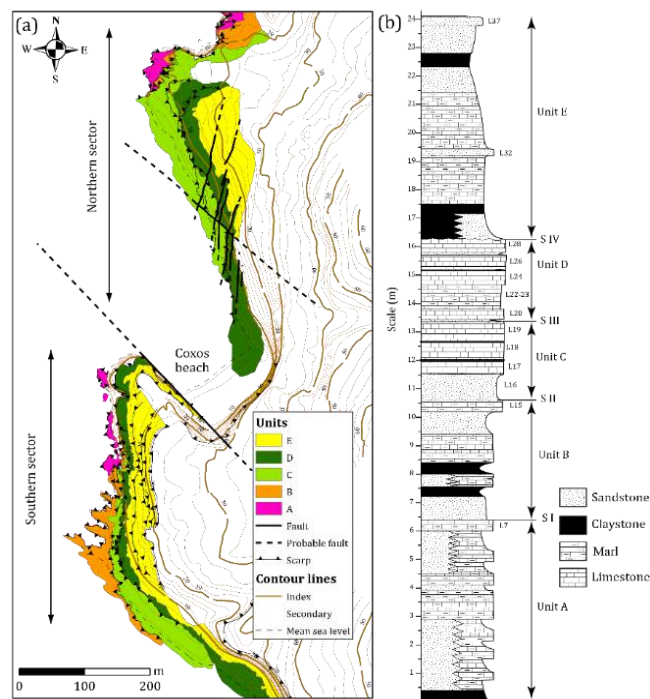


Figure 60. Map and summary log of main lithostratigraphic units (Unit A to Unit E) and structural surfaces (S I to S IV). Modified after Oliveira (2017).

Unit E contrasts in mechanical resistance, lithology and bed thickness with all underlying units. It is composed of inter-bedded thin layers of soft claystones and marls, and thin hard (though densely fractured) sandstones. This unit outcrops inland of the underlying units, due to differential erosion and faster retreat of the cliff face affecting softer Unit E sediments, exposing structural platform S IV. The cliff face also adopts a smaller angle, in relation with prevailing terrestrial erosion processes. Surface run-off and mass-wasting originate colluvium deposits consisting of clay and silt with some sand, cobbles and boulders that accumulate at the base of this slope, covering S IV. The horizontal (seaward) extension of the colluvium over S IV is variable in space and time and limited by frequent outwashing promoted by rain and wave swash.

Boulder deposit

The deposits of Praia dos Coxos consists of over 1600 boulders bearing evidence of transport against gravity and landward, which accumulated in two subsets, north and south of Coxos beach. The northern subset consists of only 34 boulders, standing at 4-11 m (mean sea level - msl), a small number in comparison with the 1580 examined, measured and geo-referenced in the southern sector by Oliveira (2017). The field visit develops in the southern sector along structural surface S IV and starts at its southern end.

The vast majority of boulders consist of massive limestone ranging in mass from 3 kg to 30 ton. The predominant source layers are the resistant beds topping Unit C (boulders accumulated over S III) and Unit D (boulders over S IV) (Fig. 60 and Fig. 61). The upward and landward distances travelled by boulders are small. Vertical distances are in the order of 1-2 m and horizontal pure cross-shore displacement is in the order of the width of the platform or less. Oblique displacement, including cross shore (landward) and longshore components (the latter developing in favor of the platform slope and frequently related with backwash) are larger, reaching tenths of meters.

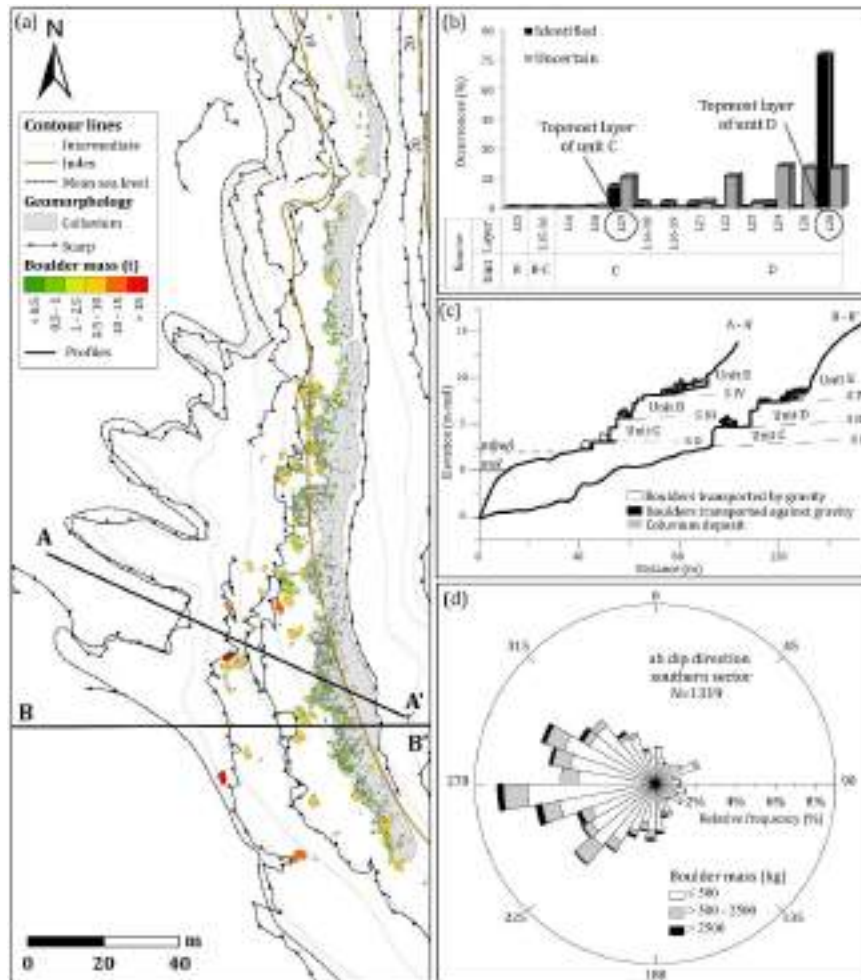


Figure 61. (a) Spatial distribution of boulder size in the southern sector; (b) Frequency distribution of boulders by source layer; (c) Profiles of the field site (profiles locations shown in (a)); (d) Rose diagram showing frequency distribution of the ab surface dip of disk-, bladed- and rod-shaped boulders. Modified after Oliveira (2017).

Source and entrainment

Data indicate that, regardless of associating to storms or tsunamis, the waves responsible for the present-day deposit mostly picked boulders from the upper region of each steep-sloped reach of the stepped cliffs, and especially from their uppermost edges, rather than sweeping and nourishing on loosened rock masses along the whole cliff face.

Moreover, in cases where unequivocal point source-deposit relationship was established, observations show that the width of displaced boulders often exceeds the width of the socket. This indicates that, at least in part, these boulders correspond to former overhangs, and in many cases the bedding plane separating the underlying layer from the (overlying) source layers is deeply karstified and exhumed, providing accommodation space for water and air injected by each wave impact. This suggests that the mechanical effects of incoming waves and that wave ability to entrain and displace large rock pieces may have been substantially increased by both water wedge effects and momentum increase of flow-induced forces acting upon the basal surface of overhangs and top surface of exhumed bedding planes.

Similar processes may occur elsewhere along the cliff face where overhangs and under-excitation features exist at lower altitudes. However, if a suitable accommodation space (a structural platform or bench) is not present in the vicinity and at a short distance above the source, these particles will move upwards for a brief time interval after being plucked from the cliff face and eventually fall down, adding to the toe deposits.

Both differential erosion and karst features vary in expression along the study area, and are relevant in determining which compartment of the study area offers ideal geomorphological settings to promote the entrainment of boulders when impacted by high-energy waves. Once the cliff surface becomes leveled from crest to toe, its reactivation becomes more difficult, regardless of the frequency distribution of extreme events. It is reasonable to assume that weathering and erosion will produce in due time a new set of irregularities, favoring cliff reactivation and boulder production. This implies that boulder entrainment and deposition on top of S III, and especially SIV, is discontinuous in time and space.

Scalar, vectorial and morphological properties

The height of emplacement of boulders resting upon surface S IV is about 6 to 15 m above msl, the elevation increasing northward in agreement with the general slope of the structural surface. In addition, a general northward decreasing trend of both boulder density per unit area and of boulder mass is apparent across surfaces S III and S IV (Fig. 61), despite pronounced irregularity in size-distribution at smaller spatial scales. Boulder size also depicts a general landward size-grading trend.

At first glance, this spatial distribution of boulders' mass and frequency may suggest that the deposit could have been emplaced by a single and extreme inundation event, capable of engulfing and sweeping this coastal ribbon, the incoming inundation flow progressing towards north. This hypothesis is compatible with the impact of a high-intensity tsunami with source located southwest of the study area, the AD 1755 event arising as a plausible candidate. The irregularities in size distribution found at more local

scales could be interpreted as an artifact of the small duration of the inundation event (minutes), precluding more effective and inclusive size-grading of the boulders.

However, a more detailed investigation of the parameters of the AD 1755 tsunami and of the geomorphology of the boulder accumulations makes this hypothesis implausible, despite this particular tsunami meeting the required propagation direction and maximum elevation of the sea surface at this coast, in addition to the overwhelming destruction it caused.

Actually, the boulders are not randomly nor simply scattered by size across surfaces S III and S IV. Surface S III is more frequently reached than S IV by storm waves, especially during spring high-tide, and presents the largest boulders (> 10 ton) found in the southern sector (Fig. 62). These boulders lean against or straddle the bench-edge topped by surface S III, showing minimum horizontal and vertical displacements, which mostly fail to exceed the boulder's long axis length. The size of the largest particles relates with higher thickness and lower joint frequency of their source layers in unit C. Other boulders sitting on this surface (2.5 to 10 ton) are arranged in clusters showing imbrication (Fig. 62a).



Figure 62. (a) 10-15 ton imbricated boulders originated from unit C (layers L18-19) standing on surface S III and leaning against the scarp between S III and S II; (b) Parallelepiped boulders (mass up to 10 ton) located next to, and landward of the edge of surface S IV, and respective socket in topmost layers of Unit D (Photos by T. Silveira); after Oliveira (2017).

The directional distribution of elongated and platy boulders sitting on S III and S IV (Fig. 61) (that could shed some light on flow direction) reveals three directional modes (NW, W and SW) and wide dispersion, instead of a well-defined SW-looking unimodal distribution – the expectable pattern should only one inundation episode related with an extreme southwesterly event having been responsible for the setting of the deposit. The rose diagram in figure 63 retains only directional data from stacks of imbricate boulders in surface S IV. The SW directional mode is strongly attenuated, whereas the

westerly and northwesterly modes remain (the latter rotated a few degrees clockwise) and a north to NNW mode is added to the previous diagram.

Boulders sitting over S IV may be grouped in three subpopulations based on mass, source layer, location and morphology of the accumulation (Fig. 63). One set includes boulders sitting near the bench edge. They were sourced in layer L28 (topmost layer of unit D), show straight and sharp edges and parallelepiped shape. They occur either isolated or in clusters of a few individuals, their mass ranging from 2.5 to 10 ton (Fig. 62b and Fig. 63). They are generally located near their sockets and their transport was mainly cross-shore (eventually added by a smaller longshore component matching the slope of the structural surface), the travelled distance being equal or smaller than the size of the boulder. Northward decrease in boulder size and boulder frequency is interpreted as resulting from increasing elevation of the cliff edge (thus lower frequency of run-up reaching higher sectors of the cliff edge) and larger fracture spacing in the same direction. Isolated and flatter boulders directly lying upon over structural surface S IV rest on their ab surface and thus tilt in agreement with the general attitude of that surface.

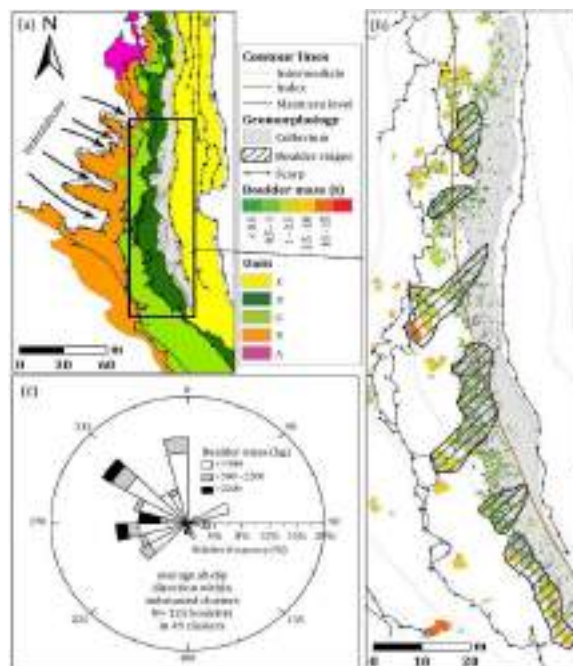


Figure 63. (a) Lithostratigraphical units and indentations on the lower structural platform and cliff face. Arrows illustrate funneling and directional effects of steep-sided and deep corridors over incoming wave bores and relations with boulder ridges over S IV; (b) Detail of (a) showing boulder ridges and spatial variation of boulder mass over S IV and within the ridges; (c) Rose diagram showing distribution of up-current directions as inferred from stacks of boulders showing imbrication. Modified after Oliveira (2017).

A second set corresponds to elongated accumulations over S IV and were categorized as boulder ridges (Fig. 63 and Fig. 64). These accumulations consist of heterometric boulders (always less than 1 ton and including cobbles) exhibiting varied shapes, in cases showing rounded edges. In many cases the source materials could not be unequivocally

identified but in every other case they were sourced in topmost layers of Unit D. Ridges attach at their landward tip to the colluviums blanketing the toe of the scarp developed in Unit E materials, and the lateral contact between both deposits is inter-fingered – an indication of alternation between slope mass movements and marine-induced input of boulders, compatible with continued construction and dismantling of the ridges. The boulder ridges are roughly aligned N-S to NE-SW, and show poorly defined, seaward sloping crests, the robustness of the accumulations also decreasing seaward (Fig. 63b).



Figure 64. Landward view of a NW-SW aligned boulder ridge. The view is approximately parallel to the ridge crest. After Oliveira (2017).

Imbrication of boulders in ridges was found correlated with ridge growth and is represented by the rose diagram in figure 63c. It relates with boulders moved from either the nearby bench edge and across the structural surface, or from more northern locations over the same platform, their movement having been stopped by immobile obstacles consisting of isolated larger particles or by the ridge itself. Landward-tilting boulders were found at the landward slope of ridges and are interpreted as corresponding to particles that were thrown over the ridge crest and came to rest over its lee slope. Ridges occur landward of, and spatially related with, deeply incised and steep-sloped excavations (referred to as indentations in Fig. 63a) affecting lithostratigraphic Unit B and, to some extent, the lower layers of Unit C. Canelas *et al.* (2014, in Oliveira, 2017) tested the ability of these indentations to modulate incoming waves and concluded that they were able to concentrate high-energy flow of wave bores, significantly increasing their ability to dislodge, entrain and transport large boulders. A third set includes boulders ranging in mass between 1 and 10 ton that align along and armor the colluviums front, locally merging with the ridges. They act as a barrier, hindering wash-out of colluvium by rain and wave swash. In locations where S IV is wider, boulder sets 2 and 3 are separated by a barren ribbon where boulder frequency is very low to null.

Chronology and origin of boulder emplacement

Besides comparing aerial photographs from 1948 onwards, age estimations of boulders' emplacement in the southern sector of Coxos were undertaken using: (i) optically stimulated luminescence (OSL) over two samples of marine sand containing "floating boulders" preserved within the colluvium materials (Fig. 65); (ii) MEM (micro erosion meters) to measure downwearing rates of fluvial silts showing a ledge developed by

differential erosion underneath one displaced large boulder (Fig. 66), and lichenometry, based on *Opegrapha durieui* colonies found in 24 boulders (Fig. 67) (see Oliveira *et al.*, 2020 for methods and results). In addition, recent storms (such as the winter 2014 *Christina* and *Nadja* storms) provided a unique opportunity to observe and measure boulder movement by storm waves.



Figure 65. Marine sand mixed with, and supporting, floating boulders. Image obtained from an excavation to sample sand for OSL dating. After Oliveira (2017).



Figure 66. Limestone boulders sitting on top of a Cretaceous very fine fluvial sandstone. The exposed surface is downwearing and protection afforded by boulder B 1509 (on the left) allowed for the development of a ledge. Vertical arrows indicate location of MEM measurements. Vertical scale is 1 m long. Modified after Oliveira (2017).



Figure 67. *Opegrapha durieui* growing on the surface of a limestone boulder. Photo by M.A. Oliveira.

Chronology results obtained from different methods are mutually consistent and allowed the identification of asynchronous periods of boulder accumulation, extending back in time to ca. 500 years. Aerial photography show that boulder movement has

occurred in the last 60 years, although not affecting all mapped and surveyed boulders. Larger particles tend to be less mobile than smaller particles, as expected. Large morphological features, such as boulder ridges, are persistent through time in aerial imagery, although there are evidences of minor changes in shape and volume of accumulations/ridges and of individual particles having been added to the ridges and others removed. In fact, addition and removal of boulders over the whole of the study site are continued processes, and the vast majority of particles at present populating the structural surfaces has been or will be affected by them.

Lichen growth data allows concluding that the absolute majority of boulders were emplaced from the last quarter of the 19th century onwards and more than half in the past 65 years. Curiously, the time window of 1740 to 1875 (that includes the time of the 1755 tsunami) is represented by a minimum in frequency (2 cases, one of which corroborated by MEM measurements) and older ages, in the time-interval of ca. 1560 to 1740, were obtained from only 5 boulders.

Altogether, the data above strongly suggest that flow responsible for the entrainment and relocation of boulders essentially relates with powerful storm waves and not the AD 1755 tsunami. And yet, the OSL ages obtained from sand beneath and above boulders, found in the middle section of the southern sector provided ages of 230 ± 20 and 290 ± 50 years that are compatible with that tsunami. However, the OSL dated sand corresponds to a unique occurrence, because it is the only mixture of a large volume of marine sand involving and supporting boulders found so far in this area, both materials having been preserved *in situ* by mass waste capping. Observed storms essentially mobilize large-sized particles and very little sand is carried onshore, no observation of deposition of a similar mixture having been recorded so far.

The uniqueness of this deposit and the age results above suggest that the 1755 tsunami effectively affected this area, but rather than contributing to increase the number of boulders in the accumulation coeval of that inundation, it must have been most effective in winnowing the rocky substrate from pre-existing boulders. This would have allowed for resetting the age of the overall accumulation, explaining the near-absence of particles older than the middle 18th century. Throughout the last 260 years, storm waves reconstructed the accumulation pattern pre-dating the 1755 tsunami, and the time interval of ca. 65 – 135 years may represent the average time interval of boulder residence on the upper structural platform.

Stop 4. Azenhas do Mar – Coastal Erosion and risk associated to sea cliff instability

Geomorphological setting (adapted from Marques, 2018)

The Azenhas do Mar (Fig. 68) is part of a 41 km long Sintra–Cascais cliff-dominated coast, located in the western coast of Portugal at approximately 30 km westwards of Lisbon (Fig. 69). The almost 40 m vertical cliff coast presents predominantly a westward facing

section with general orientation NNE-SSW to NW-SE less protected from the North Atlantic Ocean waves and storms. This cliff-dominated coast has temperate climate with a mild summer, with mean annual rainfall around 700 mm northwards of Sintra massif. The tide regime is semidiurnal mesotidal with mean amplitude of 2.1 m, with the western coast being acted upon dominant waves from NW (mean Hs of 1.7 m), with storms with the same direction and less frequently from SW (maximum Hs of 6.7 m), and in the south facing coast, waves (mean Hs of 0.7 m) and storms from SW (maximum Hs of 4.8 m). Beaches are usually small and restricted to small bays that correspond to indentations of the cliff plan contour. The geology setting of the Azenhas do Mar cliff coastal, is mainly characterized by the presence of tabular structures composed of upper Cretaceous near horizontal units of marls and limestones (Fig. 68, Fig. 69) affected by large curvature radius folding and cut by numerous near vertical faults and two generation dykes, the first mainly contemporary of Sintra massif installation and the latter related with the late Mesozoic Lisbon volcanic complex, which affected the whole study area (Marques, 2018). The Azenhas do Mar has also an exposed beach of NE-SW orientation with about 125 m of longitudinal profile and about 50 m of transversal profile. The access to this beach, is only possible during summer and at low tide (Oliveira, 2009).



Figure 68. Azenhas do Mar village and sea cliff coast. (© Sérgio Oliveira 2022).

Coastal Erosion and cliff instability

Mean annual cliff retreat rates were computed from linear regression of the spatial planimetric area lost at the cliff top for Azenhas do Mar coastal cell unit. According to Marques (2018) the retreat rate at this cell is 0.0053 m/year. The study was based on an aerial photo interpretation-based inventory of cliff retreat events occurred in a 63-year period (1947 to 2010). Nevertheless, based on the assessment of the relations between a set of predisposing factors related with cliffs geology, geomorphology, and mean annual wave power at the near offshore, and the occurrence of failures which caused cliff top retreat, in cliffs that are mainly composed of intermediate strength to strong rock masses, as it is the case, and in quite varied environmental conditions, it was found

that cliff sectors such the ones of Azenhas do Mar (Fig. 70) could present high susceptibility to cliff failure (Marques, 2018).

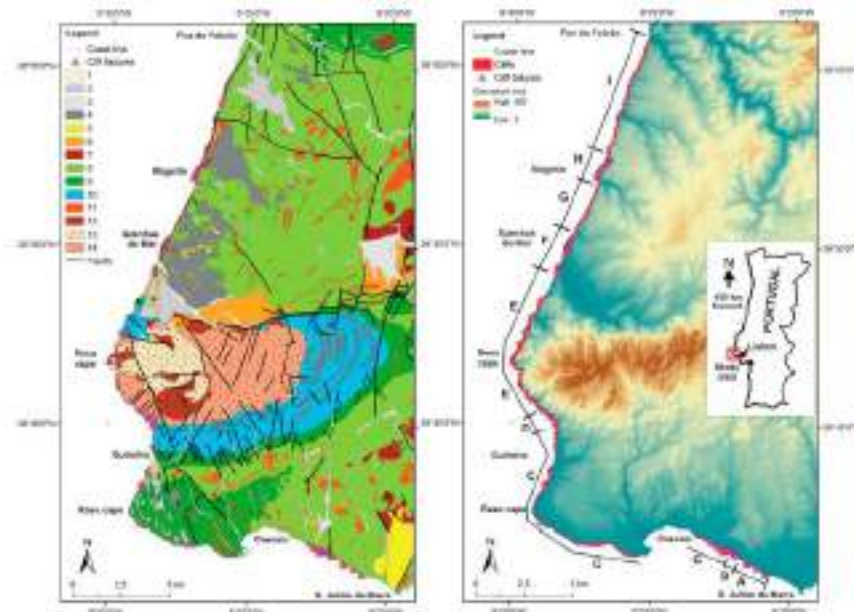


Figure 69. Localization and setting of the Sintra and Cascais coast areas. Small inset with general localization. (Left) geological map with localization of cliff failures occurred between 1947 and 2010; 1—Beach sands; 2—Dunes; 3—Alluvium; 4—Pleistocene; 5—Miocene; 6—Paleogene; 7—Lisbon volcanic complex; 8—Upper Cretaceous; 9—Lower Cretaceous; 10—Upper Jurassic; 11—Igneous dikes; 12—Gabro and diorite; 13—Sienite; 14—Granite (description in text). (Right) Cliff extent (red line) and cliff failures over digital terrain model (DTM) with cliff sectors considered for cliff retreat computing (A to I). (Marques, 2018)

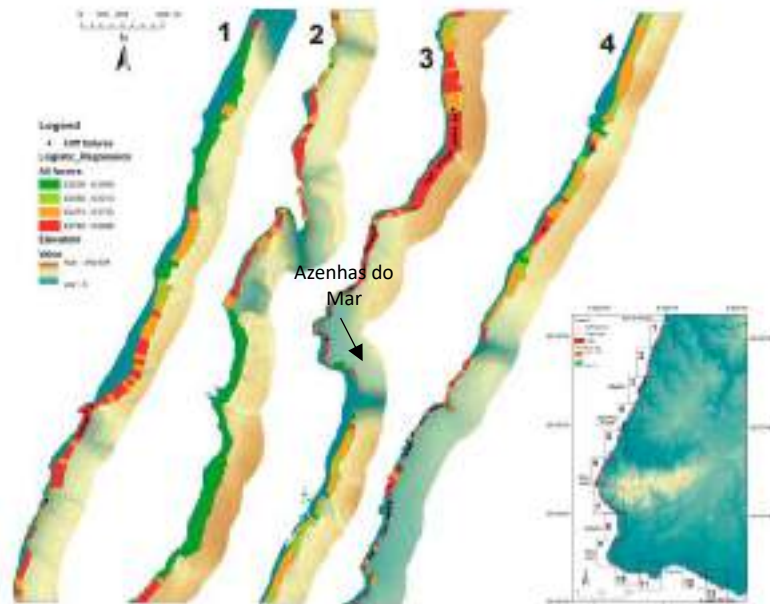


Figure 70. Susceptibility mapping based on the logistic regression model, with indication (dot) of the terrain units with cliff failures, for cliff sections 1 to 4, with general legend and localization map with numbered boxes indicating the extent of the cliff sections. Classification of logistic regression probability values in quantile-based classes. Contour line interval is 2 m. (Marques, 2018)

Risk associated to sea cliff instability

The Azenhas do Mar is an area recognized by its built-up front at risk, mainly due to its exposure to direct and indirect actions of coastal processes or dependence on coastal defence structures (MAOTDR, 2007). Risk problems are related to buildings, roads, parking and other infrastructures, namely those inserted in the DPM (Maritime Public Domain areas) or with such a proximity to the cliff that could constitute seriously threat by instability phenomena along the cliff sector. These concerns lead to the classification of this coastal sector of Azenhas do Mar as an “Potential Instability Area” in the Alcoaça-Espichel Costal Program (POC – Programa da Orla Costeira) and consequently, an area of territorial management conflict. The demolition of existing buildings is considered for conflict areas, however, in the cases of the presence of buildings of relevant historical, architectural or heritage interest, detailed studies are justified to assess slope instability phenomena, viability of treatment and design of possible slope stability intervention measures. This was considered for the Azenhas do Mar north cliff sector (APA, 2017) where the historic fisherman settlement of Azenhas do Mar is located. The maintenance of this place of scenic interest, involved in the last decade, a considerable number of interventions by the APA (Portuguese Environmental Agency) (Table III, Fig. 71), with the purpose of ensuring the stability of the cliff and adjacent buildings, but also in the south side Azenhas do Mar with the repositioning the viewpoint's limits in stable areas, not threatened by imminent risk of collapse.

Table III. POC Alcoaça – Cabo Espichel, Coastal interventions considered in the Littoral Action Plan XXI (APA, 2017).

ID	GOAL	ACTION	INTERVENTION OBJECTIVE	TYPE OF INTERVENTION	COST (€)	PERIOD
1	Cliff intervention	Stabilization of cliff north sector of Azenhas do Mar	Minimize the risk associated to sea cliff instability	Works; Inspection; Monitoring	3,441,127	2017-2019
2	Beach requalification	Requalification Intervention/Adding value – PIP (Beach Intervention Plan) of Azenhas do Mar)	Adding value areas as proposed in the Beach Intervention Plan	Works;	5,000	2018-2019
3	Requalification Intervention	Requalification Intervention of the Azenhas do Mar historic centre	Requalification of public space center, implementation of lighting equipment and urban furniture. Improvement of the electrical network and telecommunications, renewal of existing infrastructures.	Study/Project ; Works;	400,000	2019-2020
4	Requalification Intervention	Requalification intervention in the Azenhas do Mar viewpoint	Reorganization of parking and resurfacing the viewpoint, creating differentiated areas for circulation (pedestrian and cycling), for sport fishing practice and for a kiosk.	Study/Project ; Works; Inspection; Monitoring	152,000	2019-2020
5	Turism	Recovery of the ocean pool and adjacent platforms in Azenhas do Mar	Recovery of the ocean pool and adjacent platforms in Azenhas do Mar	Works	65,000	2019-2020
6	Interventions in coastal defends structures	Maintenance of structures in rockfill and concrete walls for beaches of the municipality of Sintra	Protect people and property through maintenance of structures in rockfill and concrete walls present along the beaches (not exclusively for Azenhas do Mar)	Works; Inspection	800,000	2021 - 2022



Figure 71. View of stabilization and protection works of cliff north sector of Azenhas do Mar. (<https://afaplan.com/proyecto?id=355&lang=en>, consulted in July 25th 2022).

Stop 5. Cape Roca – The westernmost point of Europe

The Cabo da Roca (140 m asl) is the westernmost tip of continental Europe. It is part of the Sintra mountain (529 m asl) that forms a E–W elongated interfluve rising about 300–350 m above the adjacent eroded landscape (Fig. 72).

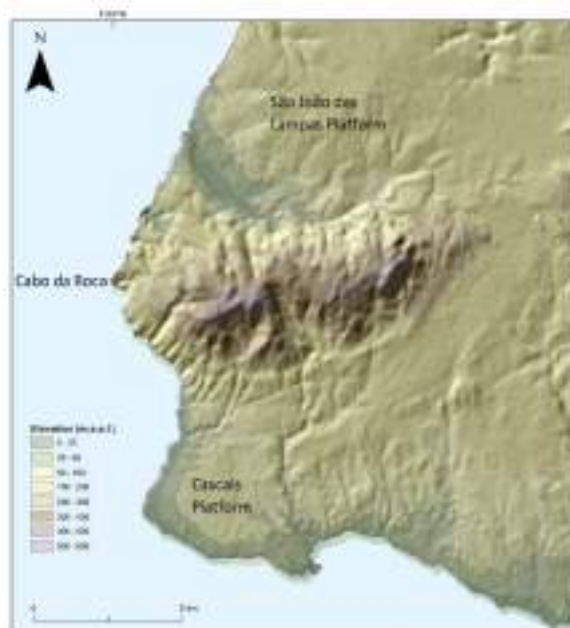


Figure 72. Digital terrain model of the Sintra mountain, showing the Cascais Platform to the South and the East, and the São João das Lampas platform to the North.

Sintra range is a residual relief that largely coincides with the cropping out of a sub-volcanic intrusion dated from the Late Cretaceous, the entirety of which was classified by UNESCO as a World Heritage Cultural Landscape (Fig. 72). It comprehends a central granite mass surrounded by syenites and gabbros that together with a dense network of radial and ring-dykes intruded Mesozoic sediments (Fig. 73) (see Ramalho *et al.*, 2001,

Kullberg and Kullberg, 2000 and references therein, for details and previous work). The landscape associated to this range evolved by differential erosion and the sub-volcanic rock mass stands out in the present-day landscape, its highest elevation reaching about 500 m above mean sea level.

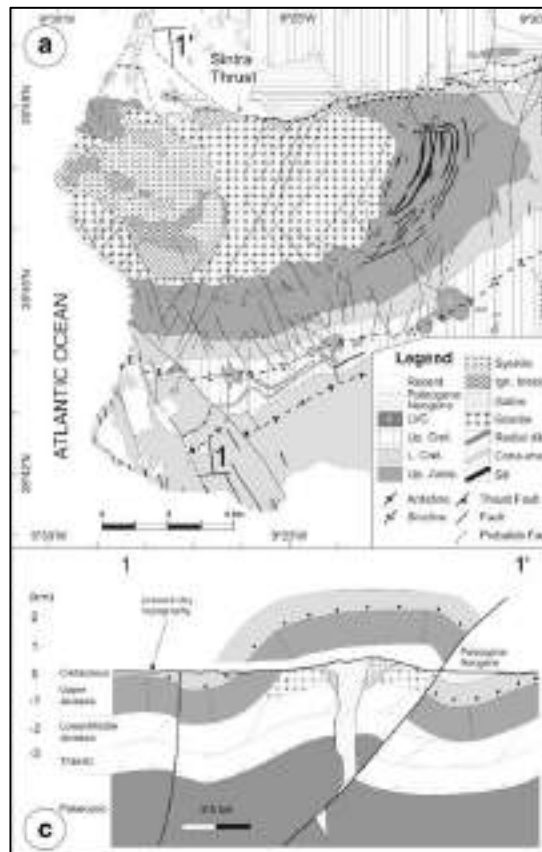


Figure 73. Geology of the Sintra Intrusive Complex (SIC). a Simplified geological map of the Sintra Intrusive Complex and host rocks, showing the location and orientation of the cross section, and c modelled geological cross section of the SIC intrusion and its sedimentary host rocks. (Adapted from Kullberg & Kullberg, 2020).

The Sintra mountain corresponds to an intrusion of a complex of alkaline igneous bodies. According to Kullberg and Kullberg (2020), the geometry of the Sintra Igneous Complex shows a composite intrusion consisting of a granite laccolith (80 Ma), elongated E–W and topping vertical gabbroic plugs and a syenite plug and laccolith (85 Ma).

The landscape of the Sintra region shows a clear lithological control, whereas the morphological evolution the progressive isostatic rebound of the mountain and the work of marine erosion combined with Quaternary fluvial retouching.

The igneous rocks are more resistant to weathering, so differential erosion controls the main traits of landforms. The eastern sector of the mountain is mainly composed of multiple granite peaks, which generally correspond to in situ clusters of large boulders, standing on the crests of the hills, forming typical tors. The western sector of the mountain is mostly composed of syenite and exhibits a slightly different morphology,

displaying rounded hill tops and almost flat surfaces, showing different reaction to weathering when compared to granites.

The bordering region of the Sintra mountain is a complex erosional surface that completely encloses the mountainous massif. To the south and the east, it is called the Cascais Platform and, to the north, the São João das Lampas Platform (Fig. 72).

In the zone between the southern slope of the Serra de Sintra and the Cascais Platform there is an alignment of peripheral hills (about 130 m–170 m asl) that are due to differential erosion. These hills formed over the metamorphosed sedimentary country rocks close to the contact with the Sintra Intrusive Complex. Here, the contact or thermal metamorphism recrystallized the calcareous host rocks of Jurassic age and enriched them with silicic components, thereby increasing their hardness (Kullberg & Kullberg, 2020).

Stop 6. Cresmina – Guincho – Cresmina aeolian corridor and headland bypassing

The coastal area extending to the NW of Lisbon until Cabo da Roca shows two main geomorphological features: the Sintra range (see Introduction chapter above) and the Cascais platform (Fig. 74).

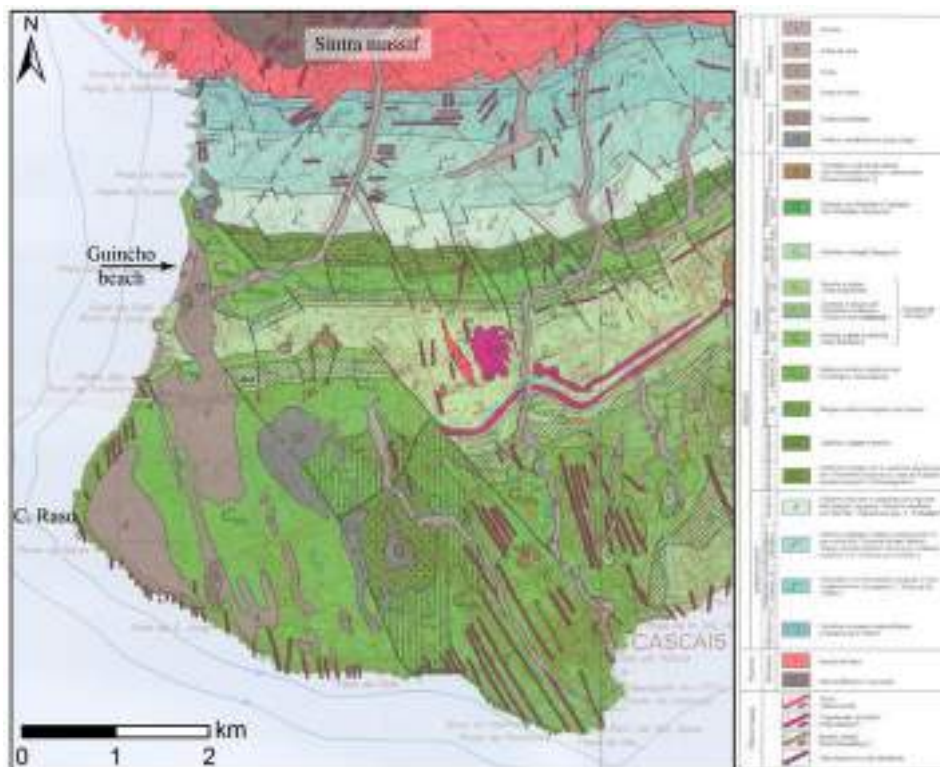


Figure 74. Geologic map of Sintra-Cascais region (adapted from the 1:50000 34-C Cascais geological map, Ramalho *et al.*, 2001). Image not to scale.

The inner region of the Cascais platform is blanketed by Holocene aeolian sand. Close to Oitavos the remnants of a Pleistocene consolidated dune (the Oitavos dune) outcrops from the Holocene sand and sits on an organic-rich paleosol, which fills karst hollows

affecting the Cretaceous rocks. Shells of pulmonate gastropod (*Helix* sp.) and organic matter in the soil were ^{14}C dated and yielded ages in the range of 16.4 to 34 kyr BP (Pereira and Angelucci, 2004, Soares *et al.*, 2006, Prudêncio *et al.*, 2007). The radiocarbon age of ca. 30 kyr BP is thus a minimum age for the development of the karst affecting platform limestones and a maximum age for the setting of the aeolian cover.

Aeolian activity across the Cascais platform has thus been persistent since the late (?) Pleistocene. This is further evidenced by abundant dreikanter and widespread aeolian grooves and polishing of limestone outcrops indicating abrasion by northerly winds. The directional spread of these ventifacts is narrow, in the range of $\text{N}10^\circ - 25^\circ\text{W}$. This directional range is in agreement with the general alignment ($\text{N}25^\circ\text{W} - \text{S}25^\circ\text{E}$) of the Guincho - Guia 4 km long and 1 km wide aeolian corridor (Fig. 74, Fig. 75), which connects the beaches of Cresmina and Guincho (at its NW tip) to the coastal reach between Oitavos and the Guia lighthouse. It is also in agreement with the morphology of stabilized parabolic dunes populating the corridor, besides coinciding with the present-day migration trend of the Guincho and Cresmina dunes and wind-regime. Aerial photographs dated from the early 1940's clearly show a blanket of aeolian sand covering a large portion of the rocky platform visited in this field trip (Fig. 76) at the downwind end of the Guincho-Guia corridor.

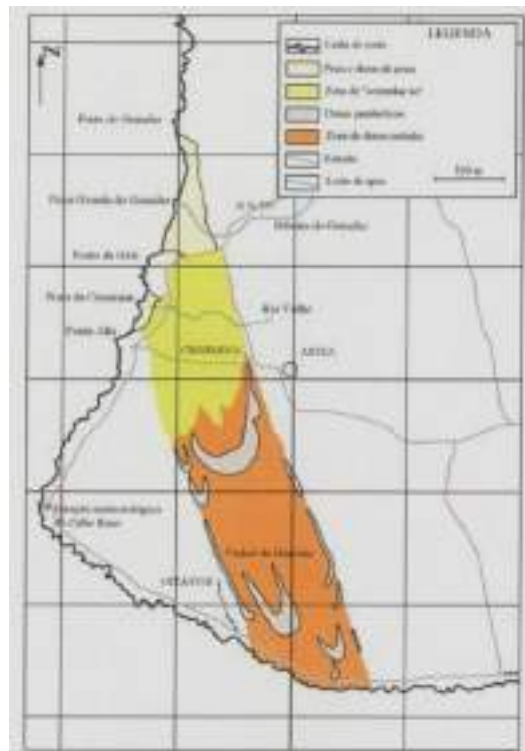


Figure 75. The Guincho-Guia aeolian corridor (Rebêlo, 2004, in Ferreira, 2019).

However, the sand cover has been since then removed by wind deflation and runoff and only a few sand patches remain captured in grikes and hollows of the lapiés-sculptured surface. This change is interpreted as resulting from human reduction of aeolian sand

transport motivated by extensive changes in land use promoted upwind and farther inland.

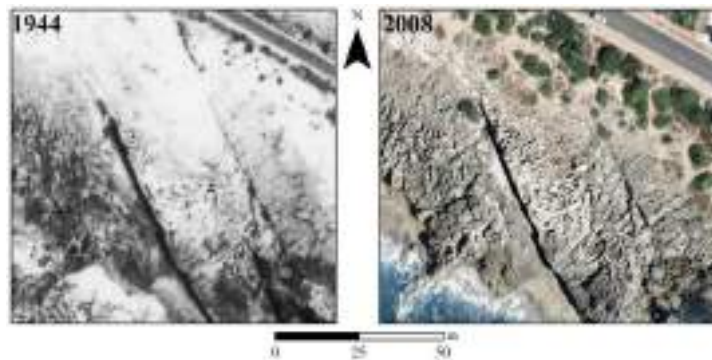


Figure 76. Aerial photographs taken in 1944 (DGOT) and 2008 (DGOT) showing wind deflation over a thin aeolian sand sheet that covered part of the rocky Cascais erosion platform south of cape Raso in the 1940's (after Oliveira and Andrade, 2017).

Aeolian activity is responsible for the huge sand volumes (ca. $1 \times 10^4 \text{ m}^3 \text{ yr}^{-1}$) that are blown every summer across the road from the Guincho beach to nourish and maintain the voluminous Guincho and Cresmina bare dunes. According to Rebêlo (2004, in Santos, 2006), Rebelo *et al.* (2002), Santos (2006) and Ferreira (2019) the Guincho and Cresmina dunes are located at the upwind region and integrate a transgressive dune system (which corresponds to a protected area).

Only the northernmost third of the aeolian corridor is at present active, and this was at least in part motivated by introduction of vegetation since at least the middle 20th century, together with construction of a golf course and development of villas and other infrastructures over Quinta da Marinha estate.

Ferreira (2019) found large similarity and excellent textural compatibility between Guincho and Cresmina beach and dune sands and investigated changes of the Guincho transgressive dune over the 1999 – 2016 period, as well as morphological changes determined by wind in its vicinity (Fig. 77). She estimated a mean rate of dune progression of about 11 m yr^{-1} and inferred sand volumes involved in dune progression of 9×10^3 to $2.7 \times 10^4 \text{ m}^3 \text{ yr}^{-1}$, in close agreement with previous estimates of aeolian solid transport potential at the downwind border of Guincho beach and computed from wind data (e.g, Rebelo, 2004, in Santos, 2006 and Santos, 2006). Linear extrapolation of these rates into the future alerts for impending risk of sand drowning of houses, roads and other infrastructures (both public and private-owned) with special relevance for facilities of D. Carlos club after 2040.

The sand surface mobilized by eolian processes is wider than the two main sand bodies of Guincho and Cresmina. Actually, it is also populated by numerous patches of lag deposits, nebkhas (herein incorporating sand mounds of varying size, temporarily held by vegetation and lacking peculiar cross-sectional shape) and shadow dunes, as well as blowouts and related prograding sand lobes, together with small parabolic forms. All

these forms exhibit intermittent mobility separated by periods of “freezing” (related with growth of vegetation) and their volume and shape pronouncedly changed in time and space. While the activity of both transgressive larger sand bodies may be characterized as representing sand “advection”, entrainment and transport of sand over the remnant surface is more similar to “diffusion”. At the SE limit of the aeolian sand field, persistent development of a large blowout led sand masses to affect infrastructures at the outskirts of Orbitur camping site.

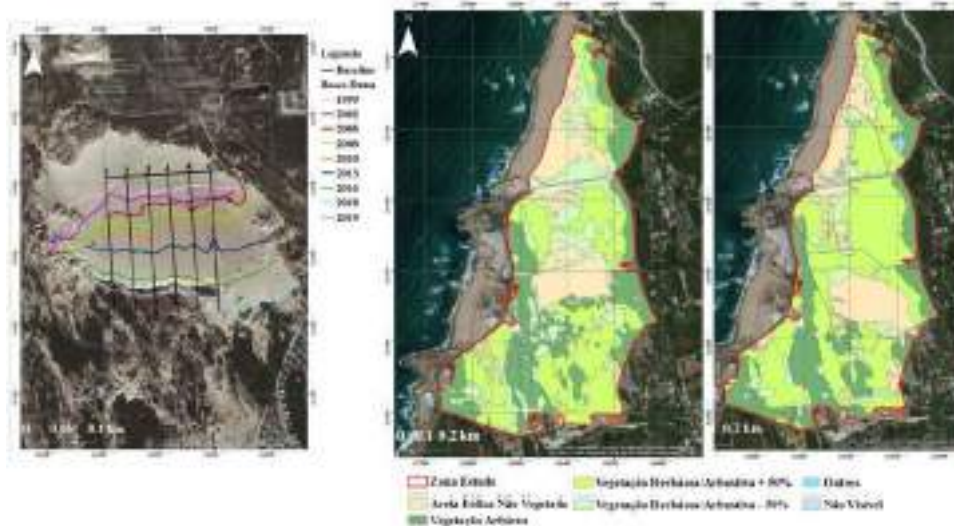


Figure 77. Left – displacement of Guincho transgressive dune toe; right: maps showing dune mobility and changes in vegetation cover between 1999 and 2016 (Ferreira, 2019).

Despite its protection statute and pathways designed to avoid indiscriminate crossing over, dune forms show evident and abundant traces of trampling by both people and horses, and Ferreira (2019) showed that these disturbances are related with destabilization of vegetation and (re)setting of dune mobility.

Sand driven by longshore currents bypasses cape Roca but not cape Raso (the southern boundary of coastal cell #4 referred above (cf. Introduction Chapter). Thus, Guincho and Cresmina beaches must be nourished from external sources, and to the best of our knowledge the most relevant source consists of water-driven erosion of the thick sand and gravel-rich regolith blanketing the slopes of the Sintra range. In turn, wind-blown sand bypassing cape Raso plays a crucial role in supplying sand to the coast extending to the east of the Guia lighthouse. This sand is distributed further eastward by littoral drift up to São Julião da Barra Fort and headland, very close to the northern margin of the Tagus inlet channel.

Stop 7. Cape Raso – The Cascais platform

Cretaceous beds outcropping southward of Sintra range (see Fig. 74) essentially consist of inner shelf fossiliferous carbonates, including reefs, together with few sandstone and marl layers representing occasional return to more littoral facies, albeit systematically

related with shallow, carbonate-rich and peri-littoral environments (see Rey, 2007 and Rey *et al.*, 2009, for details on lithostratigraphy and palaeogeographic reconstructions). These rocks have been subjected to extensive dolomitization that partially obliterated original textural, lithological and paleontological features.

In broad terms, the Mesozoic sequence tilts 15-20° towards S and SSW the dip angle increasing south of cape Raso. Cretaceous layers are densely fractured and faulted and intruded by dykes, most of which exploited dextral strike-slip faults trending N30°W. At present, these dykes frequently correspond to “matacães” (the Portuguese word equivalent to the French “calanque”) where they meet the coastline: elongated differential erosion excavations limited by vertical walls, developed by combined action of weathering and marine erosion, added by roof collapse of endokarst features.

The Cascais platform is a polygenic erosion surface carved on these lower Cretaceous rocks, though it also affects Jurassic beds closer to the Sintra range. This surface develops from ca. 80 m above mean sea level inland of the coast and gently slopes towards SW until meeting the crest of low plunging cliffs (Fig. 78).



Figure 78. Image of the gently sloping Cascais platform close to the coastline, where the surface is more degraded by weathering and marine action (Photo by M. A. Oliveira).

Cascais platform comprises a staircase of poorly preserved Late Pliocene (?) and Pleistocene marine terraces (terraces T1 to T4 in Fig. 79, see also Fig. 80) that developed in relation with marine high-stand episodes (Ramalho *et al.*, 2001, Duarte *et al.*, 2014, Cunha *et al.*, 2015 and references therein provide details on previous work and discuss morphology and age of these marine terraces, which are a matter of debate until present). North of Guincho beach, marine terraces preserve remnants of marine pebbles and sand, but further south they essentially correspond to erosive features. However, sand patches of marine facies containing rounded and disk-shaped pebbles may be found, their thickness increasing landward and showing better preservation close to the road.

Limestones outcropping and underlying the Cascais erosion platform have been subjected to denudation and solution testified by abundant surface and endokarst features, such as lapiés (karren), sinkholes and galleries. Karst hollows contain infills and coatings of well cemented and resistant, iron-rich, black to brown sediment, especially

at the seaward (lower) region of the rocky platform. The precise age of formation of this infill is unknown but they should correspond to Late Pliocene or Pleistocene paleo-karst deposits.



Figure 79. Pleistocene marine terraces along the Guincho-Cascais coastal reach. Adapted from Cunha *et al.* (2015).



Figure 80. Wave-cut surface (T3 in Figure) truncating Cretaceous beds (in Duarte *et al.*, 2014).

In places where karst galleries were exhumed these materials are overlain by a mat of well-rounded quartz sand of marine facies, including gritt, occasional small and rounded, disk-shaped quartz pebbles, and marine shell fragments. The elevation of these particular occurrences was surveyed to about 7 m above msl and they are interpreted as representing sedimentation coeval of Pleistocene higher-than-present sea level stands. Patches of this sediment are found adhering to the surface of megaclasts populating the erosion platform, suggesting that they may represent geological signatures of Pleistocene storms.

The field visit essentially mostly runs over marine terrace T3 whose inner edge stands ca. 20 m above mean sea level. This surface cuts the Cretaceous limestone and degrades progressively seawards, in tune with the increase in intensity of present-day karst processes and quarrying of limestone slabs, the latter mechanism favouring the exposure of structural surfaces. Ramalho *et al.* (2001) report the existence of a lower

terrace, preserved in discontinuous patches at 4 to 6 m above msl, locally covered by well cemented shelly marine gravel. This feature (terrace T4 in Fig. 79) may represent stage MIS 5e, during which sea level remained about 4 to 6 m higher than present (Siddall *et al.*, 2006), although Duarte *et al.* (2014) propose the same stage as responsible for the setting of T3. Ramalho *et al.* (2001) report numerous evidences of human occupation since the Paleolithic and extending up to modern times in relation with marine terraces, including worked pebbles, quartzite tools, remnants of cooking fireplaces together with accumulations of marine shells, and pottery.

DAY 3 – THE COAST SOUTH OF LISBON

Stop 1. Capuchos viewpoint – Caparica strandplain

Capuchos viewpoint provides a broad panorama over the region of Costa da Caparica and of the coast extending further south until cape Espichel, and to the north, until the Tagus inlet. Similarly to the Espichel-Sines segment, the coast in this region is arcuate and its dynamics depends to a large extent of sheltering offered by both Roca and Raso headlands regarding West to Northwest swell. The northern region of this coast is low-lying and sandy, featuring a continuous sand beach, whereas the southern region is essentially rocky with few gravel and cobble pocket beaches.

Geomorphology of the northern half is dominated by two main geological and morphological units that converge at the fossil cliff hosting the Capuchos viewpoint: (i) a raised platform extending landward (eastward) of the fossil cliff edge and (ii) a low-lying strandplain margining the toe of the cliff and extending westwards (Fig. 81).

The raised platform covers fluvial sediments of the pre-Tagus system deposited prior to the reorganization of the Tagus drainage network to its present-day framework (Formação de Santa Marta, Fig. 81). These sediments, which rest upon Miocene materials, mostly correspond to a poorly organized Pliocene fluvial system with multiple interweaving and anastomosing channels dissecting a wide floodplain and multiple outlets to the ocean (Azevêdo, 1983). Atop, a thinner cover of fluvial conglomerates (“Conglomerado de Belverde” in Fig. 81) containing clasts sourced from the Sintra range and peripheral metamorphic rocks was attributed to the late Pliocene or early Pleistocene (Pais *et al.*, 2006, Cabral, 1995). They represent the last episode of fluvial sedimentation of the pre-Tagus system before it shifted to the present-day inlet channel. The thick Pliocene deposits accumulated in tune with subsidence of the lower Tagus basin but this trend was reversed in the Early Pleistocene (Cabral, 1995), when regional uplift allowed for the capture of the lower Tagus drainage system by a stream

located approximately on the present-day Tagus inlet channel. This determined a major change of the general drainage pattern to the ocean.

Holocene dunes (at present vegetated and fixed by human action since de 18th century) form the most recent cover of this raised platform, their age and genesis having been investigated by Costas *et al.* (2012). These authors used ground penetration radar and OSL dating to investigate their stratigraphy and proposed that they correspond to a cliff-top coastal transgressive dune field containing evidence of multiple phases of aeolian activity since ca. 12600 BP, related to coastal instability and enhanced westerlies.

The fossil cliff corresponds to a high-angle slope running NW-SE that affects Pleistocene and Pliocene sediments in its northern section and becomes active some 10 km southward, close to Fonte da Telha (Fig. 82). It remains active further southward, where Miocene layers are cut by marine action and outcrop at the cliff face. At present, in the northern sector, the cliff is separated from the ocean by a coastal plain (actually, a strandplain) and the cliff shows numerous gullies and scars of slope mass movements. Colluvium and stream deposits amour its base and the lower region of the slope; altogether, they supply sand to this coast where the width of the strandplain is small. The cliff is of marine origin and it was probably reactivated by marine erosion in the late Pleistocene (namely during the EEmian sea-level high-stand) and Holocene prior to the on setting of the Caparica strandplain.

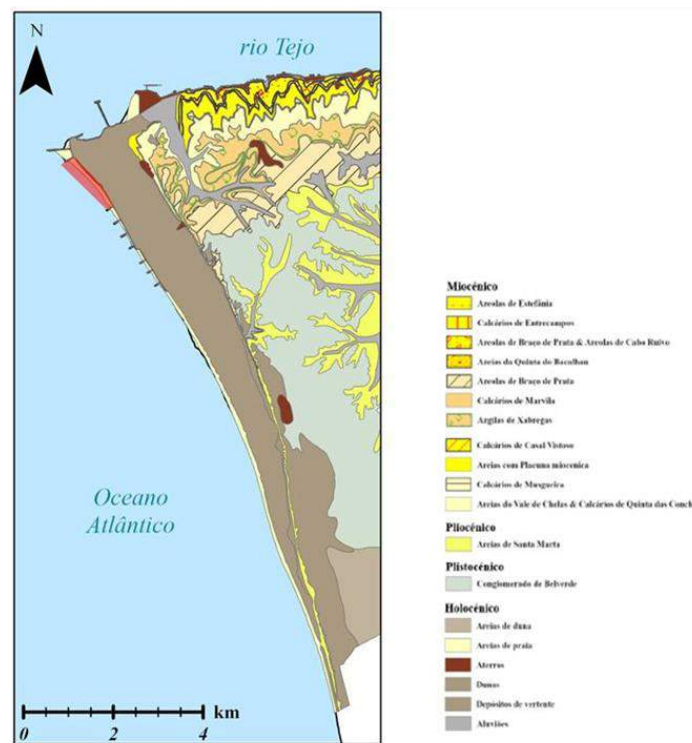


Figure 81. Geological map of the western region of the Setúbal peninsula (after CMA, 2005, in Pais, 2021). Red polygon highlights São João beach-dune system.

The coastal area extending to the West of the fossil cliff and from São João to Fonte da Telha corresponds to a roughly triangular platform formed by multiple sand ridges (beach and foredunes) and swales, part of which were reactivated by wind to form numerous blowouts and parabolic sand dunes. The origin of this strandplain is still not fully investigated but it most probably developed by incorporation of sediment sourced from cliffs along the southern half of the Caparica-Espichel coast and transported northwards by drift currents, in a broad context of northward decreasing transport potential. The on setting and earlier development stages of the strandplain are most probably contemporaneous of the stabilization of sea level ca. 7000 yrs BP, in combination with sheltering offered by capes Roca and Raso and development of the Tagus outer shoals.

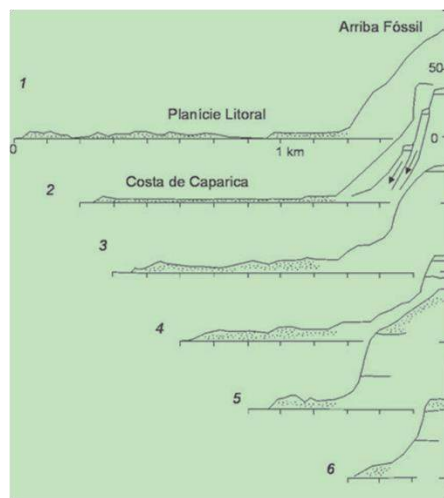


Figure 82. Profiles illustrating relations between the fossil cliff and the strandplain of Caparica (Ramos Pereira, 1988).

The following summary on the occupation of Caparica and coastal protection works is essentially based on the works by Freire (1986), Veloso-Gomes and Taveira-Pinto (2004), Pinto *et al.* (2007) and Palma *et al.* (2021). Caparica strandplain was to a large extent scarcely occupied until the 18th century, when a small settlement of fishermen (also dedicated to agriculture) started to grow. Up to the 20th century dunes were considered as valueless features and intense aeolian activity over the strandplain (which was to a large extent unvegetated) viewed as harmful for agriculture. Major attempts to control dune mobility and aeolian sand transport by introducing forestation started in the late 1800's and continued until the 1940's, when the village of Costa da Caparica started to expand to accommodate a growing industry of tourism, first based on the therapeutic properties of sea baths and later for recreational and leisure activities. In a very short time Costa da Caparica changed from a poor fishing village (Fig. 83) to a fashionable seaside resort and unwise (sometimes illegal) occupation of the coastal area by houses, condominiums, camping parks and hotels peaked in the second half of the 1960's, following the construction of the Tagus bridge. Further unwise development continued

in time expanding occupation north and south of Costa da Caparica until the earlier coastal management plans came into force, in the 1980's.



Figure 83. Costa da Caparica village in the 1930's viewed from the top of the fossil cliff (photo: <https://mar-da-costa.blogspot.com/2016/07/>).

Stop 2. São João da Caparica – Coping with long term beach erosion

First news on retreat of the coast and storm-related inundations were published in 1947 and 1948 newspapers and triggered studies on the dynamics of this coast. However, coastal retreat initiated earlier, in the transition to the 20th century (Fig. 84). In contrast with the first period of instability - that may speculatively be attributed to the end of the Little Ice Age, the cause for the onset of a permanent trend for retreat since the mid 20th century is of human nature and related with massive sand extraction from the Tagus outer shoals well above the closure depth of the coastal system (Fig. 84).

First (experimental) interventions to manage and oppose coastal change targeted the northernmost tip of the coast (Cova do Vapor, end of the 1950's) and consisted in placement of earth, sand and rubble dikes. They were replaced in 1959-1963 by two long groins rooted in a seawall, aiming at blocking drift sand and promoting updrift beach widening. However, this solution proved insufficient to halt coastal retreat and inhibit flooding of Costa da Caparica village and a second larger set of hard engineering structures was constructed between 1959 and 1971 to protect the seafront of the village. This consisted of a seawall armed with seven groins. In general terms, this solution was efficient in halting retreat of the engineered coastline until the 1980's, despite several emergency interventions (including repair works) having taken place until 2007, when a major refurbishment of the groin field was undertaken (see Veloso-Gomes *et al.*, 2006 for details) in combination with an artificial nourishment operation. Hard structures increase reflection of wave energy, so it was not a surprise to watch beach enclosed between groins decreasing in supratidal area and volume. Furthermore, from the 1980' onwards, the beach-dune area downdrift (northward) of the seawall (São João) resumed erosion (Pinto *et al.*, 2007).

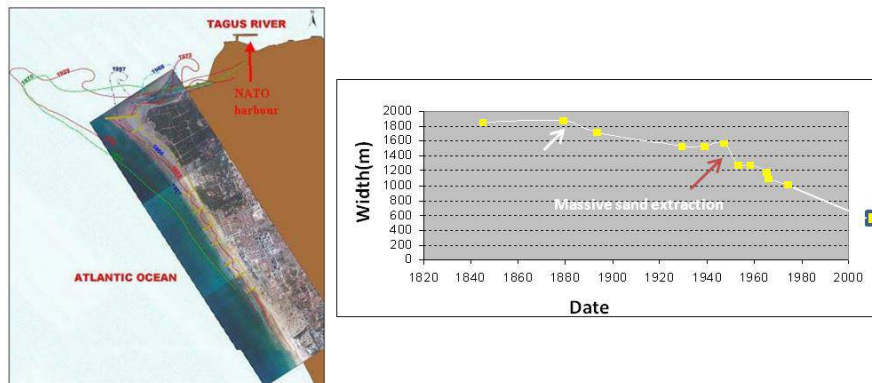


Figure 84. Left panel: coastal retreat between 1870 and 1972 in Caparica region (Veloso-Gomes, Taveira Pinto, 2004). Right panel: changes in width of the Caparica strandplain (1850 to present), data from Freire (1989), Veloso Gomes, Taveira Pinto (2004).

Since the 1990's the strategy of coastal intervention in Portugal switched to beach nourishment and dune restoration, adopted as adaptation methods to cope with impacts of long-term erosion, storm-driven inundation, damages to hard engineering structures and preservation of beach recreational value (Pinto *et al.*, 2020). In agreement, São João beach and all beaches extending further south along the Caparica seawall for 3.9 km were artificially nourished (berm-only option) in the summers of 2007 to 2009 (total ~2.5 M m³), 2014 and 2019 (1 M m³ each). Nourishments used dredged sand made available by the Lisbon port authority in the scope of channel maintenance operations (Pinto *et al.* 2020).

Monitoring of São João beach changes over time (e.g. under the COSMO monitoring programme, <https://cosmo.apambiente.pt/>, see also Pais et al., 2022 for previous studies) indicates the existence of a persistent negative sediment budget that is superimposed by shorter-term, cross-shore dominated changes in volume related with seasonal wave regime and beach rotation. Periods of sand loss are separated by abrupt increases in volume, height and width determined by artificial sand replenishment of the beach berm (Fig. 85).

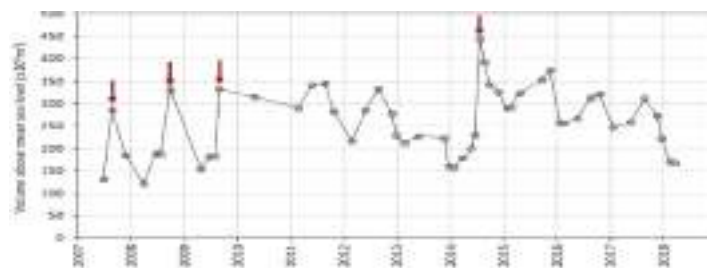


Figure 85. Time changes in sand volume above msl recorded at São João beach. Arrows indicate nourishment operations (Pinto *et al.*, 2020).

The southern beach sector shows higher susceptibility to erosion and resumes pre-nourishment morphology and volume shortly after post-replenishment storms. This is

due to the seawall enhancing reflection of wave energy and precluding temporary profile retreat during storms together with blockage of northward net littoral drift promoted by the groin at the southern beach end; it also explains the higher performance of nourishments at the northern beach section. Estimations of beach volume losses over time suggest that the longevity of each nourishment performed so far is of ca. 5 years, and that a new replenishment should be required not later than 2024 to maintain protection offered by the beach to the hinterland, to control coastline location and to allow for unconstrained beach-foredune aeolian sand transport.

Sand fences and vegetation were introduced in 2015 under ReDuna restoration project, following severe erosion and breaching of the São João foredune by the February 2014 Christina storm (Fig. 86). The restoration project (a joint project involving Almada municipality and the ministry of Environment) aimed at promoting dune growth and to provide a resilient, nature-based obstacle to oceanographic forcing.



Figure 86. Placement of native vegetation and sand fences shortly after completion of ReDUNA project (photo: Almada municipality available at <https://www.jf-charnecacaparica-sobreda.pt/images/joomlart/article/4693ba70fe7ccf8c5461d5f42e16af89.jpg>).

Restoration works led to *in situ* growth of a small primary dune, shifting the coastline 10-20 m seaward. This considerably reduced sand supply to dunes located further inland, which evolved at lower rates. The new dune grew rapidly in the first year following fence and plant deployment and more slowly in the following two years (Rato, 2017). Storm erosion and dune overtopping in 2017 and 2018 interrupted the growth pattern at the centre and southern dune sections. Fences were reconstructed after damaging episodes, allowing for aeolian processes to resume. Following the 2019 replenishment, a second positive pulse in dune growth is noticeable (Pais *et al.*, 2022) (Fig. 87, Fig. 88), especially concentrated over the beach-dune boundary.

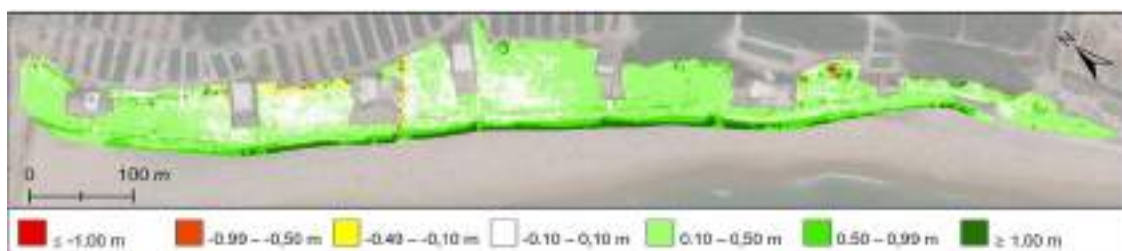


Figure 87. Spatial distribution of elevation differences measured over the São João foredune, October 2019- July 2021 (Pais *et al.*, 2022).

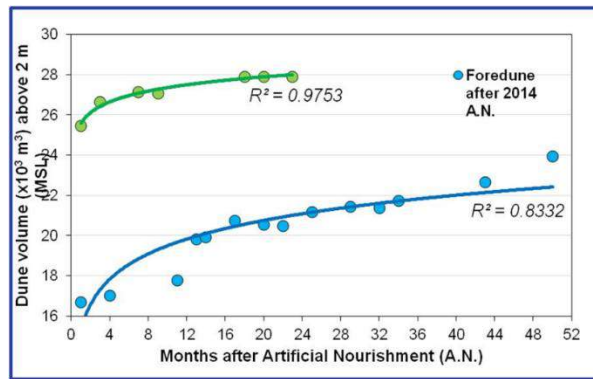


Figure 88. Time-series of volumetric change observed in the foredune following the 2014 (blue) and 2019 (green) artificial nourishments with logarithmic regression lines (Pais *et al.*, 2022).

Decreasing grow rates of the intervened foredune may reflect different wind regimes, persistent decrease in berm width (and thus in beach fetch distance offered to cross-shore wind) or both. The datasets available so far do not allow disentangling these hypotheses.

Field observations indicate that despite erosion and overtopping, the obstacle provided by this dune was quite effective in protecting the dune ridges located further landward and in managing coastline translation.

Stop 3. *Outão – Sado estuary and Troia sandspit*

This stop offers a panoramic view over the Sado estuary, Tróia sandspit and the coast extending further south until cape Sines, a non-bypassed headland defined by a sub-volcanic rock intrusion contemporaneous of Sintra. North of Sines the coast is sand-abundant, whereas south of that headland it is rocky, cliffed and sand-starved.

Sado river runs along 180 km before meeting the ocean south of Setubal, where it forms the second larger Portuguese estuary (Moreira, 1992, Psuty and Moreira, 2000, Andrade *et al.*, 2006a,b, Freitas and Andrade, 2008, Neto *et al.*, 2020 and references therein provide further data on Sado river and estuary and Tróia spit that were summarized herein). The drainage basin covers ca. 7600 km² and river flow is interrupted by 14 dams. Mean freshwater discharge is small, even in peak discharge, and the spring marine tidal prism is of 4×10⁸ m³ prevailing over fresh water input at every tidal cycle. Dynamic tide reaches about 40 km upstream of the inlet and salinity of estuarine water is similar to open marine water. This estuary intersects three protected areas (Arrábida National Park, Sado Estuary Natural Reserve and Natura 2000 site of Comporta-Galé) illustrating its role in preservation of natural values.

Besides Sado at the northern tip, no other relevant river system outlets north of Sines, and stream activity is limited to small rivulets (in part forming barred small estuaries or lagoons, e.g. Santo André) and gullies (Fig. 89). This coastal ribbon is almost homothetic

of the Raso – Espichel coast in shape, geomorphological contents and limits. However, one major and significant difference between both coastal segments is the intensity of human-interference with the coastal sediment budget over the last century, which was very significant in the case of the Tagus estuary and nearby coast but negligible in the case of Sado.

The coast extending between Sado end Sines consists of a 64 km-long continuous and reflective sand beach backed by (active) cliffs and dunes. Cliffs affect poorly consolidated Plio-Pleistocene sandstones and occur essentially along the southern section, whereas dunes are more frequent along the northern section. North of Carvalhal the beach detaches from mainland, forming the 25 km-long Tróia sand spit, which shelters the Sado estuary and confines its inlet.

Immediately north of Sines the open coast trends perpendicular to the mean wave power and develops an arcuate shape further north as a consequence of differential sheltering determined by the pronounced westward offset of the coast extending to the north of cape Espichel and W-E trend of the Arrábida range.

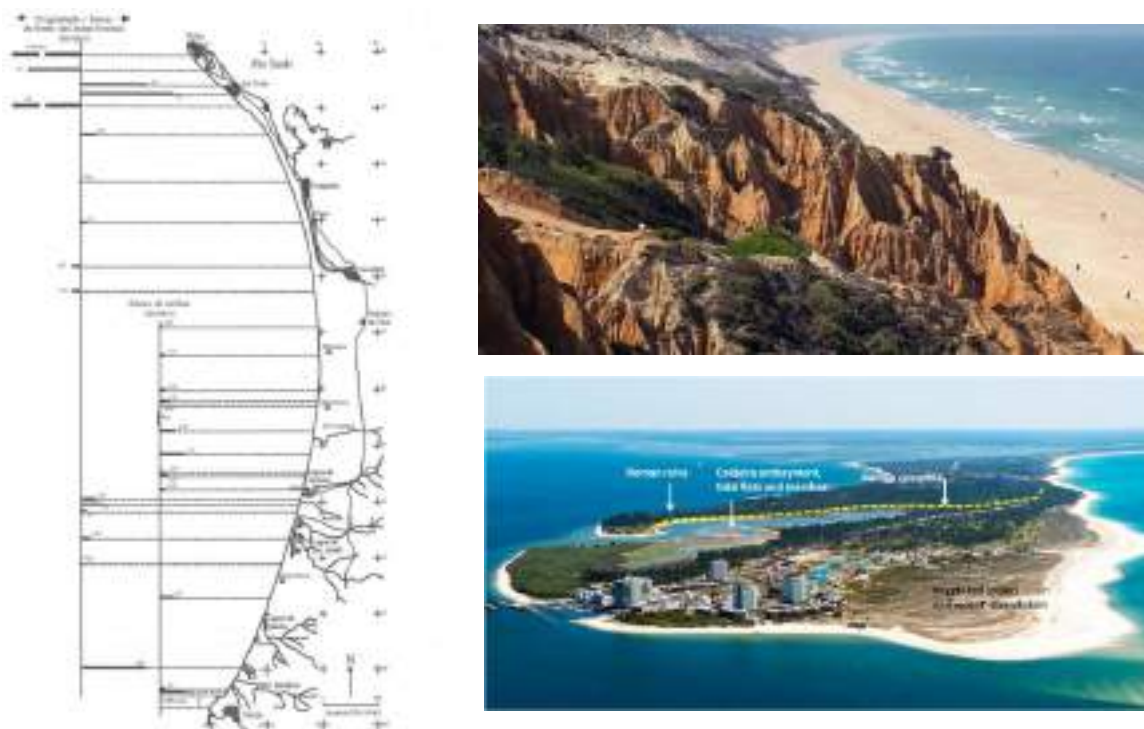


Figure 89. Left: Coastline evolution (cliffs and beach/dunes) between 1947/48 and 1987/88 inferred by comparison of aerial photographs (Marques, 2000). Right, upper panel: Galé coast showing intense gulling of soft sandstones (source: <https://mapio.net/pic/p-11046265/>); lower panel: aerial view of Tróia northern tip (source: <https://discoverportugal2day.com/visitar-troia/>); note recent tourist development, the Caldeira embayment, Roman shoreline, and post Roman extension of the spit and significant seaward progradation of the beach.

The coast facing the Atlantic is wave-dominated, the magnitude of sheltering increasing (though non-linearly) northwards. Net mean yearly littoral drift is directed northward,

and the absence of relevant external sediment sources explain concentration of cliff erosion over the southern 2/3 of this coast, whereas the northern 1/3 shows stability or prograding/accretion patterns (Marques *et al.*, 1995, Marques, 2000), (Fig. 89).

At the downdrift end of Tróia sand spit, archaeological works uncovered a Roman settlement buried under dune ridges. The exact paleogeography of the Tróia barrier at this time (a single spit rooted at its southern end or a set of barrier-islands that later welded to form the present day continuous spit is still a matter of debate). The settlement corresponds to the largest known Roman facility that produced and exported fish products to the whole Roman world between the 1st and 4th (5th?) centuries AD (Etienne *et al.*, 1994, Pinto *et al.*, 2011 provide further references on the Roman settlement, see also <https://www.atlas.cimal.pt/drupal/?q=pt-pt/node/109>). Following the abandonment of Roman settlement, relevant occupation and land use changes over of the spit resumed only in the last quarter of the 20th century and were driven by tourism, in contrast with the continuous occupation and diverse land-uses of the landward margins (Fig. 90).



Figure 90. Sado channel and estuary showing different soil occupations (Andrade *et al.*, 2006).

Key: Brown – intertidal shoals; light green – rice fields (formerly salt marshes); dark green – tidal flats and marshes; red – urban/industrial areas; yellow – salt pans and aquaculture facilities. CC – Comporta channel; CAL – Alcácer channel; CM – Marateca channel. Note the asymmetry in the intensity of occupation over the spit and landward margins of the estuary: whereas the former shows minimum development, the latter has been transformed for rice-fields and aquaculture, urban and industrial facilities, including port and shipyards, thermoelectric, paper and cement plants, as well as numerous quarries and chemical industrial facilities.

Sado inlet channel bifurcates upstream the gorge in a northern, ebb-dominated channel and a southern, flow-dominated channel (CN and CS, respectively, in Fig. 90). The nature and distribution of inner estuarine bottom sediments has not been investigated in full but available data indicate that they are essentially sandy and of marine provenance, especially over the seaward subtidal area. Sand and muddy sand intertidal flats and marshes occupy about 1/3 of the estuarine region and concentrate at the margins. The estuary is very shallow and exhibits an overall trend for siltation that also affects both

main tidal channels. Boundaries separating intertidal flats and marshes are dynamical and low marsh expansions have been yielding area to non-vegetated intertidal flats, although the surface of both marshes and flats show vertical accretion (Freitas *et al.*, 2008). In contrast with the oceanic façade, the estuarine margin of the spit is swept by drift currents directed southward and related with locally generated waves. Siltation intensity over the estuarine domain is variable in time and space but locally reached up to $1 \times 10^0 \text{ cm yr}^{-1}$, indicating that the estuarine basin is a relevant sink for marine sediment (Andrade *et al.*, 2006). Estuarine filling progressed in tune with decrease of tidal prism, in turn decreasing the equilibrium cross section of the inlet and the ability of tidal currents to limit spit lengthening; altogether, this allowed for northward extension of the sand spit during the last 2000 yrs (Fig. 89).

In contrast with the limited expression of the flood delta, outer shoals (ebb delta) of the Sado estuary are very large and shallow. This sand body is broadly triangular in plan shape and its terminal lobe attaches to the spit close to Sol-Tróia development. The outer inlet channel is narrow and deep and intensity of tidal currents precludes the need for regular dredging, with the exception of its terminal lobe. At a broader time-scale, formation of the ebb delta has been related with formation and northward elongation episodes of the Tróia sand spit, a process that occurred intermittently in time (Costas *et al.*, 2015, see also Rebêlo *et al.*, 2009, Brito, 2010, Freitas and Andrade, 2008). Costas *et al.* (2015) dated the formation of the Tróia sand spit to about 6500 cal years BP, in coincidence with the marked reduction in sea-level rise rate (Fig. 4, Fig. 91). Later development consisted of episodes of northward extension and seaward progradation, intercalated by episodes of coastal stabilization and recession. Definition and evolution of the Sado inlet and ebb delta is proposed in this study to have progressed throughout the last 3300 years.

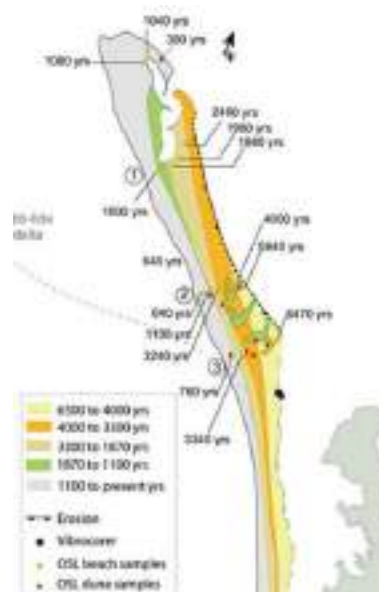


Figure 91. Major episodes of elongation and progradation of Tróia sand spit (Costas *et al.*, 2015).

Spit elongation provoked the enclosure of a former bay and setting of a single inlet, which in turn prejudiced barrier elongation and favored the accumulation of the ebb delta at the cost of sediment previously consumed by spit growth.

Stop 4. Arrábida – Structural landforms of an Alpine chain

Geological setting

The Meso-Cenozoic sedimentation reflects the complex tectonic and eustatic history that affected the Setúbal peninsula, comprised between the Tagus estuary to the north and the Sado estuary to the south. The lower Jurassic is formed by an evaporitic sequence (i.e. marls and clay) followed by compact, oolitic and coral limestone of middle to upper Jurassic age (Fig. 92). The upper Jurassic and Cretaceous deposits present strong lateral facies variations, related to differences in the depositional environments between the western (marine) and the eastern (fluviomarine) zones of the Arrábida Chain. While to the west bedrock lithology is mostly composed by limestone with fine pelitic intercalations, surface geology in the east is characterised by poorly consolidated sandstone and sandy limestone (Fig. 92). Cropping out in the eastern sector of the chain, the Paleogene and Miocene strata are characterised by coarse-grained conglomeratic deposits and by shallow marine sequences (i.e. marls and coral limestone).

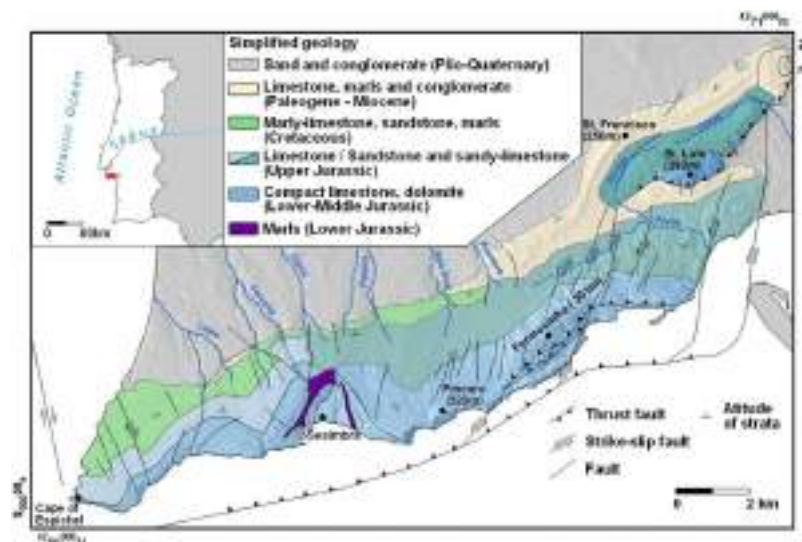


Figure 92. Structure and simplified geology of the Arrábida Chain (extracted from Fonseca *et al.* 2020)

The Pliocene and lower Quaternary sedimentation in the Setúbal peninsula were related to the paleo-drainage system of the Tagus River. Before its establishment along the Tagus gorge (north bounding the Setúbal Peninsula), the Tagus River reached the Atlantic Ocean in the vicinity of the Arrábida Chain. During this period, sediment accumulation to the north of the Chain was controlled by tectonic subsidence in the Tagus plain.

The Arrábida chain

Although small, with 35 km in length and 7 km in width, the Arrábida Chain is a WSW-ENE Alpine orogenic belt that exposes an almost complete sedimentary sequence from the lower Jurassic to the Pliocene. From the structural point of view, the chain is limited in the west and east by strike-slip structures, to the south by the Arrábida thrust and to the north by the Lagoa de Albufeira syncline (Fig. 92).

The tectonic deformation and main uplift phase of the Arrábida Chain occurred during the Middle to Late Miocene in response to the convergence between Africa and Eurasia. Two stages of deformation are identified: (1) Burdigalian (17–16 Ma)—uplift and formation of the south-verging Formosinho anticline (Fig. 93) in response to N–S compression (Antunes *et al.* 1995); and (2) upper Tortonian (8–7 Ma)—change in the shortening direction from N–S to NW–SE, causing uplift in the eastern part of the Chain and the formation of the São Luís anticline (Choffat 1908)(Fig. 93). Plio-Quaternary tectonic activity is associated with displacements along both E-W thrust faults and NNE-SSW to NNW-SSE sinistral strike-slip faults, together with a regional tilting towards NNW, in response to both the tectonic subsidence of the Tagus River basin and the uplift of the Arrábida Chain (Manuppella *et al.*, 1999).

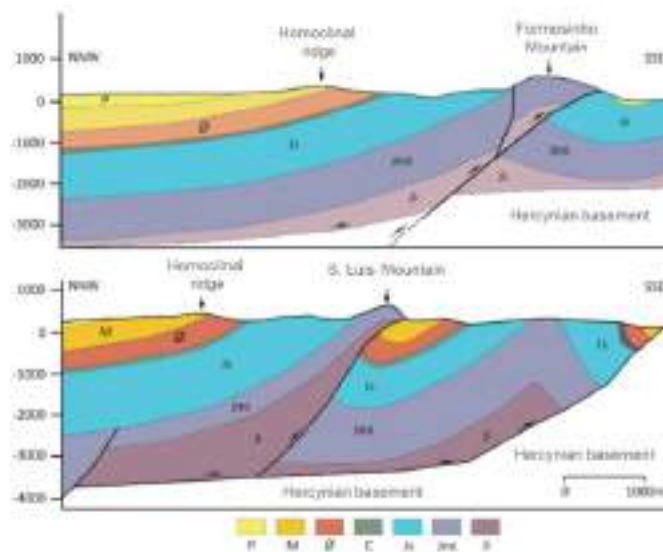


Figure 93. Geologic profiles of Arrábida (adapted from Kullberg *et al.*, (2000). P) Pliocene; M) Miocene; Φ) Palaeogene; C) Cretaceous; Js) Upper Jurassic; Jmi) Middle-Lower Jurassic; Ji) Lower Jurassic.

Structural Landforms

The Formosinho mountain (501 masl) (Fig. 94) and the São Luis Mountain (392 masl) are the highest landforms within the Arrábida chain. These two mountains are structural landforms where lithology, fold and fault geometry control the present-day topography. Formed by lower to middle Jurassic compact limestone and dolomitic units, these structures survived the action of erosional processes acting since the earliest stages of

uplift. The progressive exposure of the anticline core led to the present-day topographic setting, with the asymmetry of both the Formosinho and São Luís explained by the southerly vergence of the anticline folds and associated thrusts (Fonseca *et al.*, 2020). Along the northern flank of the Formosinho, the erosion of upper Jurassic units led to the formation of typical hogback and chevron landforms supported by compact limestone and dolomitic layers. These rocky outcrops were the source of relict scree deposits that extend to the base of the slopes, presently fed by occasional rockfalls and rockslides (Fonseca *et al.*, 2020). To the north of Formosinho and São Luís mountains, the upper Jurassic to Miocene layers strike roughly ENE–WSW and dip to the north. The dip is highest in the vicinity of the anticline folds and diminishes to the north (75–50°). Differences in bedrock erodibility played a crucial role in the evolution of this sector of the chain by imposing limits to drainage network incision. While the less competent units of the upper Jurassic, Cretaceous and Miocene (i.e. sand, conglomerates and clay) gave place to strike valleys formed by prolonged drainage incision, the competent limestone and sandy limestone belonging to Cretaceous, Paleogene and Miocene beds were left untouched forming parallel sets of homoclinal ridges (Fig. 95) (Fonseca *et al.*, 2014, 2015, 2020).



Figure 94. Southern flank of the Arrábida Chain and beach of Portinho da Arrábida. Notice the lower to middle Jurassic limestone strata forming the axis of the Arrábida anticline and thrust. Photograph credits Duarte Fernandes Pinto, A Terceira Dimensão, <http://portugalfotografiaaerea.blogspot.com> (Fonseca *et al.*, 2020)

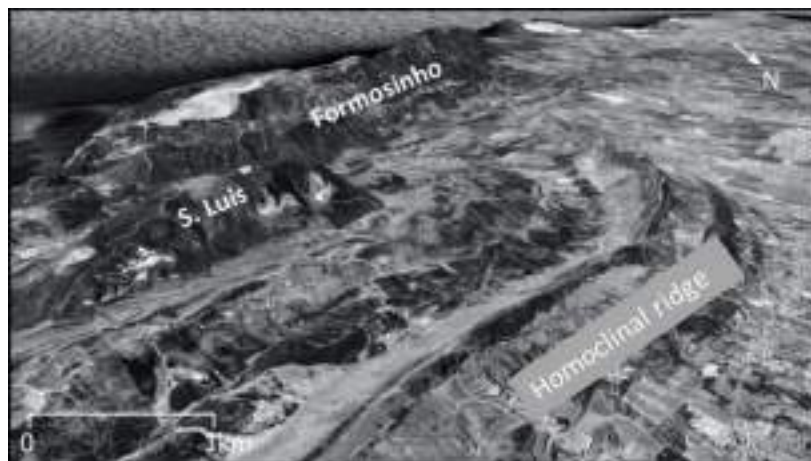


Figure 95. Bird-eye view of the Arrábida chain indicating the main structural landforms (Fonseca *et al.*, 2015).

Stop 5. Cape Espichel – The Cape Platform

Following the paroxysmal phase of tectonic deformation in the Late Miocene, vertical movements persisted in the Setúbal Peninsula during the Plio–Quaternary through the uplift of the Arrábida Chain and subsidence in the Tagus basin. Large-scale geomorphic evidence of surface uplift is provided by four erosion surfaces (L1—190 to 220 m; L2—140 to 170 m; L3—70 to 110 m; L4—30 to 50 m) perched above the present-day drainage network (Fonseca *et al.*, 2014, 2015, 2020). The preservation of these geomorphic markers is strongly associated with differences in bedrock resistance to erosion, particularly in the case of the uppermost level (L1). While to the west, the compact units of Jurassic limestone and dolomite allowed its preservation, to the east, the upper Jurassic sandstones and poorly consolidated conglomerates favoured drainage network incision, limiting geomorphic evidence of L1 to the lower flank of Mount Formosinho and São Luís.

One of the most striking stages in the evolution of the landforms of the Arrábida chain is the development of the erosive level L1, around 190 - 220 meters, named as the Cape Platform (Fig. 96), which is the oldest erosive level preserved in the region. This erosive landform (Fig. 97) extends from Cape Espichel to the base of the São Luís Mount at c. 190–220 m asl. The fact that it has developed within the compact limestone and dolomitic unit of lower to middle Jurassic age, forming a nearly flat surface, has led geomorphologists to classify it as a paleo-marine level (Ribeiro, 1968; Daveau and Azevedo, 1980–1981; Pereira, 1988; Cabral, 1993). Besides the occasional quartz pebble, the lack of stratigraphic references hampers the definition of a clear time frame for this erosional phase. Nevertheless, given that the L1 cuts the northern flank of the St. Luís anticline, a post-Tortonian age and possible association with the high sea-level stands of upper Miocene and/or Pliocene (Fonseca *et al.*, 2015) are suggested.

The intermediate surface (L2) descends from the northern edge of the upper level (L1) and towards the top of the homoclinal ridges, suggesting a degradation phase of L1, connected with a northerly-directed drainage during the Late Pliocene and Early Pleistocene time (Daveau and Azevedo, 1980–1981; Fonseca *et al.*, 2014, 2015).

The external level (L3) cuts the Pliocene terrain and the Belverde Formation along the northern flank of the Arrábida Chain and is fossilised by the torrential deposits of the Marco Furado formation. The lack of absolute ages for the Belverde (lower Pleistocene) and Marco Furado (middle Pleistocene) formations hinders the definition of a specific timeframe for the elaboration of L3 (Fonseca *et al.*, 2014).

The lowest level (L4) represents a degradation of L3 in response to Pleistocene sea-level lowering, leading to the formation of the Lagoa de Albufeira during the Holocene.

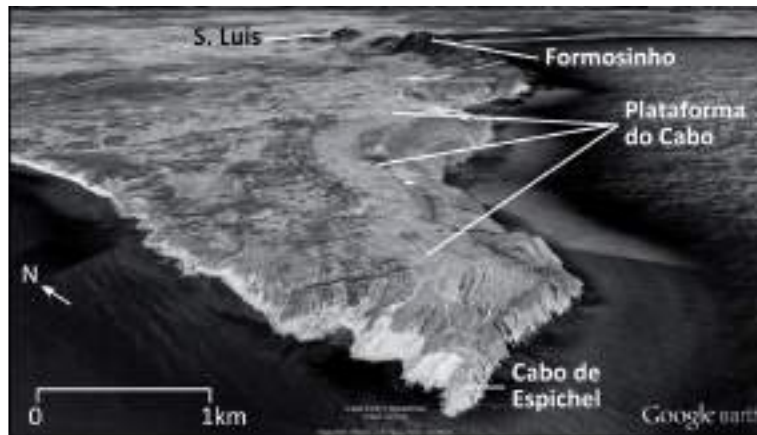


Figure 96. Bird-eye view of the Cabo platform in the west part of the Arrábida (Fonseca *et al.*, 2015).



Figure 97. Cape Espichel. Notice the upper Jurassic limestone strata dipping to the north. The erosion surface along the top corresponds to the Cabo Platform. Photograph credits Duarte Fernandes Pinto, A Terceira Dimensão, <http://portugalfotografiaaerea.blogspot.com> (Fonseca *et al.*, 2020).

Stop 6. Cristo Rei viewpoint – Lisbon and the Tagus

The location of Lisbon - close to the open coast and Tagus estuary - as well as its geomorphology, conditioned to a large extent the history of occupation and development of this city. Almeida (1991), Guerra *et al.* (2019-2022) and Vaz and Zêzere (2020) provide extensive information on the geology and geomorphology of Lisbon, in addition to details on its human occupation since pre-History until Roman times underpinning the following description. Lisbon developed and expanded over Mesozoic and Caenozoic sedimentary rocks ranging in facies from shallow marine to lagoonal and estuarine, with only brief excursions to terrestrial sedimentation and erosive episodes. These sediments were subsequently folded and fractured over the last ca. 100 M years. In very broad terms, the southwestern region developed over the Monsanto anticline (where the highest elevation is reached, ca. 227 m above msl), which features a Cenomanian limestone nuclei surrounded by basalt (s.l.) lava flows and pyroclasts, whereas the eastern region expanded over layers of Paleogene and Miocene conglomerates, clays, marls, bioclastic sandstones and calcarenites, all of which dip gently towards S and SE (Fig. 98).

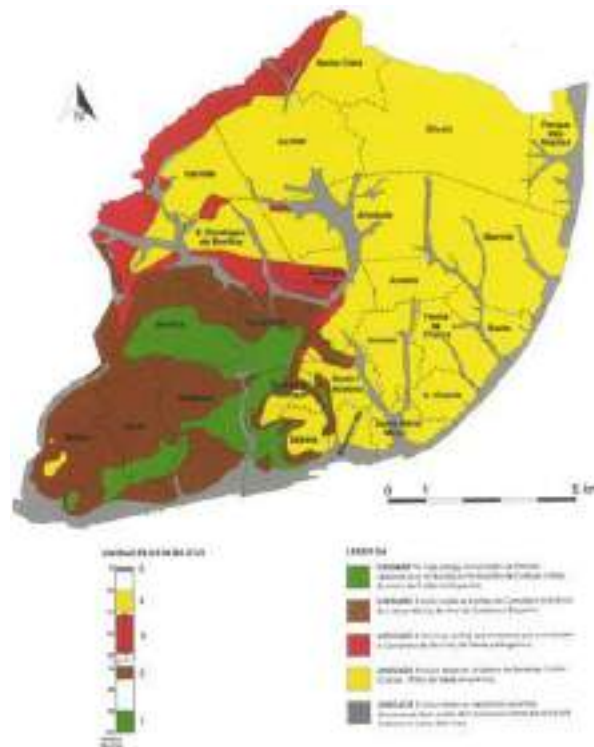


Figure 98. Schematic distribution of main lithostratigraphic units of the Lisbon area (Guerra *et al.*, 2012-2022). Key: green – Upper Cretaceous carbonate rocks; brown – Late Cretaceous/Paleocene lava flows and tephra of the Lisbon Volcanic Complex; red – Palaeogene fluvial detritic rocks; yellow – Miocene sediments; grey – alluvial deposits and landfills.

Contrasting resistance to weathering and erosion offered by different lithotypes (often outcropping side by side due to fault-controlled offset) determined a rugged landscape, showing pronounced structural and lithological controls that the urban mythology refers to as the “seven hills of Lisbon”. Hill tops and higher points correspond to outcrops of resistant rocks. Examples of this are the crystalline reef limestones of Monsanto anticline and the well cemented Miocene calcarenites that provide foundations for the São Jorge castle. Hills were first used for defense and also hosted churches and convents. They are separated by deeply incised flat-floored valleys that provided soil for agriculture. They frequently exhibit steep slopes, in cases forming canyons, such as the Alcantara valley; the iconic avenues of Almirante de Reis and Liberdade, leading to Lisbon downtown, align with the bottom of ancient streams (Valverde and Arroios) that merged further south into the wide tide-influenced channel of “Esteio da Baixa”. This channel made a serious obstacle to East-West circulation and was first extensively intervened in Roman times and later completely rectified and landfilled. Differential erosion is also responsible for the development of pronounced escarpments (designated in Portuguese by the word “costa”, like in “Costa do Castelo”) controlled atop by hard detritic limestones resting over thick and softer sediments. A number of these scarps and high-angle slopes conditioned construction of staircases and elevators. In general terms, the hydrographic network is dendritic and exploits contacts between different lithologies or weaker lineaments along fractures and drains towards S and SW, into the estuary. The northern margin of the estuary was subjected to successive landfills, which

started during Roman occupation and progressed in time and area until present. Romans also significantly changed the geomorphology by means of excavations, landfills and channeling of streams, establishing a primary framework upon which the city expanded.

Looking from the viewpoint of Cristo Rei, a clear asymmetry is apparent in the relief exhibited by the slopes margining the Tagus inlet channel: whereas the land surface to the north gently slopes towards the river following the general attitude of the Meso-Cenozoic layers, the south embankment is scarped and affects only Miocene sediments. This slope shows numerous signals of instability, related with creeping and slope mass movements. Slope instabilities determined extensive engineering works because of risk for port facilities and small urban settlements along this embankment.

The asymmetry above results from the river having cut and deepened the gorge channel subparallel to the general strike of the sedimentary sequence, exploiting E-W subvertical faults (Fig. 99).



Figure 99. Cross section of the Tagus gorge (Moitinho de Almeida, 1986)

The scarp is hold atop by outcrops of resistant detritic limestones of the Miocene sequence that make the northern section of the Albufeira syncline (Fig. 100).

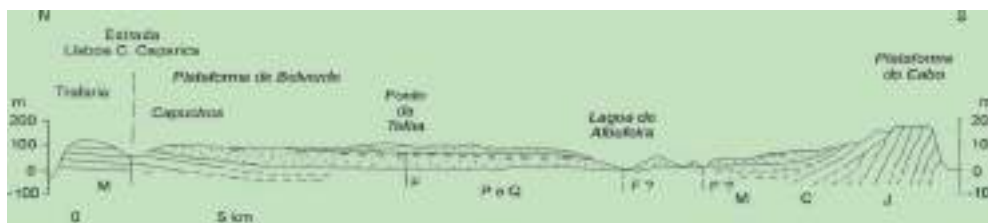


Figure 100. N-S schematic cross section of the Albufeira syncline and Arrábida range.

According to Freire (1999), Costa (1999) and Taborda *et al.* (2009) the Tagus estuary develops over a wide (320 km²) and shallow basin (mean depth of ca. 10m). It is a semidiurnal, mesotidal system, with tidal amplitudes of 1.0 m (neap tide) to about 3.5 m (spring tide) at the mouth. The average tidal prism was estimated in 7 x 10⁸ m³ and generates high renewal of estuarine water at every tidal cycle. The dynamic tide reaches 80 km upstream of the mouth and salinity is just slightly lower than that of marine water until V. F. Xira, but it decreases very rapidly upstream.

The Tagus estuary is peculiar in plan shape: margin separation along the NNE-SSW direction increases up to 15 km and decreases markedly downstream until meeting the narrow fault-controlled and deep inlet channel trending E-W (Fig. 101).

Extensive mudflats and salt marshes developed along both margins due to fluvial input of suspended sediment delivered by the main channel and numerous small creeks with modest watersheds, especially along the southern margin. There is net export into the open ocean of fine-grained sediments, in contrast with the long residence time and entrapment of coarse sediments. Coarse sediment entrapment is especially relevant where the main river channel meets the estuarine basin and encouraged the development of a bay-head delta (Fig. 101). Estuarine margins are extensively artificialized with most of the waterfront being at present engineered by seawalls, dykes, breakwaters, jetties and various rock-armored structures, which were built for aquaculture, port and urban protection and to shelter farmland; “natural” margin environments (salt marshes, beach and cliff) represent about one third of the estuarine perimeter with cliffs being dominant at the estuarine channel, whereas salt marshes and tidal flats are most frequent in the left embankment of the inner estuary.

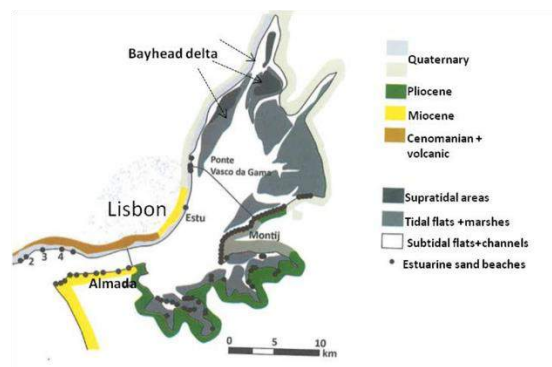


Figure 101. Main morphosedimentary domains of the Tagus estuary and location of principal estuarine sand beaches, (adapted from Guerra *et al.*, 2019-2022, Taborda *et al.*, 2009).

Sand retention within the estuarine domain has been increasing in tune with works for flow regularization and control, and construction of multiple dams for water storage. Thus, and regardless of the vast extension of the catchment area, the Tagus is not a relevant sand source for the coastal segments exposed to the Atlantic and extending north and south of the inlet.

The narrow Tagus inlet channel operates as an effective diffraction window regarding ocean swell. However, its geomorphology offers a sufficiently wide fetch for prevailing (northerly) winds to generate local waves that are responsible for cliff erosion and accumulation of sandy beaches and spits, especially along the left embankment (cf. Taborda *et al.*, 2009 for details and further references). These features are almost absent on the right embankment due to poor potential of the northern margin outcrops as sand sources. In contrast, the left margin shows a crenulated shape due to incision of several tributaries and its potential as sediment source is high, regarding the degree of

erodibility and textural compatibility of gravels, sandstones, conglomerates, silt and clay that constitute Pleistocene, Miocene and Pliocene formations affected by stream erosion and locally generated waves.

The relative importance of fluvial and marine processes in shaping this transitional depositional system varied in time and the following summary is mostly based on the studies by Vis *et al.* (2008) and Vis (2009). The very deep incision (about 70 m in the Lisbon region) of the Tagus river channel at around 20 000 BP, when mean sea level dropped to about -120 m provided space to accommodate a thick sedimentary sequence preserving signatures of environmental changes and shifting depocenters (Fig. 102).

During the 20000 BP low-stand and until about 12000 BP the narrow width of the exposed shelf provided bypassing of fluvial sediments into the heads of Lisbon and Cascais canyons, adjacent slope and abyssal plain, which formed the essential depocentres for about 8000 years (Fig. 103). Between 12000 and 7000 BP sea-level rose from ca. -40 m to about its present day position and the sedimentary record contains evidence of an earlier shift of the main depocenter to the continental shelf that persisted until ca. 10000 BP; the transgressive pulse continued in time and a second shift allowed for the drowning of the river valley by marine water to about 100 km upstream of the mouth, that lasted until ca. 7000 BP.

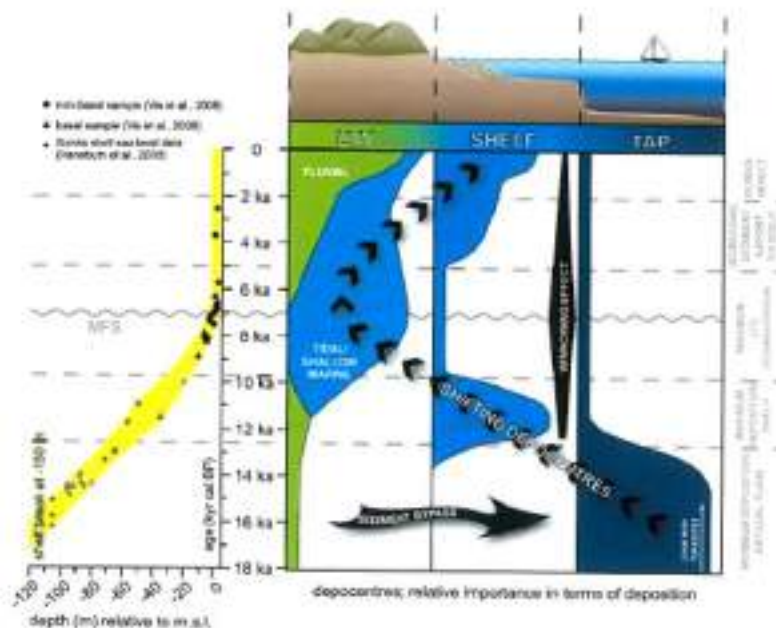


Figure 102. Time shifts in Tagus depocenters since 18000 BP, varying between the lower valley reach, the estuary, the nearby shelf/slope and abyssal plain (Vis, 2011).

After 7000 BP, relative stability in msl combined with fluvial activity and an inundated basin determined the onset of a forced regression (Fig. 102, Fig. 103), with downstream progradation of the bayhead delta and accumulation and expansion of overbank

deposits that steadily progressed downstream. Estuarine sedimentation responded essentially to changes in rate and nature of sediment supply determined by climate change, to which human interference with vegetation and land-use should be added, in particular following Roman colonization. While the inner estuary has been operating as an efficient sink for coarse sediment, fine-grained sediment exported via the gorge channel accumulated on the outer estuary, resulting in the growth of a large sediment bulge from about 7000 BP onwards, forming the foundations of the present-day Tagus ebb tidal delta.

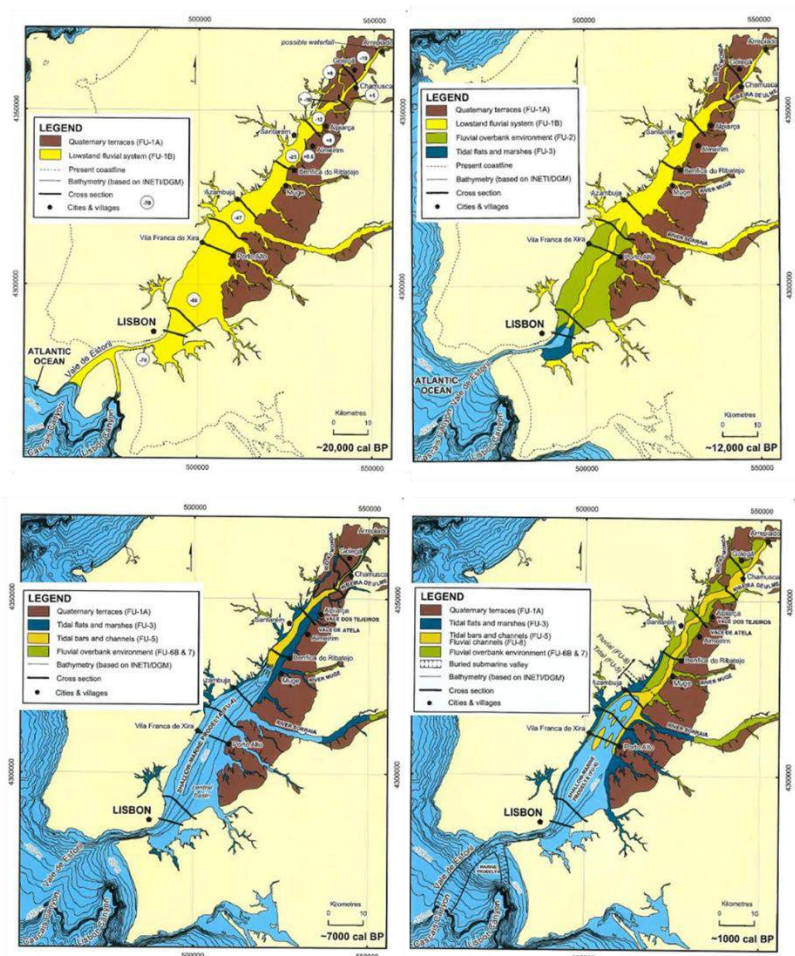


Figure 103. Paleogeography of the Tagus lower domain, estuary and shelf throughout the Holocene (after Vis, 2011)

References

- Abecasis, F. (1987) O regime aluvionar na costa portuguesa entre Peniche e a foz do Mira. *Ingenium*, 8, 4-18.
- Almeida, I. M. (1991). Características geotécnicas dos solos de Lisboa. PhD thesis, Faculdade de Ciências da Universidade de Lisboa.
- Alonso, E.E., Pineda, J.A., Cardoso, R. (2010) Degradation of marls; two case studies from the Iberian Peninsula. In: Calcaterra D, Parise M (eds) *Weathering as a predisposing factor to slope movements*, Geological Society, London, Eng. *Geol.Special Publications* 23, pp 47–75.

- Andrade, C., Freitas, M. C., Brito, P., Amorim, A., Barata, A. & Cabaço, G. (2006) – Estudo de Caso da Região do Sado – Zonas costeiras. In: Santos, F. D., Miranda, P. (Eds). Alterações Climáticas em Portugal. Cenários, Impactos e Medidas de Adaptação. Projecto SIAM II, Gradiva: 423-438.
- Andrade, C., Freitas, M.C., Cachado, C., Cardoso, A., Monteiro, J., Brito, P., Rebelo, L. (2002) Coastal zones. In: Santos, F.D., Forbes, K., Moita, R. (eds.), Climate Change in Portugal. Scenarios, Impacts and Adaptation Measures, Gradiva, Lisboa, 173–219.
- Andrade, C., Pires, H. O., Silva, P., Taborda, R. & Freitas, M. C. (2006a) – Zonas Costeiras. In: Santos, F. D. & Miranda, P. (Eds). Alterações Climáticas em Portugal. Cenários, Impactos e Medidas de Adaptação. Projecto SIAM II, Gradiva, pp. 169-208.
- Antunes MT, Elderfield H, Legoinha P, Pais J (1995) Datações isotópicas com Sr do Miocénico do flanco sul da Serra da Arrábida. Comunicações Instituto Geológico e Mineiro 81:73–78
- APA (2017) Plano de ação litoral XXI. Agência Portuguesa do Ambiente.
- Azevedo TM (1982) O Sinclinal de Albufeira. Evolução Pós-Miocénica e Reconstituição Paleogeográfica. Dissertação de doutoramento, Centro de Geologia, Fac. de Ciências de Lisboa, p 302
- Azevedo, M. T. (1983) -O Sinclinal de Albufeira- evolução pós-miocénica e reconstituição paleogeográfica. PhD thesis, Faculdade de Ciências da Universidade de Lisboa, 321 p.
- Bastos, A.P., Taborda, R., Silva, A.N., Ponte Lira, C., Andrade, C., Calvão, J.M. (2022) - A punctuated equilibrium model for storm response of geologically controlled beaches: application to western Portuguese beaches. *Geomorphology*, 404, 108184.
- Breuil, A., Zbyszewski, G. (1943) Le quaternaire de Santo Antão do Tojal. *Com Serv Geol Port XXIV*, Lisboa, 43–70.
- Breuil, H.; Zbyszewski, G. (1942 – 45) Contribution à l'étude des industries paléolithiques du Portugal et de leurs rapports avec la géologie quaternaire. *Comunicações dos Serviços Geológicos de Portugal*, 23 e 26, Lisboa
- Brito P (2010) Na Fronteira do Mar – Evolução geológica do estuário do Sado e da plataforma continental entre Sesimbra e o Canhão de Setúbal nos últimos ~ 50000 anos. Câmara Municipal de Sesimbra, Sesimbra, Portugal.
- Cabral J (1993) Neotectónica de Portugal Continental. Dissertação de doutoramento, Departamento de Geologia, Faculdade de Ciências da Universidade de Lisboa, p 435
- Cabral, J. (1995). Neotectónica em Portugal continental. *Memórias do Instituto Geológico e Mineiro*, 31, Lisboa, 265 p.
- Cabral, J. (2012) Neotectonics of mainland Portugal: state of the art and future perspectives *Journal of Iberian Geology*, 38 (1): 71-74.
- Carvalho J, Barceló J (1966) Agitação marítima na costa W de Portugal. *Memórias do L.N.E.C.*, 290, 34p.;
- Choffat P (1908) Essai sur la tectonique de la Chaîne de l'Arrabida. *Memórias dos Serviços Geológicos Portugueses*, p 89
- Chung, C.F., Fabbri, A.G. (1993) The representation of geoscience information for data integration. *Nonrenewable Resources*, 2(2), 122-139.
- CMA (Câmara Municipal de Almada) (2005). Carta Geológica do Concelho de Almada na escala 1:20 000. Departamento de Estratégia e Gestão Ambiental Sustentável da Câmara Municipal de Almada / Centro de Estudos Geológicos da Faculdade de Ciências e Tecnologia da Universidade Nova de Lisboa.
- Coelho, A.G. (1979) Análise cartográfica de estabilidade de taludes para o planeamento urbano. *Geotecnia*, 26, 75-89.
- Costa M (1987) Análise de um ano de dados de agitação marítima na Figueira da Foz. *Anais do Instituto Hidrográfico*, 8: 23 28.
- Costa M (1994) Agitação marítima na costa portuguesa. *Anais do Instituto Hidrográfico*, 13: 35 – 40.
- Costa, M. J. (1999). O estuário do Tejo. Ed. Cotovia, Lisboa, 196 p.
- Costa, M., Esteves, R. (2009) Clima de agitação marítima na costa oeste de Portugal Continental. *Actas, XI Jornadas Técnicas de Engenharia Naval*. Instituto Superior Técnico, Lisboa.
- Costas, S., Ferreira, Ó, Plomaritis, T., Leorri, E. (2016) Coastal barrier stratigraphy for Holocene high-resolution sea-level reconstruction. *Nature Scientific Reports*, 6, 38726.

- Costas, S., Jerez, S., Trigo, R.M., Goble, R., Rebêlo, L. (2012). Sand invasion along the Portuguese coast forced by westerly shifts during cold climate events. *Quaternary Science Reviews*, 42: 15-28.
- Costas, S., Rebêlo, I., Brito, P., Burbidge, C., Prudêncio, M., FitzGerald, D. (2015) The Joint history of Tróia Peninsula and Sado ebb-delta. In: Randazzo, G. et al. (eds.) *Sand and Gravel Spits, Coastal Research Library*, 12, Springer.
- Cunha, P., Martins, A., Cabral, J., Gouveia, M., Buylaert, J-P., Murray, A. (2015). Staircases of wave-cut platforms in western central Portugal (Cape Mondego to Cape Espichel) – relevance as indicators of crustal uplift. *Proceedings, VIII Simposio Margem Ibérico Atlântico (MIA15)*, Málaga: 137 -144.
- Daveau, S. (1973) Quelques exemples d'évolution quaternaire des versantes au Portugal. *Separata de Finisterra. Revista Portuguesa de Geografia*. Vol.VIII, nº 15, Lisboa, 47p.
- Daveau, S. (1980) Espaço e tempo – evolução do ambiente geográfico de Portugal ao longo dos tempos pré-históricos. C. L. I. O. - *Revista de História da Universidade de Lisboa*, Vol. 2, Lisboa, p. 13 – 37
- Daveau S, Azevedo T (1980–81) Aspectos e evolução do relevo da extremidade sudoeste da Arrábida (Portugal). *Bol. Soc. Geol. Port.*, volume de homenagem aos Professor Carlos Teixeira, Lisboa, pp 163–180
- Daveau, S. (1985) Critères géomorphologiques de déformations tectoniques récentes dans les montagnes de schistes de la Cordilheira Central (Portugal). *Bulletin de l'AFEQ*, nº24, 4, 229 – 238
- Daveau, S., Almeida, G., Feio, M., Rebelo, F., Silva, E., Sobrinho, A. (1978) Os temporais de Fevereiro / Março de 1978. *Finisterra*, 13 (26): 236-260.
- Daveau, S.; Pereira, A. R.; Zbyszewski, G (1983) Datation au C14 du site archéologique de la plage de Magoito (Portugal) scélée par une dune consolidée, C. L. I. O. - *Revista de História da Universidade de Lisboa*, Vol. 4, Lisboa
- Dewey, J. F., Helman, M. L., Knott, S. D., Turco, E., & Hutton, D. H. W. (1989) Kinematics of the western Mediterranean. *Geological Society, London, Special Publications*, 45(1), 265-283.
- Dias, A. (1985) Registos da migração da linha de costa nos últimos 18.000 anos na plataforma continental portuguesa setentrional. I Reunião do Quaternário Ibérico - Actas, Vol. I, Grupo de Trabalho para o Estudo do Quaternário, Instituto Nacional de Investigação Científica, Fundação Calouste Gulbenkian, Lisboa, p. 281 – 295
- Dias, A. (1990) A evolução actual do litoral português. *Geonovas*, 11, p. 15 – 28
- Dias, A.; Taborda, R. (1988) Evolução recente do nível médio do mar em Portugal. *Anais do Instituto Hidrográfico*, 9, Lisboa, p. 83 - 97
- Dias, R., Madeira, J. (1982) Cartografia geológica da zona compreendida entre o Cabo da Roca e a Praia das maças. Relatório de estágio de licenciatura em geologia, FCUL (não publicado).
- Dias, R., Oliveira, J., Matos, J., Ressureição, R., Machado, S., Pais, J., Manupella, G. (2016) Notícia Explicativa da Carta 42-A (Grândola), Carta Geológica de Portugal à escala de 1:50 000, Laboratório nacional de Energia e Geologia, Lisboa.
- Diogo, Z., Bastos, A., Lira, C., Taborda, R., Freire de Andrade, C., Silveira, T., Ribeiro, M., Silva, A.N., Carapuço, M.M., Pinto, C., Freitas, M.C. (2014) Morphological impacts of Christina storm on the beaches of the central western Portuguese coast. *Comunicações Geológicas*, 101, Sp. Iss. 3, 1445-1448. ISSN: 0873-948X; e-ISSN: 1647-581X
- Dodet, G., Bertin, X., Taborda, R. (2010) Wave climate variability in the North East Atlantic Ocean over the last six decades. *Ocean Modelling*, 31, 120–131.
- Duarte, D., Volochay, K., Magalhães, R., Amaro, S., Cabral, J. (2014). Caracterização de terraços marinhos entre Cascais e o Cabo da Roca com recurso a elementos cartográficos e de detecção remota. *Implicações neotectónicas. Geonovas, Rev. Assoc. Portuguesa de Geólogos*, 27: 39-46.
- Étienne, R., Makaroun, Y., Mayet, F. (1994).- *Un grand complexe industriel à Tróia (Portugal)*. Éditions de Boccard, Paris.
- Fabbri, A.G., Chung, C.F., Napolitano, P., Remondo, J., Zêzere, J. L. (2002) Prediction rate functions of landslide susceptibility applied in the Iberian Peninsula. *WIT Transactions on Modelling and Simulation*, 31.
- Ferreira, A. (2019) Dinâmica sedimentar e morfológica do campo de dunas da Crismina-Guincho. MSc dissertation, Faculdade de Ciências da Universidade de Lisboa, 130 p.
- Ferreira, A. B. (1984) Découverte d'un littoral a 250 m sur le piemont occidental de la Serra de Sintra. *Finisterra*, XIX (37), 83-88.
- Ferreira, A.B. (1984) Mouvements de terrain dans la région au Nord de Lisbonne—conditions morphostructurales et climatiques. *Documents-BRGM*, (83), 485-494.

- Ferreira, A.B., Zêzere, J.L., Rodrigues, M.L. (1987) Instabilidade dos versantes na região ao Nord de Lisboa. Essai de cartographie geomorphologique, *Finisterra* 22(44), 227–246.
- Ferreira, A.B., Zêzere, J.L., Rodrigues, M.L. (1996) The Calhandriz landslide (Metropolitan area of Lisbon). *Landslides*, Balkema, Rotterdam, 31–38.
- Ferreira, O., Voudoukas, M., Ciavola, P. (2009) Micore review of climate change impacts on storm occurrence (open access, deliverable wp1. 4). <http://www.micore.eu/file.php?id=4>
- Figueiredo, P., Cabral, J., Rockwell, T., Ponte Lira, F. (2019) Morphotectonics in a low tectonic rate area: analysis of the southern Portuguese Atlantic coastal region. *Geomorphology*, 326, 132–151.
- Fonseca AF, Zêzere JL, Neves M (2014) Geomorphology of the Arrábida Chain. *J Maps* 10(1):103–108.
- Fonseca AF, Zêzere JL, Neves M (2015) Contribution to the knowledge of the geomorphology of the Arrábida Chain (Portugal): Geomorphological mapping and geomorphometry. *Rev Bras Geomorfol* 16 (1):137–163.
- Fonseca, A. F., Zêzere, J. L., Neves, M. (2020) The Arrábida Chain: The Alpine Orogeny in the Vicinity of the Atlantic Ocean. In *Landscapes and Landforms of Portugal* (pp. 273–278). Springer, Cham.
- Freire, M. (1986) – A Planície litoral entre a Trafaria e a Lagoa de Albufeira- estudo de geomorfologia litoral. Dissertação de Mestrado, Faculdade de Letras da uiversidade de Lisboa, 204 p.
- Freire, P. (1999). Evolução morfo-sedimentar de margens estuarinas (estuário do Tejo, Portugal). Tese de Doutoramento, Faculdade de Ciências da Universidade de Lisboa, 320p.
- Freitas, J.G., Dias, J.A. (2013) 1941 windstorm effects on the Portuguese coast. What lessons for the future? *Journal of Coastal Research*, SI65: 714–719.
- Freitas, M. C., Andrade, C. (2008) - O estuário do Sado. In Soares, J. (Coord.), *Embarcações tradicionais no contexto físico-cultural do estuário do Sado*. MAEDS, ADS, APSS: 20–29.
- Freitas, M.C., Andrade, C., Cruces, A., Munhá, J., Sousa, M.J., Moreira, S., Jouanneau, J.M., Martins, L. (2008). Anthropogenic influence in the Sado Estuary (Portugal): a geochemical approach. *Journal of Iberian Geology*, 34(2): 271–286.
- Friedman, G.; Sanders, J. (1978) *Principles of Sedimentology*. John Wiley & Sons, New York, 792p.
- Gama C, Dias J, Ferreira Ó, Taborda R (1994) Analysis of storm surge in Portugal, between June 1986 and May 1988. *Proceedings of Littoral*, 94: 26–29.
- Gama, C., Taborda, R., Andrade, C. (2006) Longshore sediment transport in the Tróia-Sines littoral ribbon (SW Portugal). Abstracts, VII Congresso Nacional de Geologia, Estremoz, Portugal.
- Garcia, R.A.C., Oliveira, S.C. (2020) Portugal Landslide Hazardscapes. In *Landscapes and Landforms of Portugal* (pp. 63–71). Springer, Cham.
- Girão, A. A. (1949 – 1951) *Geografia de Portugal*. 2ª. edição, Portucalence Editora, Porto, 510p.
- Guerra, A., Freitas, M.C. and Cachão, M. (2019–2022) (coord.) *Lisboa Romana*. Felicitas Julia Olisipo, II. O Território e a Memória. Câmara Municipal de Lisboa, Lisboa, 157 p. ISBN: 978-989-658-644-7. <https://dunesopenarchive.letras.ulisboa.pt/portal/apps/Cascade/index.html?appid=2b49dabba6a74a868ccba6fbdf13e332>.
- Kullberg MC (1996) *Estudos Tectónicos e Fotogeológicos nas Serras de Sintra e Arrábida*. Tese de Doutoramento. Faculdade de Ciências da Universidade de Lisboa.
- Kullberg MC, Kullberg J, Terrinha P (2000) Tectónica da Cadeia da Arrábida. In *Tectónica das regiões de Sintra e Arrábida*, *Memórias Geociências*. Museu Nac Hist Nat Univ Lisboa 2:35–84
- Kullberg MC, Kullberg JC (2000) Tectónica da região de Sintra. In: *Tectónica das Regiões de Sintra e Arrábida*, vol 2. Museu Nacional de História Natural, Lisboa, *Memórias de Geociências*, pp 1–34
- Kullberg MC, Kullberg JC (2000) Tectónica da Região de Sintra. In *Tectónica das regiões de Sintra e Arrábida*. *Mem Geociências Univ. Lisboa* 2:01–34.
- Kullberg, M. C., Kullberg, J. C. (2020) Landforms and geology of the Serra de Sintra and its surroundings. In *Landscapes and Landforms of Portugal* (pp. 251–264). Springer, Cham.
- Kullberg, J.C., Rocha, R.B., Soares, A.F., Rey, J., Terrinha, P., Callapez, P., Martins, L. (2006) A Bacia Lusitaniana: Estratigrafia, Paleogeografia e Tectónica in Dias R; Araújo A; Terrinha P, Kullberg JC (Eds.) *Geologia de Portugal no contexto da Ibéria*. Universidade de Évora: 317 – 368.

- Leorri, E., Cearreta, A., Milne, G. (2012) Field observations and modelling of Holocene sea-level changes in the southern Bay of Biscay: implication for understanding current rates of relative sea-level change and vertical land motion along the Atlantic coast of SW Europe. *Quaternary Science Reviews* 42, 59–73. Doi: <http://dx.doi.org/10.1016/j.quascirev.2012.03.014>.
- Lopes, L., Oliveira, S.C., Neto, C., Zêzere, J.L. (2020) Vegetation evolution by ecological succession as a potential bioindicator of landslides relative age in Southwestern Mediterranean region. *Natural Haz.* 103: 599–622.
- Manuppella G, Antunes MT, Pais, Ramalho MM, Rey J (1999) Carta geológica de Portugal na escala 1:50 000. Notícia explicativa da folha 38-B Setúbal. Instituto Geológico e Mineiro, p 143
- Manuppella, G.; Antunes, M.; Pais, J.; Ramalho, M.; Rey, J. (1999) Notícia explicativa da folha 30-A (Lourinhã) da Carta Geológica de Portugal. Esc. 1:50 000. Serviços Geológicos de Portugal
- MAOTDR (2007) GIZC - Bases para a estratégia de Gestão Integrada da Zona Costeira Nacional. Ministério do Ambiente, do Ordenamento do Território e do Desenvolvimento Regional.
- Marques, F. (2000). Evolução das arribas e da linha de costa no arco litoral Tróia-Sines (Portugal). In: Carvalho, G. , Gomes, F., Pinto, F. (eds.) *A Zona Costeira do Alentejo. Proceedings, Seminário sobre a Zona Costeira do Alentejo, Sines, 16-18 June 1999: 69-80, Associação Eurocoast-Portugal.*
- Marques, F. (2018) Regional Scale Sea Cliff Hazard Assessment at Sintra and Cascais Counties, Western Coast of Portugal. *Geosciences* 8: 80; doi:10.3390/geosciences8030080.
- Marques, F., Almeida, I.M., Boléo-Tomé, A. (1995). Evolução das arribas do arco litoral Tróia-Sines: resultados preliminares. IV Congresso Nacional de Geologia, Porto, Dezembro de 1995. Mus. Lab. Min. Geol. Fac. Ciências Univ. Porto, *Memória* 4: 421-425.
- Martins, K., Blenkinsopp, C.E., Almar, R., Zang, J. (2017). The influence of swash-based reflection on surf zone hydrodynamics: a wave-by-wave approach. *Coastal Engineering*, 122, 27–43. <https://doi.org/10.1016/j.coastaleng.2017.01.006>.
- Miranda, R., Valadares, V., Terrinha, P., Mata, J., Azevedo, M.R., Kullberg, J.C., Ribeiro, C. (2009) Age constraints on the Late Cretaceous alkaline magmatism on the West Iberia Margin. *Cretac Res* 30:575–586.
- Moitinho de Almeida, F. (1986) Carta Geológica do Concelho de Lisboa na escala 1:10000. Serviços Geológicos de Portugal, Lisboa.
- Moreira, M. E. (1992). Recent salt marsh changes and sedimentation rates in the Sado estuary. *Journal of Coastal Research*, 8 (3): 631-640.
- Neto, C., Geraldès, M., Almeida, D. (2020). The Tróia peninsula – an aeolian sedimentological legacy. In: . In: Vieira, G., Zêzere, J.L., Mora, C.. (eds.) *Landscapes and landforms of Portugal*, Springer: 99-108.
- Oliveira, L.M.E.T. (2009) Estudo Morfodinâmico e Sedimentar das Praias do Concelho de Sintra. Mestrado em Geologia do Ambiente, Riscos Geológicos e Ordenamento do Território. https://repositorio.ul.pt/bitstream/10451/3310/1/ulfc055508_tm_ligia_oliveira.pdf
- Oliveira, M.A. (2017) - Boulder deposits related to extreme marine events in the western coast of Portugal. PhD thesis, Faculdade de Ciências da Universidade de Lisboa, 369 p.
- Oliveira, M.A., Andrade, C. (2017). Boulder deposits in the Lisbon region. In: Costa, P. and Andrade, C. (eds.) *Field trip guide for the 5th International Tsunami Field Symposium, Lisboa, September 2017*, pp. 8-42. ISBN: 978-989-20-7817-15.
- Oliveira, M.A., Llop, E., Andrade, C., Branquinho, C., Goble, R., Queiroz, S., E., Freitas, M.C., Pinho, P. (2020). Estimating the age and mechanism of boulder transport related with extreme waves using lichenometry. *Progress in Physical Geography*, 44(6): 870–897. <https://doi.org/10.1177/0309133320927629>.
- Oliveira, M.A., Scotto, M.G., Barbosa, S., Andrade, C., Freitas, M.C. (2020) Morphological controls and statistical modelling of boulder transport by extreme storms. *Marine Geology*, 426, pp 1-16.
- Oliveira, S.C. (2012) Incidência espacial e temporal da instabilidade geomorfológica na bacia do rio Grande da Pipa (Arruda dos Vinhos). PhD thesis in Physical Geography, IGOT, Universidade de Lisboa, 452p.
- Oliveira, S.C., Zêzere, J.L., Catalão, J., Nico, G. (2015) The contribution of PSInSAR interferometry to landslide hazard in weak rock-dominated areas. *Landslides* 12(4):703–719.
- Pais, D. (2021). Evolução do sistema praia-duna de São João da Caparica após alimentação artificial. MSc dissertation, Departamento de Geologia, Faculdade de Ciências da Universidade de Lisboa.
- Pais, D., Andrade, C., Pinto, C. (2022). Evolution of a beach-dune system after artificial nourishment: the case of São João da Caparica (Portugal). In: Strypsteen, G., Roest, B., Bonte, D., Rauwoens, P. (Ees.). *Book of abstracts:*

- Building Coastal Resilience 2022. Bruges, Belgium, 12-13 April. VLIZ Special Publication 89. KU Leuven, Leuven / Flanders Marine Institute (VLIZ), Oostende, Belgium: 50-52.
- Pais, J., Moniz, C., Cabral, J., Cardoso, J., Legoinha, P., Machado, S., Morais, M., Lourenço, C., Ribeiro, M., Henriques, P., Falé, P. (2006). Notícia Explicativa da Folha 34-D (Lisboa) da Carta Geológica de Portugal na Escala 1:50 000 (2ª edição). Lisboa, Portugal: Departamento de Geologia/Instituto Nacional de Engenharia, Tecnologia e Inovação.
- Palma, M., Marcelino, A., Sampath, D.M.R., Dias, J.A., Freitas, J.G. (2021) The Sand of Caparica: A history of human intervention in beach-dune system (Portugal), Storymap, DUNES Project,
- Paredes, D., Trigo, R. M., Garcia-Herrera, R., & Trigo, I. F. (2006) Understanding precipitation changes in Iberia in early spring: weather typing and storm-tracking approaches. *Journal of Hydrometeorology*, 7(1), 101-113.
- Pereira AR (1988) Aspectos do relevo de Portugal. Litorais ocidental e meridionais da Península de Setúbal. *Finisterra* 23(46):335–349
- Pereira, A. R. (1983) Enquadramento geomorfológico do sítio datado por C14 na praia de Magoito. *Cuadernos do Laboratório Xeológico de Laxe, nº5, VI Reunião do Grupo Espanhol de Trabalho do Quaternário, Vigo*, p. 551 – 563
- Pereira, A.R. (1988) Aspectos do relevo de Portugal. Litorais ocidental e meridionais da Península de Setúbal. *Finisterra* 23(46):335–349
- Pereira, A. R.; Correia, E. B. (1985) Duas gerações de dunas consolidadas em S. Julião, Ericeira (Portugal). I Reunião do Quaternário Ibérico – Actas. Vol. I, Grupo de Trabalho para o Estudo do Quaternário, Instituto Nacional de Investigação Científica, Fundação Calouste Gulbenkian, Lisboa, p. 323 – 337
- Pereira, A., Angelucci, D. (2004). Formações dunares no litoral português, do final do Plistocénico e inícios do Holocénico, como indicadores paleoclimáticos e paleogeográficos. In: Tavares, A., Ferro Tavares, A., Cardoso, J. (eds.) - *Evolução geohistórica do litoral português e fenómenos correlativos*. Geologia, História, Arqueologia e Climatologia, Universidade Aberta, Lisboa: 220-256.
- Pinto, C. (2014) Registo das ocorrências no litoral - Temporal de 3 a 7 de janeiro de 2014. (Record of damages on Portuguese Coastline during Hercules Storm (3 - 7 January 2014)). Technical report, Agência portuguesa do Ambiente, 123 p.
- Pinto, I., Magalhães, A., Brum, P. (2011). O complexo industrial de Tróia desde os tempos dos Cornélii Bocchi, escritor Lusitano da Idade de Prata da Literatura Latina. In: Cardoso J., Almagro-Gorbea, M. (eds.) *Lucius Cornelius Bocchus*. Academia Portuguesa da História e Real Academia de la Historia, Lisboa e Madrid, 133–167.
- Pinto, C. A., Taborde, R., Andrade, C. (2007). Evolução recente da linha de costa no troço Cova do Vapor – Costa da Caparica. *Actas, . 5ª Jorn. Port. Engenharia. Costeira e Portuária*, Lisboa, 13 p.
- Pinto, C.A., Silveira, T.M., Teixeira, S.B. (2020) Beach nourishment practice in mainland Portugal (1950–2017): overview and retrospective. *Ocean & Coastal Management*, 192, 105211.
- Pinto, C.A., Silveira, T.M., Teixeira, S.B. (2020). Beach nourishment practice in mainland Portugal (1950–2017): Overview and retrospective. *Ocean & Coastal Management*, 192(2020) 105211. doi.org/10.1016/j.ocecoaman.2020.105211.
- Pita C, Santos J (1989) Análise dos temporais da costa oeste de Portugal Continental. Report 1/89 A, Instituto Hidrográfico/LNEC, Lisboa.
- Prudêncio, I. Marques, R., Rebelo, L., Cook, G., Cardoso, G., Naysmith, P., Freeman, S., Franco, D., Brito, P., Dias, M. (2007). Radiocarbon and Blue Optically Stimulated Luminescence chronologies of the Oitavos consolidated dune (Western Portugal). *Radiocarbon*, 49 (2): 1145-1151.
- Psuty, N., Moreira, M.E. (2000). Holocene sedimentation and sea level rise in the Sado estuary, Portugal. *Journal of Coastal Research*, 16 (1): 125-138.
- Ramalho, M., Rey, J., Zbyszewski, G., Matos Alves, C., Palácios, T., Moitinho de Almeida, F., Costa, C., Kullberg, C. (2001). Carta Geológica e Notícia Explicativa da Folha 34-C (Cascais) na escala 1: 50000. Instituto Geológico e Mineiro, Lisboa.
- Ramos Pereira, A. (1988) Aspectos do relevo de Portugal. Litorais ocidental e meridional da Península de Setúbal. *Finisterra*, XXII, 46: 335-349.
- Ramos, C., Ramos-Pereira, A. (2020) Landscapes of Portugal: Paleogeographic Evolution, Tectonics and Geomorphology. In *Landscapes and Landforms of Portugal* (pp. 3-31). Springer, Cham.

- Ramos-Pereira, A. (2005) Cabo da Roca headland and its surroundings. In: A. Ramos-Pereira, J. Trindade and J. Neves, eds. (2005) Portugal: coastal dynamics. Field trip guide A1, 6th International Conference on geomorphology, Zaragoza, 38-40.
- Rato, D. (2017). Monitorização da Duna de São João da Caparica. MSc dissertation, Faculdade de Ciências da Universidade de Lisboa.
- Rau, V.; Zbyszewski, G. (1949) Estremadura et Ribatejo (Livret-guide de l'excursion D). XVI Congrès International de Géographie, Lisboa, 146p.
- Rebêlo, L. P. (2004) Evolução e Dinâmica dos Sistemas Dunares da Manta Rota e do Guincho-Oitavos: Dois Sistemas Distintos na Evolução das Dunas Costeiras em Portugal. Instituto Geográfico e Mineiro, Lisboa. 205p.
- Rebêlo, L., Brito, P., Monteiro, J. (2002) - Monitoring the Cresmina dune evolution (Portugal) using differential GPS. Journal of Coastal Research, SI 36: 591-604.
- Rebêlo, L., Ferraz, M., Brito, P. (2009). Tróia peninsula evolution: the dune morphology record. Journal of Coastal Research, SI56:352–355.
- Ressureição, R., Cabral, J., Dias, R. (2012) Plio-Pleistocene marine terraces at the Melides-Vila Nova de Milfontes (Alentejo, SW, Portugal): neotectonic implications. Abstracts, 7th Symposium on the Iberian Atlantic Margin, Lisbon.
- Rey, J. (2007) - Stratigraphie séquentielle et séquences de dépôt dans le Crétacé inférieur du Bassin Lusitanien. Ciências da Terra, Vol. Esp. VI, Universidade Nova de Lisboa, Lisboa, 120p.
- Rey, J., Caetano, P., Callapez, P., Dinis, J. (2009) – Le Crétacé du Bassin Lusitanien (Portugal). Excursion du Groupe Français du Crétacé, 100 p., <https://hal.archives-ouvertes.fr/hal-00452152>
- Rey, J., Gracinsky, P., Jacquin, T. (2003) - Les sequences de depot dans le Crétacé inférieur du Bassin Lusitanien. Comunicações do Instituto Geológico e Mineiro, Lisboa, 90: 15-42.
- Ribeiro A (2013) Evolução geodinâmica de Portugal: os ciclos Meso-Cenozóicos. In: Dias R, Araújo A, Terrinha P, Kullberg JC (eds) Geologia de Portugal, vol II, Geologia Meso-cenozóica de Portugal. Escolar Editora, Lisboa, pp 9–27
- Ribeiro, A. (1984) Néotectonique du Portugal. In: Livro de Homenagem a Orlando Ribeiro, Vol. 1, Centro de Estudos Geográficos, Lisboa, p. 173 – 182
- Ribeiro A, Antunes MT, Ferreira MP, Rocha RB, Soares AF, Zbyszewski G, Moitinho de Almeida F, Carvalho D, Monteiro JH (1979) Introduction à la Géologie Générale du Portugal. Serviços Geológicos de Portugal, Lisboa
- Ribeiro, M. (2017) Headland sediment bypassing processes. PhD thesis, University of Lisbon, 210p.
- Ribeiro, M., Taborda, R., Rodrigues, A., Silveira, T. (2014). Insights on sediment bypassing at headland-bay beaches: an example at the Portuguese west coast. Proceedings, 3 Jornadas de Engenharia Hidrográfica, Lisboa: 301-304.
- Ribeiro, O. (1968). Excursão à Arrábida. Finisterra, 3(6).
- Righetti, A. (2022) The geology and environmental processes that govern the origin of the continental shelf of Iberia. PhD thesis, University of Lisbon.
- Rock, N.M.S. (1982) The Late Cretaceous alkaline igneous province in the Iberian Peninsula, and its tectonic significance. Lithos 15:111–131
- Santos, M. (2006). Caracterização e quantificação do transporte sólido eólico na duna da Cresmina. Relatório de Estágio, Curso de Especialização Pós-graduada em Geologia Aplicada, Departamento de Geologia, Faculdade de Ciências da Universidade de Lisboa, 55 p.
- Santos, F., Mota Lopes, A., Moniz, G., Ramos, L., Taborda, R. (2014) Gestão da zona costeira. O desafio da mudança. Relatório do Grupo de Trabalho do Litoral. Technical report (in Portuguese), 237 p, prepared for the Portuguese Ministry of Environment, available at: https://apambiente.pt/sites/default/files/_SNIAMB_Agua/DLPC/ENGIZC/GTL_RF20150416.pdf
- Siddall, M., Chappell, J., Potter, E.-K. (2006). Eustatic sea level during past Interglacials. In: Sirocko, F., Claussen, M., Litt, T., Sanchez-Goni, M. (eds.) - The Climate of Past Interglacials, vol. 7. Developments in Quaternary Science, Elsevier Science: 75-92. ISBN: 9780080468068.
- Silva, C. F. (2015) Dinâmica Sedimentar em Sistemas Dunares Litorais – Aplicação ao Sistema Dunar da Praia do Guincho, Cascais. MSc Dissertation - Arquitetura Paisagista. Instituto Superior de Agronomia da Universidade de Lisboa, 120p.

- Silva, A.N., Taborda, R., Castelle, B., Dodet, G., 2020. Wave directional spreading importance on sheltered embayed beaches. *J. Coast. Res.* SI 95, 1536–1541.
- Silveira, T. M. (2017) Geomorphological framework control on beach dynamics. PhD thesis, University of Lisbon, 368 p.
- Silveira, T.M., Diogo, Z.S., Taborda, R., Andrade, C.F., Sousa, H., Carapuço, A.M., Silva, A.N., (2013). Entregável 1.2.3.e. - Caracterização da variabilidade morfodinâmica sazonal das praias-piloto representativas do litoral em estudo. Relatório técnico, Projeto Criação e implementação de um sistema de monitorização no litoral abrangido pela área de jurisdição da Administração da Região Hidrográfica do Tejo. FFCUL/APA, I.P., Lisboa. Technical Report (in Portuguese).
- Soares A (1999) Caracterização do clima de agitação marítima em Portugal continental utilizando os resultados do modelo numérico MAR3G.2. Nota técnica VAM2 – 2/99, Instituto de Meteorologia.
- Soares, A., Moniz, C., Cabral, J. (2006). A duna consolidada de Oitavos, a Oeste de Cascais, região de Lisboa : a sua datação pelo método do radiocarbono. *Comunicações Geológicas* 93, Laboratório Nacional de Engenharia e Geologia: 105-118. <http://hdl.handle.net/10400.9/886>
- Taborda, R., Andrade, C., Marques, F., Freitas, M.C., Rodrigues, R., Antunes, C., Pólvora, C. (2010) Plano estratégico do concelho de Cascais face às alterações climáticas. Unpublished technical report, CeGUL, LATTEX, DEGGE, FCUL – C. M. Cascais.
- Taborda, R., Andrade, C.F., Silva, A.N., Silveira, T.M., Lira, C., Freitas, M.C., Pinto, C. (2014) - Modelo de circulação sedimentar litoral no arco Caparica-Espichel. *Comunicações Geológicas*, 101, Especial II: 641-644.
- Taborda, R., Freire, P., Silva, A., Andrade, C. and Freitas, M.C. (2009). Origin and evolution of Tagus estuarine beaches. *Journal of Coastal Research*, SI 56 (Proceedings of the 10th International Coastal Symposium), 213 – 217. ISSN 0749-0258.
- Taborda, R., Freire, P., Silva, A., Andrade, C. and Freitas, M.C. (2009). Origin and evolution of Tagus estuarine beaches. *Journal of Coastal Research*, SI 56 (Proceedings of the 10th International Coastal Symposium), 213 – 217. ISSN 0749-0258.
- Teixeira S (1990) Dinâmica das praias da Península de Setúbal (Portugal). Dissertação de Mestrado, Universidade de Lisboa.
- Teixeira, S., Gaspar, P., Rosa, M. (2005) Holocene sea-level index points on the Quarteira coast (Algarve, Portugal). In: Freitas, M.C., Drago, T. Andrade, C. (eds.) *Proceedings, Coastal Hope Conference*, 24-29 July, University of Lisbon, 125-127.
- Terrinha P, Pueyo EL, Aranguren A, Kullberg JC, Kullberg MC, Casas-Sainz A, Azevedo MR (2018) Gravimetric and magnetic fabric study of the Sintra Igneous complex: laccolith-plug emplacement in the Western Iberian passive margin. *Int J Earth Sci* 107 (5):1807–1833
- Trigo, R. M., Pozo-Vázquez, D., Osborn, T. J., Castro-Díez, Y., Gámiz-Fortis, S., & Esteban-Parra, M. J. (2004) North Atlantic Oscillation influence on precipitation, river flow and water resources in the Iberian Peninsula. *International Journal of Climatology: A Journal of the Royal Meteorological Society*, 24(8), 925-944.
- Trigo, R. M., Ramos, C., Pereira, S. S., Ramos, A. M., Zêzere, J. L., Liberato, M. L. (2016) The deadliest storm of the 20th century striking Portugal: Flood impacts and atmospheric circulation. *Journal of Hydrology*, 541, 597-610.
- Trigo, R. M., Zêzere, J. L., Rodrigues, M. L., & Trigo, I. F. (2005) The influence of the North Atlantic Oscillation on rainfall triggering of landslides near Lisbon. *Natural Hazards*, 36(3), 331-354.
- Trindade, J. (2001) Evolução geomorfológica do sector terminal da bacia do rio Alcabrichel. Dissertação de Mestrado. FLUL. 121p.
- Trindade, J. (2010) Dinâmica morfossedimentar de praias dominadas por sistemas de arriba (Peniche – Cascais). Tese de Doutoramento. Universidade Aberta. 322p.
- Trindade, J.; Pereira, A. R. (2013) Inundation and erosion susceptibility in wave dominated beaches. *Finisterra*, XLVIII, 95, 2013, pp. 81 100
- Van Drunen, M. (2000) Landslides in urbanized areas north of Lisbon (Portugal). University of Lisbon. Report not published.
- Vaney, J. P.; Mougnot, D. (1981) La Plate-Forme continentale du Portugal et les provinces adjacentes. Analyse géomorphologique. *Memórias, Serviços Geológicos de Portugal*, nº28, Lisboa
- Vaz, T., & Zêzere, J.L. (2016) Landslides and other geomorphologic and hydrologic effects induced by earthquakes in Portugal. *Natural Hazards*, 81(1), 71-98.

- Vaz, T., Zêzere, J. L., Pereira, S., Oliveira, S. C., Garcia, R. A., & Quaresma, I. (2018) Regional rainfall thresholds for landslide occurrence using a centenary database. *Natural Hazards and Earth System Sciences*, 18(4), 1037-1054.
- Vaz, T., Zêzere, J.L. (2020). The urban geomorphological landscape of Lisbon. In: Vieira, G., Zêzere, J.L., Mora, C.. (eds.) *Landscapes and landforms of Portugal*, Springer: 295-303.
- Veloso Gomes, F., Taveira Pinto, F. (2004) Cova do Vapor case-study, Costa da Caparica (Portugal). Report, EuroSION Case Study, EUROSION - A European initiative for sustainable coastal erosion management. <http://www.euroSION.org/shoreline/40covadovapor.html>.
- Veloso Gomes, F., Taveira Pinto, F., Pais-Barbosa, J., Costa, J., Rodrigues, A. (2006). Estudo das intervenções na Costa da Caparica. *Actas, 1^{as} Jornadas de Hidráulica, Recursos Hídricos e Ambiente*, Faculdade de Engenharia da Universidade do Porto, Porto: 27-35.
- Vieira, R., Antunes, C., Taborda, R., Andrade, C. (2013) Sobreelevação meteorológica. Unpublished Technical report, project CIRAC (Floods and Risk in Climate Change Scenarios), Fundação da FCUL- Associação Portuguesa de Seguradores, 7 p.IS
- Vis, G.-J. (2009). Fluvial and marine sedimentation at a passive continental margin: the Late Quaternary Tagus depositional system. PhD Thesis, VU University of Amsterdam, 246 p.
- Vis, G.-J. (2011). A geo-gastronomical fieldtrip to the Tagus river in Portugal. A modern analogue for an incised valley-fill: from proximal to distal domain. *Petroleum Geologische Kring*, 60 p.
- Vis, G.-J., Kasse, C., Vandenberghe, J. (2008) Late Pleistocene and Holocene palaeogeography of the Lower Tagus valley (Portugal): effects of relative sea level, valley morphology and sediment supply. *Quaternary Science Reviews* 27, 1682–1709.
- Vitorino J, Oliveira A, Jouanneau J, Drago T (2002) Winter dynamics on the northern Portuguese shelf. Part 1: physical processes. *Progress in Oceanography*, 52: 129 153.
- Wilson, R. (1979) A reconnaissance study of Upper Jurassic sediments of the Lusitanian Basin. *Ciências da Terra*, 5, p. 53 – 84
- Zbyszewski, G. (1964) Notícia explicativa da Folha 2 Loures (Carta Geológica dos Arredores de Lisboa). *Serv Geol Portugal, Lisboa*
- Zbyszewski, G., Assunção, C.T. (1965) Notícia explicativa da folha 30-D (Alenquer). *Carta Geológica de Portugal (1:50 000)*. Serviços Geológicos de Portugal. Lisboa.
- Zbyszewski, G., Moitinho de Almeida, F., Torre de Assunção, C. (1955) – Notícia explicativa da Folha 30 – C (Torres Vedras) da Carta Geológica de Portugal na escala de 1: 50000. *Serviços Geológicos de Portugal, Lisboa*.
- Zêzere J.L. (1988) As costeiras a Norte de Lisboa. Dinâmica de vertentes e cartografia geomorfológica. *Dissertação Mestrado Geografia Física e Regional, Universidade de Lisboa*.
- Zêzere, J.L. (1991) As costeiras do Norte de Lisboa: evolução quaternária e dinâmica actual das vertentes. *Finisterra* 26(51), 27–56.
- Zêzere, J.L. (2001) Evolução geomorfológica da Bacia de Loures no decurso do Quaternário. *Redescobrir a Várzea de Loures: ambiente, geologia e pré-história antiga na Várzea: rios, riachos e ribeiros de Loures*, 33-40.
- Zêzere J.L. (2001) Distribuição e ritmo dos movimentos de vertente na região a Norte de Lisboa. *Centro de Estudos Geográficos, Lisboa*.
- Zêzere, J.L. (2020) The North of Lisbon Region—A Dynamic Landscape. In *Landscapes and Landforms of Portugal* (pp. 265-272). Springer, Cham.
- Zêzere, J.L., Garcia, R.A.C., Oliveira, S.C., Reis, E. (2008) Probabilistic landslide risk analysis considering direct costs in the area north of Lisbon (Portugal). *Geomorphology*, 94(3-4), 467-495.
- Zêzere, J.L., Oliveira, S.C., Garcia, R.A., Reis, E. (2007) Landslide risk analysis in the area North of Lisbon (Portugal): evaluation of direct and indirect costs resulting from a motorway disruption by slope movements. *Landslides*, 4(2), 123-136.
- Zêzere, J.L., Pereira, S., Tavares, A.O., Bateira, C., Trigo, R.M., Quaresma, I., Santos, P.P., Santos, M., Verde, J. (2014) DISASTER: a GIS database on hydro-geomorphologic disasters in Portugal. *Nat. Hazards*. 72, 503–532.
- Zêzere, J.L., Reis, E., Garcia, R., Oliveira, S., Rodrigues, M.L., Vieira, G., Ferreira, A.B. (2004) Integration of spatial and temporal data for the definition of different landslide hazard scenarios in the area north of Lisbon (Portugal). *Natural Hazards and Earth System Sciences*, 4(1), 133-146.

- Zêzere J.L., Trigo R. (2011) Impacts of the North Atlantic oscillation on landslides. In: Vicente-Serrano S, Trigo R (eds) Hydrological, socioeconomic and ecological impacts of the North Atlantic Oscillation in the Mediterranean Region, *Advances in Global Change Research*, Vol 46. Springer, Berlin, pp 199–212.
- Zêzere, J.L., Trigo, R.M., Trigo, I.F. (2005) Shallow and deep landslides induced by rainfall in the Lisbon region (Portugal): assessment of relationships with the North Atlantic Oscillation. *Natural Hazards and Earth System Sciences*, 5(3), 331-344.
- Zêzere, J.L., Vaz, T., Pereira, S., Oliveira, S.C., Marques, R., & Garcia, R.A. (2015) Rainfall thresholds for landslide activity in Portugal: a state of the art. *Environmental Earth Sciences*, 73(6), 2917-2936.

Index

Itinerary and schedule	7
Introduction	9
<u>Day 1.</u> Landslides and floods in the north of Lisbon	24
Stop 1. Loures - Cuestas landscape and the Loures basin	24
Stop 2. Trancão Valley - Landslides and landslide susceptibility assessment in the Fanhões-Trancão area	27
Stop 3. Roucas - Calhandriz – The Calhandriz Landslide	32
Stop 4. Mata - Landslides and landslide susceptibility assessment in the Grande da Pipa River (GPR) basin, Arruda dos Vinhos	36
Stop 5. Quintas - Disastrous flash flood occurred in November 1967	44
<u>Day 2.</u> The coast north of Lisbon	48
Stop 1. Maceira – Structural and erosional landforms	48
Stop 2. Santa Rita beach -recent and present-day coastal dynamics	60
Stop 3. Coxos – Sand and boulder dynamics on a rocky shore	67
Stop 4. Azenhas do Mar – Coastal Erosion and risk associated to sea cliff instability	82
Stop 5. Cape Roca – The westernmost point of Europe	86
Stop 6. Cresmina – Guincho – Cresmina aeolian corridor and headland by passing	88
Stop 7. Cape Raso – The Cascais platform	91

<u>Day 3. The coast south of Lisbon</u>	94
Stop 1. Capuchos viewpoint – Caparica strandplain	94
Stop 2. São João da Caparica – Coping with long term beach erosion	97
Stop 3. Outão – Sado estuary and Troia sandspit	100
Stop 4. Arrábida – Structural landforms of an Alpine chain	104
Stop 5. Cape Espichel – The Cape Platform	107
Stop 6. Cristo Rei viewpoint – Lisbon and the Tagus	108
References	113



Photo by Sérgio Brito

ORGANIZATION AND SUPPORTERS:





10th IAG INTERNATIONAL CONFERENCE ON GEOMORPHOLOGY

Photo by Sérgio Brito

COIMBRA - PORTUGAL
« GEOMORPHOLOGY AND GLOBAL CHANGE »

FIELDTRIP GUIDEBOOK **Littoral (Figueira da Foz – Barra) and Bairrada** 14 September 2022

Pedro A. Dinis
A. Campar Almeida



Pedro A. Dinis
A. Campar Almeida

10th International Conference on Geomorphology
Fieldtrip Guidebook – Littoral (Figueira da Foz –
Barra) and Bairrada

14 September 2022



Coimbra, 2022

Edition notice:

Title: *10th International Conference on Geomorphology. Fieldtrip Guidebook – Littoral (Figueira da Foz – Barra) and Bairrada*

Authors: *Pedro A. Dinis and A. Campar Almeida (University of Coimbra)*

Fieldtrip guided by: *Pedro A. Dinis and A. Campar Almeida (University of Coimbra)*

Edition: *Universidade de Coimbra, Faculdade de Letras*

Fieldtrip and Guidebook Coordination: *António Vieira (University of Minho)*

Cover: *Village of Costa Nova (photograph by António Campar Almeida)*

ISBN: *978-989-8511-03-4*

Introductory Note

The 10th International Conference on Geomorphology will take place in Coimbra (Portugal) from 12th to 16th September 2022, under the theme "Geomorphology and Global Change" and it is organized by the International Association of Geomorphologists (IAG) and the Portuguese Association of Geomorphologists (APGeom).

As in previous international conferences on Geomorphology, and as is the tradition in many geomorphological events organized around the world, the organizing committee of the 10th International Conference on Geomorphology proposed several fieldtrips to the participants, occurring before, during and after the main event.

These fieldtrips intend, above all, to show to geomorphologists from all over the world the diversity and richness of the geomorphological elements of the Portuguese territory (and also from Cape Verde) and to allow an exchange of experiences between the specialists that investigate these territories and the visitors, contributing for mutual scientific enrichment and for the valorization of this international conference.

The pre-conference fieldtrip is dedicated to the islands of Santiago and Fogo, in the Archipelago of Cape Verde. It will take place from 6th to 9th September and will be led by colleagues from the University of Cape Verde (Vera Alfama, Sónia Victória, Sílvia Monteiro, José Maria Semedo and Romualdo Correia). The volcanic geomorphology will dominate the visit (including well conserved structural volcanic forms such as cones, domes, craters and calderas), especially in the island of Fogo where recent volcanic activity has been registered.

The one-day mid-conference fieldtrips will take the visitors around the Portuguese mainland territory, the 14th September, allowing the visit of four different geomorphological realities.

In the Arouca UNESCO Global Geopark, internationally recognized territory since 2009, participants will be able to visit unique geological and geomorphological features (such as planation surfaces, bowl-shaped valleys and narrow river valleys) and witness the remarkable effort of protection and promotion of natural (abiotic and biotic) and cultural (tangible and intangible) heritage. The visit to the "516 Arouca" suspension bridge will be an excellent opportunity to observe the magnificent landscapes of this mountainous territory. This fieldtrip will be led by Artur A. Sá, António Vieira and Daniela Rocha.

The field trip to coastal areas of central Portugal will be led by Pedro Dinis and António Campar Almeida. Their proposal is to observe the different morphotectonic units of central west Portugal, namely the Coastal Mountain of Serra da Boa Viagem (revealing karstification features), the littoral plain (with aeolian dunes associated with some

reliefs with higher elevation), the Cértima subsiding area (structurally-controlled morphology), and the Buçaco region (with the Syncline of Buçaco).

The visit to the Schist Mountains of Central Portugal will be centered in the mountains of Lousã and Açor, and will be conducted by Luciano Lourenço and Bruno Martins. It is proposed the observation of the main contrasts of the landscape, especially in terms of its physical geography, translated into geological, hypsometric, geomorphological, and hydrographic differentiation, or the land use and occupation and evolution of vegetation cover, namely following the recurrent large forest fires and the subsequent erosive processes they caused.

The fourth one-day fieldtrip will be oriented to the Estrela UNESCO Global Geopark, and led by Gonçalo Vieira, Emanuel Castro and Fábio Loureiro. The main geoheritage significance of the Estrela UGGp is the extent and richness of the Late Pleistocene glaciation(s) landforms and deposits (with spectacular morphological features such as the Zêzere glacial valley or the glacial cirques, moraine boulders, erratics or *roches moutounnées*) as well as the peculiar long-term geological evolution (revealing a significant diversity of granite types and landforms).

The three post-conference fieldtrips include a visit to the Lisbon Region, Serra da Estrela and, finally, Minho and Galicia (Spain), and will take place from 17th to 19th September.

The fieldtrip to the Lisbon Region will be guided by José Luís Zêzere, César Andrade, Sérgio Oliveira, Jorge Trindade and Ricardo Garcia, and will cover topics related with slope instability and landslides that affect the region of Lisbon, the floods occurring in the area north of Lisbon, and the coastal dynamics, morphology, cliff instability and beach erosion at north and south of Lisbon.

The three days field trip to the Serra da Estrela is led by Gonçalo Vieira, Emanuel Castro and Fábio Loureiro. Participants will be taken to visit some of the Geopark's most inaccessible geosites and observe breathtaking landscapes during two hikes: one in the Zêzere valley and the other between Penhas Douradas and Lagoa Comprida. The different geosites to visit include features of glacial, periglacial, granite weathering, fluvial, hydrogeological, petrological and tectonic themes, and aspects related with the management of a UNESCO Global Geopark will be discussed.

The third three-days fieldtrip is destined to the northwestern part of Portugal and the Spanish region of Galicia. Guided by Alberto Gomes and Antonio Perez Alberti, will be mainly devoted to the coastal area and to the observation and discussion of issues related to coastal dynamics, marine terrace staircases, differential uplift of coastal blocks, coastal geoheritage, coastal geoarchaeology, coastal erosion and coastal land planning.

It is our expectation that these visits will please all participants and promote the scientific enrichment of all involved, allowing a better understanding of the topics covered in each one.

We also hope that this set of fieldtrip guidebooks can help in the understanding of the themes discussed and that they can be a testimony of the commitment and dedication shown by all the scientific responsible for the several visits, to whom the organizing committee of the International Conference on Geomorphology expresses its greatest recognition and gratitude.

have a good fieldtrip!

Lúcio José Sobral da Cunha
António Vieira

on behalf of the ICG2022 Organizing Committee

ITINERARY AND SCHEDULE

Itinerary

08:00 - Departure from Coimbra (Largo D. Dinis)

9:15 – 9:45 - Stop 1 – Doline in Serra da Boa Viagem

10:00 – 10:20 - Stop 2 – Viewpoint of Bandeira

10:35 – 11:10 - Stop 3 – “Casa dos Cogumelos”

11:25 – 11:40 - Stop 4 – Pond of Braças (Quiaios dunes)

12:10 – 12:20 - Stop 5 – Vagueira

12:30 – 13:00 - Stop 6 – Barra de Aveiro

13:00 – 14:30 - (Technical stop and lunch)

14:50 – 15:15 - Stop 7 - “Pateira de Fermentelos”

15:35 – 15:50 - Stop 8 – Arcos de Anadia

16:30 – 16:50 - Stop 9 – Cruz Alta

17:15 – 17:35 - Stop 10 – Chã da Mata

18:00 - Arrival in Coimbra

Introduction

The field trip Littoral-Bairrada (Fig. 1) will cover different morphotectonic units of central west Portugal (Fig. 2). Considering the order of the stops, these units are: (1) the Coastal Mountain of Serra da Boa Viagem, which is associated with a northward thrusting in the Quiaios Fault, (2) the littoral plain, a very dynamic low elevation region, strongly affected by coastal processes, where aeolian dunes are associated with some of the reliefs with higher elevation and the outcrop of the phreatic level in lower locations allowed the development of small freshwater lakes; (3) the Cértima subsiding area, characterized by several structurally controlled sectors that experienced independent geomorphological evolution during the late Pliocene-Quaternary; and (4) the Buçaco region, where the Porto-Tomar Fault Zone, underlining the limit between the Variscan Massif and the Meso-Cenozoic coastal margin, and the quartzites of Buçaco syncline have a major influence on local geomorphology.

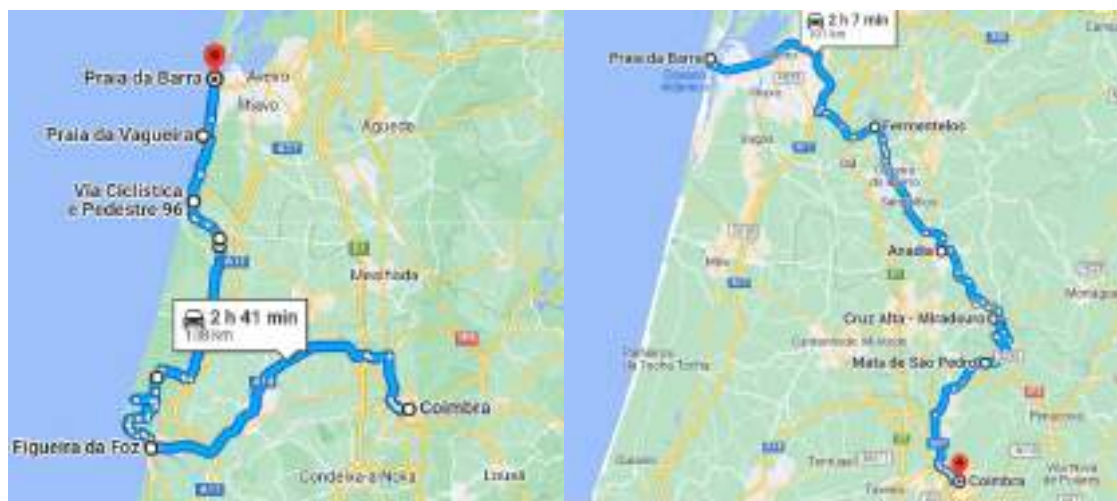


Figure 1. Morning itinerary (L) and afternoon itinerary (R) (Source: Google Maps).

Ten stops were selected for this field trip in order to provide snapshots of key positions for the understanding of the geomorphological evolution of West Iberia. Some of the following topics will be addressed:

- The Variscan deformation, which culminated with Pangea amalgamation, and its present imprint on the geomorphology of West Iberia;
- The Pangea break-up and the opening of the Atlantic Ocean, with reactivation of Variscan structures and deposition of diverse carbonate and siliciclastic series in the Lusitanian Basin of west Iberia;
- The sub-aerial exposure of Mesozoic carbonate successions and its karstification conditions, which affected even units with relatively high clay content

- The Neotectonic activity and the way it shaped drainage patterns in the fringe at the contact between the Atlantic Margin and the Variscan Massif;
- The Pliocene-Pleistocene landforms and nearshore deposits presently preserved in elevated regions of littoral mountains (Serra da Boa Viagem), in the eastern edge of the Variscan Massif, and in flattened regions between these reliefs;
- The history of aeolian sand invasion and its relation with the development of small and shallow freshwater lakes;
- The present forms of human occupation and use near a coastline that displays features typical of wave-dominated high energy settings with undoubtful associated risks.

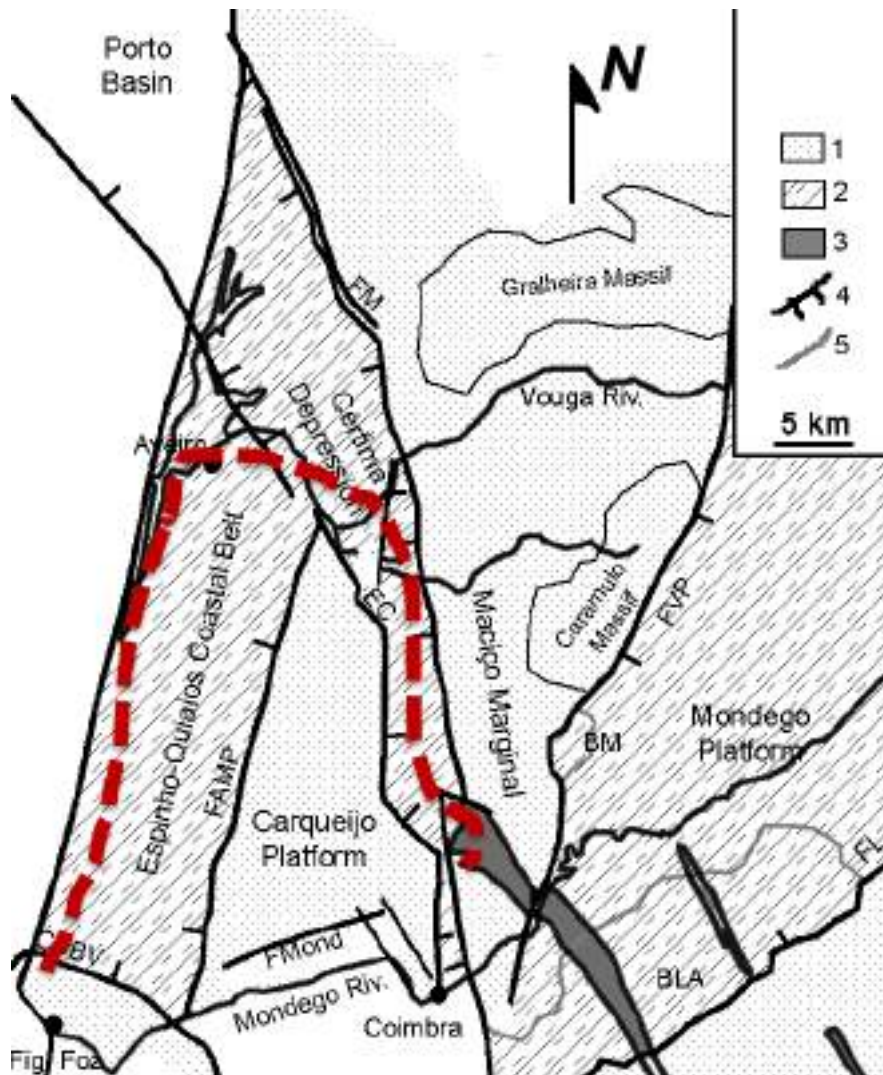


Figure 2. Main morphostructural units observed in the field trip. Approximate path indicated by dashed red line. 1: Uplifted sectors; 2: Subsiding sectors; 3: Quartzite ridge; 4: Major tectonic structure; 5: Main rivers; FM: Marginal Fault; FVP: Verin Penacova fault; FL: Lousã Fault; EAMP: Arunca Montemor Palhaça axis; CSBV: Serra da Boa Viagem thrust; Fmond: Mondego Flexure; BM: Mortágua Basin; BLA: Lousã Arganil Basin.

Stops are described below.

Stop 1. Dolines, karstification

The Serra da Boa Viagem with a carbonate succession that is covered by sandstones, particularly in the southern slope. Despite occasionally high clay and sand content, these units show an important karstification, especially with dolines. Nevertheless, other karst landforms are present such as lapies, swallow holes and caves. The lapies are spread through the upper surface and in the quaternary platforms. They are rounded because of the sandy cover and wave erosion when the sea was building these platforms during Quaternary interglacial periods. They can be classified as buried lapies (Cunha, 1988).

The swallow holes make, often, the linkage between dolines and caves because most of the dolines have a hole in their deepest points. The caves, which can be seen one or two in the landscape, are deduced when opened swallow holes let us listen water running in the depth. They must be narrow caves because the marly limestones are not favourable to the karstification.

There are about 150 dolines over the Serra da Boa Viagem (Fig. 3). Groups of them are oriented particularly W-E and N-S, which is more or less parallel to main geological lineaments and according to some transverse faults, respectively. In fact, the thicker and carbonate-enriched Bathonian, Oxfordian Kimmeridgian units allowed more intense chemical decomposition and faulting promoted water infiltration and thus increased rock dissolution. In general, the dolines can vary in size between 2 and 85 m length and 0.5 and 15 m in depth (Almeida, 1997). Curiously, the greatest ones appear in sandstones from the lower part of the Kimmeridgian succession (Fig. 4).

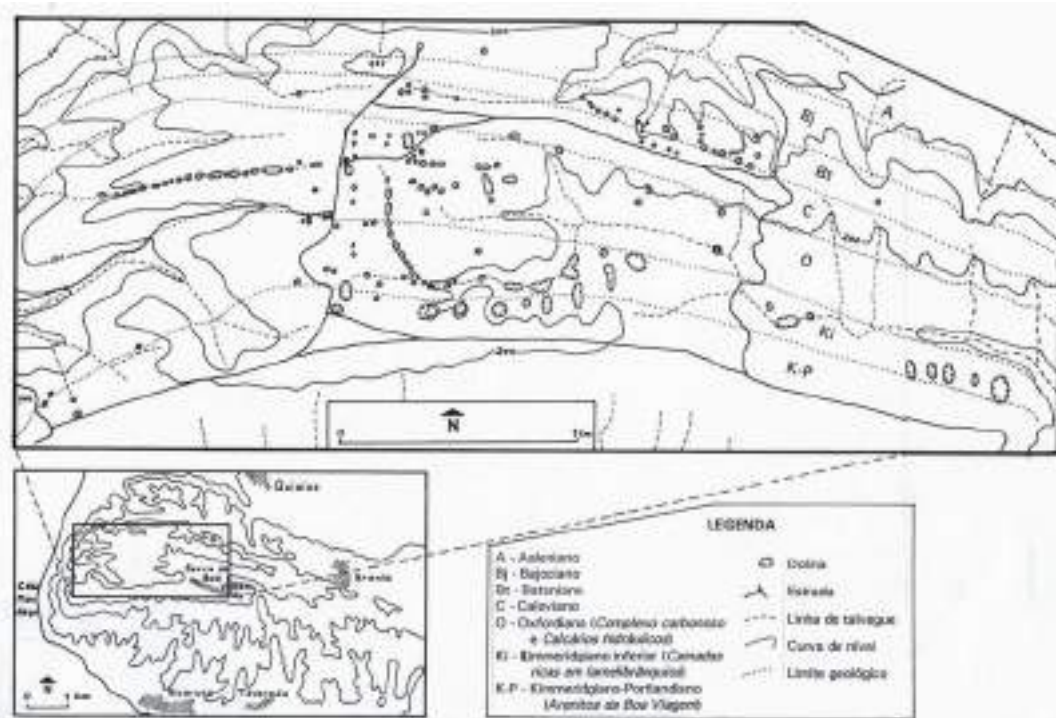


Figure 3. Doline distribution on the Boa Viagem mountain. From Almeida (2001).

Three types of dolines can be seen: funnel-shaped dolines, dish-shaped dolines and asymmetrical dolines. A lot of them are composite dolines with a funnel-shaped doline embedded into a dish-shaped doline (Almeida, 2001).

Usually, the holes in the dolines absorb all the water that flows on local watersheds.



Figure 4. A funnel shape doline, a year after a wildfire, and a swallow hole at the deepest point of a doline.

Genetic process

The dolines have almost all been developed on the upper part of the hill, between 257 m and 170 m above sea level. The beginning of its formation took place only after the retreat of the sea that had sculpted the surfaces where they stand, which is witnessed by coarse sandy to conglomeratic nearshore deposits, attributed to the end of the Pliocene or the early Pleistocene. With the marine regression, a fluvial incision developed with wide valleys that display rounded floors and, at the same time, the limestones were chemically attacked under a sandy permeable cover. The dish-shaped dolines would then have formed in this process. With the starting or continuation of the Serra da Boa Viagem uplift, the karstification deepened through the digging of pits and caves whose action has accelerated the vertical development of the dolines. A funnel shaped form can be ascribed to the fact that each doline has a little swallow hole in their bottom where the water flows down. The funnel-shaped dolines embedded in the dish-shaped dolines also resulted from the appearance of a swallow hole inside them.

A curious aspect is the presence of some of the largest dolines, such as the one to be visited, located in the outcrops of Upper Jurassic sandstones (Kimmeridgian- Tithonian), without calcium carbonate component. The explanation can be found in the local fracturing of these sandstones which allowed the attack of the underlying limestones, also fractured, and therefore with a greater surface of exposure to aggressive waters.

Stop 2. Viewpoint of Bandeira

Right below the viewpoint, a very steep scarp, about 150 m height, is very evident (Fig. 5, L). Its genesis has been attributed to an erosion scarp, but the contribution of a faulty movement must not be completely excluded. The possibility of thrusting of the Middle

Jurassic units over the marly Toarcian can be considered, but it still requires confirmation. Just at the northern end of the Serra da Boa Viagem, a lower scarp put in contact the Lower Jurassic limestones with Quaternary sands of Gândara. This contact also probably resulted from the action of an inverse fault (Cabral, 1993).



Figure 5. Scarp of Bandeira and scarp of Serra da Boa Viagem and Gândara in the background.

Looking to the northeast, a flat surface north of the Serra da Boa Viagem can easily be observed, where several villages stand out, interspersed with agricultural land and pine or eucalyptus forests (Fig. 5, R). It is Gândara, a term that etymologically means unproductive sandy land, despite offering various agricultural and animal productions at the expense of much effort on the part of its inhabitants. It consists of essentially parabolic dunes associated with transport from northwest to southeast, already very eroded by runoff (Fig. 6). Gândara sands are associated with the oldest generation of dunes whose age has been attributed to the last glacial period (G. S. Carvalho, 1964) or, at least, a thousand years ago, if they are equivalent to dunes with similar soils near Cortegaça (Carvalho and Granja, 1997). In fact, they display well-developed podzols with a thick ferruginous hard horizon, Bs, which differentiates them from other more recent dune generations located to the west until the ocean (Almeida, 1997). At its western limit there is a sequence of interdune ponds which are thought to have been created by the advance of the most recent dunes to the east, having blocked the circulation of water towards the sea and contributed to the groundwater rising in the oldest dune forms.

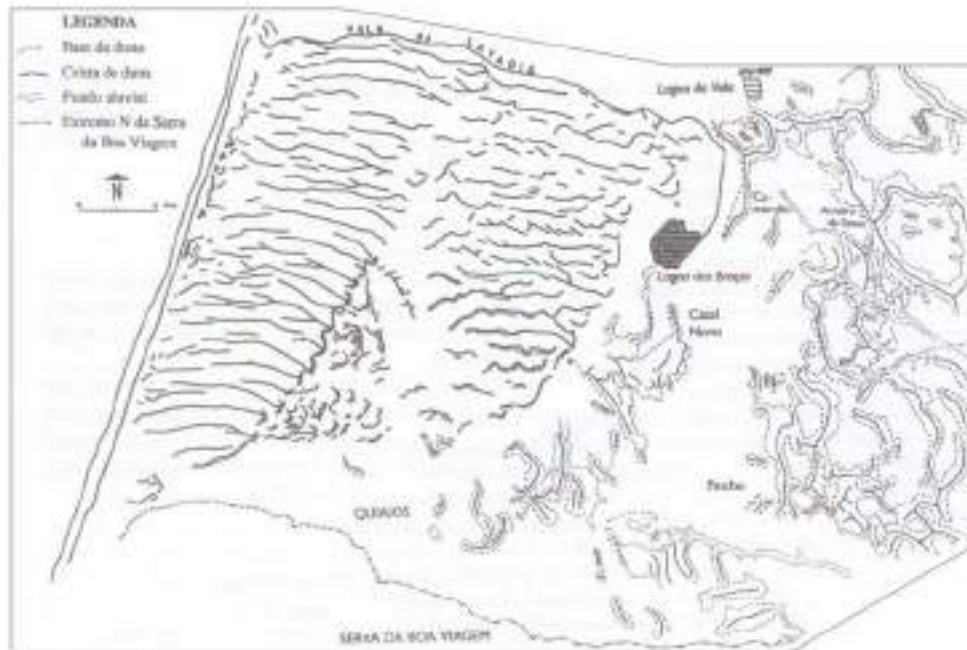


Figure 6. Dunes immediately north of Serra da Boa Viagem. From Almeida (1997).

Stop 3. Casa dos Cogumelos (Mushrooms' House)

At about 8 m high, there is a marine abrasion surface sculpted on the Jurassic limestones that is a few tens of meters wide and finishes inland by a paleo-cliff close to Casa dos Cogumelos, easily remarkable where it was exhumed (Fig. 7). The abrasion surface is covered by coarse sand with well-rounded quartz pebbles, passing upwards to well sorted finer-grained sands, considered to be of aeolian origin. These deposits record a former beach level, Praia da Murtinheira, attributed to the last interglacial period and, thus, equivalent of the lower elevation fluvial terrace in Mondego valley (i.e., M5 level of Ramos *et al.*, 2010). Occasionally, the beach succession at Praia da Murtinheira reaches a thickness of more than 1 m, and these sediments can be intercalated with heterometric calcareous and solifluxive beds (Soares *et al.*, 1993).

Heterometric deposits covering the beach units were deposited in a continental environment, during marine regression and with a nearby source. At the base of the paleo-cliff, clasts are disposed chaotically, with limestone blocks and pebbled and some aeolian sandy matrix. It seems to be associated with talus deposits at the bottom of the cliff, after it was abandoned by the sea in sharp retreat.

Immediately to the west, the stratification begins to be noticed, revealing paraconglomeratic and orthoconglomeratic beds that are intercalated with aeolian sands. Sometimes, sands are observed only as the matrix of the coarser strata. The low percentage of fines, the persistence of aeolian sands, at least as a matrix, and the paraconglomeratic-orthoconglomeratic character of the coarser levels indicate a cold and dry environment (Soares *et al.*, 1993).



Figure 7. Deposit of Casa dos Cogumelos above the present calcareous cliff.

Above and more or less in the middle of the deposit, there is a muddy-clayey, greyish-brownish sequence, with rhizoconcretions, which can be associated with a paleosoil, suggesting warmer and more humid period (idem, ibidem). The upper part of the deposit, better stratified and enriched in fine-grained matrix relative to the lower part, is organized in fining-upward sequences, suggesting transport by water and a topography already shaped by stream incision, with the cliff being practically fossilized. This would be the result of deposition by solifluction movements and torrential flows. Climatic conditions are said to be cold and humid (Soares *et al.*, 1993).

Apparently independent of the development of the referred deposits, the Vale de Anta presents its slopes with frequent cryoclastic materials, in particular at the base of ledges (layer cliffs) (Ramos *et al.*, 2018). They were formed by gravity fall and are constituted by angular calcareous clasts, with more or less fine sandy matrix, mostly aeolian. These deposits seem to be younger than the Casa dos Cogumelos unit but also belonging to the last glacial period (Almeida, 1997). More studies are required to improve their stratigraphic assignments.

Stop 4. Pond of Braças (Quiaios dunes)

The dune field developed to the north of Quiaios is composed of aeolian sands which were carried and deposited under favourable conditions at least since the last Quaternary glacial period. Using a methodology based on the analysis of borehole lithological sequences, of C14 dating and of palynological data it was possible to establish a coherent history of the dunes and pond formation in Quiaios region (Danielsen *et al.*, 2012).

The truncated dunes from the Gândara were formed during the Pleistocene, mainly by the time of the Younger Dryas crisis. The last major sea retreat exposed wide beach and nearshore sediments that could be blown by strong winds. In fact, these sands cover a lacustrine layer with the minimum age of about 12000 yr BP (idem, ibidem).

In a triangular area north of Quiaios (Fig. 6) and in other small areas east of the recent dune field, there are generally parabolic dunes with a dominant SE orientation, lower in altitude than the younger dunes and showing more evolved soils (Almeida, 1997). This is a second generation of dunes, which would have developed after a phase of intense deforestation, which ended around 1600 yr BP, followed by a sparse heath favorable to the development of parabolic dunes (Danielsen *et al.*, 2012).

Westwards from the lakes and up to the foredune, a 6 km wide dune field is maintained, with an undulating morphology thanks to the existence of linear dunes that overall strike W-E (Fig. 5). The degradation of the heathlands and the climate conditions around 500 yr BP, with the beginning of the Little Ice Age and the prevalence of a negative NAO (North Atlantic Oscillation) (Clarke & Rendell, 2006), allowed the rapid development of the third generation of dunes (Danielsen *et al.*, 2012). At the beginning of the 20th century, they were still moving inland, which led to human intervention through maritime pine seedlings, from 1924 to 1940, to fix them (Rei, 1940). The interdune lakes of Braças and Vela (Fig. 8), as the others to the north, were successively pushed to east because of the inland sand drifting (Danielsen *et al.*, 2012).



Figure 8. Interdune lake of Vela, which is 1500x500 m long.

Stop 5. Vagueira beach

In 1978 was built the seawall of Vagueira and one year after a groin at its south. It was the result of the fast coastline retreat, the weakening or even disappearance of the foredune and the missing of sand on the beach. Nevertheless, the retention of the little longshore drifting sand in front of Vagueira has increased the downdrift coastline retreat

and forced the construction of another groin on Labrego beach in 2002. After storms in 2001 and in October 2011 the spit just south of this groin was cut and the sea and Aveiro lagoon connected temporarily (Fig. 9, L). The deposition of sediments to rebuild the foredune was performed and that channel was closed. Finally, in 2015 an artificial foredune was raised between Labrego and Areão beach, with the contribution of dredged sediments from the lagoon of Aveiro. Numerous palisades have allowed the increasing of the dune height through the accumulation of aeolian sands (Fig. 9, R).



Figure 9. Road cut by the sea overtopping in Labrego (Nov. 2011) and artificial foredune close to Areão beach (2018).



Figure 10. The Vagueira seawall in collapsing process (Feb. 2014) and the new dyke (nowadays).

The surface where is settled Vagueira is only 3 to 5 meters above mean sea level, which is a major problem under the scenario of possible sea level rising of 1 m until 2100 (Andrade *et al.*, 2006). At this moment, during the highest tides the sea water almost reaches that level in some places. In addition, it must be considered the effect of storm surges which may reach a little more than 1 m in northern Portugal (Gama *et al.*, 1997). Thus, what must be done in the future to protect Vagueira? A dyke along the coast (Fig. 10) and another along the lagoon edge? How much costs the building and maintenance of this kind of hard structures? Is this sustainable?

An economical approach developed by Maia *et al.* (2015), comparing the costs and benefits in scenarios of protected coast and not protected coast, concluded that for Vagueira in the near future, although negative, the Net Present Value should be much

lower in a not protected coast than in a protected coast. The difference could be about -2,4 million euros against -15,7 million euros, respectively.

Stop 6. Barra de Aveiro

With the stabilisation of the sea level for 3000-5000 yr BP (Dias *et al.*, 2012), after the Flandrian rising, the coastline started evolving according to the balance between the sediment removal by coastal agents and sediment feeding. At least in the 9th century (eventually after the 1st/2nd centuries) a spit started to form southwards from Espinho, as a result of the south-directed littoral drift. In 1200 the spit tip was located in Torreira, in 1500 in S. Jacinto, in 1643 in Vagueira and, finally in 1757 it reached Mira, almost closing the Aveiro lagoon (Pereira *et al.*, 2020). During the first period of evolution of this spit, corresponding to the Medieval Climatic Optimum, the progression rate was the greatest (130 m/yr), decreasing significantly during the Transition period (40 m/yr) and increasing again during the Little Ice Age (70 m/yr) (*idem*, *ibidem*). The lagoon closure can be seen as a consequence of its natural evolution as a result of the action of oceanic and continental drivers. Due to the economic weight of Aveiro and its region, in 1808 was opened an artificial outlet close to this city. Its maintenance was not easy during the 19th century and the first half of the 20th, but in 1958 a jetty was built, to stop sand entrance in the inlet, which was increased in 1987, because the drift sands were entering again. Dredging has been maintained to ensure access conditions for the ships that use the port of Aveiro.

The jetties building started the coastline retreat to the south of the outlet. A maximum erosional rate of 10 m/yr happened between 1958 and 1973 (Oliveira *et al.*, 1982, *apud* Dias *et al.*, 2012). This coastline retreat forced the building of groins to hold the sands in front of Barra and Costa Nova towns. Other issues that are affecting natural foredune evolution in these beaches are the installation of walkways and cafés over the foredune (Fig. 11). These hard structures difficult or inhibit the growth of vegetation characteristic of this environment, such as the marram grass (*Ammophila arenaria* subsp. *arundinacea* H. Lindb.) the main dune builder. In front of the cafés, the vegetation growth is hindered to maintain the sea sight. In this case, the aeolian sand flow faster to inland, threatening houses located just at the back of the dune. An extreme situation can be seen in Costa Nova, where the foredune was cut to install a residential quarter (Fig. 12). All these examples have increased very much regional wave and wind exposure, turning the risk of being overtopped very high.



Figure 11. Walkway and cafés over the foredune in Barra (Nov. 2021).



Figure 12. Costa Nova. A residential quarter where there was the foredune and cafés over the beach.

Stop 7. “Pateira de Fermentelos”

“Pateira de Fermentelos” is a small lake in a subsiding area at the downstream sector of the structurally-controlled Cértima River valley. It is placed at the confluence of Cértima and Águeda rivers. Strictly speaking, the Pateira is 3.5 km long, but in a broader perspective it is related to a narrow subsiding strip that extends from further south for 12 km². In the vicinity of “Pateira de Fermentelos”, the course of Cértima is influenced by tectonic structures striking roughly NW-SE and NE-SW, which also control the shape of the small lake (Fig. 13).

When the Águeda River crosses the constraint imposed by a SW uplifted block, its sediment load is directed to the “Pateira de Fermentelos”, developing a deltaic accumulation with approximately 2 km². The Cértima River does not have the same capacity to build deltaic accumulations in the small lake, mainly because the sediment

loads are transported along a subsiding corridor, with a trend for being deposited before reaching the maximum subsidence sector of “Pateira de Fermentelos”. Furthermore, the average altitude and area of Cértimas’s catchment are lower than those of the Águeda River, hence carrying less sediment.

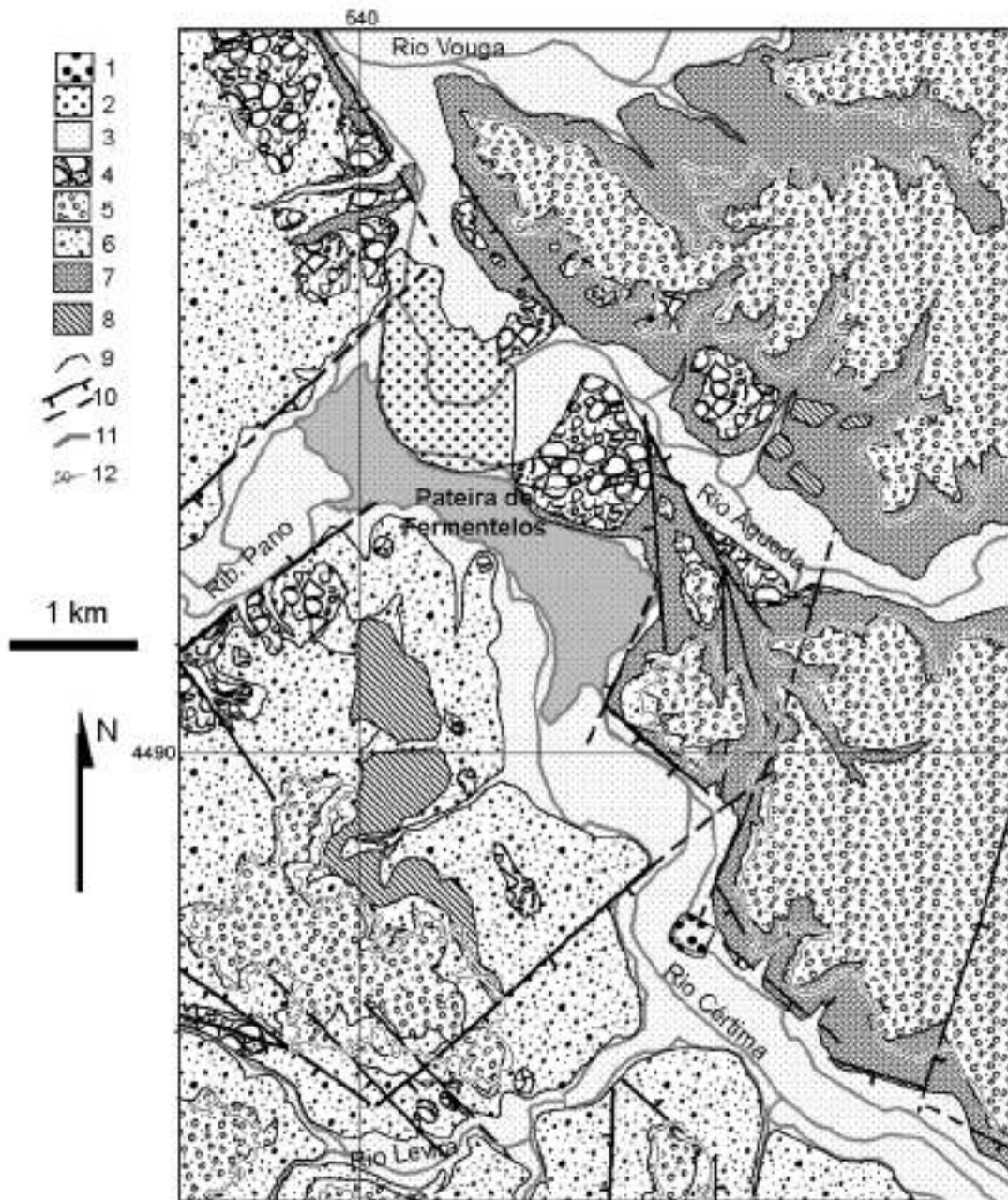


Figure 13. Morpho-sedimentary units in Pateira de Fermentelos. 1: Talus cone; 2: Águeda Delta in “Pateira de Fermentelos”; 3: Alluvium; 4: Terrace; 5: Pliocene and Quaternary sediments that precede fluvial incision; 6: Cretaceous; 7: Triassic; 8: Strath terrace associated with the fluvial incision level; 9: Geological contact; 10: Fault (with indication of the downed block)/hidden fault; 11: Hydrography. 12: 50 meters elevation. From Dinis (2004).

If today the “Pateira de Fermentelos” is a water body detached from the “Ria de Aveiro” (Vouga estuary), during the final stages of the Flandrian transgression (~5-3 ka), when the river valleys were not so filled with sediment, it must have been associated with an arm of that coastal system. About a century ago it was already argued that the outlet of the Vouga was placed in a wide gulf that extend through the lower reaches of rivers Águeda and Cértima (Girão, 1922; Souto, 1923). By the time of the maximum of the Flandrian transgression, the “Pateira de Fermentelos” would be linked to an arm of a structural estuary (Estuary of Vouga), with its limits conditioned by variations in sea level and sediment yields, but above all by tectonic activity.

Stop 8. Arcos de Anadia

Within the wide subsiding area of Cértima, some uplifted sectors are also recognized. The best examples are the horsts of Arcos and Quintela das Lapas. The Horst of Arcos is a tilted block with Upper Triassic to Lower Jurassic outliers that separates subsiding sectors where rivers Cértima and Serra are presently emplaced.

To the NW of Arcos Horst there is a linear valley, approximately 1-1.5 km wide, which follows the contact between two platforms at distinct elevation and where the trainline was constructed. The cross-sectional morphology of that valley does not seem compatible with the small stream that flows there, but is comparable to that of the Cértima valley upstream from the confluence with the Serra River. Given the position of the various uplifted and subsiding areas around Arcos Horst, is conceivable to assume that the valley to the NNW with the trainline records a former path of Cértima River (Fig. 14). Two sub-parallel north-flowing rivers were then separated by the Sangalhos Platform, which is aligned with Arcos Horst and displays similar width.

Diverse mud-dominated alluvial-lacustrine units, which can be intercalated with sand and gravel deposits, in particular in upper portions of the succession and closer to the uplifted marginal Massif were deposited in Pliocene-Pleistocene analogues of the Pateira de Fermentelos. The large variations in the thickness of these units in the region indicate that their deposition took place under strong structural control. Thickness is greater in the Cértima Depression, decreasing to the East and West, being highest (~50 m) in small localized sectors, allowing the definition of discrete sub-basins. This alluvial-lacustrine succession covers inner shelf to fluvial sand-dominated deposits that does not show significant variations in thickness, indicating that they precede the main phases of tectonic activity (Fig. 15).

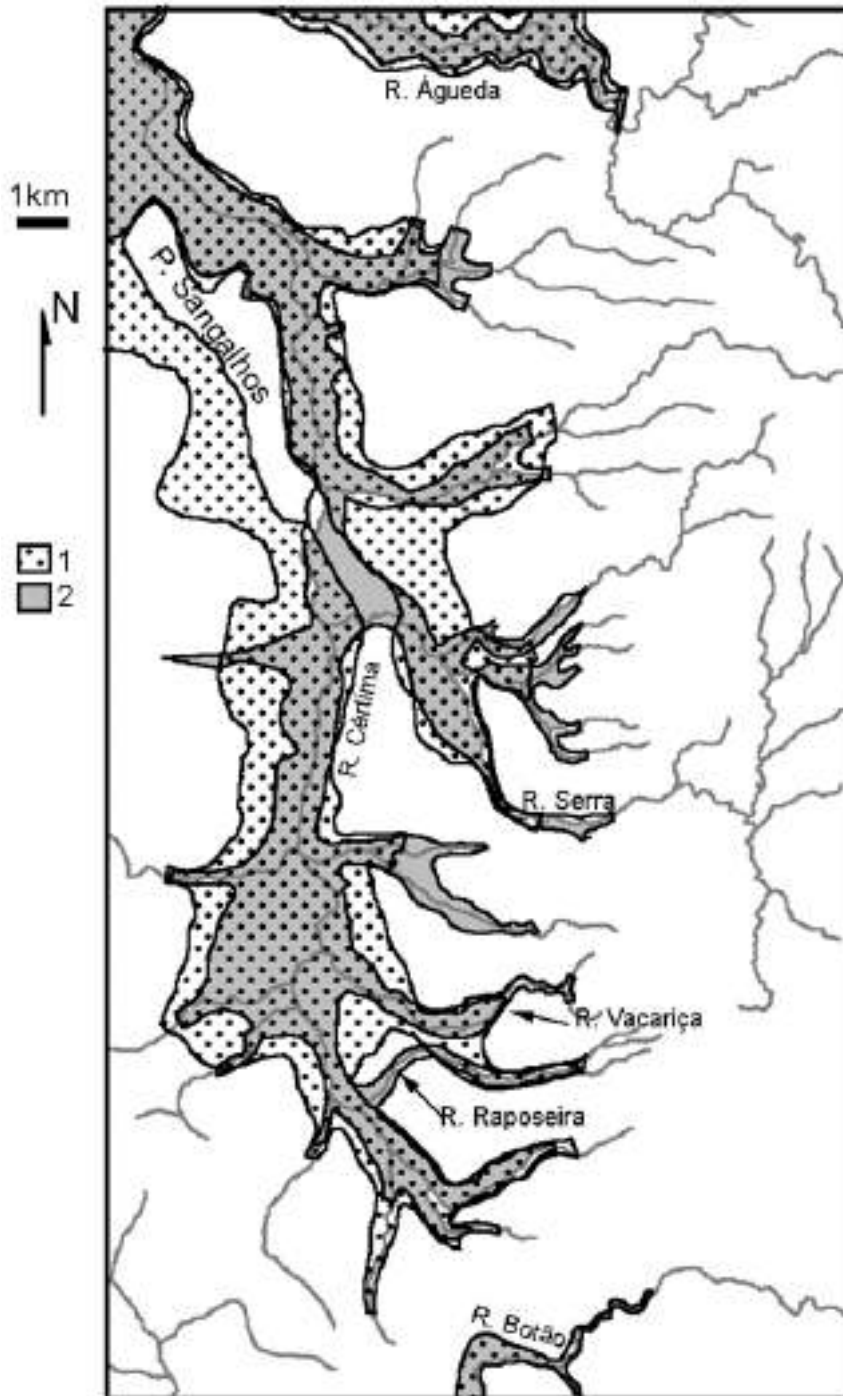


Figure 14. Different paths of the main rivers within the Cértima subsiding area based on the distribution of Pleistocene terrace deposits and alluvial-lacustrine units that precede Quaternary fluvial incision. 1: A former situation with Cértima path along a graben to the west of the uplifted Sangalhos area, which is aligned with the Arcos horst. The confluence of Cértima and Serra rivers took place in “Pateira de Fermentelos”; 2: Paths similar to present conditions. From Dinis (2004).

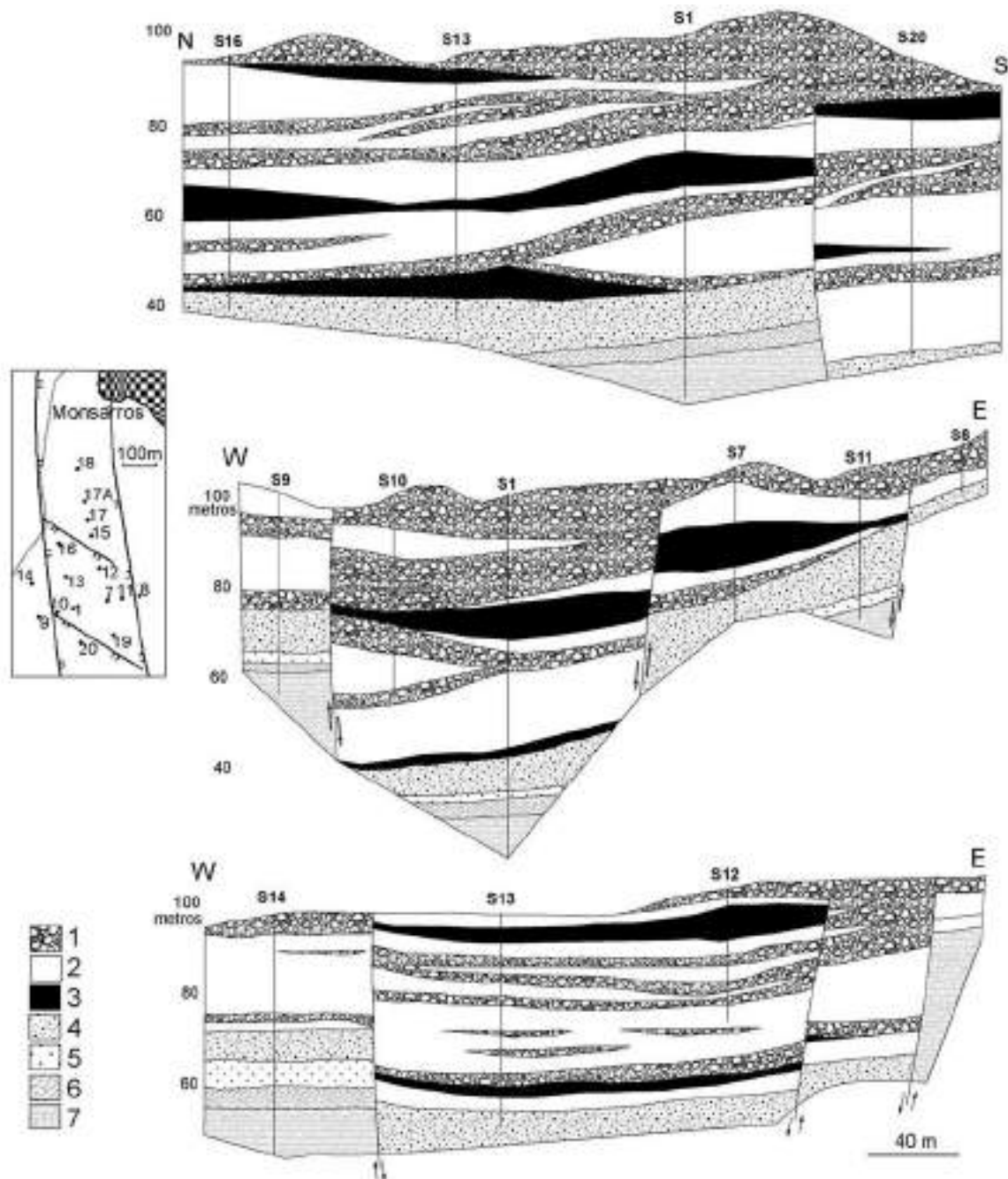


Figure 15. Synthetic, transverse and longitudinal geological sections of a graben (oriented North South) to the south of Arcos Horst. Sections based on field and borehole data. 1: Alluvial fan conglomerates; 2: Sandy-muds, usually stained; 3: Black clays and lignite; 4: Moderately sorted medium to coarse sands; 5: Fine to very fine inner shelf sands; 6: Decalcification clays covered pebbly-sands; 7: Jurassic marls and limestone. From Dinis (2004).

Stop 9. Cruz Alta

Cruz Alta is placed at the NNW end of “Serra do Buçaco”, a ridge associated with the NE flank of Buçaco syncline. Orographically, Serra do Buçaco reaches its maximum elevation in the proximity of the Cruz Alta gate (560 m). It is associated with Ordovician quartzites that are commonly found close to the axes of major folds of the Variscan Massif of Iberia supporting quartzitic reliefs.

These reliefs are considered to result from the contrast in terms of resistance to mechanical breakdown and chemical decomposition between these rocks and the evolving and covering units, with tectonics playing a minor role (Molina *et al.*, 1989; Martín Serrano, 2000). However, at the contact between the Marginal Massif and the coastal region to the west we can see numerous evidences of deformation, which are known for long (Biro, 1949; Ferreira, 1991; Daveau *et al.*, 1985-86; Soares *et al.*, 1993). Thus, tectonics must have played a supplementary role, contributing to the uplift of the Syncline of Buçaco relative to the regions to the west and east (Fig. 16). Basically, the syncline of Buçaco was formed during the first phase of Variscan deformation (Ribeiro *et al.*, 1990; Simancas, 2019). It was then reshaped later Variscan or Alpine tectonic movements. Presently the axis of the syncline is oriented NW-SE, dipping NW. The ridge in the eastern flank of the syncline is responsible for the longest and most prominent relief – the “Serra do Buçaco”.

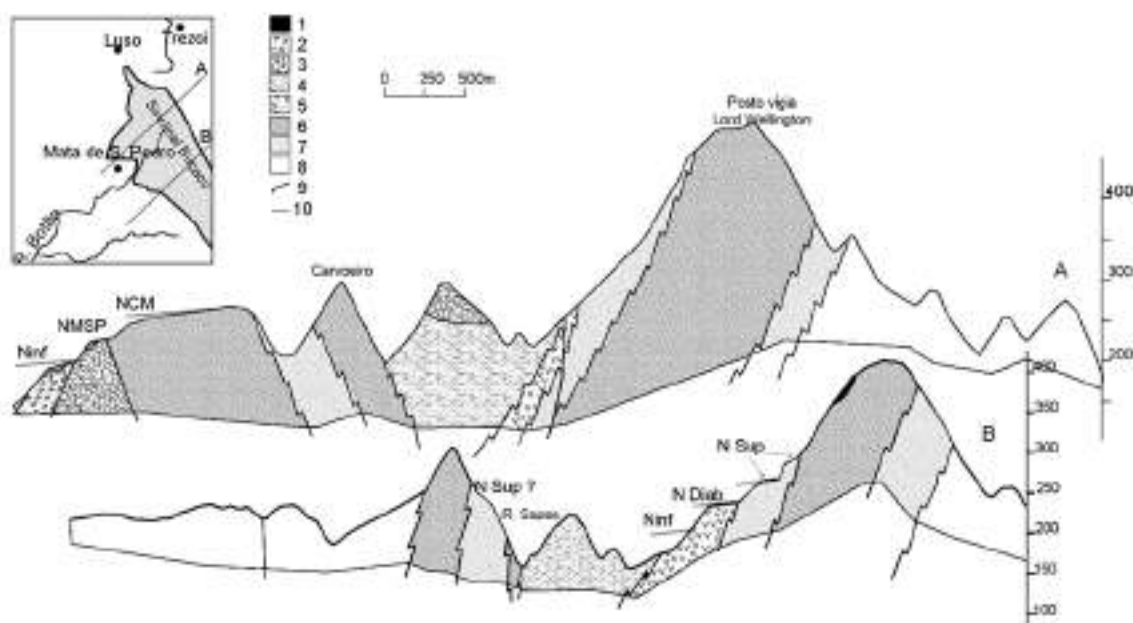


Figure 16. Geological cross-sections of the Buçaco Syncline. 1: Neogene alluvial fan deposits; 2: Triassic; 3: Upper Carboniferous; 4: Upper Ordovician-Silurian metasediments; 5: Ordovician diabbases and schists with diabbases; 6: Ordovician quartzites; 7: Ordovician schist, quartzite and greywacke; 8: Precambrian Metasediments; 9: Geological contact; 10: Strath terrace. From Dinis (2004).

The Ordovician quartzites are probably among the harder rocks that can endure best mechanical breakdown in the Variscan basement. The quartzites in the NE flank of the Buçaco syncline were thrust over western units, complicating geological boundaries that otherwise presented linear N-S strike and probably affecting the distribution of uplifted and subsiding sectors in the western region with Mesocenozoic sedimentary units. The SW flank of the syncline does not have the same influence on the structure of the Mesocenozoic fringe due to its orientation closer to E-W.

In the view point of Cruz Alta and in other elevated locations of the quartzitic ridge is possible to have a general perspective of the western region that was crossed before in this field trip (Fig. 17). Another remarkable feature that is observed in the vicinity of Cruz Alta are silicifications affecting Upper Cretaceous alluvial units. The silicification resulted from prolonged weathering under hot weather (Cunha, 1992; Cunha *et al.*, 1993). The formations affected by these exogenous processes probably extended over wide areas, but are now better preserved in the vicinity of quartzite reliefs.

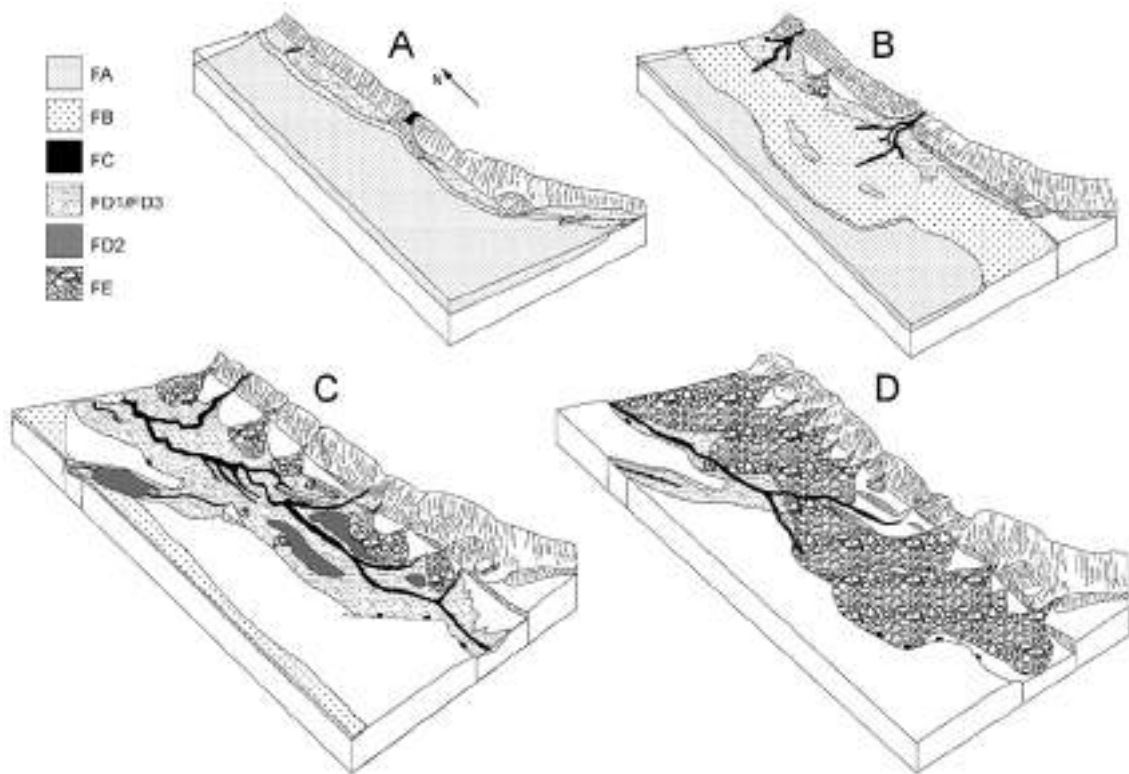


Figure 17. Paleogeographic evolution of the region seen from Cruz Alta viewpoint to the west. FA: Inner shelf; FB: Beach to transitional sand dominated; FC: Fluvial and transitional distributary channels; FD: Floodplain and lacustrine; FE: Alluvial fan. From Dinis (2006).

Stop 10. Chã da Mata

Chã da Mata is located in the western end of a fragment of the southern flank of the Buçaco Syncline, which is isolated from its eastern portion by the Ponte da Mata-Carvalheiras fault. This is a right strike-slip fault striking N-S to NNE SSW. This isolated fragment of the SW flank of Buçaco syncline is also cut by several N-S structures influenced by the Porto-Tomar Fault zone. Part of them control the outcropping area of the Upper Carboniferous continental basin and the contacts of this Basin with the Variscan Basement. They also mark the inner edge of the Iberian Atlantic Margin (Fig. 18).

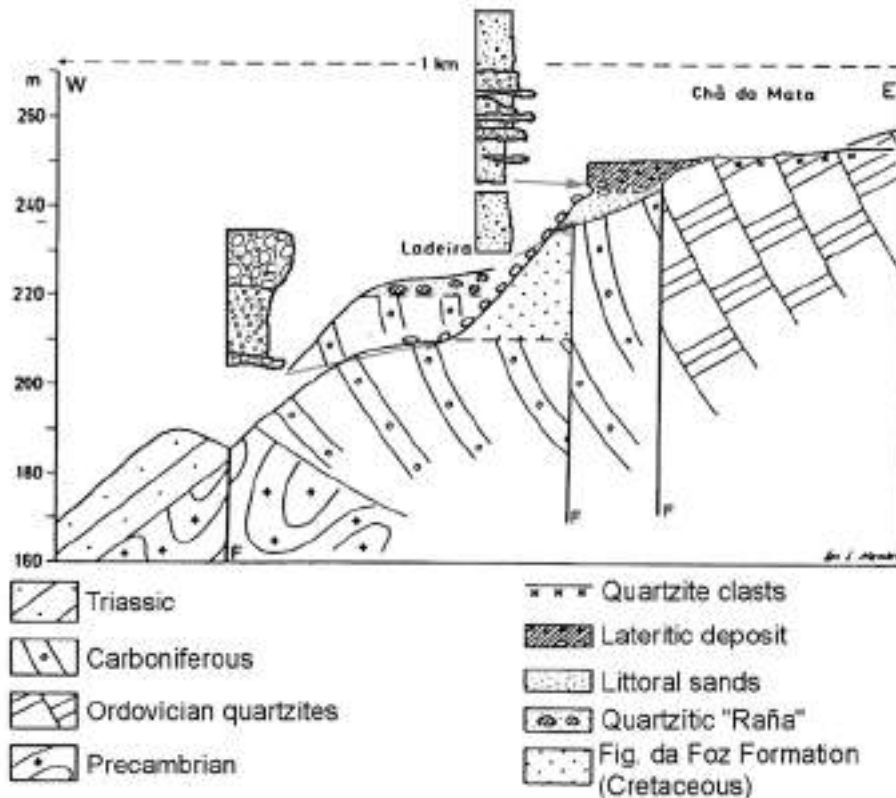


Figure 18. Cross sectional sketch at the latitude of Chã da Mata with the littoral levels of Chã da Mata and Serra da Vila (Adapted from Daveau et al., 1985-86) and the stratigraphic profiles for the deposits that record these two former littorals.

The Chã da Mata deposit and evolving area have unique characteristics. In this region it is possible to recognise two former littoral deposits that have been ascribed to the Piacenzian and Calabrian (Daveau *et al.*, 1985-86; Dinis, 2004). The Upper Chã da Mata deposit also displays an unusual ferruginization. The diabases and some Fe-rich metasediments are probably the most important sources of iron for the Chã da Mata and the transport may have been accomplished both through permeable surface deposits and deep circulation favoured by existing faults (Fig. 19).

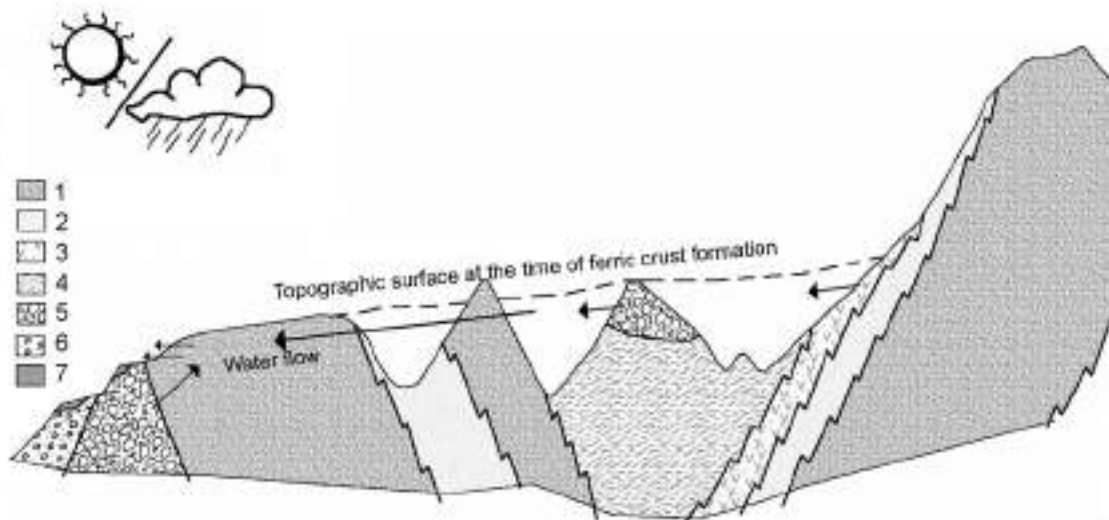


Figure 19. Explanatory model of cementation in Chã da Mata. Iron is fed by a phreatic circulation, from the East. There may be additional availability, linked to the mineralized waters circulating with spring in the Upper Carboniferous. Iron accumulation on the edge of flattened areas under oxidizing and slightly acidic or alkaline conditions. 1: Ordovician quartzites; 2: Ordovician with slates and quartzites; 3: Diabase, sometimes intercalated with shales; 4: Silurian shales; 5: Upper Carboniferous continental units; 6: Silves Group (Triassic); 7: Pliocene and Quaternary sediments. The arrows indicate water circulation associated to Fe-precipitation.

References

- Almeida, A. Campar (1997). *Dunas de Quiaios, Gândara e Serra da Boa Viagem. Uma abordagem ecológica da paisagem.* Lisboa, F. C. Gulbenkian/JNICT.
- Almeida, A. Campar (2001). *A carsificação da Serra da Boa Viagem: um processo quaternário.* *Estudos do Quaternário*, 4, 29-33.
- Andrade, C., Pires, H.O., Silva, P., Taborda, R., Freitas, M.C. (2006). *Zonas costeiras.* In F.D. Santos & P. Miranda (eds). *Alterações Climáticas em Portugal. Cenários, Impactos e Medidas de Adaptação.* Projecto SIAM II, (pp. 169-208), Gradiva, Lisboa.
- Biot, P. (1949). *Les surfaces d'érosion au Portugal Central et Septentrional.* *Rapport de la Commission pour la Cartographie des surfaces d'aplanissement.* *Actas Congr. Intern. Géographie*, 9-116.
- Cabral, João M.C. (1993). *Neotectónica de Portugal Continental.* PhD Thesis, Faculty of Sciences of University of Lisbon.
- Carvalho, G.S. & Granja, H. (1997). *Terraços versus litostratigrafia e geocronologia do Plistocénico e do Holocénico da zona costeira do Minho (Portugal).* *Estudos do Quaternário*, 1, 25-40.
- Carvalho, Gaspar S. (1964). *Areias da Gândara (Portugal) – (Uma formação eólica quaternária).* Porto, *Publ. Mus. Lab. Min. Geol. Fac. Ciências do Porto*, LXXXI – 4^a Série, 7-32.

- Clarke, M.L. and Rendell, H.M. (2006). Effects of storminess, sand supply and the North Atlantic Oscillation on sand invasion and coastal dune accretion in western Portugal. *The Holocene*, 16(3), 341–355.
- Cunha, L. (1988). As serras calcárias de Condeixa – Sicó – Alvaiázere. Estudo de Geomorfologia. Coimbra, FLUC, PhD thesis.
- Cunha, P.P. (1992). Estratigrafia e sedimentologia dos depósitos do Cretácico Superior de Portugal central a leste de Coimbra. PhD thesis, University of Coimbra.
- Cunha, P.P., Barbosa, B.P., Reis, R.P., (1993). Synthesis of the Piacenzian onshore record, between the Aveiro and Setúbal parallels (Western Portuguese margin). *Ciências da Terra* 12, 35-43.
- Danielsen, R., Castilho, A.M., Dinis, P.A., Almeida, A.C., Callapez, P.M. (2012). Holocene interplay between a dune field and coastal lakes in the Quiaios-Tocha region, central littoral Portugal. *The Holocene* 22(4), 383-395.
- Daveau, S., Birot, P., Ribeiro, O., (1985-86). Les bassins de Lousã et Arganil . Recherches géomorphologiques et sédimentologiques sur le massif ancien et sa couverture a l'est de Coimbra. *Mem. Centro Estudos Geográficos*, 8, 1-450.
- Dias, J.A., Bastos, M.R., Bernardes, C., Freitas, J.G., Martins, V. (2012). Interações Homem-Meio em zonas costeiras: o caso de Aveiro, Portugal. In M.A.C. Rodrigues, S.D. Pereira (eds). *Baía de Sepetiba: Estado da Arte* (pp. 215-235), Ed. Corbã, Rio de Janeiro, Brasil.
- Dinis, P. A. (2004). Evolução pliocénica e quaternária do vale do Cértima. PhD thesis, University of Coimbra.
- Dinis, P. A. (2006). Depósitos neogénicos anteriores à incisão fluvial actual entre Coimbra e Aveiro: fácies, arquitectura deposicional e controlos sobre a sedimentação. *Comunicações Geológicas* 93, 81-104.
- Ferreira, A. B., (1991). Neotectonics in Northern Portugal. A geomorphological approach. *Z. Geomorphologie*, v. Suppl. Bd. 82, 73-85.
- Gama, C., Taborda, R., Dias, J. M. A. (1997). Sobreelevação do nível do mar de origem meteorológica (“storm surge”), em Portugal Continental. In G. Soares Carvalho, F. Veloso Gomes & F. Taveira Pinto (eds). *Colectânea de Ideias sobre a Zona Costeira de Portugal*, (pp. 131-149), Assoc. Eurocoast-Portugal.
- Girão, A. (1922). *Bacia do Vouga: estudo geográfico*. PhD thesis, Univ. Coimbra.
- Maia, A., Bernardes, C., Alves, M. (2015). Cost-benefit analysis of coastal defenses on the Vagueira and Labrego beaches in North West Portugal. *Revista de Gestão Costeira Integrada*, 15(1), 81-90.
- Martín-Serrano, A. (2000). El paisaje del área fuente cenozoica, evolución e implicaciones; correlación con el registro sedimentario de las cuencas. *Ciências da Terra (UNL)*, 14, 25-38.
- Molina, E., Vicente, A., Cantano, M., & Martín-Serrano, A. (1989). Importancia y implicaciones de las paleoalteraciones y de los sedimentos siderolíticos del paso Mesozoico-Terciario en el borde suroeste de la Cuenca del Duero y Macizo Hercínico Iberico. *Studia Geol. Salmant.*, 5, 177-186.

- Pereira, O. N. A., Bastos, M. R., & Dias, J. A. (2020). E o clima deu à costa! Impacto do “Pequeno Ótimo Climático” e da “Pequena Idade do Gelo” na formação e evolução da Laguna de Aveiro (Portugal). *Ambiente e Educação. Revista de Educação Ambiental*, 25(3): 55-78.
- Pinheiro, L. M., Wilson, R. C. L., Reis, R. P., Whitmarsh, R. B., & Ribeiro, A. (1996). The western Iberia margin: a geophysical and geological overview. In: R. B. Whitmarsh, D. S. Sawyer, A. Klaus, D. G. Masson (eds.), *Proceedings of the Ocean Drilling Program, Scientific Results*, 149, 3-23.
- Ramos, A., Almeida, A. C., Lopes, F. C., & Cunha, L. (2018). Livret-Guide. Voyage d'étude Littoral du centre du Portugal: Serra da Boa Viagem – Nazaré. Vème colloque de l'AFGP Géographie physique et Société : des risques naturels au patrimoine naturel Coimbra (Portugal) du 20 au 22 septembre 2018.
- Ramos, A., Cunha, P. P., Gomes, A. A., & Cunha, L. (2010, Maio). Caracterização geomorfológica e sedimentológica da escadaria de terraços da margem direita do rio Mondego, no sector entre Maiorca e Vila Verde. VI Seminário Latino Americano de Geografia Física, II Seminário Ibero Americano de Geografia Física, Universidade de Coimbra, Maio de 2010.
- Rei, Manuel Alberto (1940). *Arborização. Alguns artigos de propaganda regionalista. Figueira da Foz.*
- Ribeiro, A., Quesada, C., & Dallemeyer, R. D. (1990). Geodynamic evolution of the Iberian Massif. In: R. D. Dallmeyer & E. Martínez García (eds.), *Pre-Mesozoic geology of Iberia* (pp. 399–409), Springer-Verlag.
- Simancas, J. F. (2019). Variscan Cycle. In C. Quesada & J. Oliveira (Eds.), *The Geology of Iberia: A Geodynamic Approach. Regional Geology Reviews*. Springer.
- Soares, A. F., Cunha, L., Marques, J. F., Almeida, A. C., & Lapa, M. L. R. (1993). Depósitos de vertente no Cabo Mondego. Integração no modelo evolutivo do Quaternário do Baixo Mondego. *Actas da 3ª Reunião do Quaternário Ibérico, Coimbra*, 199-208.
- Souto, Alberto (1923). *Origens da Ria de Aveiro (subsídios para o estudo do problema)*. Livraria João Vieira da Cunha.

Index

Itinerary and schedule	7
Introduction	8
Stop 1. Dolines, karstification	10
Stop 2. Viewpoint of Bandeira	11
Stop 3. Casa dos Cogumelos (Mushrooms' House)	13
Stop 4. Pond of Braças (Quiaios dunes)	14
Stop 5. Vagueira beach	15
Stop 6. Barra de Aveiro	17
Stop 7. “Pateira de Fermentelos”	18
Stop 8. Arcos de Anadia	20
Stop 9. Cruz Alta	22
Stop 10. Chã da Mata	24
References	26



Photo by Sérgio Brito

ORGANIZATION AND SUPPORTERS:





**10th IAG INTERNATIONAL
CONFERENCE ON GEOMORPHOLOGY**

Photo by Sérgio Brito

COIMBRA - PORTUGAL
« GEOMORPHOLOGY AND GLOBAL CHANGE »

FIELDTRIP GUIDEBOOK
Minho (Portugal) and Galicia (Spain) Regions
17-19 September 2022

Alberto Gomes
Alejandro Gómez Pazo,
Augusto Pérez-Alberti
(collaboration of Maria Assunção Araújo and Ricardo Carvalho)



Coimbra, 2022

Alberto Gomes

Alejandro Gómez Pazo

Augusto Pérez-Alberti

(collaboration of Maria Assunção Araújo and Ricardo Carvalho)

10th International Conference on Geomorphology Fieldtrip Guidebook – Minho (Portugal) and Galicia (Spain) Regions

17-19 September 2022



Coimbra, 2022

Edition notice:

Title: *10th International Conference on Geomorphology. Fieldtrip Guidebook – Minho (Portugal) and Galicia (Spain) Regions*

Authors: Alberto Gomes (UPorto), Alejandro Gómez Pazo (US Compostela), Augusto Pérez-Alberti (US Compostela)

Fieldtrip guided by: Alberto Gomes (UPorto), Alejandro Gómez Pazo (US Compostela), Augusto Pérez-Alberti (US Compostela)

Edition: *Universidade de Coimbra, Faculdade de Letras*

Fieldtrip and Guidebook Coordination: *António Vieira (University of Minho)*

Cover: *Perspective of the boulder beach of Laxe Brava, Galicia (photograph by Augusto Pérez-Alberti)*

ISBN: 978-989-8511-05-8

Introductory Note

The 10th International Conference on Geomorphology will take place in Coimbra (Portugal) from 12th to 16th September 2022, under the theme "*Geomorphology and Global Change*" and it is organized by the International Association of Geomorphologists (IAG) and the Portuguese Association of Geomorphologists (APGeom).

As in previous international conferences on Geomorphology, and as is the tradition in many geomorphological events organized around the world, the organizing committee of the 10th International Conference on Geomorphology proposed several fieldtrips to the participants, occurring before, during and after the main event.

These fieldtrips intend, above all, to show to geomorphologists from all over the world the diversity and richness of the geomorphological elements of the Portuguese territory (and also from Cape Verde) and to allow an exchange of experiences between the specialists that investigate these territories and the visitors, contributing for mutual scientific enrichment and for the valorization of this international conference.

The pre-conference fieldtrip is dedicated to the islands of Santiago and Fogo, in the Archipelago of Cape Verde. It will take place from 6th to 9th September and will be led by colleagues from the University of Cape Verde (Vera Alfama, Sónia Victória, Sílvia Monteiro, José Maria Semedo and Romualdo Correia). The volcanic geomorphology will dominate the visit (including well conserved structural volcanic forms such as cones, domes, craters and calderas), especially in the island of Fogo where recent volcanic activity has been registered.

The one-day mid-conference fieldtrips will take the visitors around the Portuguese mainland territory, the 14th September, allowing the visit of four different geomorphological realities.

In the Arouca UNESCO Global Geopark, internationally recognized territory since 2009, participants will be able to visit unique geological and geomorphological features (such as planation surfaces, bowl-shaped valleys and narrow river valleys) and witness the remarkable effort of protection and promotion of natural (abiotic and biotic) and cultural (tangible and intangible) heritage. The visit to the "516 Arouca" suspension bridge will be an excellent opportunity to observe the magnificent landscapes of this mountainous territory. This fieldtrip will be led by Artur A. Sá, António Vieira and Daniela Rocha.

The field trip to coastal areas of central Portugal will be led by Pedro Dinis and António Campar Almeida. Their proposal is to observe the different morphotectonic units of central west Portugal, namely the Coastal Mountain of Serra da Boa Viagem (revealing karstification features), the littoral plain (with aeolian dunes associated with some reliefs with higher elevation), the Cértima subsiding area (structurally-controlled morphology), and the Buçaco region (with the Syncline of Buçaco).

The visit to the Schist Mountains of Central Portugal will be centered in the mountains of Lousã and Açor, and will be conducted by Luciano Lourenço and Bruno Martins. It is proposed the observation of the main contrasts of the landscape, especially in terms of its physical geography, translated into geological, hypsometric, geomorphological, and hydrographic differentiation, or the land use and occupation and evolution of vegetation cover, namely following the recurrent large forest fires and the subsequent erosive processes they caused.

The fourth one-day fieldtrip will be oriented to the Estrela UNESCO Global Geopark, and led by Gonçalo Vieira, Emanuel Castro and Fábio Loureiro. The main geoheritage significance of the Estrela UGGp is the extent and richness of the Late Pleistocene glaciation(s) landforms and deposits (with spectacular morphological features such as the Zêzere glacial valley or the glacial cirques, moraine boulders, erratics or *roches moutonnées*) as well as the peculiar long-term geological evolution (revealing a significant diversity of granite types and landforms).

The three post-conference fieldtrips include a visit to the Lisbon Region, Serra da Estrela and, finally, Minho and Galicia (Spain), and will take place from 17th to 19th September.

The fieldtrip to the Lisbon Region will be guided by José Luís Zêzere, César Andrade, Sérgio Oliveira, Jorge Trindade and Ricardo Garcia, and will cover topics related with slope instability and landslides that affect the region of Lisbon, the floods occurring in the area north of Lisbon, and the coastal dynamics, morphology, cliff instability and beach erosion at north and south of Lisbon.

The three days field trip to the Serra da Estrela is led by Gonçalo Vieira, Emanuel Castro and Fábio Loureiro. Participants will be taken to visit some of the Geopark's most inaccessible geosites and observe breathtaking landscapes during two hikes: one in the Zêzere valley and the other between Penhas Douradas and Lagoa Comprida. The different geosites to visit include features of glacial, periglacial, granite weathering, fluvial, hydrogeological, petrological and tectonic themes, and aspects related with the management of a UNESCO Global Geopark will be discussed.

The third three-days fieldtrip is to the northwestern coast of Portugal and the Spanish region of Galicia. Guided by Alberto Gomes, Alejandro Gómez Pazo and Augusto Perez Alberti, will be mainly devoted to the observation and discussion of issues related to coastal dynamics, marine terrace staircases, differential uplift of coastal blocks, coastal geoheritage, coastal geoarchaeology, coastal erosion and coastal land planning.

It is our expectation that these visits will please all participants and promote the scientific enrichment of all involved, allowing a better understanding of the topics covered in each one.

We also hope that this set of fieldtrip guidebooks can help in the understanding of the themes discussed and that they can be a testimony of the commitment and dedication shown by all the scientific responsible for the several visits, to whom the organizing committee of the International Conference on Geomorphology expresses its greatest recognition and gratitude.

Have a good fieldtrip!

Lúcio José Sobral da Cunha
António Vieira

on behalf of the ICG2022 Organizing Committee

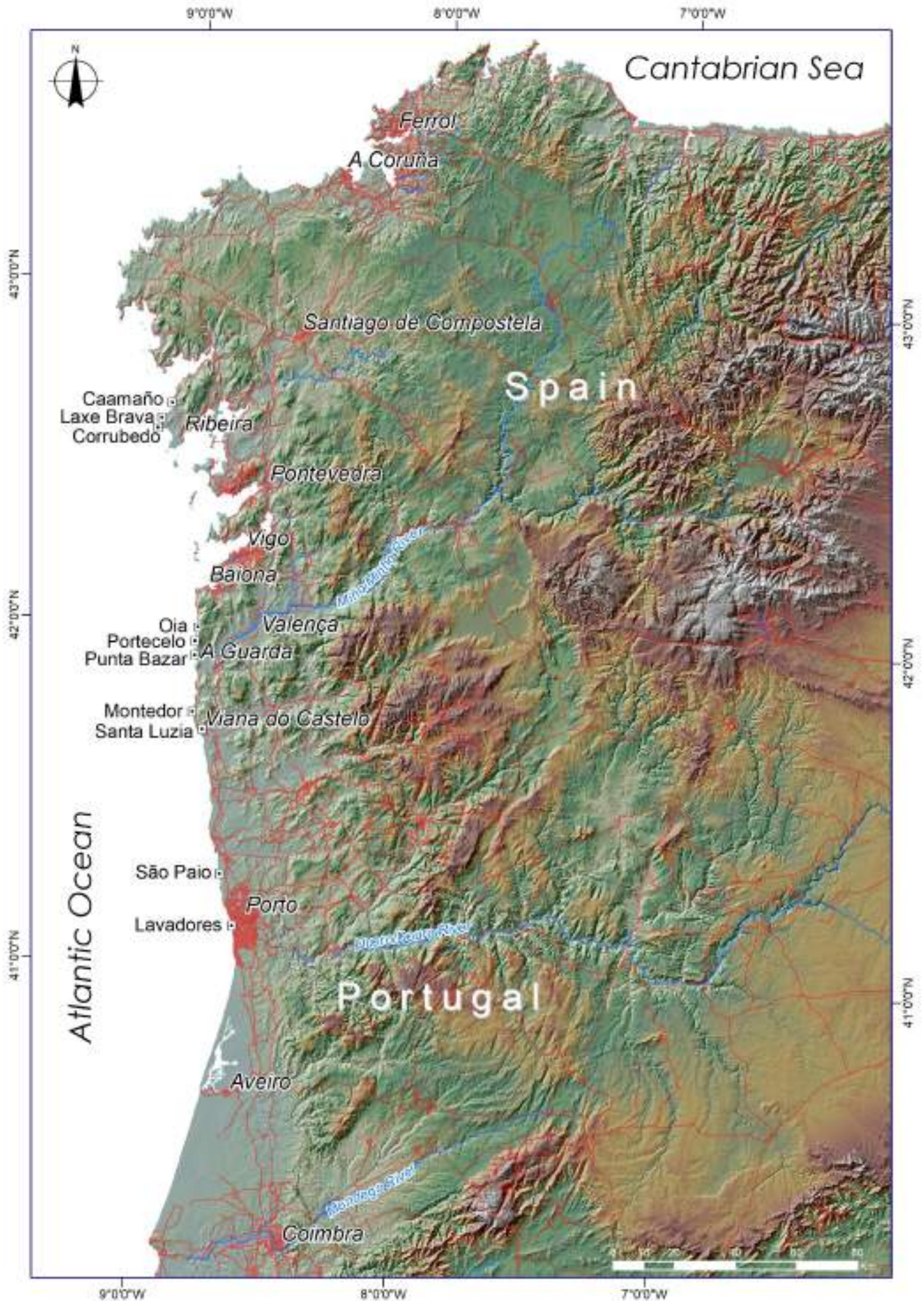


Figure 1. Itinerary of the field trip.

FIELD TRIP SCHEDULE

17 September - Saturday

km	Place	Travel Time
122	COIMBRA	1h30min
	Lavadores	
22		30 min
	São Paio - Labruge	
63		1h
	Santa Luzia	
12		20min
	Montedor	
52		1h
	VALENÇA	
	(HOTEL VALENÇA DO MINHO)	
271	Total	4h20min

18 September - Sunday

km	Place	Travel Time
126	VALENÇA	1h30min
	Caamaño	
10		30min
	Laxe Brava	
5		15 min
	Faro Corrubedo	
102		1h30min
	VIGO	
	(HOTEL HESPERIA)	
243	Total	3h45min

19 September - Monday

km	Place	Travel Time
52	VIGO	1h
	Oia	
6		15 min
	Portecelo	
5		15 min
	Punta do Bazar	
113		1h15min
	(Porto Airport)	
138		1h30min
	COIMBRA	
314	Total	4h15min

Portugal Maps

<https://apps.apple.com/us/app/mapas-lneg/id1502752420>
<https://geoportal.lneg.pt/>
<https://geoportal.lneg.pt/mapa/#>

Spain Maps

<https://play.google.com/store/apps/details?id=com.orux.oruxmapsIGN&hl=es&gl=US>
<http://mapas.igme.es/servicios/default.aspx?lang=spa>
https://mapas.igme.es/gis/rest/services/Cartografia_Geologica/IGME_MAGNA_50/MapServer/kml/mapImage.kmz

Connections Coimbra -> Lisbon (Schedules)

CP (Train): <https://www.cp.pt/passageiros/en/train-times/Train-time-results>
 Express buses: <https://rede-expressos.pt/en/timetables>
<https://www.flixbus.pt/>

Mobile Phones nº

(AG) +351 938514731
 (AGP) +34 645040653
 (APA) +34 692007159

Hotel Valenca do Minho - North of Portugal

Av. Miguel Dantas, 4930-678 Valença
 Phone: +351 251824211

Hotel Hesperia - Galicia

Av. da Florida, 60, 36210 Vigo, Pontevedra, Spain
 Phone: +34 986296600



1. Introduction

The geomorphologic contrast between the Galician and Northern Portuguese coasts is a challenge that intrigued many researchers during the last century.

North Coast of Portugal

The North Coast of Portugal (NCP), which stretches *ca.* 122 km from Caminha to Espinho, has a rectilinear pattern of low rocky coast with irregular sandy stretches, which are mainly located at south of the principal rivers mouth. The coast follows the general NNW-SSE direction determined by the Hercynian tectonic setting. The coastline alternates between sandy and rocky areas, and comprises estuaries of different shapes and sizes. The estuaries have wide valleys and well-developed marshes to the north, while they are entrenched and sinuous up to the mouth to the south. The pattern of the coastal drift is N-S.

The NCP, is classified as mesotidal, with a mean tidal range of 2.5 m and a maximal range of around 4 m. The swell waves mainly arise from the northwest and, less often, from the west and southwest. High waves ($H_s > 4$ m) mainly occur in winter and are generated by depressions moving from northwest and western directions. In January of 2014, during the storm Hercules, it has been recorded high waves with 13.5 m of H_{max} (buoy of Leixões).

The humid climate in the northwest of Portugal (1000-2000 mm precipitation per year) feeds rivers with significant flows, which served as sources of sediment supply for the coast in the past. Today, numerous dams obstruct the free flow of sediments and contribute to an imbalance in coastal sediment supply (Mota-Oliveira, 1990). This factor, along with the artificialization of the coastline (housing, coastal protection works, and harbours), speeds up the current process of coastal erosion.

For the Portuguese coast, the travel includes visiting low rocky coastal areas and pocket beaches. We will observe staircases of marine terraces, actual and relict wave-cut platforms in different lithologies, and other geomorphological markers of sea level. The journey tries to highlight the relevance of quaternary sea-level variation by the sedimentary and rock markers of this littoral, emphasizing the influence of the structural control in the coastal shape and the sedimentary contribution of the main rivers to the present sedimentary (un)balance of this littoral, discussing problems of coastal erosion and management.

Galician coast

The coastline of Galicia has more than 2100 km long. Two broad types of coasts can be differentiated: zones with Rías and zones without Rías. Marine inlets dominate in the former, whereas rectilinear stretches dominate in the latter, and only small coves or estuaries occur. The mega forms of coastal relief in northwest Spain are determined by the tectonic structure, whereas lithological differentiation has played a predominant role in the meso and microforms (Pérez-Alberti and Blanco-Chao, 2005). The coastline shaping is determined firstly by the tectonic processes related to the differential erosion, and the different geomorphological processes determine the forms and their distribution in different environments.

The Galician coast is classified as mesotidal, with a mean tidal range of 2.5 m and a maximal range of around 4 m. The swell waves mainly arise from the northwest and less often from the west and southwest. High waves (> 3 m) mainly occur in winter and are generated by depressions moving from northwest and western directions. The largest waves have been recorded at Cabo Vilán (13.5 m in 2009), Estaca de Bares (2.9 m in 2008) and Cabo Silleiro (12.01 m in 2014).

2. Brief characterization of the area

Northern of Portugal stops

The itinerary on the NCP will be focus on three main coastal geomorphological elements - marine terraces, rocky markers of ancient sea levels and coastal deposits. Meanwhile, the geoconservation actions and policies implemented along this coast will address our attention. Potential occurrence of differential uplift between coastal blocks will be highlighted and discussed.

Tides along the Portuguese coast are semidiurnal. The maximum tidal range at Leixões harbour, situated at the Leça River mouth, is about 3.8 m. At neap tides, the tidal range is substantially lower and equals 0.8 m. Low spring tides are very good times to explore the marine platforms and rocky notches the sea excavates, exploiting fractures and faults in hard granitic and metamorphic rocks. In fact, between Caminha (mouth of the river Minho) and Espinho, the bedrock is present below beach sands and in almost half of the area it contacts directly with the sea or outcrops beneath beach deposits.

The high-energetic wave regime at the western coast of Portugal induces a net potential littoral drift directed southward that can reach up to $10^6 \text{ m}^3 \text{ year}^{-1}$ (Litoral, 2014). The erosion trend in the low-lying sandy sectors of the NCP (Pires et al., 2009), is particularly seen on the dune fields located at south of rivers mouth, like the Amorosa dune field, observed from Santa Luzia. Lira et al. (2014), estimate for this areas of the NCP, a maximum erosion rate of *ca.* 2 m, by the comparison of digital aerial photos of 1928 with orthophotomaps of 2010.

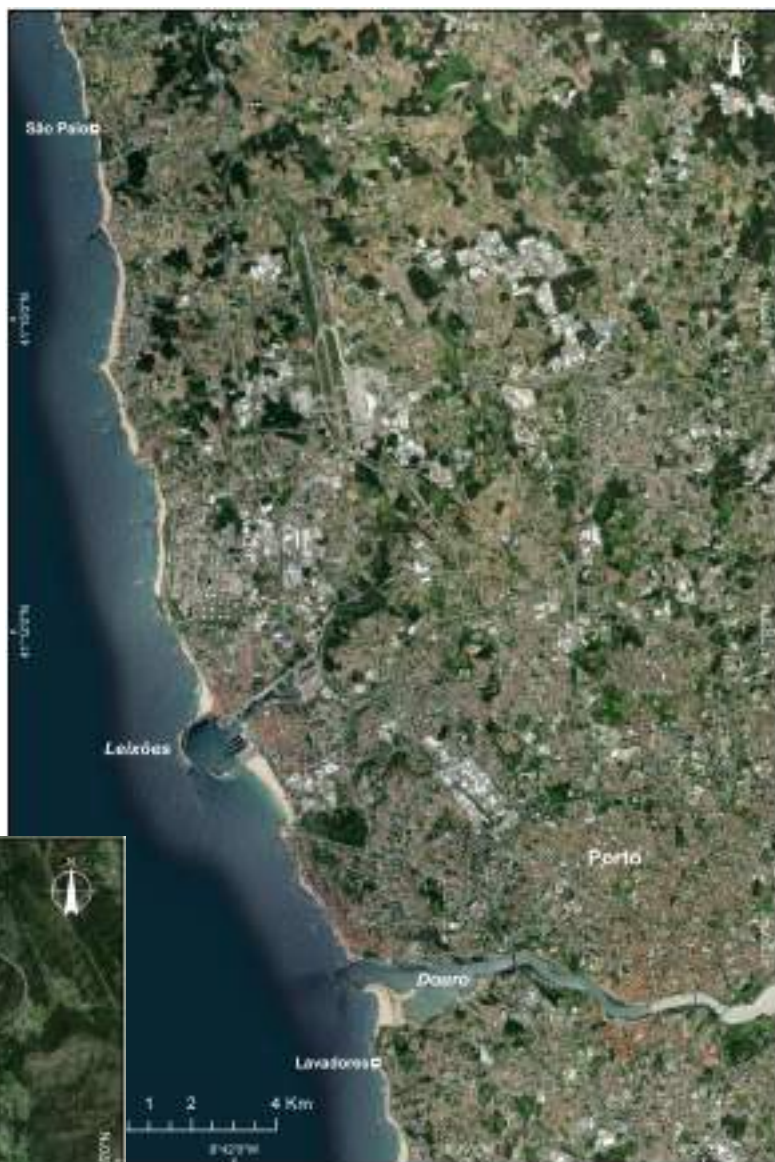
Along this littoral, an elevated platform of Plio-quaternary age develops, similar to the Spanish "Rasa", formed before the incision of the current hydrographic network (Araújo et al., 2003). On this Rasa, we can find a higher staircase of fluvial and alluvial deposits, and a lower staircase of marine terraces with 5/6 levels in the Lavadores coastal area, below the 30 m of altitude. Covering these deposits, there are post MIS 5 sediments and environments related with the marine regression and the accentuation of cold climate conditions, *e.g.* coastal loess, dunes, cold colluviums, *Pinus silvestris* forests and lagoons (Thomas et al., 2008, Araújo, 2020, Granja, 2022).

Quaternary sea level variation, coastal terrace staircases arrangement (marine and fluvial), marine erosion platforms, notches at various altitudes, incision stages of the main rivers, and the geomorphological evolution of the coastal landscape will also be highlighted during the NCP Itinerary.

This coastal region exhibits an abundance of sedimentary terraces that are irregularly spaced out and stand out in areas like Lavadores, Labruge, São Paio, Esposende and Montedor.

From Espinho, a little south of Oporto, till Caminha, near the Spanish border, the altitude difference between the littoral platform and the relief that limits it from the east, the Marginal Relief, gets greater. This arrangement can suggest the existence of a flexure that may be more active to the north (Araújo, 2020). This flexure may represent a meridian direction active during the Quaternary overprinted on older directions (Galician "Rias" and Northern Portuguese rivers).

Figure 2. Stops on the coastal sector of Porto.



Along the NCP it's possible to observe the typical forms of a low rocky coastal sectors, such as present-day and relict notches and pot-holes, relict sea urchin niches of the intertidal area, low cliffs, and shore platforms cut on igneous and metamorphic resistant basement. The geomorphic remains and their relative position opens the discussion about the role of the differentiated uplift on a passive margin.

In resistant metamorphic rocks, marine erosion guided by fractures and faults can create some spectacular notches. The rocky outcrops are extremely fractured and some of the lineaments are not simply the result of weak rock scouring by the marine action. In some places, recent vertical movements, along old Late Variscan directions, seem to have uplifted marine platforms (Araújo & Gomes, 2009).

The significant geological and geomorphological diversity of this coast, has been object of several inventories and publications (<https://www.progeo.pt/>), which lead to the implementation of geoconservation actions like the geosite trail on Lavadores, and the creation of the Coastal Geopark of Viana do Castelo (Carvalhido et al., 2014, 2016).

Figure 3. Stops on the coastal sector of Viana do Castelo.



Photo 1 - Shore platform on Lavadores (NP)



Photo 2 - Pocket beach guided by the structure on São Paio (NP)



Photo 3 - Relict notches on Montedor (NP)



Photo 4 - Shoreplatform .of Caamaño (Galicia)



Photo 5 - Boulders on the Laxe Brava (Galicia)



Photo 6 - Rocky coast of Portecelo (Galicia)



Figure 4. The littoral of the field trip.

The itinerary on the Galician coast focuses on two main coastal forms, the shore platforms and the boulder beaches.

There are different theories based on the shore platform shape and evolution in relation to the shore platforms. Mainly the discussion is about the factors that determine their behaviour. Authors and Trenhaile (1973, 1982, 1987) attempted to establish a relationship between the diverse parameters of the geometry of the platforms based on mathematical models and statistical techniques. According to these investigations, the tidal range is the main factor determining the platform slope and is more important than structure or lithology. Other aspects, such as the mean elevation of the platform or its uniformity or width, will depend to a greater extent on local conditions. Considering the evidence from the Galician coast, it is regarded that, as for cliff retreat, the formation and evolution of coastal platforms are largely determined by the balance between the previous weathering of the rock, structural factors, and wave energy.

The existence in some sites of ancient deposits on the platforms (Trenhaile et al., 1999) indicates that these are polygenic forms formed during the Eemian inter-glacial period (Perez-Alberti et al., 2010) and are currently being reshaped. In recent years, various analyses have been carried out in shore platform areas, such as Gómez-Pazo et al. (2021), where the authors compare the main characteristics of the three closest shore platforms with different lithological characteristics.

Boulder beaches are zones characterized by important boulder accumulations and are relatively frequented in the Atlantic coast context. These areas are named in Galicia as *coidos*. In the Galician zone, it is possible to differentiate between the boulder beaches related to weathering of the layer of granite rock, the dismantling of granite platforms, and the remobilization of cliff deposits, mainly of periglacial or snow origin (Blanco-Chao et al., 2002; Pérez-Alberti and Bedoya, 2004). Generally, the boulder beaches in this journey are formed by heteromeric boulders with different origins; for example, in Laxe Brava, the boulders are related to the erosion of the shore platform; meanwhile, in Oia a large part of boulders come from the back cliff. As also occurs in other coastal forms, in boulder beaches is possible to identify at least five morphological types (Pérez-Alberti & Gómez-Pazo, 2019): longitudinal, double-peaked, bow-shaped, channel-type, and simple peaked.

The stops in Galicia can be divided into two main sectors: the Barbanza Peninsula sector and, on the last day, the south coast area, closest to the Portugal boundary. In Barbanza Peninsula, we will visit three sectors. Two characterized for boulder accumulations and another where the shore platform has the major relevance.

In the Caamaño zone, we will visit a great example of a shore platform developed on schists and with some granite outcrops that marked their evolution and shape (Gómez-Pazo et al., 2021a).



Figure 5. Barbanza Peninsula sector.



In Laxe Brava, we visited a small shore platform related to a boulder beach exposed to the winter storms and that has been previously analyzed in several publications (Pérez-Alberti et al., 2012; Pérez-Alberti & Trenhaile, 2015a; Pérez-Alberti & Trenhaile, 2015b; Gómez-Pazo & Pérez-Alberti, 2019). The last stop in this Peninsula will be in Faro Corrubedo; in the zone of this lighthouse appear a great boulder accumulation in simple peak form with homogeneous boulders related to the granite evolution.

The second day in the Galicia region will run along the south coast, the sector between Cabo Silleiro and the Miño/Minho River estuary. This coast is characterized by a rectilinear design with several shore platforms and boulder beaches. In this area, we will make three stops.

Firstly, the Oia boulder beach sector, one of the most analyzed boulder beaches in Galicia with several publications in the last years (Pérez-Alberti & Trenhaile, 2015a; Pérez-Alberti & Trenhaile, 2015b; Gómez-Pazo et al., 2019; Gómez-Pazo et al., 2021b).

The second stop will be in Portecelo, a rocky coast sector with a shore platform associated to mega forms, as domes or corridors, and different boulder accumulations.

The last stop in the Galicia sector will be in Punta Bazar, a sector close to Portecelo. This area includes boulders above 57 t in different elevations and different boulder ages accumulations.

Figure 6. South Galician coast area with the visiting sectors.

3. Portugal characteristics and stops.

The itinerary for the North of Portugal includes one day with four stops. The first two stops will be in the Porto Metropolitan Area. The vast majority of this littoral is made up of urban areas, a significant harbor, and isolated patches of agricultural or forestry land.

The last two stops will be on the municipality of Viana do Castelo's coast. Despite heavy human intervention, this region has sizable portions of the littoral covered in natural vegetation, agricultural land, and forestry.

At each of the stops, we'll walk a short distance. The tide level will affect the route we take along each stop.

Stop 1. Lavadores

Coordinates: 41.130886; -8.669872
 High tidal time and height: 8:08 (2.7 m)
 Low tidal time and height: 14:24 (1.4 m)

The rocky sector of Lavadores, immediately at the south of the Douro River mouth, has a great geological and geomorphological significance. The post-tectonic granites dominated (298 ± 11 Ma age) the landscape, and their emplacement was controlled by a major mechanical anisotropy formed by transtensional structures associated with the Porto-Tomar shear zone (Martins et al., 2011). In the contact belt, the surrounding metasedimentary rocks exhibit spectacular deformational structures. The rocky coastal landforms of this sector, such as cliffs, shore platforms, pot-holes, arches, notches, tafonis and dispersal boulders, clearly show the influence of structure, weathering, and wave dynamics.

The littoral of Lavadores shows a staircase of marine terraces composed of well sorted deposits of gravels, pebbles and sands, massive or stratified, and with herringbone structures, comprising the following levels (a.s.l.): T1, 27-30 m; T2, 20-23 m; T3, 15-19 m; T4, 10,5-13 m; T5, 5-7 m; T6, 0-3 m. OSL dating of these terraces are ongoing, and preliminary results gets T5 on MIS 7 and T3 on MIS 11. The terraces T6 and T7, normally are iron cemented and fossilize fractures and small entrenched embayment's of the rocky shore. In the colluvium overlying T2 it was found *Acheulian* industry (Monteiro-Rodrigues et al., 2014).

Till now, the chronological and sedimentological features allowed to date the deposits from the Middle/Upper Pleistocene until the last glacial period, being observed an evolution from a depositional setting in a marine intertidal zone, passing to a fluvial environment and ending in a palustrine/lagoon environment with possible periglacial influence (Ribeiro et al., 2018).

Figure 7. Marine terrace of Lavadores site at 15-19m (photo of 2005)



Stop 2. São Paio and Labruge

Coordinates: 41.280518; -8.729674
High tidal time and height: 8:08 (2.7 m)
Low tidal time and height: 14:24 (1.4 m)

The rocky sector of São Paio-Labruge is a small geodiversity hotspot. It is the highest point at northern Portuguese coast (21m at the geodesic mark), contacting with the sea by a staircase of small platforms. Granite and metamorphic outcrops are strictly controlled by sharp directions, mostly NNE-SSW. The cliffs, sometimes more than 10 m high are rectilinear looking very much like fault scarps.

Looking carefully, it is possible to find small relicts of sediments of different ages and paleo-environments. The most interesting sequence has a marine deposit at its base at ca. 5 m a.s.l., overlain by a solifluction unit and above it by an aeolian deposit. The latter was TL dated for 84 k BP, showing that the underlying marine deposit may be from the last interglacial (MIS-5e, often designed as Eemian). A fossil notch carved in fresh granite hanging at 9-11 m a.s.l. and fossilised by a marine pebble deposit can be found just 100 metres to the south of this outcrop. A steep scarp with a straight NNE-SSW direction runs between the notch and the former outcrop.

At the top of the small promontory, we can find another marine deposit, ca 19m high.

It should be crucial to have reliable data from OSL of most of these small relicts of deposits. Like in Lavadores, at south, OSL dating of these deposits are ongoing. However, the idea of a small uplifting block is the first that comes to one's mind when we see marine deposits at different altitudes separated by "structural cliffs".

The observation of another beach to the south (Labruge) may show a more "normal" display of a probable Eemien old beach, made up with big blocks at its base, remaining at an altitude of about 6 m.

Walking from the north, we see a "Castro" of an iron age establishment at the planned surface in the top of the first relief. The geoarchaeological significance of the site, combined with its scenic and geomorphologic values, provided an incentive for its preservation and the establishment of an interpretive centre.

**Stop 3. Santa Luzia****Stop 4. Montedor**

Coordinates SL: 41.750055; -8.878260
Coordinates Mont: 41.700998; -8.834694
High tidal time and height: 8:08 (2.7 m)
Low tidal time and height: 14:28 (1.4 m)

Figure 9. Lima River estuary and coastal area to the south of the Santa Luzia belvedere.



The typical major landforms of the NCP can be seen from the Santa Luzia belvedere (about 180 m asl): a) the marginal reliefs structured in erosion surfaces progressively higher to the east, defining a staircase (Darque Platform ~ 20 m; Vila Fria ~ 50 m; Ola ~ 75 m; Faro de Anha ~ 100 m; Além do Rio ~ 160 m; St. Mamede ~ 270 m; St. Luzia ~ 470 m and Arga ~ 800 m), formed between upper Pleistocene (~410 ma) and Paleocene (~60 Ma?) and carved by a fluvial network installed on Palaeozoic fractures, sub-perpendicularly NW-SE / ENE-OSO and with huge slopes (>30%); b) the littoral platform (Rasa) with gentle slope to the west, where upper pleistocene coastal platforms are preserved; c) the wide estuary of Lima River, oriented ENE-OSO, with iconic longitudinal (and transverse) bars and margin salt-marshes (and river meadows and lagoons), both historically used to agricultural activities (and aviation!) and the production of salt, respectively; also important wetlands in the county, vital for birdlife; d) the extensive dune field (actual and Little Ice Age dunes) to the south of the river mouth.

Between the mouths of the Minho and Neiva rivers, the coastal deposits record continental (small alluvial fans and streams) and transitional (aeolian dunes, interdune ponds, estuary, sandy and gravelly beaches) paleoenvironments (Carvalhido et al., 2014).

A staircase of coastal terraces (abrasion shore platforms) was identified (altimetry, a.s.l.) preserved at the lower Erosion Surface – Darque Surface and ascribed to the following probable Marine Isotope Stages (MIS): T1, 20-18 m (MIS11); T2, ca. 13 m (MIS9); T3, 9.3-7.3 m (MIS7); T4, 5.5-4.5 m (MIS5); T5, 3.5-2.0 m (MIS5). The terraces have some preserved sedimentary facies, including coeval beach sediments on the lowest four. A late Pleistocene to Holocene sedimentary cover comprises four sub-units: a) the lower sub-unit, corresponding to ferruginous stream deposits and aeolian dunes dated ca. 67-61 ka (MIS4), probably related to sub-humid to arid mid-cold conditions; b) on the slopes, the lower sub-unit is overlapped by sandy-silty colluvium and sandy alluvial deposits dated ca. 56-28 ka (MIS3) and probably reflecting cold/mid-cold and wet/dry climate conditions; c) soliflucted lobes top this sub-unit and sandy-silty/silty deposits recording cold and dry climate dated 20-13 ka (MIS2), and d) a top sub-unit dated to 16-18th century, recording Little Ice Age events, consisting of fluvial sediments coeval with temperate climate evolving to aeolian dunes from the Maunder Minimum (cold windy dry conditions).

The altitude of T4 & T5 abrasion shore platforms indicated above, refers to the northern coastal margin of River Lima, as at its southern altitude reference values, lower ~1 m. This finding reveals a very low seismic activity at the river Lima fault (~ 0,05 mm/y) since MIS5 (Carvalhido et al, 2014).

A geosite inventory done in the coastal area of the Viana do Castelo district revealed important geodiversity elements, mainly geomorphological features such as granite, tectonic, fluvial, aeolian, and cultural landforms (Carvalhido et al., 2016). The quantitative assessment showed that among 35 geosites, 13 of them have exceptional scientific value, high to very high potential for tourism and educational uses, and medium to high risk of degradation. Based on these results, the Viana do Castelo municipality has decided to designate these 13 geosites as local natural monuments, according to the Portuguese legislation of nature conservation (Aviso 4658/2016, de 6 de Abril & Aviso n.º 1212/2018 de 25 de janeiro).

Figure 10. Montedor coastal cliff and shore platforms.



4. Galician stops description

Galician travel plan includes two journeys. First day the visit starting in Ribeira, Barbanza Peninsula, and visit the sectors of Laxe Brava, Caamaño and Faro Corrubedo sector.

On the second day, the visit is focused on the south part of the Galician coast. The three stops are very close and are Oia, Portecelo and Punta de Bazar.

Stops in the Galician section depending on the tides.

Las paradas de la parte gallega del viaje estarán condicionadas.

Stop 1. Caamaño

Coordinates: 42.654630; -9.040880
 High tidal time and height: 10:25 (2.7 m)
 Low tidal time and height: 16:56 (1.6 m)

In the Caamaño area, the main element in this visit will be the shore platform. This sector is in on Barbanza Peninsula, oriented towards the west, exposed to the dominant NW-SE waves, and about 600 in length (Gómez-Pazo et al., 2021a). Caamaño shore platform lacks extensive sedimentary deposits and, in some areas, small accumulations of boulders and medium-coarse sand appear in depressions and against topographic obstructions.

The main part of the Caamaño platform is developed in schists with some outcrops of fine to medium grain granites. The dominant joint system in this sector agrees with the dominant waves (NW-SE), and the average joint length is 8.46 m.

Figure 11. Caamaño detailed zone.



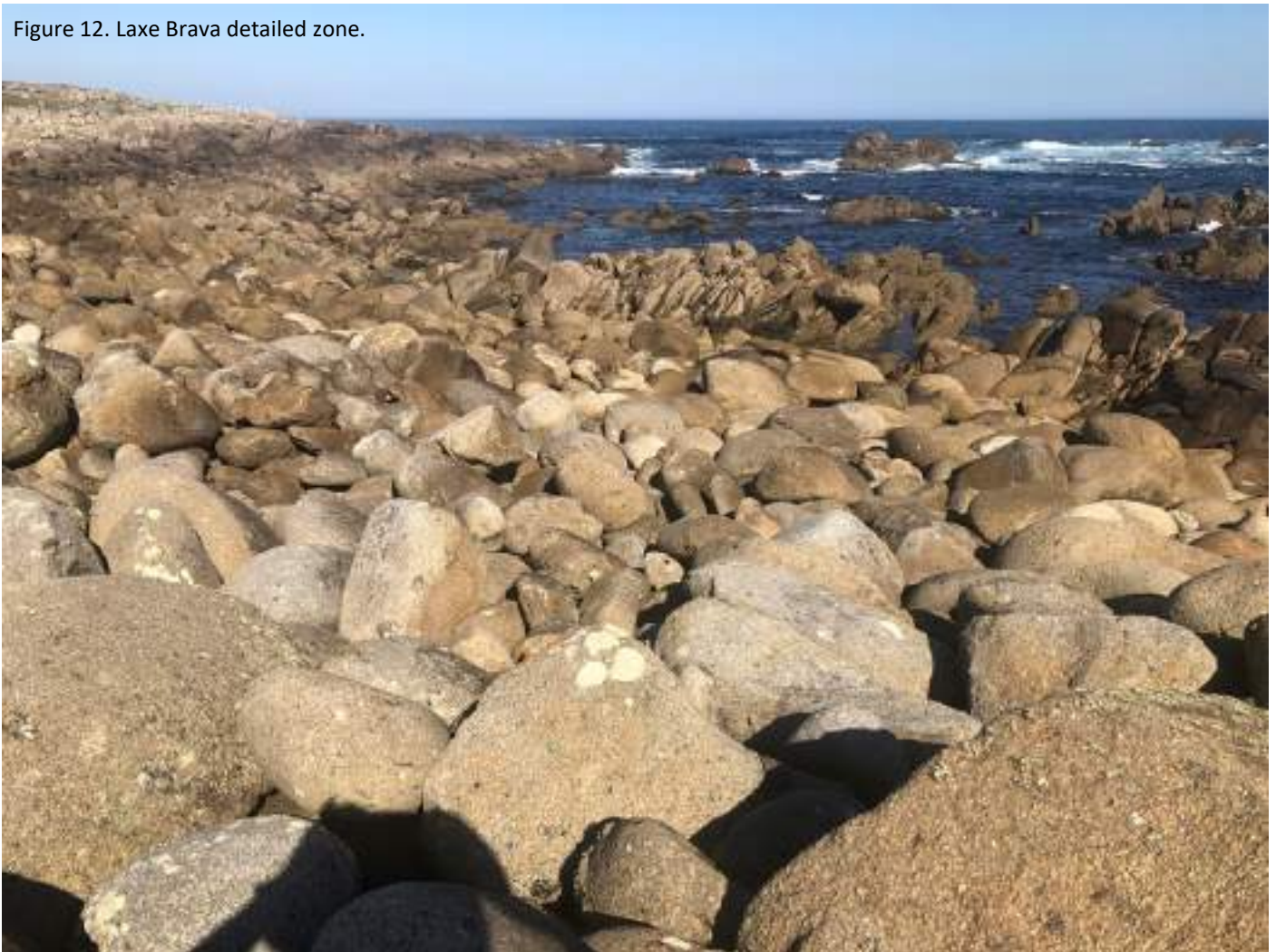
Stop 2. Laxe Brava

Coordinates: 42.598167; -9.074373 High tidal time and height: 10:25 (2.7 m) Low tidal time and height: 16:56 (1.6 m)
--

Laxe Brava is located in the Barbanza Peninsula, on the south edge of Coruña province. This area is characterized by the great relevance of winter storms with waves above 8 m during various hours. As in a major part of this coastal section, the granites dominate the sector and configure their evolution concerning the marine forces and the continental processes.

The Laxe Brava boulder beach faces northwards to northwestwards and is exposed to large storm waves from the northwest. In relation to the southwest storms, this beach is partially protected by a rocky promontory at the bay's western end (Pérez-Alberti & Trenhaile, 2015b). Laxe Brava sector boulders depend on wave quarrying on the rocky foreshore. The beach extends up to several meters above the high spring tidal level with a beach gradient of about 8° and boulders with a mean intermediate axis of around 0.66 m (Pérez-Alberti & Trenhaile, 2015a).

Figure 12. Laxe Brava detailed zone.

**Stop 3. Faro Corrubedo**

Coordinates: 42.576541; -9.090619 High tidal time and height: 10:25 (2.7 m)
--

This area is the final sector included in Barbanza Peninsula. In this case, Faro Corrubedo is closest to the Natural Park of Corrubedo, distinguished by the large shifting dune (Pérez-Alberti et al., 2020). The Faro Corrubedo sector is a perfect example of simple peaked boulder accumulation (Pérez-Alberti & Gómez-Pazo, 2019). The boulder beach has a maximum width of 40 m, and its elevation varies to a maximum of 5 m. In this case, the boulder's size is more homogeneous, with a normal diameter below 1 m.

Figure 13. Punta Corrubedo detailed zone



Figure 14. Punta Corrubedo boulder channel

Stop 4. Oia

Coordinates: 41.998084; -8.879724
 High tidal time and height: 11:50 (2.6 m)
 Low tidal time and height: 18:36 (1.7 m)

Oia sector is located in south-western Galicia, only 12 km from the Miño/Minho River estuary. In this context, the study area is a boulder beach extending approximately 90 m along the rear of a shallow bay. The beach, approximately 20 m wide, runs along the upper fore-shore and backshore and lies on top of a shore platform related to the Eemiense interglacial period (Blanco-Chao et al., 2007). The platform is exposed, and some boulder accumulations appear, especially in structural depressions. Both the shore platform and the boulders are granitic, and the boulders increase their size northwards and from the beach to the front of the beach (Pérez-Alberti & Trenhaile, 2015a). A great amount of the beach material is related to unconsolidated Weichselian peri-glacial and fluvial-nival sediments in an eight m-high cliff running along the back of the bay (Blanco-Chao et al., 2007).

The boulder beach is delimited by two rocky outcrops and oriented almost perpendicular to the dominant waves. In this area, the storm waves are generated from the northwest by low-pressure systems during the winter.

This area was analyzed using different techniques and methods over the last decades. First from a description of forms and evolution (Pérez-Alberti et al., 2012), then with the analysis of boulder position and their changes using photointerpretation techniques and UAVs images (Pérez-Alberti & Trenhaile, 2015a, 2015b). The volumetric differences were analyzed by Gómez-Pazo et al., 2019, and the most recent work used RFID sensors to identify the boulder displacements in this sector (Gómez-Pazo et al., 2021b).

Figure 15 Oia detailed zone.



Stop 5. Portecelo

Coordinates: 41.962654; -8.886528
High tidal time and height: 11:50 (2.6 m)
Low tidal time and height: 18:36 (1.7 m)

Portecelo is located south of Oia boulder beach. In this case, the wave and tidal characteristics are very similar. In Portecelo, there is also a shore platform, but with a large extension and the boulder accumulations vary in relation to the previous area (Gómez Pazo & Pérez-Alberti, 2022). In this case, the analysis carried out in this zone showed the relation between the joint patterns and the boulders. Also, in this sector, we can distinguish various boulder accumulations in relation to the active moment. One accumulation in the seaward, with smallest boulders and major movement currently and another accumulation zone with larger boulders in the upper platform part, in a currently static zone, only with a few boulders displacements in the storm events.



Figure 16. Portecelo detailed zone.

Stop 6. Punta de Bazar

Coordinates: 41.916954; -8.884847 High tidal time and height: 11:50 (2.6 m) Low tidal time and height: 18:36 (1.7 m)
--

Punta de Bazar is the last area on the Galician coast and the closest site to A Guarda, the last city in the Galicia margin. The wave's characteristics are like the ones mentioned previously in the Oia case because the coastline orientation is similar. This area is marked for the succession of domes and corridors in granite rocks and some dikes. At this zone, rocks ranging from coarse boulders to medium blocks with long axes generally oriented towards the east-northeast are perched on top of a gently curving structural dome. The largest of these blocks has a mass of over 57 t (Pérez-Alberti et al., 2012). It is probably the area with the biggest boulders, and in this part, we can see different examples of actual and Eemiense boulder accumulations (Gómez-Pazo & Pérez-Alberti, 2022).

Figure 17. Punta de Bazar detailed zone.



References

- Araújo, M. A., Gomes, A., Chaminé, H. I., Fonseca, P. E., Pereira, L. C., & Jesus, A. (2003). Geomorfologia e geologia regional do sector de Porto-Espinho (W de Portugal): implicações morfoestruturais na cobertura sedimentar cenozóica. *Cadernos Lab. Xeolóxico de Laxe Coruña*, 28, 79-105
- Araújo, M. D. A., & Gomes, A. (2009). The use of the GPS in the identification of fossil shore platforms and its tectonic deformation: an example from the Northern Portuguese coast. *Journal of Coastal Research*, 688-692.
- Araújo, M. A. (2020). The Northwest Portuguese Coast: A Longitudinal Coastline and Its Diversity. *In Landscapes and Landforms of Portugal*, Springer, 83-98
- Blanco-Chao, R., Costa Casais, M., Martínez Cortizas, A., Pérez-Alberti, A., & Vázquez Paz, M. (2002). Holocene evolution in Galician coast (NW Spain): An example of paraglacial dynamics. *Quaternary International*, 93-94, 149-159.
- Blanco-Chao, R., Pérez-Alberti, A., Trenhaile, A. S., Costa-Casais, M., & Valcárcel-Díaz, M. (2007). Shore platform abrasion in a para-periglacial environment, Galicia, northwestern Spain. *Geomorphology*, 83(1-2), 136-151. <https://doi.org/10.1016/j.geomorph.2006.06.028>
- Carvalhido, R. P., Pereira, D. I., Cunha, P. P., Buylaert, J. P., & Murray, A. S. (2014). Characterization and dating of coastal deposits of NW Portugal (Minho-Neiva area): A record of climate, eustasy and crustal uplift during the Quaternary. *Quaternary International*, 328, 94-106.
- Carvalhido, R. J., Brilha, J. B., & Pereira, D. I. (2016). Designation of natural monuments by the local administration: the example of Viana do Castelo municipality and its engagement with geoconservation (NW Portugal). *Geoheritage*, 8(3), 279-290.

- Granja, H., Gómez-Orellana, L., Costa, A. L., Morais, R., Oliveira, C., Ramil-Rego, P., & Pinho, J. L. (2022). Holocene evolution of the Cávado estuary (NW Portugal). *Quaternary International*, 622, 36-50.
- Gómez-Pazo, A. (2022). *Aplicación de novas tecnoloxías no estudo da costa de Galicia dirixidas a unha nova xestión no contexto do cambio global*. Universidade de Santiago de Compostela.
- Gómez-Pazo, A., & Perez-Alberti, A. (2019). El uso de imágenes de alta resolución en el estudio de los cambios volumétricos en playas de bloques. El ejemplo de Laxe Brava (Ribeira, NO Península Ibérica). In R. Durán, J. Guillén, & G. Simarro (Eds.), *X Jornadas de Geomorfología Litoral* (pp. 201–204). <https://doi.org/10.20350/digitalCSIC/8956>
- Gómez-Pazo, A., & Perez-Alberti, A. (2022). Control estructural, mega bloques y dinámica costera del sector Oia – A Guarda. In Blanco-Chao et al. (Eds.), *Actas de la XI Jornadas de Geomorfología Litoral*
- Gómez-Pazo, A., Pérez-Alberti, A., & Trenhaile, A. (2019). Recording inter-annual changes on a boulder beach in Galicia, NW Spain using an unmanned aerial vehicle. *Earth Surface Processes and Landforms*, 44(5), 1004–1014. <https://doi.org/10.1002/esp.4549>
- Gómez-Pazo, A., Pérez-Alberti, A., & Trenhaile, A. (2021a). High resolution mapping and analysis of shore platform morphology in Galicia, northwestern Spain. *Marine Geology*, 436(March), 106471. <https://doi.org/10.1016/j.margeo.2021.106471>
- Gómez-Pazo, A., Pérez-Alberti, A., & Trenhaile, A. (2021b). Tracking clast mobility using RFID sensors on a boulder beach in Galicia, NW Spain. *Geomorphology*, 373, 107514. <https://doi.org/10.1016/j.geomorph.2020.107514>
- Gómez-Pazo, A., Pérez-Alberti, A., Freitas, L., & Chaminé, H.I. (2022). Geostructural control in the rocky coast evolution: combination between UAVs and field survey techniques. *10th International conference on Geomorphology*. Coimbra, Portugal.
- Lira, C. P., Nobre Silva, A., Taborda, R., & Freire de Andrade, C. (2016). Coastline evolution of Portuguese low-lying sandy coast in the last 50 years: an integrated approach. *Earth System Science Data*, 8(1), 265-278.
- Litoral, G. T. (2014). Relatório do Grupo de Trabalho do Litoral. *Gestão da zona costeira, o desafio da mudança*. Agência Portuguesa do Ambiente, 255 p.
- Martins, H. C., Sant’Ovaia, H., Abreu, J., Oliveira, M., & Noronha, F. (2011). Emplacement of the Lavadores granite (NW Portugal): U/Pb and AMS results. *Comptes Rendus Geoscience*, 343(6), 387-396.
- Monteiro-Rodrigues, S., & Cunha-Ribeiro, J. P. (2014). A Estação Paleolítica do Cerro (Vila Nova de Gaia, Noroeste de Portugal): Caracterização preliminar dos utensílios com configuração bifacial. *Estudos do Quaternário*, 11, 3-18.
- Mota-Oliveira IB (1990) Erosão costeira no litoral Norte: considerações sobre a sua génese e controlo. *Actas do 1º Simpósio sobre a protecção e revalorização da faixa costeira do Minho ao Liz*. Inst. Hidráulica e Recursos Hídricos, Porto, pp 201–221
- Pérez-Alberti, A., & Bedoya, L. J. (2004). Caracterización de las playas de Cantos y bloques (coídos) en el noroeste de la Península Ibérica. In R. Blanco-Chao, J. López Bedoya, A. Pérez-Alberti (Eds.), *Procesos geomorfológicos y evolución costera: actas de la II Reunión de Geomorfología Litoral* (pp. 371–400). Santiago de Compostela.
- Perez-Alberti, A., & Blanco-Chao, R. (2005). Controles y balances geomorfológicos en costas rocosas de macizos antiguos. El ejemplo de Galicia (Noroeste de la Península Ibérica). In *Geomorfología litoral i quaternari* (pp. 333–349). Universitat de Valencia.
- Pérez-Alberti, A., Cunha, P. P., Murray, A. S., & Buylaert, J. P. (2010). On the coastal evolution of NW Iberia (Galicia) during the late Pleistocene. In 18 International Sedimentological Congress. Mendoza (Argentina).
- Perez-Alberti, A., Trenhaile, A. S., Pires, A., Lopez-Bedoya, J., Chamine, H. I., & Gomes, A. (2012). The effect of boulders on shore platform development and morphology in Galicia, north west Spain. *Continental Shelf Research*, 48, 122–137. <https://doi.org/10.1016/j.csr.2012.07.014>
- Pérez-Alberti, A., & Trenhaile, A. S. (2015a). An initial evaluation of drone-based monitoring of boulder beaches in Galicia, north-western Spain. *Earth Surface Processes and Landforms*, 40(1), 105–111. <https://doi.org/10.1002/esp.3654>
- Pérez-Alberti, A., & Trenhaile, A. S. (2015b). Clast mobility within boulder beaches over two winters in Galicia, northwestern Spain. *Geomorphology*, 248, 411–426. <https://doi.org/10.1016/j.geomorph.2015.08.001>
- Perez-Alberti, A., & Gómez-Pazo, A. (2019). The Rocky Coasts of Northwest Spain. In *The Spanish Coastal Systems* (pp. 27–47).
- Pérez-Alberti, A., Gómez-Pazo, A., & Otero, X. L. (2020). Natural and Anthropogenic Variations in the Large Shifting Dune in the Corrubedo Natural Park, NW Iberian Peninsula (1956–2017). *Applied Sciences*, 11(1), 34. <https://doi.org/10.3390/app11010034>

Pires, A. C., Gomes, A., & Chamine, H. I. (2009). Dynamics of coastal systems using GIS analysis and geomaterials evaluation for groins. *Environmental & Engineering Geoscience*, 15(4), 245-260.

Ribeiro, H., Pinto de Jesus, A., Sanjurjo, J., Abreu, I., Vidal Romani, J. R., & Noronha, F. (2019). Multidisciplinary study of the quaternary deposits of the Vila Nova de Gaia, NW Portugal, and its climate significance. *Journal of Iberian Geology*, 45 (4), 553-563.

Thomas, P. J., Murray, A. S., Granja, H. M., & Jain, M. (2008). Optical dating of Late Quaternary coastal deposits in northwestern Portugal. *Journal of Coastal Research*, 24 (10024), 134-144.

Trenhaile, A.S. (1973). The geometry of shore platforms in England and Wales. *The Transactions of the Institute of British Geographers*, 62, 129-142.

Trenhaile, A. S. (1982). The width of shore platforms; a theoretical approach. *Geografiska Annaler. Series A. Physical Geography*, 147-158.

Trenhaile, A. S. (1987). *The geomorphology of rock coasts*. Oxford University Press, USA.

Trenhaile, A. S., Perez-Alberti, A., Martínez-Cortizas, A., Costa-Casais, M., & Blanco-Chao, R. (1999). Rock coast inheritance: An example from Galicia, northwestern Spain. *Earth Surface Processes and Landforms*, 24(7), 605-621.

Links

Geosite of Lavadores

(vídeo) - <https://youtu.be/5tbDYj7aFQU>

<https://geossitiolavadores.pt/>

Littoral GeoPark of Viana do Castelo

<https://www.geoparquecostalviana.pt/en/>

<https://www.progeo.pt/>

<https://www.researchgate.net/profile/Alberto-Gomes-3/research>

<https://www.researchgate.net/profile/Maria-Araujo-33>

<https://www.researchgate.net/profile/Alejandro-Gomez-Pazo>

<https://www.researchgate.net/profile/Augusto-Perez-Alberti>

<https://www.researchgate.net/profile/Ricardo-Carvalho>





ORGANIZATION AND SUPPORTERS:





10th IAG INTERNATIONAL CONFERENCE ON GEOMORPHOLOGY

Photo by Sérgio Brito

COIMBRA - PORTUGAL
« GEOMORPHOLOGY AND GLOBAL CHANGE »

FIELDTRIP GUIDEBOOK **Schist Mountains of Central Portugal** 14 September 2022

Luciano Lourenço
Bruno Martins



Coimbra, 2022

Luciano Lourenço
Bruno Martins

10th International Conference on Geomorphology Fieldtrip Guidebook – Schist Mountains of Central Portugal

Geomorphological aspects of the Northwest slope of the Schist Mountains
(Lousã-Açor)

14 September 2022



Coimbra, 2022

Edition notice:

Title: *10th International Conference on Geomorphology. Fieldtrip Guidebook – Schist Mountains of Central Portugal*

Authors: *Luciano Lourenço (University of Coimbra) and Bruno Martins (ISCED/UMinho)*

Fieldtrip guided by: *Luciano Lourenço (University of Coimbra) and Bruno Martins (ISCED/UMinho)*

Edition: *Universidade de Coimbra, Faculdade de Letras*

Fieldtrip and Guidebook Coordination: *António Vieira (University of Minho)*

Cover: *Landscape of the Schist Mountains (photograph by Luciano Lourenço)*

ISBN: *978-989-8511-04-1*

Introductory Note

The 10th International Conference on Geomorphology will take place in Coimbra (Portugal) from 12th to 16th September 2022, under the theme "Geomorphology and Global Change" and it is organized by the International Association of Geomorphologists (IAG) and the Portuguese Association of Geomorphologists (APGeom).

As in previous international conferences on Geomorphology, and as is the tradition in many geomorphological events organized around the world, the organizing committee of the 10th International Conference on Geomorphology proposed several fieldtrips to the participants, occurring before, during and after the main event.

These fieldtrips intend, above all, to show to geomorphologists from all over the world the diversity and richness of the geomorphological elements of the Portuguese territory (and also from Cape Verde) and to allow an exchange of experiences between the specialists that investigate these territories and the visitors, contributing for mutual scientific enrichment and for the valorization of this international conference.

The pre-conference fieldtrip is dedicated to the islands of Santiago and Fogo, in the Archipelago of Cape Verde. It will take place from 6th to 9th September and will be led by colleagues from the University of Cape Verde (Vera Alfama, Sónia Victória, Sílvia Monteiro, José Maria Semedo and Romualdo Correia). The volcanic geomorphology will dominate the visit (including well conserved structural volcanic forms such as cones, domes, craters and calderas), especially in the island of Fogo where recent volcanic activity has been registered.

The one-day mid-conference fieldtrips will take the visitors around the Portuguese mainland territory, the 14th September, allowing the visit of four different geomorphological realities.

In the Arouca UNESCO Global Geopark, internationally recognized territory since 2009, participants will be able to visit unique geological and geomorphological features (such as planation surfaces, bowl-shaped valleys and narrow river valleys) and witness the remarkable effort of protection and promotion of natural (abiotic and biotic) and cultural (tangible and intangible) heritage. The visit to the "516 Arouca" suspension bridge will be an excellent opportunity to observe the magnificent landscapes of this mountainous territory. This fieldtrip will be led by Artur A. Sá, António Vieira and Daniela Rocha.

The field trip to coastal areas of central Portugal will be led by Pedro Dinis and António Campar Almeida. Their proposal is to observe the different morphotectonic units of central west Portugal, namely the Coastal Mountain of Serra da Boa Viagem (revealing karstification features), the littoral plain (with aeolian dunes associated with some

reliefs with higher elevation), the Cértima subsiding area (structurally-controlled morphology), and the Buçaco region (with the Syncline of Buçaco).

The visit to the Schist Mountains of Central Portugal will be centered in the mountains of Lousã and Açor, and will be conducted by Luciano Lourenço and Bruno Martins. It is proposed the observation of the main contrasts of the landscape, especially in terms of its physical geography, translated into geological, hypsometric, geomorphological, and hydrographic differentiation, or the land use and occupation and evolution of vegetation cover, namely following the recurrent large forest fires and the subsequent erosive processes they caused.

The fourth one-day fieldtrip will be oriented to the Estrela UNESCO Global Geopark, and led by Gonçalo Vieira, Emanuel Castro and Fábio Loureiro. The main geoheritage significance of the Estrela UGGp is the extent and richness of the Late Pleistocene glaciation(s) landforms and deposits (with spectacular morphological features such as the Zêzere glacial valley or the glacial cirques, moraine boulders, erratics or *roches moutounnées*) as well as the peculiar long-term geological evolution (revealing a significant diversity of granite types and landforms).

The three post-conference fieldtrips include a visit to the Lisbon Region, Serra da Estrela and, finally, Minho and Galicia (Spain), and will take place from 17th to 19th September.

The fieldtrip to the Lisbon Region will be guided by José Luís Zêzere, César Andrade, Sérgio Oliveira, Jorge Trindade and Ricardo Garcia, and will cover topics related with slope instability and landslides that affect the region of Lisbon, the floods occurring in the area north of Lisbon, and the coastal dynamics, morphology, cliff instability and beach erosion at north and south of Lisbon.

The three days field trip to the Serra da Estrela is led by Gonçalo Vieira, Emanuel Castro and Fábio Loureiro. Participants will be taken to visit some of the Geopark's most inaccessible geosites and observe breathtaking landscapes during two hikes: one in the Zêzere valley and the other between Penhas Douradas and Lagoa Comprida. The different geosites to visit include features of glacial, periglacial, granite weathering, fluvial, hydrogeological, petrological and tectonic themes, and aspects related with the management of a UNESCO Global Geopark will be discussed.

The third three-days fieldtrip is destined to the northwestern part of Portugal and the Spanish region of Galicia. Guided by Alberto Gomes and Antonio Perez Alberti, will be mainly devoted to the coastal area and to the observation and discussion of issues related to coastal dynamics, marine terrace staircases, differential uplift of coastal blocks, coastal geoheritage, coastal geoarchaeology, coastal erosion and coastal land planning.

It is our expectation that these visits will please all participants and promote the scientific enrichment of all involved, allowing a better understanding of the topics covered in each one.

We also hope that this set of fieldtrip guidebooks can help in the understanding of the themes discussed and that they can be a testimony of the commitment and dedication shown by all the scientific responsible for the several visits, to whom the organizing committee of the International Conference on Geomorphology expresses its greatest recognition and gratitude.

have a good fieldtrip!

Lúcio José Sobral da Cunha
António Vieira

on behalf of the ICG2022 Organizing Committee

ITINERARY AND SCHEDULE

Itinerary (Fig. 1)

08h00 – Departure from Coimbra

08h45 – Bacia da Lousã

09h00 –09h30 – Senhora da Candosa

10h00 – 10h30 – Góis (café)

11h00 – Arganil

11h30 – Folques

12h00 - Coja

12h30 – Mata da Margaraça – lunch pick-nick

14h00 – Piódão

15h00 – Departure from Piódão

16h00 – Barriosa

17h00 – Vide

17h30 – Alvoco

18h00 – Varandas de Avô

19h00 – Aguieira

19h30 – Penacova

20h00 – Arrival to Coimbra

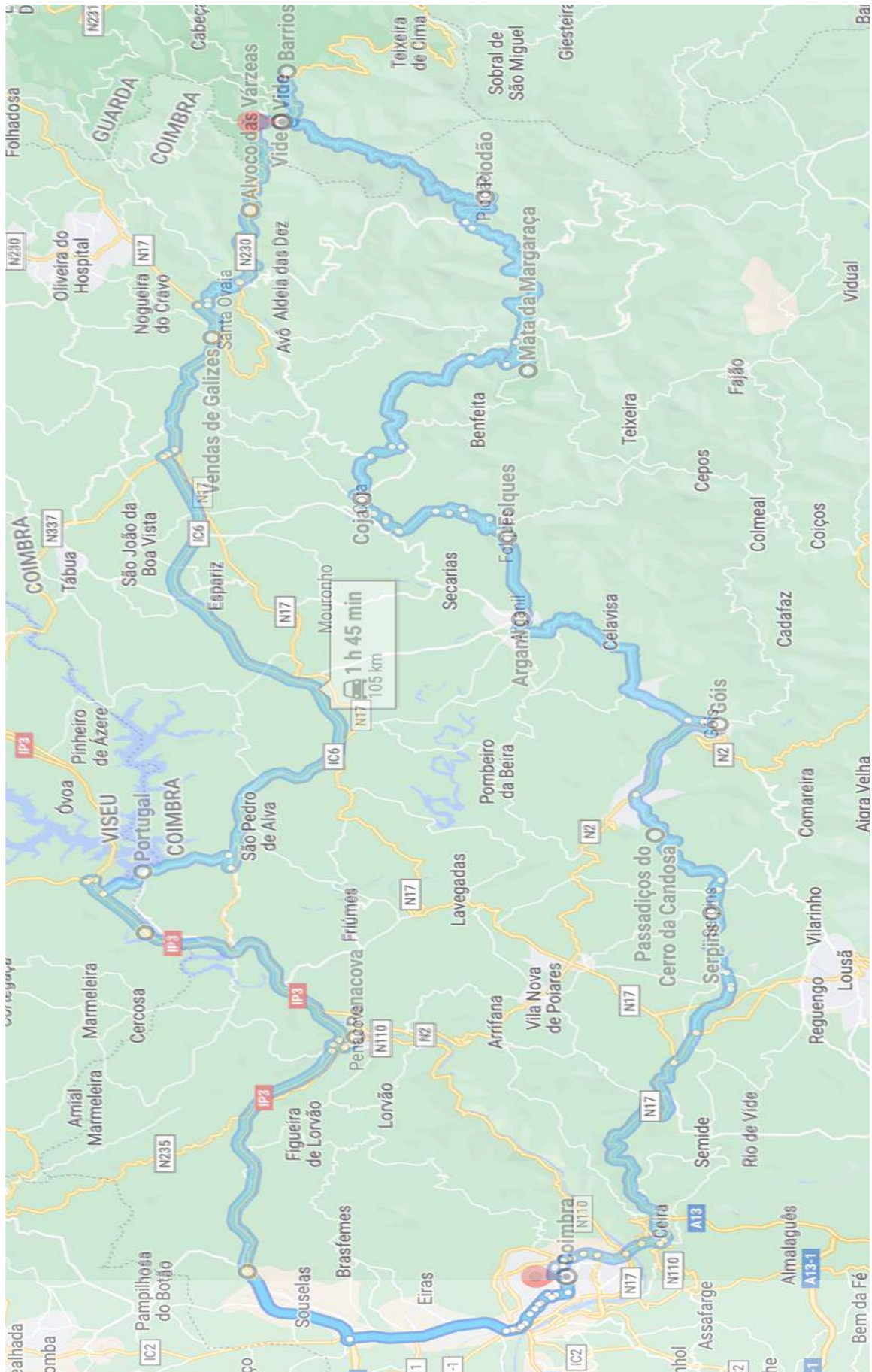


Figure 1. Map of the itinerary (Adapted from Google Maps).

Purpose

The purpose of this technical and scientific tour is to show, via direct observation, some aspects of the geography of the northwestern slope of the Schist Mountains (Serras de Xisto) of the Portuguese Cordillera Central, specifically the mountains of Lousã and Açor, as well as its base, corresponding to the Miranda do Corvo - Lousã - Góis - Arganil - Coja basin.

As such, it aims at observing the main contrasts of the landscape, mainly in terms of its physical geography, reflected in the geological, hypsometric, geomorphologic, hydrographic or soil use and occupation differences. It will also allow noting some aspects of the human geography, namely regarding contrasts in the distribution of the settlement, in the evolution of the population and its activities, or in the evolution of the vegetation cover, namely following the recurrent large forest fires and the subsequent erosive processes they caused.

Throughout the tour, the method of direct observation is preferred, be it of the nuances of the successive landscapes that can be seen from the bus, or by making stops here and there, which allow not only a more detailed analysis of places of particular interest, but also their photographic recording with greater precision and quality.

This guide does not aim to compile all the available information on the subject, as it only aims to provide some elements that may help to better understand the aspects that will be covered during the tour.

Those interested in delving deeper into the themes that will be addressed may find in the bibliography complementary elements that will not only increase their knowledge of this beautiful region but will also provide many other references for them to consult and, as such, complement the contents presented here.

Introduction

The trip takes place in the drainage basin of the Mondego river, and in particular in its two main tributaries on the left bank, the rivers Alva and Ceira (Fig. 2).

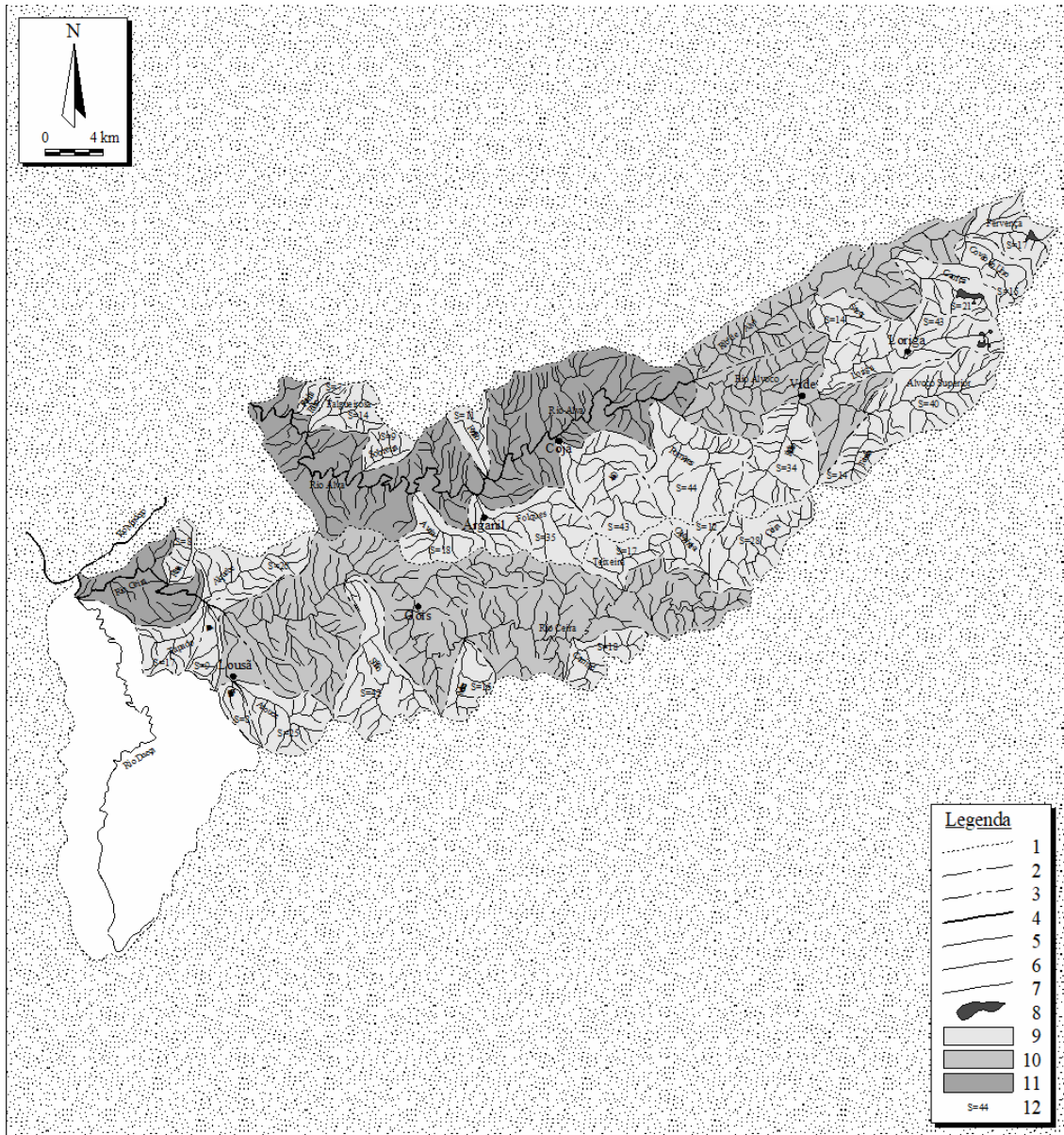


Figure 2. Delimitation of the drainage basins of order ≥ 5 , tributaries to rivers Alva and Ceira. 1 - Basin boundary of order 7; 2 - of order 6; 3 - of order 5; 4 - channel of order 7; 5 - of order 6; 6 - of order 5; 7 - of order less than 5; 8 - reservoirs; 9 - drainage basins of order 5; 10 - drained area for channel of order 6; 11 - drained area for channel of order 7; 12 - surface of basins of order 5. (Source: Lourenço, 2018)

The tour begins with an ascent of the Ceira, after it meets the Mondego at Portela (Fig. 3), where we leave the Meso-Cenozoic Rim to enter the Ancient Iberian Massif, or

Hesperian Massif, where the river flows into the tectonic basin of Lousã-Góis-Arganil (Daveau, 1986).

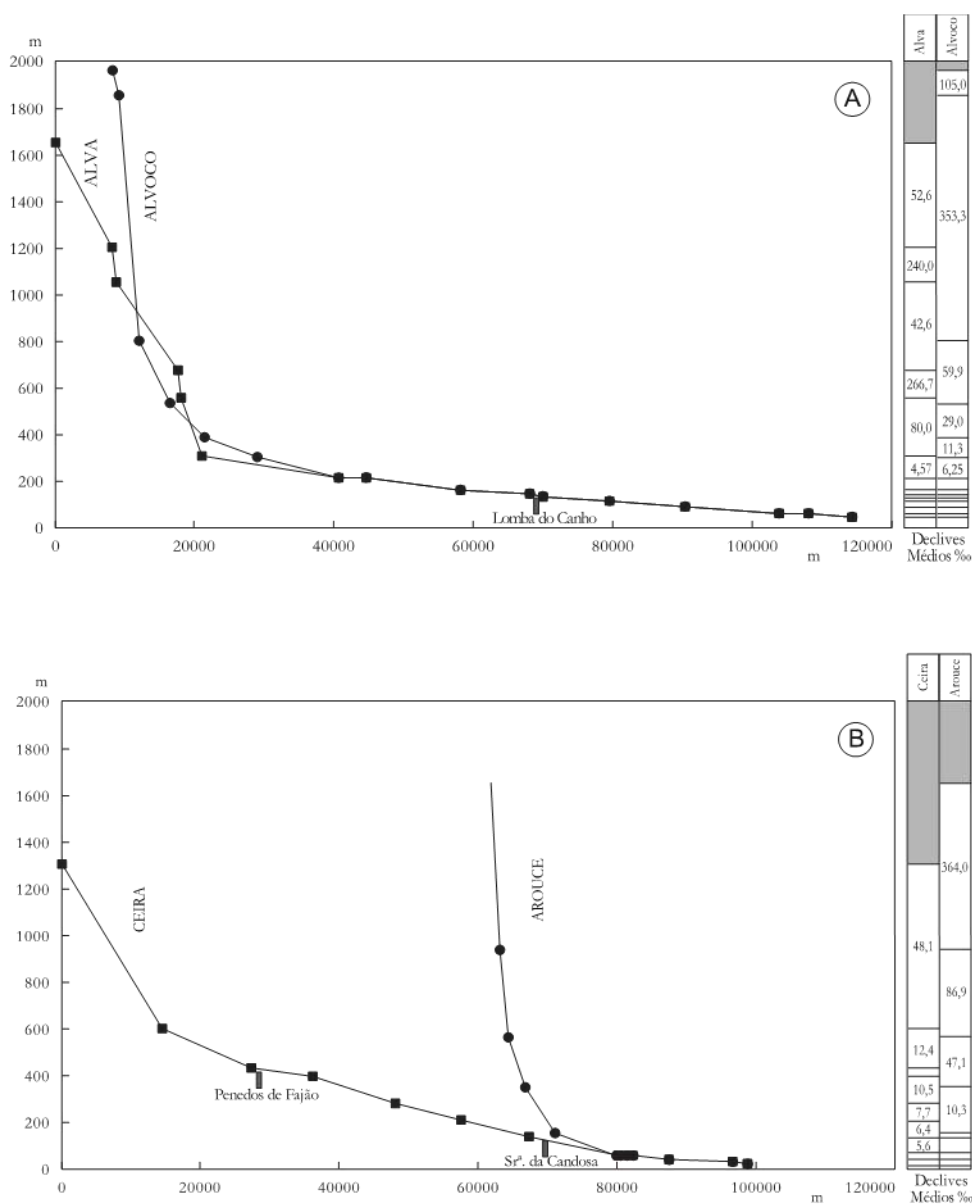


Figure 3. Schematic longitudinal profiles of the rivers Alva (A) and Ceira (B). (Source: Lourenço, 2018).

In this basin we can find arkose sediments, that date back to the Eocene, and conglomerate sediments, that attest to the uplift of the schist mountains, whose re-configuration can be traced on the quartzite crest that culminates in the Penedos de Góis and that the Ceira runs through at the epigenetic gorge of Senhora da Candosa, precisely because its drainage route took place over these deposits.

After going through Góis, one leaves the basin of the river Ceira and enters the basin of the river Alva, which, upstream of Arganil, at Pedras Negras, also crosses a secondary

quartzite crest, that of Santa Eufémia, fossilised by the "*raña de xisto*" (sedimentary landform) of Folques, and that, to the SE of the river with the same name, rises on the Monte Alto.

Next, in the vicinity of Coja, you will find *conheiras* (area made up of pebbles), made up essentially of quartz exudation, which attest to the ancient Roman gold exploitation carried out in the colluvial deposits of the Alva basin. This explains the existence of a Roman camp at Lomba do Canho, located precisely on the quartzite crest, south of the river Alva.

From here on, with the start of the ascent of the mountain range, one leaves the tectonic basin and the geomorphological picture changes, as one enters the domain of slope deposits, many of them with periglacial features. As the altitude increases, the sight reaches the sloping platform where the Mondego river flows and, closing the horizon, one can spot the Caramulo mountain range. The summits correspond to community land (wasteland), much of which is under the administration of the Local Communities or under co-management with the Portuguese State, via the Institute for Nature Conservation and Forests.

Halfway through the last century, these wastelands were subject to intense maritime pine plantations. As of the last quarter of that century, this whole area has been the scene of numerous and violent fires. The first of them to exceed a burnt area of 10 thousand hectares occurred in 1987, a situation that, in the following year, favoured the violent action of erosive processes, with incidence in the headwaters of the Pomares stream. In 2005, another major fire once again burnt a substantial part of this area and, in 2006, violent erosion processes again affected the Pomares and Piódão streams. And "*to add insult to injury*", in 2017 all this extensive area was the stage of a new and vigorous fire, and, in its sequence, there were, once again, violent erosive effects in the headwaters of the Pomares stream and, more sporadically, in other areas.

After observing some geomorphological aspects of the headwaters of the Pomares stream, we will descend to the historic village of Piódão, with its picturesque houses built of schist and covered with slate slabs. We will then follow the stream of the same name, an impressive fracture valley, running in a straight line, until we reach the Alvoco river, where we will have the opportunity to observe two levels of abandoned meanders:

- 1) An upper level, cut off naturally and partly still fossilized by colluvium, which sometimes also develop on river terraces, which have been the object of gold mining, as attested by the existing *conheiras*, and
- 2) A lower level, artificially cut by human intervention, therefore of anthropic origin.

Near Alvoco de Várzeas the valley, very structurally limited, widens until it reaches the metaphorical connection halo of the Avô plutonite, where it narrows and then becomes

embedded until it reaches the Alva river, at the Ponte das Três Entradas, which runs through a narrow tectonic rift.

Once we leave the Alva valley, the route continues along the watershed between the basins of the river Alva and a group of small tributaries that also drain into the river Mondego, which we will cross at the Aguieira dam, an important construction that, together with the Fronhas dam on the river Alva, makes it possible to regulate the flow of the river, damping down the autumn-winter flood peaks and providing water during the summer.

Immediately downstream, the Mondego river forms a whimsical meander, structurally limited, where the Raiva dams and the Coiço small hydro are located, which complement this system's hydraulic energy production system.

On the return to Coimbra, we will cross the quartzite crest that extends from Buçaco to Penedos de Góis, at the place called *Livraria do Mondego*, and the visit will end at the viewpoint of Penacova, overlooking quartzite, where we will be able to observe the adjustments that the river undergoes, before continuing its embedded course to Portela, just outside Coimbra, where we begin our journey in the morning, at its confluence with the Ceira.

The main aspects of this description will be the subject of stops, where the mentioned aspects are detailed and illustrated below.

1. Setting of the main stops and their observation topics

Departure from Coimbra via the EN17. At Portela: connection between the Meso-Cenozoic Rim and the Ancient Massif; the embedded valley of the Mondego river in Coimbra's Marginal Massif.

A tour along the Ceira river, towards the Lousã (topographic, tectonic and sedimentary) basin.

1st Stop - Lousã Basin: Observation of the arkose deposit.

2nd Stop - Senhora da Candosa: Quartzite crest and fanglomeratic sediments; Epigenesis of the Ceira river.

3rd Stop - Góis (coffee shop): Lousã-Góis-Arganil Rift.

4th Stop – Arganil: Quartzite crest (Montalto).

5th Stop – Folques: Raña of schists.

6th Stop – Coja: Terrace, colluvium and concheiras deposits.

7th Stop - Mata da Margaraça (lunch): A relic of preserved native flora.

A tour taking place close to the summit of the Açor mountain range: observation of the contrasts in the landscape:

- Steep slopes, which have been settled with slope deposits (periglacial);
- Deep valleys and mountain villages
- Major forest fires (1987, 2005 and 2017). Subsequent violent erosive processes (1988 and 2006)

8th Stop – Piódão: Uniqueness of the location.

The tour takes you through the fracture valley, virtually straight, of the Piódão stream.

9th Stop – Barriosa: River Alvoco - colluvium deposits and old meanders abandoned naturally (upper) and by human action (lower).

10th Stop – Vide: Old meander naturally abandoned; Colluvium, river terrace deposit and Conheiras.

11th Stop – Alvoco: Colluvium, river terrace deposit and Conheiras.

12th Stop - Varandas de Avô: Plutonite, confluence of the Pomares stream with the Alva river.

13th Stop – Aguieira: Hydroelectric and hydroagricultural dam.

14th Stop – Penacova: Mondego river and quartzite crests.

2. Departure from Coimbra and the Coimbra Marginal Massif

- Geology: Meso-Cenozoic Rim (Secondary) and Iberian Ancient Massif (Precambrian) connection
- Geomorphology: Embedded valley of the river Mondego and the Coimbra Marginal Massif
- Hydrography: Confluence of the Ceira river with the Mondego river

The major relief lines in the Coimbra area are intrinsically linked to the relatively recent uplift of the Coimbra Marginal Massif, in contrast with the indistinct subsidence of the whole seafront (Biro, 1949).

This Massif is an almost triangular cluster, set between the complex N-S landform, which runs through the eastern part of Coimbra, the Buçaco-Penacova quartzite crest, and the late-Hercynian foliation from Penacova to the Lousã Basin. Carved in schist, it rises to elevations higher than 500 meters, reaching a maximum of 549 meters, in Buçaco, due to the hardness of the Ordovician quartzite, underlined by the Cretaceous silicified

sandstone (Daveau, 1976). South of the Mondego the highest elevations are 100 meters below those found in the north (Ribeiro, 1985) (Fig. 4).

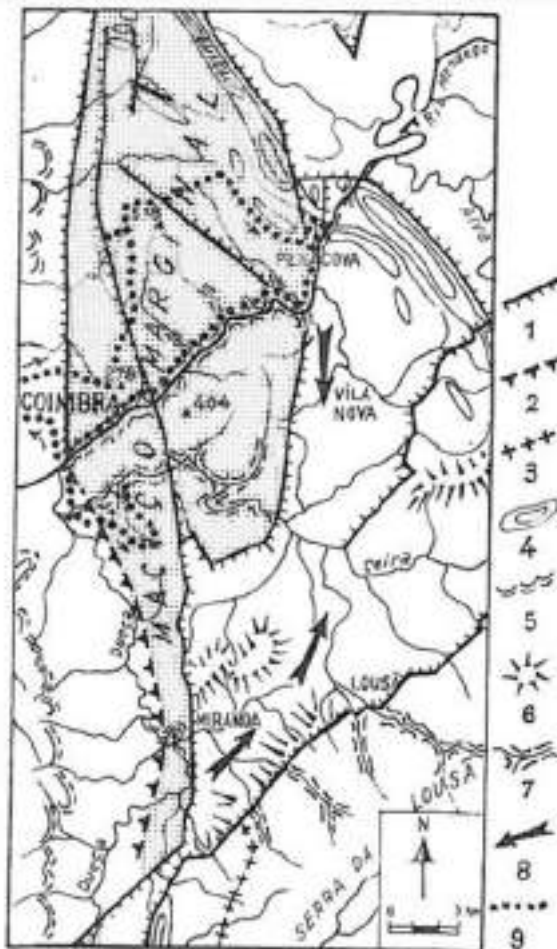


Figure 4

FIG. 1 – Bacia Marginal de Coimbra e áreas limítrofes. 1 – Falhas com expressão tectónica geral; 2 – escarpamento ocidental de Senhor da Serra; 3 – limite de basaltos graníticos; 4 – cristais quartzíticos; 5 – frente de cuestas das calcárias lísticas; 6 – colina constricta por depósitos; 7 – principais rios em granito; 8 – antiga direcção de drenagem primária; 9 – contorno segundo os rios de estudo de dia 7 de Novembro de 1981 (Figura original a adaptação de E. DAVEAU, 1976, fig. 1).

3. Tour along the Ceira river, towards the Lousã basin (topographic, tectonic and sedimentary) and the Cordillera Central

Geomorphological setting:

- Eocene (Late Tertiary): Broad surface flattening, evidenced by existing arkose sediments to the northwest and southeast of the Cordillera Central;
- Villafranchian (transition from Tertiary to Quaternary) - Start of the uplift (horts) of the Cordillera Central (Lousã, Açor and Estrela mountains, to the Northwest; Alvelos, Cabeço Rainho and Gardunha mountain ranges, to the Southeast), subsidence (grabens) of the marginal basins (Lousã-Góis-Coja and Seia-Pinhanços, to the Northwest; Sarzedas, to the Southeast) and middle Zêzere rift (graben) between the Northwest and Southeast mountain ranges;
- Pre-Ceira and river terraces (Chã do Freixo, with an airfield for fighting forest fires).

Stop 1. Lousã Basin, observation of deposits

The diversity of forms that characterises the Cordillera Central shows the importance of the lithology factor, defining the two main groups of the mountain relief: the schist, found in the Lousã and Açor mountains, and the granite, in the Estrela mountains (Fig. 5). The structure has a significant weight, since the tectonics also plays an important role, as the Cordillera Central is a large and complex horst, often limited by tectonic basins (Figs. 6 and 7).

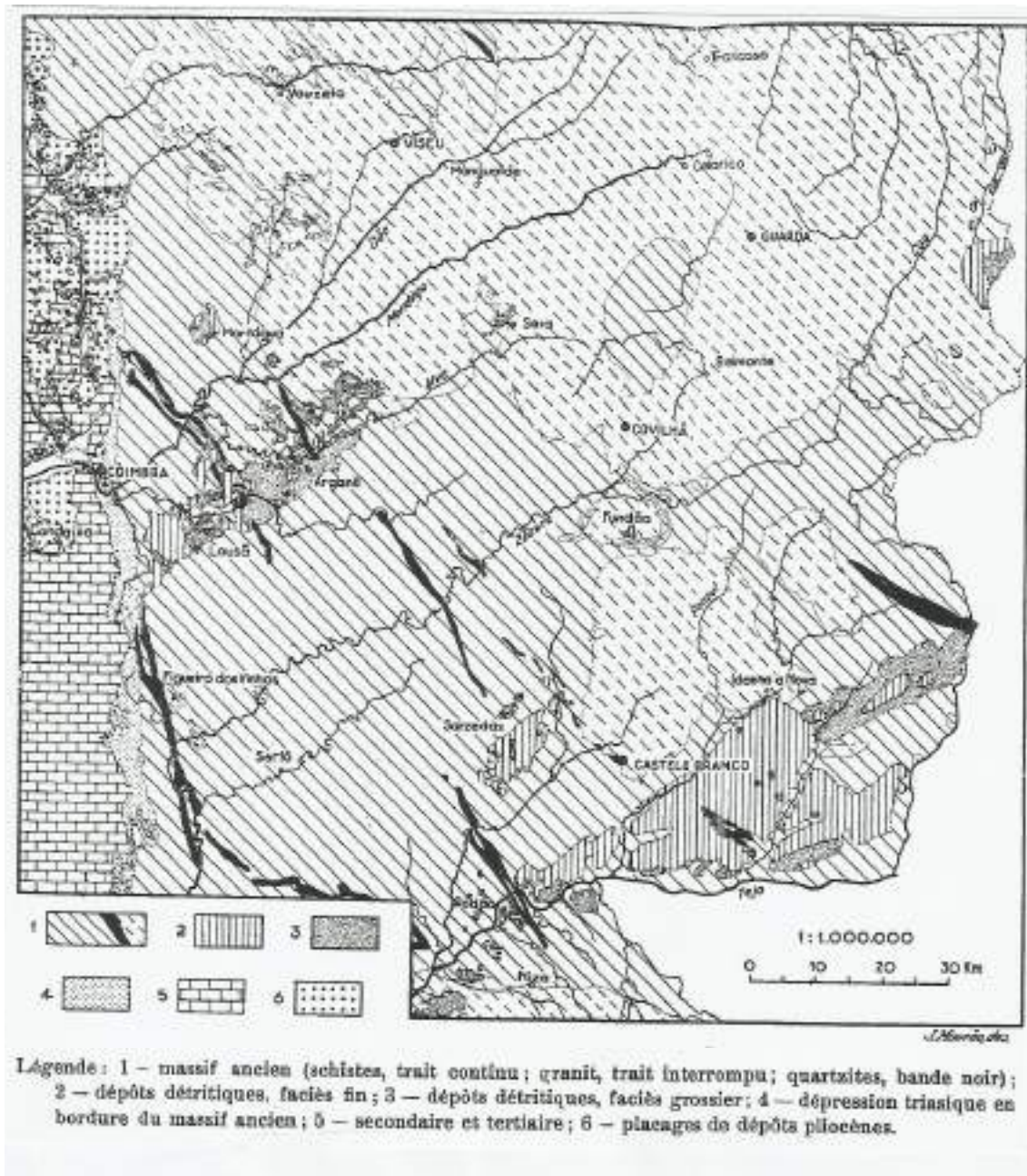


Figure 5. Schematic geological section of Central Portugal, according to O. Ribeiro (1949).

Nevertheless, many forms are closely correlated with climate, because, as will be seen, the presence of deposits makes it possible to infer previous paleogeographic and paleoclimatic conditions. In the Lousã basin, deposits are found (Fig. 8) that represent excellent landmarks for the interpretation of the uplift of the Cordillera. However, the various deposits are not easy to distinguish, not only because of the similarity of facies, but also because of their incomplete scaling. There is a predominance of light-coloured, quartz sandstones, sometimes feldspathic, and somewhat clayey. Relatively inconsistent and permeable, except when hardening occurs through silicification.

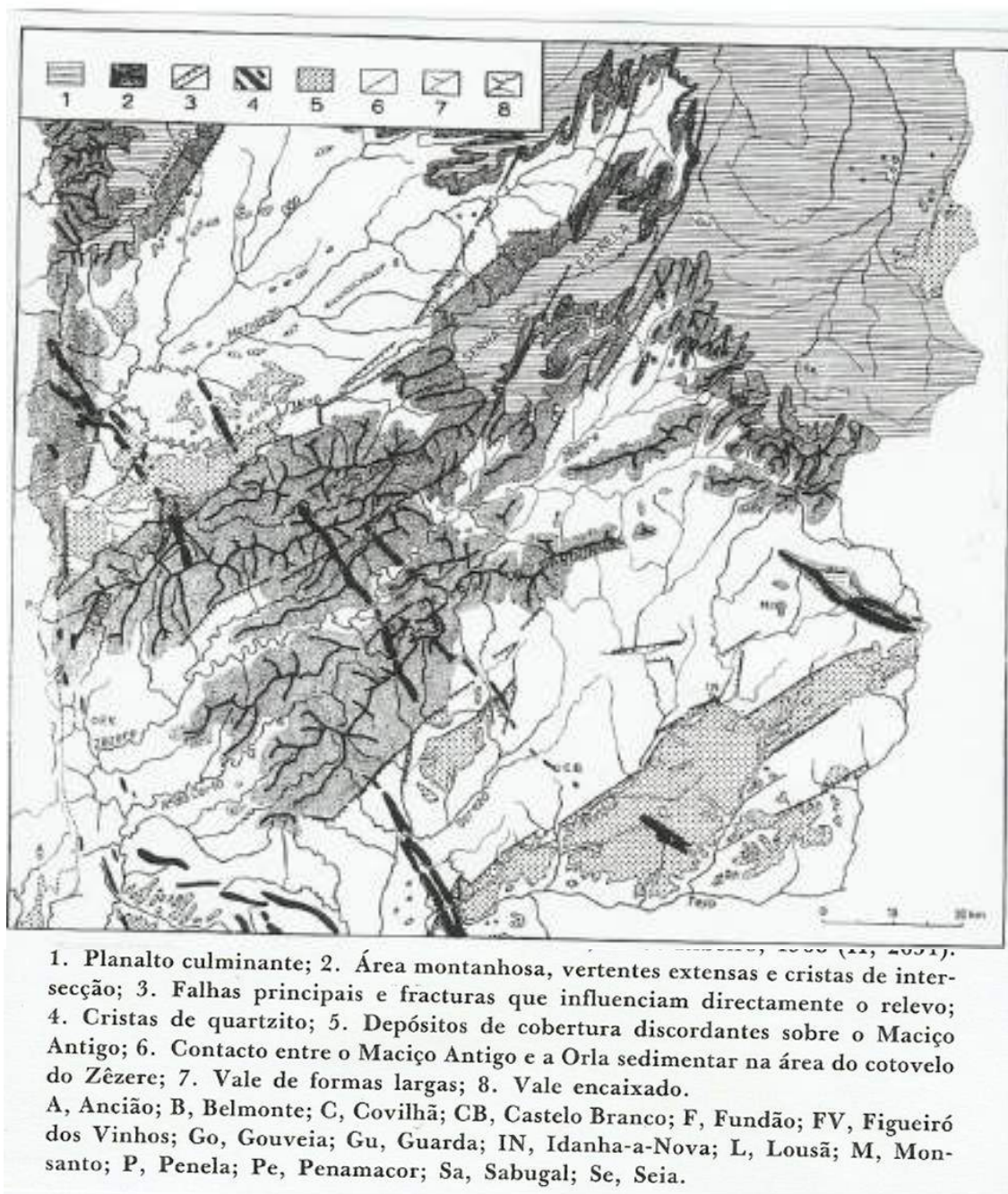


Figure 6. Morphological sketch of Central Portugal (S. Daveau and O. Ribeiro, in Ribeiro, 1968, II, p. 2651)

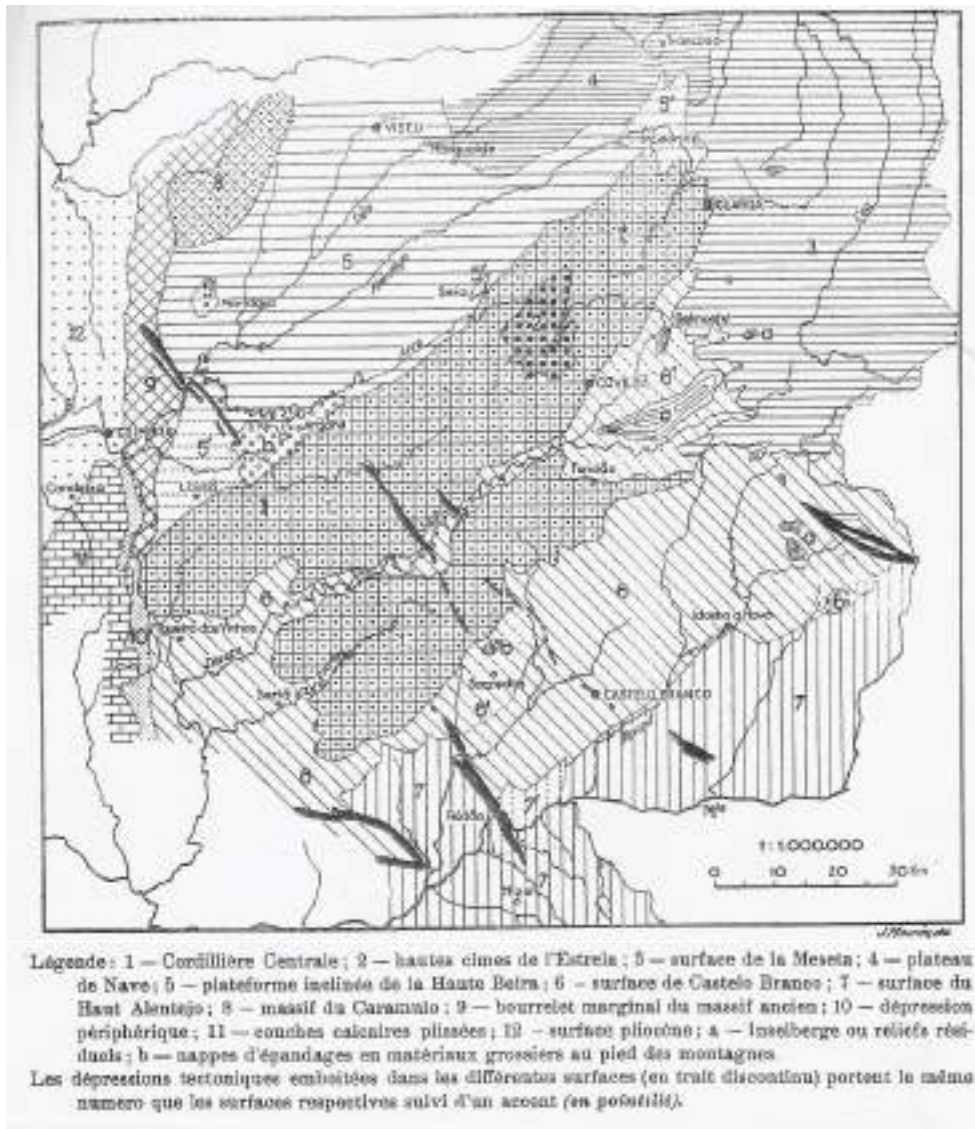
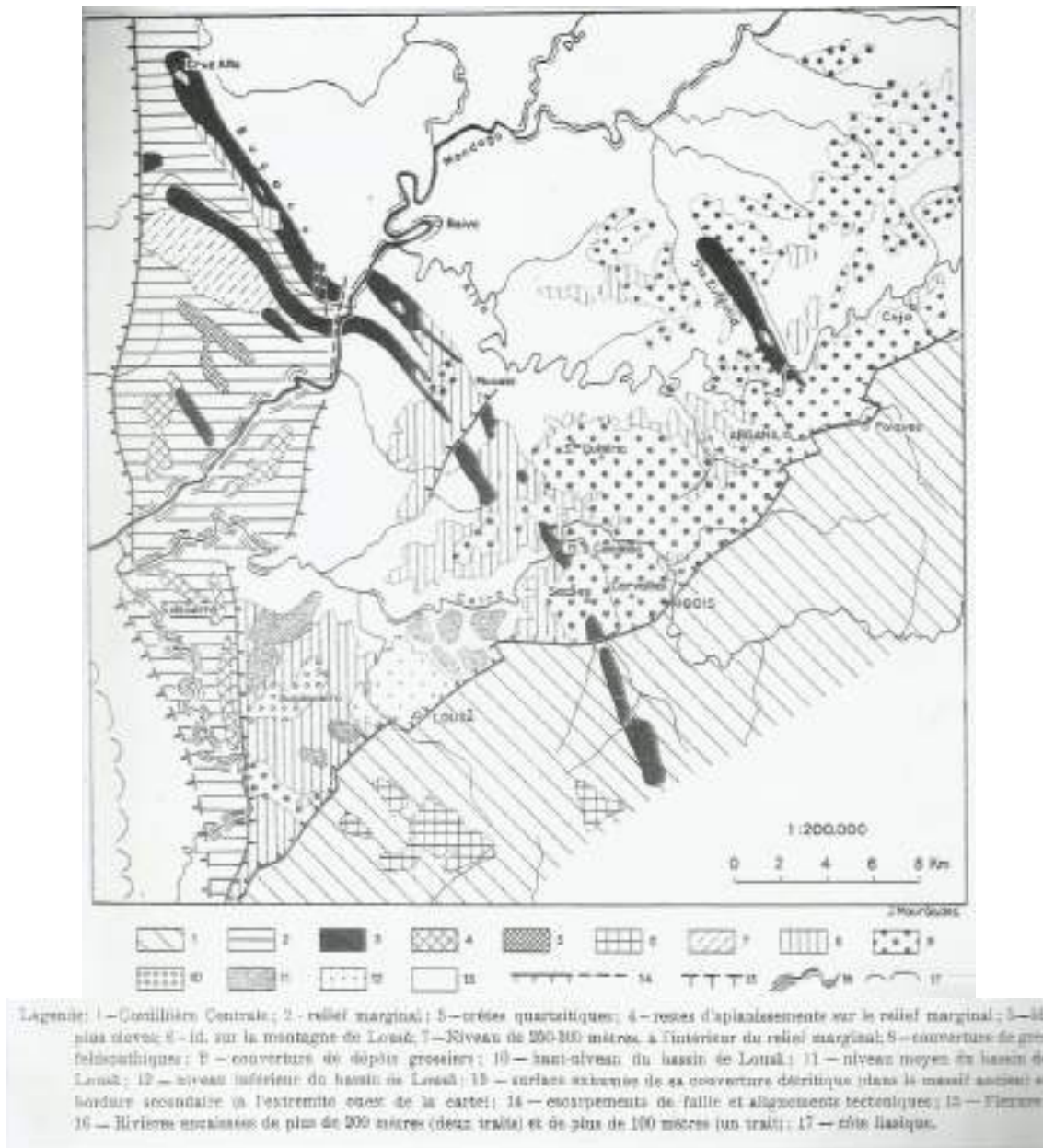


Figure 7. Morphological units of Central Portugal, according to O. Ribeiro (1949).



Stop 2. Senhora da Candosa

- First contact with quartzite;
- Epigenesis of "Cabril do Ceira";
- Epigenesis of the Ceira river;
- Quartzite crest and fanglomeratic sediments (Fig. 9);
- Lousã-Góis-Arganil Rift.

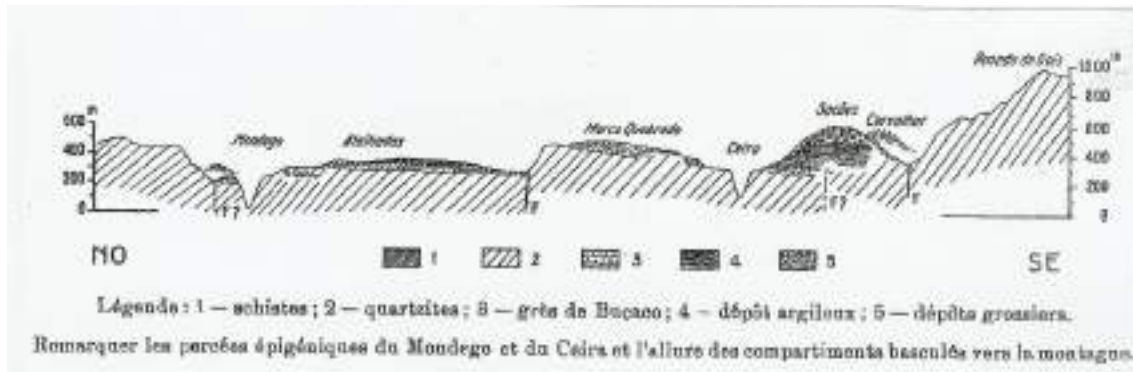


Figure 9. Schematic section along the quartzite crest of Buçaco according to O. Ribeiro (1949).

The arkose formation in Coja contains conglomerates with clasts of quartzite, milky quartz, feldspar, schist and granite. The sands are made up of quartz, feldspar, muscovite and biotite. The formation reaches 60 m thickness in the area between Vila Nova de Ceira and Arganil. Very coarse sandstones predominate, generally solid and gravelly, with relatively rare concave interbedded stratification. They have a significant silty fraction. The colour is whitish green, sometimes yellowish.

The Coja Arkoses are a detrital sequence essentially composed of arkoses and microconglomerates, which were transported by water, mainly by bottom charges. The facies and palaeocurrents suggest deposition by a fluvial system with braided watercourses and low sinuosity (Cunha, 1991; 1992).

It is possible to identify three sedimentary sequences limited by discordances, the Campelo Formation, greso-conglomeratic, dating from the upper Tortonian-lower Messinian; the second sequence, dating from the Messinian upper-Zanclean, made up of arenolite facies; and finally, the third, dating from the Piacenzian (lower Villafranchian), and which comprises a deposition based on coarse conglomerates with quartzite elements and gravelly sandstones, with rare interlayers of lutite.

The analysis of these formations allows us to infer that the great uplift of the Cordillera Central (Fig. 10) occurred in the Tortonian (upper Miocene), about 10 MA ago (Carvalho *et al.*, 1983), when compression reached its peak, although the compressive behaviour continues, as we have seen, until today. Consequently, several uplift phases can be observed, recorded through several regional sedimentary breaks, clearly erosive, which can affect the basement (Cunha, 1992, p. 212).

Later, in the Pliocene, the most recent uplift of the Cordillera Central determined the reactivation of the marginal faults of the Ordovician outcrops, leading to the over-elevation of the crests and, in the vicinity of these, to the formation of foothill deposits and summit deposits, rañas, traced to the upper Villafranchian, which precede the recent fluvial entrenchment (Cunha, 1987). Some authors consider that certain raña type formations may be associated with periglacial phenomena of cryoclastic and solifluction, in an arid and cold type morphogenesis (Muñoz-Jimenez, 1976, p. 87), hypothesising

that the top may be the result of a pasty outflow, carried out on frozen ground (Vaudour, 1979), which, in the Schist Mountains of the Cordillera Central, may have occurred during the first cold periods of the Quaternary.

(Adapted from L. Lourenço, 2018).

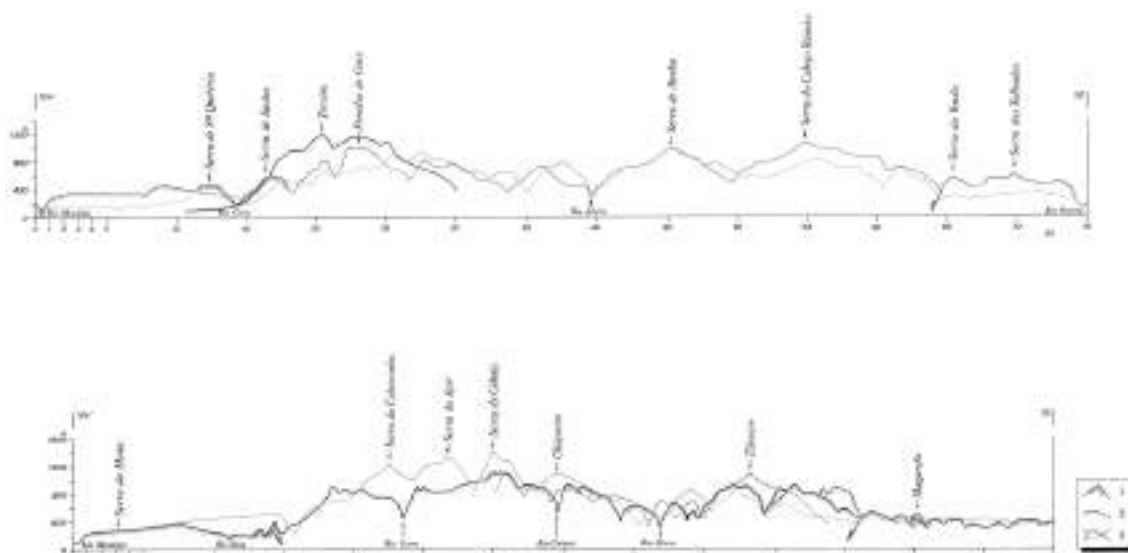


Figure 10. Cross-sections of the Schist Mountains (heights $\times 5$). A - Western sector; B - Eastern sector. 1 - Coarse deposits hills; 2 - Quartzite crests 3 - Schist Mountains. (Source: Lourenço, 2018).

Stop 3. Góis

Stop 4. Arganil

- Quartzite crest (Santa Eufémia - Montalto) - Comparative analysis with the crest of Penedos de Góis (the Great Rocks of Góis) (Fig. 11)

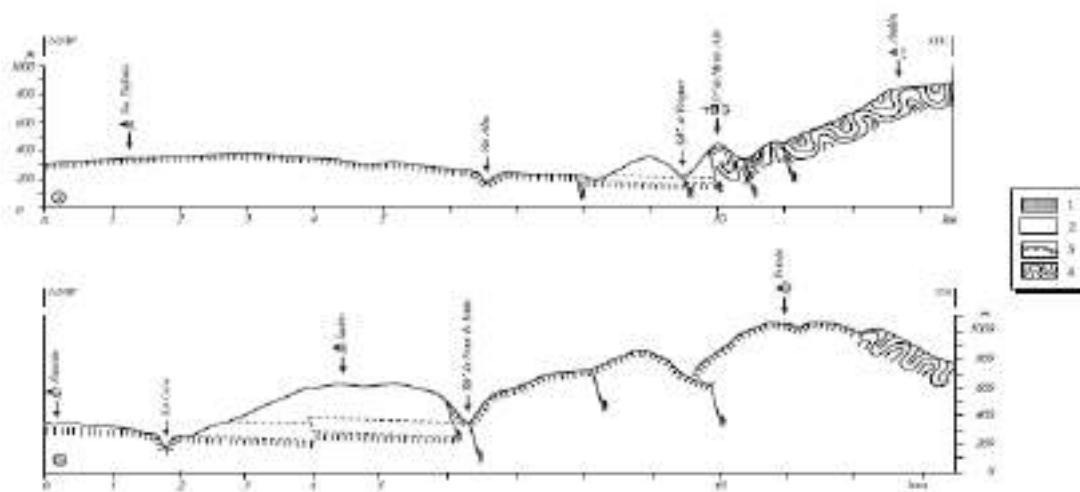


Figure 11. Longitudinal profiles of the quartzite crests of: A - Moita Mountain; B - Penedos de Góis. 1 - Coarse deposits; 2 - Arkose deposits; 3 - Quartzite crests; 4 - Schist mountains. (Source: Lourenço, 2018).

Stop 5. Folques

- Raña de xisto

Near Folques, coarse deposits of the raña type also occur, but formed essentially of schist, a distinctive feature that makes them unique in the context of coarse deposits.

Stop 6. Salgueiral/Coja

- Alva river
- Terrace, colluvium and conheiras deposits

Gold mining seems to still justify the presence of piles of rounded pebbles, devoid of clay matrix, which seem to indicate their probable being washed for gold prospecting. These are found not only in the Alva river, but also in the Alvoco river, its tributary, as well as in other rivers (Lourenço, 2018).

Stop 7 .Mata da Margaraça

- A relic of preserved native flora

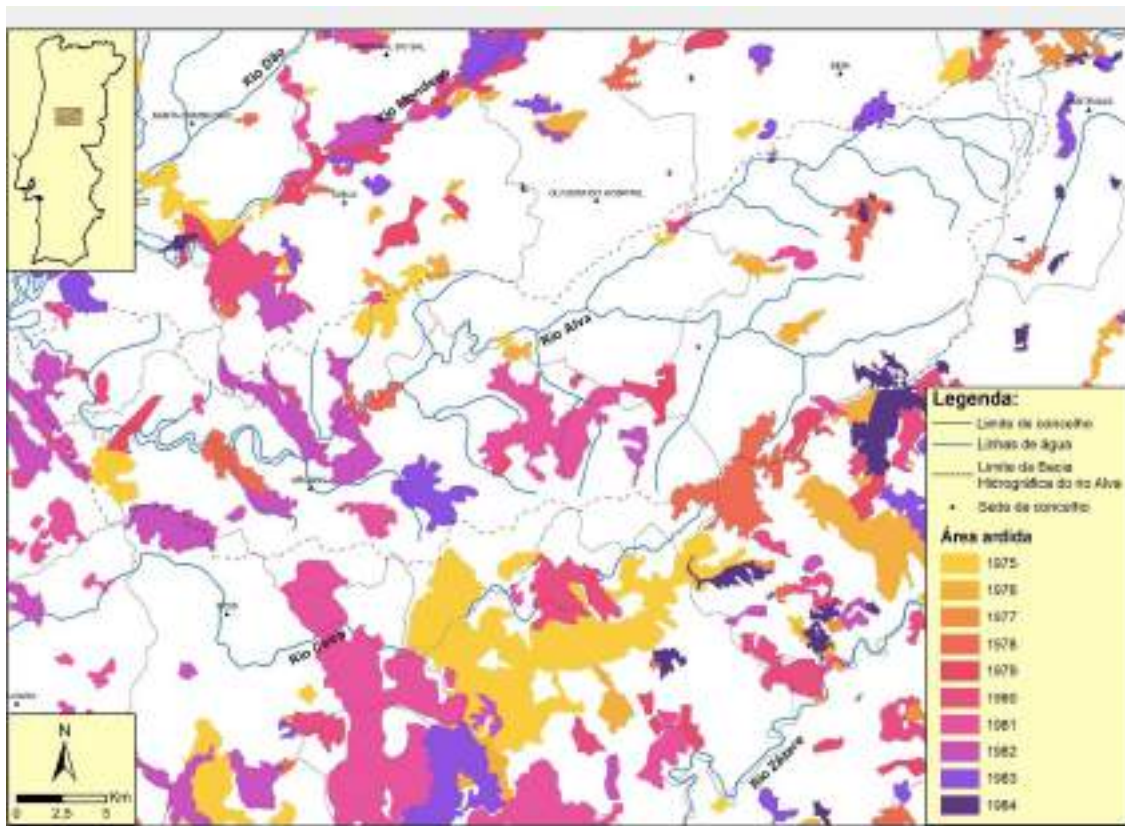
Establishing itself as one of the most luxuriant woodlands in the Beiras. Its vegetation is made up of a mixture called Rusco-Quercetum-roboris which is part of the Quercion robori-pyrenaicae grouping, characteristic of the nord-west part of Iberian Peninsula. These woods are, in fact, the best example of such area in Portugal. It is, therefore, a rare and important specimen of what used to be the covering vegetation of the hillsides in the centre of Portugal. It belonged to the Count-Bishops of Coimbra, from the reign of D. Afonso III and seems to have remained in much some condition until the nineteenth century. At that time, the liberal regime considered it part of the national estate and incorporated it into the public heritage. The bishopric made a further attempt to assert its claim for possession, but it passed into private hands after public auction. Since 1985, the woodland has been the property of the ICNF - Instituto de Conservação da Natureza e das Florestas (Institute for the Conservation of Nature and Forests).

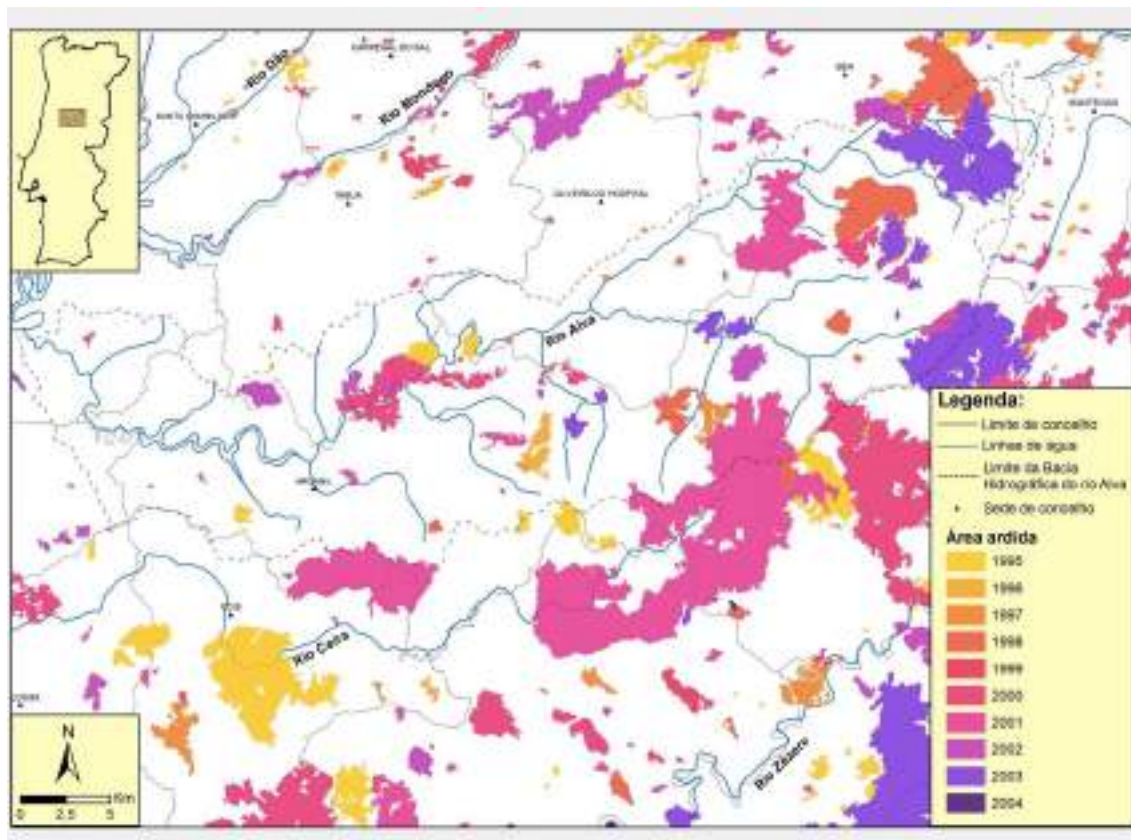
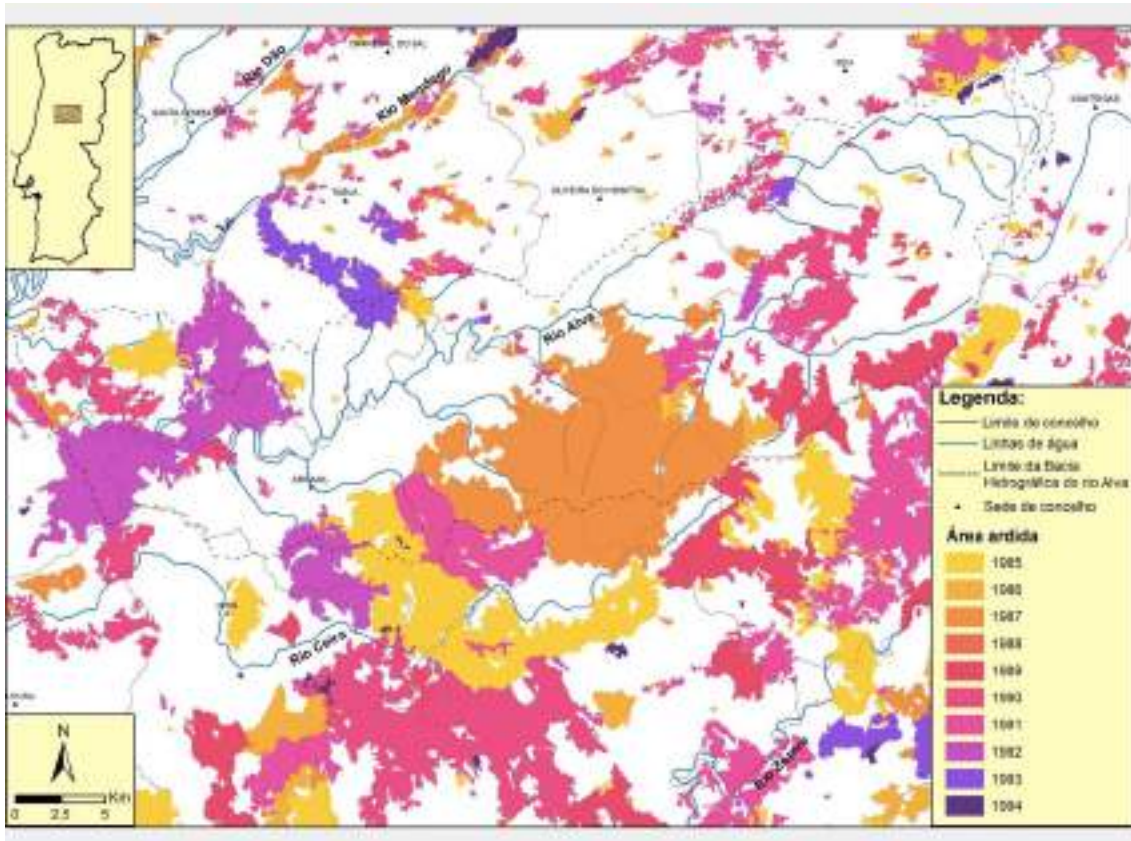
This tour takes place close to the summit of the Açor mountain range, with observation of:

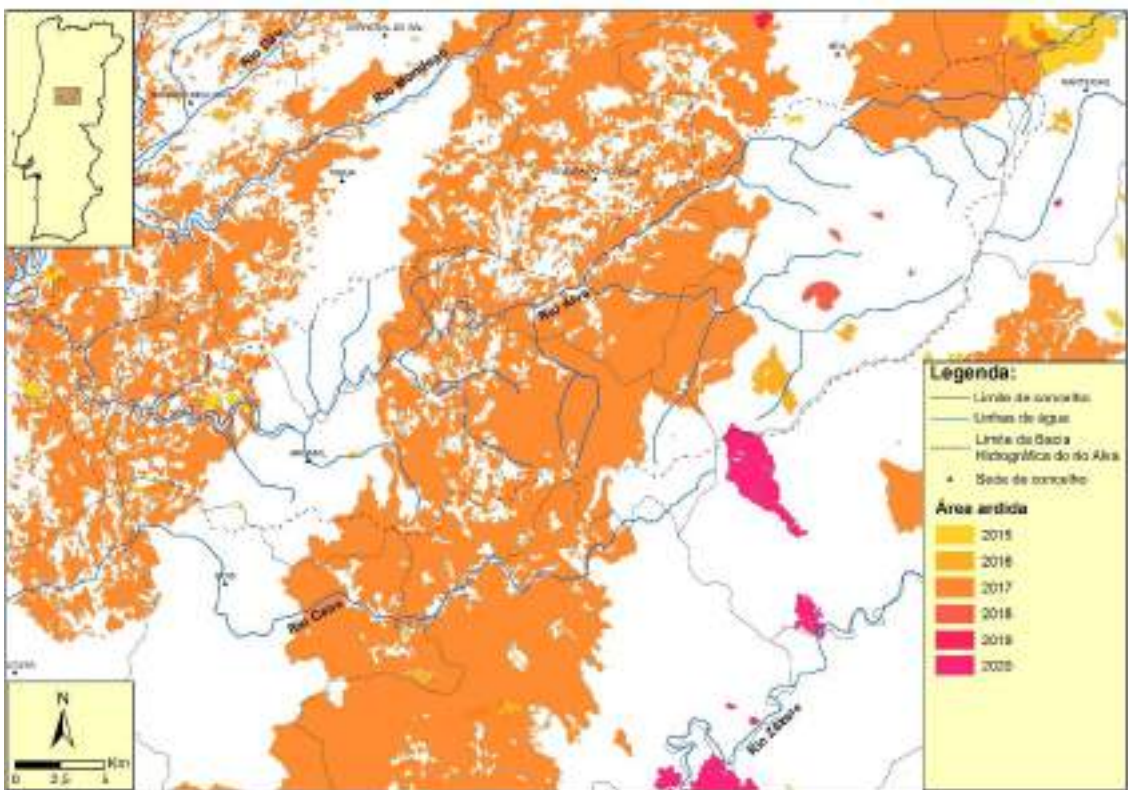
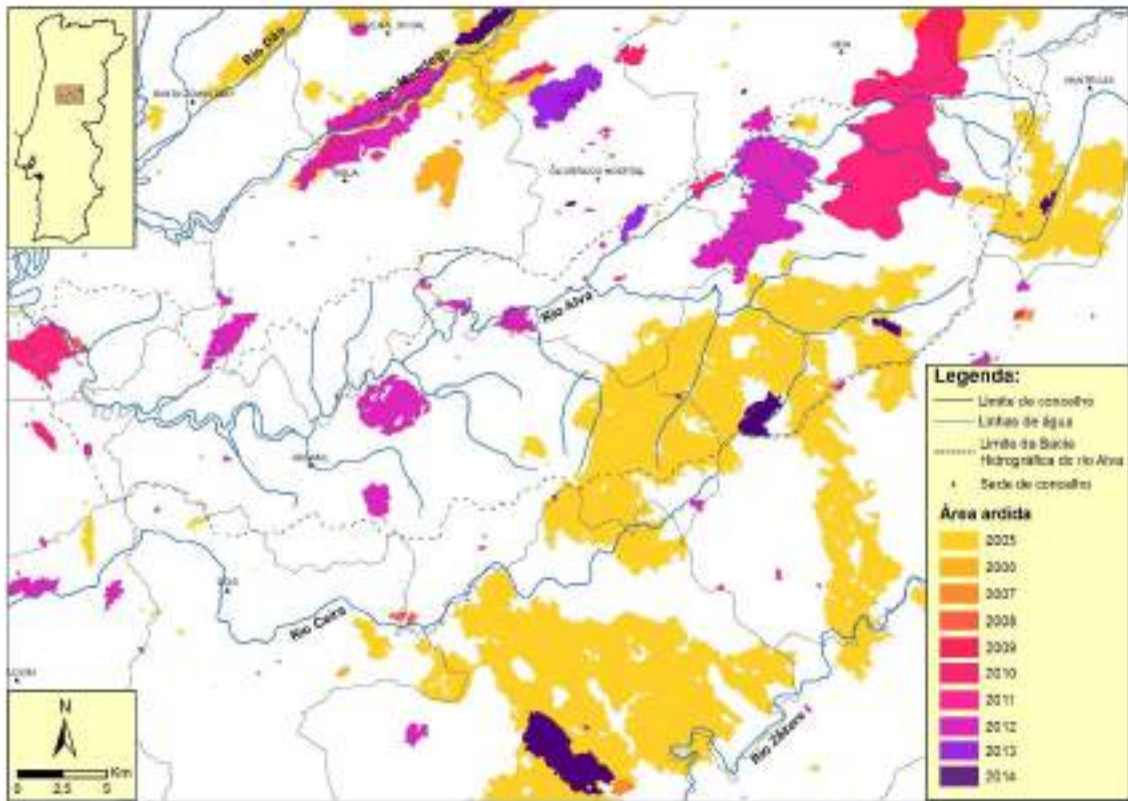
- Landscape contrasts;
- Steep slopes, which have been settled with slope deposits (periglacial) (Photo 1);
- Deep valleys, embedded and tectonically shaped;
- Violent erosive processes following the great fires (1988 and 2006).



Photograph 1. Overview of the curviflow deposit of Estrada Vide - Pedras Lavradas, (Source: Lourenço, 2018).







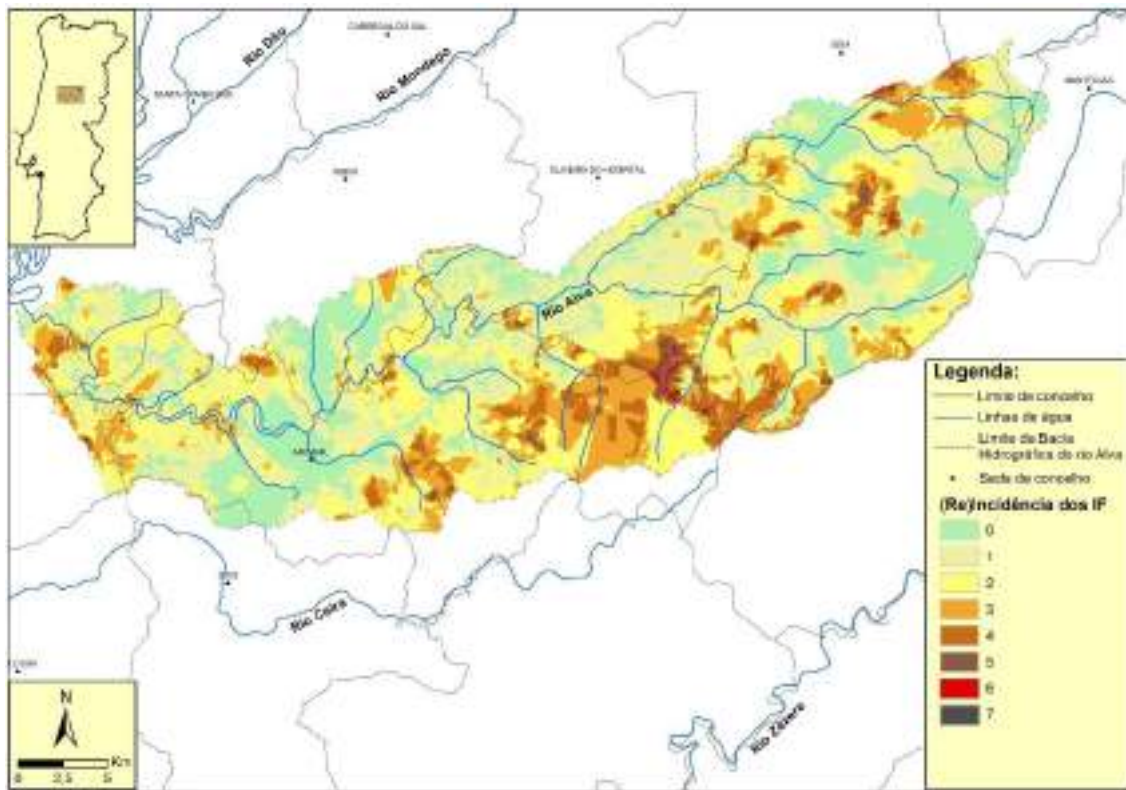


Figure 12. Annual mapping of the major forest fires, grouped in decennia, and their recurrence in the Alva river basin (Source: Adapted from Lourenço *et al.*, 2020).

Stop 8. Piódão

- Uniqueness of the location: isolated and inaccessible until the end of the 20th century;
- Top of the Açor Mountain: S. Pedro do Açor (1342 m) and Cabeço do Gondufo (1342 m);
- Headwaters of the Piódão stream: slopes settled with deposits, steep slopes, deeply embedded fracture valley, downstream of Piódão;
- Forestry suitability; major forest fires and post-fire erosion.

The tour runs along the virtually straight fracture valley of the Piódão stream and then along the Alvoco river (Fig. 13).

- Abandoned meanders: naturally and by human intervention;
- Slope and valley bottom deposits: river terrace, colluvium and conheiras.

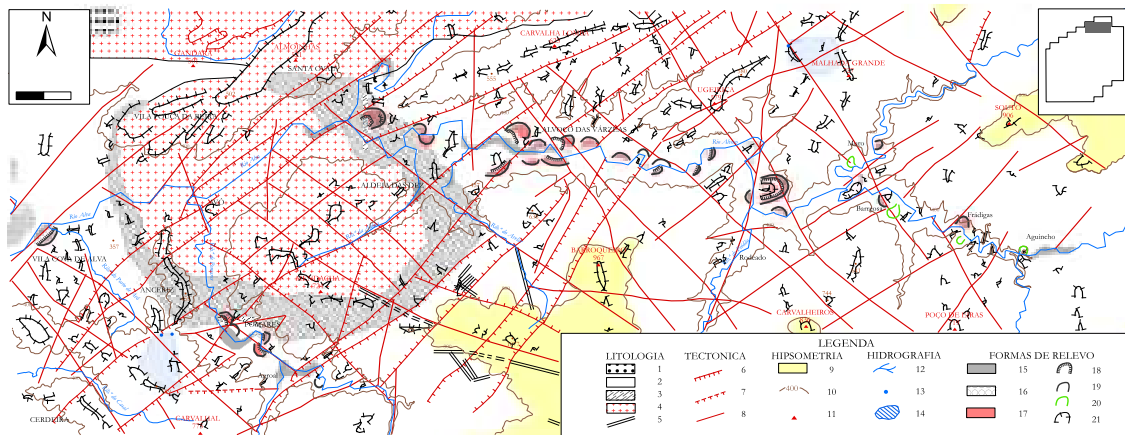


Figure 13. Geomorphological sketch, very simplified, of the vestibular parts of the Alvoco river and the Pomares stream. 1 - topsoil deposits (plateau gravels); 2 - schists and graywacke; 3 - contact metamorphic rocks (Avô plutonite); 4 - granitoid rocks; 5 - basic rock veins; 6 - rift; 7 - probable rift; 8 - significant fracture; 9 - altitude above 800 metres; 10 - contour line of 400 metres; 11 - geodesic vertex and respective altitude in metres; 12 - main hydrographic network; 13 - probable capture; 14 - river basin threatened with capture; 15 - alluvial bottom; 16 - remixed terrace; 17 - red deposit; 18 - deposit exploitation front; 19 - margin of old meander; 20 - meander artificially abandoned, by man-made cutting, in trench; 21 - tableland. In chart: location of the figure relative to the studied area. (Source: Lourenço, 2018).

Stop 9. Barreosa

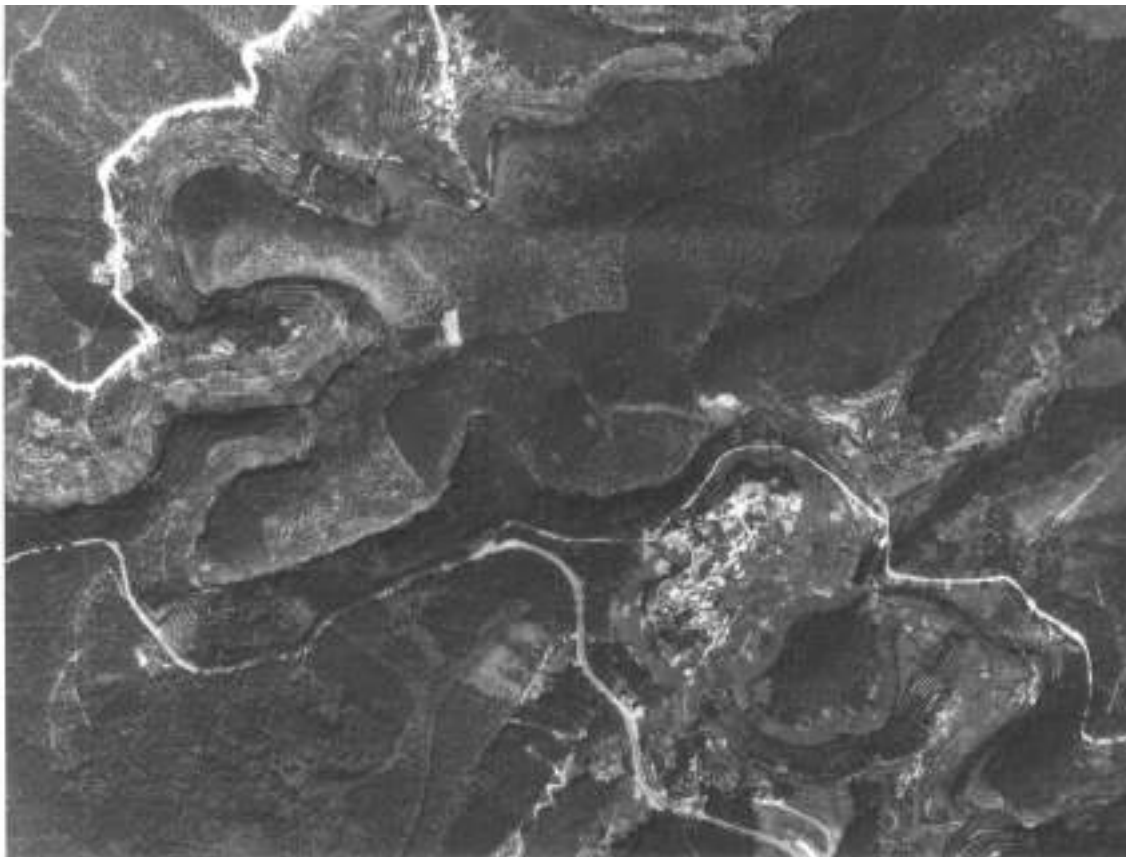
- River Alvoco: colluvium deposits and old meanders abandoned naturally (upper level) and by human action (lower level);

The evolution of meanders seems to be mainly based on tectonic criteria, as can be inferred from the analysis of several examples collected along the rivers and streams that drain the Schist Mountains. However, other factors also appear to be important for the evolution of meanders, for their downstream migration. One that warrants our particular attention, perhaps because it also corresponds to one of the least known aspects of the recent evolution of the drainage network, was the abandoned lobes, especially when this process was of human origin, thus being artificial and relatively recent.

From the outset we noted the existence of two different processes by which humans manually cut the peduncles of the meander. The most frequent, in a trench, was dug in the open air, while the less usual consisted of digging an underground gallery, in a tunnel. This second process was only used in cases where the peduncle thickness was more substantial and where, if the trench technique were to be used, it would require the removal of much larger volumes of earth, the extraction and transport of which would substantially increase the cost of these impressive hydraulic and agricultural engineering works.

As for us, although the immediate purpose of the many trenches and tunnels dug in the rock was to divert the flow of rivers and streams, the main objective was, essentially, to achieve a place where a portion of flat land could be created, easily transformable into agricultural land and irrigable with plenty of water. These aspects, of little importance in flat areas, are fundamental where flattened surfaces are scarce and where water for irrigation is rarely abundant, aims that were achieved concurrently, via the execution of the openings. Naturally, the unevenness caused by the artificial cut was often taken advantage of to install horizontal wheel water mills.

Two examples of these artificial cuts can be found in the Loriga stream, downstream of the village of Muro, and in the Alvoco river, near Barreosa (Photo 2), a place where we can also find the remains of an ancient, naturally abandoned meander, which has been fossilized by slope deposits, of the colluvium type, and which were most probably subject to gold mining, which led to the unveiling, at the entrance of Barreosa, of part of the route of this ancient meander from pre-Alvoco (Photo 2).



Photograph 2. Aerial view of the confluence of the Loriga stream with the Alvoco river.
(Source: Lourenço, 2018).

The material from the deposit that filled the abandoned meander of Barreosa was almost completely dismantled, with only small fringe areas remaining. Based on observations made on barriers pertaining to these fringes, preserved on either bank of

the meander and about thirty metres apart, an attempt was made to reconstruct the deposit and the possible conditions under which the material was deposited (Fig. 14).

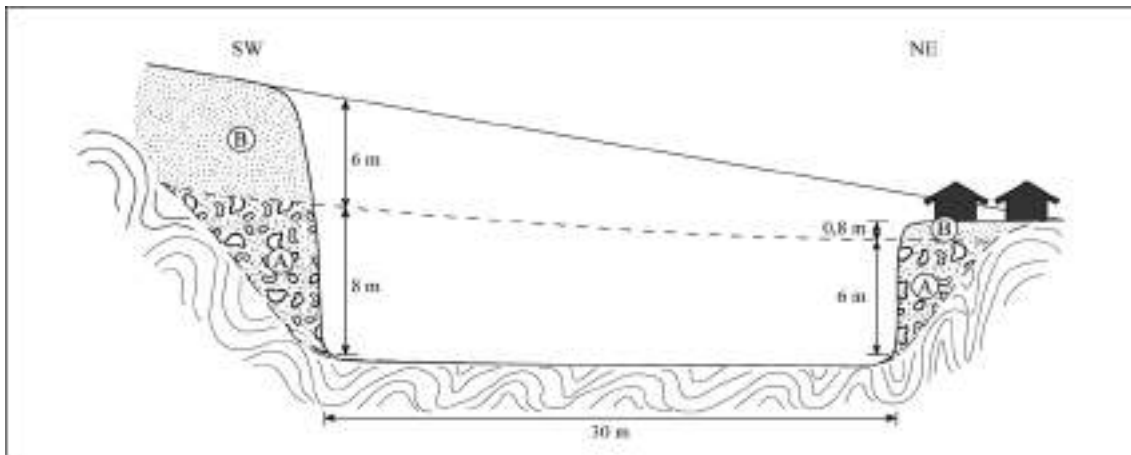


Figure 14. Schematic section of the old Barreosa Meander deposit (Source: Lourenço, 2018).
A - compact, greyish or yellowish conglomerate; B - red conglomerate.

From the outset, it is possible to identify two completely different episodes. At the base, a compact, heterometric, greyish (A), sometimes whitish or yellowish, conglomerate is observed, formed by schist plates, with the largest ones around 5 cm. The thickness of this conglomerate is about 8 metres in the barrier located to the SW and about 6 metres in the NE.

Over it rests a conglomerate also heterometric, but of a red colour, immature (B), formed of schist pebbles (80%) and quartz (20%), and with a variable matrix percentage between 30 and 60%.

Analysis of a sample from this deposit (233- 01) showed about 10% coarse material, greater than 4mm, 30% sand and 60% silty-clayey material. In the same sample two clay minerals were identified: illite and kaolinite. While the former is abundant, the latter is rare.

The pebbles are rarely rounded, and the largest ones are about 30 cm. The thickness of the deposit in the SW barrier is around 6 metres, while in the NE, where the top of the deposit was destroyed, it varies between 50 and 80 cm.

These circumstances suggest that the reconstitution of the deposit points to a general movement of the material from SW to NE, although on closer examination it could have moved in other directions, particularly to SE, as the intermingling of the pebbles in one of the observed locations seems to indicate.

(Adapted from L. Lourenço, 2018)

Stop 10. Vide

- Old meander, naturally abandoned (Photo 3);



Photograph 3. Aerial view of the abandoned meander of Vide, on the Alvoco river. The old mining front still preserves great rigidity, especially to the SE. 1 - Watercourses; 2 - Mining front of the deposit; 3 - Limits of the old meander. (Source: Lourenço, 2018).

- Colluvium

At the exit of Vide, towards Alvoco das Várzeas, the base of the colluvium is about 320 meters high, about 25 meters above the current bed of the Alvoco, in an extension of 300 meters along the road, with slight disruptions and lateral variations, and with an average thickness of about 4 to 5 meters. The primary interest of this deposit lies in its

SW end, the one closest to Vide, because it is there that we can observe the relation between three deposits: A, B and C (Fig. 15).

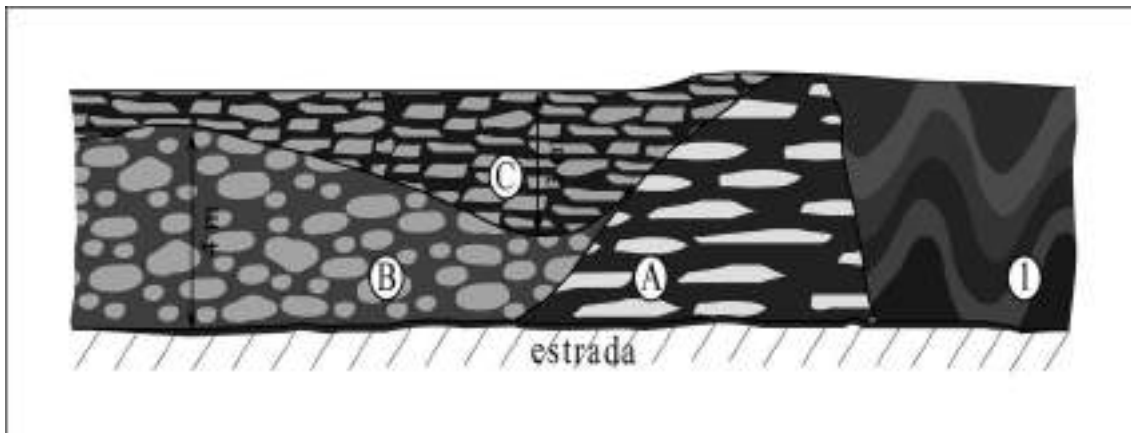


Figure 15. Schematic section of the Vide deposit, located at Km 126.9. 1 - schist; A - immature, subcompact, brownish conglomerate; B - submature, polymictic, greyish conglomerate; C - conglomeratic pelite, immature, reddish. (Source: Lourenço, 2018).

So, over the schist, a remnant of immature, subcompact, brownish conglomerate with yellowish spots and angular pebbles is preserved (A). A submature, polymictic, heterometric conglomerate with a coarse to very coarse, greyish arkose and sandstone matrix develops to the NE (B).

In this conglomerate rounded pebbles are predominant, consisting of schist (87%), quartz (8%) and granite (5%). The matrix is variable (10-40%) and the size of the coarser materials varies as follows: 1 to 2 cm - 15%; 2 to 4 cm - 20%; 4 to 8 cm - 40%; 8 to 16 cm - 15%; 16 to 32 cm - 10% and 32 to 64 cm - <1%. Sandy lenticules are sometimes interspersed within the cluster. The top of these two occurrences is cracked in the shape of a wide belly, which is filled with an immature, reddish, conglomeratic pelite with yellowish spots (C).

The fact that the submature conglomerate lies beneath the immature conglomerate makes this deposit a key piece, providing a fundamental contribution to the clarification of the natural order of overlap of the three sedimentation episodes.

Regarding clay minerals, all samples revealed illite, always very abundant, rare vermiculite and chlorite and kaolinite, both vestigial.

(Adapted from L. Lourenço, 2018).

Stop 11. Alvoco das Várzeas

- Relation between the river terrace deposit and the colluvium.

The terrace deposit of the Alvoco river, which can be observed next to the road, has a material that behaves like a subcompact to compact conglomerate, with an arkosic-sandy matrix of a red-brown or greyish-red tone common to this location, with a thickness of about 1.7 metres. The material is essentially schist (85%), granitoids (10%) and quartz (5%). Traces of altered feldspar were also found in the sand. The pebbles are very rounded (10%), rounded (70%), subrounded (15%) and subangular (5%). As for their size, we observed the following distribution: 1 to 2 cm - 5%; 2 to 4 cm - 20%; 4 to 8 cm - 50%; 8 to 16 cm - 12%; 16 to 32 cm - 10% and 32 to 64 cm - 3%.

Therefore, there is a predominance of pebbles with sizes between 4 and 8 cm, but their distribution is not homogeneous within the deposit, as from the bottom to the top there is a progressive decrease in granulometry, which is accompanied by an increase in the matrix percentage. In fact, at about 1/3 of the height of the deposit, more specifically at 50 cm from the base, the matrix percentage is about 15% and the largest dimension of the pebbles is about 25 cm. Approximately at 2/3 of the height, i.e., one meter above the base, the matrix percentage doubles, increasing to about 30%, while the largest dimension of the pebbles is reduced to 10 cm. At the top, at a height of about 1.7 m, the matrix percentage doubles again to 60% and the size of the pebbles decreases slightly to 8 cm.

As such, this deposit shows a significant loss of transport capacity by the Alvoco river, probably due to a progressive reduction in its flow.

(Adapted from L. Lourenço, 2018).

Summary of Quaternary deposits (Fig. 16)

We accept as a highly probable hypothesis that, during the Riss-Würm interglacial, the hydrographic network evolved as a result of a major recurrence of erosion, responsible for the break in slope exhibited at the midslope by many valleys.

In fact, the embedding that took place during the Riss-Würm interglacial is well marked, both by a level of naturally abandoned meanders, which testify to the beginning of the embedding, and by a very frequent terrace level, situated at about 40 metres, which corresponds to the end of the interglacial, given that, towards the top, it shows a marked loss of competence.

Meanwhile, on the slopes, the progressive increase in temperature has led to a generalised alteration in the pedogenesis, witnessed by the clayey pelites and mottled soils, sometimes superimposed on the terrace deposit.

It is followed by the two most important gelifraction stages identified by S. Daveau (1973, p. 20), which exhibit distinct characteristics.

The first stage, which we think should be attributed to the Lower and Middle Pleniglacial, as it exhibits interstage characteristics (Mateus and Queiroz, 1993, p. 123), allows us to associate it with hot and humid episodes, in a cold and humid temperate

climate (Diniz, 1992), which would allow the formation of small gelic materials with a clay matrix and solifluctions capable of displacing great quantities of this material, or other material inherited from previous stages, to the base of the slopes where, locally, they are preserved, forming the deposit we called red colluvium.

The deposit often features two sequences, separated by a break, corresponding to the Würm I/Würm II interstage.

In the end, the interstage characteristics must have further accentuated and led to the deep crevassing of the top of the deposit, marking the transition to the upper Pleniglacial, during which a cold and dry climate must have been predominant.

Among those described "this would be the coldest and driest" (Rebelo, 1986, p. 135), corresponding to "a more rigorous climate [than that of the middle Pleniglacial] with substages of variable intensity of cold and dryness" (Mateus and Queiroz, 1993, p. 124). It would have been the one that established the conditions for the formation of most of the deposits preserved today.

These deposits of plates are widely distributed but are most frequently found at altitudes above 700 m, fossilising palaeotopographies, often corresponding to small valley ditches.

By contrast, the underlying conglomerate, red colluvium, is found preferentially at lower elevations, in old, abandoned meanders or at the bottom of wider valleys, corresponding to small tectonic basins, tilted upstream.

The deposits of plates end in a break, which can be attributed to the transition between the upper Pleniglacial and the early Tardiglacial, as conditions were created that allowed the erosion of the upper part of the deposit, due to the fact that the climate registered a rapid warming (Cordeiro, 1990, pp. 58), and greater amounts of precipitation (Pedrosa, 1993, pp. 425), which favoured seepage and river runoff to the detriment of ice-related processes.

Several authors (H. Nonn, 1966; Y. Guillien *et al.*, 1978, M. Garmendia, 1989) cited by A. Pedrosa (1993, pp. 425), suggest a new climatic crisis around 11 000 BP, which may have been responsible for the formation of the curviflow deposits. In fact, these are only located at higher altitudes, preferably on north-facing slopes, displaying alternating climatic conditions, resulting in colder and drier periods and milder and wetter conditions, due to the existence of beds made up essentially of plates and others with a relatively abundant clay-sandy fraction.

This alternating pattern suggests the existence of a climate in which colder and drier periods would alternate with others in which snowfall would play an important role in the morphogenesis process, especially when melting.

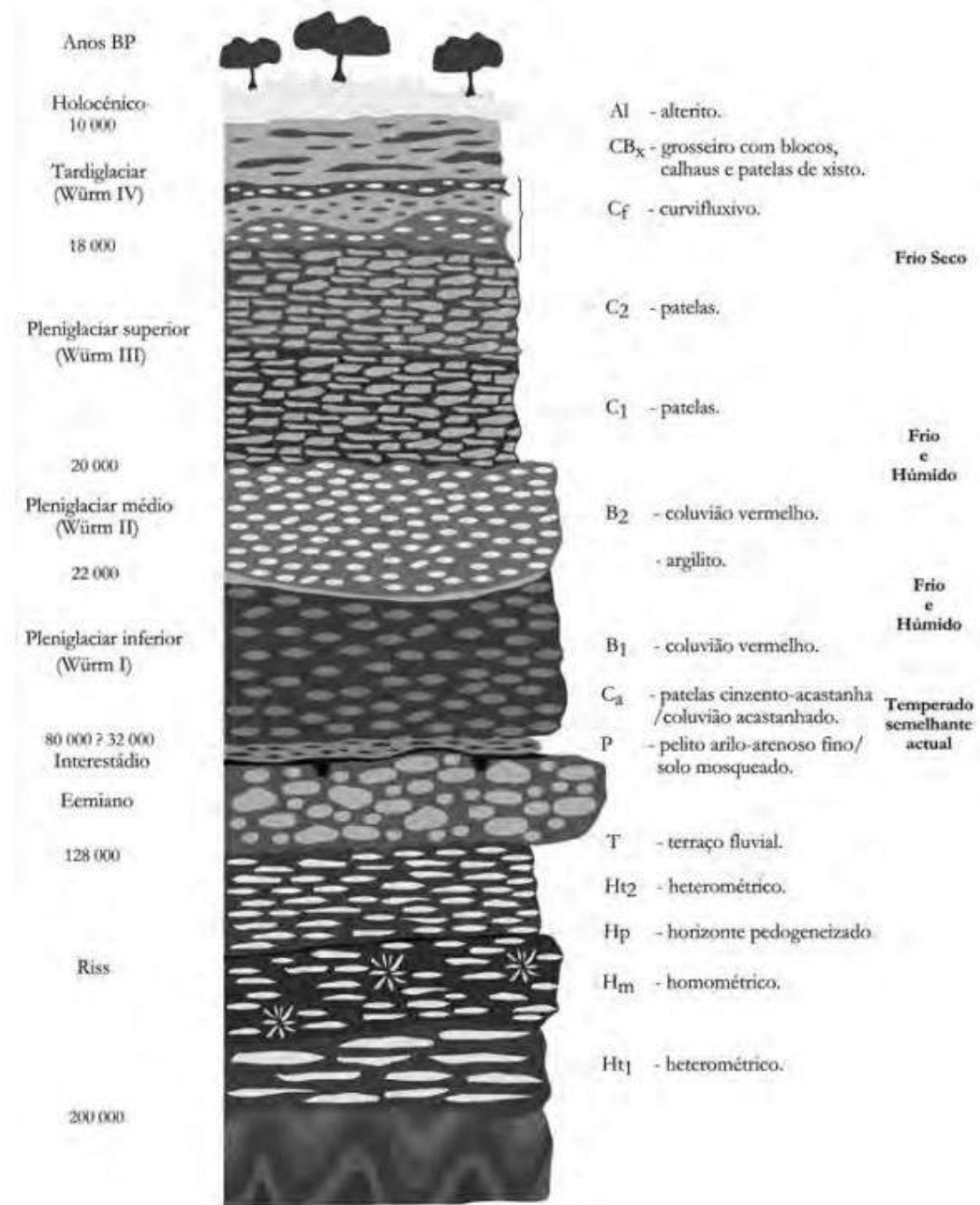


Figure 16. Interpretative sketch of the deposition that took place within the Schist Mountains at the end of the Quaternary (Source: Lourenço, 2018).

In such circumstances, the water flow within the deposits that fossilised the ancient water lines, in situations of more intense cold, could freeze within the deposits, causing the structure to swell and arch the thinner levels.

The climatic conditions at the beginning of the Tardiglacial in the Schist Mountains therefore seem favourable for the development of the curviflow deposit. It is followed by a period more prone to the occurrence of solifluctions, although the Tardiglacial, in situations of lower altitude and greater proximity to the ocean, may have presented two

favourable moments for the development of solifluctions, the early and the recent ones (Rebelo, 1986, p. 136), of which we found no records worthy of mention. It is likely that they have stirred up and transported materials left over from previous processes to the base of the slopes, where the processes associated with fluvial dynamics have evacuated them, or they have filled up old ditches, preserving them as deposits which we have labelled as uncharacteristic, which help to level the slopes. Later, a significant change in climatic conditions, as well as an increasing intervention of man over nature, have profoundly changed the framework of the natural evolution of relief forms.

Stop 12. Varandas de Avô

View over:

- The Plutonite from figure 13;
- The valley of the Pomares stream, with the Açor mountain range in the background;
- The riverside beach, at the confluence of the Pomares stream with the river Alva;
- The village of Avô and the surrounding terraces.

Stop 13. Aguieira

- Hydroelectric and hydroagricultural dam;

The Aguieira dam is located about 35 km upstream from Coimbra. It has a maximum height of 89 m (2) above the foundations and about 400 metres of total length at the crest, located at a level of 126.56, which includes a road with a seven-metre carriageway and respective pavements. It creates a reservoir that floods an area of 2,000 hectares and has a capacity of 450 million cubic metres, of which 234 are usable volume. Between levels 117.50 and 126.00 it holds 150 million cubic metres, a volume that fully covers the 100-year flood (with a peak at 2 500 m³/s), with a maximum discharge of 600 m³/s, and the 1000-year flood (with a peak at 3 500 m³/s), with a maximum discharge of 200 m³/s.

In order to control the floods, the water in the reservoir must remain at a level of 117.5 in winter. In April and May, it can fill up to level 125.0, reaching a maximum level of 126.0 in the months of June, July and August. This safety curve against floods ends up dropping until mid-October to level 125.0, and from then on, progressively, to level 117.5. The dam was built between 1972 and 1982. It is a multiple-arch dam and consists of three double-curved arches, the central one with a span of 90 metres, supported on the banks and on two buttresses located in the riverbed. The minimum thickness of the arch is 4.5 metres at the head of the dam and the maximum is 8 metres at the base. Two flood spillways, each with a flow capacity of 1 000 m³/s, are installed above them. The

discharge is made through ski-jump dissipators, directed towards the centre of the river. In addition to these two main surface dischargers, there is a bottom discharge whose flow capacity is 180 m³/s. The power station, of the dam-toe type, occupies part of the space delimited by the central arch and the buttresses, its foundation is more than 30 metres below the riverbed, and it is equipped with three reversible pump-turbines. In turbine operation, the maximum power supplied by the power station for normal reservoir levels is around 270 MW, corresponding to a flow of around 450 m³/s. With the reservoir at its maximum level (126.0), maximum power could reach 321 MW with a turbine flow of 525 m³/s. The reversible operation of these pump-turbines allows an average flow of about 3 x 140 m³/s to be pumped into the Aguieira dam from the Raiva dam, each motor absorbing a power of approximately 94 MW. Excluding pumping, the average yearly producible energy in Aguieira is around 260 GWh.

References

- Carvalho, A. M. Galopim de e Cabral, J. (1983) – “Evolução paleogeográfica da bacia Cenozóica do Tejo- Sado” (Com. 1.º Cong. Nac. Geol., Aveiro). Boletim da Sociedade Geológica de Portugal, Lisboa, xxiv, p. 209- 212.
- Cordeiro, A. M. Rochette (1990) – “O depósito de Varzielas (serra do Caramulo) – Contribuição para o estudo do Tardiglacial Würmiano em Portugal”. Cadernos de Geografia, Coimbra, 9, p. 49 60.
- Cunha, P. M. R. R. Proença (1987) – “Evolução Tectono- Sedimentar Terciária da Região de Sarzedas (Portugal)”. Comunicações dos Serviços Geológicos de Portugal, Lisboa, t. 73, fasc. 1/2, p. 67- 84.
- Cunha, P. M. R. R. Proença (1992) – Estratigrafia e Sedimentologia dos Depósitos do Cretácico Superior e Terciário de Portugal Central, a Leste de Coimbra. Dissertação de Doutoramento, Centro de Geociências da Universidade de Coimbra, Coimbra, 262 p. (inédito).
- Daveau, S. (1971) – “La glaciation de la Serra da Estrela”. Finisterra, Lisboa, vi, 11, p. 5-40.
- Daveau, S. (1973) – “Quelques exemples d'évolution quaternaire des versants au Portugal”. Finisterra, Lisboa, viii, 15, p. 5 47.
- Daveau, Suzanne (1987). As Formas de Relevo, Geografia de Portugal, I. A Posição Geográfica e o Território, Edições João Sá da Costa, Lisboa.
- Daveau, Suzanne (1987). Comentários e Actualização, Geografia de Portugal, I. A Posição Geográfica e o Território, Edições João Sá da Costa, Lisboa.
- Diniz, F. (1992) – “Pollen analyses of Pleistocene sediments from the western coast of Portugal”. Program and Abstracts, VIII International Palynological Congress, Aix en Provence (resumo).

- Lourenço Luciano (2018). *As Serras de Xisto do Centro de Portugal*, Imprensa da Universidade, Coimbra
- Lourenço, Luciano; Pinto, Carlos e Saloio, Pedro (2020). *Risco de Incêndio Florestal no Pinhal Interior. Livro-Guia da visita técnica n.º 5*. Coimbra. RISCOS – Associação Portuguesa de Riscos, Prevenção e Segurança.
- Mateus, J. E. e Queiroz, P. F. (1993) – “Os estudos da vegetação quaternária em Portugal; Contextos, Balanço de resultados, Perspectivas”. *O Quaternário em Portugal, Balanço e Perspectivas*, Colibri, Lisboa, p. 105- 131.
- Muñoz- Jimenez, J. (1976) – *Los montes de Toledo*. Departamento de Geografia de la Universidad de Oviedo e Instituto J. S. Elcano (C.S.I.C.), Oviedo, 500 p.
- Pedrosa, A. Sousa (1993) – *Serra do Marão. Estudo de Geomorfologia*, Dissertação de Doutoramento, Porto, 478 p. +119 p. de Anexos + Mapas. (inédito)
- Rebello, F. (1986) – “Modelado periglacial de baixa altitude em Portugal”. *Cadernos de Geografia*, Coimbra, 5, p. 127 137.
- Ribeiro, O. (1949). *Le Portugal central (Livret-guide de l’excursion C)*. Congrès International de Géographie de Lisbonne, Union Géographique International, Lisbonne, 180 p. + 22 estampas + 10 mapas (Reimpressão em 1982).
- Vaudour, J. (1979) – *Le région de Madrid: altérations, sols et paléosols. Contribution à l’étude géomorphologique d’une région méditerranéenne semi-aride*. Ed. Ophrys, Paris, 390 p.

Index

Purpose	9
Introduction	10
1. Setting of the main stops and their observation topics	13
2. Departure from Coimbra and the Coimbra Marginal Massif	14
3. Tour along the Ceira river, towards the Lousã basin (topographic, tectonic and sedimentary) and the Cordillera Central	15
Stop 1. Lousã Basin, observation of deposits	16
Stop 2. Senhora da Candosa	19
Stop 3. Góis	21
Stop 4. Arganil	21
Stop 5. Folques	22
Stop 6. Salgueiral/Coja	22
Stop 7 .Mata da Margaraça	22
Stop 8. Piódão	26
Stop 9. Barreosa	27
Stop 10. Vide	30
Stop 11. Alvoco das Várzeas	31
Stop 12. Varandas de Avô	35
Stop 13. Agueira	35
References	36



Photo by Sérgio Brito

ORGANIZATION AND SUPPORTERS:





10th IAG INTERNATIONAL CONFERENCE ON GEOMORPHOLOGY

Photo by Sérgio Brito

COIMBRA - PORTUGAL
« GEOMORPHOLOGY AND GLOBAL CHANGE »

FIELDTRIP GUIDEBOOK
Serra da Estrela
(The Pleistocene glaciation of the Estrela UNESCO Global Geopark)
14 September 2022

Gonçalo Vieira
Emanuel de Castro
Fábio Loureiro



Gonçalo Vieira
Emanuel de Castro
Fábio Loureiro

10th International Conference on Geomorphology
Fieldtrip Guidebook – Serra da Estrela
(The Pleistocene glaciation of the Estrela UNESCO Global Geopark)

14 September 2022



Coimbra, 2022

Edition notice:

Title: *10th International Conference on Geomorphology. Fieldtrip Guidebook – Serra da Estrela (The Pleistocene glaciation of the Estrela UNESCO Global Geopark)*

Authors: *Gonçalo Vieira (University of Lisbon), Emanuel de Castro (Estrela Geopark) and Fábio Loureiro (Estrela Geopark)*

Fieldtrip guided by: *Gonçalo Vieira (University of Lisbon), Emanuel de Castro (Estrela Geopark) and Fábio Loureiro (Estrela Geopark)*

Edition: *Universidade de Coimbra, Faculdade de Letras*

Fieldtrip and Guidebook Coordination: *António Vieira (University of Minho)*

Cover: *Alto da Torre plateau (photograph by Joel Santos)*

ISBN: *978-989-8511-06-5*

Introductory Note

The 10th International Conference on Geomorphology will take place in Coimbra (Portugal) from 12th to 16th September 2022, under the theme "Geomorphology and Global Change" and it is organized by the International Association of Geomorphologists (IAG) and the Portuguese Association of Geomorphologists (APGeom).

As in previous international conferences on Geomorphology, and as is the tradition in many geomorphological events organized around the world, the organizing committee of the 10th International Conference on Geomorphology proposed several fieldtrips to the participants, occurring before, during and after the main event.

These fieldtrips intend, above all, to show to geomorphologists from all over the world the diversity and richness of the geomorphological elements of the Portuguese territory (and also from Cape Verde) and to allow an exchange of experiences between the specialists that investigate these territories and the visitors, contributing for mutual scientific enrichment and for the valorization of this international conference.

The pre-conference fieldtrip is dedicated to the islands of Santiago and Fogo, in the Archipelago of Cape Verde. It will take place from 6th to 9th September and will be led by colleagues from the University of Cape Verde (Vera Alfama, Sónia Victória, Sílvia Monteiro, José Maria Semedo and Romualdo Correia). The volcanic geomorphology will dominate the visit (including well conserved structural volcanic forms such as cones, domes, craters and calderas), especially in the island of Fogo where recent volcanic activity has been registered.

The one-day mid-conference fieldtrips will take the visitors around the Portuguese mainland territory, the 14th September, allowing the visit of four different geomorphological realities.

In the Arouca UNESCO Global Geopark, internationally recognized territory since 2009, participants will be able to visit unique geological and geomorphological features (such as planation surfaces, bowl-shaped valleys and narrow river valleys) and witness the remarkable effort of protection and promotion of natural (abiotic and biotic) and cultural (tangible and intangible) heritage. The visit to the "516 Arouca" suspension bridge will be an excellent opportunity to observe the magnificent landscapes of this mountainous territory. This fieldtrip will be led by Artur A. Sá, António Vieira and Daniela Rocha.

The field trip to coastal areas of central Portugal will be led by Pedro Dinis and António Campar Almeida. Their proposal is to observe the different morphotectonic units of central west Portugal, namely the Coastal Mountain of Serra da Boa Viagem (revealing karstification features), the littoral plain (with aeolian dunes associated with some

reliefs with higher elevation), the Cértima subsiding area (structurally-controlled morphology), and the Buçaco region (with the Syncline of Buçaco).

The visit to the Schist Mountains of Central Portugal will be centered in the mountains of Lousã and Açor, and will be conducted by Luciano Lourenço and Bruno Martins. It is proposed the observation of the main contrasts of the landscape, especially in terms of its physical geography, translated into geological, hypsometric, geomorphological, and hydrographic differentiation, or the land use and occupation and evolution of vegetation cover, namely following the recurrent large forest fires and the subsequent erosive processes they caused.

The fourth one-day fieldtrip will be oriented to the Estrela UNESCO Global Geopark, and led by Gonçalo Vieira, Emanuel Castro and Fábio Loureiro. The main geoheritage significance of the Estrela UGGp is the extent and richness of the Late Pleistocene glaciation(s) landforms and deposits (with spectacular morphological features such as the Zêzere glacial valley or the glacial cirques, moraine boulders, erratics or *roches moutounnées*) as well as the peculiar long-term geological evolution (revealing a significant diversity of granite types and landforms).

The three post-conference fieldtrips include a visit to the Lisbon Region, Serra da Estrela and, finally, Minho and Galicia (Spain), and will take place from 17th to 19th September.

The fieldtrip to the Lisbon Region will be guided by José Luís Zêzere, César Andrade, Sérgio Oliveira, Jorge Trindade and Ricardo Garcia, and will cover topics related with slope instability and landslides that affect the region of Lisbon, the floods occurring in the area north of Lisbon, and the coastal dynamics, morphology, cliff instability and beach erosion at north and south of Lisbon.

The three days field trip to the Serra da Estrela is led by Gonçalo Vieira, Emanuel Castro and Fábio Loureiro. Participants will be taken to visit some of the Geopark's most inaccessible geosites and observe breathtaking landscapes during two hikes: one in the Zêzere valley and the other between Penhas Douradas and Lagoa Comprida. The different geosites to visit include features of glacial, periglacial, granite weathering, fluvial, hydrogeological, petrological and tectonic themes, and aspects related with the management of a UNESCO Global Geopark will be discussed.

The third three-days fieldtrip is destined to the northwestern part of Portugal and the Spanish region of Galicia. Guided by Alberto Gomes and Antonio Perez Alberti, will be mainly devoted to the coastal area and to the observation and discussion of issues related to coastal dynamics, marine terrace staircases, differential uplift of coastal blocks, coastal geoheritage, coastal geoarchaeology, coastal erosion and coastal land planning.

It is our expectation that these visits will please all participants and promote the scientific enrichment of all involved, allowing a better understanding of the topics covered in each one.

We also hope that this set of fieldtrip guidebooks can help in the understanding of the themes discussed and that they can be a testimony of the commitment and dedication shown by all the scientific responsible for the several visits, to whom the organizing committee of the International Conference on Geomorphology expresses its greatest recognition and gratitude.

have a good fieldtrip!

Lúcio José Sobral da Cunha
António Vieira

on behalf of the ICG2022 Organizing Committee

ITINERARY AND SCHEDULE

Itinerary

08:00 Departure from Coimbra (Largo D. Dinis) (Fig.1 and 2)

Stop 1 – Senhora do Espinheiro

Stop 2 – Sabugueiro/Covão do Urso Panorama

Stop 3 – Lagoa Comprida

Stop 4 – Salgadeiras

Stop 5 – Alto da Torre

Stop 6 – Covão do Boi

Stop 7 – Piornos

Stop 8 – Covão da Ametade

Stop 9 – Penhas Douradas

20:30 - Return to Coimbra



Figure 1. Serra da Estrela field trip itinerary.

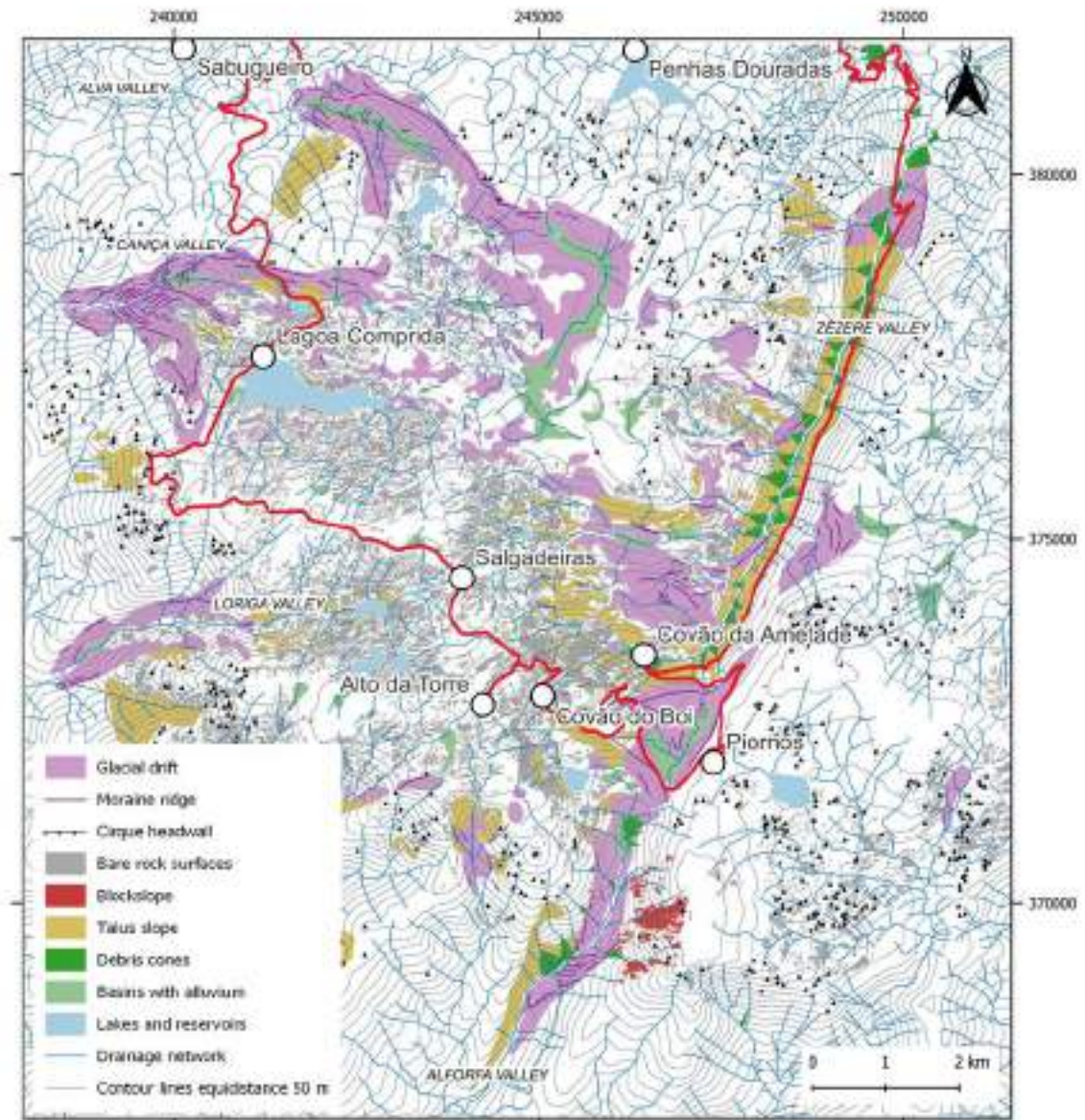


Figure 2. Geomorphology of the Serra da Estrela and main stops in the field trip (stop 1 not shown) (after Vieira, 2004).

1. The geology and geomorphology of the Serra da Estrela

1.1. Introduction

The Estrela UNESCO Global Geopark (Estrela UGGp) is located in Central Portugal and is part of the Iberian Central System, a mountain range that extends from Guadarrama, north of Madrid, to Montejunto, northeast of Lisbon. The Serra da Estrela is the highest mountain in mainland Portugal, rising to 1993 m a.s.l. at Alto da Torre, but the Estrela UGGp is a larger and encompassing area. Its boundaries include the major elements of the geology that contributed to the present-day landforms, but also to reflect how geology shaped the human nature of the Estrela inhabitants and the regional socio-economy (Fig. 3). The Estrela UGGp integrates the Estrela mountain range from its SW limits at the border with the Açor mountain, to the NE contact with the Meseta surface, as well as the piedmont regions that bound the Estrela to the NW and SE and where, for millennia humans lived in an intimate relationship with the mountain and with what it had to offer (Fig. 4).

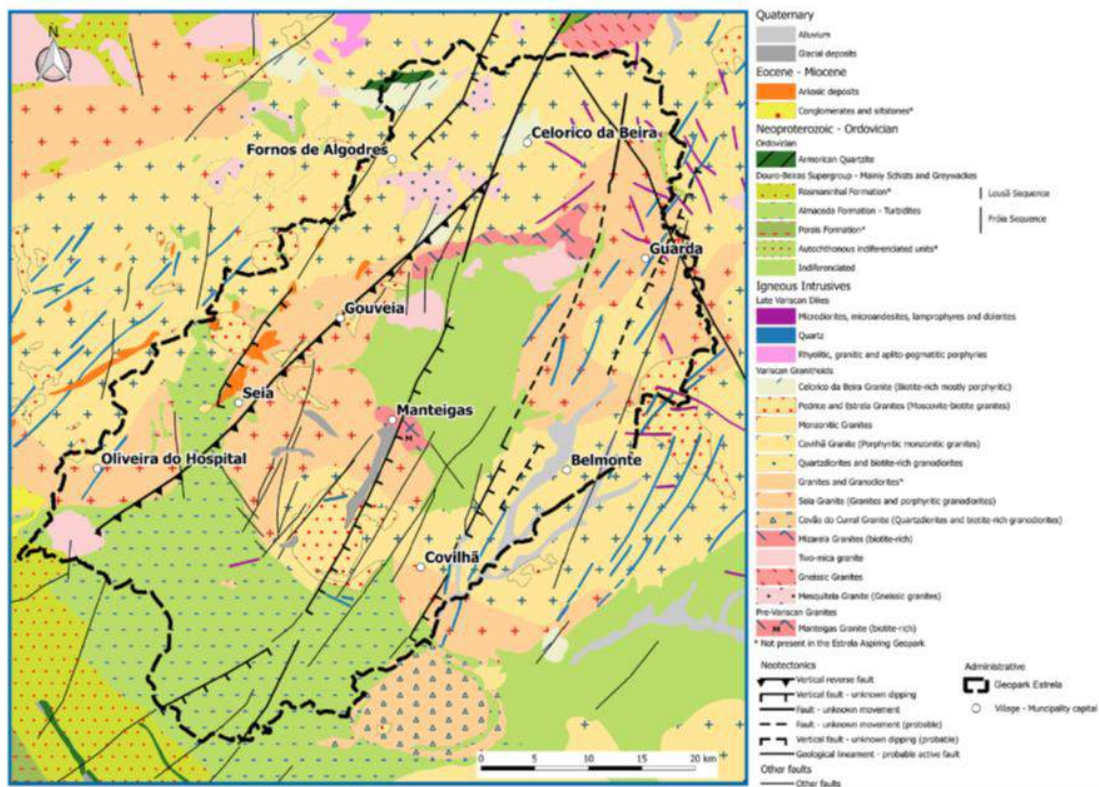


Figure 3. Geology of the Estrela UNESCO Global Geopark (based on Geological Map of Portugal 1:500.000).

The main geological originality of the Estrela UGGp is the breadth and richness of the Late Pleistocene glaciation(s) landforms and deposits, of high pedagogical and scenic values and with a remarkable scientific value, when considering the geographical

position at the SW limit of Europe. However, the glaciation and geodiversity of the Estrela UGGp would not have been possible without the peculiar long-term geological evolution from the distant past to the recent landscape evolution (Table I).

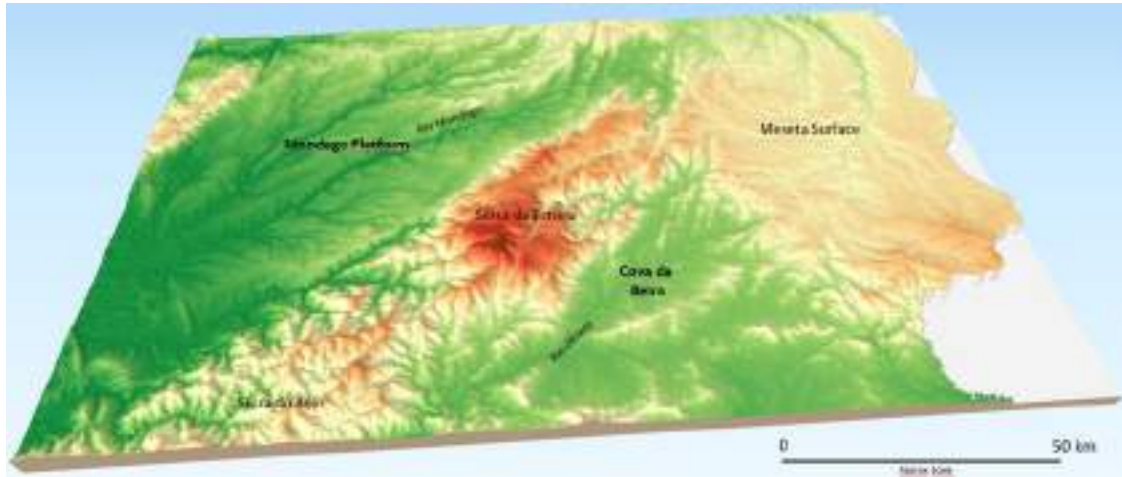


Figure 4. Overview of the Serra da Estrela topography from south to north. The Estrela rises to almost 2000 m asl and the Mondego platform averages 400-500 m asl.

1.2. The Variscan orogen heritage: a precursor of the present-day dynamics

After over 270 million years, the Variscan orogeny still shows a significant imprint in the geology of Western Iberia and jointly with the effects of Paleogene planation and Alpine tectonics, is responsible for the major features of the large-scale morphostructures and hence, for the major patterns of ecosystems, history and cultural heritage in Central Portugal.

The Estrela UGGp is located in the Central Iberian Zone (CIZ), which represents in the tectonic and paleogeographic zoning of the Iberian Peninsula, the axial zone of the Variscan orogen. This large scale orogen resulted from continental collision after the opening and subsequent closing of the Rheic and Paleothethys oceans (Ribeiro, 2013), within the context of a passage from an active continental margin (Late Precambrian) to a continental collision (Martínez-Catalán *et al.*, 2009). The resulting amalgamation of the continental masses of Laurentia, Baltica and Gondwana gave origin to the Pangea supercontinent.

In Iberia, the Variscan basement is named Iberian or Hesperian Massif and due to its paleogeographic setting is a key sector in the definition of the Palaeozoic peri-Atlantic orogens (Ribeiro, 2013). At the end of the Palaeozoic, Iberia occupied a position at the junction of the Appalachians (to the SW), the Caledonides (to the NW) and the Variscan (to the NE) (Martínez-Catalán *et al.*, 2009). Today, the Iberian Massif is present in most of the Western part of the Iberian Peninsula, with the tectono-stratigraphic model of Jullivert *et al.* (1974)(Fig. 5) dividing it into five broadly parallel zones following the Variscan structures:

- The Cantabrian and the South Portuguese zones are the external zones of the Iberian Variscan belt, with well-developed upper Palaeozoic sedimentary sequences, low-grade metamorphic and scarce sin-orogenic granite intrusions. The former is a Gondwanan overthrust foreland belt, while the later initially developed as a foredeep basin and later as an accretionary complex (Martínez-Catalán *et al.*, 2009).

Table I. Synthesis of the geological history of the Estrela UNESCO Global Geopark (EAG in the table) (AGE, 2017).

eon	era	Period	Epech	Age (Ma)	Wilson cycles	Paleogeography	Geoheritage phenomena in the EAG	
Phanerozoic	Cenozoic	Quaternary	Holocene	0.01 - today	Alpine Cycle	Fluvial erosion and slope processes (alluvial, colluvial, and debris cones), human action in the landscape, soil erosion.	Climate stability and recent human-induced climate change.	Alluvial and slope deposits.
			Pleistocene	2.6 - 0.01		Quaternary glaciations, uplift, sea-level change, fluvial erosion and stream piracy.	General cooling trend.	Glacial, fluvioglacial and periglacial deposits and landforms, active fault systems.
		Neogene	Pliocene	5.3 - 2.6		Beginning of incision of the present-day river system.	Hot climate with marked seasonality.	Formation of the main valley systems, piedmont deposition.
			Miocene	23 - 5.3		Reactivation of Variscan fault systems with main uplift of Estrela.		
		Paleogene		66 - 23		Beginning of the Alpine compression - reverse faulting. Erosion of the deep weathering mantles and retouching of the glanation surfaces.	Tropical climate with dry season.	Deposition of Arkosic clays. Planation surfaces and inselbergs.
	Mesozoic	Cretaceous		145 - 66		Opening of the Gulf of Gascony. Formation of the Iberian microplate.	No evidence in the EAG.	
		Jurassic		201 - 145		Opening of the Atlantic (Upper Jurassic). Fragmentation of the Pangea and basic volcanism with dolerites and lamprophyres.	Pre-Cretaceous glanation surface. Wet and warm climate with deep weathering and regolith formation.	Intrusion of apitic pegmatite and siliceous (quartz) veins.
		Triassic		252 - 201		Brittle deformation of the Variscan basement (faults NNE-SSW to ENE-WSW and NNW-SSC to NW-SE) formation of the basement.	Bragança - Vilaça - Mantegás fault and other lineaments.	
	Palaeozoic	Permian		299 - 252		Variscan Cycle	Erosion and full planation of the Variscan Belt with sedimentation in the Dúrcio-Beirão Carboniferous zone (Late Permian). D3 compressive phase (315-305 Ma) with Granite intrusions (310-290 Ma).	No evidence in the EAG. Contact metamorphic: hornfels and schists. Faults and folds in metasedimentary rocks. Most granite types of Serra da Estrela.
		Carboniferous		359 - 299			D2 extensional phase (335-315 Ma) with crustal thinning and exhumation with regional metamorphism. D1 compressive phase (360-350 Ma) with Barrovian.	Gneissic-migmatitic complex and Dúrcio Beirão metamorphic Supergroup.
		Devonian		419 - 359			Formation of the Parípea.	No evidence in the EAG.
		Silurian		443 - 419			Deposition of quartz sands in coastal environments. Granite intrusions.	Quartzites with Skolithos. Mantegás Granite.
		Ordovician		485 - 443			Sediment deposition in the Rheic and Paleotethys oceans.	Douro-Beiras Supergroup (SGC).
		Cambrian		541 - 485				
Proterozoic	Neoproterozoic			1000 - 541	Sediment deposition in marine environment, that will become the metasedimentary rocks.	Undifferentiated Neoproterozoic units of schists, greywackes, conglomerates and quartzite rocks.		
				2500 - 1000				
Archaean			4000 - 2500		First life forms on Earth.			
	Hadaic		4550 - 4000		Earth planet formation.			

- The West Asturian-Leonese, the Central Iberian and the Ossa-Morena zones, are the internal zones, with prevailing terrains of Pre-Cambrian and Lower Palaeozoic ages. In these zones, the Variscan deformation was stronger, while high-grade metamorphism is present and sin-orogenic granite plutons are frequent.

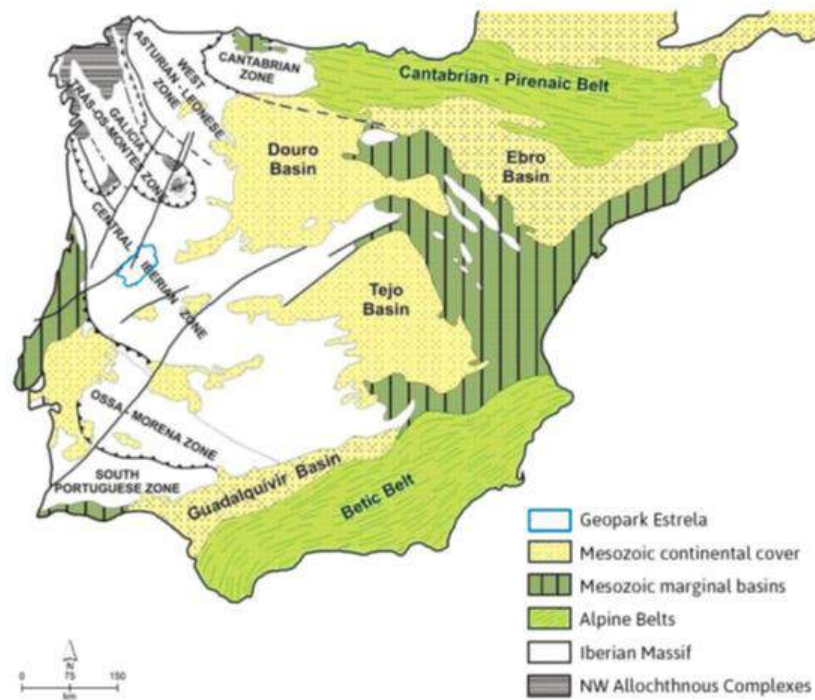


Figure 5. Tectonic and stratigraphic zoning of the Iberian Peninsula according to Julivert *et al.* 1974 (adapted from Santos and Tassinari, 2012).

1.3. The Pre-Ordovician autochthonous

The Central Iberian Zone, of special significance to the Estrela UGGp, extends from northwest to central Spain, covering most of the centre and north of Portugal and is ca. 400 km wide in the centre of the massif. Based in stratigraphic criteria and on the lithology of the autochthonous sequences underlying the Lower Ordovician quartzites, the CIZ is divided into (Martínez-Catalán *et al.*, 2009):

- The Schist-Greywacke Complex Domain (Complexo Xisto-Grauváquico, Carrington da Costa, 1950; Teixeira, 1955), a thick terrigenous sequence, currently named in Portugal the Douro-Beiras Supergroup, Sousa e Sequeira, 1987; Oliveira *et al.*, 1992). This sedimentary sequence from the Upper Precambrian to the Lower Cambrian is divided into the Douro (to the N) and the Beiras Groups (to the S), characterized as turbiditic lithofacies accumulated in two basins (Neiva *et al.*, 2013). The former shows calciturbitic occurrences and is probably upper Neoproterozoic to lower (middle?) Cambrian, while the latter is traditionally considered as monotonous non-carbonated deeper facies sequence dating from

the Neoproterozoic. Recent studies reported the existence of two distinct stratigraphic sequences bounded by a first rank unconformity (Meireles *et al.*, 2014), which is confirmed in the current 1:200.000 geological map of Portugal.

- The Ollo de Sapo Domain, a volcano-sedimentary complex, located to the N and NE of the CIZ.
- The Meridional allochthonous unit, composed by Upper Neoproterozoic to Lower Cambrian rocks with close relation to the Ossa-Morena Zone.

1.4. A wealth of granite intrusions at the late stages of the orogeny

The Variscan orogen was active in Iberia from the lower Devonian to the end of the Carboniferous and showed three major phases of deformation (D1, D2 and D3). The crustal thickening generated metamorphism and synorogenic magmatism, resulting in extensive formation of granitic rocks. Late and post-tectonic magmatism was widespread from 310 to 290 Ma, with the CIZ being the section of the European Variscan chain where granitic rocks show a wider diversity and outcrop in larger areas (Azevedo and Aguado, 2006).

The classical petrographical and geochemical classification for the granitoids of northwest Iberia groups the Variscan granites in two large categories (Capdevila and Floor, 1970; Capdevila *et al.*, 1973):

- Two mica granitoids related with migmatites and high-grade metamorphic terrains.
- Granodiorites and biotitic calc-alkaline granites (sin- and late-post-kinematic), frequently associated to mafic and intermediate igneous rocks.

Recent studies showed that the Variscan plutonism is associated with the last ductile deformation stage (D3). Hence, the Variscan granites can be divided into four groups [32]: pre-D3, sin-D3, late-D3 and post-D3. As for the scarce intrusions dating from the upper Proterozoic to the lower Palaeozoic, they are broadly classified as pre-Variscan [29] (Table II). Pre-D3 granites show similar characteristics to sin-D3 but are almost lacking in Portugal. Most of the large batholiths of peraluminous two-mica granites and leucogranites, as well as some granodiorite and biotitic granite masses are sin-D3 (320-310 Ma). The late-post-D3 granites (310-290 Ma) frequently form composite zoned massifs with contact metamorphism zones and are mainly non-deformed granodiorites and biotitic granites. They are low to moderate peraluminous, showing frequent association with basic and intermediate composition rocks. Intrusions of biotite-muscovite granites and two-mica granites, which are late- to post-D3 are also included in this group (Azevedo and Aguado, 2006).

Table II. Granites of the Estrela UNESCO Global Geopark following (Oliveira *et al.*, 1992) (* Not mapped at 1:500000 Geological map of Portugal).

Main granite types	Regional classification	Orogenic phase	
Porphyritic biotite granites	Celorico da Beira granite	late- to post-D3	Fragile fractures
Muscovite-biotite granites	Pedrice and Estrela granites	late to post-D3	Ductile shears
Monzonitic granites with megacrysts	-		
Porphyritic monzonitic granite	Covilhã granite		
Quartzdiorites and biotite granodiorites	-		
Granites and granodiorites	-	sin-D3 (intermediate series)	Ductile shears
Porphyritic granites and granodiorites	Seia granite		
Quartzdiorites and biotite granodiorites	Covão do Curral granite		
Biotite granodiorites	Mizarela granite	sin-D3 (early series)	Two-mica granitoids with xenoliths
Two-mica granites	-	sin-D3	
Granites and Migmatites*	-	sin-D3	
Gneissic granites	-	sin-D2	
Gneissic granites	Mesquitela granite	pre- to sin-D1	Two-mica granitoids with xenoliths
Ortogneisses and granites	Manteigas granite	pre-Variscan	

A large area of the Estrela UGGp is in the granitic batholith of the Beiras that intrudes metasediments from the Upper Proterozoic/Lower Cambrian to the Upper Carboniferous, which were variously affected by the polyphasic Variscan deformation (D1, D2 and D3). The tectono-magmatic evolution of the Beiras Batholith during the Variscan Orogeny showed the following phases (Azevedo and Aguado, 2006):

- Deformation phase D1 (~360-335 Ma), with a compressive regime inducing crustal thickening and Barrovian type metamorphism of the pre-Carboniferous metasediments, with partial crustal melting.
- Extensional phase D2 (~335-315 Ma) marked by a large-scale gravitational collapse, generating crustal thinning, exhumation of the orogen, which was the climax of the regional metamorphism with intense migmatization.
- Compressive phase D3 (~315-305 Ma), marked by significant crustal melting, which allowed for separation from the solid residuum. At this stage, peraluminous granite magmas (type-S) rose, suffered differentiation and consolidated, forming large two-mica leucogranite batholiths. Simultaneously, the lithospheric mantle,

separated from the crust inducing the ascension of basaltic magmas that intruded the interface crust-mantle in a process of underplating. This heat source induced the melting of the lower crust rocks and mixing and mingling of mantle and crustal magmas, generating I-S type magmas, forming calc-alkaline granodiorites and biotitic monzogranites (sin-D3). This pulse is present at the Estrela UGGp at the Maceira massif installed sin-cinematically at the Juzbado-Penalva do Castelo shear zone and is interpreted as evidence of the continuation of the tectonic exhumation. At the late D3 with the continuation of isostatic rebound and exhumation, the decompression of the asthenosphere generated basic magmas that hybridized with the molten felsic crust, forming calc-alkaline metaluminous to slightly peraluminous magmas. Their ascension occurred post-D3 generating the late-post-kinematic composite hybrid biotitic granite massifs of the Beiras batholith at 306 Ma. A period of ca. 20 Ma dominated by hydrothermal activity followed the deformation acting mainly along the major Variscan fault zones (Sant'Ovaia *et al.*, 2013).

Despite the Variscan age of most granitic rocks in the CIZ, the Manteigas granite, a medium to coarse-grained slightly porphyritic biotite granodiorite, outcropping in a small mass at the Estrela UGGp, is Ordovician (481.1 ± 5.9 Ma), hence completely unrelated with the Variscan Orogeny (Neiva *et al.*, 2009). This granite and the Mizarela granite are considered the same unit in the geological map of Portugal (Oliveira *et al.*, 1992), which was the base map for the Estrela UGGp. The current 1:200.000 map in the works, with the support of LNEG, will allow the differentiation of several of these lithologies.

1.5. The planation at the end of the Variscan cycle

The full cycle of the Variscan orogeny ended in the Late Permian with the planation of the mountain belt. This erosional phase is marked in continental sedimentation in intramontane basins such as the Dúrico-Beirão Carboniferous zone (Ferreira, 2005). This pre-Triassic planation surface is currently very deformed in Portugal, where it only occurs fossilized by Triassic sedimentation, while in Spain is still visible at the surface.

At the end of the orogenesis the Iberian Massif was affected by brittle tectonic deformation, giving origin to two main fault systems: an older set of NNE-SSW to ENE-WSW sinistral lateral strike-slip faults, and a younger set of NNW-SSE to NW-SE dextral lateral strike-slip faults. The former was much more significant for the subsequent geomorphological evolution in the Estrela UGGp (Ferreira, 2005), which reflects the changing tectonic and paleogeographical conditions following faulting at the end of the Variscan cycle.

In the Mesozoic, a new Wilson cycle started with rifting south and west of the present boundaries of the Iberian Massif initiating the breakup of Pangea. The stage lasted from

the Triassic to the Middle Jurassic, while a second stage associated with the opening of the Atlantic, started at the Upper Jurassic. The continuous formation of oceanic lithosphere west of Iberia and the opening of the Gulf of Gascony induced the anticlockwise rotation of Iberia, forming the Iberian microplate in the Lower Cretaceous (Ribeiro, 2013).

The current relief of the Estrela UGGp is mainly a result of the evolution since the Paleogene and particularly of the interplay between climate and tectonics, controlled by the Variscan structures. During large part of the Jurassic, the western part of the Iberian Massif was subject to intense chemical and biochemical weathering in a warm and wet climate, generating thick regoliths and the deposition of carbonates in the continental margin (Ferreira, 2005). These conditions lasted until the end of the Mesozoic (Martin-Serrano, 1988), with the deep weathering probably being the cause for the pre-Cretaceous planation surface, as an etch surface. Following tectonic activity and lasting until the Middle Tortonian (Pais *et al.*, 2012), climate changed to a tropical climate with dry season, and an erosional regime installed, removing the weathering mantles (Ferreira, 2005).

The pre-Cretaceous surface was retouched during the Paleogene and gave origin to subsequent planation surfaces that are key geomorphological features of the Iberian Massif today, with the oldest correlative deposits being the Coja arkoses (Upper Eocene). These deposits cover patches of the Paleogene planation surface, which is present from northern to southern Portugal and from which the main present-day mountains in the Iberian Massif developed. In the Estrela UGGp, these Paleogene deposits occur in the NW piedmont, mainly in the Seia-Pinhanços graben where they were protected from erosion.

Planation surfaces are divided in two major types (Ferreira, 1978, 2005): i. polygenic surfaces formed in tectonically stable areas, where deformation was consistently planated by prevailing erosional processes, and ii. stepped surfaces, where deformation was stronger and the various planation phases did not fully erode the newly formed relief, resulting in several planation surfaces forming at lower positions.

Polygenic surfaces are well represented in the Iberian Massif, with good examples being the Meseta Surface and the Mondego Platform, while stepped surfaces are also frequent, for example in the Central Portuguese Plateaux in the northern edge of the Estrela UGGp (Ferreira, 1978, 1991). Stepped surfaces prevail to the north of the Estrela UGGp, where uplift has been stronger, while polygenic surfaces prevail to the south, such as is the case of the Castelo Branco Surface (Ribeiro, 1949) in the Naturtejo Geopark or the Baixo Alentejo Penplain (Feio, 1952). The planation surfaces, especially to the south of the Serra da Estrela, show some good examples of residual reliefs (inselbergs) such as the Belmonte inselberg at the Estrela UGGp.

1.6. Collision with Africa and the rise of a new mountain

Regional compression in the Oligocene caused by the collision with the African plate initiated crustal shortening and rejuvenation of the Variscan tectonic structures (De Vicente and Vegas, 2009). One of the main features uplifting from the Central Iberian Zone Paleogene planation surface was the Iberian Central System (Cordilheira Central in Portugal), taking place possibly from the Middle to Upper Miocene (Martin-Gonzalez, 2009). Some authors, consider that the westernmost part of the Iberian Massif maintained continuous uplift during the whole Cainozoic (De Vicente *et al.*, 2007), while others place the peak of the Alpine compression in the Portuguese mainland in the Tortonian (Pais *et al.*, 2012, Cunha *et al.*, 2000). These changes were drastic for the continental topography of Iberia, which had an elevation close to the sea-level until the end of the Cretaceous [Cunha and Pena dos Reis, 1995; Dinis *et al.*, 2008) and suffered a general uplift of the planation surface between 100 and 600 m (De Vicente *et al.*, 2011).

During the so-called Alpine compression, several fault directions were reactivated: i. NE-SW to ENE-WSW oriented, as thrusts, ii. NNE-SSW, as sinistral strike-slip faults, and iii. NW-SE, as dextral strike-slip faults (Pais *et al.*, 2012). Thrusts controlled the uplift of the Central System, since they were reactivated as reverse faults. South of the Central System, the SE-verging and NW-dipping Ponsul fault flattens at depth while converging with the Seia-Lousã fault that is NW-verging and SE-dipping and located in the north (Fig. 6). The result was the formation of a large horst uplifting as a pop-up structure along a system of parallel faults (Ribeiro *et al.*, 1990). A whole section of the planation surface was displaced and is still visible in the summits of the Estrela forming a plateau, which dips slightly to the northeast, but which is well-preserved in granites. This plateau is quintessential for the Pleistocene evolution of the Estrela, due to its controls on climate and snow regime, influencing the glaciation style, dynamics and geomorphological features, key elements of the Estrela UGGp.

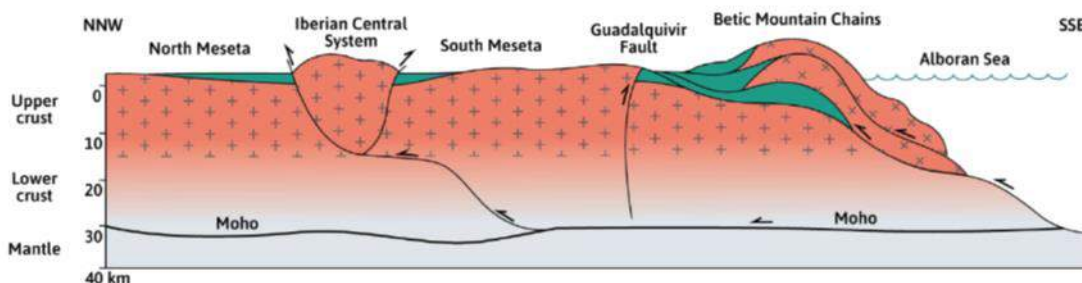


Figure 6. Schematic cross-section showing the pop-up structure of the Iberian Central System following the reactivation of Variscan faults (adapted from Ribeiro 1988).

The strike-slip fault systems show predominantly horizontal displacements that weakened the basement rocks, enabling differential erosion to carve long, deep and

linear valleys, especially where the faults affect granites. One of such examples is the 250 km long Bragança-Vilariça-Manteigas fault (BVMF) that cross-cuts the Estrela along a NNE-SSW direction giving origin to the valleys of the Zêzere and Alforfa (Daveau, 1969, Migon and Vieira, 2014) (Fig. 7). The BVMF also suffered a vertical component in the deformation that displaced the upper Estrela plateaus by about 150-200 m (Ribeiro *et al.*, 1990).

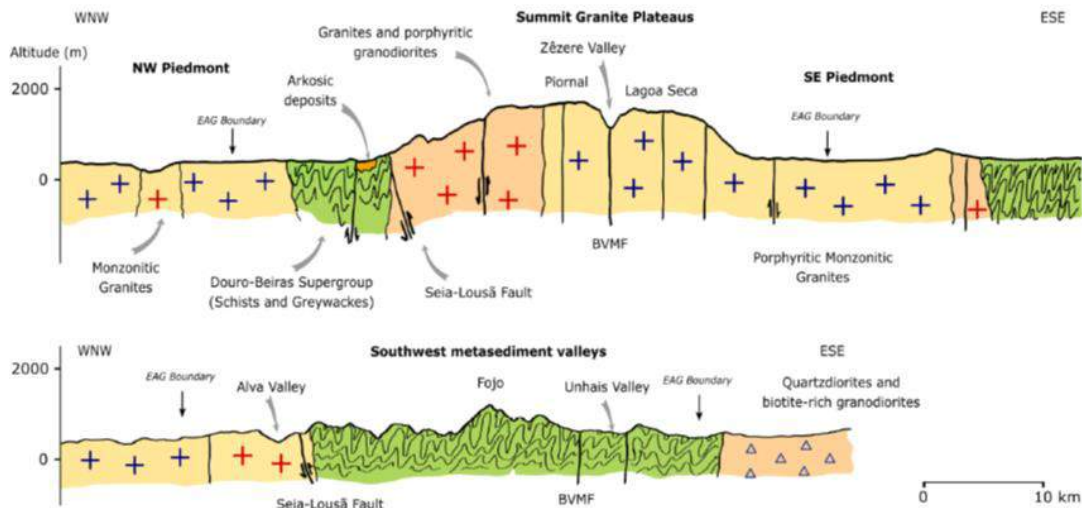


Figure 7. Simplified geological cross-sections of the Estrela UNESCO Global Geopark showing the controls of tectonics and rock type on morphology (base data from the Geological map of Portugal 1:500.000).

1.7. Towards the present-day relief organization

The Late Miocene and the Zanclean were characterized by a hot climate with marked seasonality, resulting in sedimentation occurring mainly at the foot of the fault scarps (Pais *et al.*, 2012). At the time, the main fluvial systems were endorheic draining into the interior of Iberia. In the Piacenzian the climate became hot and very wet and an exorheic fluvial network developed, with broad valleys developing in the mountains and numerous catchments forming in endorheic inland basins. In the Upper Pleistocene, the climate became colder and the continuing uplift and sea-level changes promoted a strong fluvial incision, regressive erosion and stream piracy (Pais *et al.*, 2012), defining the landform organization in Central Portugal and in the Estrela UGGp.

The tectonic deformation continued during the Quaternary with vertical movements resulting both from large scale folding and isostatic adjustments, and from active faulting. Inferred uplift rates for the last 3 Ma are of 0.1-0.2 mm/yr, with the largest deformation occurring in the centre and north of Portugal, with the Estrela UGGp territory showing values of up to 600 m, especially in the higher parts of the Estrela (Cabral, 2012; Rockwell *et al.*, 2009). Active faulting shows a predominance of ~E-W to NE-SW faults with reverse component and left-lateral strike-slip faults ~N-S to NNE-SSW.

The Seia-Lousã fault that bounds the Serra da Estrela in the north is an example of the former, while the BVMF fault is an example of the later.

The long-term geological evolution explains the general organization of the landforms in the Estrela UGGp, with the important control exerted by Alpine tectonics over reactivated Variscan faults, which generated the segmentation of the Paleogene planation indifferent steps up to the summit of the mountain (Fig. 8). One of the main geomorphological differences within the Estrela UGGp is the contrast between granites and the shales, schists and greywackes (Ribeiro, 1954; Daveau, 1969). Granite terrains show typically well-preserved remnants of the planation surfaces, both in the summit areas and in steps and erosional terraces. The valleys are rectilinear, with sharp bends, reflecting the tectonic control. On the other hand, metasedimentary terrains show sharp ridges and a dense drainage network, with scarce remnants of planation surfaces and deeply incised meandering valleys.

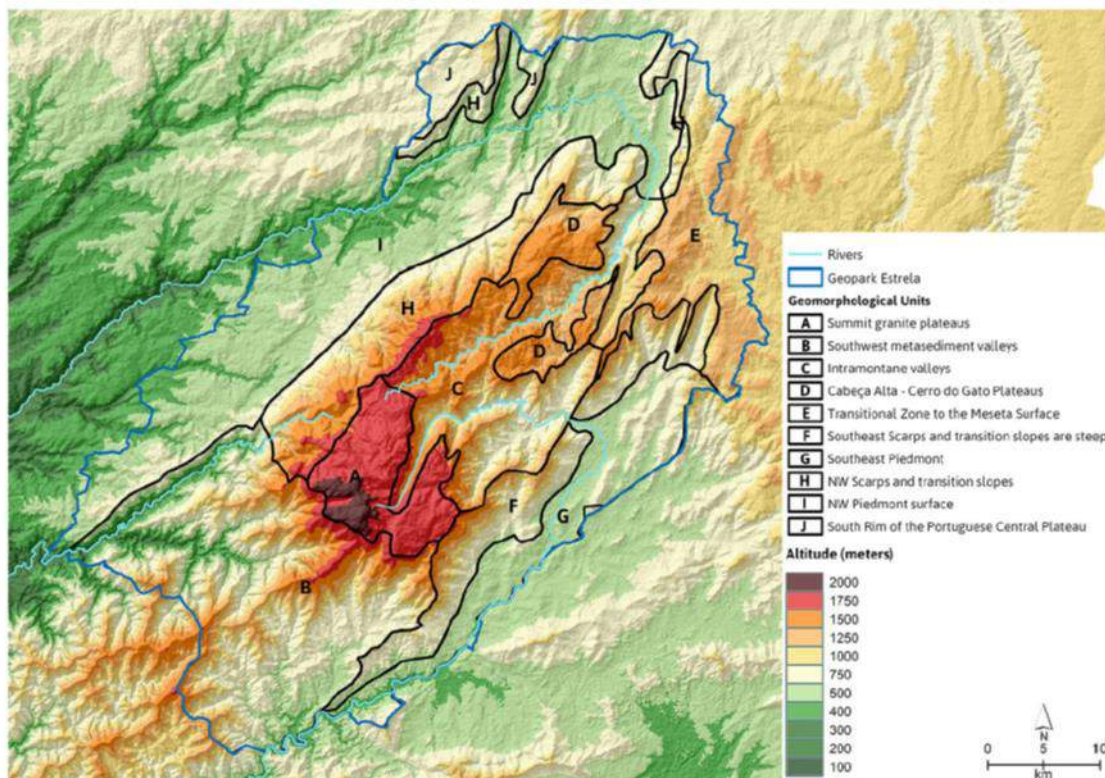


Figure 8. Geomorphological units of the Estrela UNESCO Global Geopark.

1.8. The richness of granite types and the diversity of landforms

The richness of the Estrela UGGp in granite types (Table II) with different geochemistry, age and tectonic history has allowed researchers to dig deeper into rock control on the granite geomorphology across different spatial scales. Such a granite diversity within a small area facing similar climate conditions makes the Estrela unique for assessing the effects of rock control on landforms (Migon and Vieira, 2014). Differences in granite

texture were shown to exert a major control on the occurrence of relict periglacial phenomena (Vieira, 2004), an observation with important impacts for paleoenvironmental reconstruction in granite terrains. At similar topographical settings, fine-grained granite variants show the development of blockfield and blockslopes, while coarse-grained granites show evidence of granular weathering, generating stratified slope deposits instead. Granite types also result in different tor morphologies (Migon and Vieira, 2014) (Fig. 9).



Figure 9. Examples of granite landforms in the Estrela Geopark: A. Fraga das Penhas tor and castle-koppie, B. Penedo do Sino pedestal rock, C. Terroeiro.

Although tors are not unique to the Estrela UGGp they provide, together with other granite landforms, an excellent setting for research. In the Estrela plateaus, the interplay between long-term weathering in different granite variants and the Late Pleistocene glaciation, generated important landscape differences, as well as a good dating framework. Lautensach (1929) noted that tor distribution in the Estrela showed clearly the controls of glacial erosion, with tors almost completely absent within the Pleistocene glacier boundaries. Vieira (2004) mapped over 600 tors in the plateaus confirming Lautensach's observations. However, tors were also found within the glacial limits, such as is the case of the Covão do Boi columns or the tors at the upper Candieira catchment. These formed by post-glacial erosion of the granite weathering mantle which survived under the Pleistocene glaciers (Ferreira and Vieira, 1999; Vieira, 2004). In fact, the singularity of the geomorphological setting and evolution of the Covão do Boi area, makes it one of the key geosites of international significance at the Estrela UGGp.

1.9. The originality of the last glaciation in the Serra da Estrela

a) History of research

Evidence of a glaciation at the Estrela UGGp was mentioned for the first time in 1884 by Cabral in a study about glaciations in Portugal. According to Lautensach (1929), Penck, also in 1884, had pointed evidence of glaciations in the Central System, both in Estrela and Guadarrama. In 1916, Fleury worked on Cabral's observations and described the general features of the Estrela glaciation. However, the first systematic scientific analysis of the Estrela glaciation was only made in 1929 by Hermann Lautensach, a German

geographer that spent three months in area in 1927 and 1928. He identified several features of the glaciation and mapped glacier extent and thickness. Following this work and for almost four decades, the Estrela glaciation did not attract new research, until the important paper by Suzanne Daveau in 1971 – “La glaciation de la Serra da Estrela”. Daveau added up to previous works based on better topographic maps, on field work and on systematic aerial photo interpretation. Most of the results of Daveau’s mapping are still valid today, especially in what concerns to the glacial extent outside the Zêzere valley. In the mid-1990’s, Gonçalo Vieira continued Daveau’s research and in the framework of a doctoral dissertation, using GIS, aerial photography, digital high resolution orthophotos and sedimentological analysis, supported by field work, presented the current view of the Estrela glaciation (Fig. 10). After the works of Vieira [2004, 2008), research on the glaciation has been more sporadic and deeply affected by research funding shortage. The implementation of the Estrela UGGp has resulted in increased research in the Estrela, with several recent publications and projects (Nieuwendam *et al.*, 2020; Santos *et al.*, 2020; Vieira *et al.*, 2020, 2021; Vieira and Woronko, 2021; Raab *et al.*, 2022).

b) Characteristics of the glaciation

Contrary to other mountains in Portugal, such as the Gerês and Peneda, where the glaciation generated controversies that lasted for decades (Ferreira, 1993), the glaciation of the Serra da Estrela shows widespread clear glacial geoheritage, of high scenic, pedagogical and scientific significance. For example, the remarkable U-shaped Zêzere valley has been frequently used in national and international scientific publications and is a text book example of a glacial trough.

The glaciation style of the Estrela is a result of both: i. its geographical setting in the western margin of Iberia, being the first mountain to affect the inland movement of the moist Atlantic air masses, but also, ii. of the altitude of the plateau between 1400 and ~2000 m. This altitudinal range, just above the paleo-equilibrium line altitude (ELA) of ~1650 m for the last maximum glacial extent, was perfect for the development of the Late Pleistocene glaciers (Vieira, 2008). The western plateau was especially significant for the glaciation and very sensitive to snow accumulation (as it is today) and hence to glacial inception. This is because once the ELA descends below the plateau surface, a very large accumulation area develops, providing enough ice mass for an ice-field to form. Since several valleys radiate from the plateau, conditions existed for ice streams to channel into valley glaciers (e.g. Zêzere, Alforfa, Alvoco, Loriga, Caniça and Covão do Urso).

However, the plateau also induces a large sensitivity for glacial retreat. A decrease in winter precipitation or an increase in summer ablation, with a resulting increase in the ELA, show rapid impacts in glacier mass balance, inducing the fast starvation of the valley glaciers and of the plateau ice-field. Hence, the Estrela has functioned in the

Pleistocene cold phases has a perfect « barometer » for climate variability in Western Iberia. On the contrary, if it would be a ridge style mountain (as most Alpine and Iberian mountains), it wouldn't show this behaviour that makes it unique.

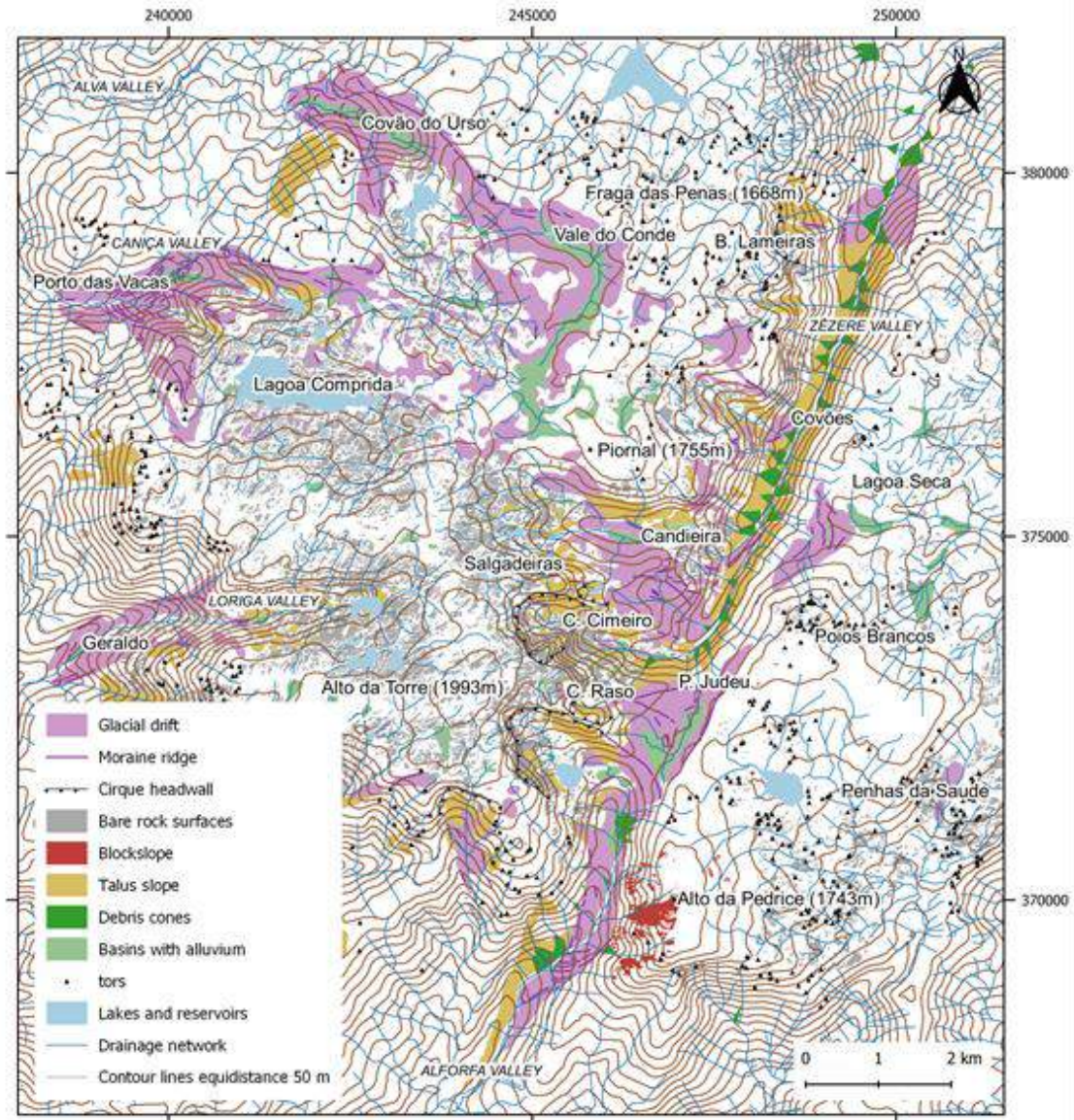


Figure 10. Main features of the glacial and periglacial geomorphology of the Serra da Estrela (after Vieira, 2004).

The Last Maximum of the Glaciation of the Serra da Estrela (LMGSE) was initially dated using thermoluminescence of fluvio-glacial sediments from the Lagoa Seca at ~30 ka BP (Fig. 11, Vieira, 2004). More recent cosmogenic isotope exposure dating from moraine boulders at the same site, support a similar age (Vieira *et al.*, 2021). This shows that the LMGSE pre-dates the LGM, a fact also supported by glacial evidence from southwest Europe and Iberia, showing that the LGM was probably cold and dry in Iberia, thus generating glacier recession.



Figure 11. The Lagoa Seca intermoraine basin and moraine ridges.

At the LMGSE, the western plateau of the Estrela had a plateau ice-field with several valley glaciers, from which the Zêzere glacier, ending close to the village of Manteigas, was the longest, with 11.3 km. The ice-field and glaciers were 66 km², with about 90 m ice thickness at the Alto da Torre and with ice thickness reaching 340 m at the Zêzere glacier (Vieira, 2008).

Glaciers left clear erosional marks in the extensive bare granite outcrops of the western plateau and valley heads, originating diverse glacial landforms, such as roches moutonnées, polished surfaces, grooves and striations (e.g. Salgadeiras and Lagoa Comprida). The contact zones between the western plateau and the main glacial valleys are marked by steep and deep cirques, especially in the eastern side, where snow accumulation was favoured by the prevailing west-winds. The best examples, are the Covão do Ferro and Covão Cimeiro, which are over 1 km wide, 240 to 290 m deep.

The glacial valleys of the Estrela show steep slopes and frequently U-shape cross-section, with the most typical being the Zêzere valley. Overdeepenings occur especially above the paleo-ELA and are infilled by post-glacial deposits that are a mixture of moraine boulders, rockfalls and sandy-gravels washed from the slope taluses. Organic sediments from overdeepenings in the plateau and at Charco da Candieira enabled the paleoenvironmental reconstruction since 14.8 ka BP. Peaks rising above the glacier surface where the ice-field drained into the Zêzere and Alforfa valleys, with nunataks at the Cântaros (pots) Gordo (fat), Raso (flat) and Magro (thin) and Piornal.

Moraines are widespread in the Estrela UGGp, occurring both along the glacial valleys and in several sectors of the western plateau (Lagoa Comprida and Vale do Conde), away from the dispersion centres of the ice-field. Most moraines are composed of large boulders (1 to over 5 m), lying on a coarse sandy-gravelly-bouldery deformation till. Most moraines show the effects of post-glacial runoff that eroded fines, sands and gravels.

Four types of moraines occur in the Estrela UGGp: i. lateral moraines, present along the larger valleys, with the best examples at Covão do Urso (4 km long), Covão Grande and Nave de Santo António, ii. Latero-frontal moraines, close to the terminus of the main valley glaciers (e.g. Manteigas and Alforfa), iii. Recessional moraine groups, present in most valleys as a series of frontal moraines, forming sets of up to 12 ridges (Caniça, Nave Travessa, Alforfa, Loriga and Lagoa Seca), iv. Marginal moraine complexes (Vale do Conde and Teleférico moraine at Nave de Santo António), and v. Sparse moraine covers, normally below 1650 m and without ridges (e.g. Lagoa Comprida, Azimbres, Vale do Conde).

Till exposures occur at the Estrela UGGp, but due to the mountain setting, limited number of outcrops and fast shrub growth, most are not easily to observe. Key outcrops such as the Cerro Rebolado flow till at the northern margin of the plateau ice-field, the Alforfa lodgement and flow tills, and the Lagoa Seca lodgement and flow tills, are excellent examples of mountain tills and of the wet-based dynamics of the glacial environment. The analysis of quartz grains from the later provided evidence that subglacial transport and erosion mobilised grains that had previously evolved in the regolith, controlled by chemical weathering (Vieira, 2004). This supports Daveau's interpretation for the saprolitic origin of the very large rounded boulders, so typical of the Estrela moraines. Such saprolites are still visible at some sites outside the glaciated area, even in the highest parts of the mountain.

Kame terraces that allow to infer the paleo valley glacier position are present in many valleys and their relation to human occupation is noteworthy, being typically used for agriculture, due to their gentle sloping surfaces, soil development and water availability.

Fluvioglacial terraces occur in Manteigas, Unhais da Serra, Alvoco and in the Alva valleys, being formed by decametric sub-rounded boulders, gravels and coarse sands, poorly stratified and forming terraces (used for agriculture and more recently to urban settlements) a few meters above the current valley floor. Three terrace generations occur in Manteigas, with a post-glacial fluvial incision of about 6 to 8 m. Fluvioglacial deposits in filling the intermorainic depression of Lagoa Seca allowed to identify the age of the last maximum glacial extent in the Estrela (Vieira, 2004).

But the glacial geoheritage of the Estrela UGGp is not limited to the LMGSE, as evidence shows ages from an earlier glacial (Vieira, 2004, 2021). At Penhas da Saúde the micromorphological analysis of a diamicton showed the presence of probably subglacial deformation microstructures. The lack of clear landforms associated to glacial erosion in the area, suggest a pre-LMGSE age for the deposit. At the Cântaro Raso and Barroca das Lameiras, linear accumulations of boulders without matrix have been interpreted as possible earlier moraines. At the Lagoa Seca, the most external of five moraine ridges, showing deeper weathering pits than the three internal ridges, was recently dated using ^{36}Cl , providing minimum ages of 138.9 ± 14.1 to 146.7 ± 17.8 ka, supporting a pre-Weichselian age (Vieira *et al.*, 2021).

c) Chronology

The following main stages in the Estrela glaciation may be (Vieira, 2004; Vieira *et al.*, 2021):

- The external stage, oldest and pre-Weichselian (c. 140 ka), without clear glacial landforms, but identified based on the presence of sectors of large boulders interpreted as moraines, on the till of Penhas da Saúde and with absolute age datings.
- The Last Maximum of the Serra da Estrela Glaciation (LMGSE), corresponding to the maximum extent of the glaciers, as seen in well-preserved moraine features and kame terraces (c. 30 ka BP).
- The Internal stage 1, marked by numerous moraine ridge complexes in the valleys in positions inside the LMGSE maximum.
- The Internal stage 2, identifiable at some latero-frontal moraines in the Zêzere and Alforfa valleys.
- The deglaciation of the plateau at the Bølling-Allerød Interstadial (14.6–12.9 ka).

Contrary to other mountains in Iberia, at the Estrela UGGp moraines close to or inside the glacial cirques are very scarce. This fact should be related to the style of deglaciation associated to the plateau ice-field, which given a rise in the ELA would have quickly been affected by an ablation regime in a large area, inducing ice-stagnation in the valleys and areolar melting resulting in abandoned bodies of dead-ice. These condition would have seen limited erosion in the cirques and consequently, no significant moraine deposits.

d) The Periglaciation

The significance of relict periglacial phenomena in the Estrela UGGp area was reported for the first time by Daveau (1973, 1978) that described the Pedrice blockslope, stratified slope deposits and screes in the Zêzere Valley and showed that frost action played a role in Late Pleistocene morphogenesis. Since most phenomena occurred outside the glaciated area and very few inside it, they should be, at least, synchronous to the LMGSE or older. More recently, Vieira (2004) presented a systematic survey and analysis of the periglacial deposits and landforms and identified a wider relict periglacial activity in Estrela, with block fields, stone-banked solifluction lobes, head-type, stratified slope deposits and debris-flow deposits. Traces of permafrost action, possibly of Late Pleistocene age are present in lamellar structures in slope deposits above 1200 m (Vieira, 2004; Nieuwendam *et al.*, 2019; Vieira and Nieuwendam, 2020), together with other features, such as a bouldery accumulation interpreted as a paleorockglacier at Alforfa.

1.10. Postglacial evolution

The Charco da Candieira deposits from the Candieira valley at 1409 m offer a good insight into the paleoenvironmental evolution of the Estrela UGGp since about 14.8 ka BP (Van den Brink and Janssen, 1985; Vand der Knaap and Van Leeuwen, 1997):

- At 14.8 ka BP glaciers were still present at the upper areas of the catchment.
- Until the Younger Dryas, climate conditions varied, with altitudinal shifting of the periglacial zone, which was more active in the Bølling and in the Younger Dryas, with open grassland formations. Between both these stadials, in warmer and wetter conditions, open woodlands occupied the valleys.
- At the onset of the Holocene, open woodlands expanded in the mountain and Quercus forests colonized the lower valleys.
- Around 7.6 ka BP Cerealia pollen increased and the forest became less dense. At 5.6 ka BP humans became the main driving force on forest dynamics.
- At 3.3 ka BP large-scale deforestation took place, first at 1400 m, climbing to 1750 m at 2.8 ka BP.
- Subsequent phases reflected successive waves of deforestation, especially at 0.8 and 0.6 ka BP, culminating at 0.34 BP with increased soil erosion.

2. Itinerary description

Stop 1. Senhora do Espinheiro

General geological and geomorphological setting, planation surfaces, regional tectonics.

The Senhora do Espinheiro area allows for an excellent observation over the Mondego platform to the northwest, and its contact with the Serra da Estrela, allowing for an understanding of the main regional geomorphological features of Central Portugal. The contact with the Serra da Estrela is a fault scarp associated to the Lousã-Seia fault, along which the range has uplifted.

Stop 2. Sabugueiro/Covão do Urso Panorama

Glaciated vs non-glaciated landscape. Introduction to the Estrela glaciation. Lateral moraine of Covão do Urso and northwest limit of the plateau ice-field.

The viewpoint allows to analyse northwest sector of the plateau ice-field and the contrast between the Late Pleistocene glaciated and non-glaciated landscape. The stop is located in the non-glaciated area, where a typical granite weathering morphology prevails, with the widespread presence of boulders and tors in convex locations. Towards the southeast, the Covão do Urso valley drained the plateau ice-field, with a glacier flowing to close to the village of Sabugueiro. A 4 km long lateral moraine is visible

in the north interfluvium of the valley, continuing up to the Vale do Conde in the plateau. Several lateral and frontal moraine ridges occur along the valley floor. This area is currently being mapped using drones and sampled for cosmogenic isotope exposure dating in a collaboration between the universities of Lisbon (G. Vieira) and Zurich (M. Egli).

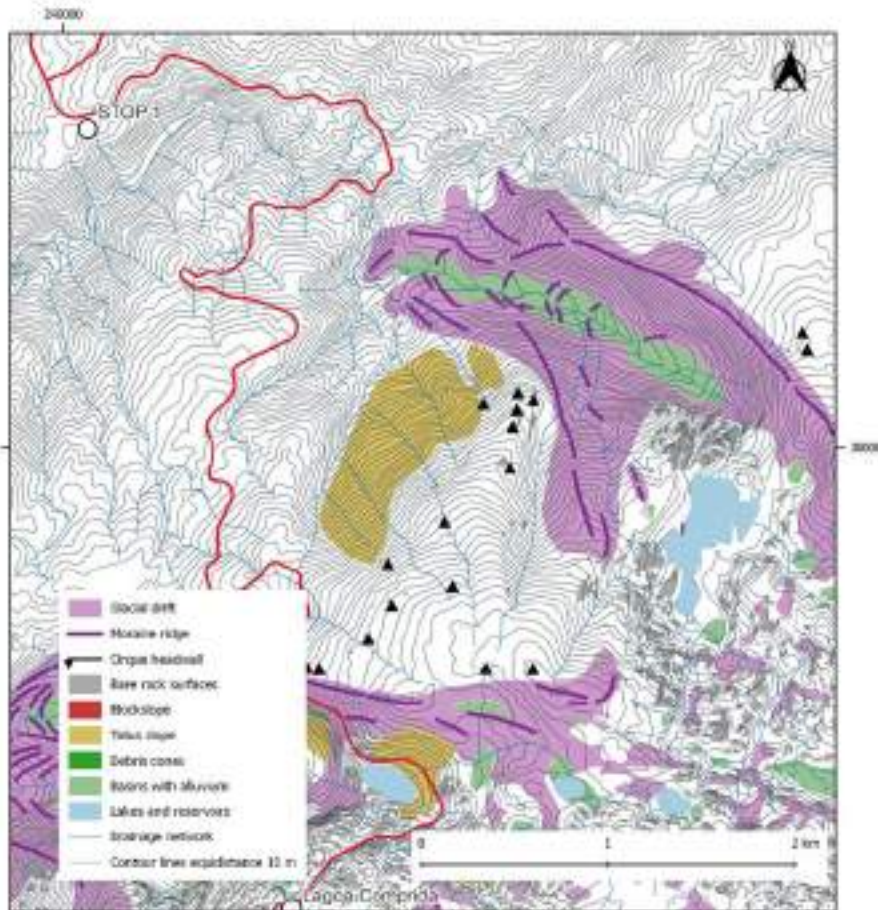


Figure 12. Main features of the glacial geomorphology of the Covão do Urso (adapted from Vieira 2004).

Stop 3. Lagoa Comprida (short walk)

Plateau ice-field, glacial erosion, glacial cirques and valleys, moraine boulders, erratics, roches moutonnées.

This is one of the geosites that best exemplifies glacial erosion in Serra da Estrela, with extensive glacial polished surfaces, overdeepenings, erratic boulders and roches moutonnées. The short walk allows for a first insight into the glacial erosion area of the plateau and for assessing the impacts of the plateau ice-field in sloping terrain, followed by the flow constrained by the valleys that drain the plateau.

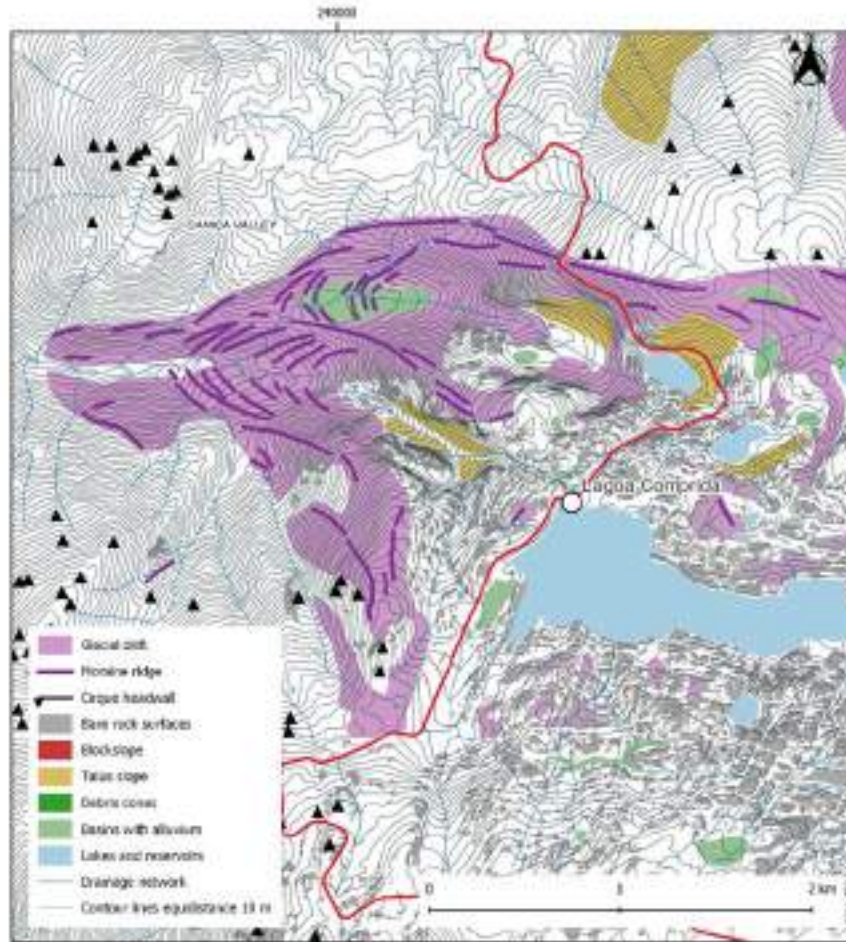


Figure 13. Main features of the glacial geomorphology of the Lagoa Comprida (adapted from Vieira 2004).

Stop 4. Salgadeiras – Lagoas do Covão da Clareza

Plateau ice-field, glacial erosion, hanging valleys, overdeepenings, deglaciation, Holocene evolution of the Serra da Estrela.

The Salgadeiras - Lagoas do Covão da Clareza area at c. 1800 m a.s.l. shows a typical landscape of glacial erosion in the plateau, resembling a Scandinavian fjell. The area shows extensively glacially scoured granite outcrops, marked by overdeepenings with numerous small ponds and lakes, which provide valuable sedimentary archives of the postglacial evolution of the Estrela. The area is also part of the biogenetic reserve and part of the Natura 2000 network and protected as a RAMSAR site.

The deglaciation of the Salgadeiras has occurred after 14.2 ka (Vieira *et al.*, 2021), with glacierets possibly surviving in niches for longer. New rock samples from polished rock outcrops and a small moraine in the Salgadeiras are currently under investigation for cosmogenic isotope exposure dating (Vieira and Egli).

The Holocene evolution of the Serra da Estrela has been studied from a 14 m core from the Charco da Candieira at 1,410 m a.s.l. with the reconstruction of the

paleoenvironmental conditions after c. 14.8 ka (Van der Knaap and Van Leeuwen, 1997). More recently, within the project HOLMODRIVE, an international team lead by the University of Lisbon, has been analyzing new sediment cores from Lagoa do Peixão between the Charco da Candieira and Salgadeiras, at c. 1,660 m a.s.l.

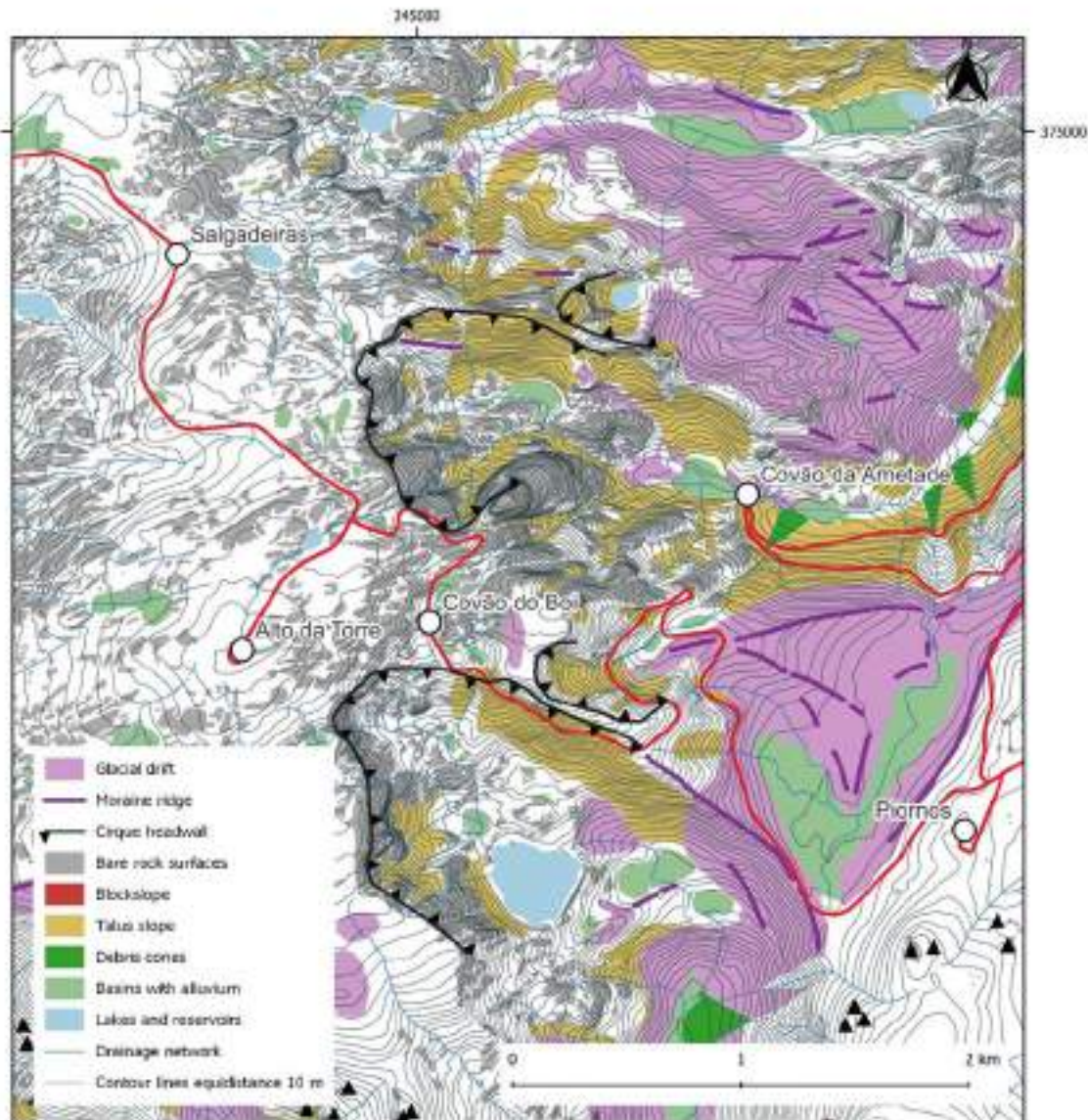


Figure 14. Main features of the glacial geomorphology of the Alto da Torre and its surroundings (adapted from Vieira 2004).

Stop 5. Alto da Torre

Elevated planation surfaces. Panorama to the Central Iberian Cordillera.

The Western Plateau with an elevation rising from about 1,500 m in the north, at Penhas Douradas, to 1993 m at Alto da Torre, is the highest summit in mainland Portugal. The area is the highest remnant of the uplifted Paleogene planation surface, which has been stripped by erosion and still preserves wide flat areas, interrupted by several steps.

These are controlled by tectonics, as well as lithology. Overall in the Estrela, the differences between the metasedimentary (schists, greywackes, shales) and the granites, prevail. Wide plateaus and rectilinear valleys have developed in the latter, while the former have generated narrow linear interfluves, deeply dissected by v-shaped and irregular valley, with a dense river network and meanders. In the plateaus, the different granite-types, together with tectonics, gave origin to the different in the landscape (Migon and Vieira, 2014).



Figure 15. The Alto da Torre plateau viewed towards the north.

Stop 6. Covão do Boi and Cântaro Raso

Granite columns, glacial and post-glacial erosion, glacial evolution of the Zêzere valley, the Lagoa Seca col, Pre-Weichselian glacial evidence.

At 1,840 m a.s.l., between the Alto da Torre, the glacial cirque of Covão do Ferro, the Zêzere glacial valley and the Cântaro Raso, a small, but very relevant col shows up - the Covão do Boi. In this remarkable geosite, we find a set of granite columns, with diameters of 2 to 5 m and between 4 and 8 m in height, constituting a rare set of landforms. Before they surfaced, the granite columns were shaped under the surface due to the deep weathering of the granite, along a dense orthogonal joint network, that formed a thick weathering mantle. During the last glaciation the col was razed by glacial erosion that removed part of the weathering mantle and cut the top of fresh granite corestones. Following glacial retreat, water erosion continued the removal of the weathering mantle and the granite columns started to form at the surface. These granite columns are locally called cheese-piles, because they resemble, in a nutshell, the form of a stack of typical Serra da Estrela cheeses. The granite columns have been sampled

for cosmogenic isotope exposure dating in 2020, confirming the postglacial age of the columns, and a manuscript is currently in preparation by Raab and colleagues.



Figure 16. Granite columns of Covão do Boi.

Stop 7. Piornos

Panorama to Nave de Santo António. Glacial cirques. Moraines. Problems of pre-Weichselian glaciations.

Piornos offers a good panorama towards the eastern margin of the Torre plateau, allowing for the observation of the Covão do Ferro glacial cirque, the three paleonunataks formed by Cântaro Raso, Cântaro Magro and Cântaro Gordo, and to the complex moraine infill of the Nave de Santo António. It also allows for analyzing the contrasts of the landforms between the western (Torre) and eastern (Penhas da Saúde) plateaus, as well as an understanding of the tectonic significance of the Alforfa and Zêzere valleys.

Stop 8. Covão da Ametade

U-shaped glacial valleys, glacial overdeepening, riegels.

Generally, in the Estrela, the so-called “covões” correspond to glacial overdeepenings, which are normally infilled by post-glacial deposition. The Covão da Ametade provides a good view towards the Cântaro Magro and marks the contrast between the zones of glacial erosion and deposition in the upper catchment of the Zêzere valley.



Figure 17. View from Covão da Ametade towards the Cântaro Magro.

Stop 9. Penhas Douradas

Granite weathering landscape, tors and castle-koppies.

The Penhas Douradas sector of the western plateau, at about 1,500 m a.s.l. shows excellent examples of granite weathering landforms, such as tors, nubbins, boulders and castle koppies. In the Estrela, the best examples of granite landforms occur in coarse grained granite variants, such as the Seia granite that outcrops in this non-glaciated sector of the plateau. The age of tor exhumation is being studied by cosmogenic isotope exposure dating by Raab *et al.*, with a manuscript under preparation.

References

- AGE (2017). Aspiring Geopark Estrela Application Dossier for UNESCO Global Geopark. Associação Geopark Estrela, Portugal.
- Azevedo, M.R; Valle Aguado, B. (2006). Origem e Instalação de Granitóides Variscos na Zona Centro-Ibérica. In: Dias R, Araújo A, Terrinha P, Kullberg J.C, (Coord.), Geologia de Portugal no Contexto da Ibéria. 107-122p.
- Cabral, F.A.V.P. (1884). Vestígios glaciários na Serra da Estrela. Revista de Obras Públicas e Minas, Lisboa. 435-459p.
- Cabral, J. (2012). Neotectonics of mainland Portugal: state of the art and future perspectives. Neotectónica de Portugal peninsular: estado de la cuestión y perspectivas de futuro. Journal of Iberian Geology 38 (1). 71-84p.

- Capdevila, R.; Corretge, G.; Floor, P. (1973). Les granitoides varisques de la Meseta Iberique. Bull. Soc. Geol. France. 209-228p.
- Capdevila, R.; Floor, P. (1970). Les differents types de granites hercyniens et leur distribution dans le nord-ouest de l'Espagne. Bol. Geol. Miner. Espana 81. 215-225p.
- Carrington da Costa, M. (1950). Notícia sobre uma carta geológica do Buçaco de Nery Delgado. Comunicações dos Serviços Geológicos de Portugal. 1-28p.
- Cunha P.P.; Pena dos Reis, R. (1995). Cretaceous sedimentary and tectonic evolution of the northern sector of the Lusitanian Basin (Portugal). Cretaceous Research 16. 155-170p.
- Cunha, P.P.; Pimentel, N.; Pereira, D.I. (2000). Sedimentary and tectonic signature of the betic compression climax in Portugal: the late Vallesian-Turolian sedimentary discontinuity. Ciências da Terra 14. Univ. Nova Lisboa. 61-72p.
- Daveau, S. (1969). Structure et relief de la Serra da Estrela. Finisterra 4(7). 33-197p.
- Daveau, S. (1971). La glaciation de la Serra da Estrela. Finisterra. Revista Portuguesa de Geografia 6 (11). 5-40p.
- Daveau, S. (1973). Quelques exemples d'évolution quaternaire des versants au Portugal. Finisterra, Lisboa. 5-45p.
- Daveau, S. (1978). Le périglaciaire d'altitude au Portugal. Colloque sur le périglaciaire d'altitude du domaine méditerranéen et abords, Strasbourg.
- De Vicente, G.; Cloetingh, S.; Van Wees, J.D.; Cunha, P.P. (2011). Tectonic classification of Cenozoic Iberian foreland basins. Tectonophysics 502(1-2). 38-61p.
- De Vicente, G.; Vegas, R.; Muñoz-Martín, A.; Silva, P.G.; Andriessen, P.; Cloetingh, S.; González-Casado, J.M.; Van Wees, J.D.; Álvarez, J.; Carbó, A.; Olaiz, A. (2007). Cenozoic thick-skinned and topography evolution of the Spanish Central System. Glob. Planet. Change 58. 335-381p.
- De Vincente, G.; Vegas, R. (2009). Large-scale distributed deformation controlled topography along the western Africa–Eurasia limit: tectonic constraints. Tectonophysics 474. 124-143p.
- Dias, R.; Ribeiro A. (2013). O Varisco do sector norte de Portugal. In: Dias R, Araújo A, Terrinha P, Kullberg J.C, (Eds). Geologia de Portugal, vol1, Escolar Edit. 59-71p.
- Dinis, J.; Rey, J.; Cunha, P.P.; Callapez, P.; Pena dos Reis, R. (2008). Stratigraphy and allogenic controls of the western Portugal Cretaceous: an updated synthesis. Cretaceous Research 29. 772-780p.
- Feio, M. (1952). A evolução do relevo do baixo Alentejo e algarve. Com. ser. geológicos Portugal 32, Lisboa.
- Ferreira A.B. (1991). Neotectonics in northern Portugal. A geomorphological approach. Geomorph. N.F, Berlim, Estugarda, Suppl. BD.82. 73-85p.
- Ferreira A.B. (1993). Manifestações geomorfológicas glaciárias e periglaciárias em Portugal. In: Carvalho G.S, Ferreira A.B, Senna-Martínez J.C, (eds.). O Quaternário em Portugal: Balanço e perspectivas. A.P.E.Q., Ed. Colibri. 75-84p.

- Ferreira A.B. (2005). O Ambiente Físico. Vol1. Geografia de Portugal, (coord.) Medeiros C.A, Lisboa, Círculo de Leitores. 495p.
- Ferreira, A.B. (1978). Planaltos e Montanhas da Beira, estudo de Geomorfologia. Mem. Centro Estudos Geográficos 4. 374p.
- Ferreira, N.; Iglésias, M.; Noronha, F.; Pereira, E.; Ribeiro, A.; Ribeiro, M.L. (1987). Granitóides da Zona Centro Ibérica e seu enquadramento geodinâmico. In: Bea F, Carnicero A, Gonzalo J, Lopez Plaza M, Rodriguez Alonso M, (Eds.) Geologia de los Granitóides y Rocas asociadas del Macizo Hespérico, Rueda, Madrid. 37-51p.
- Ferreira, N.; Vieira, G. (1999). Guia geológico e geomorfológico do Parque Natural da Serra da Estrela. PNSE-ICN, Ministério da Economia, Inst. Geológico e Mineiro. 111p.
- Fleury, E. (1916). Sur les anciennes glaciations de la Serra d'Estrela. Paris, 162. 599-601p.
- Julivert, M., Fontbote J., Ribeiro, A., Conde, L. (1974). Memória explicativa del Mapa Tectonico de la Peninsula Iberica y Baleares, Escala 1:1000000. Instituto Geológico y Minero de España, Madrid.
- Lautensach, H. (1929). Eiszeitstudien in der Serra da Estrela (Portugal). Zeitschrift für Gletcherkunde 17. 324-369p.
- Martínez-Catalán J.R, Aller J, Alonso J.L, Bastida F. (2009). The Iberian Variscan orogen. In: García-Cortés A, (Ed.) Spanish Geological Frameworks and Geosites - An Approach to Spanish Geological Heritage of International Relevance. IGME.
- Martín-González, F. (2009). Cenozoic tectonic activity in a Variscan basement: evidence from geomorphological markers and structural mapping (NW Iberian Massif). *Geomorphology* 107. 210-225p.
- Martin-Serrano, A. (1988). El relieve de la region occidental zamorana. La evolucion morfológica de um borde del macizo hespérico. Inst. Estudios Zamoranos Florian de Ocampo, Zamora. 311p.
- Meireles, C.; Castro, P.; Ferreira, N. (2014). On the presence of cadomian angular unconformity in Beiras Group (Central Portugal): cartographic, lithostratigraphic and structural evidences. *Comunicações Geológicas* 101, Esp. I. 495-498p.
- Migoñ, P.; Vieira, G. (2014). Granite geomorphology and its geological controls, Serra da Estrela, Portugal. *Geomorphology* 226. 1–14p.
- Neiva A.M.R, Teixeira R.J.S, Lima S.M, Silva P.B. (2013). Idade, Origem e Protólitos de granitos variscos de três áreas portuguesas, Academia das Ciências de Lisboa. 13p.
- Neiva, A.M.R.; Williams, I.S.; Ramos, J.M.F.; Gomes, M.E.P.; Silva, M.M.V.G.; Antunes, I.M.H.R. (2009). Geochemical and isotopic constraints on the petrogenesis of Early Ordovician granodiorite and Variscan two-mica granites from the Gouveia area, central Portugal. *Lithos* 11. 186-202p.
- Nieuwendam, A., Vieira, G.; Woronko, B., Schaefer, C., & Johansson, M. (2020). Reconstructing cold climate paleoenvironments from micromorphological analysis of relict slope deposits (Serra da Estrela, Central Portugal). *Permafrost and Periglacial Processes*. <https://doi.org/10.1002/ppp.2054>

- Oliveira J.T, Pereira E, Ramalho M, Antunes M.T, Monteiro J.H. (1992). Notícia Explicativa da Carta Geológica de Portugal, escala 1/500000, Serviços Geológicos de Portugal.
- Pais, J.; Cunha, P.P.; Pereira, D.; Legoinha, P.; Dias, R.; Moura, D., Silveira A.B, Kullberg J.C, González-Delgado J.A. (2012). The Paleogene and Neogene of Western Iberia (Portugal). A Cenozoic record in the European Atlantic domain. Springer, Heidelberg. 156p.
- Raab G., Dollenmeier W., Tikhomirov D., Vieira G., Migoñ P., Ketterer M.E., Christl M., Stutz J., Egli M. (2022). Contrasting soil dynamics in a formerly glaciated and non-glaciated Mediterranean mountain plateau (Serra da Estrela, Portugal). *Catena*. <https://doi.org/10.1016/j.catena.2022.106314>
- Ribeiro, A. (2013). A Evolução Geodinâmica de Portugal; os ciclos ante-mesozóicos. In: Dias R, Araújo A, Terrinha P, Kullberg J.C, (Eds.). *Geologia de Portugal no contexto da Ibéria*. Univ. Évora. 15-57p.
- Ribeiro, A.; Kullberg, M.C.; Kullberg, J.C.; Manuppella, G.; Phipps, S. (1990). A review of Alpine tectonics in Portugal: Foreland detachment in basement and cover rocks. *Tectonophysics* 184. 357-366p.
- Ribeiro, O. (1949). Le Portugal Central (livret-guide de l'excursion C). XVI Cong. Inter. Géogr. Lisboa.
- Ribeiro, O. (1954). Estrutura e Relevo da Serra da Estrela. *Bol. Real Soc. Esp. Hist. Nat.* (homenaje Hernández-Pacheco), Madrid. 549-566p.
- Rockwell, T.; Fonseca, J.; Madden, C.; Dawson, T.; Owen, L.A.; Vilanova, S.; Figueiredo P. (2009). Palaeoseismology of the Vilarica segment of the Manteigas-Bragança Fault in northeastern Portugal. In: Reicherter K, Michetti A.M, Silva P.G, (eds.) *Palaeoseismology: Historical and Prehistorical Records of Earthquake Ground Effects for Seismic Hazard Assessment*. The Geological Society London, Special Publications 316. 237-258p.
- Sant'Ovaia, H.; Martins, H.C.B.; Noronha, F. (2013). Oxidized and reduced Portuguese Hercynian granites associated with W and Sn hydrothermal mineralizations. *Comunicações Geológicas*, 100(1). 33-39p.
- Santos, J.B.; Vieira, G.; Santos-González, J.; Woronko, B.; Redondo-Vega, J.M. (2020). Macrofabric and grain size analysis of moraines and other till deposits in the Serra da Estrela Mountains, central Portugal, *Physical Geography*, <https://doi.org/10.1080/02723646.2020.1838136>
- Santos, R.M.P.; Tassinari, C.C.G. (2012). Different lead sources in an abandoned uranium mine (Urgeiriça, Central Portugal) and its environment impact, isotopic evidence. *Geochemistry: Exploration, Environment Analysis* 12. 241-252p.
- Sousa M.B, Sequeira A.J.D. (1987). Carta Geológica de Portugal à escala 1/50000, Folha 10D – Alijó. Serv. Geol. Portugal, Lisboa.
- Teixeira, C. (1955). Notas sobre a Geologia de Portugal: O Complexo Xisto-Grauváquico ante-Ordovícico. Porto (Eds.) Lisboa. 50p.

- Van Den Brink, L.M.; Janssen, C.R. (1985). The effect of human activities during cultural phases on the development of montane vegetation in the Serra da Estrela, Portugal. *Review of Palaeobotany and Palinology* 44. 193-205p.
- Van der Knaap, W.O.; Van Leeuwen, J.F.N. (1997). Holocene vegetation successions, altitudinal vegetation zonation, and climatic change in the Serra da Estrela. *Review of Palaeobotany and Palinology*, 97. 239-285p.
- Vieira, G. (2004). Geomorfologia dos planaltos e altos vales da Serra da Estrela. Ambientes frios do Plistocénico Superior e dinâmica actual. PhD in Geography. University of Lisbon, 724p.
- Vieira, G. (2008). Combined numerical and geomorphological reconstruction of the Serra da Estrela plateau ice-field, Portugal. *Geomorphology* 97. 190-207p.
- Vieira, G.; de Castro, E.; Gomes, H.; Loureiro, F.; Fernandes, M.; Patrocínio, F.; Firmino, G.; Forte, J.P. (2020). The Estrela Geopark—From planation surfaces to glacial erosion. in Vieira G., Zêzere, J.L. & Mora, C. (Eds.), *Landforms and Landscapes of Portugal*, Springer: 341-357.
- Vieira, G.; Nieuwendam, A. (2020). Glacial and Periglacial landscapes of the Serra da Estrela. in Vieira G., Zêzere, J.L. & Mora, C. (Eds.), *Landforms and Landscapes of Portugal*, Springer: 185-198.
- Vieira, G.; Palacios, D.; Andrés, N.; Mora, C.; Vázquez Selem, L.; Woronko, B.; Soncco, C.; Úbeda, J.; Go-yanes, G. (2021). Penultimate Glacial Cycle glacier extent in the Iberian Peninsula: new evidence from the Serra da Estrela (Central System, Portugal), *Geomorphology*, 388, <https://doi.org/10.1016/j.geomorph.2021.107781>.
- Vieira, G.; Woronko, B. (2021). The glaciers of Serra da Estrela, in Oliva, M., Palacios, D. & Fernández-Fernández, J.M. (Eds.), *Iberia, Land of Glaciers*, Elsevier, <https://doi.org/10.1016/B978-0-12-821941-6.00020-7>

Index

Itinerary and schedule	7
1. The geology and geomorphology of the Serra da Estrela	10
1.1. Introduction	10
1.2. The Variscan orogen heritage: a precursor of the present-day dynamics	11
1.3. The Pre-Ordovician autochthonous	13
1.4. A wealth of granite intrusions at the late stages of the orogeny	14
1.5. The planation at the end of the Variscan cycle	16
1.6. Collision with Africa and the rise of a new mountain	18
1.7. Towards the present-day relief organization	19
1.8. The richness of granite types and the diversity of landforms	20
1.9. The originality of the last glaciation in the Serra da Estrela	21
a) History of research	21
b) Characteristics of the glaciation	22
c) Chronology	26
d) The Periglaciation	26
1.10. Postglacial evolution	27
2. Itinerary description	27
Stop 1. Senhora do Espinheiro	27
Stop 2. Sabugueiro/Covão do Urso Panorama	27
Stop 3. Lagoa Comprida (short walk)	28
Stop 4. Salgadeiras – Lagoas do Covão da Clareza	29

Stop 5. Alto da Torre	30
Stop 6. Covão do Boi and Cântaro Raso	31
Stop 7. Piornos	32
Stop 8. Covão da Ametade	32
Stop 9. Penhas Douradas	33
References	33



Photo by Sérgio Brito

ORGANIZATION AND SUPPORTERS:

